School of Applied Geology

STRUCTURAL GEOLOGY AND GOLD MINERALISATION OF THE ORA BANDA AND ZULEIKA DISTRICTS, EASTERN GOLDFIELDS, WESTERN AUSTRALIA

Gerard Ignatius Tripp

This thesis is presented as part of the requirements for the award of the Degree of Master of Science, of the Curtin University of Technology

March 2000

ABSTRACT

Late-Archaean deformation at Ora Banda 69km northwest of Kalgoorlie, Western Australia, resulted in upright folds (D2), ductile shear zones (D3), and a regional-scale brittle-ductile fault network (D4). Early low-angle faults (D^E, D1), documented in the surrounding Coolgardie, Kambalda and Boorara Domains are not developed in the Ora Banda Domain, and the fabrics reflect only the latest ENE-WSW shortening event. The western limb of the regional-scale ESE-plunging Kurrawang syncline (D2), is truncated by the Zuleika Shear Zone (D3), a within-greenstone ductile shear zone located 10km southeast of Ora Banda. The shear zone has a much greater strike length (250km) than depth extent, as seismic imagery reveals a sharp truncation against a mid-crustal décollement at a depth of 6km-depth below surface. The Zuleika Shear Zone is a NW-SE trending band of anastomosing S-C mylonite zones formed in conjugate sets of NW-SE trending sinistral and N-S trending dextral shear zones. Widely distributed flattening strains and more restricted zones of non-coaxial shear in the Zuleika Shear Zone, suggest deformation-path partitioning typical of a transpressional tectonic environment. Late-tectonic brittle-ductile faults (D4) cross-cut the Zuleika Shear Zone and surrounding greenstones, and hence are not Riedel structures or other lower order faults genetically related to the ductile shearing. Gold mineralisation of the Zuleika Shear Zone began during the ductile deformation (D3), continued through peak metamorphism that post-dates the shearing, and finally ceased after the brittle-ductile faulting event (D4). Gold deposits are primarily located where brittle-ductile faults intersect the Zuleika Shear Zone.

Brittle-ductile faults (D4), are developed in three principal structural orientations: N-S (dextral), NE-SW (dextral) and E-W (sinistral). These faults display mutual cross-cutting relationships and were formed synchronously during a single regional shortening event. The brittle-ductile fault network is developed unevenly over the region, being localised in packets of high fracture-density referred to as structural zones. The Ora Banda structural zone is an area of high density faulting in the vicinity of Ora Banda, composed of a network of interlinked faults in which alternating ductile and brittle conditions produced cataclasite, breccia and quartz vein systems overprinting mylonite and schistosity.

Other areas of high fracture-density (eg. Grants Patch and Mount Pleasant structural zones), are located within the NW-SE trending Ora Banda mafic sequence and spaced at 10km intervals to the southeast of Ora Banda. This spatial periodicity of high fracture-density within the mafic sequence may have developed as a result of layer-parallel extension during ENE-WSW regional shortening. Gold deposits are concentrated in the Ora Banda, Grants Patch and Mount Pleasant structural zones. Gold distribution within the Ora Banda structural zone traces out the distribution of brittle-ductile faults, indicating that the fault network was the major pathway for fluid flow during mineralisation. Hydrothermal minerals are integral components of fault fabrics within the structural zone, and textures indicate that the faults were formed under conditions of high fluid pressure and, for much of the deformation, may have been fluid-generated.

At Ora Banda the Enterprise gold deposit (40 tonnes Au) highlights the control of mesoscopic-scale fractures on gold distribution. On aeromagnetic imagery, the Enterprise fault zone appears as a narrow fault structure, but at a mesoscopic-scale, it is a broad zone of interlinked brittle-ductile faults and quartz veins. Fabrics developed in the layered, differentiated dolerite host rocks of the Enterprise fault zone, range from cataclasite to banded mylonite with a major component of net-veined breccia (mesofracturing). Kinematic analyses of fault slip lineations reveal an 055° directed (ENE-WSW) maximum shortening axis during brittle-ductile faulting. Microfabrics of the faults show extensive recrystallisation with significant post-deformation recovery that may be related to late to post – tectonic intrusion of the adjacent Lone Hand Monzogranite. Deformation mechanisms indicate that the D4 event occurred at a low-to-moderate temperature, in a low strain-rate environment typical of mid to upper-greenschist facies crustal conditions. Gold mineralisation in the Enterprise deposit is controlled by faults with high-grade shoot development at the intersection of faults and host rock contacts that may represent gradients in tensile rock-strength. Although gold distribution indicates that faults are a major control on mineralisation, at a microscopic-scale, the control is by a linked network of microfractures that pervades the host rocks.

Fry analysis of gold deposits within the Ora Banda mafic sequence shows clustering into groups with about 10km spacing. Coincidence of high fracture-density zones and gold deposits in 10km spaced-corridors reveals the regional-scale nature of gold mineralisation

within the brittle-ductile fault network. Fluid-pressure gradients generated by pressure release during high-density fracturing, may have effectively increased fluid-rock ratios by focussing of metamorphic fluids through these areas. The largest gold deposits in the Ora Banda mafic sequence are hosted by 060°-090° trending brittle-ductile faults with dilational textures (hydraulic breccia), and minor evidence of slip with negligible offsets. The orientation of these structures is sub-parallel to the regional axis of maximum shortening, hence an environment of fluid overpressuring in the presence of a far-field stress system produced conditions where fluid pressure is greater than or equal to the combined minimum compressive stress and the tensile rock strength. Such conditions are conducive to multiple failure episodes with fluid-pressure cycling and transient permeability as a consequence of fault reactivation. Formation of the brittle-ductile fault network occurred as a result of a delicate balance between deviatoric stress and fluid pressure, hence incremental fault development contributed to, and was a consequence of, the gold mineralisation event.

The geometric relations of shear zones, brittle-ductile faults and gold mineralised zones are similar across all scales of observation from regional to microscopic and are therefore fractal. Fractal geometry indicates that deformation and gold mineralisation are temporally and genetically associated, and this combined with the textural relationships of the gold ores indicates that the sites of gold deposition were not structurally prepared prior to mineralisation. Development of early ductile to later brittle-ductile structures indicates changing conditions of deformation typical of decreasing crustal depth, or a variation of strain rate with time. The lack of a significant change in orientation of the maximum shortening direction and continuance of gold mineralisation throughout ductile and brittle deformation events, implies that deformation was progressive during a bulk shortening that accompanied uplift of the crust.

ACKNOWLEDGEMENTS

Special thanks to my wife Jodene, and my children for support and tolerance during the course of this project.

I would like to thank my supervisors; Peter Collins the principal supervisor of the project, and Julian Vearncombe for giving generously of his time and effort to both my professional and academic development whilst running a busy consultancy.

Centaur Mining and Exploration provided financial and technical assistance, and special thanks is due to Bradley Toms for seeing the value of this study from its inception and for his full support through to its completion. Thanks to Neil Phillips for providing essential focus to the research and expedient editing of the thesis. Special thanks to Taihe Zhou for many helpful discussions that increased my understanding of gold chemistry, and mineralisation and tectonics. Andrew Radonjic afforded invaluable logistical support including data on the Mount Pleasant gold mines. Garry Adams supplied structural data on the Nazzaris deposit, rock samples and thin sections from the Bullant deposit, and helpful advice on figure production. Steve Arnott assisted with data manipulation using Geotech. Tom Gibbins and David Williams supplied computer support, and field assistance was rendered by Doug Meyer and Chris Gamble. Thanks to Kelly Stanhope, Maria Medak, Karina Reid, Lee Forster and Paul Evans for drafting the diagrams.

Bob Crossley produced all the polished thin sections to an exceptional standard of quality, and helped with the petrology. Jeff Vaughan is thanked for providing access to laboratory facilities at Curtin University of Technology in Kalgoorlie. Data and images from the Kalgoorlie seismic transect were generously provided by Bruce Goleby of AGSO.

Critical and helpful discussions were held with Garry Adams, Steve Arnott, Stephen Burke, Greg Chintock, Peter Collins, Bob Crossley, Mal Dickie, David Hobby, Ted Hansen, Paul McMillen, Jayson Meyers, Phil Moffit, Andrew Owen, Steven Oxenburgh, Neil Phillips, Steve Reddy, Cees Swager, Michael Taylor, Bradley Toms, Julian Vearncombe, Wally Witt, and Taihe Zhou.

CONTENTS

LIST OF FIGURES

LIST OF TABLES

1 INTRODUCTION

This research is focussed on the relationships between structural geology and gold mineralisation in the Ora Banda and Zuleika districts, two important gold mining districts in terms of historic production and current resources. The two mining districts are located in the southwestern area of the Norseman – Wiluna greenstone belt, one of the best documented Archaean greenstone belts in the world. Historic and current mining, exploration and academic activity ensure a maintained, high-level of both economic and scientific interest in these areas well into the future.

A significant aspect of this research is the use of data sets of structure and gold distribution from regional to microscopic scales. Recently acquired, high-resolution aeromagnetic data has provided new images that show fine details of the distribution and geometry of structure and magnetic rock units, used for regional-scale geological interpretation. This interpretation is coupled with structural analysis of outcrop and mine exposures (mesoscopic and microscopic), to interpret the deformation of the Archaean greenstone sequence. Recent mining and exploration activity in the Ora Banda and Zuleika districts involving high-density drilling of the regolith to un-weathered rock, has shown the distribution of gold mineralisation to a level of detail unrivaled in the past. Correlation of these data sets provides a unique opportunity for understanding the structural controls on gold mineralisation at all scales.

1.1 AIMS AND OBJECTIVES

The aims and objectives of this study are;

1. To document the structural geology and gold mineralisation of the Zuleika Shear Zone, demonstrating the relationships between regional-scale ductile shear zones and mesoscopic brittle-ductile faults.
2. To document the structural geology and gold mineralisation of the Ora Banda district as an example of a high fracture-density structural zone.
3. To document the structural geology and gold mineralisation of the Enterprise gold deposit to determine mesoscopic structural relationships.

4. To assess the distribution and geometry of structures compared to gold deposits in the Ora Banda – Zuleika district for the purpose of determining correlations between the two.
5. To analyse the distribution of structure and gold mineralisation at all scales.

1.2 RESEARCH METHODOLOGY

1.2.1 Study area

The study area is broadly centered on the northwestern Kalgoorlie region, but changes significantly across different scales of observation. A regional-scale aeromagnetic interpretation by Vearncombe (1998b) used in this study covers an area of 100km x 75km (Figure 1.1). At a mine-corridor scale, two major areas are assessed at Zuleika (2km x 11km) and Ora Banda (6km x 5km) (Figure 1.1), and at a mesoscopic scale, individual mines are assessed as areas of key outcrop within each of the mine-corridors (Figure 1.2). A major part of the study at mesoscopic and microscopic scales is focussed on the Enterprise gold deposit (Figure 1.2). Data on structural styles and gold mineralisation (Witt 1993b) at Siberia, Grants Patch and Mount Pleasant are assessed, but these areas were not studied in detail.

1.2.2 Data collection techniques

Interpretations of remote sensing data in this study include aerial photography, aeromagnetic and ground magnetic data and a seismic reflection profile. The data sets comprise aerial photography flown at 1:25,000 and 1:10,000 scales, detailed aeromagnetics at 1:50,000 scale (50m spaced flight lines) and groundmagnetics at 1:5,000 scale (25m spaced lines). Interpretations are focussed on specific areas (mining centres) and as such broad scale plans are not produced. A 1:100,000 aeromagnetic interpretation by Vearncombe (1998b) is used as the main data set from which many of the regional inferences in this study are drawn.

Field observation of critical exposures with documentation of mesoscopic relationships was undertaken to provide a database from which geological and structural relationships

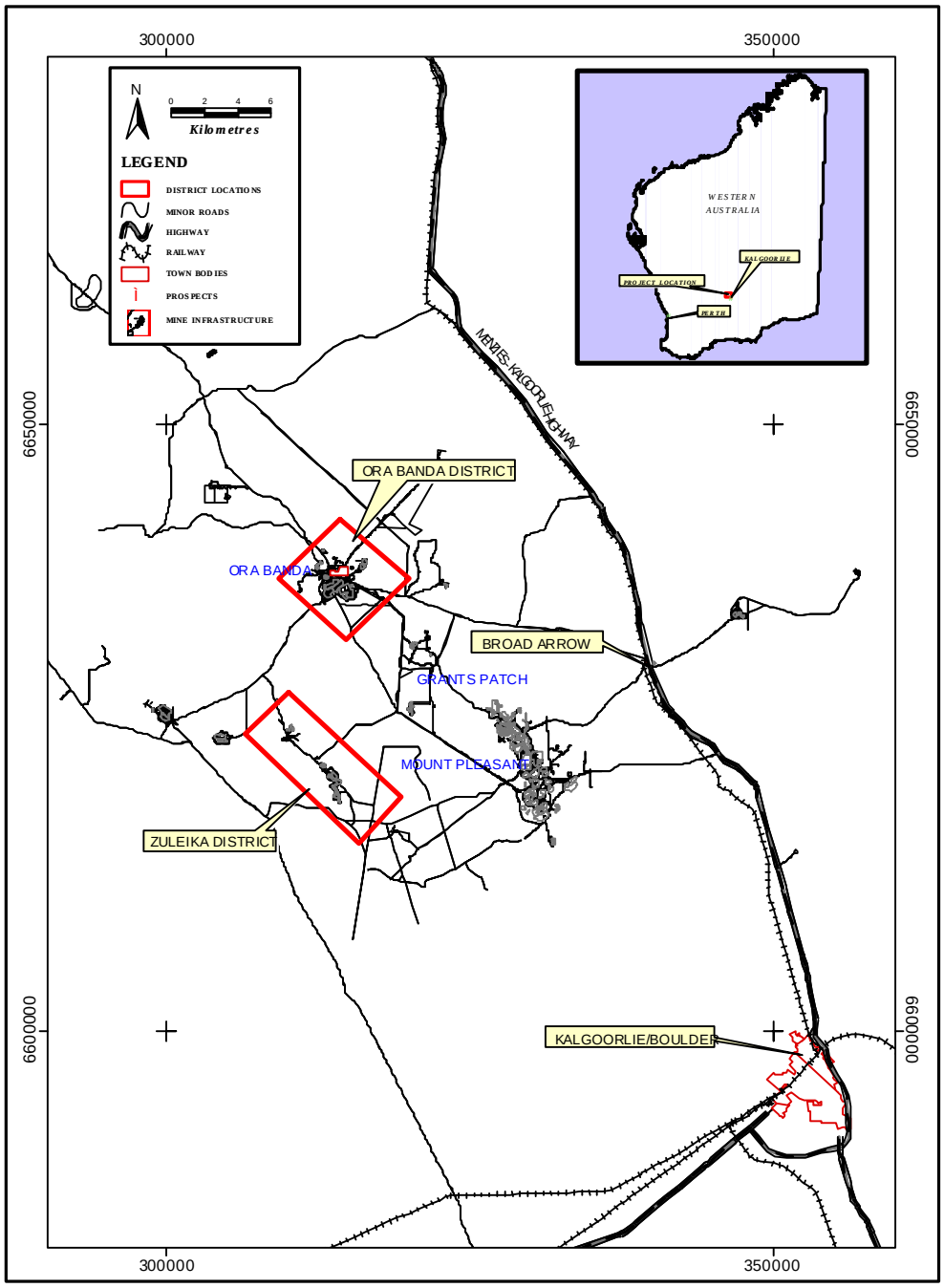

Figure 1.1 - Location map of the Ora Banda and Zuleika districts, north Kalgoorlie.

3

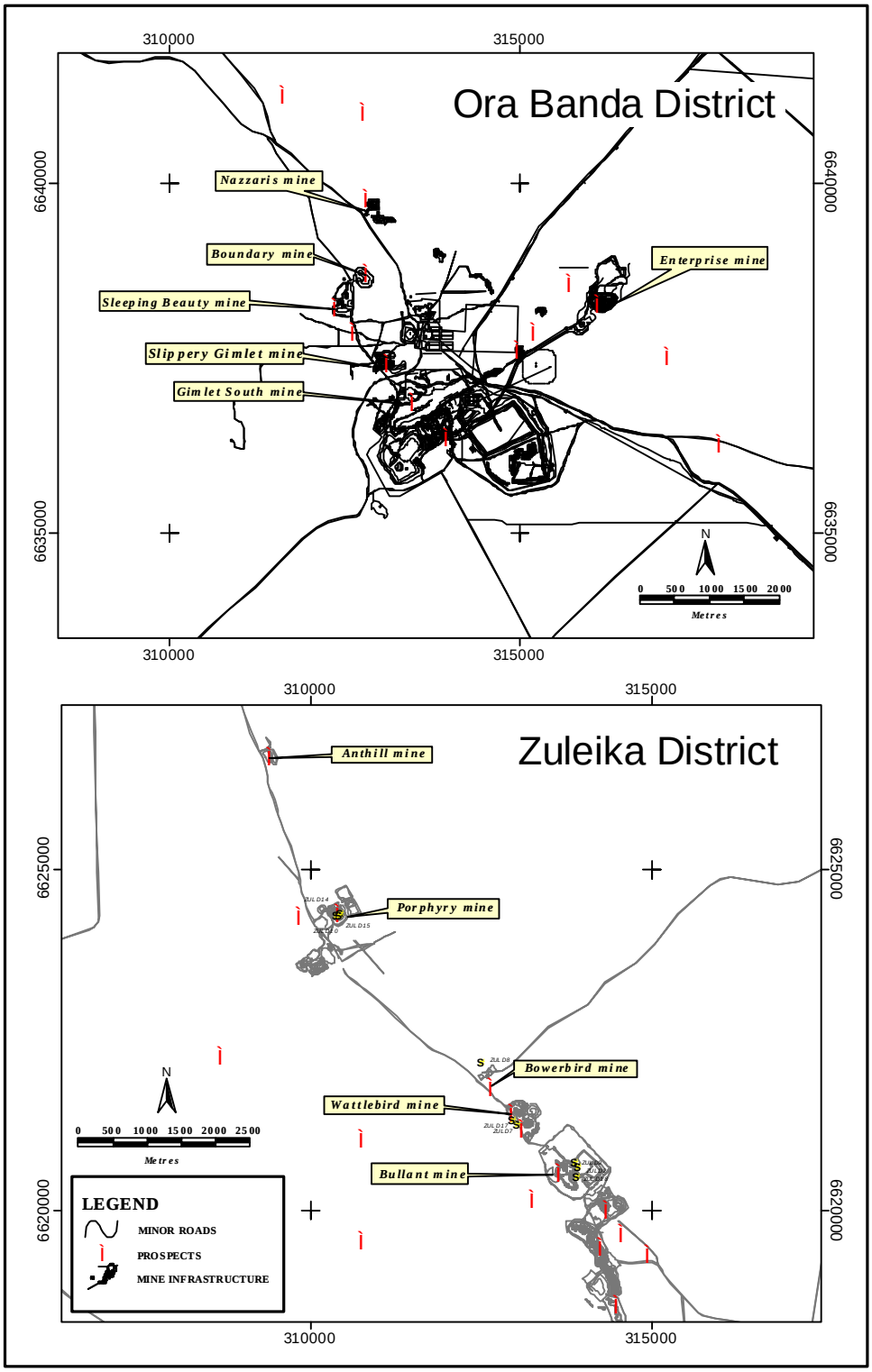

Figure 1.2 - Location of areas of detailed study within the Ora Banda and Zuleika districts

4

can be interpreted. Geological mapping areas include eight open-pit mines and one underground mine; Anthill, Porphyry, Bowerbird, Wattlebird and Bullant mines in the Zuleika Area, and Gimlet South (open-pit/underground), Sleeping Beauty, Boundary, Nazzaris, Slippery Gimlet and Enterprise mines in the Ora Banda district.

Oriented diamond drill core is used as an important adjunct to open-pit and underground mine exposures. Most open-pit mines are in strongly weathered rocks with un-weathered rocks only in the bottom of the pits. These open-pit mines provide exposure in the walls around the main ore-bearing structures, yet the prime objects of interest have been removed by mining. In these cases diamond drill core preserves the structures in pristine state, and in most deposits diamond drilling is targeted at depth extensions giving a cross-sectional view of the structures.

The majority of diamond drill core assessed in this study was planned and drilled by the author in the course of company exploration on the mining leases, hence full core was examined before cutting and sampling. Structural data were collected using the Alpha/Beta method, with a focus on minimising data-collection errors as discussed in Appendix 1.1 (p.258). Analysis of the data including drillhole rotation and stereonet plotting was done using DIPS 3.1 structural analysis software. In all drillholes, data conversion from Alpha/Beta to dip/dip direction was corrected for drillhole deviation using Eastman downhole camera surveys, or where available DEMS (Digital electronic multishot survey) or Maxibore downhole survey data.

Geological mapping and diamond core logging included the collection of a range of geological data additional to structural orientations. The data were converted into digital format for analysis by computer software programs: Excel, Micromine, Geotech, StereoNett and DIPS. The last three computer programs were used for graphical presentation of structural data. Geotech was used for plotting plans of dip/strike data, StereoNett for presentation stereograms and DIPS for presentation stereograms, and structural analysis. Structural readings were processed in Micromine for plotting against drillhole information and calculation of unique Australian Map Grid co-ordinates for each reading. Excel spreadsheets were used for handling large data sets, plotting graphs, file-

type conversion and data sorting/filtering based on the geological parameters recorded during mapping.

Since the majority of mapping in open-pit mines was in weathered rock, nearly all oriented thin section samples were taken from diamond drill core with few exceptions. Using a top-of-core orientation mark, the core was re-oriented to its true plunge/plunge direction and from this position the best angle for cutting and sampling was determined. For shear zones and schistosity the samples were cut parallel to the elongation lineation if visible (or possible) and orthogonal to the shear foliation to determine movement sense and to define the constituent mineralogy of foliations. Samples were selected mainly from structures of known orientation and gold grade so that detailed analyses could be made of the variation of gold grade and type of structures within each principal structural orientation and possible relationships determined.

Microstructural analysis of thin-section samples was carried out comprising petrographic description of constituent mineral phases including morphology, internal structure, alteration and inter/intragranular relationships, and microfabric analysis to determine the pre/syn/post-kinematic timing of mineral growth with respect to development of the fabric elements. Supplementary to microfabric analysis was the determination of components of foliations and lineations, morphology of individual fabric elements and overprinting relations between fabric elements. Microstructural analysis combined with observations of metamorphic and gold-related alteration minerals allows determination of the timing of deformation, metamorphism and gold mineralisation.

For several of the gold deposits studied, particularly Slippery Gimlet and Enterprise, Micromine and Vulcan computer programs were used to analyse the geometry, gold grade distribution and geology of the orebodies. Micromine was used for plan and cross-section analysis, and Vulcan for 3-dimensional viewing of the drillhole database and orebody interpretations. SpaDiS spatial analysis software was used to analyse the regional distribution of gold deposits, to model the envelope of gold ore in the Enterprise deposit and to identify anisotropy in gold grade distribution (eg. high-grade shoot directions).

1.2.3 Scope of the study and limitations

Some key geological questions are addressed by this study. For example, the nature and tectonic implications of the regional-scale Zuleika Shear Zone, the nature and distribution of late-tectonic brittle-ductile faults and their relationships with regional-scale ductile shear zones, and the regional and local structural controls on Archaean gold deposits. Recent mining on the Zuleika Shear Zone has provided good exposure of the cross-cutting relationships between a regional-scale, within-greenstone-belt ductile shear zone and late oblique brittle-ductile faults. Previous literature has highlighted a lack of studies of cross-cutting relationships and therefore a gap in knowledge of the timing of structural development (eg. Libby *et al.* 1990)

Whereas good exposure may provide some answers to geological questions, two major limitations of this study are; the amount of available exposure in the Archaean greenstone belt, and the number of mining areas available for detailed study. By necessity, open-pit mines and exploration diamond drillholes are the only exposures where fresh un-weathered rocks can be studied. These exposures are selected from as many localities as possible to afford some degree of representative sampling, however the locations of these exposures are highly biased by their intrinsic nature as targets of gold-exploration companies. A factor that may diminish the bias is that in any given gold deposit, only a small number of the total mappable structures are mineralised.

Geological structures in individual gold deposits are used to characterise the types of deformation fabrics produced during regional deformation, hence regional extrapolation of these local data must proceed with caution when using aeromagnetic interpretation. The application of new processing techniques to high-resolution aeromagnetic data has enabled interpreted features to be extended out from areas where the geology is known.

1.3 PREVIOUS WORK

The Ora Banda and Zuleika districts have been worked for gold since 1893, however large-scale mining operations were not initiated until 1982 when BHP Gold took control of mining leases at Ora Banda. This phase of mining activity included studies of geology, structure and mineralisation of the deposits at Ora Banda and Zuleika undertaken mostly by

BHP Research. Several studies have also been completed by subsequent leaseholders. In the late 1980's to the early 1990's, many long-term studies of the Kalgoorlie area were completed by government geological survey organisations that resulted in generation of new ideas and geological models for the region. The number of individual works from these sources is too numerous to list, but several reports that include the Ora Banda and Zuleika districts are important references for the area. Regional geological studies include works by Witt (1987, 1990), Swager *et al.* (1990), Morris (1993) and Swager (1994). Local geological studies include works by Jutson (1914), Harrison (1982, 1987), and Smit (1984). Witt (1993 a-b) produced an assessment of gold mineralisation for the Menzies-Kambalda region, with significant components included from the Ora Banda and Zuleika districts. Mineralisation studies of the local mine area were completed by Harrison *et al.* (1990), Swager (1993), Gilbert (1983) and Laing (1994). Geochemical studies by Harrison (1983, 1984), Muhling (1980) and Oliver (1993) included some petrography, but major petrographic studies were done by Gilbert (1983), Muhling (1982), Barron (1995) and Collins (1995).

Studies of the structure and geophysics of the Ora Banda and Zuleika districts are relatively few, but significant work on the structure of the areas is included in the reports by Witt (1993a-b), Swager *et al.* (1990) and Swager (1997). Local structural studies include works by Harrison (1987), Baxter (1989) and Bogacz (1995). Studies on the geophysical signature of lode mineralisation were carried out by Label (1984), Irvine (1979), Winer (1980) and Wynne and Isles (1986).

1.4 THESIS OUTLINE

This thesis follows a systematic assessment of the structural geology from regional-scale to microscopic-scale, to test similarities at all scales. The structural geology and gold geology are treated separately to avoid ambiguity with colloquial terminology (lode, reef, blow, spur, leader, stringer etc.), commonly employed to describe the gold deposits. The reason for this is to allow the structures that are hosts to gold deposits, to be assessed in the context of the current literature and classified appropriately.

Chapter 2 presents the regional and local geological settings with a brief description of the rock types, some new data on the rock units (from this study) are presented where

appropriate. Chapter 3 outlines the regional structure as determined from aeromagnetic interpretation and presents documentation of gold mineralisation along the Zuleika Shear Zone. The structural framework presented is supported by mesoscopic and microscopic observations from the Zuleika Shear Zone to demonstrate cross-cutting relations between the major structural elements. Chapter 4 presents a detailed study of the Ora Banda structural zone identified as a zone of high fracture-density in Chapter 3, and presents data on gold mines within the Ora Banda district. Several structural zones are interpreted as forming a distinct macroscopic structural anisotropy, and their coincidence with gold mining centres is of particular interest to this study. In Chapter 5, the Enterprise fault zone is discussed to illustrate mesoscopic structural development within the Ora Banda structural zone, and details of the Enterprise gold deposit are presented. Chapter 6 is totally concerned with gold deposits and the relationships between deformation and gold mineralisation using the similarities between gold geometry and distribution, and structural geometry and distribution at all scales, as demonstrated in Chapters 3, 4 and 5. Chapter 7 presents a summary and discussion of the major findings of the research, and Chapter 8 lists the conclusions of the thesis.

1.5 DEFINITIONS

1.5.1 High fracture-density ‘structural zones’

The structural zones referred to in this study are areas with a higher-density of faulting and shearing than the surrounding areas. Structural zones are parts of the regional deformation fabric and are zones of anisotropy in the late tectonic brittle-ductile fault network. In some areas (eg. Mount Pleasant) the structural zones have corridor geometry with a greater length than width, whereas in other areas (eg. Ora Banda) the structural zones have no defined long axis but are equi-dimensional (in plan view).

1.5.2 Ductile shear zones and brittle-ductile faults

The main thrust of this thesis examines the structural development of the Ora Banda and Zuleika districts that occurred in the final stages of orogenesis and during progressive uplift of the supracrustal sequence. Structural features reflect a progression of styles from early ductile to later brittle with considerable overlap in the brittle-ductile regime. Two main

pulses of shortening resulted in the development of ductile fabrics; the earlier pulse produced mostly regional-scale folds whereas the later pulse produced ductile fabrics in regional-scale shear zones. Hence, ‘ductile shear zone’ in this study refers to NW-SE trending zones of ductile shearing that are generally layer-parallel and have significant width (i.e. tens to thousands of metres). Smaller-scale fractals of the regional structures are ‘shear zones’ by definition, usually located along bedding contacts in interflow sedimentary rocks: these also are included in this definition.

Examples of ‘shear zones’ abound in mesoscopic exposures of late-tectonic cross-cutting structures, but the mesoscopic shear zones are usually integral components of brittle-ductile faults that may include breccia, cataclasite or quartz veins overprinting wallrocks that exhibit ductile strain fabrics. Whereas the structures are ‘ductile zones of simple shear’ by definition, at the regional scale they are insignificant in terms of width and offset and are therefore termed ‘brittle-ductile faults’ to avoid confusion with references to regional-scale ductile shear zones.

‘Brittle-ductile’ is taken to mean a combination of continuous and discontinuous deformation. Whereas this usage is somewhat ambiguous in terms of lacking a quantification of scale, mineralogy, strain rate, deformation continuity and deformation mechanism, it is useful to convey that the faults display a combination of brittle and ductile fabrics in a hand specimen. The two fabric types within a given fault can be mutually overprinting and hence are ‘the same fault’ for the purpose of defining broad structural controls.

1.5.3 Scales of observation

Data at several scales of observation are assessed in this study, and it is important that these scales are defined to avoid confusion. Since outcrop in Archaean terrains is scant, the necessary use of drillholes, mines and old workings to gain subsurface information leads to an unspecific scale terminology (eg. mine-scale, mine-corridor-scale, regional-scale) and the relationships between each scale in terms of orders of magnitude change in length and area generally remain undefined. In the following chapters, references are made to these unspecific scales that can span up to four orders of magnitude as listed in Table 1.1.

The numerical scale is determined by using the metre as the basic unit of division, i.e. 1 metre on a plan equals 1 metre on the ground at 1:1 (no increase or decrease in length or area). From these definitions, regional scale could include scales smaller than 1:100,000 however this is the smallest scale assessed in this study. Mesoscopic-scale spans four orders of magnitude from mine-scale (~ km) to hand specimen-scale (cm). Microscopic is taken to include x10 hand lens magnification and higher.

Table 1.1 – Defined scales of observation

Scale of observation	Physical equivalent	Numerical scale	Order of magnitude (m)
Regional	regional plans	1:100,000	10^5
Macroscopic	mine corridor	1:10,000	10^4
Mesoscopic	mine scale outcrop hand specimen	1:1000 1:100 1:10 1:1	10^3 10^2 10^1 1
Microscopic	thin section	1: 0.1 1: 0.01	10^{-1} 10^{-2}

2 GEOLOGICAL SETTING

2.1 REGIONAL GEOLOGY

The Ora Banda and Zuleika districts are located in the Eastern Goldfields Province of the Yilgarn Craton in south central Western Australia (Figure 2.1). The Yilgarn Craton is a regionally extensive crustal unit composed essentially of two main tectonic subdivisions. The majority of the craton consists of Archaean granite-greenstone terrane, and Archaean gneissic rocks that form the western margin of the craton. The Eastern Goldfields Province is the easternmost of three greenstone provinces, and contains large areas of granitoid rocks interspersed with abundant belts of greenstones up to 150 km wide.

The Ora Banda and Zuleika districts (Figure 2.2) form part of the Norseman-Wiluna greenstone Belt of the Eastern Goldfields Province (Figure 2.1). The belt was interpreted as a trough or graben association by Williams (1974) based on a komatiite-rich sequence without development of banded-iron-formation (BIF). The basement to the greenstones was considered to be sialic (Archibald *et al.*1981, Gee *et al.* 1981). Witt (1990) described the Norseman-Wiluna Belt as a tectonically and volcanically active trough during the Archaean, flanked by more stable parts of the Yilgarn Craton. The general stratigraphic sequence that is documented within the fault-bounded terranes of the Norseman-Wiluna Belt has a lower basalt unit that is overlain by a komatiite unit, an upper basalt unit and a felsic volcanosedimentary formation with mafic/ultramafic sills unconformably overlain by a coarse clastic sedimentary unit (Table 2.1). The presence of non-vesicular pillow basalts and abundant komatiites within the Norseman-Wiluna greenstone belt has led some authors to suggest that the mafic and ultramafic sequences were deposited in a deep marine basin (eg. Groves and Batt 1984). Abundant BIF and a paucity of komatiite in surrounding areas such as the Callion Terrane, Norseman Terrane and the Kurnalpie Terrane has led to a platform-phase interpretation of these areas. Barley and Groves (1988) and Barley *et al.* (1989) proposed a marginal rift-basin model for the Norseman-Wiluna greenstone belt. The Kurnalpie Terrane to the east is characterised by restricted komatiite and bi-modal volcanic rocks and is thought to represent a volcanic arc at a continental margin (Morris 1993; Swager 1995). The greenstones in the Kalgoorlie Terrane were deposited around 2.7 Ga, with the main period of deformation, granitoid intrusion, metamorphism and gold mineralisation between 2.66 to 2.64 Ga (Swager *et al.* 1990).

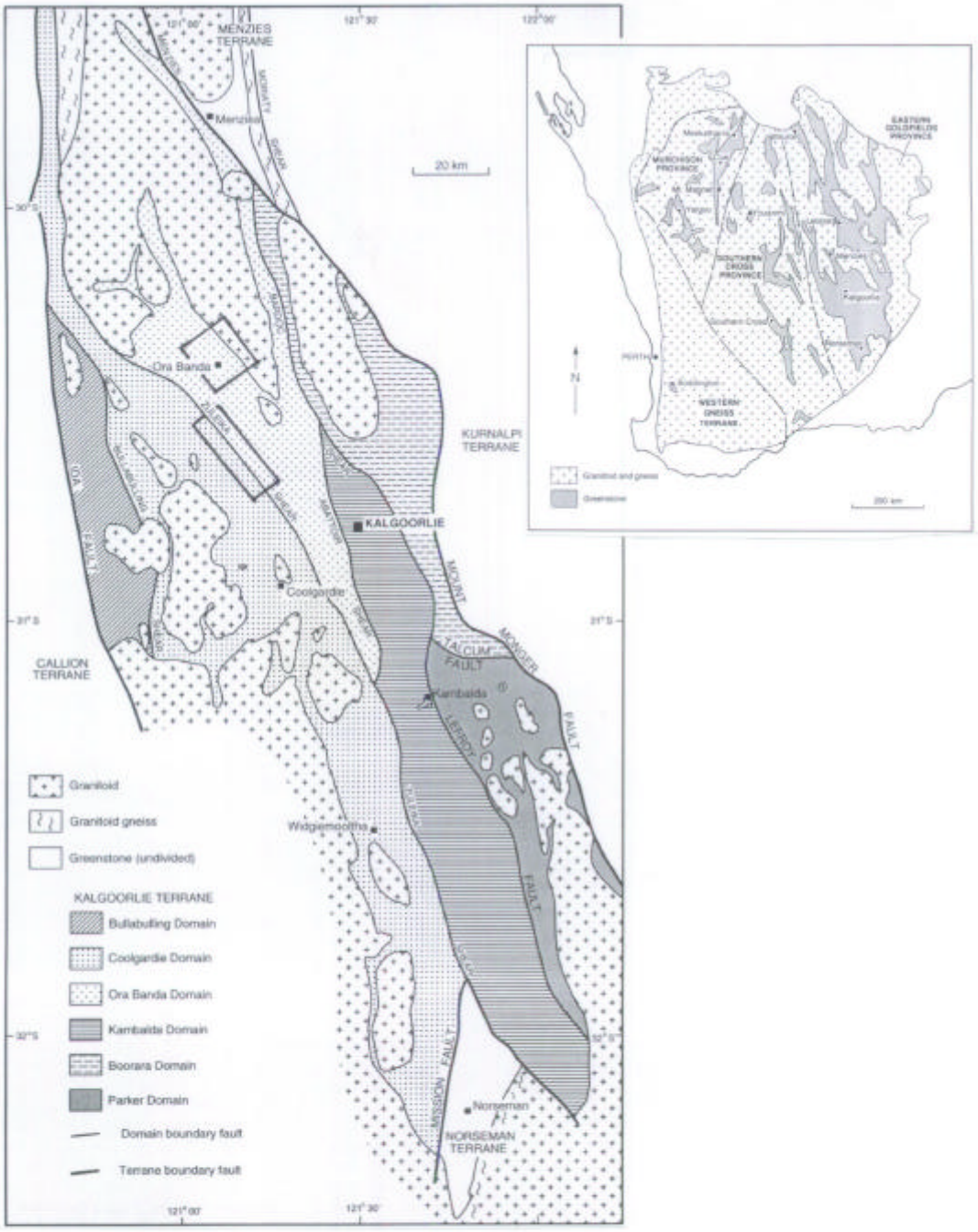

Figure 2.1 – Map of the Kalgoorlie Terrane showing distribution of tectonostratigraphic domains. Box encloses approximate location of the study area. Inset showing major tectonic subdivisions of the Yilgarn Craton with the location of the Kalgoorlie Terrane (after Swager *et al.* 1990).

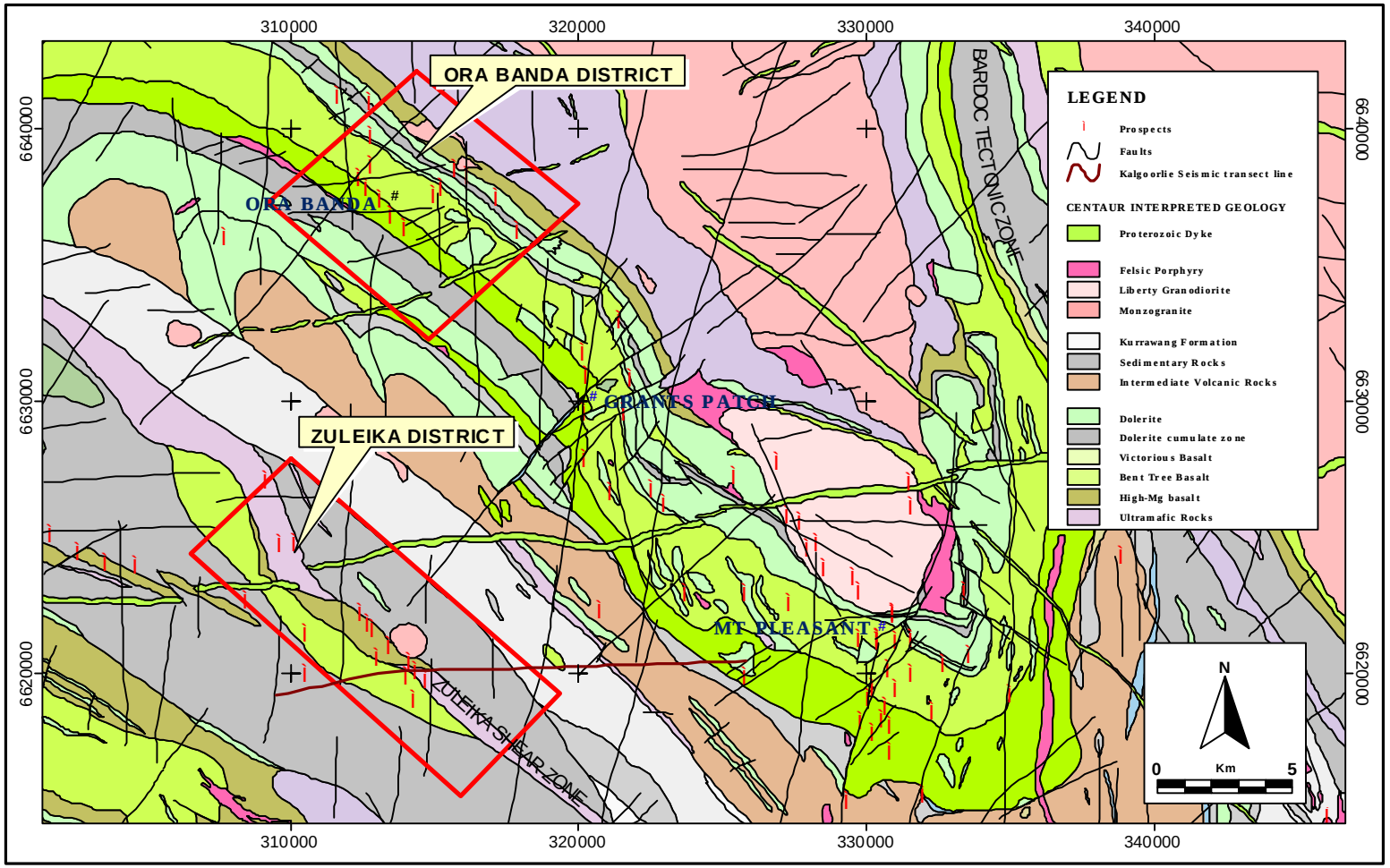

Figure 2.2 - Geology of the Ora Banda and Zuleika districts, northwest Kalgoorlie. Detailed study areas outlined.

Table 2.1 – Stratigraphic correlation of rock successions across tectonostratigraphic domains of the Kalgoorlie Terrane, modified from Swager *et al*. (1990).

Stratigraphic succession	Characteristic rock types	Ora Banda Domain	Kambalda Domain	Coolgardie Domain	Boorara Domain
Polymictic conglomerate unit	Polymictic conglomerate, immature sandstone: coarse trough cross beds, graded beds	Kurrawang Formation	Merougil Conglomerate	Absent	Absent
Felsic volcanic and sedimentary unit	Felsic volcaniclastic sedimentary rocks, ranging from coarse-clastic sandstone to interbedded sand/siltstone. Rhyolite to dacite, locally andesite; lava, tuff,agglomerate	BLACK FLAG GROUP: Pipeline Andesite; Orinda Sill; Ora Banda Sill	BLACK FLAG GROUP: Junction Dolerite; Condenser Dolerite; Golden Mile Dolerite; Triumph Gabbro	BLACK FLAG GROUP: White Flag Formation; Powder Sill; Spargoville Formation	Felsic unit, volcanic and sedimentary rocks
Upper basalt unit	High-Mg and tholeiitic basalt; massive, pillowed and vesicular lavas	GRANTS PATCH GROUP: Victorious basalt; Bent Tree Basalt; Mt Pleasant Sill; Mt Ellis Sill / Enterprise dolerite	KALGOORLIE GROUP: Paringa Basalt; Defiance Dolerite; Williamstown Dolerite	COOLGARDIE GROUP: Absent or thin and discontinuous	Absent or thin and discontinuous
Komatiite unit	High-Mg basalt at top; then thin komatiite flows with minor interflow sedimentary beds, overlying thicker komatiite flows and / or massive olivine adcumulate	LINGER AND DIE GROUP: Big Dick Basalt; Siberia Komatiite; Walter Williams Formation	KALGOORLIE GROUP: Devon Consols Basalt; Kambalda Komatiite	COOLGARDIE GROUP: Hampton Formation	Highway ultramafics
Lower basalt unit	Tholeiitic and high-Mg basalt flows, subaqueous	POLE GROUP: Missouri Basalt; Wongi Basalt	KALGOORLIE GROUP: Lunnon Basalt	COOLGARDIE GROUP: Golden Bar Sill; Burbanks Formation; Three Mile Sill	Scotia Basalt
References		Witt (1987, 1994) Gregory (1998) Harrison (1983, 1984, 1987)	Roberts (1988) Woodall(1965) Langsford (1989)	Hunter (1993)	Christie (1975) Witt (1994)

2.2 GEOLOGY OF THE ZULEIKA DISTRICT

2.2.1 Geological setting

The Zuleika district is located on the Zuleika Shear Zone, a regional-scale within-greenstone-belt ductile shear zone (Figure 2.2 p.14). Intense tectonic interleaving of ultramafic, mafic and intermediate rocks prevents the construction of a local stratigraphic section and the strike continuity and younging direction are undetermined, however very broadly the progression from west to east is high-magnesium basalt, talc-chlorite schist and felsic volcaniclastic rocks. All rocks types are extensively carbonate altered, with alteration distribution closely associated with shear zones.

Ultramafic rocks

Ultramafic rocks in the Zuleika area comprise intensely sheared talc-chlorite schist with localised brecciation. Relict spinifex textures in breccia clasts indicate that the protolith was ultramafic komatiite, and therefore the rocks are possibly remnants of the regional ultramafic marker unit. Evidence of pre-shearing brecciation abounds, with flattened clasts of ultramafic rocks and talc-carbonate veins filling the voids. The texture is typical of the majority exposures of ultramafic rocks and is most evident in diamond drill core. The brecciation may be either auto-brecciation related to volcanism in a sub-aqueous environment or a later tectonic fabric.

High magnesium basalt

Basaltic rocks include high-magnesium pillow basalt with local interpillow breccia and variolitic texture. The basalts form a generally continuous layer but also are mapped as discontinuous mega-boudins within talc-chlorite schist in the Wattlebird area.

Pillow margins are glassy and locally vesicular with zeolite infill minerals and quartz-calcite +/-epidote in the interpillow voids. The basaltic rocks are extensively muscovite-calcite altered in the vicinity of shear zones.

Intrusive albitite porphyry

Porphyritic felsic intrusive rocks are localised discontinuous bodies that are intrusive into talc-chlorite schist. The porphyries commonly are weakly foliated to undeformed with contact relationships that indicate late-to-post tectonic intrusion. Several large (<1km-scale) bodies of porphyritic granodiorite intrude the Zuleika Shear Zone in the study area but many smaller stocks are also exposed in drilling and open-pits. Some examples of mylonitic, felsic porphyritic rocks indicate intrusion over a broad period that began during the waning stages of ductile deformation (D3).

2.3 GEOLOGY OF THE ORA BANDA DISTRICT

The geology of the Ora Banda district is dominated by a moderately southwest-dipping sequence of late Archaean age (Figure 2.2 p.14, Figure 4.6 p100). The sequence locally known as the 'Ora Banda mafic sequence' is typified by weak deformation with preserved primary depositional features and igneous textures (Figure 2.3). The succession is right-way-up younging to the southwest with ultramafic rocks at the base (Linger and Die Group), overlain by tholeiitic igneous rocks (Grants Patch Group), and intermediate to felsic igneous rocks to the west (Black Flag Group). The composition of the extrusive sequence evolves as the rocks get younger from early ultramafic to later felsic, and is typical of Archaean supracrustal successions around the world (Annhaeusser 1971).

2.3.1 Stratigraphic succession

Linger and Die Group

The Linger and Die Group (Witt 1990) is a regional ultramafic marker unit with internal compositional variation including adcumulate dunite, spinifex-textured komatiite and high-magnesium basalt. The group is visible on aeromagnetic imagery as a thick internally complex zone of high magnetic response. In the study area only the upper units of the Linger and Die Group are exposed.

Siberia Komatiite (Figure 4.6 p.100) is a sequence of spinifex textured, olivine-komatiite flow rocks with localised gabbro and high-magnesium basalt. The unit is approximately

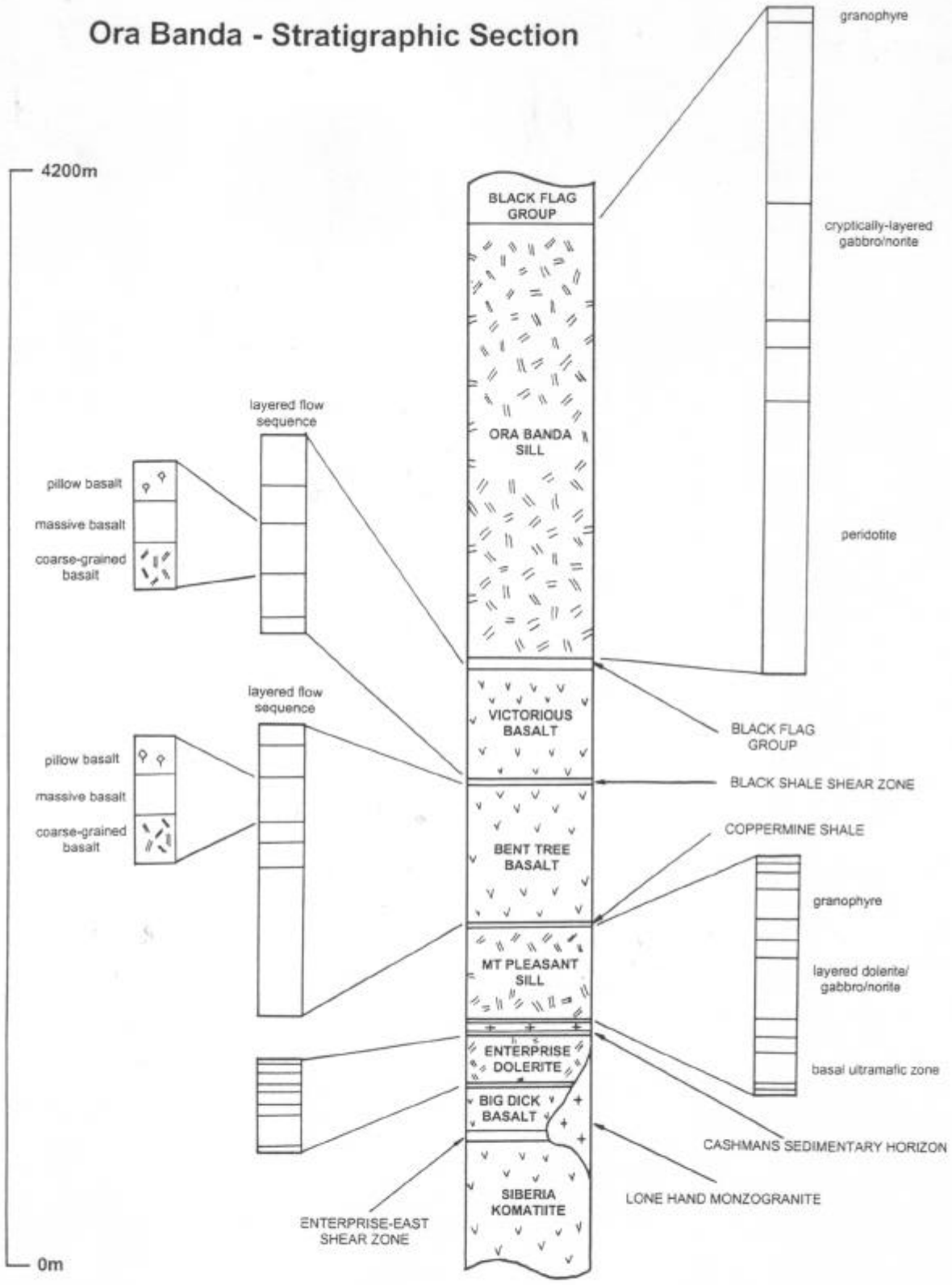

Figure 2.3 – Stratigraphic section of the Ora Banda mafic sequence. Detailed enlargements of main section show position of layers within basalt flow units and layered, differentiated sills.

2600m thick at Ora Banda and is significantly thickened in the hinge of the Kurrawang Syncline. Individual flow units are well differentiated, 1 to 5m-thick flows with olivine and clinopyroxene spinifex textures (Hill *et al.* 1987). Localised interflow sedimentary rocks and discontinuous intrusive doleritic sills disrupt the lower part of the sequence.

Big Dick Basalt (Figure 4.6 p.100) is a 500m thick sequence of interbedded basalt flow rocks. The flows consist of massive to pillowed high-magnesium basalt with variolitic texture. The pillow margins are locally deformed with initially spherical varioles becoming flattened elliptical shapes with progressive shearing. Interflow sedimentary rocks are common within the sequence. Geochemically, the unit is high-magnesium basalt with 9-18% MgO (Witt 1990) and forms the upper-most unit of the Linger and Die Group ultramafic sequence.

Grants Patch Group

The Grants Patch Group (Witt1990) is a layered mafic sequence with over 70km of strike extent, comprising interbedded basaltic flow rocks with syn-volcanic intrusive doleritic sills. The doleritic sills post-date the deposition of the flows and are therefore discussed later with intrusive rocks.

The Bent Tree Basalt (Figure 4.6 p.100) the lowermost unit of the Grants Patch Group, is a 675m thick sequence consisting of a lower gabbroic layer overlain by intercalated basaltic flow rocks that define a distinct volcanic stratigraphy (Harrison 1983). Up to six flow layers have been identified at the Gimlet South mine with each flow layer comprising a coarse-grained basal unit, massive dolerite in the middle, and pillow-basalt at the top locally with flow-top breccia. Chemical analyses indicate tholeiitic chemistry with similarities to the overlying Victorious Basalt.

Victorious Basalt (Figure 4.6 p.100) is a 450m thick succession of basaltic flow rocks with distinct flow layering similar to Bent Tree Basalt. The unit is coarsely plagioclase phyric with phenocrysts up to 5cm diameter. Flow units consist of lower coarse-grained porphyritic rocks, massive porphyritic-dolerite in the middle, and porphyritic-pillowed basalt at the top. Geochemically the unit is tholeiitic with weak calc-alkaline affinity (Harrison 1983).

Black Flag Group

The Black Flag Group (Figure 4.6 p.100) is a 2000m thick unit of felsic to intermediate volcanic and volcaniclastic rocks including epiclastic greywacke, siltstone and shale. At Ora Banda the unit is represented by a thin sliver of altered siliceous metasedimentary rocks at the upper contact of the Victorious Basalt. In the Ora Banda district, the Black Flag Group rocks are intruded by mafic/ultramafic sills.

Interflow sedimentary rocks

Interflow sedimentary rocks are developed extensively in the Ora Banda Domain at basalt flow contacts, and represent intermittent pauses in volcanic activity. Widespread black shales and cherts indicate deep-water deposition onto the volcanic substrate. Common layered sulphidic bands may be exhalative in origin (Bavinton 1979; Gilbert 1983) however some may have a diagenetic origin with pyrite replacement of graded-bedding in sedimentary rocks.

The Cashmans Sedimentary Horizon (Figure 4.6 p.100) is located between the Big Dick Basalt and Bent Tree Basalt, and comprises fine-grained silicified, sulphidic interflow sedimentary rock units with interbedded chert bands and locally convolute laminations. The stratigraphic position is a significant locus for intrusion with three intrusive episodes including Enterprise dolerite, Mount Pleasant Sill and felsic porphyritic dykes and sills, each of which has split the sedimentary horizon into successively thinner slices, moving the same unit to widely separated locations. The unit is variably exposed for up to 15 km of strike length and forms an important regional marker horizon.

Regionally, the Cashmans Sedimentary Horizon occupies a similar stratigraphic position to the Kapai Slate at Kambalda and shares similar textural and lithological relationships (Bavinton 1979). Locally, the unit is 1 to 5m thick with laminae of pyrite in thicker bands of silicified chert. Weathered exposures show isoclinal folds and bedding-parallel cleavage defined by aligned micas that may reflect localised bedding-parallel shearing. A thin slice of Cashmans Sedimentary Horizon is located at the Big Dick Basalt / Enterprise Dolerite contact with banded pyrite and chert layers.

The Coppermine Shale (Figure 4.6 p.100) is a 1-10m thick black shale unit between the Bent Tree Basalt and Mount Pleasant Sill, and is possibly a slice of Cashmans Sedimentary Horizon separated from the stratigraphically lower unit with intrusion of the Mount Pleasant Sill. The unit does not crop out in the Ora Banda district, but several drillholes have intercepts of carbonaceous pyritic shale with intense slaty cleavage. Outcrops of fine-grained silicified black chert north of Grants Patch, are correlated with the same unit at Ora Banda. The shale is deformed by strong bedding-parallel cleavage and locally contains stretched angular fragments of schistose mafic rocks to 20cm diameter, at the lower contact with Mount Pleasant Sill. Ellipsoidal quartz (chert?) pebbles are contained within the foliated sediment. Thin chert bands with pinch and swell structure are common with rounded isoclinal fold hingelines trending 24°→165°. The unit is deformed by three prominent cleavages including bedding-parallel cleavage trending 160°/63°W, cross-cut by pervasive schistosity trending 133°/60°W. Both are cross-cut by a late spaced cleavage trending 130°/72°SW.

A 1 to 5m thick carbonaceous black shale layer locally known as the ‘Black shale’ separates the Bent Tree Basalt and Victorious Basalt (Figure 4.6 p.100). The shale unit is significantly sheared with thrust-style fabrics described in detail in Chapter 4.4.2 (p.107). Shearing is common in most interflow sedimentary rocks and mesoscopic structures (lineations and isoclinal fold axes) indicate that the shearing may be related to flexural slip movement along bedding contacts during regional folding. The Black shale does not crop out but is exposed in several open pit mines (eg. Gimlet South, Slippery Gimlet and Sleeping Beauty mines) and in underground exposures at the Gimlet South mine.

2.3.2 Intrusive rocks

Dolerite sills

Layered, differentiated dolerite sills are common and make up a significant proportion of the stratigraphic succession in the Ora Banda Domain. The mafic and ultramafic sills are layer-parallel marker units that can be traced for several tens of kilometres along strike and around the hinges of major folds. Moderate shearing localised at the intrusive contact, is a common feature of the sills. Four sills have intruded interflow sedimentary rocks of the Ora

Banda mafic sequence, and the petrology, geochemistry and phase layering of the sills are documented by Williams and Hallberg (1973), Witt (1987,1990) and Witt *et al.* (1991).

The Enterprise dolerite (Figure 4.6 p.100) is a layered mafic sill that intruded the Cashmans Sedimentary Horizon at the contact between the Big Dick Basalt and Bent Tree Basalt. The unit is identifiable in subcrops that extend from Whitehaven to Denver City, but the generally poor exposure has resulted in the unit not being mapped in previous studies. New exposures in Enterprise open pit and in over 180 diamond drill holes have permitted detailed mapping of the layering and phase variation within the unit. Eight layers have been identified within the sill (Figure 2.4), which has a tholeiitic affinity (Gregory 1988). The sill appears to be slightly transgressive of bedding with rare drillhole intercepts of Big Dick Basalt stratigraphically above the Enterprise dolerite. Gabbroic layers within the sill have textural and geochemical similarities with the Mount Ellis Sill (Gregory 1998), which has been mapped between Grants Patch and Mount Pleasant (Witt 1990). The Mount Ellis Sill (Witt 1990), is a 600m thick dolerite sill of tholeiitic composition that has intruded the contact between the Big Dick Basalt and Bent Tree Basalt, and may represent a southern extension of the Enterprise dolerite.

The Mount Pleasant Sill (Figure 4.6 p.100), is a well-differentiated dolerite sill up to 600m thick, has petrographic evidence of simultaneous crystallisation from the roof and floor of the intrusion, and is divided into twelve distinct layered units based on petrology and chemistry (Witt *et al*. 1991). Phase layering and rhythmic layering are common throughout the sill (Williams and Hallberg 1973) which has lower ultramafic hornblende-peridotite layers that grade upwards into gabbro and quartz dolerite. The layers are important indicators of younging direction and form regional stratigraphic marker horizons.

The Ora Banda Sill (Figure 4.6 p.100), is the largest of the mafic/ultramafic sills with a maximum thickness of 2000m (Williams and Hallberg 1973; Witt 1990). Five distinct layers are present with cryptic layering defined by compositional variations in mineralogy within the sill. The Ora Banda Sill intruded volcanic and volcaniclastic rocks at the base of the Black Flag Group with local melting of wallrocks on the upper contact.

The Orinda Sill is a 250m thick phase-layered gabbroic unit that intruded the middle to upper portions of the Black Flag Group (Witt 1990).

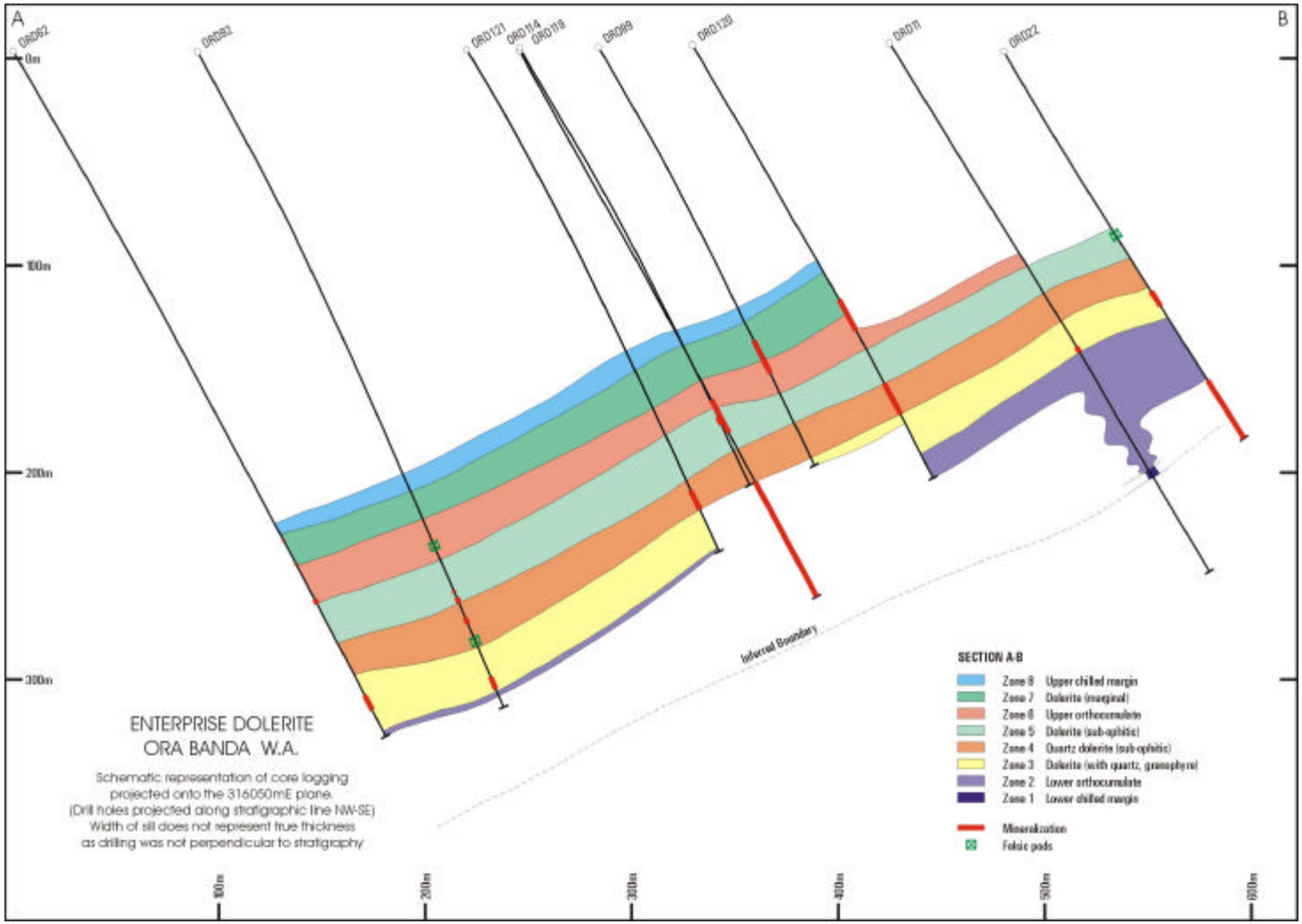

Figure 2.4 – Stratigraphic section of the Enterprise dolerite sill (from Gregory 1998)

Granitoid rocks

Several small stocks and thin bedding-parallel sills of late to post-tectonic granitoid have been emplaced into the Ora Banda mafic sequence. The Lone Hand Monzogranite (LHM) (Figure 4.6 p.100) is a NW plunging teardrop-shaped body of biotite granite with some porphyry. The stock intruded the eastern end of Ora Banda structural zone and its location indicates significant dilation in the area. Most early ductile fabrics do not affect the LHM, however late faults and shear zones cross-cut the LHM and are also intruded by the porphyritic stocks. The Lone Hand Monzogranite has intruded along the Enterprise-east shear zone, and a large fragment of schistose mafic rocks (300m x 50m) is contained within the western margin. Several large porphyry dykes with variable shearing are intruded into the Enterprise east shear zone indicating syn to post kinematic intrusion.

Granitoid-related calcite-fluorite veins are ubiquitous in the Enterprise area and are associated with muscovite-calcite alteration haloes that overprint most brittle-ductile faults. Limited reactivation and shearing of the veins further support syn to post kinematic intrusion. Abundant molybdenite is closely associated with quartz veins forming <1mm wide halos on vein margins and pressure solution seams within the veins indicating significant quartz vein development with porphyry intrusion.

Felsic porphyry dykes and sills

Quartz-feldspar porphyry dykes are common in the Enterprise area and have intruded Enterprise dolerite at several stratigraphic levels. The dykes are usually less than 1m wide and have cross-cut pre-existing quartz veins with pervasive muscovite alteration and associated fluorite and molybdenite. A 10m-thick quartz-feldspar porphyry sill has intruded the Cashmans Sedimentary Horizon, and can be traced for most of the length of this unit. Geochemical data (Centaur) indicate distinctly different trends between the porphyry sills and stocks with fractionation processes evident in the stocks and single-pulse clustering in the sills. At Zuleika, felsic porphyritic rocks have intruded ultramafic rocks along the Zuleika Shear Zone but the chemical composition of the dykes is significantly different to those at Ora Banda. Similar contact relationships of porphyritic intrusions at Ora Banda and Zuleika indicate syn to post-tectonic timing of intrusion yet the widely spaced nature of

the outcrops precludes direct correlation of the rock types except as a district-wide episode of syn to late-tectonic granitoid and porphyry intrusion.

Proterozoic dolerite dykes

Widely-spaced Proterozoic dolerite dykes rarely crop out in the Ora Banda Domain, and most are identified from regional aeromagnetic imagery as lineaments of very high or very low magnetic response. Drillhole intersections north of the Enterprise mine, show the dykes as up to several tens of centimetres thick with a very fine-grained dark mineralogy including phenocrysts of (?)olivine. Localised zones of silicification of the wallrocks and 1-2cm wide reaction zone within the dykes indicate high temperature intrusion.

2.4 DEFORMATION

Deformation in the Norseman-Wiluna greenstone belt is well-documented (Archibald *et al*. 1978; Swager 1989; Swager and Griffin 1990; Witt 1990), and most authors recognise up to four phases of shortening with less well-documented evidence of early and intervening extensional episodes (eg. Hammond and Nisbet 1992; Williams and Whitaker 1993) (Table 2.2). The absence of early thrust faults in the Ora Banda and Zuleika districts is anomalous, however the terminology of Swager *et al*. (1990) is continued here to allow correlation with other notation systems. D1 thrust faults produced duplexes and stratigraphic repetition in the Boorara, Kambalda and Coolgardie Domains only. In the Ora Banda and Zuleika districts, the sequence of deformation events is well constrained by early regional folds that are cross-cut by all other fabrics. The folds are therefore annotated as D2 structures and clearly are the same generation of structures as D2 folds in other domains of the Kalgoorlie Terrane.

D3 was a regional sinistral ductile-shearing event that produced ductile shear zones up to hundreds of kilometres long. The shear zones commonly separate tectonostratigraphic domains with differences in tectonic history and stratigraphic succession, however broad correlations are possible due to the presence of the regional komatiite marker unit, hence the domains are unlikely to be exotic terrane fragments. Whereas D3 produced significant shear zones without visible marker unit offsets in the Ora Banda Domain, the deformation was primarily a shortening event with widespread flattening strains documented in the D3

Table 2.2 – Regional deformation history of the Eastern Goldfields modified from Swager (1997). Only the last three shortening events D2 / D3 / D4 are recognised in this study. Details of references for extensional deformation events and granitoid age dates are given in Swager (1997).

Tectonic event	Timing Constraint
D4 ***REGIONAL SHORTENING – ENE-WSW*** regional brittle-ductile fault network, with N-S, NE-SW and E-W principal structural orientations	granite – 'post tectonic' : ca. 2620-2600 Ma (very few)
EAST-WEST EXTENSION restricted to Ida shear zone, post metamorphic orogenic collapse?	granite – 'late-tectonic' : ca. 2640 Ma
D3 ***REGIONAL SHORTENING – ENE-WSW*** strike and reverse slip, regional within-greenstone-belt ductile shear zones, en echelon folds	
LOCAL EXTENSION final uplift stage of granite-gneiss complexes	granite – 'post-regional folding' : ca. 2660 Ma
D2 ***REGIONAL SHORTENING – ENE-WSW*** upright foliation and folds, domain scale thrusting, inversion of extensional structures?	granite – 'pre to syn regional folding' : > ca. 2660 Ma
POST D1 and PRE D2 E-W EXTENSION roll-over anticlines, synclinal basins with clastic infill	post-D1 and pre-D2 felsic porphyry : 2674 +/- 6 Ma
D1 ***REGIONAL THRUSTING – N-S*** thrust stacking, recumbent folds: involves upper felsic volcanic unit with extensional structures	felsic volcanic rocks : minimum age constraints 2681+/- 5 Ma (Kalgoorlie), 2675 +/- 3 Ma (Gindalbie)
DE *EARLY EXTENSION* low-angle shearing along granite-greenstone contacts; north to south movement? Syn-volcanic granite plutonism, syn-volcanic domes, local polydirectional extension and local recumbent folds	early granites: c. 2685-2675 Ma (? ca. 2710 Ma)

structures (Eisenlohr *et al*. 1989; Skwarnecki 1987; Swager 1989; Vearncombe 1992; Vearncombe 1998a). Crustal shortening resulted in tightening of earlier D2 folds and partitioning of simple-shear deformation into high strain zones in a transpressional tectonic regime (Libby *et al*. 1990; Swager 1989). D4 is documented as an oblique faulting event with N-S trending dextral faults (Clout *et al*. 1990; Witt 1990). Most published maps show the late faults as being restricted in distribution, with only the most obvious faults mapped from known offsets. The fault event is characterised from new data in this study as brittle-ductile in nature forming a regionally developed network of interlinking faults that are primarily mesoscopic-scale structures (Table 2.2 p.26).

2.5 METAMORPHISM

Regional metamorphism in the Ora Banda Domain reached lower greenschist facies, characterised by actinolite-albite metamorphism of igneous pyroxene-plagioclase assemblages (Figure 2.5). A lower limit of prehnite-pumpellyite facies for static domains was recorded by Witt (1993a). Widespread preservation of primary igneous textures is typical at Ora Banda hence the prefix “meta” is omitted from rock descriptions here.

In the Zuleika area, the presence of biotite in felsic rocks and amphibole in mafic rocks suggests a slightly higher metamorphic grade than for rocks in the adjacent Ora Banda Domain. The Zuleika Shear Zone was interpreted by Swager *et al.* (1990) as a domain boundary, and shown as juxtaposing tectonostratigraphic domains of markedly different metamorphic grade. However, observations presented in Chapter 3 (p.29) do not record any significant change of metamorphic grade across the Zuleika Shear Zone and the interpretation of this shear zone as a metamorphic boundary is equivocal. Gold mineralisation accompanied potassium metasomatism in the form of muscovite and biotite in the Zuleika Shear Zone. Metamorphic biotite in the Kurrawang Conglomerate to the east of the Zuleika Shear Zone (Hunter 1993) suggests that the metamorphic boundary may be located at the eastern contact of the conglomerate unit or possibly further to the east. Randomly oriented actinolite sheafs overprinting ductile shear zone fabrics and hydrothermal biotite at Zuleika (Bullant mine), indicate that metamorphism outlasted deformation. Randomly oriented amphibole is commonly reported in the Kalgoorlie region (Swager 1994, Witt 1993), and may be related to post-tectonic porphyry intrusion.

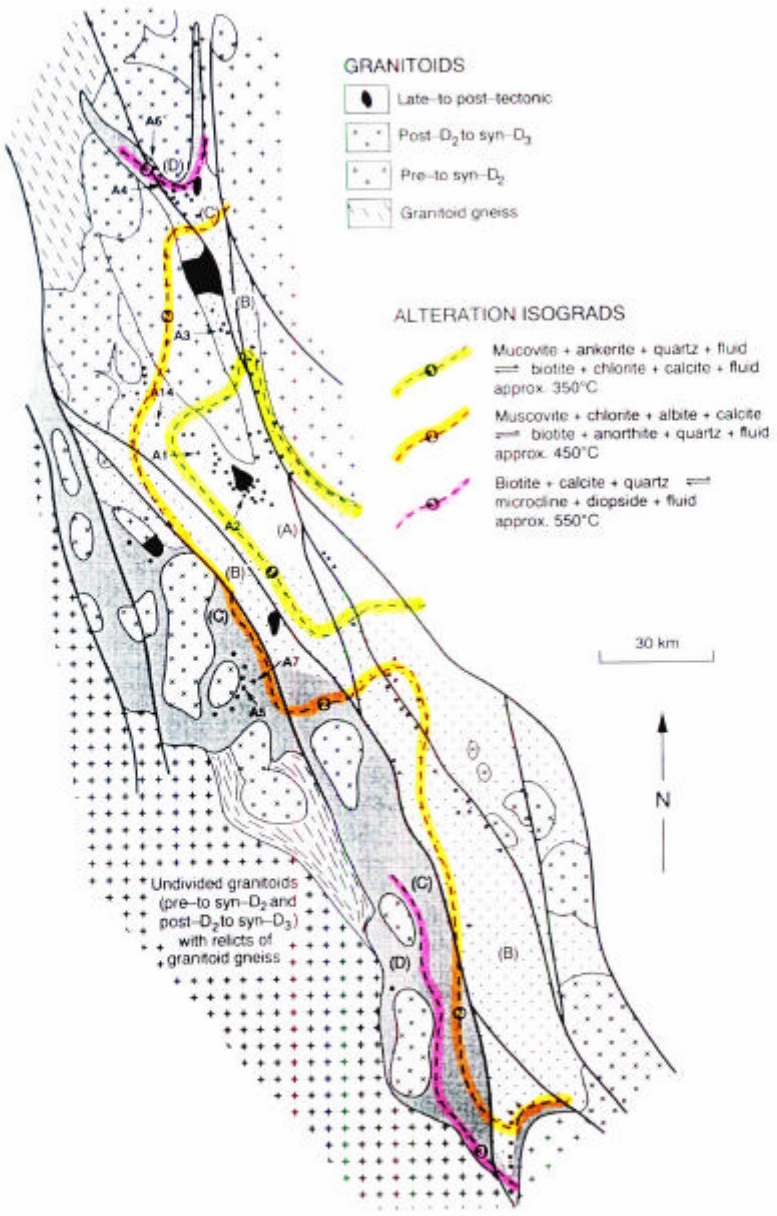

Figure 2.5 – Distribution of metamorphic facies in the Kalgoorlie terrane (from Witt *et al.* 1997)

3 REGIONAL STRUCTURAL FRAMEWORK

3.1 INTRODUCTION

This chapter investigates the deformation sequence in the northern Kalgoorlie area, using aeromagnetic imagery to determine regional-scale relationships. In the Zuleika district, the regional-scale D3 Zuleika Shear Zone is exposed in open-pit mines. These exposures show cross-cutting relationships between the shear zone and the late-tectonic brittle-ductile fault network. Regional-scale relationships are inferred from mesoscopic observations at Zuleika that document the nature of both the D3 ductile shearing event, and the D4 brittle-ductile faulting event. The D3 and D4 events are assessed at larger scales in Chapters 4 and 5 from Ora Banda, where better exposures of the D4 brittle-ductile fault network are located.

The Kalgoorlie Terrane has a prominent NNW-SSE trending structural grain that is developed over several hundred kilometres. The terrane covers a broad belt of greenstones from Norseman to Menzies and is divided into six distinct domains (Swager *et al.* 1990), each with a similar stratigraphic sequence and deformation history. The Ora Banda Domain is the northernmost of the six domains and is also one of the least deformed stratigraphic packages in the Norseman-Wiluna Belt with large tracts of intact, moderately dipping igneous and sedimentary rocks.

3.2 AEROMAGNETIC INTERPRETATION

An image of aeromagnetic data (Figure 3.1) shows good definition of rock types from the marked difference in magnetic response between ultramafic, mafic and felsic igneous rocks. Ultramafic rocks, including ultramafic zones in intrusive mafic sills, have the highest magnetic response of all rock-types, and delineate the trace of igneous layering as long sinuous belts with well-defined offsets. The Ora Banda Domain is a large area of weak deformation typified by the broad fold structure in the centre of the image (Figure 3.1). The Zuleika Shear Zone is poorly defined magnetically and appears to truncate the western limb of the Kurrawang syncline, yet the truncation may be against the eastern contact of the Kurrawang Formation. Large areas of low-to-moderate magnetic response with coarse ‘texture’ on the image are granitic rocks, and belts of ultramafic rocks have a high response. Several E-W trending linear features of marked high and low response that

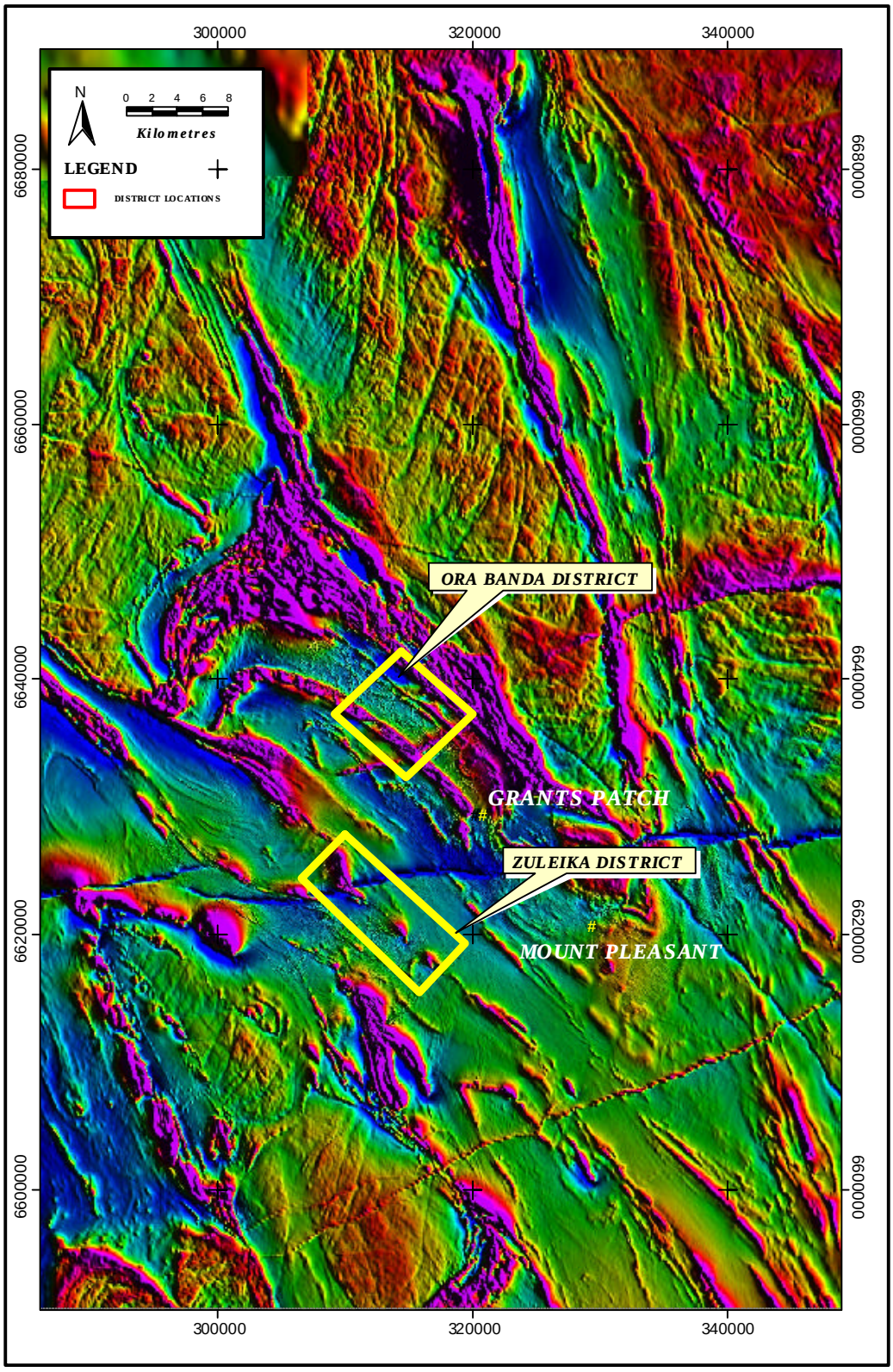

Figure 3.1 - Image of total magnetic intensity, from the north Kalgoorlie region. See appendix for survey details.

30

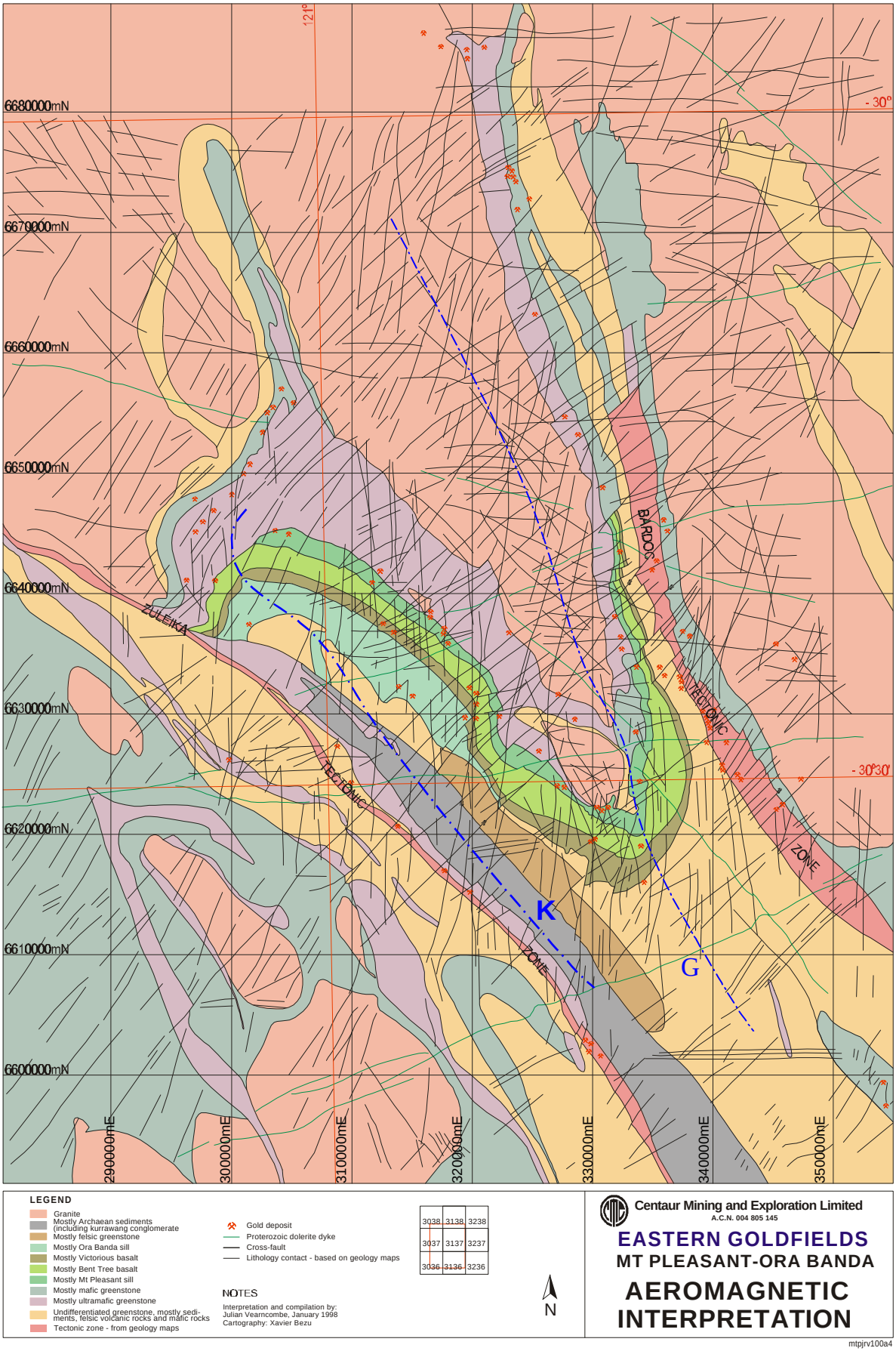

Figure 3.2 – Interpretation of aeromagnetic imagery from the north Kalgoorlie region at 1:100,000 scale after Vearncombe (1998b). The Zuleika Tectonic Zone of Vearncombe (1998b) is equivalent to the Zuleika Shear Zone in this study. **K** – Kurrawang Syncline, **G** – Goongarrie-Mt Pleasant Anticline.

cross-cut all other geological features, coincide with outcrops of Proterozoic mafic dykes. The trace of layering on the image shows a gross NNW-SSE trend that is sub-parallel to regional-scale ductile shear zones such as the Zuleika Shear Zone, Bardoc Tectonic Zone, Kunanulling Shear Zone, Boulder-Lefroy Fault and Ida Fault. A network of late tectonic brittle-ductile faults that overprints the regional-scale ductile shear zones is manifest as several groups of lineaments that are most obvious in the granitoid rocks, and are traceable through adjacent intermediate, mafic and ultramafic rocks. In some areas the lower magnetic response of the mafic and intermediate rocks masks the fault network. Local studies show the brittle-ductile structures of the fault network to have offsets of less than 100m, which are negligible at the map scale.

The validity of interpreted aeromagnetic imagery relies upon many factors including the scale of the imagery, processing techniques and quality of the raw data. The assumptions drawn from Figure 3.1 (p.30) are of regional compass and are considered valid at the scale of the image (1:100,000). However, subsets of the data at smaller scales show a higher level of detail that is not represented at 1:100,000 scale, with closer-spaced faults and offsets constrained by better defined bedding contacts.

3.3 STRUCTURES OF REGIONAL SIGNIFICANCE

Deformation features at a regional-scale include folds, ductile shear zones and a domain-wide network of mesoscopic brittle-ductile faults. The geometry and distribution of each defines the regional-scale fabric and reveals the strains produced by the major deformation events. Since some of the folds and ductile shear zones are developed on the scale of tens or hundreds of kilometres, they are best described from aeromagnetic imagery at a large scale where the structures can be observed in their entirety.

3.3.1 Kurrawang Syncline/Goongarrie–Mount Pleasant Anticline fold couplet (D2)

Regional-scale folding is the oldest recognisable deformation event in the Ora Banda Domain (Witt 1990). Regional-scale (first order) fold structures include the Kurrawang Syncline / Goongarrie-Mount Pleasant Anticline fold couplet (Figure 3.2 p.31). The folds have wavelengths of up to 18 km and are classified as close on the basis of 50° interlimb angles. The axial trace of the Goongarrie-Mount Pleasant Anticline trends 330° with a

southerly plunge of 10°-20° (Witt 1990), whereas the axial trace of the Kurrawang Syncline varies from 310° in the south to 330° in the north (Figure 3.1 p.30). Complex faulting and re-folding of the D2 folds (Plate 1A of Witt 1993a) appears to be locally developed and may be related to syn-D3 granitoid intrusion. The fold limbs are truncated to the west against the Kurrawang Formation with prominent drag folding, but are parallel with the Bardoc Tectonic Zone to the east. Folding of the Kurrawang conglomerate was interpreted as synchronous with the D2 regional folding event (Swager *et al.* 1990; Hunter 1993; Witt 1993a), yet the unit is mapped with unconformable contacts cross-cutting F2 fold form surfaces on regional maps (Witt and Davy 1997), and F2 hinge trace lines (Witt 1993a, Plate 1a).

Second order folds are developed in the less competent Black Flag Group rocks and associated intrusives. The Orinda Sill forms macroscopic folds that are parasitic on the megascopic Kurrawang Syncline, with similar geometric and geographic classifications as the regional-scale folds but different morphology. Mesoscopic-scale folds are locally developed in interflow sedimentary rocks at the contacts of major intrusive units. Examples of parasitic folds in the Cashmans Sedimentary Horizon studied at Cashmans and Denver City, south of Enterprise, show a range of fold axis orientations of 41°→ 200°, 37°→ 258° and 47°→ 280° (Figure 3.3). There is a variety of fold styles at each out-crop including chevron, buckle and isoclinal styles. These are spatially related and may have been produced by flexure of the sedimentary rocks during shearing on the nearby Cashmans Shear Zone, or alternatively the folds were formed as parasitic structures on the major regional folds and were subsequently rotated during later shear zone movements. Refolding of earlier folds is not observed, and a lack of overprinting of fold related fabrics excludes the different fold orientations as being related to separate shortening events.

3.3.2 Zuleika Shear Zone (D3)

Ductile shear zones are large-scale features in the Norseman-Wiluna greenstone belt and are traceable for hundreds of kilometres on aeromagnetic imagery. The shear zones are NW-SE to NNW-SSE trending linear zones that truncate earlier structural features. They were interpreted by Swager *et al.* (1990) as domain boundary faults and in some cases terrane boundaries, however many are layer-parallel at the local scale and are defined by sheared mafic and ultramafic rock contacts. The most prominent ductile shear zones

Figure 3.3 – Anomalous parasitic fold styles related to strike-slip shearing on the Cashmans Shear Zone at Denver City. **a)** Open fold in Cashmans Sedimentary Horizon plunging to the southeast. **b)** Small chevron fold trending 41°→200° developed in the hinge zone of the fold in a), lens cap is 55mm diameter. **c)** Isoclinal fold trending 11°→175° developed in layering within quartz porphyry intruding the Cashmans Sedimentary Horizon. Hammer handle is 330mm long.

bounding the Ora Banda Domain are the Zuleika Shear Zone, Abattoir Shear and the Bardoc Tectonic Zone. Regional folds are truncated by the Zuleika Shear Zone northwest of Ora Banda, but the role of the Bardoc Tectonic Zone as a significant truncating feature is not well established. It is poorly defined on aeromagnetic imagery as a shear zone (Vearncombe 1998b), and is sub-parallel to the regional trend of volcanic and sedimentary sequences.

Seismic interpretation

A 250-km long east-west seismic line across the Kalgoorlie Terrane (Goleby *et al.* 1993), provides a two-dimensional view of the crustal structure, approximately orthogonal to NNW-SSE trending regional fabric (Figure 2.2 p.14, Figure 3.4). Many authors have used the seismic data to interpret the structure of the crust, but several have reported problems with mapped surface geology conflicting with the apparent orientation of major shear and tectonic zones as interpreted from seismic images (Hall 1998).

An image of the seismic data across the Zuleika area is interpreted to assess the orientation and nature of the Zuleika Shear Zone in the third dimension, and to determine the relative scale and importance of the shear zone as a major crustal discontinuity. The seismic image used, is a small subset of the Kalgoorlie seismic transect that covers the Zuleika area crossing the Kurrawang formation to the east, and the western limb of the Goongarrie - Mount Pleasant Anticline (Figure 2.2 p.14, Figure 3.4). The image has a total line length of 15 km, and represents the upper crust to a depth of 12 km (4 seconds, two-way travel time), but does not cover the middle and lower crust. A significant discontinuity is located at about 6 km depth, defined by strong reflectors marking a roughly horizontal surface that truncates low angle reflectors above. Most authors (Goleby *et al.* 1993; Archibald 1998) have interpreted the surface as a basal décollement to the greenstones and a major change in the structure of the crust with imbricated duplex features below. The western limb of the Goongarrie - Mount Pleasant Anticline also is clearly visible as a series of shallow to moderately west-dipping reflectors on the eastern side of the image.

Seismic interpretation of vertical structures like the Zuleika Shear Zone is problematic, since steep features are subparallel to the propagation direction of the seismic waves, and hence are unreflective. The presence of vertical features is therefore inferred from

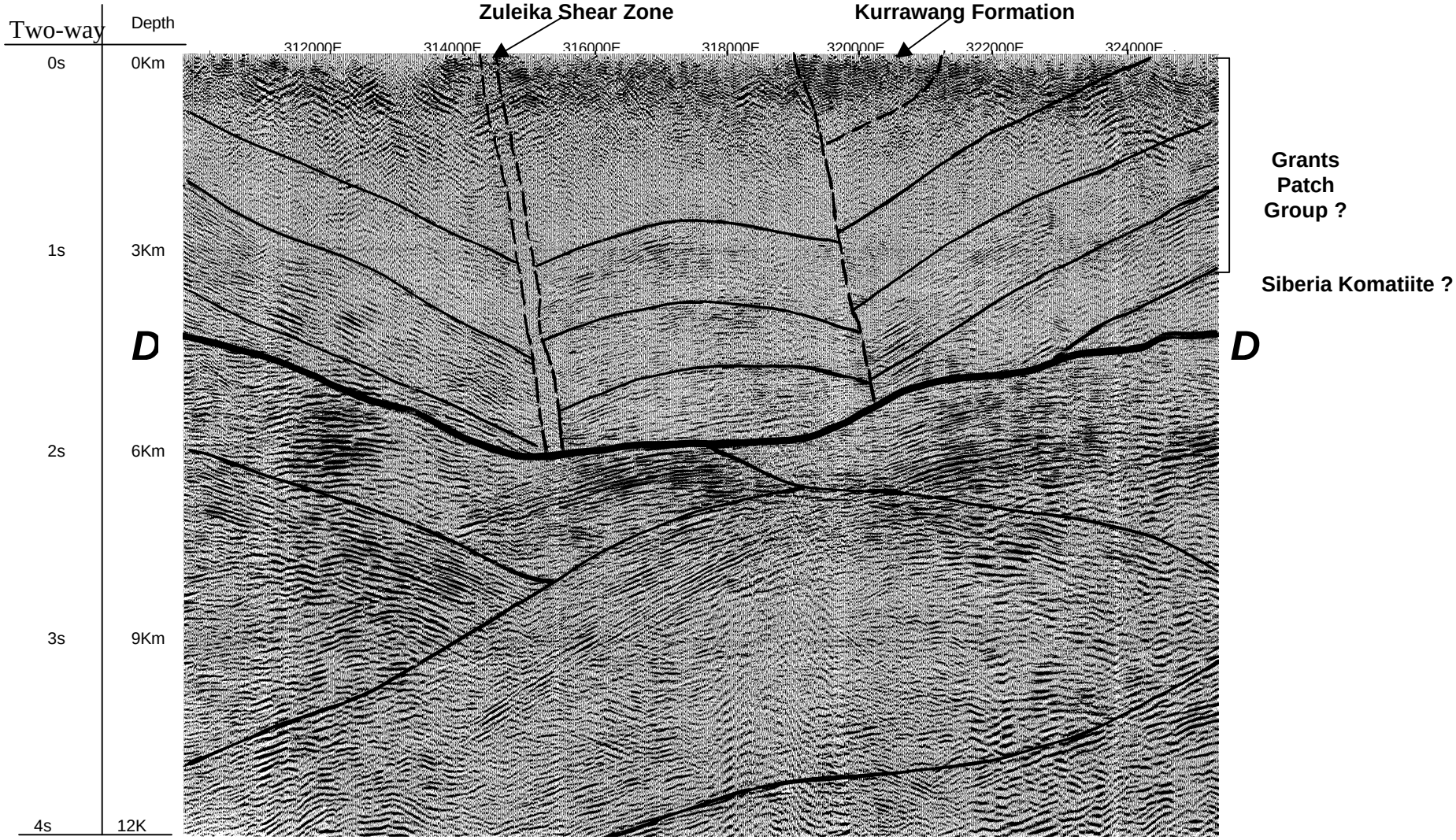

Figure 3.4 – Subset image of migrated seismic data from the Eastern Goldfields Seismic Transect – EGF1 (Goleby *et al*.1993). Eastings at the top of the image are in Australian Map Grid. The décollement (D) marks the base of the greenstones. Layering in the upper part of the image is extrapolated from surface contacts. The location of EGF1 is shown on the geological map in Figure 2.2, page 14.

truncation of horizontal reflectors (Sheriff 1982). The Zuleika Shear Zone is clearly visible as a steeply east-dipping band of non-reflection about 0.3 km wide, that truncates moderately dipping reflectors on both sides (Figure 3.4 p.36). The steep east-dip and width of the non-reflection band agrees with surface measurements of the Zuleika Shear Zone, but the nature of the intersection of the shear zone with the basal décollement is unclear. The Zuleika Shear Zone clearly does not extend below the décollement, implying that either the décollement overprints the earlier formed Zuleika Shear Zone, or it soled out against the décollement. An interpretation of the décollement overprinting within-greenstone shear zones was made by Goleby *et al.* (1993).

At the surface, the Zuleika Shear Zone is a network of shear zones enclosing lozenge-shaped areas of relatively undeformed rock with a total width of a few hundred metres, which is characteristic of major ancient fault zones (Sibson 1977; Ramsay 1980a). As the Zuleika Shear Zone does not extend at depth for greater than 6 km, and has a strike length of 250 km (Swager *et al.* 1990), its high length-to-depth ratio is consistent with the shear zone being a strike-slip fault (Sibson 1977). However, Drummond *et al.* (1997) maintain that the seismic data from deeper crustal levels are consistent with the Hammond and Nisbet (1992) interpretation of NW-SE shear zones as upturned early thrust faults.

The relatively shallow depth extension of the Zuleika Shear Zone when compared with the Bardoc Tectonic Zone and the Ida Fault, and its close association with lithologic contacts, may indicate that this shear zone is not a crustal-scale deformation zone. The 6km depth may not be its original depth, yet the shear zone is a D3 structure like the Bardoc Tectonic Zone, hence a similar timing would require consistent overprinting relationships with the mid-crustal décollement for these structures. The Zuleika Shear Zone may be a within-greenstone ductile shear zone of significance only to the upper layer of the greenstones, and its role as a deeply-tapping fluid conduit is not substantiated by the seismic data.

Surface exposures

The Zuleika Shear Zone is investigated in detail at five localities where it is exposed in the Anthill, Porphyry, Bowerbird, Wattlebird and Bullant open-pit mines along the trend of the shear zone (Figure 3.5). Elsewhere, the shear zone rarely outcrops and diamond drill holes were used to gain subsurface information in un-weathered rocks. The shear zone

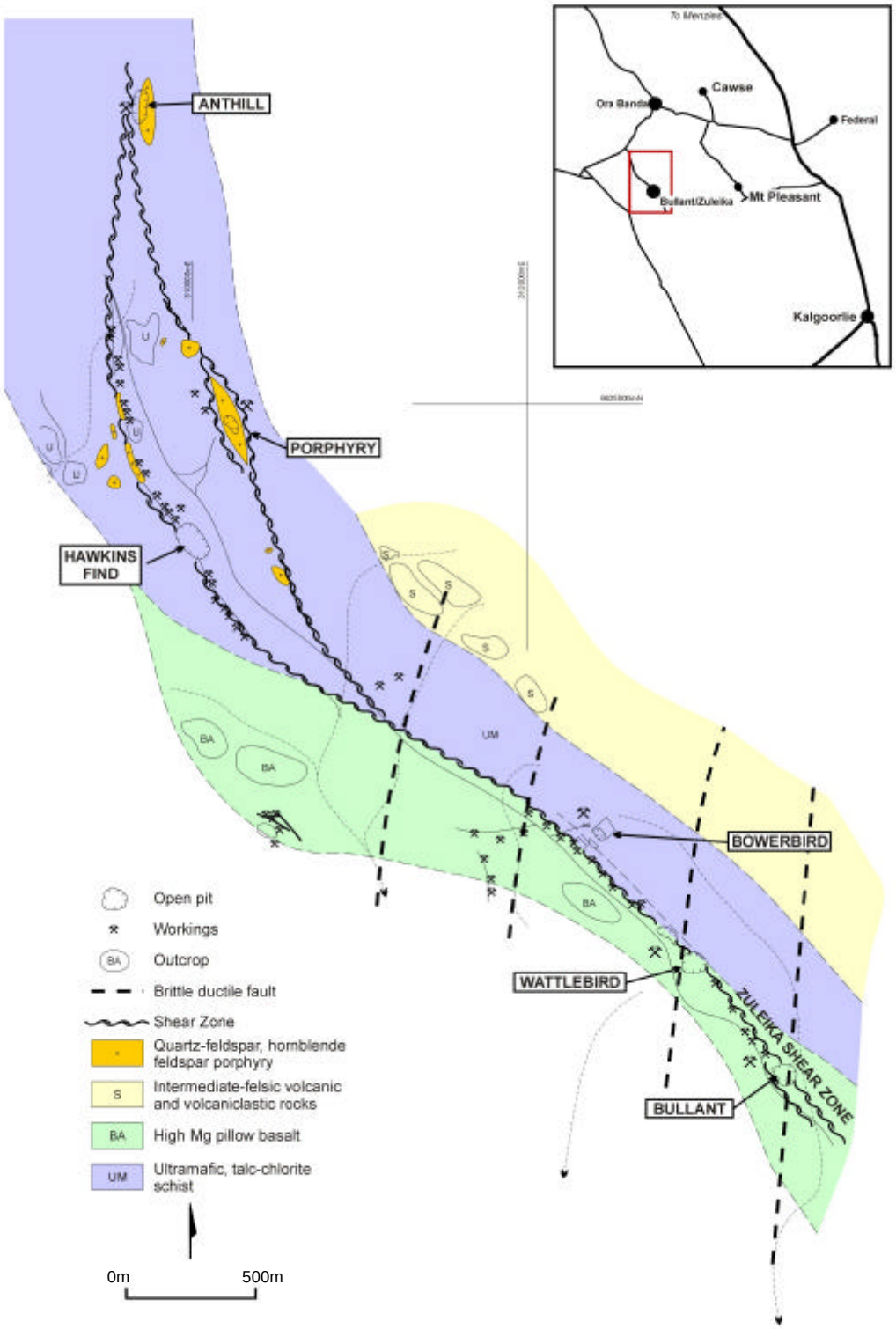

Figure 3.5 – Location map and geology of mines along the Zuleika Shear Zone. Outcrop locations after Konecny (1988).

strikes at 152° on average and its dip varies from 77°SW to 74°NE. A major change in the strike of the shear zone occurs in the Porphyry mine area where the shear zone turns to a more northward trend. Further north past the Anthill mine area the shear zone returns to a northwest trend (Figure 3.5 p.38). This change of strike correlates with a similar change of strike of igneous layering in the Grants Patch area to the east of Zuleika, and may represent a regional northeast-southwest trending kink fold. Morphologically, the Zuleika Shear Zone is defined from drilling and limited outcrop as a 300-500m wide corridor of individual anastomosing ductile shear zones, each up to 100m wide. The corridor is poorly understood in terms of the geometry and distribution of strain and the series of open-pits along the shear zone may represent discrete shear planes within a wider shear zone.

Anthill mine

At the Anthill mine (Figure 3.5 p.38, Map 1 p.262), the Zuleika Shear Zone is mostly talc-chlorite ultramafic schist with a pervasive schistosity striking 159°, and dipping steeply to sub-vertical with variable east to west dip. Quartz-feldspar porphyry has intruded the shear zone as discrete lenticular bodies, that vary in dimensions from several metres to several tens of metres long. The main schistosity is deflected around the edges of the porphyry bodies with local folding and several cross-cutting cleavages at the contact. The contacts have complex deformation of pre-existing S-C fabrics in the ultramafic rocks and contain irregular folded and sheared quartz veins, that are coeval with intrusion of the porphyry. A 10cm-wide aureole exhibiting thermal effects of the porphyry intrusion into sheared ultramafic rocks is observed with local induration and silicification, and a 3-5cm reaction halo in the porphyry (Figure 3.6a). The felsic porphyry bodies are internally deformed with a weak foliation at a moderate angle to the contacts, and cross-cutting quartz vein arrays that average 067°/76°S.

Porphyry mine

A 300m long lenticular body of porphyritic biotite-granodiorite intrudes a parallel shear plane to the east of the main Zuleika Shear Zone at the Porphyry open-pit (Figure 3.5 p.38, Map 3 p.271). The rock is coarse-grained composed of quartz, plagioclase, biotite and hornblende similar to the hornblende-plagioclase porphyry at Hawkins Find open-pit 500m southwest of the Porphyry open-pit (Witt 1992). In thin section, phenocrysts of

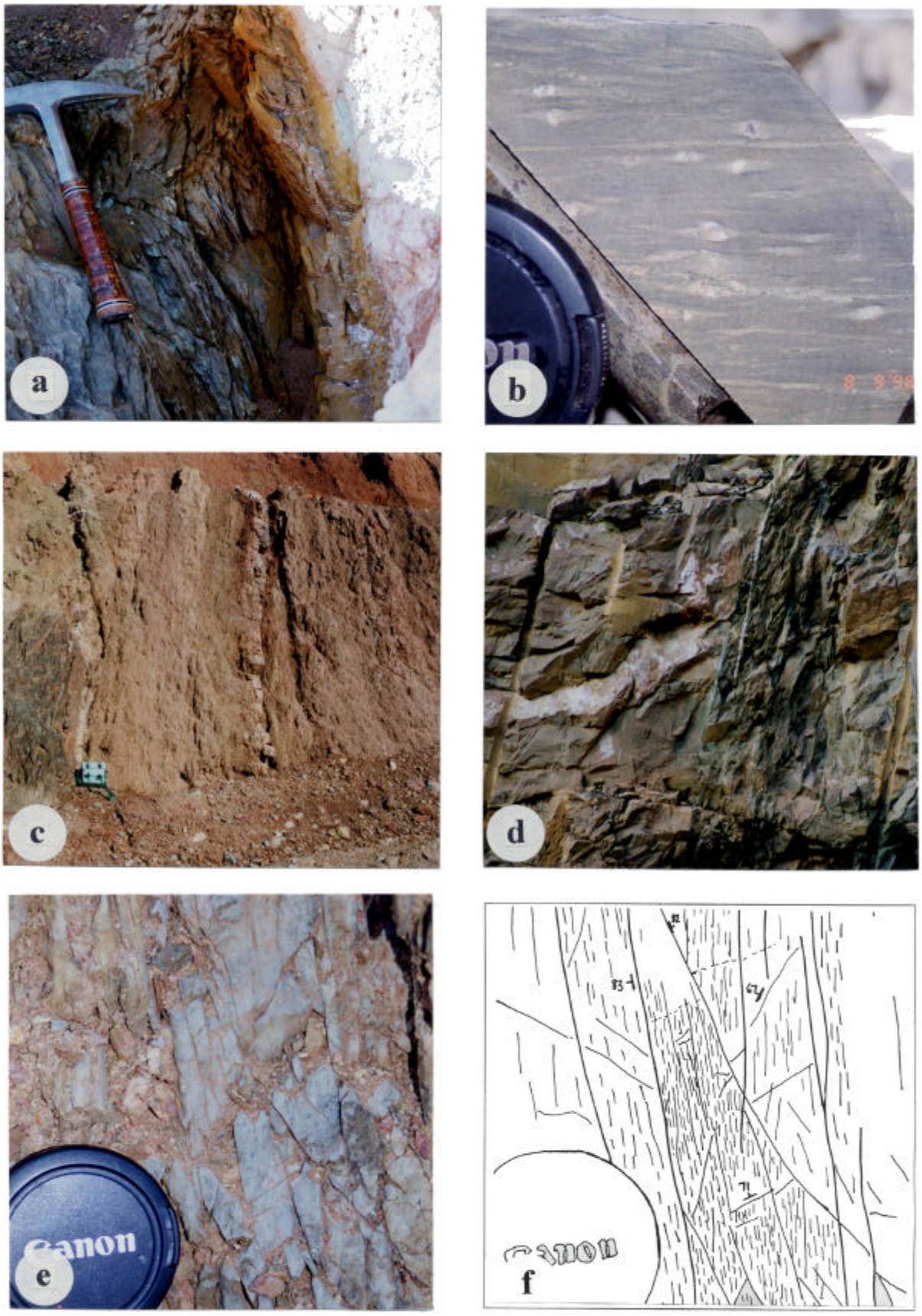

Figure 3.6 - a) Porphyry / ultramafic contact, Anthill open-pit. **b)** Type II S-C mylonite, Bowerbird diamond drill core. **c)** Zuleika Shear Zone in weathered basalt from Bullant open-pit. **d)** Zuleika Shear Zone in fresh basalt from Bullant open-pit. **e)** Multiple brittle fractures in schistose basalt, Bullant open pit. **f)** Line drawing of Figure 3.6e. See text and over-page for explanation.

Captions for figures on page 40 – Zuleika Shear Zone

Figure 3.6a
Photograph of a contact between talc-chlorite ultramafic rocks and intrusive porphyry from Anthill open-pit. The talc-chlorite ultramafic rock is intensely deformed with a disrupted S-C fabric that deviates up to 40° from the normal orientation of the Zuleika Shear Zone. The felsic porphyry contains a weak foliation at a moderate angle to the margins of the body. The contact zone is 5cm wide and in the ultramafic rock shows local thermal effects of intrusion, whilst the felsic porphyry displays a thin zone of reaction, and is discolored from white to tan. The porphyry has forcefully intruded the already sheared ultramafic rocks and a later oblique phase of deformation progressed possibly while the body was in a semi-consolidated state producing the weak foliation. Hammer is 330mm long. Top of photo points north.

Figure 3.6b
Ultramylonite in high-magnesium basalt from Bowerbird. The shear zone contains a pervasive C foliation with left lateral porphyroclast asymmetry. Porphyroclasts (<10%) are survivor fragments of plagioclase feldspar and quartz veins. Thin bands of ribbon quartz traverse the core parallel to the C foliation. A significant degree of flattening is exhibited by porphyroclasts in the bottom of the photo with strongly ellipsoidal shapes. The shear zone trending 123°/80°NE is located at 193.80m in diamond drillhole ZULD8. Lens cap for scale.

Figure 3.6c
Photograph of the Zuleika Shear Zone in pillowed high-magnesium basalt from Bullant open-pit. The shear zone is 5 metres wide and continues off to the right of the photo. A well-developed S-C fabric is prominent in the strongly weathered basalt, and the intensity increases towards the contact marked by the camera bag. At hand specimen scale the shear zone flakes easily into centimetre-size sigmoid-shaped lithons of rock formed from breakage along the intersection of the S-C planes. Large 20-30cm quartz veins are parallel to the shear zone and show weak stretching and boudinage effects indicating either minor movement on the shear zone after vein formation, or that dilatency occurred very late in the movement history. Camera bag is 200mm wide. View is looking south-east.

Figure 3.6d

Photograph of the Zuleika Shear Zone in pillowed high-magnesium basalt from Bullant open-pit. The shear zone is developed in fresh rock at the base of the pit and is a smaller parallel structure west of the main shear in 3.6c. The zone is 30cm wide and displays a well-developed C-plane trending top to bottom. The S-plane is also well developed trending top right to bottom left in between the C-planes. Thin quartz veins display minor stretching and boudinage parallel to the C-plane. Relatively undeformed-pillowed basalt has sharp contacts with the shear zone boundary. Base of photo is 1.5m wide. View is looking NW-SE.

Figure 3.6e
Brittle fractures cross-cutting schistose high-magnesium basalt in Bullant open-pit. Four distinct fracture sets are present, one set is parallel to the shear direction 155°/83°W (up the page) and the other three cross-cut obliquely 167°/67°W, 134°/82°E and 025°/71°N. The thoroughgoing fractures are parallel to the shear direction and these cross-cut the higher angle fractures, indicating that high angle fractures formed first with progressive overprinting by shallow angle fractures. The fractures are from a 4m wide ductile shear zone and as such may be considered as Riedel fractures since they are brittle in nature and are totally confined within the zone of simple shear with the correct timing sequence of development. An interpretation of the structures as Riedel fractures implies that the fractures developed with simple shear displacement on the ductile shear zone possibly at a time when the dominant mode of deformation was more brittle. The photo is looking down onto a horizontal surface, top points towards 335°. Lens cap is 55mm diameter.

Figure 3.6f
Line drawing of photograph in 3.6e showing fabric detail and overprinting relationships.

plagioclase are set in a fine groundmass of saccaroidal-textured plagioclase and quartz (Figure 3.11a-b p.47). Weak silica-albite alteration is widespread with recrystallised biotite pseudomorphing amphibole forming a well-developed tectonic foliation with irregular trend, pervasive throughout the rock (Figure 3.7). Fine-grained dyke-like phases of the porphyry up to 4m thick, are also foliated and have sharp schistose contacts against the coarser grained rock with a 2-3cm reaction halo. The finer grained porphyry clearly postdates the coarse-grained rock, but a similar foliation in each suggests a common deformation history. Sheared talc-chlorite ultramafic rocks at the boundaries of the body are contact metamorphosed to coarse-grained random-textured biotite schist, and display irregular folding with ductile shearing textures similar to fabrics observed at Anthill open-pit.

Schistosity in the porphyritic biotite-granodiorite at the Porphyry mine trends irregularly with wide variability in strike and dip. The fabric is described as a schistosity since it is defined by metamorphic biotite with a shape-preferred-orientation, but it is not schistose in the sense that coarse-grained micas dominate the rock fabric. Shear zone hosted porphyritic rocks of this type are geochemically related to pre to syn-D2 granitoid domes and late tectonic granodiorite and tonalite (Witt 1992), however the syn-to-post D3 timing suggested by structural relationships may indicate some overlap in the timing of intrusion and the D2/D3 deformation events.

The dominant stretch fabric in the surrounding sheared ultramafic rocks is predominantly sub-horizontal, but in the vicinity of the porphyry contacts, contact metamorphism has produced a randomly oriented fabric of acicular amphiboles and coarse-grained biotite that has destroyed the original shear fabric. Late shear surfaces in the ultramafic rocks defined by quartz and calcite have overprinting slip lineations that vary from 20°S to 65°N.

Bowerbird mine

At the Bowerbird mine, the Zuleika Shear Zone is 100m wide with an average orientation of 157°/74°SW (Figure 3.5 p.38, Figure 3.8). The shear zone cross-cuts intermediate volcaniclastic rocks, cherty sedimentary rocks, felsic porphyry, mafic volcanic rocks and ultramafic komatiites. The distribution of the different lithotypes is erratic with interleaving of all five rock-types over a 20m interval in diamond drillhole ZULD8.

Porphyry mine

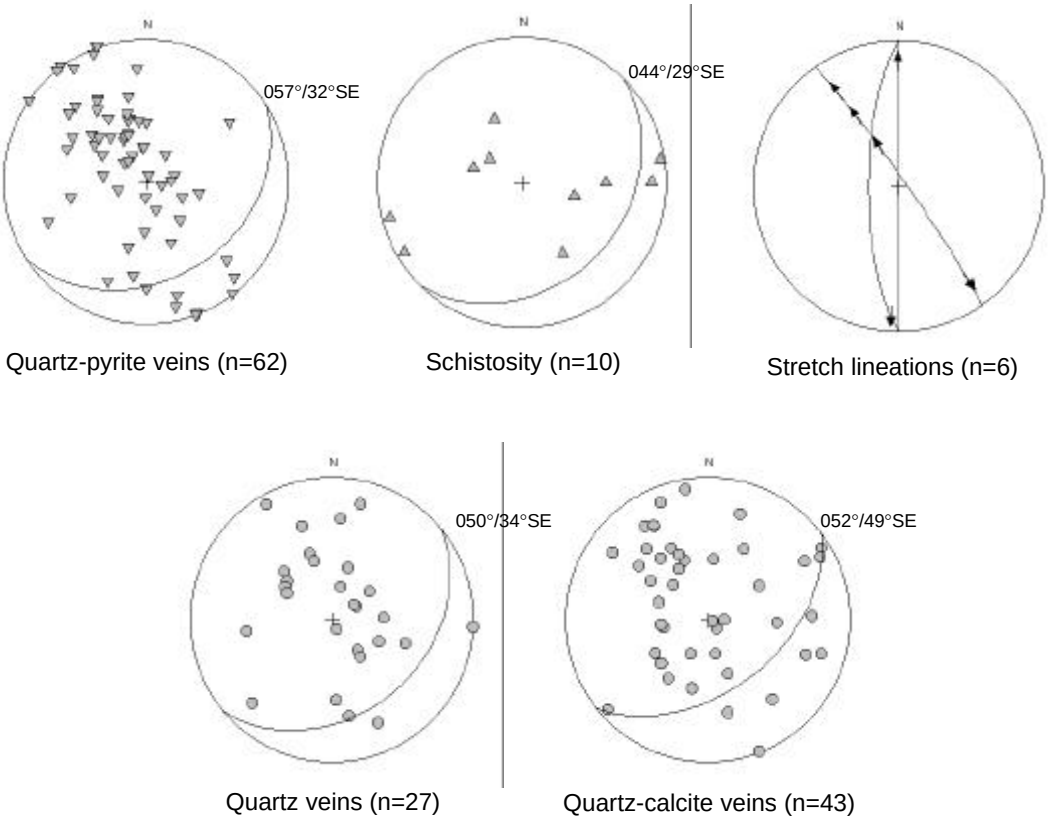

Figure 3.7 – Equal area stereograms of structural elements from Porphyry mine. Orientations are for average great circles to the major clusters, with number of measurements (n). Data measured from diamond drill core and open pit mapping. All stereograms in this thesis are lower hemisphere projections.

Bowerbird mine

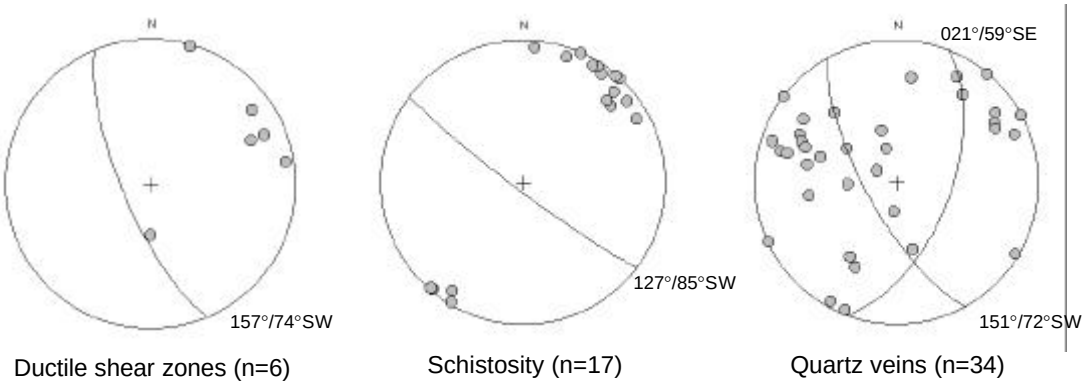

Figure 3.8 – Equal area stereograms of structural elements from the Bowerbird mine. Orientations are for average great circles to the major clusters, with number of measurements (n). Data collected from diamond drill core and open pit mapping.

Wallrocks to the east of the shear zone are strongly foliated with flattened leucoxene and biotite crystals. The foliation grades into discrete 1m wide zones of orthomylonite in intermediate volcaniclastic rocks, characterised by porphyroclasts of plagioclase and coarse-grained crystal-lithic tuff in a fine-grained matrix. Ultramylonite (50m wide), forms the most intense portion of the shear zone with ribbon quartz and asymmetric porphyroclasts. The shear zone is classified as a type II S-C mylonite (Lister and Snoke 1984), and the porphyroclasts are classified as sigma-type (Simpson 1986). Porphyroclast asymmetry indicates left-lateral offset (Figure 3.6b p.40) in sections parallel to the stretching lineation and orthogonal to the foliation. The western part of the shear zone contains interleaved felsic porphyry, mafic volcanic rocks and interflow sedimentary rocks. Sheared felsic porphyry contains previously sheared wallrock fragments of mafic volcanic and ultramafic rocks. The felsic porphyry occurs near a mafic volcanic/ultramafic contact that can be correlated with a similar stratigraphic position to the south at Wattlebird open-pit. The shear zone continues west into ultramafic komatiite but the intensity of shearing decreases across a contact with moderately brecciated pillow basalt.

Wattlebird mine

At the Wattlebird mine, the Zuleika Shear Zone trends 142°/83°SW (Figure 3.9), and is developed at a contact between brecciated talc-chlorite altered komatiite and fine-grained pillow basalt to the west (Figure 3.5 p.38, Maps 4-5 p.277-278). Thin bodies of felsic porphyry intrude the ultramafic rocks, and relict spinifex texture is common in centimetre-scale pods of deformed komatiite that are surrounded by intensely sheared talc-chlorite ultramafic rocks. Pillow basalt has round pillow shapes in the wallrocks of the shear zone, and the basalt is strongly altered to muscovite and calcite. Muscovite forms a penetrative schistosity in the basalt trending 142°/88°SW (Figure 3.9), with increased intensity towards the shear zone. A 5-15m thick mylonite zone marks the main Zuleika Shear Zone at the basalt/ultramafic contact. The contact is a 10m-wide zone of interleaved basalt and ultramafic rocks with chlorite-biotite +/-talc alteration. The margin of the shear zone in the ultramafic rocks is a sharp boundary between talc-chlorite mylonite and clast supported breccia with flattened elongated breccia clasts of ultramafic rock (Figure 3.20f p.65).

In thin section, the shear zone has a well-developed S-C fabric defined by chlorite and talc. A sample taken from the centre of the shear zone, (ZSZ-1) shows fabrics at a

Wattlebird mine

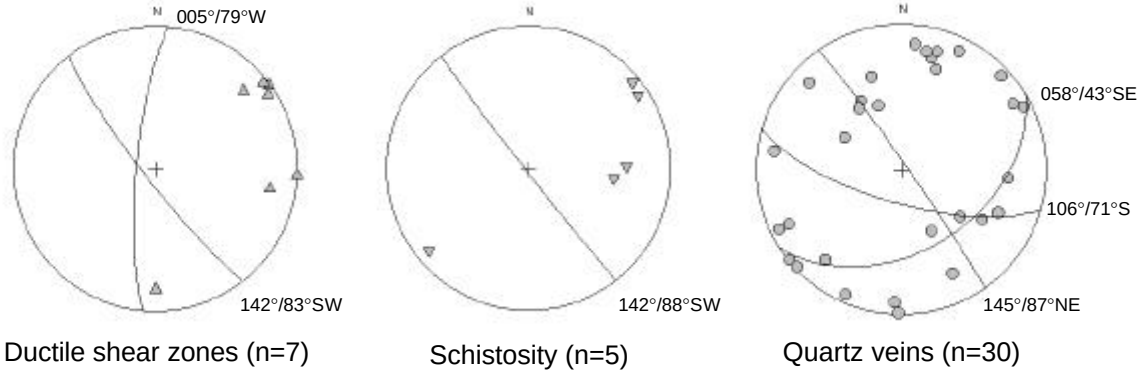

Figure 3.9 – Equal area stereograms of structural elements from Wattlebird mine. Orientations are for average great circles to the major clusters, with number of measurements (n). Data collected from diamond drill core and open pit mapping.

Bullant mine

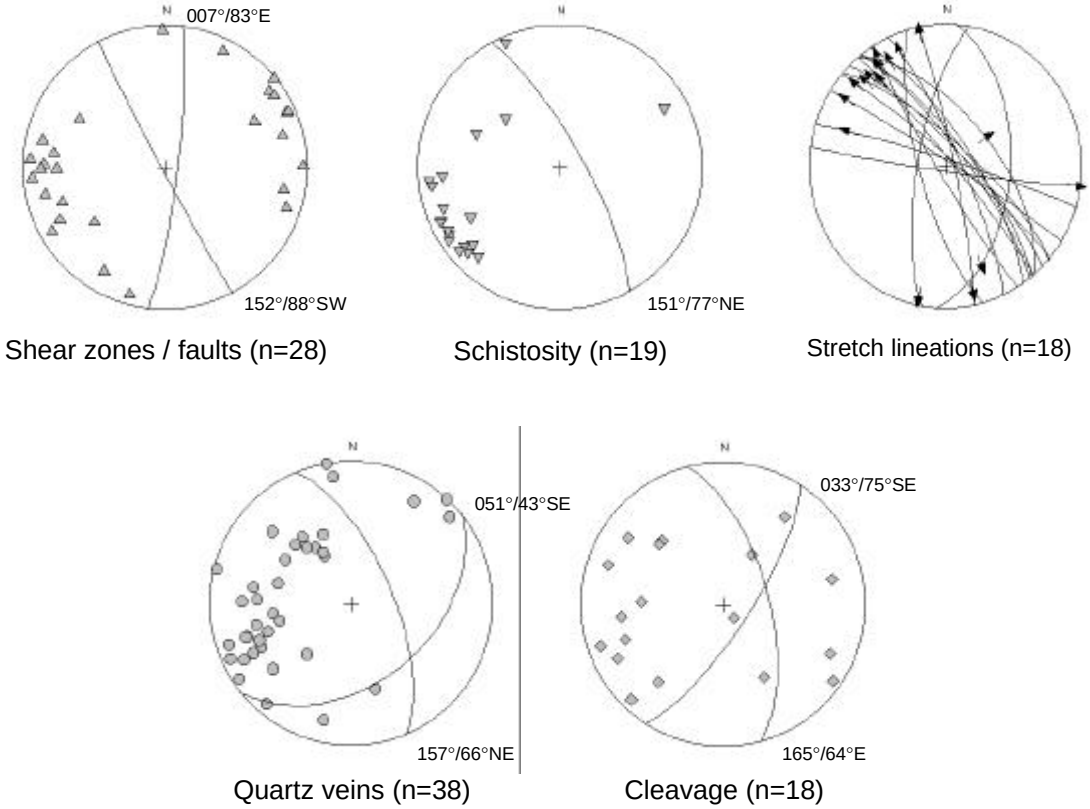

Figure 3.10 – Equal area stereograms of structural elements from Bullant mine. Orientations are for average great circles to the major clusters, with number of measurements (n). Data measured from diamond drill core and open pit mapping.

microscopic scale that emulate the interleaving of mafic and ultramafic rocks at the mesoscopic-scale (Figure 3.11c-d). The C planes of the shear zone are defined by chlorite with subordinate amounts of talc and calcite. S planes also are defined by chlorite, parallel to a weakly developed schistosity. C-plane cleavage domains account for about 40% volume of the rock and are smoothly anastomosing with a sharp transition to microlithon domains. Irregular-shaped clusters of talc overprint the chlorite C planes, but are optically continuous with them. Talc grains are poorly defined, yet individual grains are visible from divergent cleavage traces from grain to grain (Figure 3.12 p.49). Talc displays little or no intracrystalline deformation indicating almost total replacement post-dating deformation, and may indicate that this talc is a product of retrogression.

Microlithons are lens-shaped, up to 2mm long, composed of fine-grained quartz and chlorite (Figure 3.12 p.49). Quartz-rich microlithons are mostly strain-free with weak undulose extinction in about 30% of grains. The remainder is recrystallised with high-angle quartz grain boundaries pegged against chlorite in the surrounding cleavage domains. The microlithons are asymmetric, partially defining the left-lateral S-C fabric, and may be remnants of high magnesium basalt tectonically interleaved with ultramafic rocks. Calcite veins in the rock are up to 3mm-thick forming asymmetric porphyroclasts, or distended, isoclinal intrafolial folds with minor pinch-and-swell texture. The veins are composed of strain-free recrystallised calcite and ankerite, with 120° dihedral angles in highly deformed veins indicating significant post-deformation recovery. Nucleation microstructures of quartz growing at calcite triple-junctions, and irregular quartz grain-boundaries with 120° dihedral angles, indicate dynamic recrystallisation of the fabric. In most cases, the veins are parallel to the shear fabric, but also are disrupted by it. Syn to late-tectonic porphyry intrusion may have induced localised thermal recovery of the deformation fabrics.

Bullant mine

The Zuleika Shear Zone at Bullant open-pit is represented by a series of 0.5-20m wide zones of ductile shear developed within pillow basalt (Figure 3.5 p.38, Figure 3.6c-d p.40, Map 2 p.266). Ultramafic rocks are not present in the immediate mine area, but have been intersected in drill holes 100m west of the open pit. A series of shear zones spaced at 80-100m trends 152°/88°SW on average (Figure 3.10 p.45). Shallow-moderate plunging

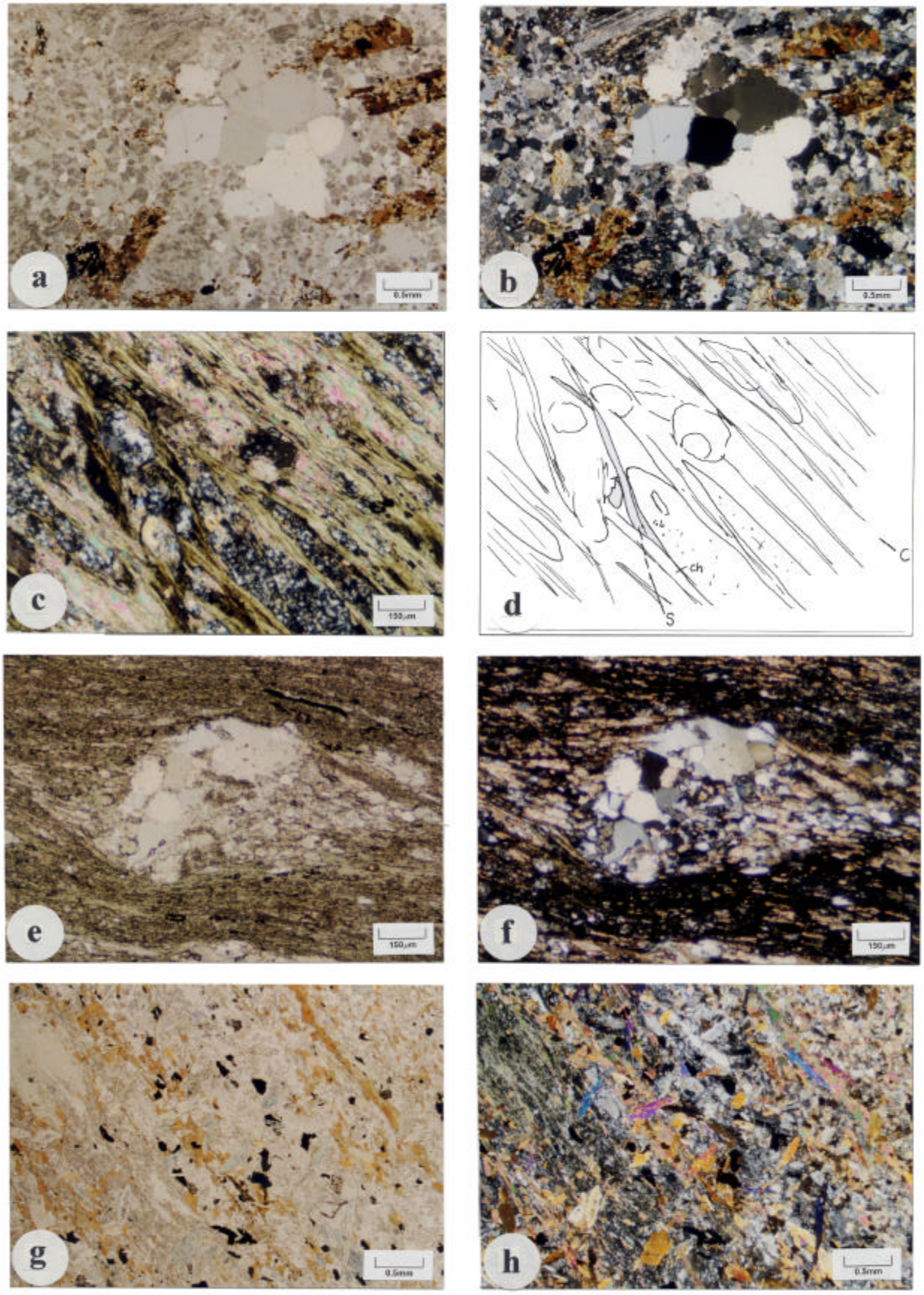

Figure 3.11 – Photomicrographs from the Zuleika shear zone. **a)** Felsic porphyry from the Porphyry mine, (PPL). **b)** Felsic porphyry from the Porphyry mine, (XPL). **c)** S-C fabric in talc-chlorite schist from the Wattlebird mine, (XPL). **d)** Line drawing of c). **e)** Assymetric porphyroclast showing dextral shear sense, from the Bullant mine, (PPL). **f)** Same as for Figure 3.11e), (XPL). **g)** Hydrothermal biotite forming the shear zone fabric, (PPL). **h)** Same as for Figure 3.11 g), (XPL). See text and over page for explanation.

Captions for figures on page 47

Figure 3.11a
Photomicrograph (PPL) of felsic porphyry from the Porphyry mine. Phenocrysts of rounded quartz and subhedral plagioclase are set in a fine-grained groundmass of saccaroidal textured quartz. Hydrothermal biotite pseudomorphs original hornblende. Sample is from 31.0m in diamond drill hole ZULD10.

Figure 3.11b
Sample as for Figure 3.11a), (XPL).

Figure 3.11c
Photomicrograph (XPL) showing S-C fabric in talc-chlorite ultramafic rock from the centre of the Zuleika Shear Zone. Films of chlorite and talc define both the S and C planes, and wrap microlithons of quartzofeldspathic material. The quartzofeldspathic material may be remnants of mafic rocks that are interleaved with ultramafic rocks in the shear zone. Sample trending 146°/84°NE is from the eastern wall of the Wattlebird south pit. ZSZ-1.

Figure 3.11d
Line drawing of the fabric relationships in Figure 3.11c).

Figure 3.11e
Photomicrograph (PPL) of an asymmetric porphyroclast in a N-S trending shear zone from the Bullant mine. The porphyroclast is a quartz vein fragment composed of strain-free recrystallised quartz grains. Quartz and calcite form pressure shadow beards around the vein fragment with asymmetry indicating dextral movement sense. Chlorite and calcite form a strong shear foliation that partially wraps the porphyroclast. Recrystallisation of the quartz indicates a degree of post-deformation recovery. A fire assay value of 0.05 g/T Au was returned for this sample. Sample trending 008°/68°E is from 209.3m in diamond drill hole ZULD9.

Figure 3.11f
Same view as for Figure 3.11e), (XPL).

Figure 3.11g
Photomicrograph (PPL) of ductile shear fabric in the Zuleika Shear Zone at the Bullant mine. Euhedral biotite forms a spaced cleavage parallel to the shear direction and smaller disseminated grains of biotite, feldspar and chlorite form the general fabric. The shear fabric is overprinted by randomly oriented actinolite indicating that peak metamorphism post-dates the shearing, and an earlier retrograde metamorphic event defined by chlorite. A fire assay value of 2.51 g/T Au was returned for this sample. Sample trending 138°/72°NE is from 202.4m in diamond drill hole ZULD9.

Figure 3.11h
Same view as for Figure 3.11g), (XPL).

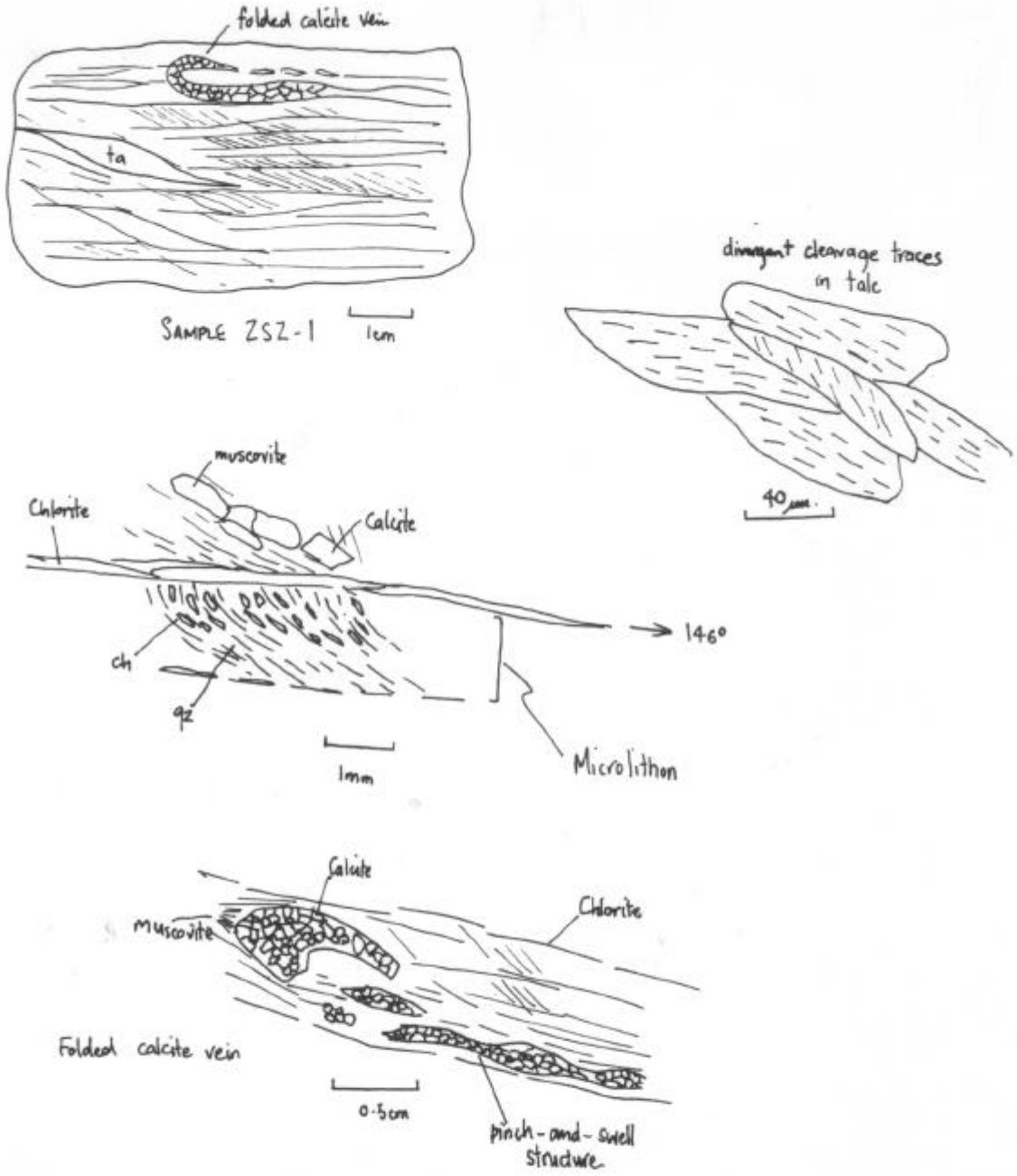

Figure 3.12 – Sketches of microfabrics from the Zuleika Shear Zone. Examples are from sample number ZSZ-1 from the Wattlebird mine.

stretching lineations in the C-plane of the shear zone indicate dominantly strike-slip movement (Figure 3.13a-b), with left-lateral offset displayed by S-C fabric asymmetry. Quartz veins are common in the plane of the shear zone trending 157°/66°NE, and cross-cutting the schistose fabric with an average trend of 051°/43°SE (Figure 3.10 p.45). Shearing-parallel quartz veins display pinch-and-swell morphology, whereas later veins are simple fracture-infill veins with non-directional controlled quartz addition textures (Vearncombe 1993) and triangular textures (Taylor 1992) displayed by hydrothermal biotite and chlorite.

An ENE-WSW trending brittle-ductile fault cross-cuts the Zuleika Shear Zone in the open-pit, with dextral offset trending sub-parallel to the S foliation. The fault bends into the main Zuleika Shear Zone, but the two may be developed as a conjugate pair (G. Adams, personal communication 1998). The later brittle-ductile fault is sub-parallel to a number of other mapped brittle-ductile faults trending 007°/83°E (Figure 3.10 p.45). Euhedral biotite defines a well-developed schistosity in the main shear zone trending 151°/77°NE (Figure 3.10 p.45) with a high proportion of silica recrystallisation of the groundmass (Figure 3.11g-h p.47). Mylonitisation is characteristic of the shear zone with flattened chlorite and white mica in poorly developed S-C fabrics.

In Bullant open-pit, the Zuleika Shear Zone is cross-cut by a late low-angle reverse fault with sub-parallel strike, that offsets the shear zone across the pit (Map 2 p.226). Spaced cleavage with about 5mm spacing defined by chloritic fractures, cross-cuts the schistose basalt with variable orientations that average 033°/75°SE (Figure 3.10 p.45).

A 4m-wide shear zone in the north wall, contains a series of fractures that may be brittle Riedel-type structures (Figures 3.6e-f p.40). The shear zone has sharp boundaries with weakly deformed basalt and the fractures appear to be contained within the shear zone, but do not extend into the wallrocks. The fractures have cross-cutting relationships with sequential development progressively approaching parallelism with the main shear zone orientation of 155°/83°W.

The detailed fabric of the shear zone in the area of strongest shearing in the pit, displays well-developed S-C fabrics and sharp planar boundaries with the wallrocks (Figure 3.6d

b

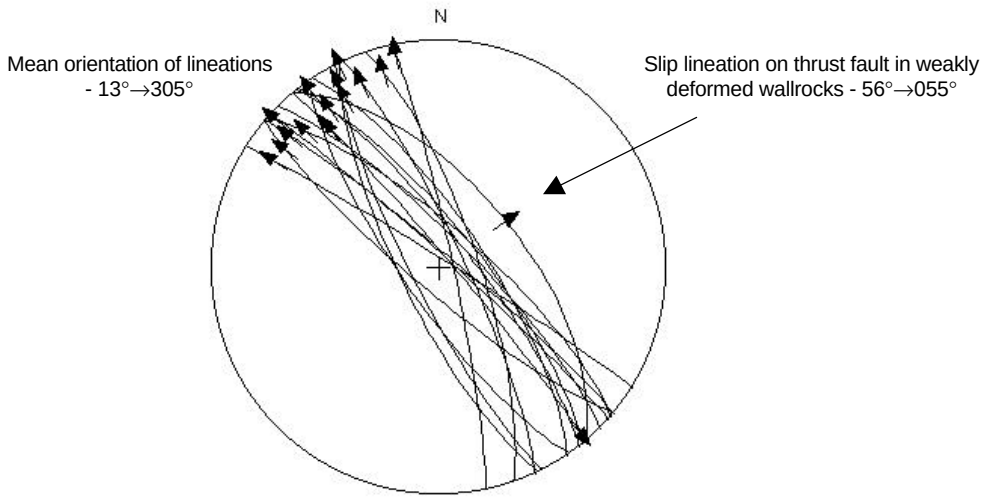

Figure 3.13- a) Photograph of stretching lineation in the plane of the Zuleika Shear Zone. The lineation trending 25°→320° is defined by aligned flakes of biotite and muscovite and quartz rods in the plane of the foliation trending 140°/86°E. **b)** Stereogram of lineations from the Zuleika Shear Zone from Anthill, Porphyry, Wattlebird and Bullant mines.

p.40). Pinch-and-swell quartz veins are common, and are developed parallel with the S-plane of the shear zone. A 20m band of schistosity in the northwest wall has discrete ductile shear zones with greater shearing-intensity spaced at about 5m.

In thin section (sample ZULD9 202.40), the shear fabric is defined by thin trails of hydrothermal biotite and calcite spaced at 1-5mm (Figure 3.11g-h p.47). Elongate flakes of brown biotite form smoothly anastomosing cleavage domains that overprint a fine-grained quartzofeldspathic matrix with up to 500*m*m long plagioclase (albite?) grains. Large un-oriented actinolite crystals up to 3mm long overprint the shear cleavage, indicating that peak metamorphism postdates the D3 shearing. The actinolite has weak undulose extinction in rare examples, but is mostly strain-free with ragged branching ends or euhedral terminations on acicular crystals.

Summary

The Zuleika Shear Zone consists of interlinked thin zones of mylonite that anastomose along strike. Strain is partitioned by rock contacts and anisotropies within basalt flow rocks including pillow margins. There is no evidence that major offset occurs across the shear zone and its location primarily at rock contacts suggests that the shearing may be a result of competency contrast between (previously) competent, olivine-rich ultramafic rocks and less competent basalt. The highly incompetent state of the ultramafic rocks seen today is a result of fluid movement through the shear zone and retrogression of the olivine during later shearing.

The shear zone was intruded by felsic porphyry bodies that appear to be mostly syn-late tectonic since cross-cutting relationships show both wrapping and truncation of the foliation. Felsic porphyries are most abundant in the Porphyry mine area where the ultramafic rock units are thickest indicating preferential intrusion into weak ultramafic schists. No logical source for the felsic porphyries is located in the vicinity of Zuleika, which is probably at depth. Randomly oriented actinolite overprinting the shear zone fabric indicates a post-D3 timing of peak metamorphism that may be related to the late porphyry intrusion.

A predominant sub-horizontal principal stretch direction is manifest as lineations, and elongate basalt pillows and ultramafic clasts, with no evidence of earlier dip-slip movement. S-C fabrics indicate left-lateral movement, but the amount of displacement may be negligible. The Zuleika Shear Zone is adequately exposed for analysis of its morphology and structural relationships, yet an appreciation of the broad structure and distribution of ductile deformation is hindered by poor surface exposure.

3.3.3 Brittle-ductile fault network (D4)

Late-tectonic brittle-ductile faults are ubiquitous throughout the Zuleika area and the Ora Banda Domain. The faults are interpreted from aeromagnetic imagery, ground-truthed in outcrop and drilling, and form a pervasive network that cross-cuts most other structures and all rock types (Fig 3.2 p.31, Chapter 4 p.86, Figure 4.1, p.87, Figure 4.6, p.100). Previous structural interpretations (Simpson *et al*. 1995; Swager *et al*. 1990) treat the faults as minor, locally developed features that do not persist through major geological and structural contacts, yet aeromagnetic images clearly show the structures extending through stratigraphic sequences over distances of tens to hundreds of kilometres.

The network of lineaments interpreted from aeromagnetic imagery (Figure 3.2 p.31) is divided into three principal structural orientations NE-SW, N-S and E-W (Figure 3.14). The number of NE-SW trending lineaments (n=374) is significantly greater than the other orientations, N-S (n=214), E-W (n=109) (Figure 3.15). A group of NW-SE trending lineaments (n=65) represents the D3 ductile shear zones

The lengths of the lineaments were analysed graphically to show the distribution of structures at a regional scale (Figure 3.15). Although some large features are interpreted (20 km, Zuleika Shear Zone) many lineaments in each of the principal structural orientations are less than 2000m long with most less than 1000m in length. In general, NE-SW and N-S trending lineaments have closer spacing than E-W trending lineaments.

These results indicate that the domain-wide fault network comprises brittle-ductile faults that individually are developed at the mesoscopic scale, but their widespread distribution indicates deformation of a regional extent. Veins, brittle-ductile faults and a poorly developed spaced cleavage cross-cut the Zuleika Shear Zone in most exposures. The late

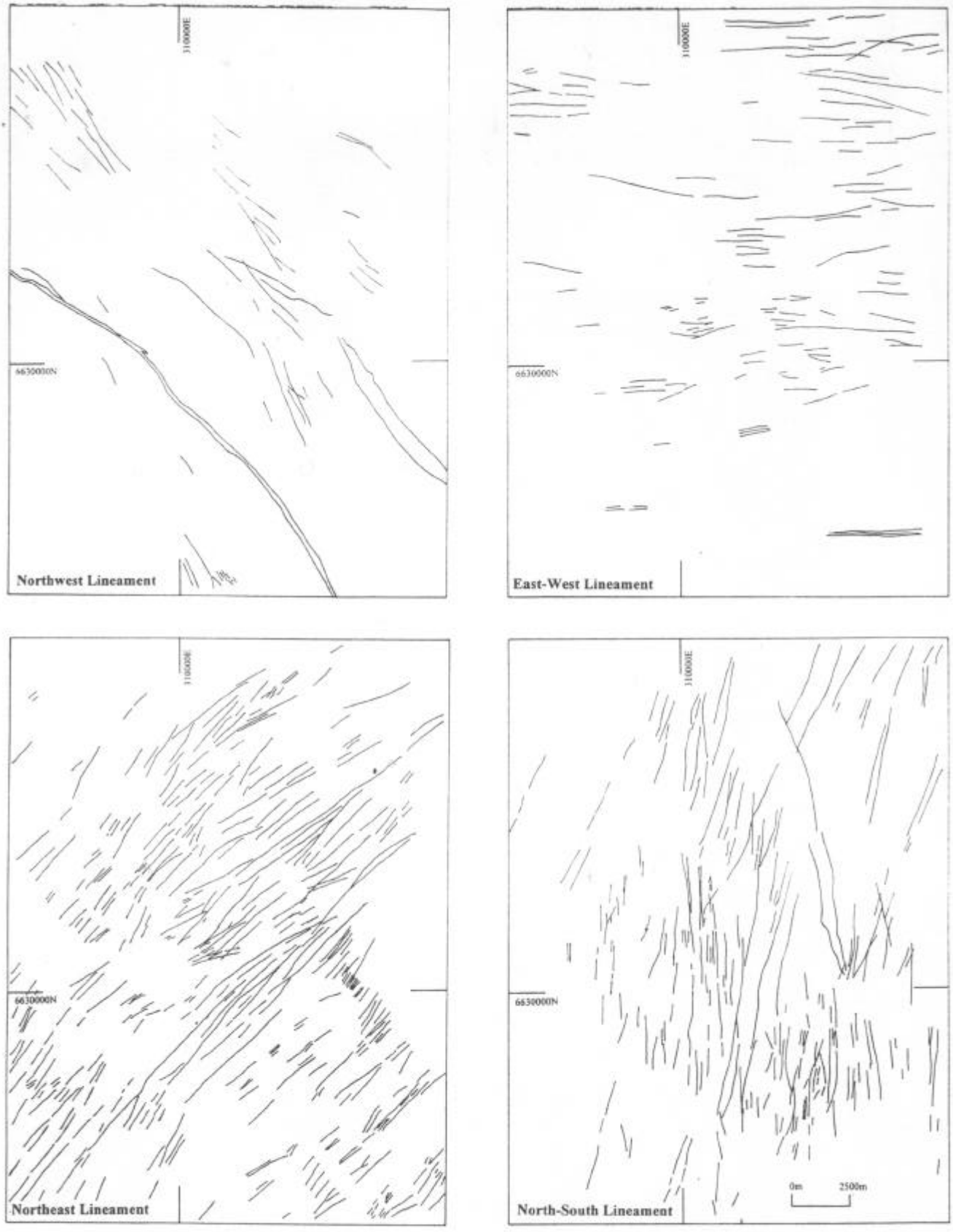

Figure 3.14 – Maps of individual lineaments from each of the four main groups interpreted from figure 3.1. Total lineaments in each group are 65 for NW-SE, 109 for E-W, 374 for NE-SW and 214 for N-S.

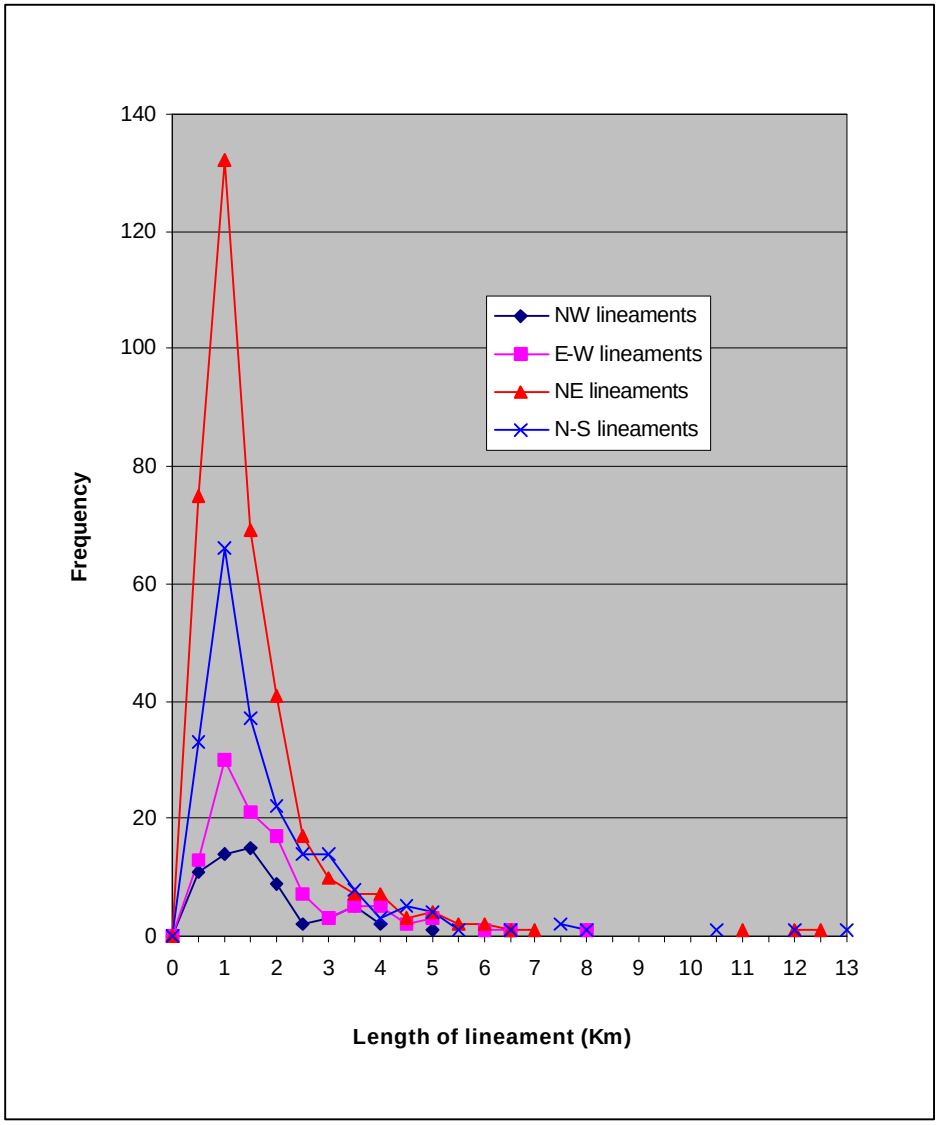

Figure 3.15– Graph of lineament lengths from maps in figure 3.14. The majority of lineaments are less than 2km long in each of the principal structural orientations.

structures have characteristic brittle-ductile textures and in some examples have either completely ductile or completely brittle fabrics.

Anthill mine

At the Anthill mine, brittle-ductile faults trending 134°/73°W cross-cut the main Zuleika Shear Zone with S-C fabrics indicating right-lateral offset (Figure 3.16c, Map 1 p.262). The late faults spaced at 0.5–1.0 metre, are up to 5cm wide and contain 10 to 20mm-thick lensoid quartz veins within parallel shear bands and fracture planes. Since sheared talc-chlorite ultramafic rocks are the dominant rock-type, the late structures developed in the ultramafic rocks have mostly ductile character. Thin lensoid quartz veins trending 067°/76°S cross-cut a weak foliation in felsic porphyry.

Porphyry mine

Structural analysis of diamond drill core from the Porphyry mine reveals three dominant structural orientations for stockwork quartz veins trending 033°/41°SE, 018°/67°NW, and 096°/45°NE (Map 3 p.271). Broadly scattered vein orientations from several drillholes have an average orientation of 057°/32°SE (Figure 3.7 p.43), and late brittle-ductile faults trend 172°/74°W and 044°/29°SE. Quartz veins at the Porphyry mine are usually thin (<5mm wide), simple fracture-sealing veins with displacement-controlled quartz addition textures. Quartz-pyrite is the dominant mineralogy with silica-albite alteration halos, but unmineralised quartz and quartz-calcite veins in fractures are also common. Fracturing of the porphyry body is more prominent in a 15-20m wide band on the western margin. The more fractured western margin may be a separate phase from the eastern part of the body (Map 3 p.271).

Bowerbird mine

Brittle-ductile features at the Bowerbird mine comprise mostly brittle-style comb-textured quartz veins that cross-cut the mylonitic shear fabric at a high angle. These veins are comb-textured with quartz fibres at a high angle to the vein walls or have recrystallised fabrics. Cataclastic textures are not observed.

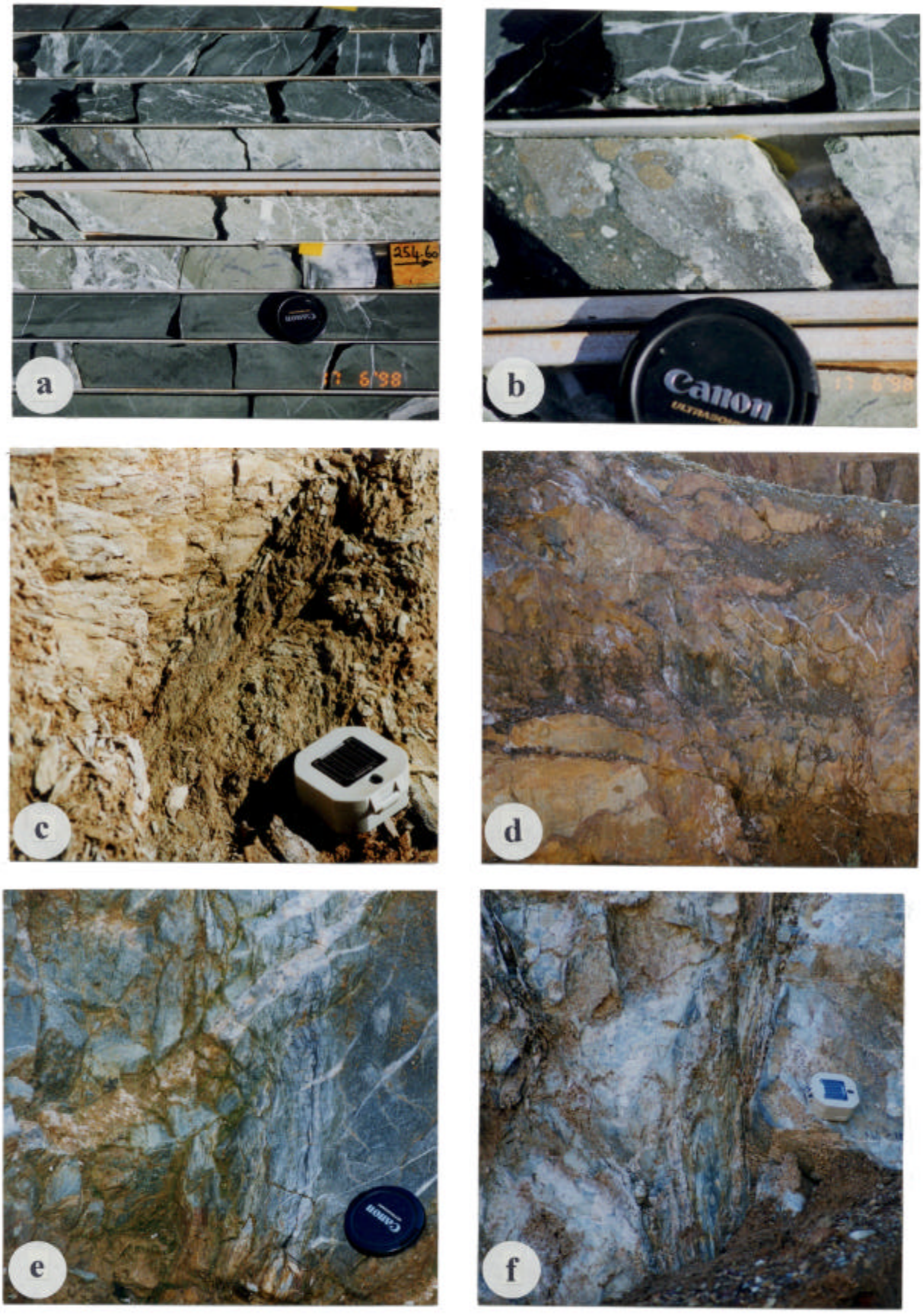

Figure 3.16 - a) Breccia zone with localised cataclasite and fault gouge crosscutting Zuleika Shear Zone, Bullant diamond drill core. **b)** Close-up of fault gouge from Figure 3.16a. **c)** Late ductile shear band cross-cutting Zuleika Shear Zone, Anthill open-pit. **d)** Quartz vein array, Wattlebird open-pit. **e)** Quartz vein array, Wattlebird open-pit. **f)** Oblique brittle-ductile shear zone on pillow margin, Bullant open-pit See text and over-page for explanation.

Captions for figures on page 57 – Brittle-ductile faults

Figure 3.16a
Brittle fault zone cross-cutting ductile fabrics related to the Zuleika Shear Zone. The fault zone is a markedly altered zone with intense muscovite-calcite alteration retrogressive after chlorite in high-magnesium basalt. Brittle fabrics include random fault breccia with cementation by hydrothermal precipitates, jigsaw puzzle textures with net-veined breccia morphology and random fault gouge with a high degree of milling of fragments and rolling of clasts. Large fragments of relatively undeformed but highly altered basalt separate zones displaying these textures. The fault trending 028°/70°SE is located at 252.30m in diamond drillhole ZULD18. Downhole direction is to the right, Lens cap is 55mm diameter.

Figure 3.16b
Close-up of fault gouge zone from 3.16a. The zone is 90mm wide and typified by cataclastic texture with several overprinting stages of cataclasis and brecciation followed by variable milling of the clasts. Zones of re-cementation of the breccia clasts occur around thin quartz-carbonate veins. Four types of clasts are present; angular to sub-rounded white-mica-altered schistose basalt, elongate rounded pyrite fragments up to 30mm long, clasts of several matrix generations (green chlorite-pyritic, dark grey pyritic and light grey pyritic), and chlorite-epidote? altered mafic. The variety of clasts of matrices to earlier failure events indicates a complex episodic movement history for the structure with several events related to mineralisation. Movement sense is undetermined at x10. A gold value of 0.21 ppm Au was returned for the fault, Lens cap is 55mm diameter.

Figure 3.16c
Photograph of an oblique brittle-ductile fault that cross-cuts penetrative schistosity in talc-chlorite ultramafic rock from Anthill open-pit. The late structure trends 134°/73°W, S-C fabric indicates right-lateral offset. The Zuleika Shear Zone trending 345°/89°W can be seen as a flat surface parallel to the plane of the photograph truncated against the C-plane of the late fault. Compass is 70mm square. View is looking west-southwest.

Figure 3.16d
Photograph of a late quartz vein array that cross-cuts the Zuleika Shear Zone from Wattlebird south-pit. The veins in the array trend parallel to the veins in Figure 5.3b but the array in total trends N-S. The quartz veins are less than 200mm thick and appear sigmoid in cross-section. Veins in the array do not have individual alteration halos but the wallrocks are pervasively altered to white-mica-carbonate in close vicinity of the Zuleika Shear Zone. The quartz vein array is 5-10m wide. View is looking NE-SW, long axis of the photograph is parallel to the Zuleika Shear Zone (north-west trend).

Figure 3.16e
Photograph of a quartz vein array that cross-cuts a discrete ductile shear zone from Wattlebird south-pit. The structures are developed in moderately schistose high-magnesium basalt. The ductile shear zone is a thin shear parallel to the main Zuleika Shear Zone to the east. Ductile fabrics include a strong shear foliation defined by slivers of chlorite interspersed with zones of highly schistose basalt and stretched elongated quartz veins. Parallel quartz veins form an array with average orientation 043°/45°S that cross-cuts the ductile shear zone. Dominantly brittle in character, the veins fill planar fractures with sharp boundaries against the fabric of the Zuleika Shear Zone. Lens cap is 55mm diameter. View is looking NW-SE.

Figure 3.16f
Photograph of an oblique brittle-ductile fault in strongly altered pillow basalt from Bullant open-pit. The shear zone 100mm wide, trends 010°/73°W with a well-developed slip-lineation plunging 9°→185° indicating dominantly strike-slip movement with a minor reverse component. The fabric of the fault is characterised by stretched elongate fragments of basalt and vein quartz, sharp boundaries and lack of a parallel planar fabric in the wallrocks, indicating strain partitioning into the plane of the shear zone. The brittle-ductile fault is localised along a pillow margin in high-magnesium basalt. Compass is 70mm square. View is looking north.

Wattlebird mine

Brittle-ductile faults trending 005°/79°W (Figure 3.9 p.45, Maps 4-5 p.277-278) and brittle fault/vein arrays trending 058°/43°SE and 106°/71°S, cross-cut the Zuleika Shear Zone at the Wattlebird mine (Figure 3.16d-e p.57). Brittle-ductile shear bands in talc-chlorite ultramafic rocks trending 090°/72°N cross-cut the S-C fabric of the shear zone. Quartz veins that trend parallel to the Zuleika Shear Zone display stretching and boudinage (Figure 3.20f p.65) and were most likely developed synchronous with the shear zone.

Bullant mine

At the Bullant mine, oblique brittle-ductile faults cross-cutting the Zuleika Shear Zone trend 007°/83°E on average (Figure 3.10 p.45, Map 2 p.266) with associated quartz veining, pervasive microfracturing and localised breccia (Map 2 p. 266). Some of these structures are predominantly ductile with porphyroclastic texture (Figure 3.11e-f p.47). An intensely muscovite-altered brittle fault zone trending 028°/70°SE has fault gouge at the margins and random textured cataclasite (Figure 3.16a-b p.57). The fault gouge contains polylithic cataclasite with fragments of pre-existing breccia matrices indicating multiple-stage failure and reworking of the fault (Figure 3.17a-b). White mica altered basalt fragments are angular with jigsaw textures and a quartz-calcite vein matrix, with rare voids infilled by euhedral prehnite (Figure 3.17c).

Late quartz veins trending 051°/43°SE have associated schistosity defined by chlorite and quartz overprinted by euhedral biotite, and quartz-calcite-biotite-pyrrhotite veining. A late brittle-ductile fault trending 010°/73°W that cross-cuts the main structure in the Bullant open-pit (Figure 3.16f p.57), can be traced across the walls of the open-pit and is persistent for several hundred metres as it has been intersected in drillholes to the north and south of the pit.

Summary

Brittle-ductile faults form an interlinked network that is pervasive at a regional scale. In outcrop the faults are single cataclasite zones, simple veins or vein array systems. The

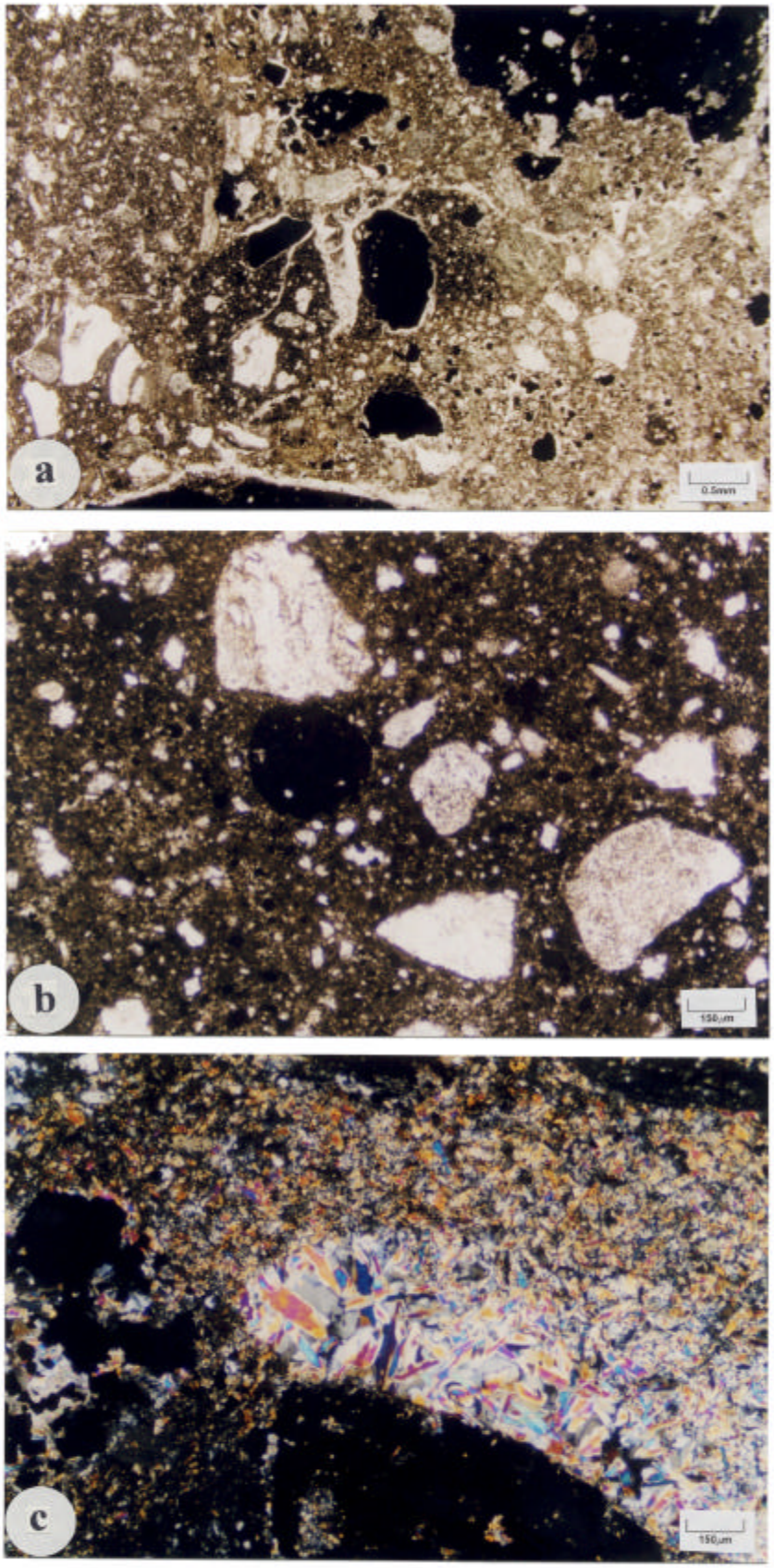

Figure 3.17 - a), b) Photomicrographs of polylithic, cataclastic breccia, from the fault in Figure 3.16b (PPL). Isotropic fragments are massive pyrite clasts. The fault shows a wide range of clast sizes and variable angularity of clasts in matrix supported breccia. **c)** Photomicrograph of a void in the rock, filled with euhedral prehnite (XPL). All photomicrographs from 252.3m in diamond drill hole ZULD18. See text for explanation.

faults group into three orientations with structural style and dimensions that are significantly different to the regional shear zones. Cross-cutting relationships indicate that the faults are later than the Zuleika Shear Zone with textural differences suggesting an increased strain rate or a crustal level different to that for the D3 shearing event.

3.4 REGIONAL MECHANICAL ANALYSIS

Three main episodes of shortening are evident in the Zuleika district. The following mechanical analysis is an attempt to assess the nature of the deformations that produced the strain fabrics and to assess possible orientations for the principal axes of strain for each deformation pulse. Mesoscopic data on the rock fabrics are from the Zuleika area only and these may be influenced by their location close to a regional-scale shear zone. Hence similar mechanical analyses are presented in Chapters 4 and 5 to compare principal shortening axes at several scales across the Ora Banda and Zuleika districts.

3.4.1 Regional folding

Folding in the Ora Banda and Zuleika districts is developed at the regional scale with only localised mesoscopic folding. The Kurrawang Syncline and Goongarrie – Mount Pleasant Anticline are close folds with 50° interlimb angles, and the fold geometry suggests a shortening of the crust in a direction orthogonal to the axial traces (Figure 3.18).

3.4.2 Ductile shearing

The Zuleika Shear Zone has been interpreted previously as a strike-slip deformation zone (Hunter 1993; Swager *et al*. 1990), however no significant mismatch of stratigraphic sequence is recorded across it. The location of the shear zone at a stratigraphic contact, and the geometry of wallrock strain markers implicate a deformation history dominated by shortening rather than one of non-coaxial strike-slip shearing.

Strain markers and flow partitioning

Strain is heterogeneously distributed in the Zuleika Shear Zone. The wallrocks of the shear zone contain markers that record a significant flattening component (pure shear) of the

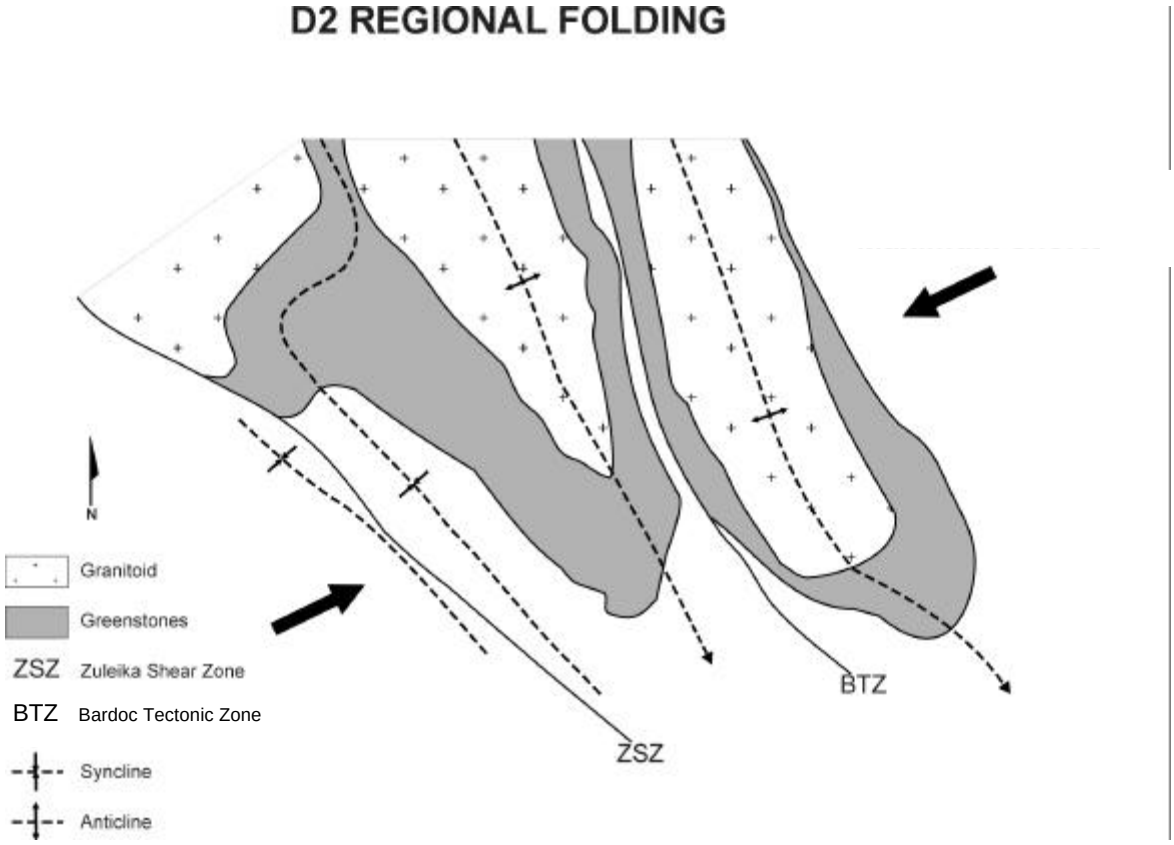

Figure 3.18 – Map of the regional folding pattern in the Ora Banda and Boorara Domains. NW-SE trending fold axes indicate that folding was produced by shortening orthogonal to the axial traces. NW-SE trending regional ductile shear zones trend sub-parallel to the fold axes, and in most cases are located in the synformal areas of the fold belt.

deformation, with the simple-shear component (non-coaxial) partitioned into discrete planar zones. Shear zones are localised mostly along rock unit boundaries but also are slightly transgressive of the contacts. Two types of strain marker at Zuleika, basalt pillow structures and varioles, are used to determine the nature of strain in the wallrocks of the shear zone (Figure 3.19).

Pillow structures in basalt are a primary depositional feature that usually form elongate tubes with long axes sub-parallel to the flow-direction (Compton 1985). Cross-sections perpendicular to the flow direction can have circular pillow shapes, but oblique cross-sections may have a variability of shapes from circular to flattened ellipsoids.

Basalt pillows at the Wattlebird mine display progressive flattening with proximity to the highest strain zone (Figures 3.20 b,c,d). Within 5-10m of the shear zone, previously round basalt pillow structures are ellipsoidal and are progressively flattened and elongated into long thin shapes as the strain increases. The cross-sectional orientation through the pillow structures may not be optimal for a quantitative strain analysis but qualitatively, the amount of flattening increases towards the zone of highest strain (simple shear). A sharp change in the axial ratios of the pillows occurs close to the shear zone indicating that although the immediate wallrock does not contain planar shear fabrics, a significant pure shear component is localised in the vicinity of the non-coaxial shear zone that decreases sharply with distance into the wallrock.

Variolitic texture (Figure 3.20a), is an igneous crystallisation phenomenon formed by spherical shaped clusters of radiating acicular amphibole or plagioclase crystals from mafic magma (Morris 1993). The spherical nature of the varioles means the structure is an excellent strain marker that records the shape of the finite strain ellipsoid, and may provide quanitative data on the component of flattening that accompanied non-coaxial simple shear. Variolitic texture is well-developed in basalt pillow margins, and groups of varioles show flattening strains developed with a common stretching axis orientation (Figure3.19a, 3.20a). Large elliptical centimetre-scale spots with elongate, flattened shapes, occur in the pillow margins of basalt in the Wattlebird north-pit (Figure 3.20e). The spots are interpreted as varioles or ocelli in the margin of the basalt pillows but they have an unusually large size and may be fragments of interpillow breccia.

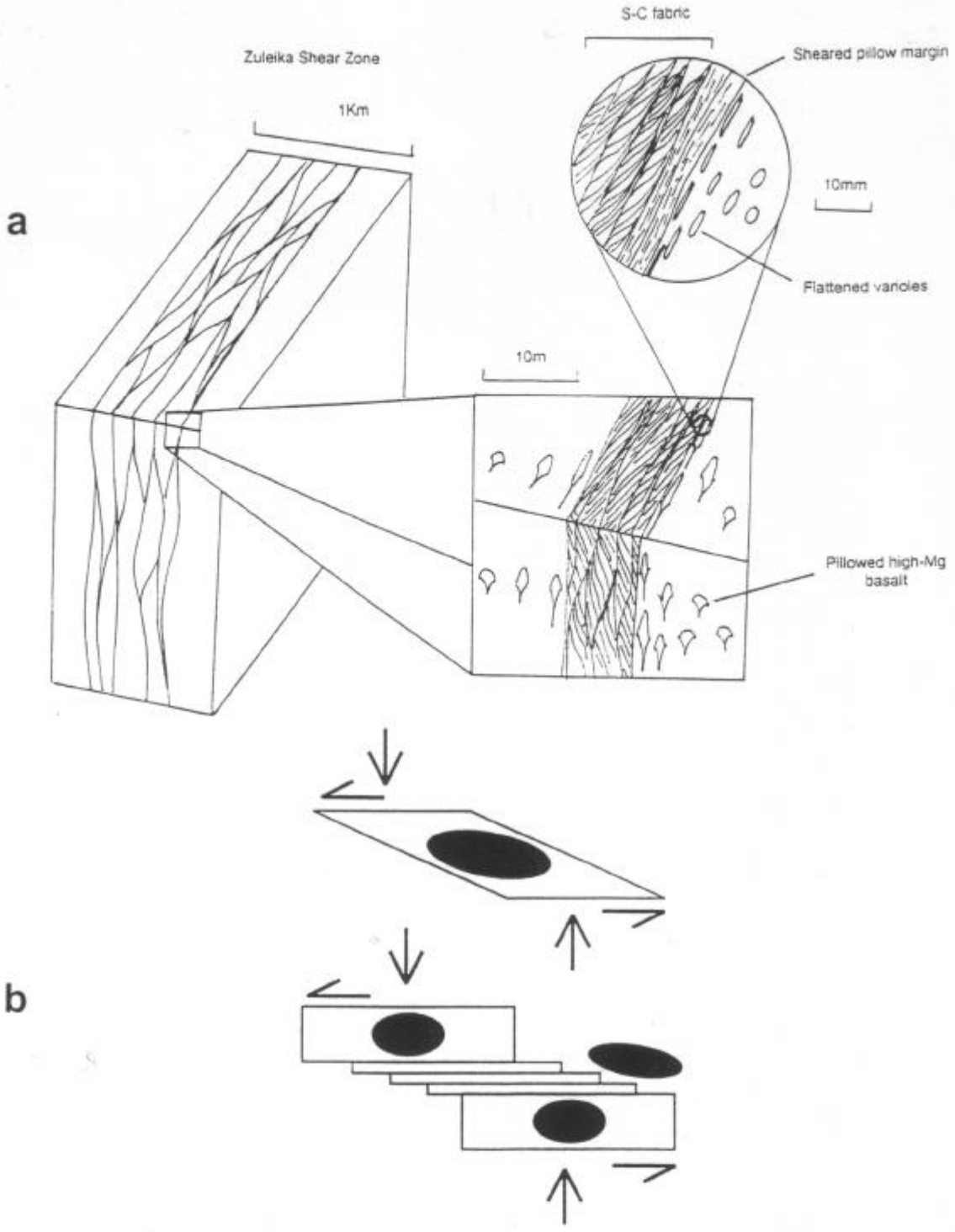

Figure 3.19 – a) Schematic diagram showing the distribution of strain markers in the Zuleika shear zone. A zone of thin shear zones enclosing lithons of weakly deformed rock consists of thin simple shear zones with flattening strains in the immediate wallrocks. b) During deformation the simple shear component of the flow was partitioned into discrete planar zones with flattening strains in the surrounding wallrocks. The relationship is typical of strain partitioning (modified from Hanmer and Passchier 1991).

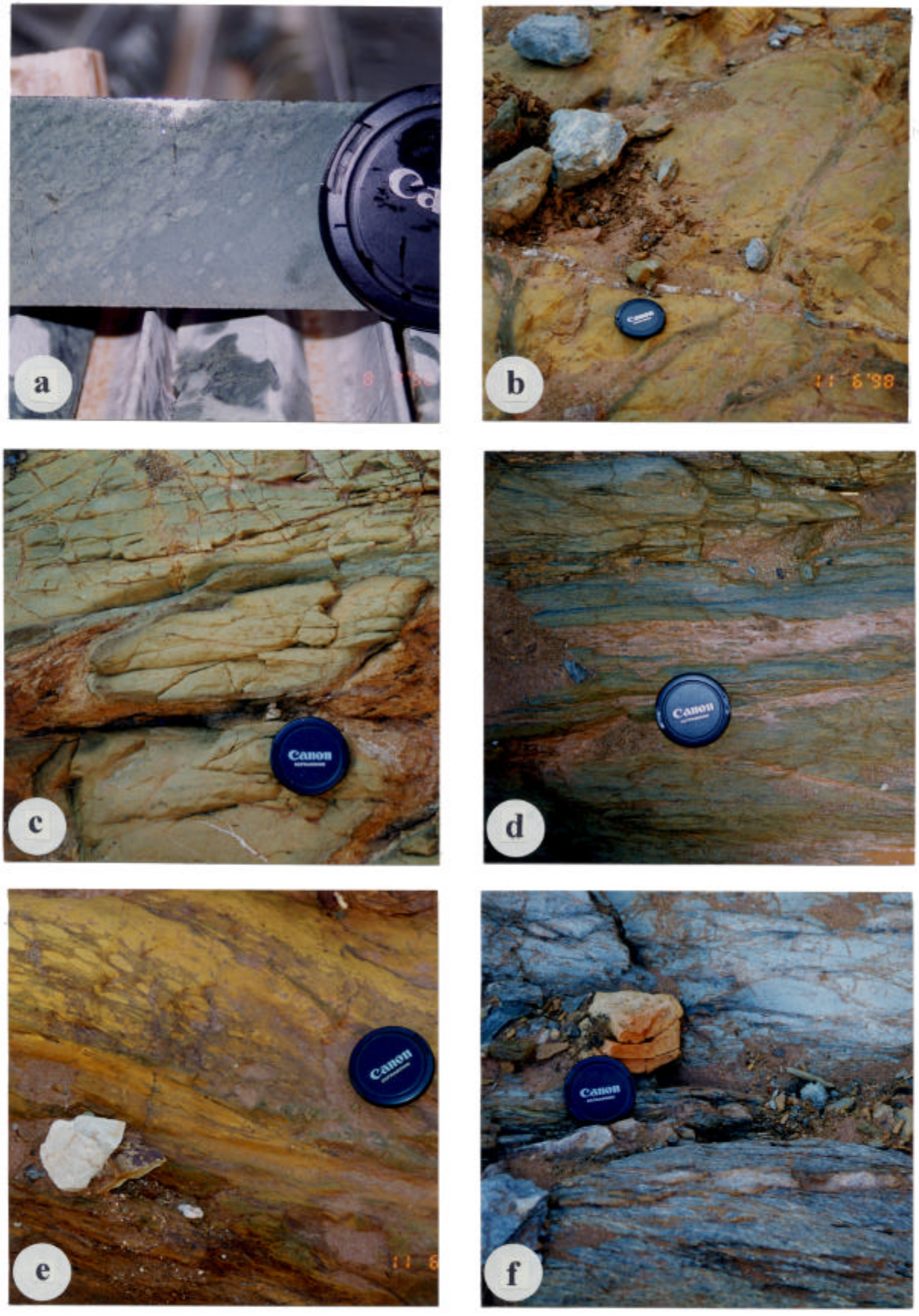

Figure 3.20 - a) Flattened varioles in high-magnesium basalt, Bullant. **b), c), d)** Basalt pillow margins from Wattlebird open-pit showing increasing degrees of flattening strain. **e)** Strained varioles / interpillow breccia material, Wattlebird north-pit. **f)** S-C mylonite / flattened ultramafic breccia contact, Wattlebird open-pit. See text and over-page for explanation.

Captions for figures on page 65 – Strain markers

Figure 3.20a

Flattened variolitic texture from a pillow margin in high-magnesium basalt, Bullant. The structure is a useful strain marker since varioles are spherical igneous crystallisation phenomena. Varioles when viewed in the correct orientation give the shape and orientation of the finite strain ellipsoid at the final stage of the deformation. The shapes of variolitic structures indicate a significant flattening component of the deformation orthogonal to the Zuleika Shear Zone. Sample is at 369.30m in diamond drillhole ZULD2.

Figure 3.20b, c and d

Series of photographs of pillow margins in high-magnesium basalt from Wattlebird south-pit. The pillow margins are zones of high chlorite concentration in strongly white mica-carbonate altered basalt. As the main Zuleika Shear Zone is approached the pillow structures are progressively flattened with aspect ratios decreasing markedly with decreasing distance from the shear zone. Within the shear zone the pillow structures are entrained parallel to the foliation. The dimensions of the basalt pillows are 800mm x 300mm, 300mm x 100mm and 900mm x 70mm for 5.2b,c and d respectively. The distance of the basalt pillows from the main shear zone is 7m, 2m and 0m for 5.2b,c,and d respectively. Long axes of the pillow margins trend sub-parallel to the weathered face in each photograph and pillow cross-sections in this plane are ellipsoidal, hence the exposure on the floor of the pit is not the optimum view for a quantitative strain analysis. The best section for viewing the pillows is a cross-section oriented at 90° to the foliation and the stretching lineation of the main shear zone. Optimum exposures were not available at Wattlebird. Lens cap is 55mm diameter. View in 5.2b is south-east, and in 5.2c and d top of photo points north-east

Figure 3.20e

Flattened varioles / interpillow breccia fragments in pillow basalt from Wattlebird north-pit. The fragments are unusually large for varioles but the weathered nature of the outcrop may mask the detailed texture of the structures. The fragments are located within a pillow margin of intensely sheared high-magnesium basalt and are flattened indicating a component of shortening orthogonal to the plane of the shear zone. Top of photo points NE-SW. Lens cap is 55mm diameter.

Figure 3.20f

Photograph of S-C fabric in sheared talc-chlorite ultramafic from Wattlebird open-pit. The outcrop demonstrates the inhomogeneous nature of the deformation on the Zuleika Shear Zone with the Lens cap at a sharp boundary of well developed S-C mylonite (below) and clast-supported breccia with coarse flattened clasts of talc-chlorite ultramafic (above). S-C fabrics indicate left-lateral offset on the Zuleika Shear Zone. A thin slightly stretched quartz vein occurs in a fracture sub-parallel to the C-plane of the shear zone. Lens cap is 55mm diameter. Top of photo points NE-SW.

An analysis of 13 varioles in a pillow margin from diamond drillhole ZULD2 – 369.3m at the Bullant mine, shows that the structures are deformed into triaxial ellipsoids with X>Y>Z where, X= axis of maximum elongation, Y=intermediate axis of elongation and Z=minimum axis of elongation. The samples plot on a Flinn diagram with K<1 (K=0.34), indicating an apparent flattening deformation. The axis of maximum elongation plunges in a direction parallel to the mineral elongation lineation defined by aligned micas in the plane of the shear zone (Figure 3.21). The mineral elongation contained within the C-plane is oriented at about 90° to the S-C intersection. Parallelism of the mineral elongation lineation (simple shear), and the axis of maximum elongation of varioles, may indicate that the two fabrics were produced during the same shortening event, and implies partitioning of the flow into rotational and irrotational components (Figure 3.19b p.64). Rotation of the variole long axes from some other angle into parallelism with the flow plane would be expected if the deformation was bulk non-coaxial, however the data are insufficient to determine this relationship.

This determination provides a general guide to the flattening component of the deformation based on relatively few samples, whereas a representative strain analysis requires a larger sample population that is not available from the current amount of exposure at Zuleika. Strain markers indicate a component of flattening approximately orthogonal to the Zuleika Shear Zone, and this combined with the development of obtuse conjugate shear zone pairs of NW-SE sinistral and NNW-SSE dextral shear zones, implies an ENE-WSW maximum shortening during the formation of the Zuleika Shear Zone (Figure 3.22).

3.4.3 Principal structural orientations of shear zones and brittle-ductile faults

Faults and shear zones in the study area cluster into four principal structural orientations: NW-SE, N-S, NE-SW and E-W trending structures (Figure 3.23, Table 3.1). These correspond to four groups of lineaments with similar orientations that have been interpreted from aeromagnetic imagery (Figure 3.2 p.31, Figure 3.14 p.54). The three principal orientations of brittle-ductile faults (N-S, NE-SW and E-W) are averages of structures with similar deformation styles that are interpreted as being formed synchronously.

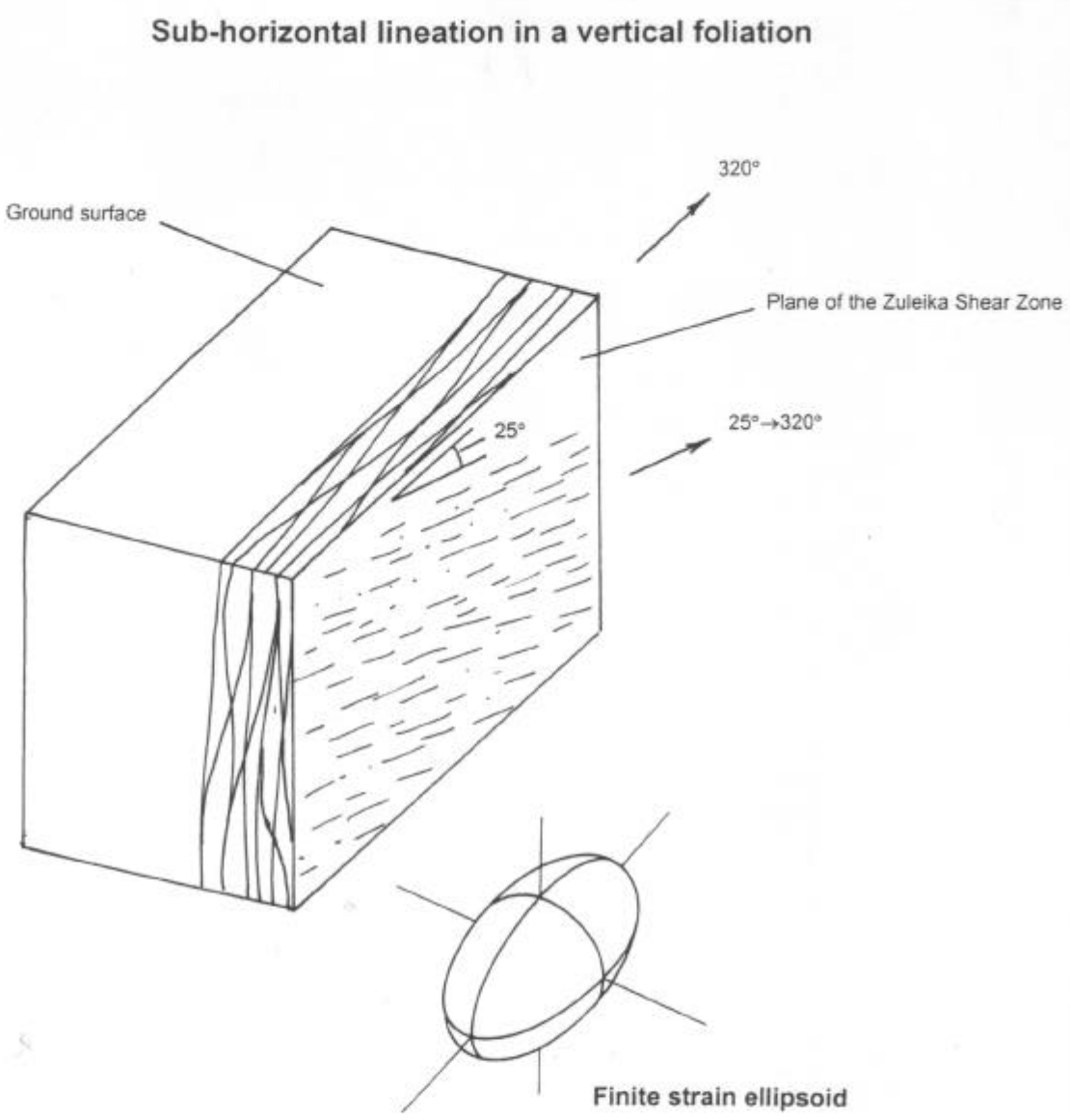

Figure 3.21 –Sketch of the slip / stretching lineation on the plane of the Zuleika Shear Zone in Bullant open pit. The geometry of varioles in high-magnesium basalt indicates that the slip lineation is sub-parallel to the local orientation of the maximum stretch axis of the finite strain ellipsoid.

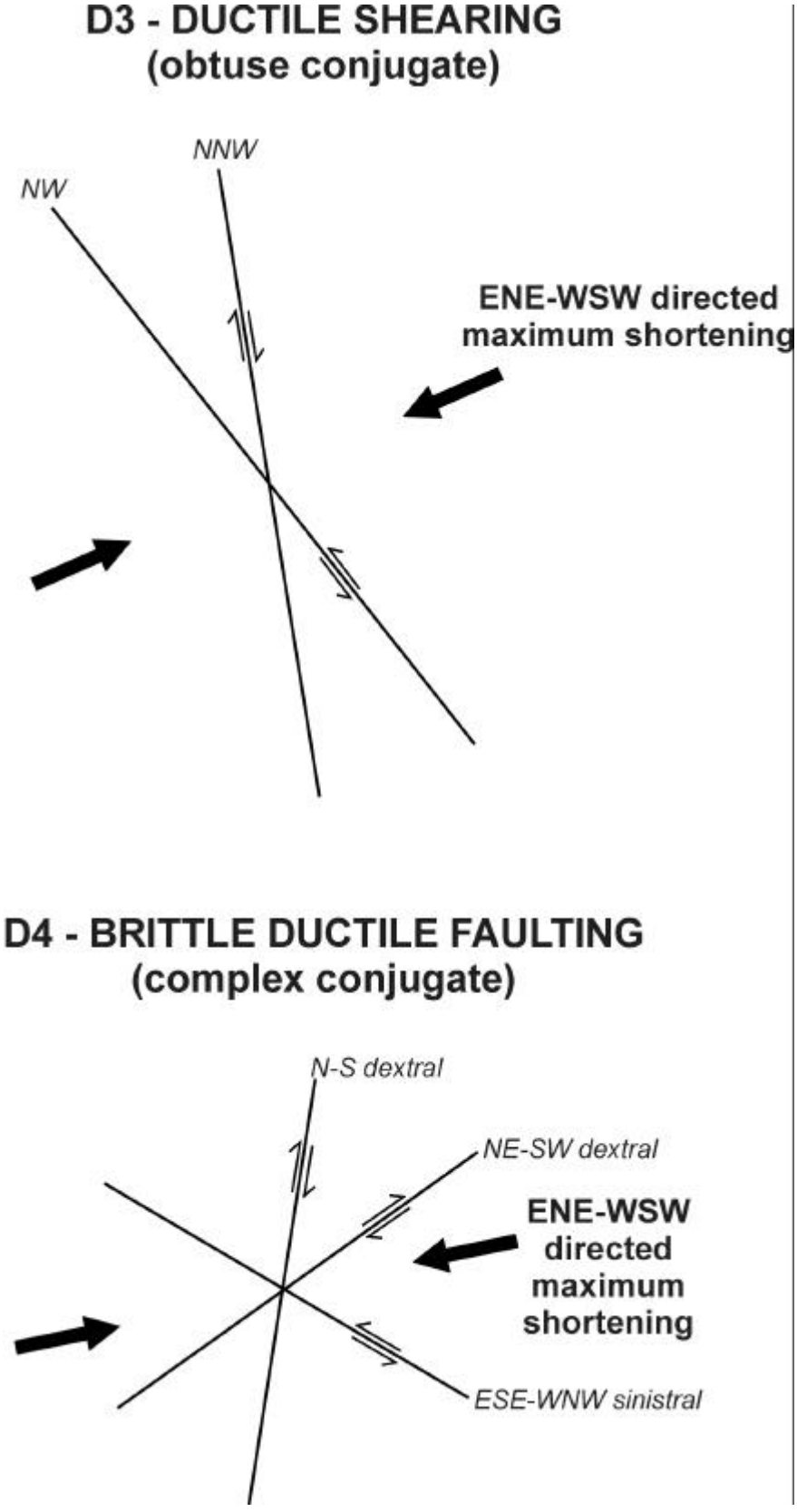

Figure 3.22 – Schematic diagrams showing the distribution and offset relationships of D3 ductile shear zones, and components of the D4 brittle-ductile fault network. Both events have orientations and sense of offset that indicate formation during ENE-WSW shortening.

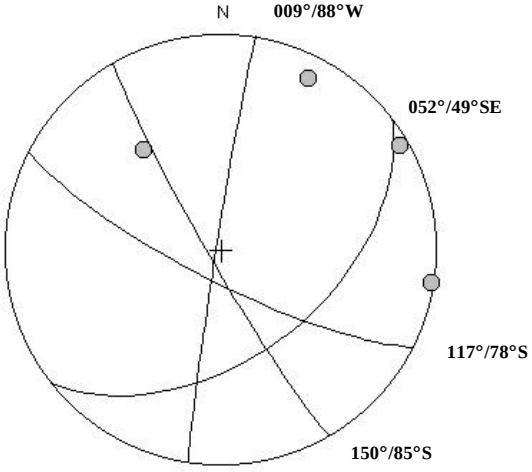

Figure 3.23 – Stereogram showing the four principal structural orientations at Zuleika. Great circles are for the average orientations listed in Table 3.1. The opposite-dipping variation for the NW-SE and N-S principal orientations are omitted for clarity.

Table 3.1 – Principal structural orientations in the Zuleika area compiled from drill-core and open pit observations, grouped by structural style. Orientations for each structural element are great circle orientations to the major clusters presented on stereograms for each prospect.

Principal Structural Orientations	NW-SE	N-S	NE-SW	E-W
Shear Zones				
Anthill	151°/68°W	015°/73°W	-	-
Porphyry	-	-	-	-
Bowerbird	157°/74°SW	-	-	-
Wattlebird	142°/83°SW	005°/79°W	-	-
Bullant	152°/88°SW	007°/83°E	-	-
Brittle Faults				
Anthill	-	-	-	-
Porphyry	-	-	057°/42°SE	-
Bowerbird	-	-	-	-
Wattlebird	-	-	-	-
Bullant	-	-	-	-
Veins				
Anthill	-	178°/72°W	067°/76°S	-
Porphyry	-	-	053°/38°SE	-
Bowerbird	151°/72°SW	021°/59°SE	-	-
Wattlebird	145°/87°NE	-	058°/43°SE	106°/71°S
Bullant	157°/66°NE	-	051°/43°SE	-
Schistosity and Cleavage				
Anthill	155°/66°W	-	-	-
Porphyry	-	-	044°/29°SE	-
Bowerbird	-	-	-	127°/85°SW
Wattlebird	142°/88°SW	-	-	-
Bullant	151°/77°NE	-	033°/75°SE	-
Average Orientations	**150°/85°SW**	**009°/88°W**	**052°/49°SE**	**117°/78°SW**

Relationships between deformation styles

Northwest-southeast trending structures have a mostly ductile character, typified by zones of schistosity and mylonite, and are represented by the Zuleika Shear Zone and conjugate shear zones. There is some evidence of minor brittle-ductile deformation related to the shear zones, such as subparallel shear veins with pinch-and-swell morphology. The other three principal orientations are brittle-ductile to brittle in character, ranging from breccia zones with localised cataclasite to fracture-fill quartz veins. A poorly developed spaced cleavage is also observed cross-cutting the earlier ductile fabrics.

Ductile features generally cluster tightly on a stereonet but brittle-ductile and brittle features may have up to 30° variability in strike with opposing dip directions. Additional scatter in orientations is produced by the anastomosing nature of foliations in shear zones especially when measured in diamond drill core. Not all of the structural styles are developed at each location, or in each of the principal orientations. Ductile shear zones trend in two main orientations; NW-SE and N-S. Some of these structures are brittle-ductile shear veins that overprint the NW-SE trending ductile shear zones, whereas others may be developed synchronously with the Zuleika Shear Zone forming an obtuse conjugate pair (eg. Ramsay 1980a). Brittle faults including rare cataclastic breccia and cataclasite seams mostly form in the NE-SW and E-W orientations. Quartz veins are ubiquitous in all of the principal structural orientations, whereas schistosity is sub-parallel to the NW-SE trending ductile shear zones. Spaced cleavage is developed sub-parallel to the NE-SW trending faults, the best examples of this being from the Bullant mine.

Overprinting relationships

Northwest-southeast trending ductile shear zones are overprinted by all other structures with rare exceptions. The other three principal orientations have mutual cross-cutting relationships that imply broadly synchronous development. Several examples were studied that demonstrate conjugate development of E-W and NE-SW trending brittle style quartz-pyrite and quartz-biotite-pyrite veins.

Offsets and displacements

The kinematic history of the Zuleika Shear Zone was predominantly left-lateral strike slip but similarities of lithological sequence across the shear zone indicate that there is not a large displacement of the wallrocks. Brittle-ductile faults in the N-S, NE-SW and E-W orientations have typically small apparent offsets from aeromagnetic imagery of the order of metres to a maximum of hundreds of metres. Mesoscopic data on offsets of the brittle-ductile fault network from Ora Banda (Chapter 4 p.86) show consistent offsets of N-S dextral, NE-SW dextral and E-W sinistral.

3.4.4 Kinematic interpretation

Regional folding produced fold structures with a geometry that suggests significant crustal shortening from an ENE-WSW orientation. The folds are the oldest deformation event in the Ora Banda Domain. Subsequent deformation events are shearing and faulting events that resulted in major disruptions to the folded sequence.

Fabrics in the Zuleika Shear Zone range from simple S-C mylonite to finely layered ultramylonite, characterised by grain size reduction and almost total destruction of primary rock fabrics with development of porphyroclastic texture. The fabric of the shear zone indicates predominantly ductile deformation which sets it apart from most other structures observed in the Zuleika area with brittle or brittle-ductile character.

The Zuleika Shear Zone has kinematic indicators with asymmetric geometry and a pronounced shallow stretching lineation in discrete high-strain zones, that indicate left-lateral strike-slip kinematics produced by inhomogeneous non-coaxial shear. Wallrock strain markers such as basalt pillows, breccia clasts in ultramafic rocks and centimetre-sized varioles from pillow margins at Wattlebird and Bullant show flattening strains that suggest part of the deformation was produced by inhomogeneous shortening (pure shear) normal to the plane of the Zuleika Shear Zone.

The two different types of strain indicate that bulk inhomogeneous shortening (Bell 1981) was an important component of the deformation coupled with inhomogeneous simple shear. A difference to the Bell (1981) model is that the Zuleika Shear Zone is a

predominantly NW-SE trending shear zone with a subordinate component of NNW-SSE trending conjugate dextral shear zones (Figure 3.22 p.69, Map 2 p.266). Sharp planar boundaries separate zones with non-coaxial strains from zones with co-axial strains (Figure 3.20f p.65). Boundaries between zones of co-axial deformation and undeformed rock are metre-scale tracts with a sharp change of strain intensity.

Various sets of mesoscopic-scale brittle-ductile faults and quartz veins that cross-cut the regional-scale Zuleika Shear Zone, support the aeromagnetic interpretation of a regional-scale network of late brittle-ductile faults, that cross-cuts both the rock sequences and earlier ductile shear zones. Late brittle-ductile faults also cross-cut the Zuleika Shear Zone to the south at the Broads Dam mine (Glasson *et al*. 1998).

Similar observations were made by Colvine *et al.* (1988) who concluded that deformation in the Ontario district produced a series of discrete tectonic structures of "regional and shield-wide extent". Early structures such as folds and major NNW-SSE trending shear zones at the Golden Mile, Kalgoorlie have also been cross-cut and offset by N-S trending oblique faults (Clout 1988).

Late faults can be grouped into three average orientations representing the strike directions of most structures, yet there is a moderate scatter of structural orientations in each group, and structures developed in a particular strike-group may display opposing dip directions. Cross-cutting relationships between the N-S, NE-SW and E-W groups are not obvious from aeromagnetic imagery since the majority of structures have small displacements of 50m or less, and timing relationships are therefore obtained only from mesoscopic observations.

The faults have varied morphologies that range from groups of small parallel faults making up a main fault zone, to single discrete fractures with or without quartz veins. Northerly trending faults are commonly developed as single discrete brittle-ductile faults with laminated quartz veins (Black Flag Fault / Quarters style), and may have a significant cataclastic component. Northeast-southwesterly and easterly trending faults may be both arrays of discrete fractures with quartz vein infill, and localised brittle-ductile faults. These late faults overprint the Zuleika Shear Zone and therefore represent a later deformation event.

Similar orientations for the resolved axes of maximum shortening for each of the deformation events may indicate a maintained regional crustal shortening from an ENE-WSW direction. Development of structural fabrics from ductile folding, cross-cut by ductile shearing and later brittle-ductile faulting may reflect a change in strain-rate, or alternatively, may be interpreted as progressive deformation during uplift and exhumation of the greenstone pile, with the structural styles recording translocation of the rocks from the lower-middle crust into the upper crustal seismogenic regime (Figure 3.24)

3.5 GOLD MINERALISATION – ZULEIKA SHEAR ZONE

The series of mines along the Zuleika Shear Zone have total gold endowment of 11 tonnes Au. Gold deposits occur in two lithological associations: those hosted by felsic porphyritic rocks and those in basalt.

3.5.1 Porphyry-hosted gold deposits

The main porphyry hosted gold deposits are at the Anthill and Porphyry mines, with other deposits at Hawkins Find, Porphyry West and in small lenticular bodies of felsic porphyry at Wattlebird. Gold mineralisation at the Porphyry mine is in a sheeted network of millimetre-scale fractures now filled with quartz-pyrite +/- chlorite. The veins trend 057°/32°SE on average (Figure 3.7 p.43) with a high vein-density in the economic envelope. Although the average orientation of the veins is NE-SW, there is wide variability in both strike and dip reflecting the complex nature of brittle fracturing and fracture-sealing processes. Silica-albite is the most common alteration assemblage with variable calcite alteration. Gold grades in quartz-pyrite veins are low (1-2ppm), however in areas of high fracture-density, the greater number of veins creates ore-grade zones. Intense ductile shear zones at the edges of the porphyry lenses also are well mineralised.

3.5.2 Basalt-hosted gold deposits

Several gold deposits in the Zuleika Shear Zone are hosted by high-magnesium basalt (eg. Bowerbird, Wattlebird and Bullant mines). The gold envelopes are elongate, trending parallel to the plane of the shear zone with high-grade zones localised in steep shoots that

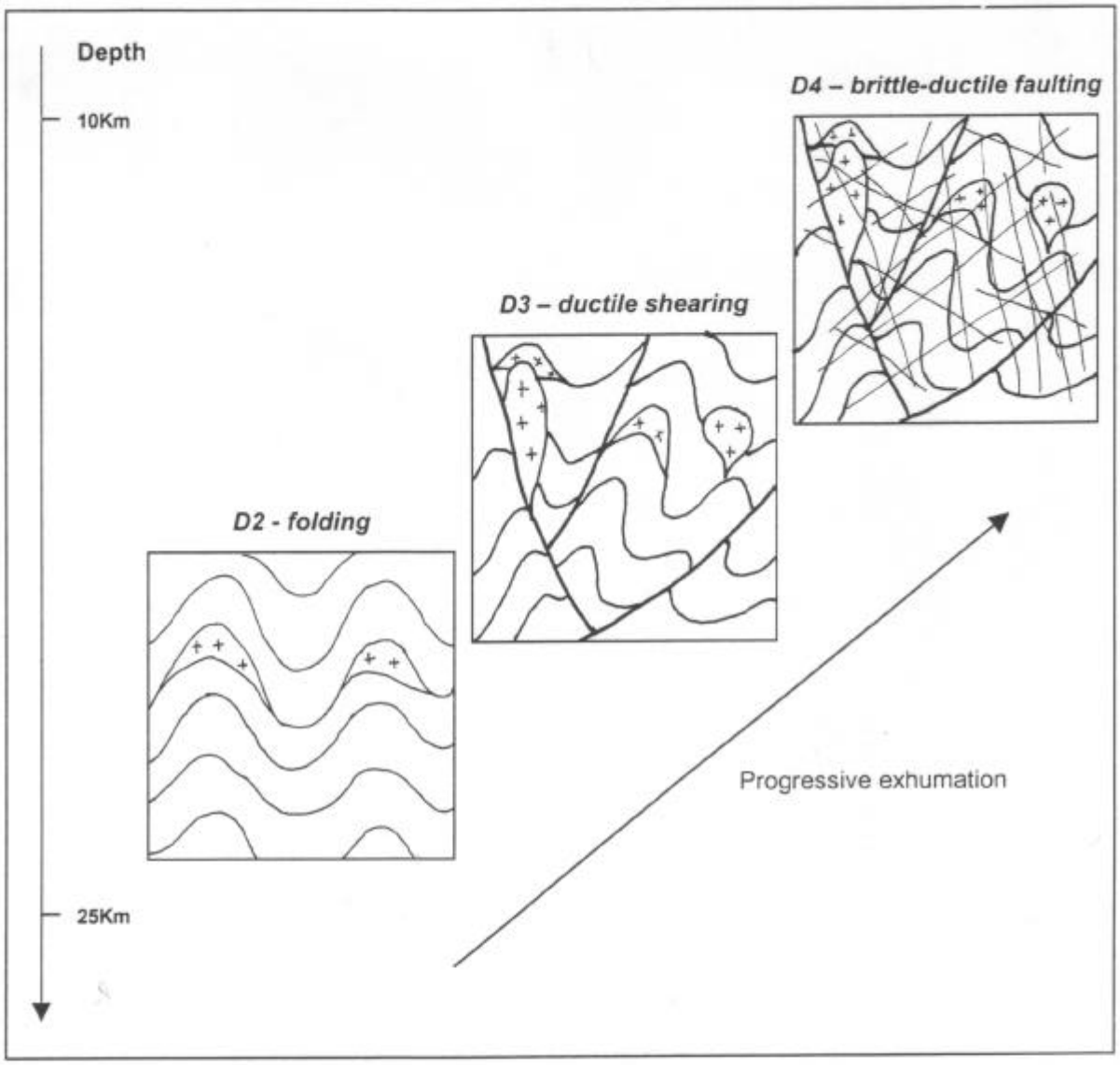

Figure 3.24 – Schematic diagram illustrating the structural development of the Ora Banda and Zuleika districts, during progressive exhumation of the Archaean supracrustal sequence. The three deformation events illustrated have finite strains specific to each episode, but form part of a progressive ENE-WSW regional shortening event.

plunge to the northwest and southeast. High-grade ore shoots occur at the intersection of the Zuleika Shear Zone with brittle-ductile faults in the three principal structural orientations. At Wattlebird, a ≈20m-wide quartz vein array with N-S trend cross-cuts the shear zone, with a high-grade shoot at the juncture of the two structures (Map 5 p.278). Gold grade is distributed away from the intersection point in the planes of both structures. Similar relationships occur at Bullant where a brittle-ductile fault trending 013°/77°E cross-cuts the main Zuleika Shear Zone. A large quartz vein in the plane of the Zuleika Shear Zone at Bullant that contains high-grade gold has associated galena, sphalerite and pyrrhotite with the vein, which is a significantly different mineralogy to the later cross-cutting structures (Figure 3.25h).

A sample of the ore zone at Bullant (sample ZULPIT-1) taken from the high-grade portion of the orebody, contains up to 14 g/T Au (G. Adams personal communication 1998). The sample displays relationships that constrain the timing of deformation, gold mineralisation and metamorphism. In thin section, the rock has a distinct domainal fabric with biotite-calcite rich domains interspersed with quartzofeldspathic (ultramylonite) domains. The mylonitised domains have undergone intense grain-size reduction during dynamic recrystallisation, with strong undulose extinction in equant to elongate quartz grains of 20*m*m average diameter. Very fine-grained ribbon texture is developed in long continuous bands. Biotite-calcite domains are mostly strain-free, have coarser grain-size and appear to overprint the ultramylonite. Pyrite (+/- marcasite) is present as elongate grains that trend parallel to the shear fabric and is assumed to represent the gold mineralisation event. The presence of marcasite indicates low-temperature alteration of the sulphides.

The shear fabric is overprinted by large, randomly oriented sheafs of actinolite that are strain free, cross-cutting both domain-types (Figure 3.25b-d). Actinolite crystals oriented at a high angle to the shear zone have very fine rims of pyrite up to 0.5*m*m thick (Figure 3.25d). The rims appear as coatings of pyrite that pseudomorph actinolite crystals on broken surfaces. Pyrite also occurs in large elongate grains closely associated with calcite, that cross-cut un-oriented actinolite sheafs (Figure 3.25g). These relationships displayed by pyrite indicate that mineralisation began with the ductile shearing, continued during metamorphism, and finally ceased after the peak of metamorphism. The elongate continuous form of the pyrite may indicate that pyrite is replacing pyrrhotite. Some secondary remobilisation of the sulphides is evident in the presence of minor marcasite.

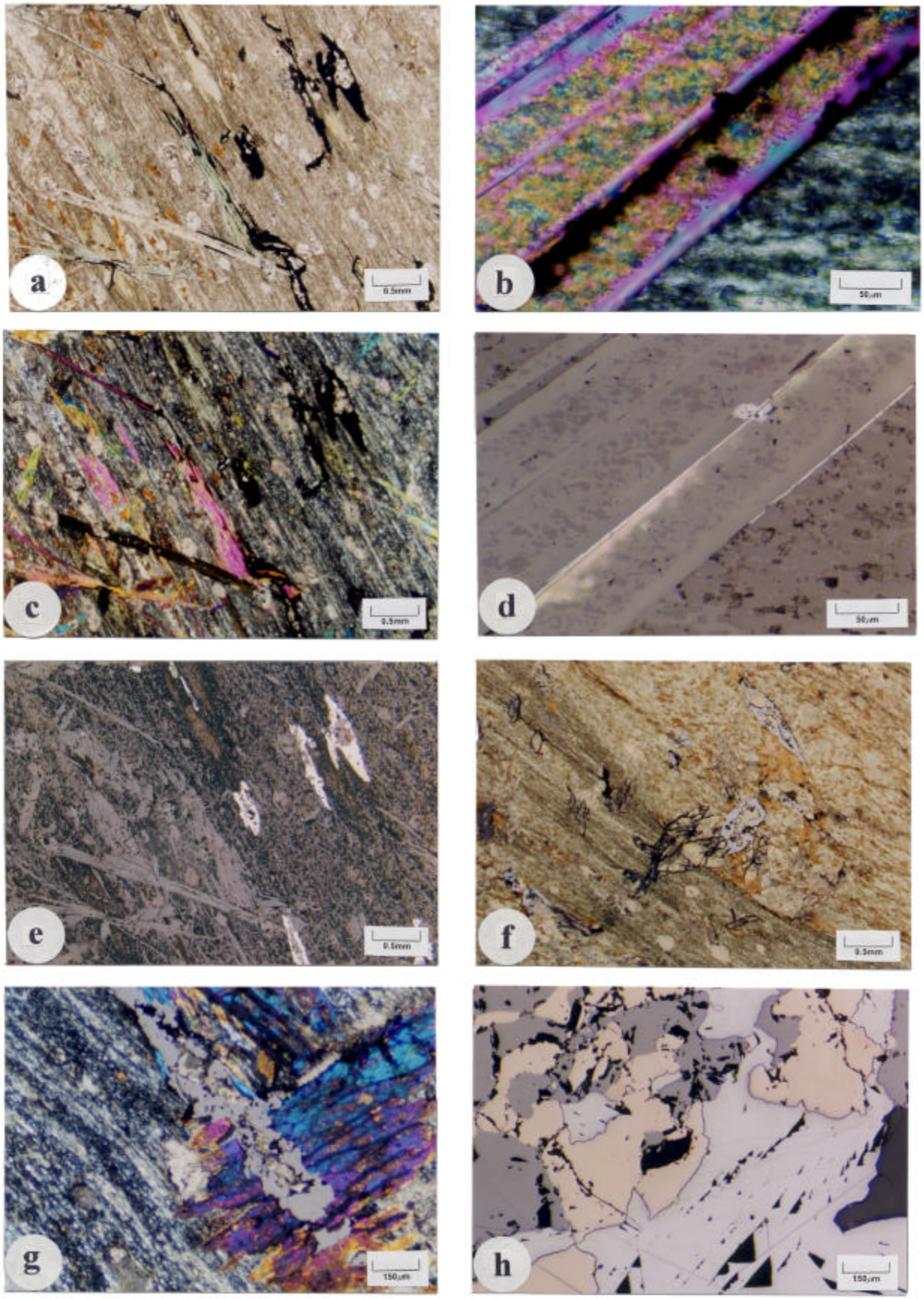

Figure 3.25 – Photomicrographs of mineralised basalt from the Bullant mine. Figures **a), c)** and **e)** are views of the same area - (PPL) in a), (XPL) in c), reflected light in e). **b)** Close up of actinolite overprinting the shear fabric at a high angle. **d)** Reflected light view of b) showing fine pyrite along actinolite margins. **f)** Pyrite overprinting biotite-calcite domains that appear to cross-cut the mylonitic fabric. **g)** Pyrite-calcite overprinting late actinolite, combined reflected and transmitted light (XPL). **h)** Massive sulphides in a mineralised quartz vein. See text and over page for explanation.

Captions for figures on page 77

Figure 3.25a, c, e,
Photomicrographs of the same area of sample ZULPIT1 (**a**-PPL, **c**-XPL, **e**-reflected light) from a high-grade ore zone in the Bullant open-pit. The samples show the relationships between deformation, metamorphism and mineralisation within the Zuleika Shear Zone. In all figures, the NW-SE trending shear fabric is clearly visible, defined by quartzofeldspathic material that has undergone intense grain-size reduction producing a mylonitic fabric. In Figure 3.25e pyrite is formed parallel to the shear zone and in some cases is stretched along it, or is replacing actinolite that is also parallel to the foliation. In Figure 3.25c actinolite is aligned along the foliation but mostly overprinting the shear fabric with random orientation.

These relationships indicate that metamorphism began late in the ductile shearing event but peak metamorphism overprints the D3 shear zone, and crystallisation of actinolite occurred in the absence of a significant stress. Pyrite in this sample is assumed to represent the gold mineralisation event and its form is significantly affected by the shearing indicating that gold mineralisation was synchronous with D3 ductile shearing. Additional evidence that supports this assertion includes the shear zone fabric being defined by hydrothermal biotite in Figure 3.11g and h.

Figure 3.25b, d
The shear zone is shown in close-up with detail of the overprinting relationships between metamorphic actinolite and the shear fabric. Dark isotropic edges of the actinolite in Figure 3.25b are revealed in Figure 3.25d as very fine films of pyrite (0.5*m*m-thick) pseudomorphing the actinolite, which indicates that the gold mineralisation event continued during peak metamorphism. Gold mineralisation also post-dates metamorphism as evinced by **Figure 3.25g** where pyrite overprints the randomly oriented actinolite. In all cases pyrite is closely associated with calcite. Pyrite also overprints biotite-calcite rich domains that appear to overprint the shear zone in **Figure 3.25f**.

Figure 3.25h
Photomicrograph of massive sulphides in a gold-bearing quartz vein from the Bullant mine. The vein is 3.3m wide and contains large inclusions of massive pyrrhotite-sphalerite and galena trending 146°/84°NE. This mineralogy is unusual for gold-bearing veins in the Zuleika Shear Zone, however the vein returned a fire assay value of 2.93 g/T Au. Sample is from 215.7m in diamond drill hole ZULD9.

3.5.3 Structural timing of gold mineralisation

Mineralogical studies by Vaughan (1988), demonstrate that gold is associated with both sulphides and silicates. Gold-related biotite and pyrite defining the Zuleika Shear Zone fabric implies that significant gold mineralisation occurred during movement on the structure. In comparison, the coincidence of significant gold at the intersection of late brittle-ductile faults with the Zuleika Shear Zone suggests a common timing of gold mineralisation and the late fault event. Hence the timing of gold mineralisation is constrained to a period during movement on the regional-scale Zuleika Shear Zone (D3), and continuing into the overprinting late fault event (D4).

3.6 DISCUSSION

Deformation in the Ora Banda Domain was heterogeneous in three distinct episodes represented by regional folding (D2), ductile shearing (D3) and brittle-ductile faulting (D4). This sequence is demonstrable from simple cross-cutting of the major structures visible in aeromagnetic imagery and outcrop. Early low-angle faults with stratigraphic repetition are not observed. Regional-scale upright folds (D2), with NNW-SSE trending axial planes suggest an ENE-WSW directed regional shortening event (Swager *et al.*1990). Ductile shearing (D3), possibly occurred along pre-existing structures that record several phases of movement and were interpreted as ancient extensional-normal-faults active during back-arc basin formation by Swager (1989).

Kinematic indicators in the D3 shear zones show that the last phase of movement was strike-slip with shallow to moderately north-plunging slip/stretch lineations, and left-lateral fabric asymmetry in S-C mylonites. Brittle and brittle-ductile fault structures (D4), in three principal structural orientations were formed synchronously, but post-dating movement on the regional ductile shear zones (D3). This relationship has resulted in four principal structural orientations that are identified at most outcrops in the north Kalgoorlie area. Finite strains indicate a deformation sequence that was ductile in the initial stages, progressing through brittle-ductile to brittle in the final stages of deformation. This sequence may indicate a change in strain-rate, or may be related to progressive uplift towards the final stages of orogenesis.

The heterogeneous distribution of strain in the Zuleika area with strong separation into high strain zones interspersed with relatively undeformed wallrocks, has contributed to the local tectonic fabric, and is analogous to the regional-scale geometry. In detail, the high strain zones have fabrics that suggest development due to bulk shortening at a high angle to the shear zones. This interpretation is significant for the Zuleika Shear Zone and the Kalgoorlie Terrane, since many regional-scale ductile shear zones are therefore implicitly low-displacement zones, with the amount of displacement unrelated to the intensity or thickness of the zones (eg. Walsh and Watterson 1988). With low displacements across major ductile shear zones, the interpretation of juxtaposed high and low strain domains requires revision. A strain gradient between the Coolgardie Domain and the Ora Banda Domain is evident if reference points are chosen well within each domain. However, the presence of a sharp strain gradient at the contact is not observed at Zuleika, which is the interpreted domain boundary between the Ora Banda and Coolgardie Domains (Swager *et al.* 1990). It is possible that the Zuleika Shear Zone is localised along a region of the crust that is both a strain and metamorphic gradient up to several kilometres wide, without the necessity for a sharp line of demarcation (however poor exposure hinders the resolution of the problem).

Although the Zuleika Shear Zone has been interpreted as coincident with a metamorphic isograd (Swager *et al.* 1990; Witt 1991; Witt 1993; Witt *et al*. 1997), data from geological mapping and drillcore logging do not support a significant change of metamorphic grade across the shear zone at Zuleika (Chapter 3 p.33-60, Tables A1.1–1.6 p.261-279). The shear zone was interpreted as a tectonic boundary between lower - middle greenschist facies rocks of the Ora Banda Domain and upper greenschist - lower amphibolite facies rocks of the Coolgardie Domain. The main indicator minerals of the change are biotite and actinolite, but these minerals are observed in exposures and drillholes on both sides of the shear zone. Furthermore, Hunter (1993) reported widespread development of metamorphic biotite in the Kurrawang Conglomerate, 3 km to the east of Zuleika. An alternative location for a metamorphic isograd juxtaposing tectonostratigraphic and metamorphic domains logically should be a shear zone or fault of regional compass, but there are no regional shear zones to the east of the Zuleika Shear Zone until the Bardoc Tectonic Zone (Figure 3.2 p.31). A previously recognised shear zone at the western contact of the Kurrawang formation (Hunter 1993) is interpreted as a significant truncating feature in the seismic image (Figure 3.4 p.36), and is a possible candidate for the metamorphic boundary, with seismic characteristics similar to the Zuleika Shear Zone. Alternatively, it is possible that

the change in metamorphic grade is a gradual one that accompanies a strain gradient with decreasing intensity towards the east.

The kinematic history of the Zuleika Shear Zone is complex, but there is at least one major phase of left-lateral movement. There is no evidence of early dip-slip events, although the fabrics of the shear zone may record only the latest movements. The later period of movement accommodated bulk shortening and was possibly related to oblique convergence during closure of the Kalgoorlie basin.

In a re-interpretation of regional-scale ductile shear zones in the central Norseman-Wiluna belt, Hammond and Nisbet (1992) identified early low-angle extensional shear zones (lags) on granite greenstone contacts. They considered that later shear zones with both vertical and horizontal stretch lineations were syn-regional folding thrust faults and upturned early thrusts, respectively. This model is important for the interpretation of fabric development in NW-SE trending structures like the Zuleika Shear Zone, since an original low-angle top-to-the-north thrust fault would display sinistral kinematics (as observed), when upturned by later E-W shortening. Conversely, most workers document kinematic indicators that lead to a strike-slip interpretation for that part of the deformation history.

The main point of contention is whether or not a regional sinistral wrenching event occurred (eg. Mueller and Harris 1987; Mueller *et al*. 1988), or the now sub-vertical structures were originally formed as basin-controlling normal faults during basin-development (Swager *et al*. 1990), and reactivated as reverse thrusts during subsequent basin closure. The problem is not easily resolved but if the model proposed by Hammond and Nisbet (1992) is correct, then an early (pre-folding) episode of gold mineralisation is implied for gold deposits hosted in regional ductile shear zones with gold-related alteration assemblages defining the shear zone fabric. The timing of gold mineralisation of the Zuleika Shear Zone is therefore dependent on the preferred interpretation, and timing of gold mineralisation becomes a major tool for resolving the tectonic history of the region. Four interpretations of the kinematic history of the Zuleika Shear Zone are possible:

1. *Early within-greenstone D^E extensional shear zone*. For an interpretation of the shear zone as an early within-greenstone D^E extensional (flat-lying) shear zone, an approximately vertical maximum shortening direction is implied, which would have

produced a top-to-the-SSE low angle shear zone (tectonic slide), and when upturned would display (apparent) dextral kinematics. Such an interpretation is inconsistent with observed field relations and strain marker geometry, and is therefore rejected.

2. *Upturned D1 thrust fault*. D1 thrusting was a north-directed shortening event that produced top-to-the-north low angle thrust faults, and resulted in widespread stratigraphic repetition. During the D1 event, the maximum shortening direction was horizontal in a direction which is at 90° to that interpreted from strain markers at Zuleika and therefore this model is also rejected. The apparent sinistral kinematics that would be produced by upturning a D1 thrust fault are however in agreement.

3. *Upturned syn-shortening D2 thrust fault*. An interpretation of the Zuleika Shear Zone as a syn-shortening D2 thrust fault is not plausible, since the observed stretching lineation is sub-horizontal whereas a steep to sub-vertical lineation would be expected. The option of the sub-horizontal stretch lineation overprinting an earlier formed sub-vertical lineation is possible, however there is no evidence of remnant early lineations, and all observed ductile fabrics and strain markers display a sub-horizontal maximum elongation direction. Furthermore, the seismic data show that the Zuleika Shear Zone is not listric at depth, and the contact with the mid crustal décollement is a sharp truncation instead of a smooth ‘soling-out’ against a sub-horizontal discontinuity, as would be expected from syn-shortening thrust faulting.

4. *Sinistral wrench fault*. Wrench tectonic interpretations have been proposed by many authors to explain the regional-scale ductile shear zones in the Eastern Goldfields Province (Swager 1989; Witt 1993b-c; Mueller and Harris 1987; Mueller *et al*. 1988). However, development of the Zuleika Shear Zone in a bulk shortening is preferred over a bulk non-coaxial wrench, since there is a lack of obvious displacement parallel to the shear zone and since there are no synchronous minor structures (Riedel structures, conjugate shears) as predicted for well-studied areas of wrench tectonism (Sylvester 1988; Mandl 1988). Strain fabrics require that the maximum shortening axis was at a high angle to the plane of the shear zone, which supports the interpretation of bulk shortening deformation with flow partitioning of non-coaxial deformation fabrics. Also, an obtuse conjugate system of ductile shear zones (320°/350°) is observed at the mesoscopic scale, interpreted at the regional-scale, and is reported for other areas in the

northern goldfields (eg. Vearncombe 1988a). In addition, the late tectonic fault network has timing and cross-cutting relationships that support a ENE-WSW directed maximum shortening. This relationship obviates the need for a major re-orientation of the stress field between ductile and brittle deformation events, but rather allows for deformation during progressive exhumation of the greenstones (or a period of increased strain rate), with a succession of overprinting structural styles from early ductile to later brittle.

The ductile shearing event as recognised at Zuleika displays cross-cutting relationships with later mesoscopic structures, that require a revised interpretation of the tectonic models applied to explain their development. Application of a model in which the far-field stress system is bulk non-coaxial in nature (wrench tectonics) is not consistent with the mesoscopic detail of structures in the Zuleika area.

The brittle-ductile fault network overprints within-greenstone-belt ductile shear zones (Zuleika Shear Zone) which is a new interpretation of the timing of development of these faults. Previously, the late faults were interpreted as second or third-order splays off 'first order' crustal deformation zones (Clarke *et al*. 1986; Mueller *et al*. 1988; Libby *et al*. 1990), or contemporaneous Riedel shears formed during strike slip deformation (Witt 1993b-c; Mueller and Harris 1987; Mueller *et al*. 1988). In some studies (Swager *et al*. 1990; Simpson *et al*. 1995) the brittle-ductile faults have been relegated to a minor role in the deformation history of the Kalgoorlie Terrane, but they are a prominent expression of strain at the outcrop, and a significant contributor to the regional fabric on aeromagnetic imagery. Problems with the interpretation of late brittle-ductile faults as low order splays off regional ductile shear zones include significant differences in magnitude, structural style and orientation. Furthermore, clear cross-cutting relations indicate that these structures postdate the regional ductile shear zones, and hence cannot have been formed during an event that they overprint.

The interpretation of the late brittle-ductile faults as Riedel structures has enjoyed popular status (Mueller *et al*. 1988; Mueller and Harris 1987; Eisenlohr 1987) but is also problematic considering the temporal evolution of structures as displayed in the original experiments by Riedel (1929) and Tchalenko (1970). Their work showed that a distinct sequence of fractures would develop at various angles to the shear direction, beginning with high-angle fractures progressively rotated to low-angle fractures and approaching sub-

parallelism with the shear direction with increasing displacement (Figure 3.26). To apply this model to the Ora Banda Domain, NW-SE trending regional ductile shear zones should overprint all other high-angle fractures, but this is not observed (see also Hagemann *et al.* 1992). Additionally, the Riedel experiment was applied to upper-crustal brittle deformation, designed to simulate the development of structures in sedimentary successions overlying deep basement faults, hence its applicability to rocks at the brittle-ductile transition is not proven (Vearncombe *et al*. 1989).

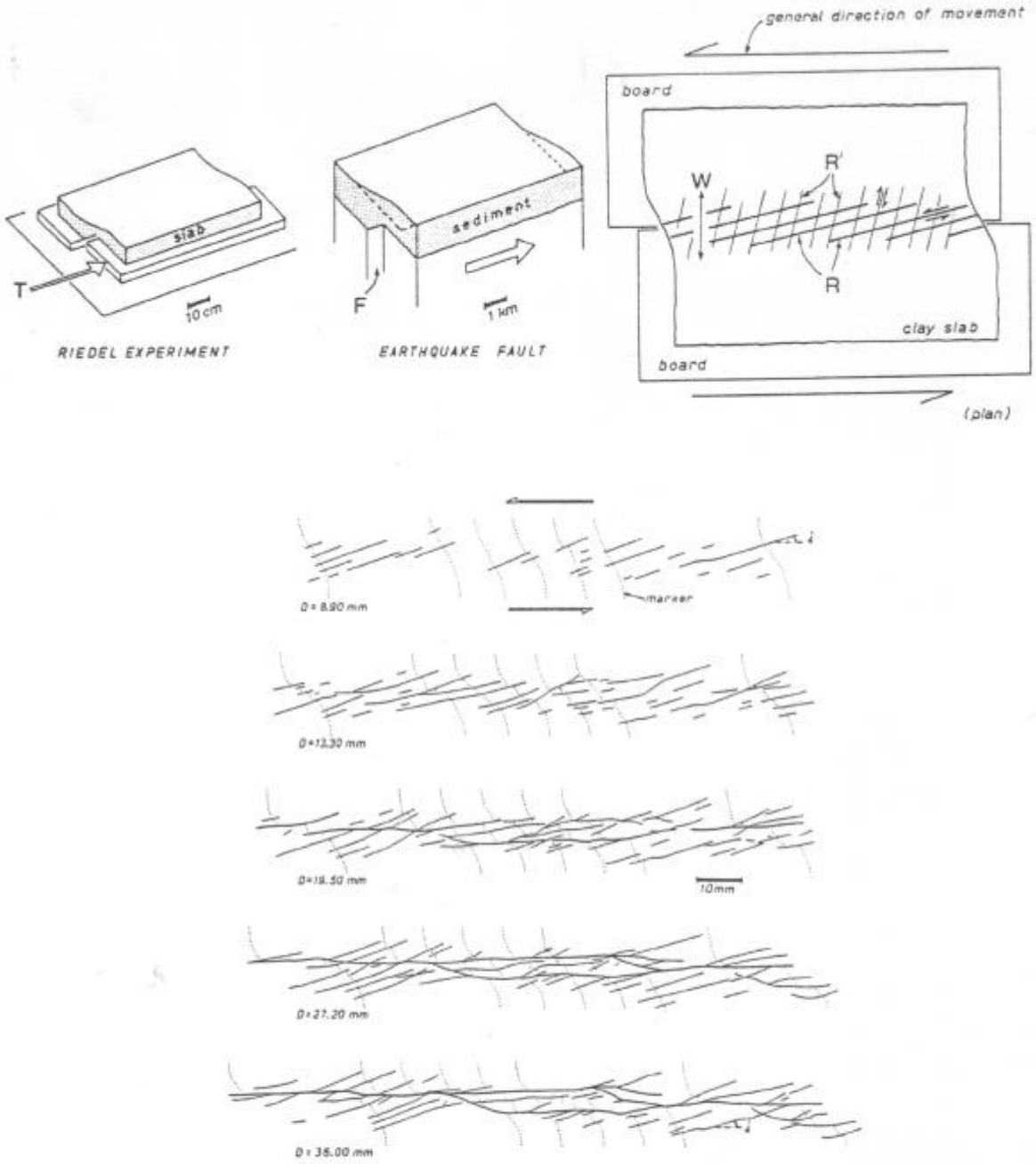

Figure 3.26 – Riedel experiment showing clay slab over movable boards to simulate a shear couple, and high angle fractures produced with the beginning of simple shear. The series of diagrams record the sequential development of fractures in clay produced with increasing displacement across the boards. High angle fractures form first followed by progressively shallower angles approaching parallelism with the direction of simple shear at maximum displacement. All diagrams reproduced from Tchalenko (1970).

4 ORA BANDA STRUCTURAL ZONE

4.1 INTRODUCTION

At a regional-scale, the brittle-ductile fault network (Chapter 3.3.3 p.53) is composed of sub-domains of faults, which intersect to form localised zones of high fracture-density. The zones have uniform relationships between sets of faults with different average orientations, and are therefore interpreted as structural zones. The term ‘structural zone’ is used to indicate that the areas are not simply chance intersections of randomly developed faults, but are considered to contain brittle-ductile faults that are related in space, time, origin and structural style.

The Ora Banda structural zone is discussed in detail in this chapter to document the D4 brittle-ductile fault network at a macroscopic scale. A group of faults intersect in the Ora Banda district and collectively form the ‘structural zone’. Geological relationships including structural style, geometry, structural orientation and cross-cutting relationships are assessed for the group of faults to test similarities, and to characterise the brittle-ductile fault network at a macroscopic scale.

The Ora Banda structural zone is a macroscopic zone of high-density faulting and shearing relative to adjacent areas (Figure 4.1). Strain distribution is heterogeneous, reflected by narrow, tabular high-strain zones (brittle-ductile faults) separating lithons of essentially undeformed rock. Faults and shear zones cross-cut the stratigraphic sequence and are also localised along rock-unit contacts especially interflow sedimentary rocks.

Two other structural zones at Grants Patch and Mount Pleasant are also coincident with gold mining centres, hence better exposure is available in these areas with well-developed fracturing. Local lithological factors control the spacing, size and geometry of the structural zones and some rock types appear particularly more sensitive to brittle-ductile deformation than others (eg. mafic versus ultramafic rocks).

Several major brittle-ductile faults make up the Ora Banda structural zone, including the Enterprise fault zone, the Gimlet South and Sleeping Beauty Faults (Harrison *et al.* 1990; Laing 1994; Bogacz 1995) and the Slippery Gimlet fault, which have good

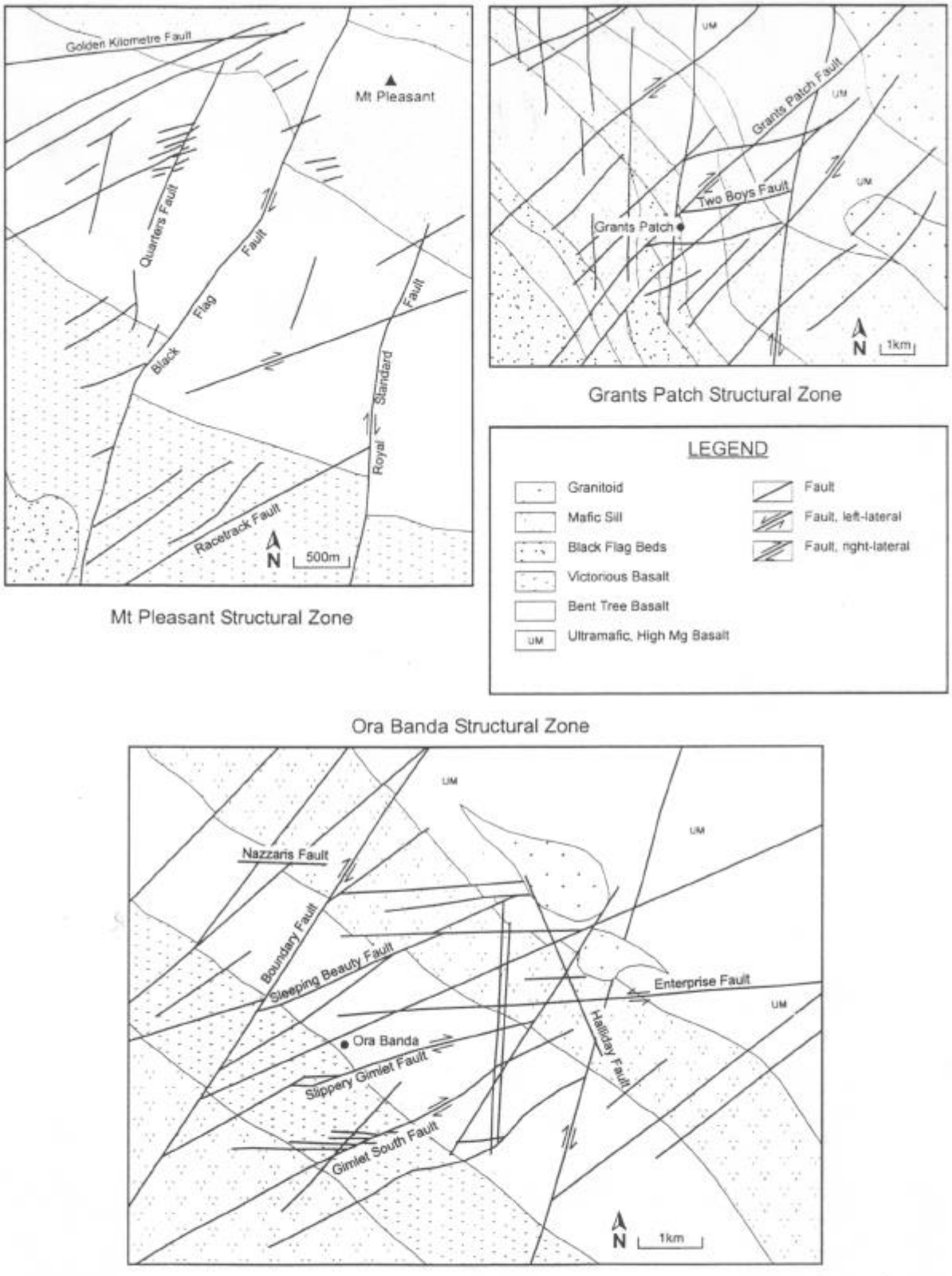

Figure 4.1 – Geological maps of structural zones at Mount Pleasant, Grants Patch and Ora Banda. The structural zones are localised zones of high fracture-density with respect to surrounding areas and contain brittle-ductile faults in similar orientations. Faults are interpreted from aeromagnetic and groundmagnetic imagery.

examples of mesoscopic structural elements developed in dolerite and basalt. Depth extensions at Nazzaris and Boundary are only recent discoveries and are at the initial stages of mine development. Bedding-parallel ductile shear zones, rarely host large gold deposits in the area and exposures are limited to chance drillhole intersections or open-pit exposures. Of these the Black shale shear zone, Cashmans Shear Zone and Enterprise-east shear zone are discussed in detail.

4.2 STRUCTURAL STYLES

Deformation in the Ora Banda structural zone is manifest in a variety of structural styles that range from ductile to brittle. The distribution of each is heterogeneous and most examples of deformed rocks exhibit a variety of fabrics. The following discussion focuses on examples of structural styles and their litho-stratigraphic relations. Fault rocks are grouped according to the classification of Passchier and Trouw (1996).

4.2.1 Brittle faults

Brittle faults occur as tabular breccia zones, cataclasite zones, discrete planar fault surfaces or wide rhomb shaped breccia ‘jogs’ in the dilatant parts of brittle-ductile shear zones. All brittle faults are cohesive types (Passchier and Trouw 1996) including breccia (c.f. Sibson 1977), with hydrothermal precipitates forming a matrix to the clasts. They have foliated and non-foliated fabrics, but most brittle structures fall into the non-foliated category. Non-foliated brittle faults are genetically related to movement on nearby shear zones, and form slip-transfer jogs where fault movement is accommodated by lateral transfer to a parallel fault or shear zone. In such transfer-jogs, dilation and brecciation was along pre-existing fractures with subsequent infill by vein material.

Brittle faults are developed primarily in basalt flows of the Grants Patch Group, which appear to fail by fracture more easily than the coarser grained intrusive dolerite/gabbro sills, that are commonly schistose. Contacts between fine-grained and coarse-grained rocks may control changes in the deformation style of high-angle faults that transect the contacts. Brittle fault textures in the Ora Banda structural zone can be grouped as; breccia, cataclasite, discrete fault planes and veins. Breccias are characterised by jigsaw textures without major comminution and rounding of the clasts.

Jigsaw breccia typically has a significant component of hydrothermal precipitates forming veins or infill matrices to large angular clasts (Figure 4.2a). The breccia zones are non-foliated tabular structures with dimensions in the order of several metres or tens of metres. Jigsaw breccia is developed at the margins of fault zones with random fabrics, closely associated with mesofracture arrays in the wallrocks. The development of jigsaw fabrics with inter-clast voids infilled by hydrothermal vein material may indicate a textural progression from incipient fracture propagation, to jigsaw breccia and finally random fragmental breccia/cataclasite towards the centre of a fault (Figures 4.2b and d). Mesofracture arrays are coincident with hydrothermal alteration of the wallrocks suggesting increased permeability facilitated by an interlinked network of fractures.

Cataclasites (Engelder 1974; Higgins 1971) are usually greater than 0.1m-wide, whereas some may be much less than 0.1m-wide (cataclasite seams). The cataclasite is characterised by 50-90% wear-abraded and rounded clasts in a weakly deformed matrix of hydrothermal precipitates. Cataclastic textures include poorly sorted conglomerate with sub-rounded to rounded fragments of quartz/carbonate veins, mafic host rocks, and variously mineralised and altered rock fragments (Figure 4.2b). Fine grained matrix materials of similar composition to the clasts are cemented in quartz and calcite and contain a variety of textures exhibited by alteration and sulphide minerals from early fracture and brecciation to post deformation infill. The zones display a greater degree of textural maturity than jigsaw breccia, with several generations of fracturing and fragmentation recorded in the clasts. Faults at Gimlet South mine contain re-brecciated breccia, and have clasts of altered basalt with parallel fractures infilled by quartz-sulphide veins (Figure 4.15c, p.114). The clasts are interspersed with fragments of re-cemented cataclasite matrices from several generations of fault movement. Such textures indicate a repetitive history of brecciation and cataclasis with subsequent healing by hydrothermal precipitates. The degree of textural maturity is displayed in the roundness of clasts and matrix/clast relationships.

Cataclasite zones usually do not have sharp boundaries but may grade into fractured wallrock adjacent to the fault. Non-foliated cataclasite typically has a higher proportion of hydrothermal precipitates than foliated types, and is probably produced by fluid assisted processes including overpressuring and wallrock implosion during fault movements. Textures indicate that the initial stages of faulting involved dilation along a series of

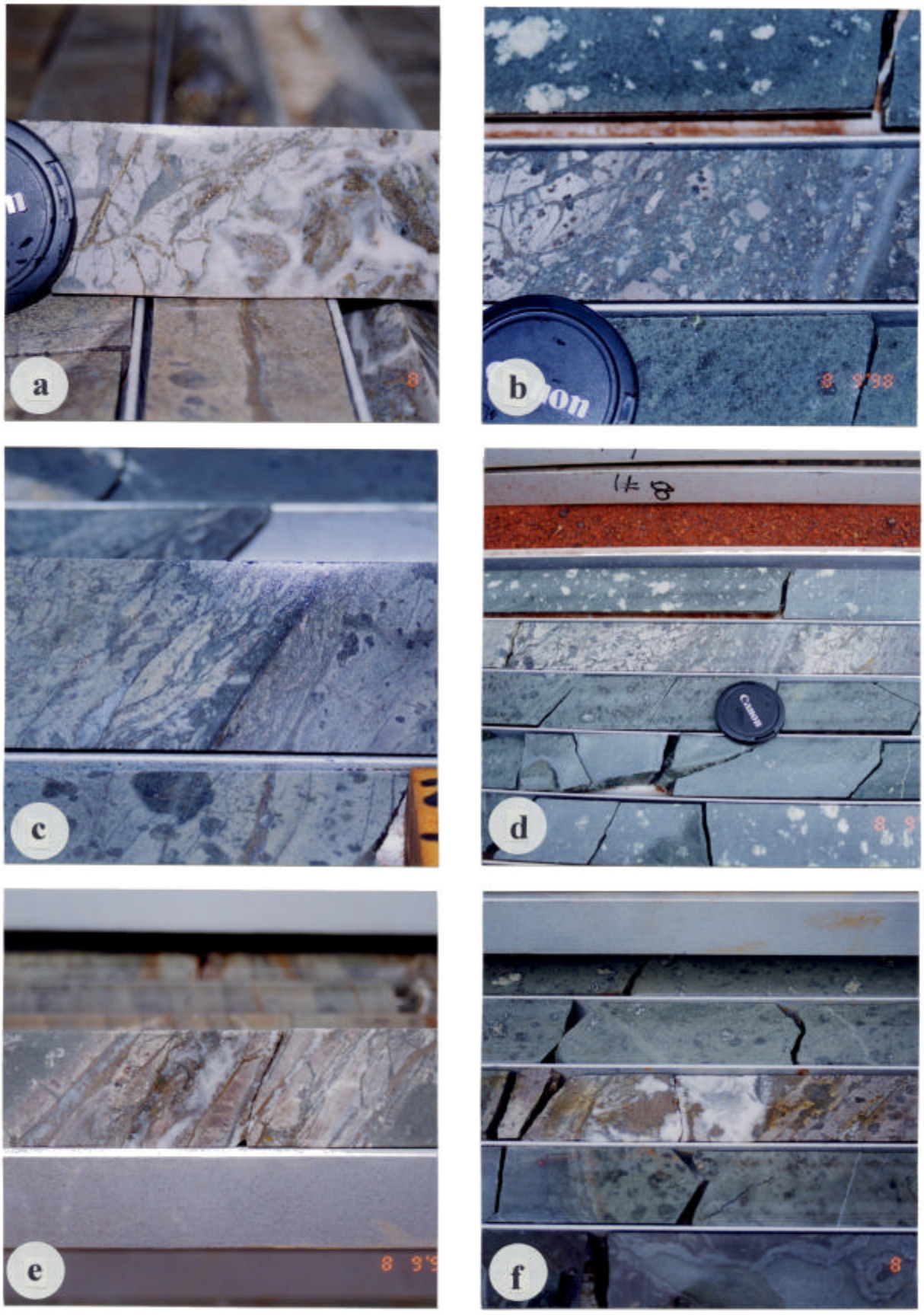

Figure 4.2 - a) Coarse-grained fragmental breccia zone from Slippery Gimlet. **b)** Cataclasite in the centre of a breccia zone, Slippery Gimlet. **c)** Ductile shear fabric at the margin of a breccia zone, Slippery Gimlet. **d)** Breccia zone in porphyritic basalt, Slippery Gimlet. **e)** Breccia zone with hydrothermal vein infill, Slippery Gimlet. **f)** Quartz-calcite vein with massive pyrrhotite, Slippery Gimlet. See text and over-page for explanation.

Captions for figures on Page 90

Figure 4.2a
Coarse-grained fragmental breccia zone from Slippery Gimlet. The zone is developed in grey muscovite-carbonate altered Victorious Basalt. Mesofracture arrays are visible in the wallrock of the zone with two orientations. The larger fractures trending parallel to the wall of the zone cross-cut an earlier fracture set trending top left to bottom right. Pyrite forms veins in the fractures, and fragments of wallrock with pyrite veins are clasts in the breccia, hence the timing of brecciation was later than fracture propagation in the wallrock. The clasts are sub-angular to rounded indicating rotation and moderate wear-abrasion. White quartz and calcite cement the breccia clasts. The breccia zone is at 222.00m in GIMD16, downhole direction is to the right. Lens cap is 55mm diameter.

Figure 4.2b
Cataclasite in the centre of a breccia zone from Slippery Gimlet. The photo is a close-up view of the breccia zone in 4.2d. Clasts comprise highly fragmented altered-basalt with a gradation of clast dimensions from <1mm to >20mm. The range of clast sizes contrasts with figure 4.2a where most clasts are up to several centimetres diameter. Clast size is distributed unevenly, decreasing towards the area of the zone marked by thin quartz veins. The quartz veins have diffuse boundaries, and with pyrrhotite and calcite appear to cement the breccia clasts. Clast morphology is mostly angular and may indicate dominance of fluid assisted brecciation over cataclasis and abrasion. The breccia zone is at 166.70m in diamond drillhole GIMD28, downhole direction is to the right. Lens cap is 55mm diameter.

Figures 4.2c
Ductile shear fabric at the edge of a breccia zone from Slippery Gimlet. Ductile deformation is evident from stretched plagioclase phenocrysts in the fine-grained basalt matrix, and from lens shaped pods of basalt separated by thin cleavage seams of chlorite and pyrrhotite. A thin cataclasite seam forms a sharp boundary with less altered basalt to the right, sub-parallel to the cleavage seams. Pyrrhotite forms veins along cleavage seams and grains disseminated throughout the rock. The shear zone oriented 043°/69°NW, is at 237.50m in diamond drillhole GIMD10. Downhole direction is to the right, base of photo is 112mm.

Figures 4.2d
Breccia zone in porphyritic basalt from Slippery Gimlet. The zone is 0.32m wide with intense muscovite-carbonate-pyrrhotite alteration in the vicinity of the structure, which grades sharply into carbonate-chlorite altered basalt in the wallrocks. Fractures in the wallrock of the fault with pyrrhotite-chlorite filled fractures at low angle to core axis, cross-cut high angle fractures. The two fracture sets are visible on both sides of the fault with constant orientation. Fracture propagation predates breccia with the pre-existing fractures forming planes of breakage during brecciation. Sample details as for figure 4.2b.

Figure 4.2e
Breccia zone in porphyritic basalt from Slippery Gimlet. Brecciation is characterised by thin slices of wallrock infilled by hydrothermal vein material. The slices have broken along fractures oriented parallel to the zone. Quartz-pyrrhotite infills previously fractured basalt with pyrrhotite veins in thin fractures. The breccia zone is at 298.00m in diamond drillhole GIMD22. Base of photo is 220mm.

Figure 4.2f
Quartz-calcite vein with massive pyrrhotite from Slippery Gimlet. The vein infills a weakly deformed zone with minor fracturing of the wallrock parallel to the vein. A large patch of pyrrhotite infills a void in the quartz-calcite vein. Few wallrock breccia fragments are present. Vein is at 253.50m in diamond drillhole GIMD22. Base of photo is 310mm.

fractures and parallel slices of wallrock in weakly deformed zones of breccia with vein infill (Figure 4.2e p.90). Subsequent dilation and brecciation produced jigsaw textures, with later significant differential displacement that resulted in cataclasis and milling of the wallrock fragments.

Cataclasite seams occur as thin restricted zones from 0.01-0.1m thick, or as fine sub-millimetre-scale seams. Most seams of cataclasite contain fragments of altered and mineralised rock. Cataclasite seams may occur in swarms defining a penetrative planar fabric or as individual zones either at the margins of large planar quartz veins or in the centre of brittle-ductile faults. The morphology of cataclasite seams is usually very fine-grained to microscopic gouge composed of sulphides (pyrrhotite and pyrite) and wallrock/vein fragments forming <1mm wide bands. Cataclasite seams are located in the centre of breccia zones (Figure 4.2b p.90), and thin bands of fine-grained fragmented sulphides and chlorite cross-cut angular breccia (Figure 4.3d). Cataclasite is also a common clast constituent in breccia zones indicating that in some examples cataclasis may be a precursor to later brecciation. The cataclasite appears to have formed channel ways for overpressurised hydrothermal fluids with subsequent implosion brecciation of the wallrocks, and there is evidence of cataclasite seams overprinting both coarse breccia zones (Figure 4.3d) and ductile shear fabrics (Figure 4.2c p.90).

Discrete fault surfaces are planar discontinuities that are usually less than 5mm wide. Slickenfibre growths, mineral lineations and stepping slickensides are characteristic of the faults, and permit determination of offset. Slickenfibres are composed of chlorite and calcite usually but may also contain quartz-carbonate veins. Cataclasite seams also form discrete fault surfaces with slickenfibre lineations of fine-grained gouge material.

Veins are relatively uncommon brittle textures in basalt hosted structural zones. The veins are usually simple fracture-fill types with thick bands of quartz or calcite/ankerite and minor amounts of pyrite, pyrrhotite, sphalerite, galena, tourmaline, chlorite, biotite, epidote and muscovite. Some veins show evidence of offset across the margins and, where movement has occurred, the vein margins have shallow-plunging slip lineations on stepping slickenfibres and variable deformation. Whereas veins are a subordinate deformation fabric, they occur in arrays or vein systems related to fault movements and are generally located in less deformed wallrocks.

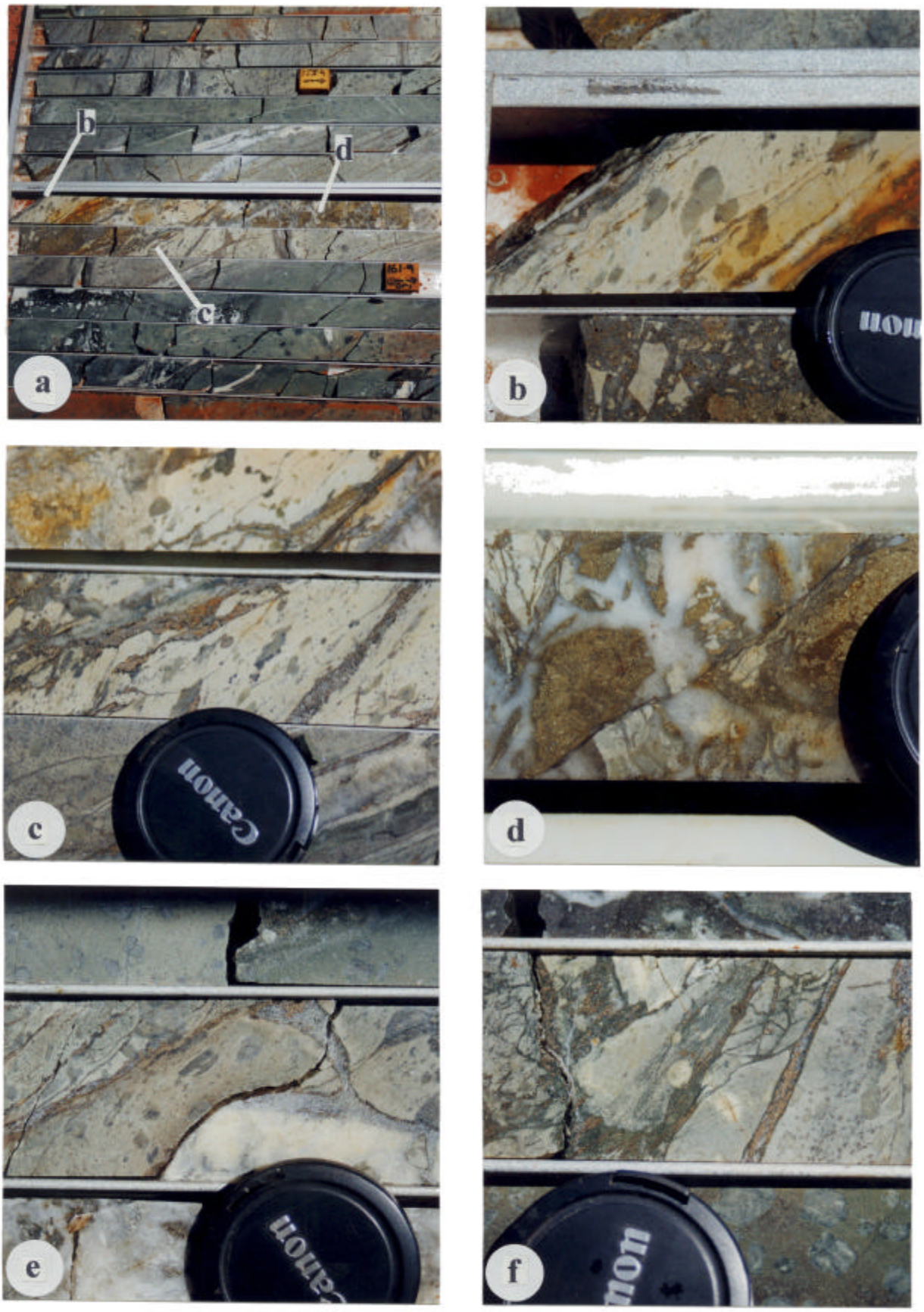

Figure 4.3 - a) Brittle-ductile fault zone, Slippery Gimlet. **b)** Ductile shear fabric at the edge of breccia zone, Slippery Gimlet. **c)** Ductile shear fabric from the edge of breccia zone, Slippery Gimlet. **d)** Central breccia zone crosscut by cataclasite seam, Slippery Gimlet. **e)** Ductile shear fabric in Victorious Basalt, Slippery Gimlet. **f)** Discrete ductile shear band in Victorious Basalt, Slippery Gimlet. See text and over-page for explanation.

Captions for figures on Page 93

Figure 4.3a
Brittle-ductile fault zone from Slippery Gimlet. The fault zone is 4m wide marked by light-grey coloured muscovite-carbonate alteration that grades into distal chlorite-carbonate alteration in porphyritic basalt. Ductile deformation manifest as aligned and stretched plagioclase phenocrysts (4.3b and c) is overprinted by brittle fault breccia and cataclasite (4.3d). Brittle fracture arrays at a shallow angle to the ductile shear fabrics extend into the wallrock of the zone. The brittle fractures cross-cut ductile fabric in 4.3b, c, e and f. This relationship was observed in many fault zones with ductile shearing usually located at the edges of fault zones implying brittle reactivation along pre-existing planes of weakness. Fragmental breccia forms the central part of the zone. The fault zone is at 159.30-160.60 in diamond drillhole GIMD29. Downhole direction is to the right, core block is 50mm wide.

Figure 4.3b
Ductile shear fabric from the area marked “b” in 4.3a. The fabric trending top to bottom is defined by aligned and stretched (flattened) plagioclase phenocrysts without development of fissile schistosity or cleavage. Quartz-calcite-pyrrhotite filled fractures oriented top-right to bottom-left overprint the ductile fabric. The ductile shear fabric trending 080°/85°S is at 159.30m in diamond drillhole GIMD29. Lens cap is 55mm diameter.

Figure 4.3c
Ductile shear fabric from the area marked “c” in 4.3a. The fabric is the same as in 4.3b and both are probably part of a pre-existing shear zone. Brittle fractures with quartz-calcite-pyrrhotite, +/- tourmaline cross-cut the ductile fabric. In contrast to 4.3b the ductile shear zone trends 086°/78°N suggesting either a small component of rotation across the fault zone or non-uniform extension during brecciation. The ductile shear fabric is at 160.60m in diamond drillhole GIMD29. Lens cap is 55mm diameter.

Figure 4.3d
Central breccia component of the fault zone marked “d” in 4.3a. Coarse clasts of fractured wallrock, massive pyrite/pyrrhotite and pre-existing breccia are cemented by hydrothermal quartz-calcite vein material. The breccia comprises angular and sub-rounded fragments of fractured/brecciated altered basalt and mineralised material indicating multiple episodes of faulting and mineralisation. A thin cataclasite seam traverses the specimen from top right to bottom left and cross-cuts the breccia fragments. Specimen is at 159.70m in diamond drillhole GIMD29. Lens cap at right of photo for scale.

Figure 4.3e
Ductile shear fabric in Victorious Basalt from Slippery Gimlet. The fabric is defined by aligned flattened phenocrysts of plagioclase with a weak planar anisotropy developed. Late white quartz with irregular morphology overprints the ductile fabric, and pyrite-pyrrhotite mineralisation is localised along thin quartz-calcite veins that also overprint the ductile shearing. The shear fabric trends 120°/84°SW at 266.80m in diamond drillhole GIMD31. Lens cap is 55mm diameter.

Figure 4.3f
Discrete ductile shear band in Victorious Basalt from Slippery Gimlet. A 5-10mm band of ductile deformation is defined by flattened plagioclase phenocrysts interspersed within a planar fabric of aligned and stretched chlorite slivers and thin flattened grains of pyrrhotite. The ductile fabric appears to overprint a small zone of fracturing to the right however some chloritic fractures cross-cut the ductile shear zone. A quartz-calcite-chlorite-pyrrhotite vein is parallel to the ductile shear zone. Pyrrhotite mineralisation occurs in veins, fractures and as part of the ductile fabric. The ductile shear band trends 092°/58°N in diamond drillhole GIMD9 at 244.65m. Lens cap is 55mm diameter.

4.2.2 Brittle-ductile faults

Brittle-ductile faults in the Ora Banda district have either mostly ductile or mostly brittle character with a subordinate component of the other. These relationships are expressed as ductile shear fabrics and schistosity cut by sub-parallel cataclasite seams (Figure 4.2c p.90) or conversely, thick breccia zones with thin ductile shear bands at the margins or centre of the breccia bodies (Figure 4.3 p.93). Shear veins are common brittle-ductile features with variably deformed quartz veins in schistose shear zones. In each case the subordinate component is an integral part of the structure, which suggests reactivation of these structures under different conditions to when the original fabric developed.

4.2.3 Ductile shear zones

A series of ductile shear zones is present in the Ora Banda structural zone developed both within and cross-cutting incompetent rocktypes such as interflow sedimentary rocks and ultramafic units. Type I S-C mylonite (Lister and Snoke 1984) is commonly developed in units with a pre-existing planar fabric or mineral composition dominated by weak minerals or phyllosilicates. S-C foliations are common in medium-grained doleritic sills but generally absent in ductile fabrics from basalt flow rocks where flattening strains dominate. The mylonite zones are discrete planar structures developed over several metres width and up to tens of kilometres long whereas ductile fabrics in basalt flows are usually restricted to zones of less than one metre width and tens of metres long. The localisation of ductile shear zones within interflow sedimentary rocks may be a factor of competence contrast as outlined by Robert *et al.* (1994), and a result of enforced shearing where strain is localised in the weaker rocks. Four of the ductile shear zones in the Ora Banda district (Black shale shear zone, Enterprise-east shear zone, Cashmans Shear Zone and Ora Banda shear zone), are discussed in Chapter 4.4 (p.99).

4.2.4 Schistosity and cleavage

Ductile deformation is accompanied by schistosity and cleavage development with heterogeneous distribution similar to high strain shear zones. The zones of foliation vary from spaced cleavage defined by thin seams of metamorphic chlorite and/or biotite less than 1mm wide, to continuous cleavage and schistosity defined by metamorphic chlorite, biotite

or muscovite penetrative over several metres. Ductile shear zones are spatially associated with zones of schistosity where the schistose zones may represent zones of preferential weakness and strain partitioning.

Schistosity and cleavage are localised primarily in doleritic parts of intrusive sills and are developed in massive basalt only at the boundaries of major shear zones. Intrusive sills have zones of cleavage and schistosity both parallel to, and overprinted by, later brittle-ductile faults and quartz veins. These relationships indicate a complex series of events that involved alternating brittle and ductile conditions with reactivation and localisation of brittle features along pre-existing ductile structures (eg. quartz veins emplaced parallel to zones of schistosity).

4.2.5 Discussion

Shear zones were classified as brittle, brittle-ductile or ductile by Ramsay (1980a), whereas Passchier and Trouw (1996) recognised only a two-fold subdivision into brittle zones (or faults), and ductile zones. The subdivision of Passchier and Trouw (1996) is based on the unique deformation processes that produce either totally brittle or totally ductile fabrics and is useful because it recognised that when exposed to stress, rock materials either flow or fail under given conditions.

In the classification of Ramsay (1980a), brittle shear zones have a clear discontinuity with unstrained or brecciated wallrocks whereas brittle-ductile shear zones have some ductile deformation in the walls of a discontinuity, and ductile shear zones have deformation and differential displacement but no visible discontinuities. He also recognised the possibility that in brittle-ductile shear zones the respective brittle and ductile parts of the deformation history may not be synchronous and that a critical limit to coherent flow may be reached after which brittle deformation proceeds. The reverse order of deformation is also possible where brittle deformation is overprinted by ductile flow. Brittle-ductile textures are therefore composite fabrics that combine elements of totally brittle and totally ductile deformation. The fabrics are characteristic of deformation at the brittle-ductile transition, an environment where brittle deformation processes and ductile deformation processes operate alternately but not synchronously, without large gaps in time, producing fabrics that show evidence of both kinds of deformation.

Since the transition between brittle and ductile deformation depends on many factors including strain rate, temperature, pressure, grain size, lithotype, fluid-pressure, pre-existing anisotropy and ambient stress conditions, the transitional environment can occur in a number of geological settings depending on conditions of deformation. This relationship means that the environment of brittle-ductile deformation is dependent on more than simply depth in the crust, hence a competent rock type that deforms in brittle fashion may be juxtaposed with a relatively incompetent rock type that flows under the same conditions. The presence of both brittle and ductile fabrics in the same lithotype where overprinting occurs in the same structure may indicate alternating conditions of deformation under a consistent prevailing stress field.

Brittle faults in the Ora Banda structural zone are developed in areas where pre-existing mesofracture arrays impart anisotropy to the rock from the intersection of two or more consistently oriented fracture sets (Figure 4.2 p.90). This process is analogous to tectonic comminution (Jebrak 1997), which includes the two processes of fracture propagation and wear abrasion (Figure 4.4). Fractures at Slippery Gimlet mine are commonly filled with pyrite or pyrrhotite with minor amounts of quartz-calcite and tourmaline with traces of sphalerite and arsenopyrite. Muscovite-calcite alteration and pyrite-pyrrhotite mineralisation in the wallrocks of the faults, show clear timing relationships between fracturing and brecciation, where breccia zones contain angular and rounded fragments of the fractured, mineralised wallrock. The jigsaw breccia / mill breccia distinction depends on the dominant clast type and the level of wear and abrasion. In the Ora Banda district, a full transition of clast morphology exists from angular blocks in jigsaw patterns with only minor infill components to poorly sorted breccia with rounded clasts and a higher matrix to clast ratio.

4.3 GEOMETRY OF THE ORA BANDA STRUCTURAL ZONE

Ora Banda structural zone has dimensions of about 6 km x 8 km, centered on Ora Banda (Figure 4.1 p.87). Felsic-intermediate sedimentary rocks to the southwest and ultramafic rocks to the northeast, flank the Ora Banda stratigraphic sequence of basalt flows and intrusive mafic sills. The structural zone is defined mostly within the mafic sequence on aeromagnetic imagery and in open-pit mines. The lower degree of brittle deformation

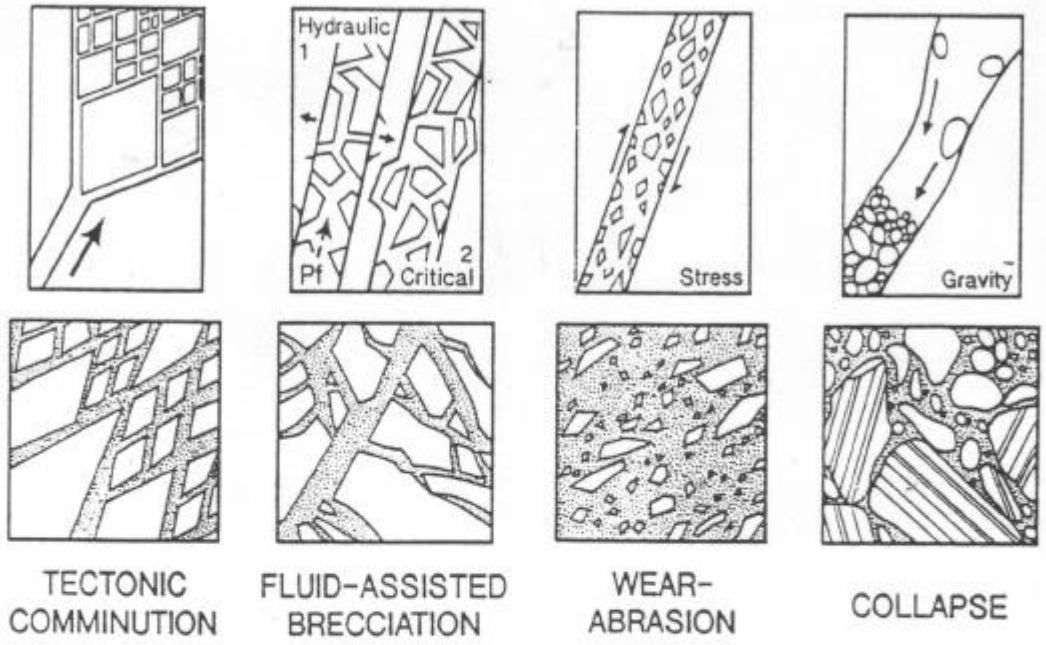

Figure 4.4 – Diagrams showing typical textures developed by various brecciation processes, modified from Jebrak (1997).

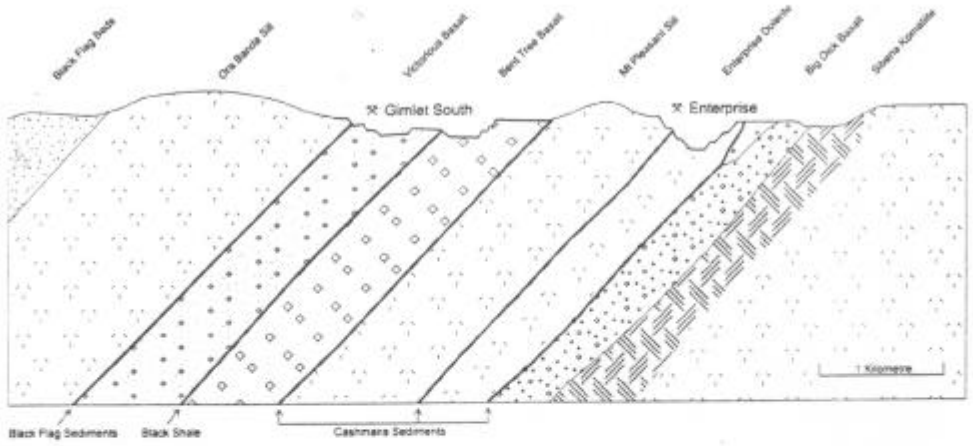

Figure 4.5 – Schematic geological cross-section through the Ora Banda structural zone

beyond the bounds of the mafic sequence may be an artifact of a lack of gold deposits in less chemically-favourable host units, and therefore fewer outcrops of critical structures always present with gold occurrences. However, remote sensing data suggest a higher density of fracturing in the mafic sequence that is diminished to the east and west. A series of brittle-ductile faults interpreted from ground magnetic imagery (Figure 4.1 p.87), extends into less competent rock types on both sides of the mafic package, but the density of faulting in these outer units appears markedly less than within the Ora Banda mafic sequence.

A schematic cross-section through the mafic sequence (Figure 4.5 p.98) shows moderately southwest dipping layers forming the limb of the Kurrawang Syncline. It is probable that the zone of high fracture-density represented at the surface as the structural zone, plunges parallel with the more brittle rocks in the layered sequence giving a pipe-like geometry to the structural zone with depth. Apparent fault offsets are determined from lateral breaks in the magnetic layers and fault slip lineations in most areas have shallow to moderate plunges indicating that much of the movement was strike-slip with subordinate oblique-slip components. Most brittle-ductile faults have offsets of less than 50m which is negligible at the scale of the map (Figure 4.1 p.87) and cross-section (Figure 4.5 p.98). A prominent feature of the Ora Banda structural zone is the array of parallel faults trending about 060° that are steeply dipping to sub-vertical with anastomosing geometry. Zones of schistosity and cleavage tend to be sub-parallel to most brittle-ductile faults and are present in restricted zones within the mafic sills. Poor distinction in magnetic imagery may be due to magnetite destruction in high strain shear zones. Several ductile shear zones trending NE-SW and NW-SE traverse the length of the structural zone and these can be traced in outcrop and drilling several tens of kilometres along strike.

4.4 Significant structures within the Ora Banda structural zone

4.4.1 Gimlet fault array (D4)

A series of five parallel faults locally known as the ‘Gimlet lodes’, dominates the structure of the Ora Banda district. These include the North Sandalwood, Gimlet South, Slippery Gimlet, Tom Allen and Sleeping Beauty faults (Figure 4.6). The faults are spaced at intervals of 500-800m trending ENE-WSW. Minor differences of size and structural

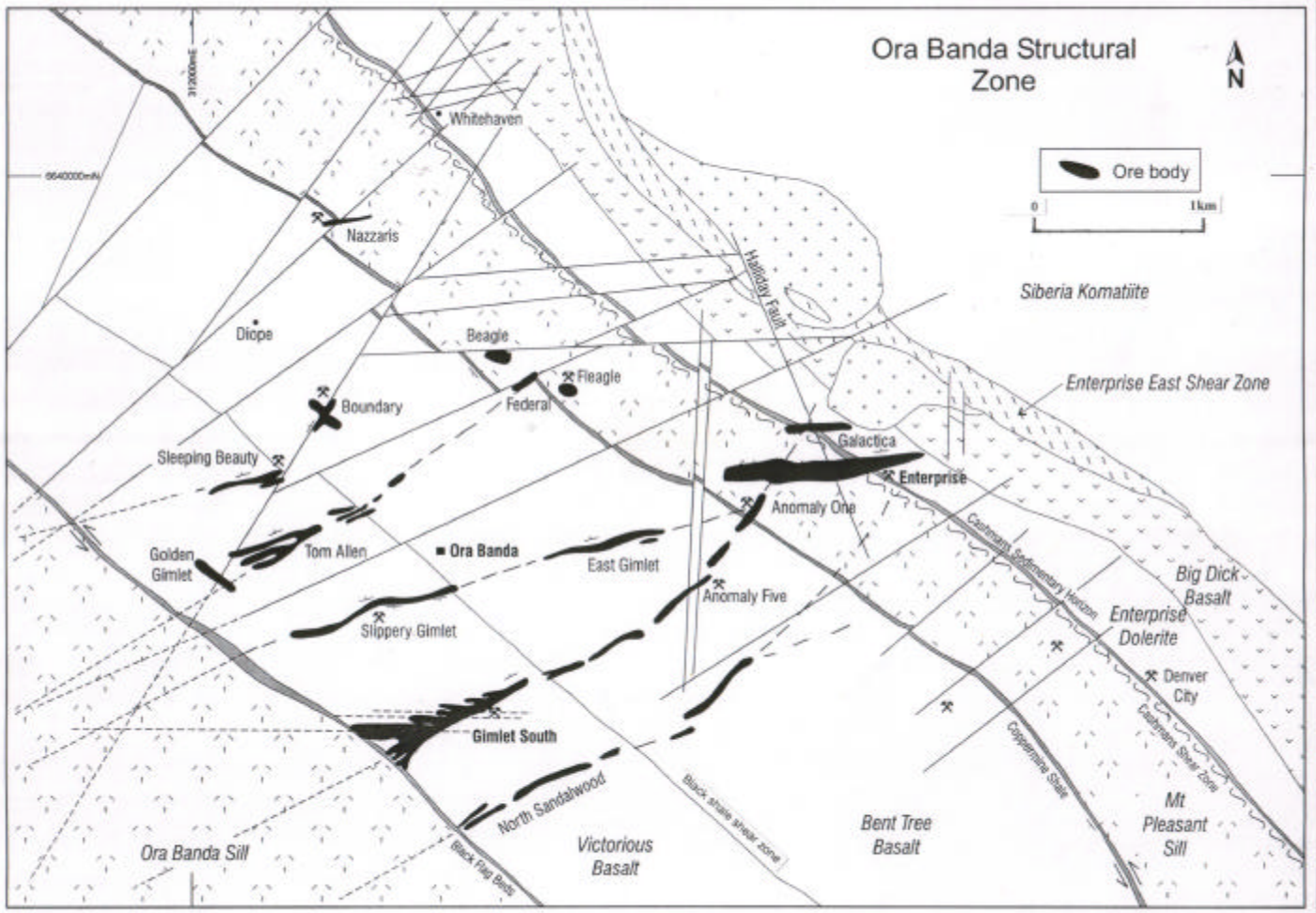

Figure 4.6 – Geological map of the Ora Banda structural zone, showing the interlinked network of brittle-ductile faults. Dip and strike symbols show general trends of igneous layering and structures.

setting distinguish the faults, however host rocks and timing are common to all five. Three of these five are discussed in some detail and are representative of the variation in style between the structures. The Black shale shear zone is also presented in detail since it provides important timing constraints on the structural development of the area.

Gimlet South and Sleeping Beauty faults (D4)

Gimlet South fault is the largest of the faults and includes a group of smaller historic prospects that are parts of the same structure (Figure 4.6 p.100). The group is collectively called "Gimlet South fault" and includes Victorious/east/deeps, Wilson's Lode, Gimlet South, Far East, Farther east, Old Mate, Corsair spur, Avenger and Hornet lodes. Full descriptions of the Gimlet South fault are given in Petersen (1987) and Harrison *et al*. (1990). Gimlet South fault and Sleeping Beauty fault have similar structural styles, but the main difference is the scale of development. Gimlet South fault is over 2 km long, up to 50m wide and known to extend to several hundred metres depth, whereas Sleeping Beauty fault is 300m long, 10m wide on average and known to about 150m depth (Figure 4.6 p.100, Map 8 p.353). The structures trend 060° and dip sub-vertical to 75° NW.

Kinematic indicators for the Gimlet South fault reported by several authors (Baxter 1989; Laing 1994; Oliver 1993), show right-lateral strike-slip offset with displacement of the basalt sequence in the order of several metres, which at the mine-corridor scale is negligible. Stereograms of structural elements compiled from underground mapping from the Gimlet South mine (Figure 4.7), show three dominant brittle-ductile fault sets striking 057°, 172° and 085°. The 057° cluster is the main trend of the structure with the weak 085° cluster representing the spur lodes. Cross-cutting brittle-ductile faults are subordinate features along the 172° trend.

Gimlet South fault and Sleeping Beauty fault are intersected by prominent E-W trending brittle-ductile faults locally known as spur lodes. The E-W faults have similar morphology to the main structures comprising fault and hydraulic breccia with components of ductile shear. Laing (1994) interpreted the E-W faults in terms of their intersection geometry with the main Gimlet South fault as either cross-cutting or asymptotic in contact with the 057° trending faults. In both cases the intersections form steeply northeast plunging, discrete shoot-style zones of high fracture-density (Figure 4.8). Slip lineations plotted on a

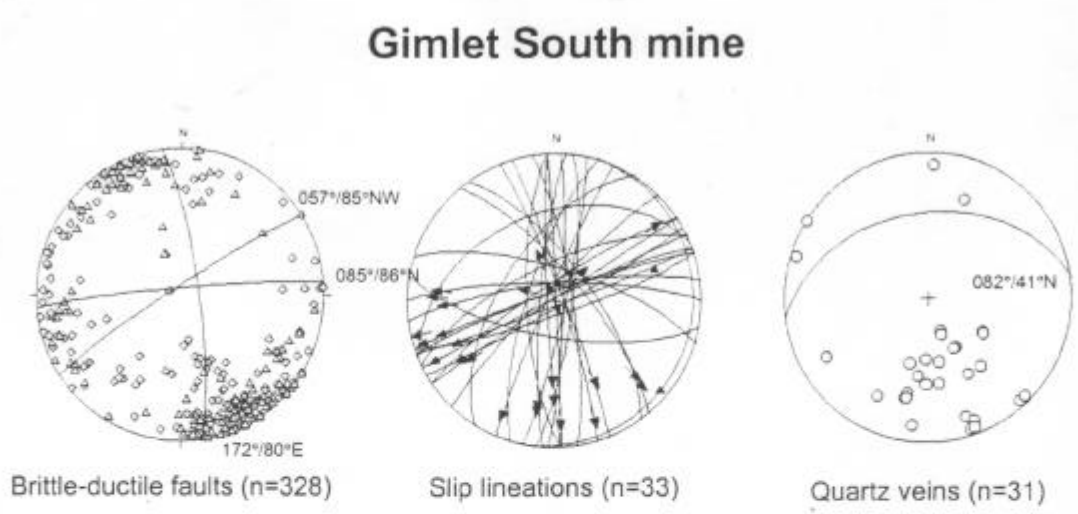

Figure 4.7 – Equal area stereograms of structural elements from the Gimlet South mine. Orientations are for average great circles to the major clusters. Squares represent faults, triangles represent shear zones. Data are compiled from several hundred underground face maps prepared by Ora Banda mine geologists. See text for explanation.

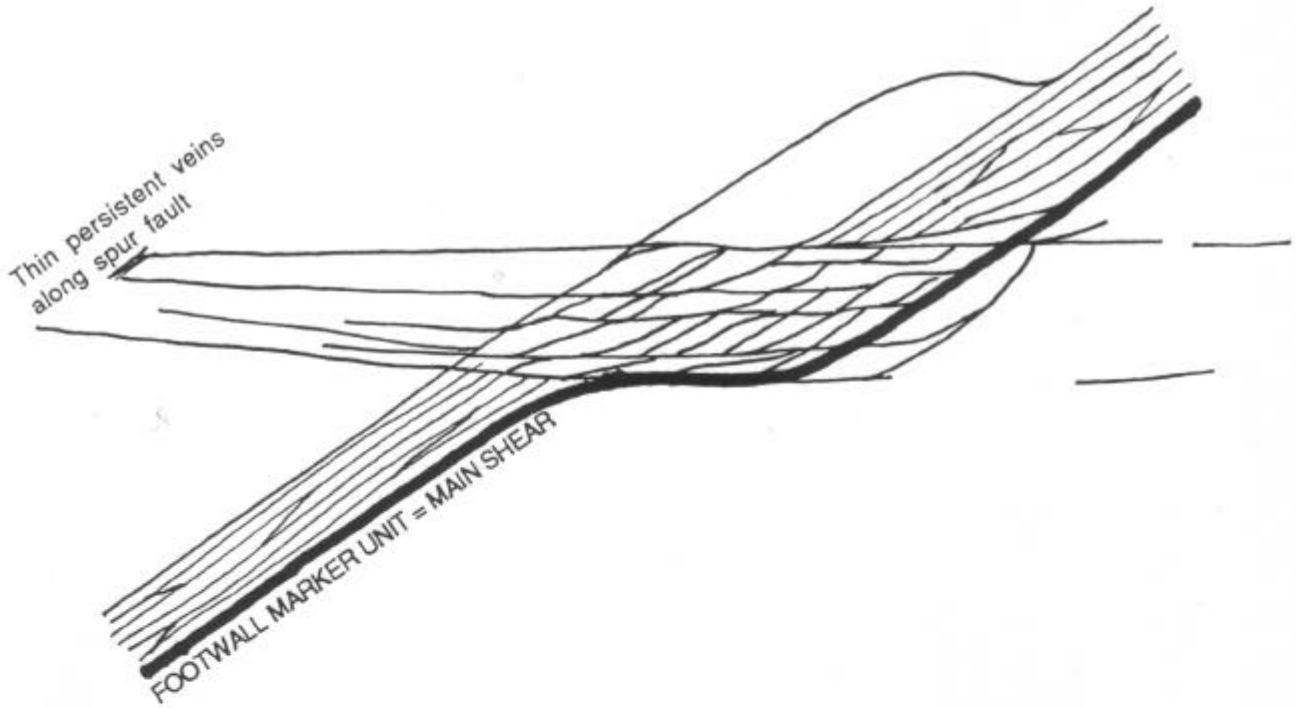

Figure 4.8 – Schematic plan view showing high fracture-density zones that form at the intersection of 057° and 085° shear zones (main lode, spur lode) from Gimlet South, and illustrating the two types of fault intersections at Gimlet South, asymptotic and cross-cutting. Modified from Laing (1994).

stereogram show one of the clusters plunging 73°→035° (Figure 4.7 p.102), indicating some fault movement parallel to ore-shoots that are developed in this orientation. Tabular quartz veins are common along sharp brittle fault planes located at the footwall boundary of the main structure, with thick breccia bodies in the hangingwall. The Gimlet South fault exhibits textures that indicate complex development of breccia lodes with a high degree of textural maturity (Figure 4.15c, p.114). Compared to the other four structures, the Gimlet South fault is the largest and most complex developed over 2 km of strike length, and probably represents a preferred locus of the most intense deformation, with the other structures decreasing in intensity away to the northwest and southeast. Gimlet South fault extends into the Mount Pleasant Sill, but changes orientation to 045° across a contact with coarse-grained gabbroic rocks in the base of the Bent Tree Basalt. The fault intersects the Enterprise fault zone in the Mount Pleasant Sill, but cross-cutting relations between the two faults have not been determined. A significant zone of faulting and fracturing is however, present at the point of intersection.

Slippery Gimlet fault (D4)

Slippery Gimlet fault is a brittle-ductile structure located 800m north of the Gimlet South fault (Figure 4.6 p.100). It is a good example of a dilational fault jog as described by Sibson (1987), with the 'jog' geometry mapped in the open-pit and interpreted from diamond drilling (Figure 4.9, Map 9 p.356). A NE-SW trending brittle-ductile fault is separated by a 35m wide jog zone. The location of the dilational jog may be controlled by a significant change in grainsize of the basalt sequence, at an intersection with the NE-SW trending fault.

The eastern segment of the NE-SW trending brittle-ductile fault oriented 067°/77°S, is a markedly deformed zone within relatively undeformed and unaltered porphyritic basalt (Figure 4.9, Map 9 p.356). The fault has a central section of intensely sheared fault gouge (0.8m wide) and outer sections of weakly to strongly sheared basalt with a total width of 1.9m. In the hanging wall of the structure (Figure 4.10) two sets of thin quartz-carbonate-chlorite filled fractures are parallel to the C and S planes of the main brittle-ductile fault. Two lineations are present on the C-plane. One is a product of the intersection between the C and S planes of the fault trending 25°→083°, and the other is a mineral elongation

Figure 4.9 – Geological map of the Slippery Gimlet open-pit. Coarse-grained units are integral parts of the basalt flow sequence.

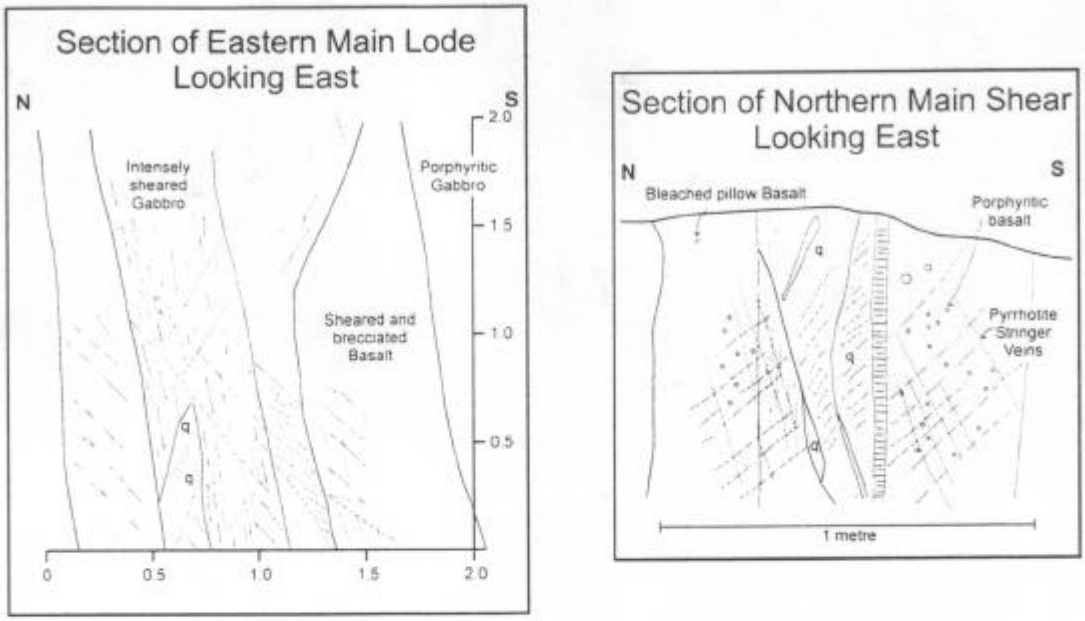

Figure 4.10 - Field sketches of cross-sections through the southern main shear zone and the northern main shear zone, Slippery Gimlet.

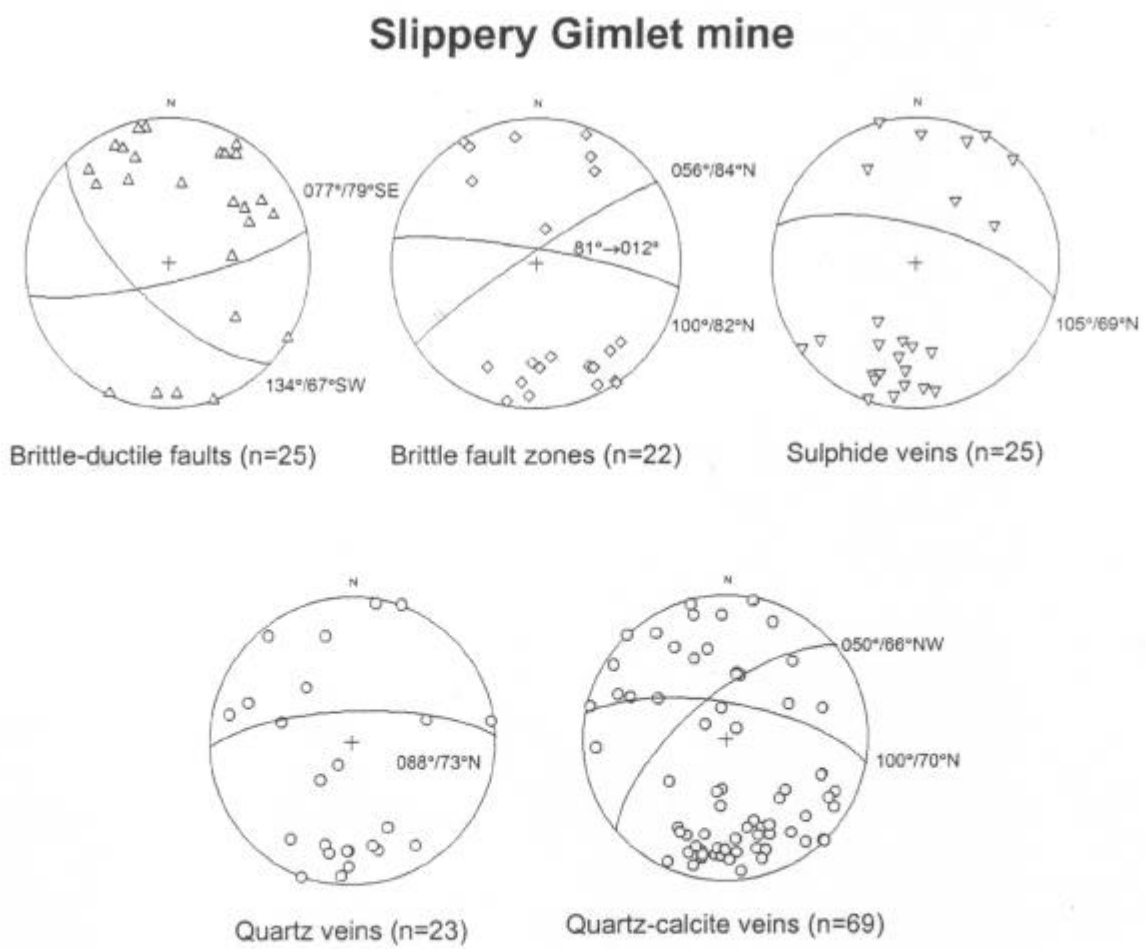

Figure 4.11 – Equal area stereograms of structural elements from Slippery Gimlet. Orientations are for average great circles to the major clusters, with number of measurements (n). Data collected from diamond drill core and open pit mapping. See text for explanation.

lineation defined by aligned micas trending 22°→245°. The S-C fabric geometry indicates right-lateral displacement, and the mineral elongation lineation confirms normal oblique-slip movement on the fault. Ferruginous quartz veins in the weathered fault are lens-shaped and appear to predate the shearing.

The western segment of the NE-SW trending brittle-ductile fault is oriented 056°/88°N and has mostly brittle textures with a higher degree of fracturing in the wallrock, but only a small <0.5m zone of schistosity and quartz veining. The structure is 1.1m wide with abundant pyrite-pyrrhotite veins and thin quartz veins. Deformation is in the form of pervasive fracturing with weakly developed jigsaw breccia. Interlinked mesofractures trend 099°/46°N and 062°/61°S.

A central rhomb shaped area (dilational jog) is enclosed by the eastern and western fault segments, which are linked by a layer-parallel brittle-ductile fault trending 122°/78°S on the northern boundary of the jog. The southern boundary is slightly sheared trending 115°/73°S (Figure 4.10 p.105). The northern boundary fault is 0.6m wide with a strong mineral elongation lineation developed in the C-plane. Strike-slip movement is indicated by this shallow NW-plunging lineation, but the sense of shear is unclear. In the central portion of the fault, the rock is intensely sheared and has sharp boundaries with outer portions of weakly foliated basalt. The fault contains abundant 5-10cm milky quartz veins and has a 0.2m wide alteration halo with carbonate-muscovite replacement of the wallrocks and intense bleaching. A greater proportion of quartz veins than the eastern segment of the NE-SW trending fault is present as thin veins with comb textured quartz growths at 90° to the vein walls, and iron oxide staining from the breakdown of pyrite. The predominance of quartz veins with open space growth textures suggests a component of dilation orthogonal to the fault. Some quartz veins are folded, indicating either that minor shearing postdated dilation, or the folded veins are an earlier generation. Quartz veins average about 088°/73°N (Figure 4.11 p.105). The western boundary of the jog area has a thin <0.1m zone with S-C fabrics that show left-lateral offset. Strong hematite-chlorite-muscovite alteration is confined to a few centimetres either side of the zone.

Within the dilational jog, a series of sub-parallel quartz veins and breccia zones are spaced at 2m intervals. Individual veins average 10mm-wide, with pyrite-pyrrhotite halos and wide calcite-muscovite-pyrrhotite alteration halos. The veins are sub-parallel to the northern

boundary fault defining a southwest plunging shoot 35m by 50m. Northeast-southwest and NW-SE trending quartz-breccia veins are not common in the open-pit but are observed in diamond drill core (Figure 4.2 p.90, Figure 4.3 p.93).

The Slippery Gimlet fault shows a wide range of brittle fault textures from weakly deformed zones with sub-parallel wallrock fragments (Figure 4.2e p.90), to complex mill breccia with rounding of clasts (Figure 4.2a p.90). Brittle-ductile faults form the boundaries to breccia zones in most instances (Figure 4.2c p.90, Figure 4.3 p.93) and the gross geometry of the structures is controlled by brittle-ductile faults that trend 077°/79°S and 134°/67°SW (Figure 4.11 p.105). A series of brittle fault zones trending 100°/82°N (Figure 4.11 p.105), are subparallel to sulphide veins trending 105°/69°N. Breccia lodes containing clasts of wallrock with sulphide filled fractures, clearly indicate that brecciation overprints an earlier phase of fracture development. However sulphidation and intense wallrock alteration also are widely developed with the formation of breccia, hence fracture propagation and subsequent brecciation are not widely separated in time. Areas of higher density fracture may become breccia loci, and breccia zones are closely associated with brittle-ductile faults. Quartz-carbonate veins are generally sub-parallel to breccia zones. A lack of hydrothermal alteration of the type associated with breccia zones indicates that the quartz carbonate veins overprint the brecciation event. The veins may have been emplaced under a similarly oriented but significantly diminished far-field stress, and localised by a pre-existing anisotropy.

4.4.2 Black shale shear zone (D2-D4?)

A thin, strike persistent interflow sedimentary shale layer separates the Victorious Basalt from the underlying Bent Tree Basalt (Figure 4.6 p.100). It is a critical structure in the Ora Banda district because pre-existing gold-bearing brittle-ductile faults are offset by the shear zone, and it therefore constrains the timing of gold mineralisation and deformation.

Morphology

The shale is generally 1m thick on average, but varies up to 5m. Along strike the unit is continuous with variable thickness and has been traced for 12km to Grants Patch, and further south at Mount Pleasant. Similar thin units of shale are mapped at various

stratigraphic levels between basalt flows, but these are generally discontinuous and irregular, some occurring as rip-up clasts within basalt. The shale has been described as carbonaceous, pyritic, chloritic, tuffaceous shale with banded pyrite horizons interpreted as exhalative in origin (Gilbert 1983).

The Black shale shear zone was investigated in the Gimlet South underground mine and diamond drill core at the Slippery Gimlet mine. An apparent 20m right-lateral offset of the main Gimlet South fault (20m) was mapped in underground development drives at the Gimlet South mine. The shear zone is an intense deformation zone with ductile fabrics characteristic of a thrust fault (Figure 4.12). Thrust-related textures and fabrics are exhibited mostly by quartz veins within the shale including boudinaged quartz veins with long axes of boudins parallel to a well developed stretching lineation, isoclinal drag folding with fold axes approximately parallel to the S-C intersection lineation, rootless intrafolial folds and ptygmatic folding. S-C relationships indicate west-over-east thrust movement (Figure 4.12). The S-plane is particularly well developed defined by slaty cleavage in graphitic shale. Isoclinal, rootless intrafolial folds are present in both the C and S planes.

Kinematics

Reverse dip-slip movement on the Black shale shear zone is confirmed by apparent right-lateral offset of the steeply north-dipping Gimlet South fault in plan view (Figure 4.6 p.100). This contrasts with an earlier interpretation of the Black shale layer as being offset by the Gimlet South fault (Gwatkin 1984; Harrison *et al*. 1990). Since known movement on the Black shale shear zone is dip-slip, determination of the true displacement (117m) and heave (83m) is possible using the throw (75m), looking orthogonal to strike. The shear zone overprints late brittle-ductile faults (Slippery Gimlet fault and Gimlet South fault) and is therefore one of the latest deformation fabrics in the Ora Banda structural zone.

The deformation is typical of bedding-parallel thrusting produced during flexural-slip folding (Tanner 1989) and may preserve evidence of continued tightening of regional D2 folds (Swager 1989; Witt 1993c). The ductile nature of the strain fabrics may reflect simply a relative strength contrast with surrounding basaltic rocks, however intense ductile

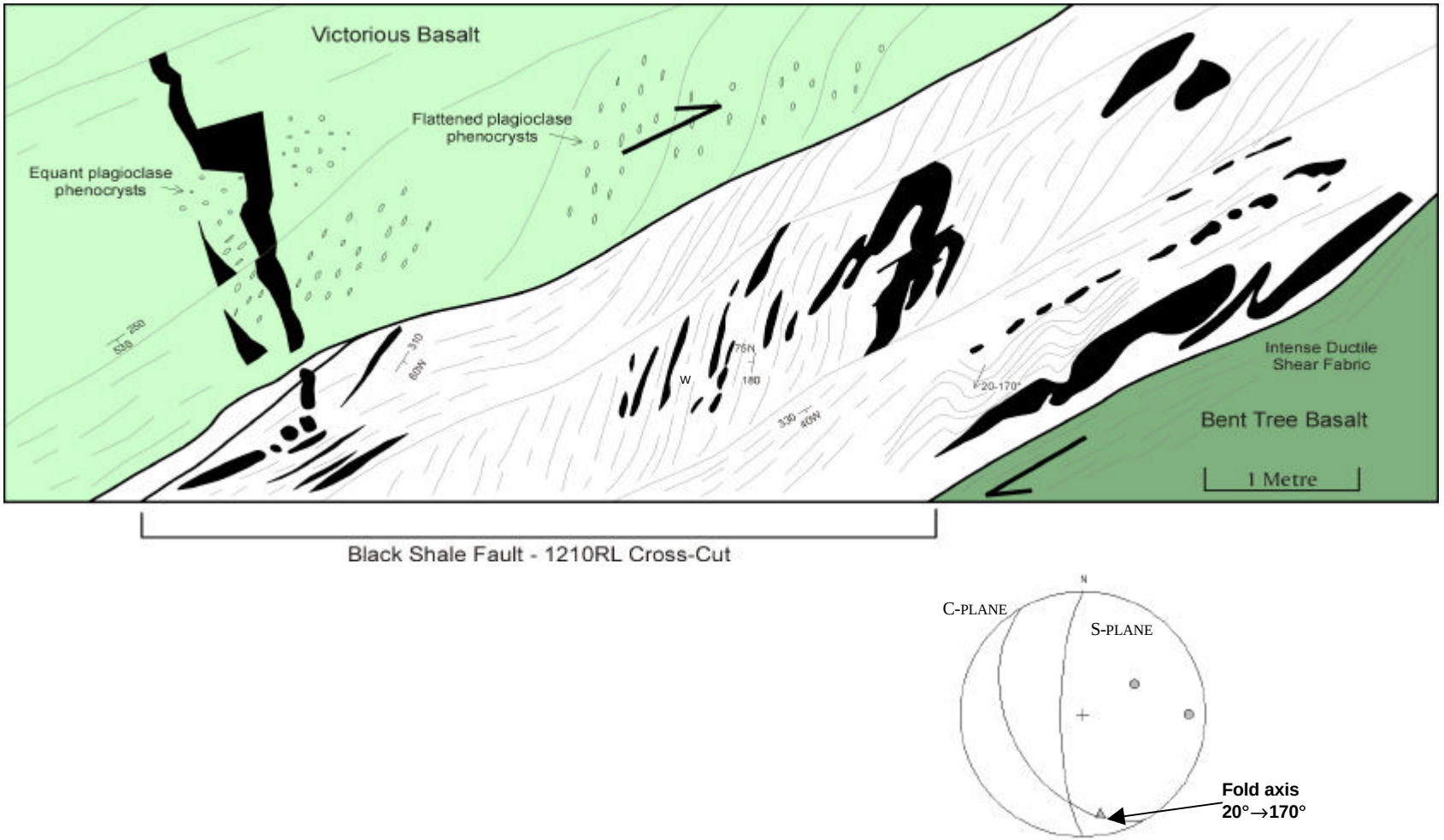

Figure 4.12 – Face map of the Black shale shear zone from an underground drive at the 1210 RL in the Gimlet South mine. Strong shearing in basalt in the immediate wallrocks of the shale, and ductile fabrics in the shale indicate west-over-east thrust movement. The stereogram shows the S-C fabric relationships, with the triangle symbol representing the fold axis orientation of bedding and folded quartz veins, approximately parallel to the S-C intersection lineation. A pre-shearing brittle quartz vein in the Victorious basalt is entrained parallel to the shear zone. View is looking towards 330°, for a plan view see Figure 4.6 (p.100).

shearing of the basalt wallrocks within 2m of the shear zone indicates significant ductile deformation. The thrust movements may have been initiated during the D2 regional folding event.

There is no evidence of strike slip movement during D3, however the Black shale shear zone is parallel to several other D3 shear zones within the Ora Banda structural zone. Kinematic analysis of the shear zone determines a direction for the maximum shortening axis at about E-W, which is similar to the ENE-WSW orientation interpreted for the Gimlet parallel-fault-array. This determination is supported by S-foliation fabrics within the shear zone and flattened plagioclase phenocrysts in the basalt wallrocks that are at angles of >45 to the shear plane, which suggests a horizontal E-W directed shortening axis. This later movement and offset of D4 faults may be a final effect of the regional ENE-WSW shortening, and may also indicate a marked decrease in strain-rate post-dating brittle-ductile faulting.

4.4.3 Enterprise fault zone (D4)

The Enterprise fault zone (Figure 4.6 p.100, Map 6 in pocket) is discussed in detail in Chapter 5 (p.145), but key features of the fault zone as they relate to the Ora Banda structural zone are presented here. The fault zone is a corridor of 080º-trending brittle-ductile faults, 1.3 km long and 50-100m wide. The Enterprise fault zone is somewhat different to most other structures as it is developed in a dolerite sill (Enterprise dolerite). Well-developed schistosity and cleavage in dolerite are typical of the fault zone, whereas breccia developed in fine-grained basalt, typical of the Gimlet parallel-fault-array, is relatively scarce.

East-west trending brittle-ductile faults that form the main structure, cross-cut the Big Dick Basalt, Enterprise dolerite and Mount Pleasant Sill, but the highest density of faulting occurs in the Enterprise dolerite. Differences in tensile strength of the rock units are displayed in the Enterprise open-pit where there is a large-scale sheeted vein system in the Enterprise dolerite, but the overlying Mount Pleasant Sill is only weakly veined. East-west trending brittle-ductile faults are cross-cut by a swarm of metre scale brittle faults and brittle-ductile faults that trend NE-SW and NW-SE on average. Localised zones of high fracture-density occur at intersections of major brittle-ductile faults and at the intersection

of major E-W faults with the Enterprise dolerite / Mount Pleasant Sill contact. The Enterprise fault zone extends west and may link up with the Sleeping Beauty fault.

4.4.4 Boundary fault (D4)

The Boundary fault is located 2.5 km north of Ora Banda and 500m east of the Sleeping Beauty fault (Figure 4.6 p.100). The structure is a brittle-ductile fault up to 5m wide with anastomosing geometry that bifurcates in several places producing a series of parallel shear planes. The main structure cross-cuts massive to pillowed chlorite-biotite altered Bent Tree Basalt and is characterised by quartz veining with intense shearing and breccia. Shear sense indicators (S-C fabrics) and stratigraphic offset show right-lateral displacement of 20-50m across the main fault trending 032°/67°NW (Figure 4.13). There is also a subsidiary set of brittle-ductile faults trending 002°/51°W but their offsets and displacements have not been determined.

Quartz veins at the Boundary mine are mostly simple crack-seal veins with laminations of chlorite parallel to the vein margins. The veins cluster about two main orientations, one parallel to NW-SE faults, which are poorly represented in the data-set, and one sub-parallel to the main brittle-ductile fault orientation at Boundary.

4.4.5 Nazzaris fault zone (D4)

The Nazzaris fault zone is a series of brittle-ductile faults located 1 km to the north of the Boundary mine (Figure 4.6 p.100, Map 7 p.347). The faults cross-cut the Mount Pleasant Sill and extend west into Bent Tree Basalt. This fault zone is typical of dolerite-hosted structures where the trend of the main zone of shearing is E-W, but also there are subsidiary faults oriented NE-SW to N-S. Similar relationships exist at Enterprise where a few large-scale brittle-ductile faults up to 1.3 km long control the main direction of gold mineralisation but at the mesoscopic scale, numerous oblique faults intersect the main brittle-ductile faults providing local structural controls.

Widely scattered fault measurements from Nazzaris have an average orientation of 003°/49°W which trends at about 90° to the main fault zone orientation (Figure 4.14). Schistosity measurements cluster tightly about 130° with moderate southwest dip,

2 GEOLOGICAL SETTING

2.1 REGIONAL GEOLOGY

The Ora Banda and Zuleika districts are located in the Eastern Goldfields Province of the Yilgarn Craton in south central Western Australia (Figure 2.1). The Yilgarn Craton is a regionally extensive crustal unit composed essentially of two main tectonic subdivisions. The majority of the craton consists of Archaean granite-greenstone terrane, and Archaean gneissic rocks that form the western margin of the craton. The Eastern Goldfields Province is the easternmost of three greenstone provinces, and contains large areas of granitoid rocks interspersed with abundant belts of greenstones up to 150 km wide.

The Ora Banda and Zuleika districts (Figure 2.2) form part of the Norseman-Wiluna greenstone Belt of the Eastern Goldfields Province (Figure 2.1). The belt was interpreted as a trough or graben association by Williams (1974) based on a komatiite-rich sequence without development of banded-iron-formation (BIF). The basement to the greenstones was considered to be sialic (Archibald *et al.*1981, Gee *et al.* 1981). Witt (1990) described the Norseman-Wiluna Belt as a tectonically and volcanically active trough during the Archaean, flanked by more stable parts of the Yilgarn Craton. The general stratigraphic sequence that is documented within the fault-bounded terranes of the Norseman-Wiluna Belt has a lower basalt unit that is overlain by a komatiite unit, an upper basalt unit and a felsic volcanosedimentary formation with mafic/ultramafic sills unconformably overlain by a coarse clastic sedimentary unit (Table 2.1). The presence of non-vesicular pillow basalts and abundant komatiites within the Norseman-Wiluna greenstone belt has led some authors to suggest that the mafic and ultramafic sequences were deposited in a deep marine basin (eg. Groves and Batt 1984). Abundant BIF and a paucity of komatiite in surrounding areas such as the Callion Terrane, Norseman Terrane and the Kurnalpie Terrane has led to a platform-phase interpretation of these areas. Barley and Groves (1988) and Barley *et al.* (1989) proposed a marginal rift-basin model for the Norseman-Wiluna greenstone belt. The Kurnalpie Terrane to the east is characterised by restricted komatiite and bi-modal volcanic rocks and is thought to represent a volcanic arc at a continental margin (Morris 1993; Swager 1995). The greenstones in the Kalgoorlie Terrane were deposited around 2.7 Ga, with the main period of deformation, granitoid intrusion, metamorphism and gold mineralisation between 2.66 to 2.64 Ga (Swager *et al.* 1990).

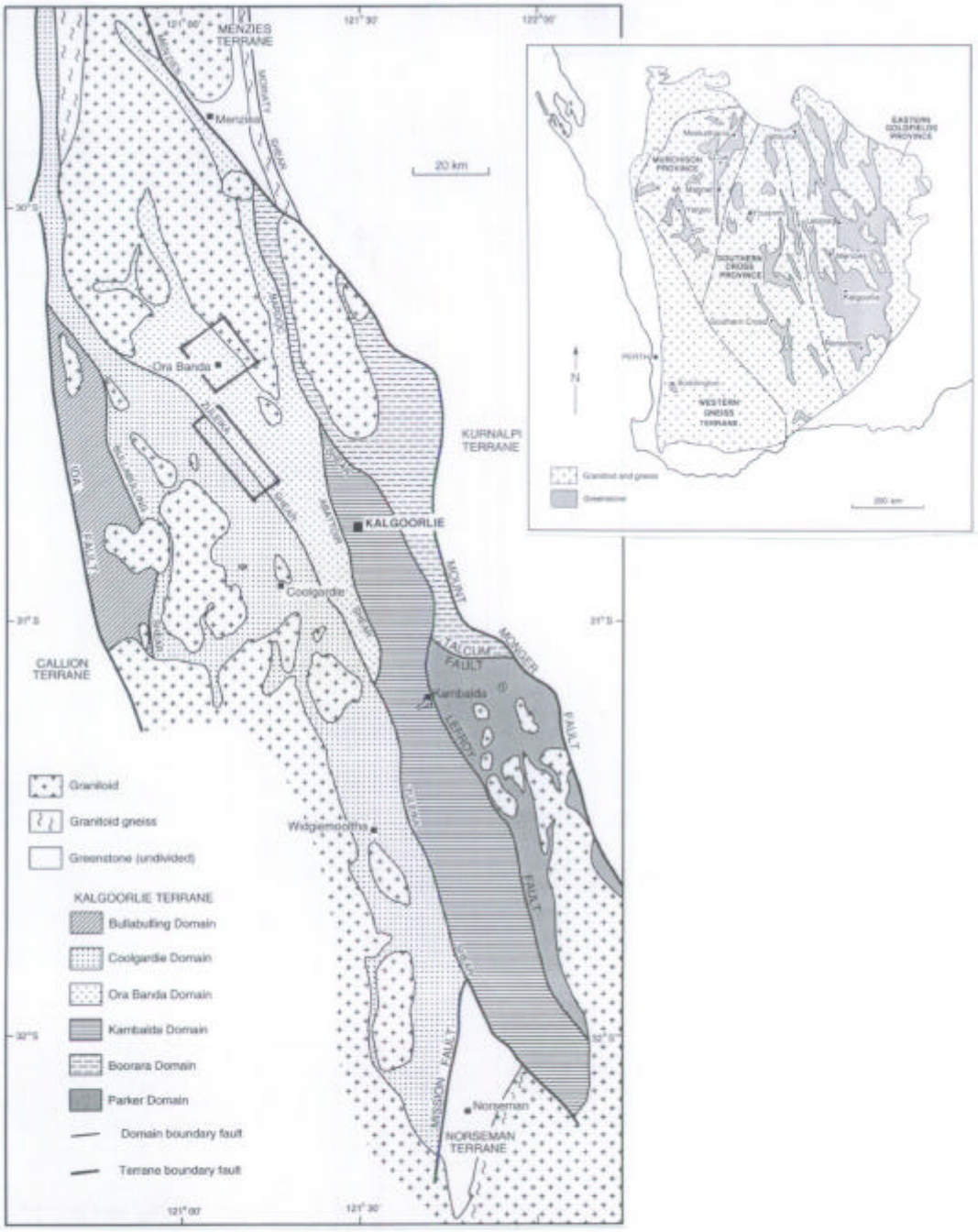

Figure 2.1 – Map of the Kalgoorlie Terrane showing distribution of tectonostratigraphic domains. Box encloses approximate location of the study area. Inset showing major tectonic subdivisions of the Yilgarn Craton with the location of the Kalgoorlie Terrane (after Swager *et al.* 1990).

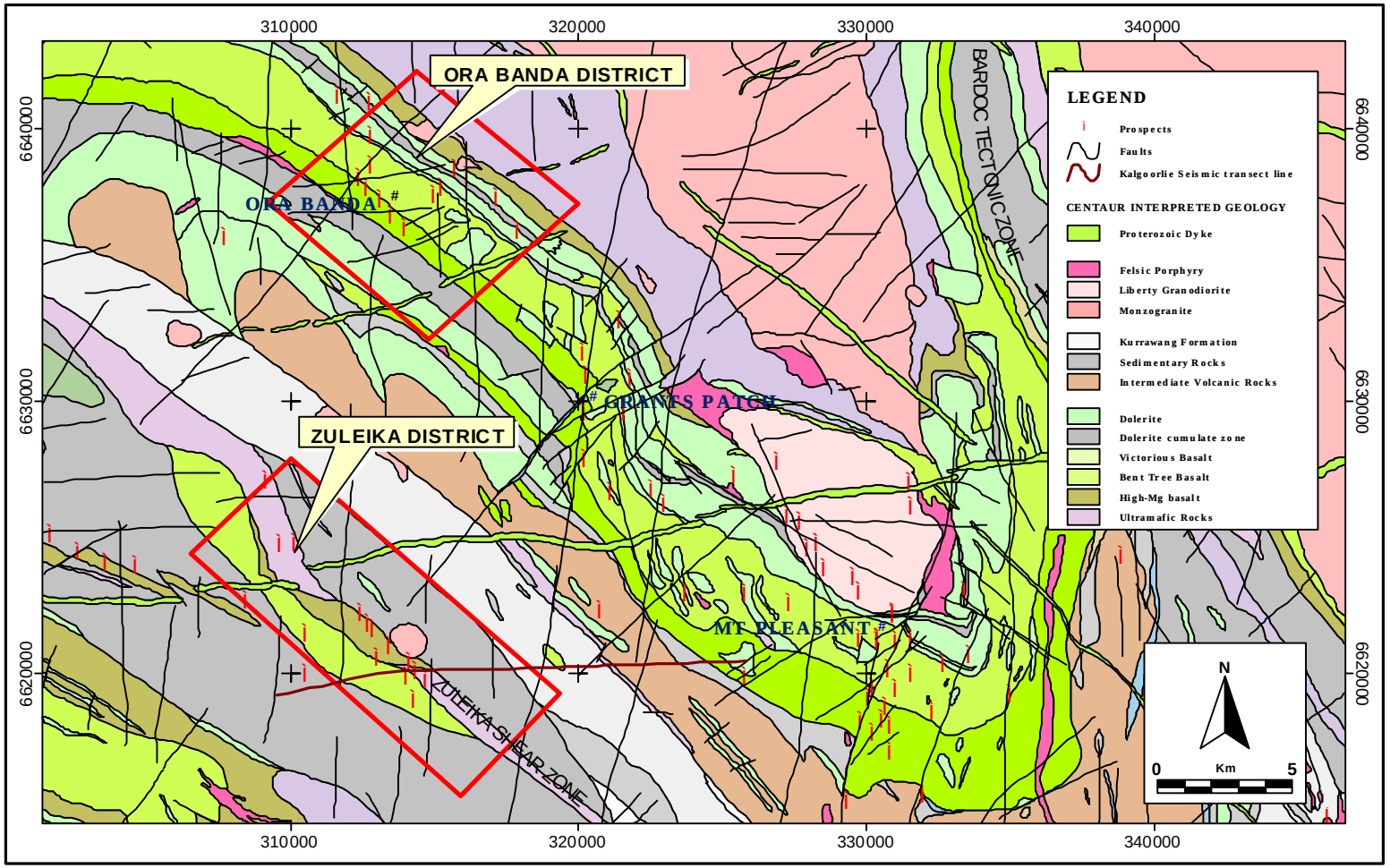

Figure 2.2 - Geology of the Ora Banda and Zuleika districts, northwest Kalgoorlie. Detailed study areas outlined.

Table 2.1 – Stratigraphic correlation of rock successions across tectonostratigraphic domains of the Kalgoorlie Terrane, modified from Swager *et al*. (1990).

Stratigraphic succession	Characteristic rock types	Ora Banda Domain	Kambalda Domain	Coolgardie Domain	Boorara Domain
Polymictic conglomerate unit	Polymictic conglomerate, immature sandstone: coarse trough cross beds, graded beds	Kurrawang Formation	Merougil Conglomerate	Absent	Absent
Felsic volcanic and sedimentary unit	Felsic volcaniclastic sedimentary rocks, ranging from coarse-clastic sandstone to interbedded sand/siltstone. Rhyolite to dacite, locally andesite; lava, tuff,agglomerate	BLACK FLAG GROUP: Pipeline Andesite; Orinda Sill; Ora Banda Sill	BLACK FLAG GROUP: Junction Dolerite; Condenser Dolerite; Golden Mile Dolerite; Triumph Gabbro	BLACK FLAG GROUP: White Flag Formation; Powder Sill; Spargoville Formation	Felsic unit, volcanic and sedimentary rocks
Upper basalt unit	High-Mg and tholeiitic basalt; massive, pillowed and vesicular lavas	GRANTS PATCH GROUP: Victorious basalt; Bent Tree Basalt; Mt Pleasant Sill; Mt Ellis Sill / Enterprise dolerite	KALGOORLIE GROUP: Paringa Basalt; Defiance Dolerite; Williamstown Dolerite	COOLGARDIE GROUP: Absent or thin and discontinuous	Absent or thin and discontinuous
Komatiite unit	High-Mg basalt at top; then thin komatiite flows with minor interflow sedimentary beds, overlying thicker komatiite flows and / or massive olivine adcumulate	LINGER AND DIE GROUP: Big Dick Basalt; Siberia Komatiite; Walter Williams Formation	KALGOORLIE GROUP: Devon Consols Basalt; Kambalda Komatiite	COOLGARDIE GROUP: Hampton Formation	Highway ultramafics
Lower basalt unit	Tholeiitic and high-Mg basalt flows, subaqueous	POLE GROUP: Missouri Basalt; Wongi Basalt	KALGOORLIE GROUP: Lunnon Basalt	COOLGARDIE GROUP: Golden Bar Sill; Burbanks Formation; Three Mile Sill	Scotia Basalt
References		Witt (1987, 1994) Gregory (1998) Harrison (1983, 1984, 1987)	Roberts (1988) Woodall(1965) Langsford (1989)	Hunter (1993)	Christie (1975) Witt (1994)

2.2 GEOLOGY OF THE ZULEIKA DISTRICT

2.2.1 Geological setting

The Zuleika district is located on the Zuleika Shear Zone, a regional-scale within-greenstone-belt ductile shear zone (Figure 2.2 p.14). Intense tectonic interleaving of ultramafic, mafic and intermediate rocks prevents the construction of a local stratigraphic section and the strike continuity and younging direction are undetermined, however very broadly the progression from west to east is high-magnesium basalt, talc-chlorite schist and felsic volcaniclastic rocks. All rocks types are extensively carbonate altered, with alteration distribution closely associated with shear zones.

Ultramafic rocks

Ultramafic rocks in the Zuleika area comprise intensely sheared talc-chlorite schist with localised brecciation. Relict spinifex textures in breccia clasts indicate that the protolith was ultramafic komatiite, and therefore the rocks are possibly remnants of the regional ultramafic marker unit. Evidence of pre-shearing brecciation abounds, with flattened clasts of ultramafic rocks and talc-carbonate veins filling the voids. The texture is typical of the majority exposures of ultramafic rocks and is most evident in diamond drill core. The brecciation may be either auto-brecciation related to volcanism in a sub-aqueous environment or a later tectonic fabric.

High magnesium basalt

Basaltic rocks include high-magnesium pillow basalt with local interpillow breccia and variolitic texture. The basalts form a generally continuous layer but also are mapped as discontinuous mega-boudins within talc-chlorite schist in the Wattlebird area.

Pillow margins are glassy and locally vesicular with zeolite infill minerals and quartz-calcite +/-epidote in the interpillow voids. The basaltic rocks are extensively muscovite-calcite altered in the vicinity of shear zones.

Intrusive albitite porphyry

Porphyritic felsic intrusive rocks are localised discontinuous bodies that are intrusive into talc-chlorite schist. The porphyries commonly are weakly foliated to undeformed with contact relationships that indicate late-to-post tectonic intrusion. Several large (<1km-scale) bodies of porphyritic granodiorite intrude the Zuleika Shear Zone in the study area but many smaller stocks are also exposed in drilling and open-pits. Some examples of mylonitic, felsic porphyritic rocks indicate intrusion over a broad period that began during the waning stages of ductile deformation (D3).

2.3 GEOLOGY OF THE ORA BANDA DISTRICT

The geology of the Ora Banda district is dominated by a moderately southwest-dipping sequence of late Archaean age (Figure 2.2 p.14, Figure 4.6 p100). The sequence locally known as the 'Ora Banda mafic sequence' is typified by weak deformation with preserved primary depositional features and igneous textures (Figure 2.3). The succession is right-way-up younging to the southwest with ultramafic rocks at the base (Linger and Die Group), overlain by tholeiitic igneous rocks (Grants Patch Group), and intermediate to felsic igneous rocks to the west (Black Flag Group). The composition of the extrusive sequence evolves as the rocks get younger from early ultramafic to later felsic, and is typical of Archaean supracrustal successions around the world (Annhaeusser 1971).

2.3.1 Stratigraphic succession

Linger and Die Group

The Linger and Die Group (Witt 1990) is a regional ultramafic marker unit with internal compositional variation including adcumulate dunite, spinifex-textured komatiite and high-magnesium basalt. The group is visible on aeromagnetic imagery as a thick internally complex zone of high magnetic response. In the study area only the upper units of the Linger and Die Group are exposed.

Siberia Komatiite (Figure 4.6 p.100) is a sequence of spinifex textured, olivine-komatiite flow rocks with localised gabbro and high-magnesium basalt. The unit is approximately

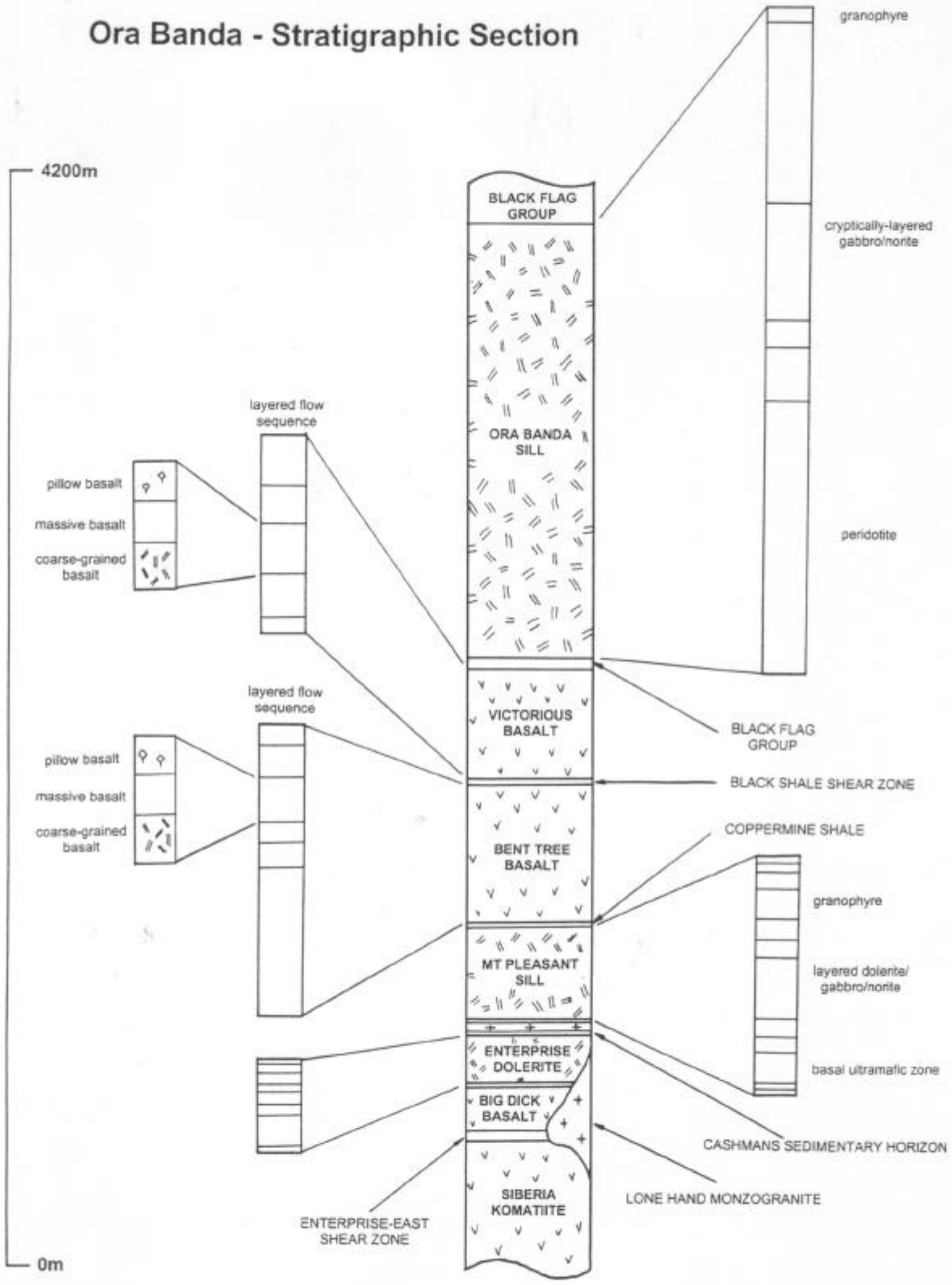

Figure 2.3 – Stratigraphic section of the Ora Banda mafic sequence. Detailed enlargements of main section show position of layers within basalt flow units and layered, differentiated sills.

2600m thick at Ora Banda and is significantly thickened in the hinge of the Kurrawang Syncline. Individual flow units are well differentiated, 1 to 5m-thick flows with olivine and clinopyroxene spinifex textures (Hill *et al.* 1987). Localised interflow sedimentary rocks and discontinuous intrusive doleritic sills disrupt the lower part of the sequence.

Big Dick Basalt (Figure 4.6 p.100) is a 500m thick sequence of interbedded basalt flow rocks. The flows consist of massive to pillowed high-magnesium basalt with variolitic texture. The pillow margins are locally deformed with initially spherical varioles becoming flattened elliptical shapes with progressive shearing. Interflow sedimentary rocks are common within the sequence. Geochemically, the unit is high-magnesium basalt with 9-18% MgO (Witt 1990) and forms the upper-most unit of the Linger and Die Group ultramafic sequence.

Grants Patch Group

The Grants Patch Group (Witt1990) is a layered mafic sequence with over 70km of strike extent, comprising interbedded basaltic flow rocks with syn-volcanic intrusive doleritic sills. The doleritic sills post-date the deposition of the flows and are therefore discussed later with intrusive rocks.

The Bent Tree Basalt (Figure 4.6 p.100) the lowermost unit of the Grants Patch Group, is a 675m thick sequence consisting of a lower gabbroic layer overlain by intercalated basaltic flow rocks that define a distinct volcanic stratigraphy (Harrison 1983). Up to six flow layers have been identified at the Gimlet South mine with each flow layer comprising a coarse-grained basal unit, massive dolerite in the middle, and pillow-basalt at the top locally with flow-top breccia. Chemical analyses indicate tholeiitic chemistry with similarities to the overlying Victorious Basalt.

Victorious Basalt (Figure 4.6 p.100) is a 450m thick succession of basaltic flow rocks with distinct flow layering similar to Bent Tree Basalt. The unit is coarsely plagioclase phyric with phenocrysts up to 5cm diameter. Flow units consist of lower coarse-grained porphyritic rocks, massive porphyritic-dolerite in the middle, and porphyritic-pillowed basalt at the top. Geochemically the unit is tholeiitic with weak calc-alkaline affinity (Harrison 1983).

Black Flag Group

The Black Flag Group (Figure 4.6 p.100) is a 2000m thick unit of felsic to intermediate volcanic and volcaniclastic rocks including epiclastic greywacke, siltstone and shale. At Ora Banda the unit is represented by a thin sliver of altered siliceous metasedimentary rocks at the upper contact of the Victorious Basalt. In the Ora Banda district, the Black Flag Group rocks are intruded by mafic/ultramafic sills.

Interflow sedimentary rocks

Interflow sedimentary rocks are developed extensively in the Ora Banda Domain at basalt flow contacts, and represent intermittent pauses in volcanic activity. Widespread black shales and cherts indicate deep-water deposition onto the volcanic substrate. Common layered sulphidic bands may be exhalative in origin (Bavinton 1979; Gilbert 1983) however some may have a diagenetic origin with pyrite replacement of graded-bedding in sedimentary rocks.

The Cashmans Sedimentary Horizon (Figure 4.6 p.100) is located between the Big Dick Basalt and Bent Tree Basalt, and comprises fine-grained silicified, sulphidic interflow sedimentary rock units with interbedded chert bands and locally convolute laminations. The stratigraphic position is a significant locus for intrusion with three intrusive episodes including Enterprise dolerite, Mount Pleasant Sill and felsic porphyritic dykes and sills, each of which has split the sedimentary horizon into successively thinner slices, moving the same unit to widely separated locations. The unit is variably exposed for up to 15 km of strike length and forms an important regional marker horizon.

Regionally, the Cashmans Sedimentary Horizon occupies a similar stratigraphic position to the Kapai Slate at Kambalda and shares similar textural and lithological relationships (Bavinton 1979). Locally, the unit is 1 to 5m thick with laminae of pyrite in thicker bands of silicified chert. Weathered exposures show isoclinal folds and bedding-parallel cleavage defined by aligned micas that may reflect localised bedding-parallel shearing. A thin slice of Cashmans Sedimentary Horizon is located at the Big Dick Basalt / Enterprise Dolerite contact with banded pyrite and chert layers.

The Coppermine Shale (Figure 4.6 p.100) is a 1-10m thick black shale unit between the Bent Tree Basalt and Mount Pleasant Sill, and is possibly a slice of Cashmans Sedimentary Horizon separated from the stratigraphically lower unit with intrusion of the Mount Pleasant Sill. The unit does not crop out in the Ora Banda district, but several drillholes have intercepts of carbonaceous pyritic shale with intense slaty cleavage. Outcrops of fine-grained silicified black chert north of Grants Patch, are correlated with the same unit at Ora Banda. The shale is deformed by strong bedding-parallel cleavage and locally contains stretched angular fragments of schistose mafic rocks to 20cm diameter, at the lower contact with Mount Pleasant Sill. Ellipsoidal quartz (chert?) pebbles are contained within the foliated sediment. Thin chert bands with pinch and swell structure are common with rounded isoclinal fold hingelines trending 24°→165°. The unit is deformed by three prominent cleavages including bedding-parallel cleavage trending 160°/63°W, cross-cut by pervasive schistosity trending 133°/60°W. Both are cross-cut by a late spaced cleavage trending 130°/72°SW.

A 1 to 5m thick carbonaceous black shale layer locally known as the ‘Black shale’ separates the Bent Tree Basalt and Victorious Basalt (Figure 4.6 p.100). The shale unit is significantly sheared with thrust-style fabrics described in detail in Chapter 4.4.2 (p.107). Shearing is common in most interflow sedimentary rocks and mesoscopic structures (lineations and isoclinal fold axes) indicate that the shearing may be related to flexural slip movement along bedding contacts during regional folding. The Black shale does not crop out but is exposed in several open pit mines (eg. Gimlet South, Slippery Gimlet and Sleeping Beauty mines) and in underground exposures at the Gimlet South mine.

2.3.2 Intrusive rocks

Dolerite sills

Layered, differentiated dolerite sills are common and make up a significant proportion of the stratigraphic succession in the Ora Banda Domain. The mafic and ultramafic sills are layer-parallel marker units that can be traced for several tens of kilometres along strike and around the hinges of major folds. Moderate shearing localised at the intrusive contact, is a common feature of the sills. Four sills have intruded interflow sedimentary rocks of the Ora

Banda mafic sequence, and the petrology, geochemistry and phase layering of the sills are documented by Williams and Hallberg (1973), Witt (1987,1990) and Witt *et al.* (1991).

The Enterprise dolerite (Figure 4.6 p.100) is a layered mafic sill that intruded the Cashmans Sedimentary Horizon at the contact between the Big Dick Basalt and Bent Tree Basalt. The unit is identifiable in subcrops that extend from Whitehaven to Denver City, but the generally poor exposure has resulted in the unit not being mapped in previous studies. New exposures in Enterprise open pit and in over 180 diamond drill holes have permitted detailed mapping of the layering and phase variation within the unit. Eight layers have been identified within the sill (Figure 2.4), which has a tholeiitic affinity (Gregory 1988). The sill appears to be slightly transgressive of bedding with rare drillhole intercepts of Big Dick Basalt stratigraphically above the Enterprise dolerite. Gabbroic layers within the sill have textural and geochemical similarities with the Mount Ellis Sill (Gregory 1998), which has been mapped between Grants Patch and Mount Pleasant (Witt 1990). The Mount Ellis Sill (Witt 1990), is a 600m thick dolerite sill of tholeiitic composition that has intruded the contact between the Big Dick Basalt and Bent Tree Basalt, and may represent a southern extension of the Enterprise dolerite.

The Mount Pleasant Sill (Figure 4.6 p.100), is a well-differentiated dolerite sill up to 600m thick, has petrographic evidence of simultaneous crystallisation from the roof and floor of the intrusion, and is divided into twelve distinct layered units based on petrology and chemistry (Witt *et al*. 1991). Phase layering and rhythmic layering are common throughout the sill (Williams and Hallberg 1973) which has lower ultramafic hornblende-peridotite layers that grade upwards into gabbro and quartz dolerite. The layers are important indicators of younging direction and form regional stratigraphic marker horizons.

The Ora Banda Sill (Figure 4.6 p.100), is the largest of the mafic/ultramafic sills with a maximum thickness of 2000m (Williams and Hallberg 1973; Witt 1990). Five distinct layers are present with cryptic layering defined by compositional variations in mineralogy within the sill. The Ora Banda Sill intruded volcanic and volcaniclastic rocks at the base of the Black Flag Group with local melting of wallrocks on the upper contact.

The Orinda Sill is a 250m thick phase-layered gabbroic unit that intruded the middle to upper portions of the Black Flag Group (Witt 1990).

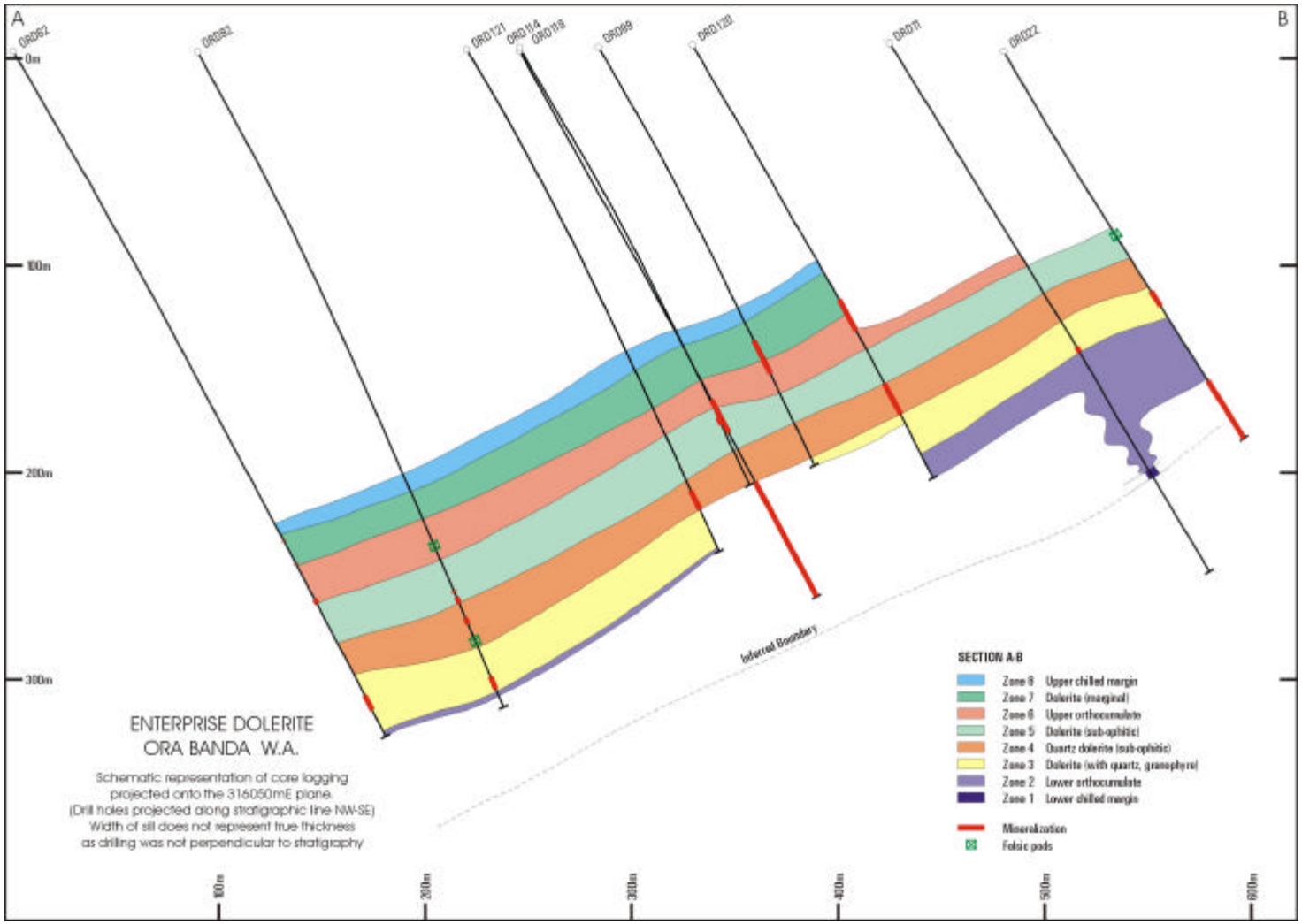

Figure 2.4 – Stratigraphic section of the Enterprise dolerite sill (from Gregory 1998)

Granitoid rocks

Several small stocks and thin bedding-parallel sills of late to post-tectonic granitoid have been emplaced into the Ora Banda mafic sequence. The Lone Hand Monzogranite (LHM) (Figure 4.6 p.100) is a NW plunging teardrop-shaped body of biotite granite with some porphyry. The stock intruded the eastern end of Ora Banda structural zone and its location indicates significant dilation in the area. Most early ductile fabrics do not affect the LHM, however late faults and shear zones cross-cut the LHM and are also intruded by the porphyritic stocks. The Lone Hand Monzogranite has intruded along the Enterprise-east shear zone, and a large fragment of schistose mafic rocks (300m x 50m) is contained within the western margin. Several large porphyry dykes with variable shearing are intruded into the Enterprise east shear zone indicating syn to post kinematic intrusion.

Granitoid-related calcite-fluorite veins are ubiquitous in the Enterprise area and are associated with muscovite-calcite alteration haloes that overprint most brittle-ductile faults. Limited reactivation and shearing of the veins further support syn to post kinematic intrusion. Abundant molybdenite is closely associated with quartz veins forming <1mm wide halos on vein margins and pressure solution seams within the veins indicating significant quartz vein development with porphyry intrusion.

Felsic porphyry dykes and sills

Quartz-feldspar porphyry dykes are common in the Enterprise area and have intruded Enterprise dolerite at several stratigraphic levels. The dykes are usually less than 1m wide and have cross-cut pre-existing quartz veins with pervasive muscovite alteration and associated fluorite and molybdenite. A 10m-thick quartz-feldspar porphyry sill has intruded the Cashmans Sedimentary Horizon, and can be traced for most of the length of this unit. Geochemical data (Centaur) indicate distinctly different trends between the porphyry sills and stocks with fractionation processes evident in the stocks and single-pulse clustering in the sills. At Zuleika, felsic porphyritic rocks have intruded ultramafic rocks along the Zuleika Shear Zone but the chemical composition of the dykes is significantly different to those at Ora Banda. Similar contact relationships of porphyritic intrusions at Ora Banda and Zuleika indicate syn to post-tectonic timing of intrusion yet the widely spaced nature of

the outcrops precludes direct correlation of the rock types except as a district-wide episode of syn to late-tectonic granitoid and porphyry intrusion.

Proterozoic dolerite dykes

Widely-spaced Proterozoic dolerite dykes rarely crop out in the Ora Banda Domain, and most are identified from regional aeromagnetic imagery as lineaments of very high or very low magnetic response. Drillhole intersections north of the Enterprise mine, show the dykes as up to several tens of centimetres thick with a very fine-grained dark mineralogy including phenocrysts of (?)olivine. Localised zones of silicification of the wallrocks and 1-2cm wide reaction zone within the dykes indicate high temperature intrusion.

2.4 DEFORMATION

Deformation in the Norseman-Wiluna greenstone belt is well-documented (Archibald *et al*. 1978; Swager 1989; Swager and Griffin 1990; Witt 1990), and most authors recognise up to four phases of shortening with less well-documented evidence of early and intervening extensional episodes (eg. Hammond and Nisbet 1992; Williams and Whitaker 1993) (Table 2.2). The absence of early thrust faults in the Ora Banda and Zuleika districts is anomalous, however the terminology of Swager *et al*. (1990) is continued here to allow correlation with other notation systems. D1 thrust faults produced duplexes and stratigraphic repetition in the Boorara, Kambalda and Coolgardie Domains only. In the Ora Banda and Zuleika districts, the sequence of deformation events is well constrained by early regional folds that are cross-cut by all other fabrics. The folds are therefore annotated as D2 structures and clearly are the same generation of structures as D2 folds in other domains of the Kalgoorlie Terrane.

D3 was a regional sinistral ductile-shearing event that produced ductile shear zones up to hundreds of kilometres long. The shear zones commonly separate tectonostratigraphic domains with differences in tectonic history and stratigraphic succession, however broad correlations are possible due to the presence of the regional komatiite marker unit, hence the domains are unlikely to be exotic terrane fragments. Whereas D3 produced significant shear zones without visible marker unit offsets in the Ora Banda Domain, the deformation was primarily a shortening event with widespread flattening strains documented in the D3

Table 2.2 – Regional deformation history of the Eastern Goldfields modified from Swager (1997). Only the last three shortening events D2 / D3 / D4 are recognised in this study. Details of references for extensional deformation events and granitoid age dates are given in Swager (1997).

Tectonic event	Timing Constraint
D4 ***REGIONAL SHORTENING – ENE-WSW*** regional brittle-ductile fault network, with N-S, NE-SW and E-W principal structural orientations	granite – 'post tectonic' : ca. 2620-2600 Ma (very few)
EAST-WEST EXTENSION restricted to Ida shear zone, post metamorphic orogenic collapse?	granite – 'late-tectonic' : ca. 2640 Ma
D3 ***REGIONAL SHORTENING – ENE-WSW*** strike and reverse slip, regional within-greenstone-belt ductile shear zones, en echelon folds	
LOCAL EXTENSION final uplift stage of granite-gneiss complexes	granite – 'post-regional folding' : ca. 2660 Ma
D2 ***REGIONAL SHORTENING – ENE-WSW*** upright foliation and folds, domain scale thrusting, inversion of extensional structures?	granite – 'pre to syn regional folding' : > ca. 2660 Ma
POST D1 and PRE D2 E-W EXTENSION roll-over anticlines, synclinal basins with clastic infill	post-D1 and pre-D2 felsic porphyry : 2674 +/- 6 Ma
D1 ***REGIONAL THRUSTING – N-S*** thrust stacking, recumbent folds: involves upper felsic volcanic unit with extensional structures	felsic volcanic rocks : minimum age constraints 2681+/- 5 Ma (Kalgoorlie), 2675 +/- 3 Ma (Gindalbie)
DE *EARLY EXTENSION* low-angle shearing along granite-greenstone contacts; north to south movement? Syn-volcanic granite plutonism, syn-volcanic domes, local polydirectional extension and local recumbent folds	early granites: c. 2685-2675 Ma (? ca. 2710 Ma)

structures (Eisenlohr *et al*. 1989; Skwarnecki 1987; Swager 1989; Vearncombe 1992; Vearncombe 1998a). Crustal shortening resulted in tightening of earlier D2 folds and partitioning of simple-shear deformation into high strain zones in a transpressional tectonic regime (Libby *et al*. 1990; Swager 1989). D4 is documented as an oblique faulting event with N-S trending dextral faults (Clout *et al*. 1990; Witt 1990). Most published maps show the late faults as being restricted in distribution, with only the most obvious faults mapped from known offsets. The fault event is characterised from new data in this study as brittle-ductile in nature forming a regionally developed network of interlinking faults that are primarily mesoscopic-scale structures (Table 2.2 p.26).

2.5 METAMORPHISM

Regional metamorphism in the Ora Banda Domain reached lower greenschist facies, characterised by actinolite-albite metamorphism of igneous pyroxene-plagioclase assemblages (Figure 2.5). A lower limit of prehnite-pumpellyite facies for static domains was recorded by Witt (1993a). Widespread preservation of primary igneous textures is typical at Ora Banda hence the prefix “meta” is omitted from rock descriptions here.

In the Zuleika area, the presence of biotite in felsic rocks and amphibole in mafic rocks suggests a slightly higher metamorphic grade than for rocks in the adjacent Ora Banda Domain. The Zuleika Shear Zone was interpreted by Swager *et al.* (1990) as a domain boundary, and shown as juxtaposing tectonostratigraphic domains of markedly different metamorphic grade. However, observations presented in Chapter 3 (p.29) do not record any significant change of metamorphic grade across the Zuleika Shear Zone and the interpretation of this shear zone as a metamorphic boundary is equivocal. Gold mineralisation accompanied potassium metasomatism in the form of muscovite and biotite in the Zuleika Shear Zone. Metamorphic biotite in the Kurrawang Conglomerate to the east of the Zuleika Shear Zone (Hunter 1993) suggests that the metamorphic boundary may be located at the eastern contact of the conglomerate unit or possibly further to the east. Randomly oriented actinolite sheafs overprinting ductile shear zone fabrics and hydrothermal biotite at Zuleika (Bullant mine), indicate that metamorphism outlasted deformation. Randomly oriented amphibole is commonly reported in the Kalgoorlie region (Swager 1994, Witt 1993), and may be related to post-tectonic porphyry intrusion.

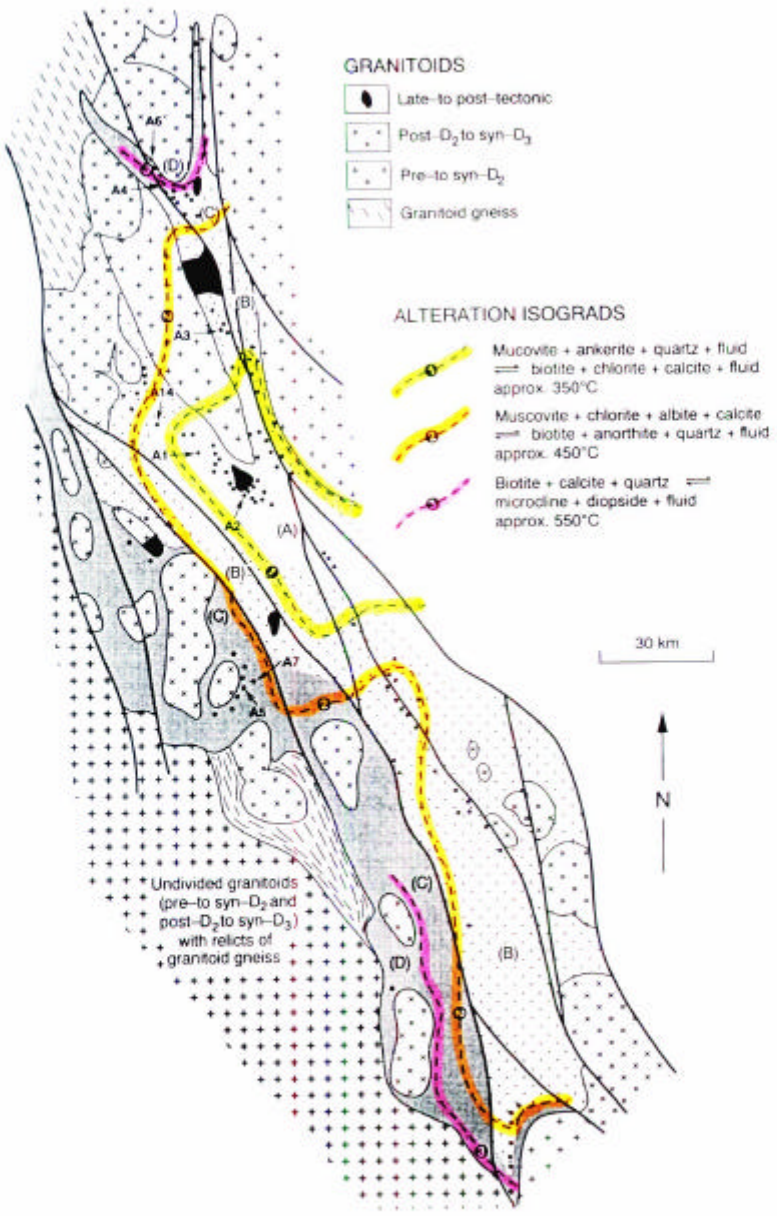

Figure 2.5 – Distribution of metamorphic facies in the Kalgoorlie terrane (from Witt *et al.* 1997)

3 REGIONAL STRUCTURAL FRAMEWORK

3.1 INTRODUCTION

This chapter investigates the deformation sequence in the northern Kalgoorlie area, using aeromagnetic imagery to determine regional-scale relationships. In the Zuleika district, the regional-scale D3 Zuleika Shear Zone is exposed in open-pit mines. These exposures show cross-cutting relationships between the shear zone and the late-tectonic brittle-ductile fault network. Regional-scale relationships are inferred from mesoscopic observations at Zuleika that document the nature of both the D3 ductile shearing event, and the D4 brittle-ductile faulting event. The D3 and D4 events are assessed at larger scales in Chapters 4 and 5 from Ora Banda, where better exposures of the D4 brittle-ductile fault network are located.

The Kalgoorlie Terrane has a prominent NNW-SSE trending structural grain that is developed over several hundred kilometres. The terrane covers a broad belt of greenstones from Norseman to Menzies and is divided into six distinct domains (Swager *et al.* 1990), each with a similar stratigraphic sequence and deformation history. The Ora Banda Domain is the northernmost of the six domains and is also one of the least deformed stratigraphic packages in the Norseman-Wiluna Belt with large tracts of intact, moderately dipping igneous and sedimentary rocks.

3.2 AEROMAGNETIC INTERPRETATION

An image of aeromagnetic data (Figure 3.1) shows good definition of rock types from the marked difference in magnetic response between ultramafic, mafic and felsic igneous rocks. Ultramafic rocks, including ultramafic zones in intrusive mafic sills, have the highest magnetic response of all rock-types, and delineate the trace of igneous layering as long sinuous belts with well-defined offsets. The Ora Banda Domain is a large area of weak deformation typified by the broad fold structure in the centre of the image (Figure 3.1). The Zuleika Shear Zone is poorly defined magnetically and appears to truncate the western limb of the Kurrawang syncline, yet the truncation may be against the eastern contact of the Kurrawang Formation. Large areas of low-to-moderate magnetic response with coarse ‘texture’ on the image are granitic rocks, and belts of ultramafic rocks have a high response. Several E-W trending linear features of marked high and low response that

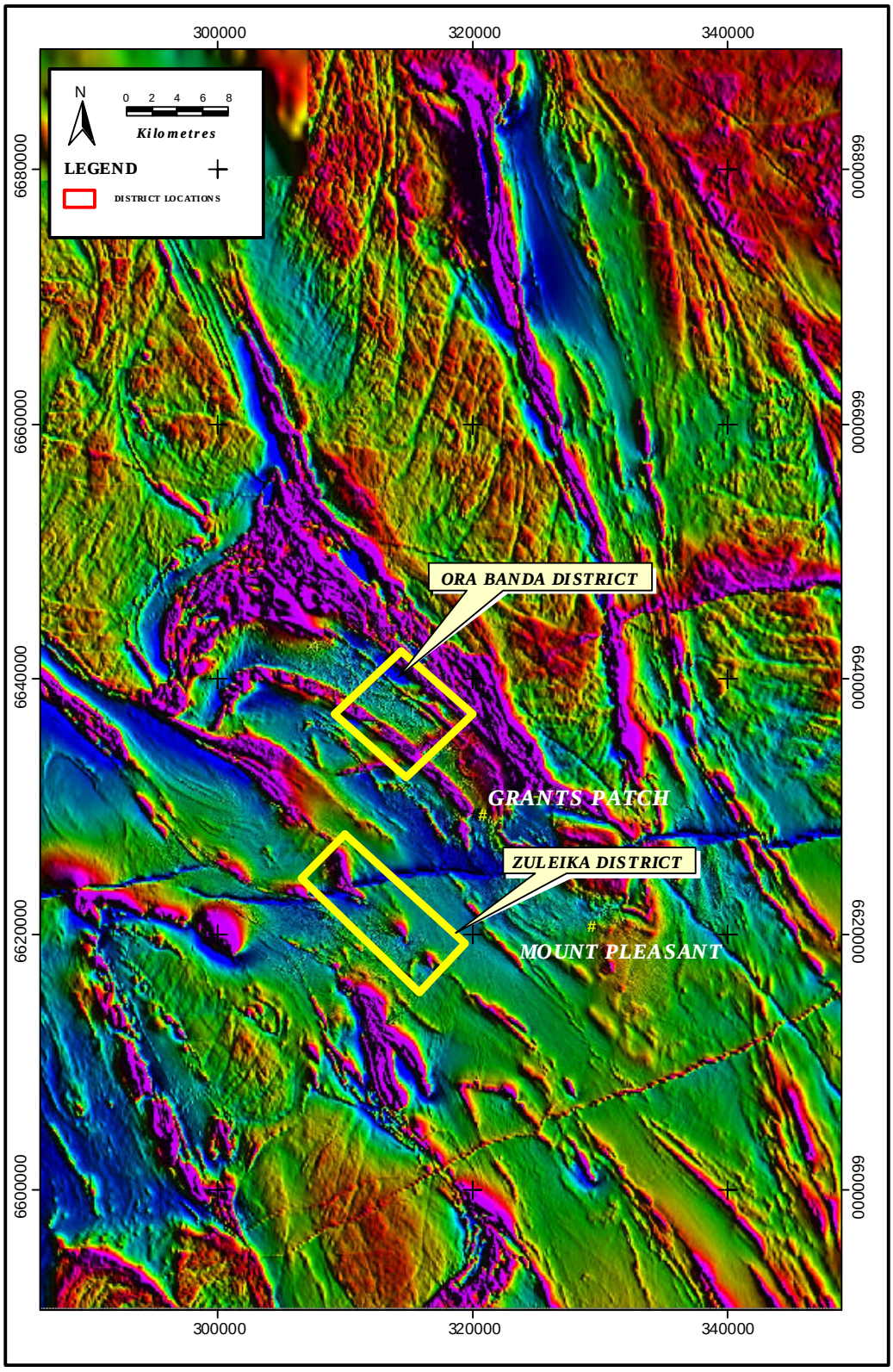

Figure 3.1 - Image of total magnetic intensity, from the north Kalgoorlie region. See appendix for survey details.

30

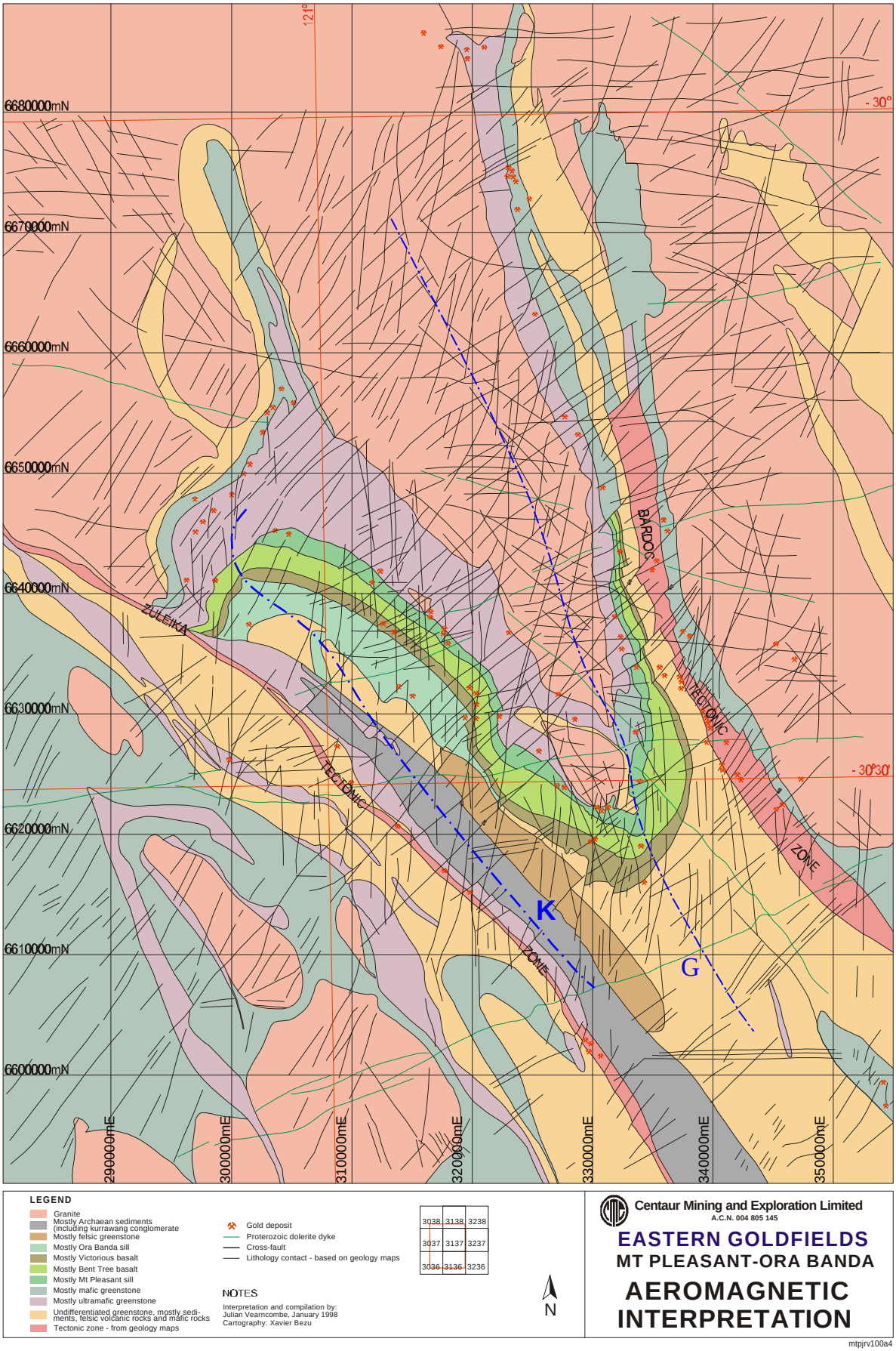

Figure 3.2 – Interpretation of aeromagnetic imagery from the north Kalgoorlie region at 1:100,000 scale after Vearncombe (1998b). The Zuleika Tectonic Zone of Vearncombe (1998b) is equivalent to the Zuleika Shear Zone in this study. **K** – Kurrawang Syncline, **G** – Goongarrie-Mt Pleasant Anticline.

cross-cut all other geological features, coincide with outcrops of Proterozoic mafic dykes. The trace of layering on the image shows a gross NNW-SSE trend that is sub-parallel to regional-scale ductile shear zones such as the Zuleika Shear Zone, Bardoc Tectonic Zone, Kunanulling Shear Zone, Boulder-Lefroy Fault and Ida Fault. A network of late tectonic brittle-ductile faults that overprints the regional-scale ductile shear zones is manifest as several groups of lineaments that are most obvious in the granitoid rocks, and are traceable through adjacent intermediate, mafic and ultramafic rocks. In some areas the lower magnetic response of the mafic and intermediate rocks masks the fault network. Local studies show the brittle-ductile structures of the fault network to have offsets of less than 100m, which are negligible at the map scale.

The validity of interpreted aeromagnetic imagery relies upon many factors including the scale of the imagery, processing techniques and quality of the raw data. The assumptions drawn from Figure 3.1 (p.30) are of regional compass and are considered valid at the scale of the image (1:100,000). However, subsets of the data at smaller scales show a higher level of detail that is not represented at 1:100,000 scale, with closer-spaced faults and offsets constrained by better defined bedding contacts.

3.3 STRUCTURES OF REGIONAL SIGNIFICANCE

Deformation features at a regional-scale include folds, ductile shear zones and a domain-wide network of mesoscopic brittle-ductile faults. The geometry and distribution of each defines the regional-scale fabric and reveals the strains produced by the major deformation events. Since some of the folds and ductile shear zones are developed on the scale of tens or hundreds of kilometres, they are best described from aeromagnetic imagery at a large scale where the structures can be observed in their entirety.

3.3.1 Kurrawang Syncline/Goongarrie–Mount Pleasant Anticline fold couplet (D2)

Regional-scale folding is the oldest recognisable deformation event in the Ora Banda Domain (Witt 1990). Regional-scale (first order) fold structures include the Kurrawang Syncline / Goongarrie-Mount Pleasant Anticline fold couplet (Figure 3.2 p.31). The folds have wavelengths of up to 18 km and are classified as close on the basis of 50° interlimb angles. The axial trace of the Goongarrie-Mount Pleasant Anticline trends 330° with a

southerly plunge of 10°-20° (Witt 1990), whereas the axial trace of the Kurrawang Syncline varies from 310° in the south to 330° in the north (Figure 3.1 p.30). Complex faulting and re-folding of the D2 folds (Plate 1A of Witt 1993a) appears to be locally developed and may be related to syn-D3 granitoid intrusion. The fold limbs are truncated to the west against the Kurrawang Formation with prominent drag folding, but are parallel with the Bardoc Tectonic Zone to the east. Folding of the Kurrawang conglomerate was interpreted as synchronous with the D2 regional folding event (Swager *et al.* 1990; Hunter 1993; Witt 1993a), yet the unit is mapped with unconformable contacts cross-cutting F2 fold form surfaces on regional maps (Witt and Davy 1997), and F2 hinge trace lines (Witt 1993a, Plate 1a).

Second order folds are developed in the less competent Black Flag Group rocks and associated intrusives. The Orinda Sill forms macroscopic folds that are parasitic on the megascopic Kurrawang Syncline, with similar geometric and geographic classifications as the regional-scale folds but different morphology. Mesoscopic-scale folds are locally developed in interflow sedimentary rocks at the contacts of major intrusive units. Examples of parasitic folds in the Cashmans Sedimentary Horizon studied at Cashmans and Denver City, south of Enterprise, show a range of fold axis orientations of 41°→ 200°, 37°→ 258° and 47°→ 280° (Figure 3.3). There is a variety of fold styles at each out-crop including chevron, buckle and isoclinal styles. These are spatially related and may have been produced by flexure of the sedimentary rocks during shearing on the nearby Cashmans Shear Zone, or alternatively the folds were formed as parasitic structures on the major regional folds and were subsequently rotated during later shear zone movements. Refolding of earlier folds is not observed, and a lack of overprinting of fold related fabrics excludes the different fold orientations as being related to separate shortening events.

3.3.2 Zuleika Shear Zone (D3)

Ductile shear zones are large-scale features in the Norseman-Wiluna greenstone belt and are traceable for hundreds of kilometres on aeromagnetic imagery. The shear zones are NW-SE to NNW-SSE trending linear zones that truncate earlier structural features. They were interpreted by Swager *et al.* (1990) as domain boundary faults and in some cases terrane boundaries, however many are layer-parallel at the local scale and are defined by sheared mafic and ultramafic rock contacts. The most prominent ductile shear zones

Figure 3.3 – Anomalous parasitic fold styles related to strike-slip shearing on the Cashmans Shear Zone at Denver City. **a)** Open fold in Cashmans Sedimentary Horizon plunging to the southeast. **b)** Small chevron fold trending 41°→200° developed in the hinge zone of the fold in a), lens cap is 55mm diameter. **c)** Isoclinal fold trending 11°→175° developed in layering within quartz porphyry intruding the Cashmans Sedimentary Horizon. Hammer handle is 330mm long.

bounding the Ora Banda Domain are the Zuleika Shear Zone, Abattoir Shear and the Bardoc Tectonic Zone. Regional folds are truncated by the Zuleika Shear Zone northwest of Ora Banda, but the role of the Bardoc Tectonic Zone as a significant truncating feature is not well established. It is poorly defined on aeromagnetic imagery as a shear zone (Vearncombe 1998b), and is sub-parallel to the regional trend of volcanic and sedimentary sequences.

Seismic interpretation

A 250-km long east-west seismic line across the Kalgoorlie Terrane (Goleby *et al.* 1993), provides a two-dimensional view of the crustal structure, approximately orthogonal to NNW-SSE trending regional fabric (Figure 2.2 p.14, Figure 3.4). Many authors have used the seismic data to interpret the structure of the crust, but several have reported problems with mapped surface geology conflicting with the apparent orientation of major shear and tectonic zones as interpreted from seismic images (Hall 1998).

An image of the seismic data across the Zuleika area is interpreted to assess the orientation and nature of the Zuleika Shear Zone in the third dimension, and to determine the relative scale and importance of the shear zone as a major crustal discontinuity. The seismic image used, is a small subset of the Kalgoorlie seismic transect that covers the Zuleika area crossing the Kurrawang formation to the east, and the western limb of the Goongarrie - Mount Pleasant Anticline (Figure 2.2 p.14, Figure 3.4). The image has a total line length of 15 km, and represents the upper crust to a depth of 12 km (4 seconds, two-way travel time), but does not cover the middle and lower crust. A significant discontinuity is located at about 6 km depth, defined by strong reflectors marking a roughly horizontal surface that truncates low angle reflectors above. Most authors (Goleby *et al.* 1993; Archibald 1998) have interpreted the surface as a basal décollement to the greenstones and a major change in the structure of the crust with imbricated duplex features below. The western limb of the Goongarrie - Mount Pleasant Anticline also is clearly visible as a series of shallow to moderately west-dipping reflectors on the eastern side of the image.

Seismic interpretation of vertical structures like the Zuleika Shear Zone is problematic, since steep features are subparallel to the propagation direction of the seismic waves, and hence are unreflective. The presence of vertical features is therefore inferred from

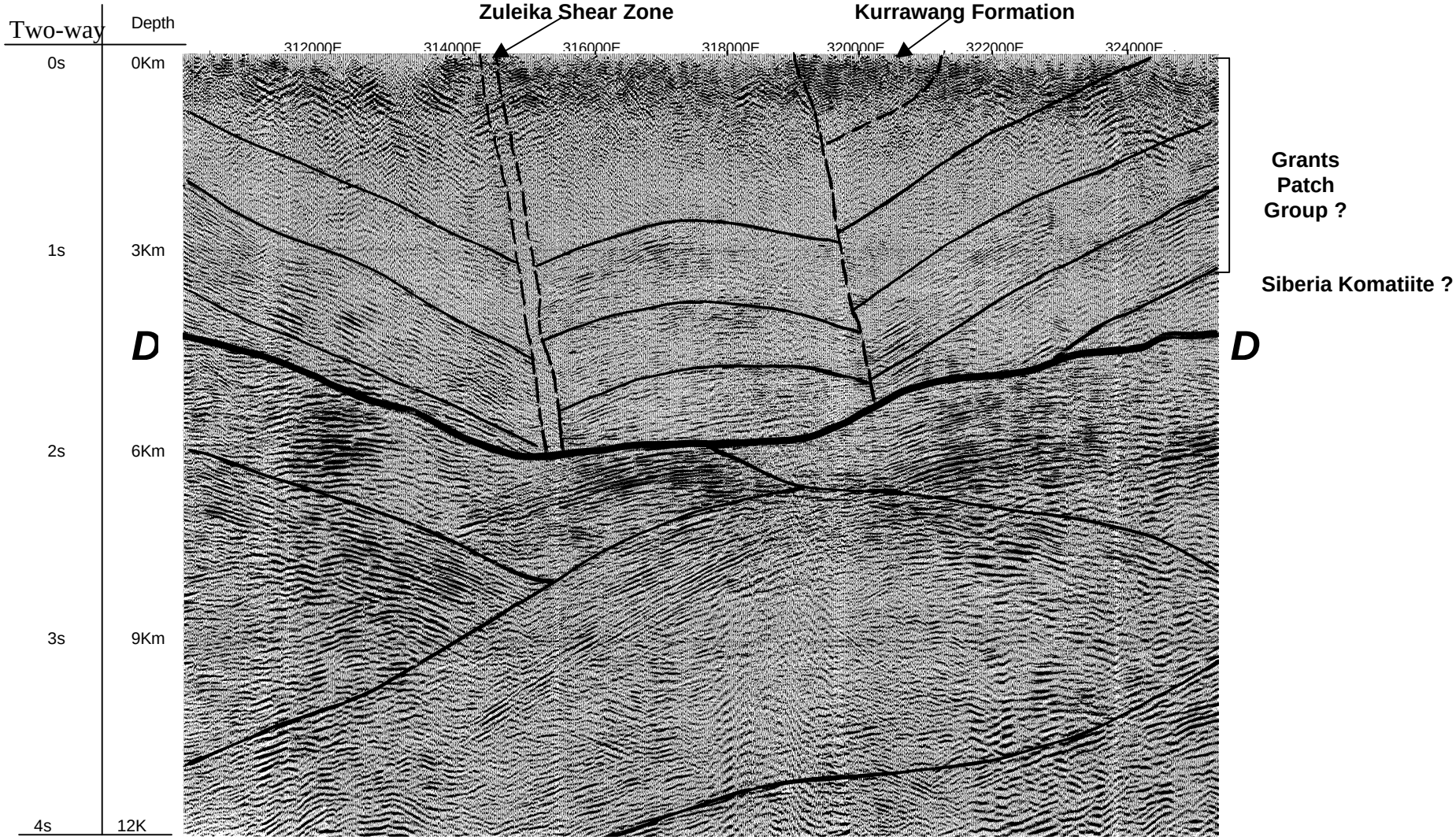

Figure 3.4 – Subset image of migrated seismic data from the Eastern Goldfields Seismic Transect – EGF1 (Goleby *et al*.1993). Eastings at the top of the image are in Australian Map Grid. The décollement (D) marks the base of the greenstones. Layering in the upper part of the image is extrapolated from surface contacts. The location of EGF1 is shown on the geological map in Figure 2.2, page 14.

truncation of horizontal reflectors (Sheriff 1982). The Zuleika Shear Zone is clearly visible as a steeply east-dipping band of non-reflection about 0.3 km wide, that truncates moderately dipping reflectors on both sides (Figure 3.4 p.36). The steep east-dip and width of the non-reflection band agrees with surface measurements of the Zuleika Shear Zone, but the nature of the intersection of the shear zone with the basal décollement is unclear. The Zuleika Shear Zone clearly does not extend below the décollement, implying that either the décollement overprints the earlier formed Zuleika Shear Zone, or it soled out against the décollement. An interpretation of the décollement overprinting within-greenstone shear zones was made by Goleby *et al.* (1993).

At the surface, the Zuleika Shear Zone is a network of shear zones enclosing lozenge-shaped areas of relatively undeformed rock with a total width of a few hundred metres, which is characteristic of major ancient fault zones (Sibson 1977; Ramsay 1980a). As the Zuleika Shear Zone does not extend at depth for greater than 6 km, and has a strike length of 250 km (Swager *et al.* 1990), its high length-to-depth ratio is consistent with the shear zone being a strike-slip fault (Sibson 1977). However, Drummond *et al.* (1997) maintain that the seismic data from deeper crustal levels are consistent with the Hammond and Nisbet (1992) interpretation of NW-SE shear zones as upturned early thrust faults.

The relatively shallow depth extension of the Zuleika Shear Zone when compared with the Bardoc Tectonic Zone and the Ida Fault, and its close association with lithologic contacts, may indicate that this shear zone is not a crustal-scale deformation zone. The 6km depth may not be its original depth, yet the shear zone is a D3 structure like the Bardoc Tectonic Zone, hence a similar timing would require consistent overprinting relationships with the mid-crustal décollement for these structures. The Zuleika Shear Zone may be a within-greenstone ductile shear zone of significance only to the upper layer of the greenstones, and its role as a deeply-tapping fluid conduit is not substantiated by the seismic data.

Surface exposures

The Zuleika Shear Zone is investigated in detail at five localities where it is exposed in the Anthill, Porphyry, Bowerbird, Wattlebird and Bullant open-pit mines along the trend of the shear zone (Figure 3.5). Elsewhere, the shear zone rarely outcrops and diamond drill holes were used to gain subsurface information in un-weathered rocks. The shear zone

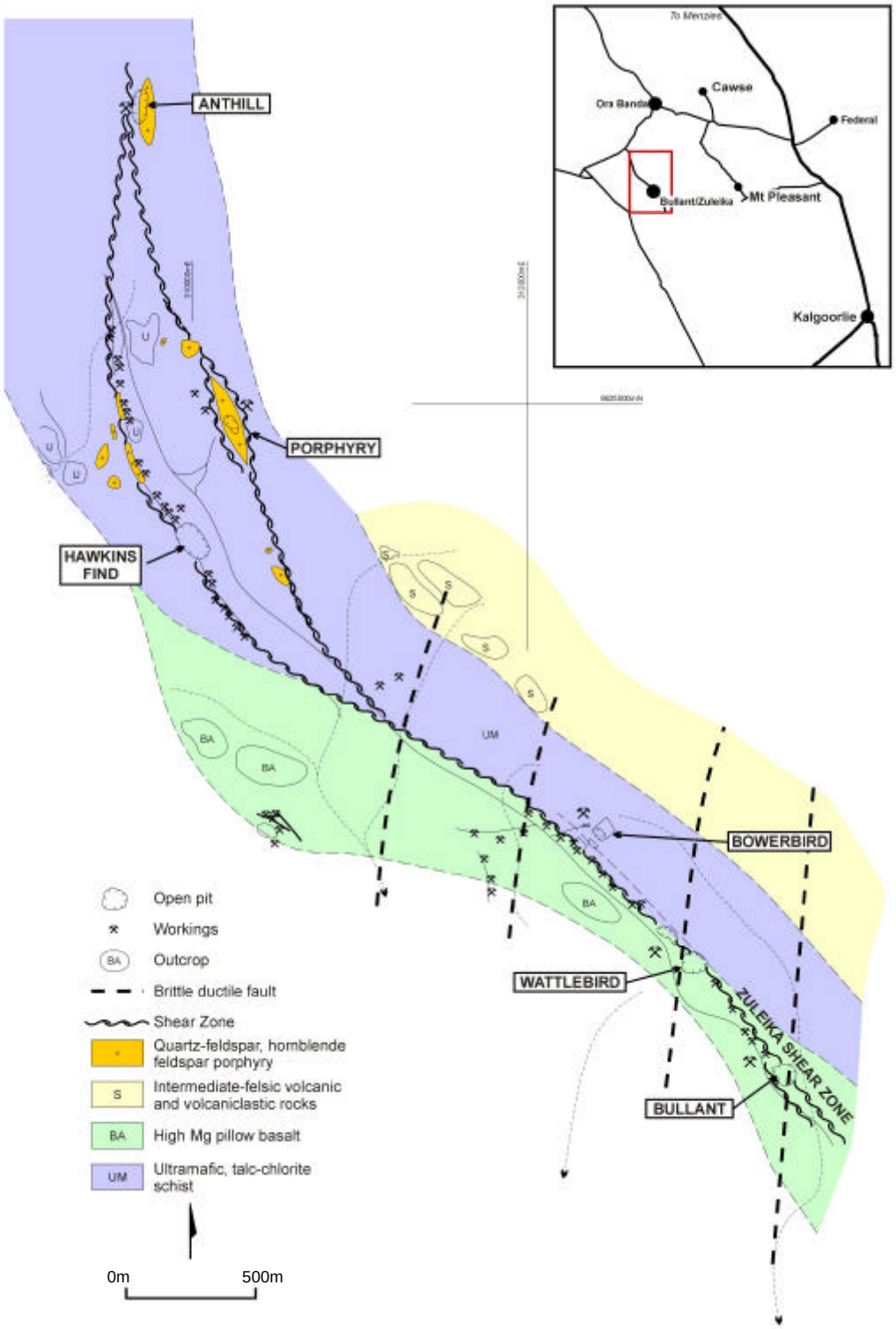

Figure 3.5 – Location map and geology of mines along the Zuleika Shear Zone. Outcrop locations after Konecny (1988).

strikes at 152° on average and its dip varies from 77°SW to 74°NE. A major change in the strike of the shear zone occurs in the Porphyry mine area where the shear zone turns to a more northward trend. Further north past the Anthill mine area the shear zone returns to a northwest trend (Figure 3.5 p.38). This change of strike correlates with a similar change of strike of igneous layering in the Grants Patch area to the east of Zuleika, and may represent a regional northeast-southwest trending kink fold. Morphologically, the Zuleika Shear Zone is defined from drilling and limited outcrop as a 300-500m wide corridor of individual anastomosing ductile shear zones, each up to 100m wide. The corridor is poorly understood in terms of the geometry and distribution of strain and the series of open-pits along the shear zone may represent discrete shear planes within a wider shear zone.

Anthill mine

At the Anthill mine (Figure 3.5 p.38, Map 1 p.262), the Zuleika Shear Zone is mostly talc-chlorite ultramafic schist with a pervasive schistosity striking 159°, and dipping steeply to sub-vertical with variable east to west dip. Quartz-feldspar porphyry has intruded the shear zone as discrete lenticular bodies, that vary in dimensions from several metres to several tens of metres long. The main schistosity is deflected around the edges of the porphyry bodies with local folding and several cross-cutting cleavages at the contact. The contacts have complex deformation of pre-existing S-C fabrics in the ultramafic rocks and contain irregular folded and sheared quartz veins, that are coeval with intrusion of the porphyry. A 10cm-wide aureole exhibiting thermal effects of the porphyry intrusion into sheared ultramafic rocks is observed with local induration and silicification, and a 3-5cm reaction halo in the porphyry (Figure 3.6a). The felsic porphyry bodies are internally deformed with a weak foliation at a moderate angle to the contacts, and cross-cutting quartz vein arrays that average 067°/76°S.

Porphyry mine

A 300m long lenticular body of porphyritic biotite-granodiorite intrudes a parallel shear plane to the east of the main Zuleika Shear Zone at the Porphyry open-pit (Figure 3.5 p.38, Map 3 p.271). The rock is coarse-grained composed of quartz, plagioclase, biotite and hornblende similar to the hornblende-plagioclase porphyry at Hawkins Find open-pit 500m southwest of the Porphyry open-pit (Witt 1992). In thin section, phenocrysts of

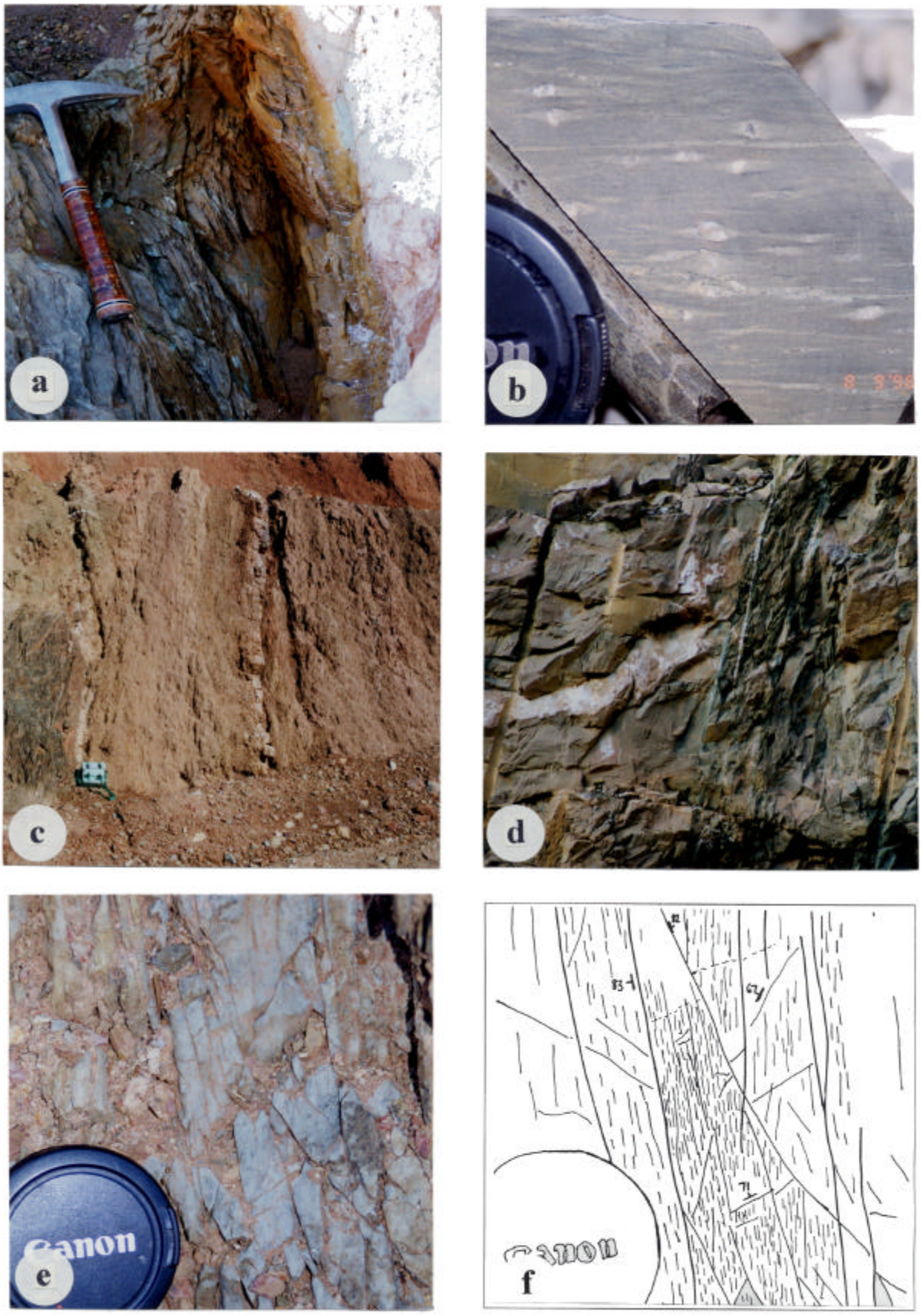

Figure 3.6 - a) Porphyry / ultramafic contact, Anthill open-pit. **b)** Type II S-C mylonite, Bowerbird diamond drill core. **c)** Zuleika Shear Zone in weathered basalt from Bullant open-pit. **d)** Zuleika Shear Zone in fresh basalt from Bullant open-pit. **e)** Multiple brittle fractures in schistose basalt, Bullant open pit. **f)** Line drawing of Figure 3.6e. See text and over-page for explanation.

Captions for figures on page 40 – Zuleika Shear Zone

Figure 3.6a
Photograph of a contact between talc-chlorite ultramafic rocks and intrusive porphyry from Anthill open-pit. The talc-chlorite ultramafic rock is intensely deformed with a disrupted S-C fabric that deviates up to 40° from the normal orientation of the Zuleika Shear Zone. The felsic porphyry contains a weak foliation at a moderate angle to the margins of the body. The contact zone is 5cm wide and in the ultramafic rock shows local thermal effects of intrusion, whilst the felsic porphyry displays a thin zone of reaction, and is discolored from white to tan. The porphyry has forcefully intruded the already sheared ultramafic rocks and a later oblique phase of deformation progressed possibly while the body was in a semi-consolidated state producing the weak foliation. Hammer is 330mm long. Top of photo points north.

Figure 3.6b
Ultramylonite in high-magnesium basalt from Bowerbird. The shear zone contains a pervasive C foliation with left lateral porphyroclast asymmetry. Porphyroclasts (<10%) are survivor fragments of plagioclase feldspar and quartz veins. Thin bands of ribbon quartz traverse the core parallel to the C foliation. A significant degree of flattening is exhibited by porphyroclasts in the bottom of the photo with strongly ellipsoidal shapes. The shear zone trending 123°/80°NE is located at 193.80m in diamond drillhole ZULD8. Lens cap for scale.

Figure 3.6c
Photograph of the Zuleika Shear Zone in pillowed high-magnesium basalt from Bullant open-pit. The shear zone is 5 metres wide and continues off to the right of the photo. A well-developed S-C fabric is prominent in the strongly weathered basalt, and the intensity increases towards the contact marked by the camera bag. At hand specimen scale the shear zone flakes easily into centimetre-size sigmoid-shaped lithons of rock formed from breakage along the intersection of the S-C planes. Large 20-30cm quartz veins are parallel to the shear zone and show weak stretching and boudinage effects indicating either minor movement on the shear zone after vein formation, or that dilatency occurred very late in the movement history. Camera bag is 200mm wide. View is looking south-east.

Figure 3.6d

Photograph of the Zuleika Shear Zone in pillowed high-magnesium basalt from Bullant open-pit. The shear zone is developed in fresh rock at the base of the pit and is a smaller parallel structure west of the main shear in 3.6c. The zone is 30cm wide and displays a well-developed C-plane trending top to bottom. The S-plane is also well developed trending top right to bottom left in between the C-planes. Thin quartz veins display minor stretching and boudinage parallel to the C-plane. Relatively undeformed-pillowed basalt has sharp contacts with the shear zone boundary. Base of photo is 1.5m wide. View is looking NW-SE.

Figure 3.6e
Brittle fractures cross-cutting schistose high-magnesium basalt in Bullant open-pit. Four distinct fracture sets are present, one set is parallel to the shear direction 155°/83°W (up the page) and the other three cross-cut obliquely 167°/67°W, 134°/82°E and 025°/71°N. The thoroughgoing fractures are parallel to the shear direction and these cross-cut the higher angle fractures, indicating that high angle fractures formed first with progressive overprinting by shallow angle fractures. The fractures are from a 4m wide ductile shear zone and as such may be considered as Riedel fractures since they are brittle in nature and are totally confined within the zone of simple shear with the correct timing sequence of development. An interpretation of the structures as Riedel fractures implies that the fractures developed with simple shear displacement on the ductile shear zone possibly at a time when the dominant mode of deformation was more brittle. The photo is looking down onto a horizontal surface, top points towards 335°. Lens cap is 55mm diameter.

Figure 3.6f
Line drawing of photograph in 3.6e showing fabric detail and overprinting relationships.

plagioclase are set in a fine groundmass of saccaroidal-textured plagioclase and quartz (Figure 3.11a-b p.47). Weak silica-albite alteration is widespread with recrystallised biotite pseudomorphing amphibole forming a well-developed tectonic foliation with irregular trend, pervasive throughout the rock (Figure 3.7). Fine-grained dyke-like phases of the porphyry up to 4m thick, are also foliated and have sharp schistose contacts against the coarser grained rock with a 2-3cm reaction halo. The finer grained porphyry clearly postdates the coarse-grained rock, but a similar foliation in each suggests a common deformation history. Sheared talc-chlorite ultramafic rocks at the boundaries of the body are contact metamorphosed to coarse-grained random-textured biotite schist, and display irregular folding with ductile shearing textures similar to fabrics observed at Anthill open-pit.

Schistosity in the porphyritic biotite-granodiorite at the Porphyry mine trends irregularly with wide variability in strike and dip. The fabric is described as a schistosity since it is defined by metamorphic biotite with a shape-preferred-orientation, but it is not schistose in the sense that coarse-grained micas dominate the rock fabric. Shear zone hosted porphyritic rocks of this type are geochemically related to pre to syn-D2 granitoid domes and late tectonic granodiorite and tonalite (Witt 1992), however the syn-to-post D3 timing suggested by structural relationships may indicate some overlap in the timing of intrusion and the D2/D3 deformation events.

The dominant stretch fabric in the surrounding sheared ultramafic rocks is predominantly sub-horizontal, but in the vicinity of the porphyry contacts, contact metamorphism has produced a randomly oriented fabric of acicular amphiboles and coarse-grained biotite that has destroyed the original shear fabric. Late shear surfaces in the ultramafic rocks defined by quartz and calcite have overprinting slip lineations that vary from 20°S to 65°N.

Bowerbird mine

At the Bowerbird mine, the Zuleika Shear Zone is 100m wide with an average orientation of 157°/74°SW (Figure 3.5 p.38, Figure 3.8). The shear zone cross-cuts intermediate volcaniclastic rocks, cherty sedimentary rocks, felsic porphyry, mafic volcanic rocks and ultramafic komatiites. The distribution of the different lithotypes is erratic with interleaving of all five rock-types over a 20m interval in diamond drillhole ZULD8.

Porphyry mine

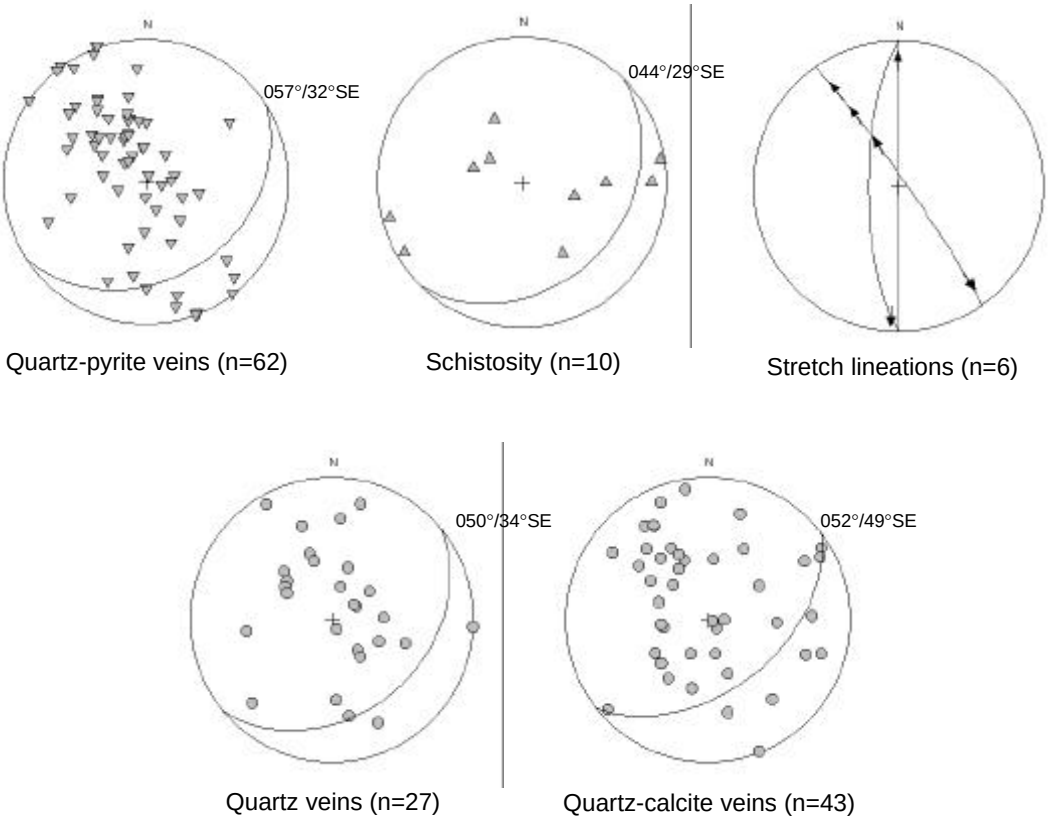

Figure 3.7 – Equal area stereograms of structural elements from Porphyry mine. Orientations are for average great circles to the major clusters, with number of measurements (n). Data measured from diamond drill core and open pit mapping. All stereograms in this thesis are lower hemisphere projections.

Bowerbird mine

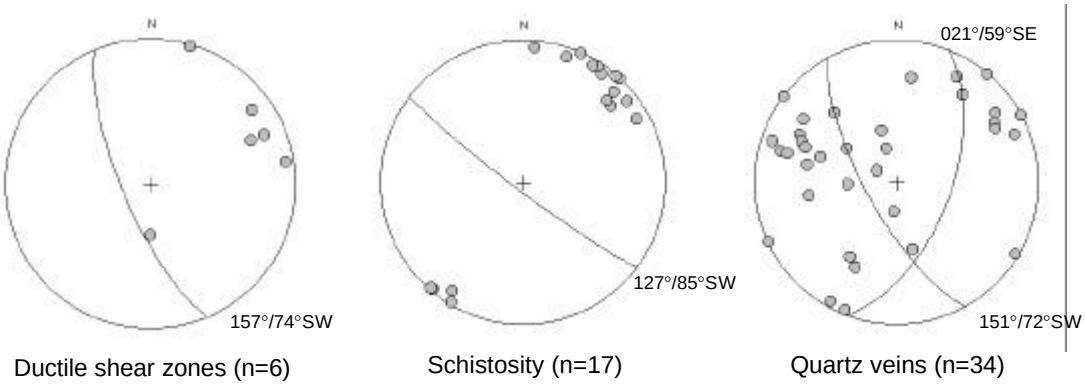

Figure 3.8 – Equal area stereograms of structural elements from the Bowerbird mine. Orientations are for average great circles to the major clusters, with number of measurements (n). Data collected from diamond drill core and open pit mapping.

Wallrocks to the east of the shear zone are strongly foliated with flattened leucoxene and biotite crystals. The foliation grades into discrete 1m wide zones of orthomylonite in intermediate volcaniclastic rocks, characterised by porphyroclasts of plagioclase and coarse-grained crystal-lithic tuff in a fine-grained matrix. Ultramylonite (50m wide), forms the most intense portion of the shear zone with ribbon quartz and asymmetric porphyroclasts. The shear zone is classified as a type II S-C mylonite (Lister and Snoke 1984), and the porphyroclasts are classified as sigma-type (Simpson 1986). Porphyroclast asymmetry indicates left-lateral offset (Figure 3.6b p.40) in sections parallel to the stretching lineation and orthogonal to the foliation. The western part of the shear zone contains interleaved felsic porphyry, mafic volcanic rocks and interflow sedimentary rocks. Sheared felsic porphyry contains previously sheared wallrock fragments of mafic volcanic and ultramafic rocks. The felsic porphyry occurs near a mafic volcanic/ultramafic contact that can be correlated with a similar stratigraphic position to the south at Wattlebird open-pit. The shear zone continues west into ultramafic komatiite but the intensity of shearing decreases across a contact with moderately brecciated pillow basalt.

Wattlebird mine

At the Wattlebird mine, the Zuleika Shear Zone trends 142°/83°SW (Figure 3.9), and is developed at a contact between brecciated talc-chlorite altered komatiite and fine-grained pillow basalt to the west (Figure 3.5 p.38, Maps 4-5 p.277-278). Thin bodies of felsic porphyry intrude the ultramafic rocks, and relict spinifex texture is common in centimetre-scale pods of deformed komatiite that are surrounded by intensely sheared talc-chlorite ultramafic rocks. Pillow basalt has round pillow shapes in the wallrocks of the shear zone, and the basalt is strongly altered to muscovite and calcite. Muscovite forms a penetrative schistosity in the basalt trending 142°/88°SW (Figure 3.9), with increased intensity towards the shear zone. A 5-15m thick mylonite zone marks the main Zuleika Shear Zone at the basalt/ultramafic contact. The contact is a 10m-wide zone of interleaved basalt and ultramafic rocks with chlorite-biotite +/-talc alteration. The margin of the shear zone in the ultramafic rocks is a sharp boundary between talc-chlorite mylonite and clast supported breccia with flattened elongated breccia clasts of ultramafic rock (Figure 3.20f p.65).

In thin section, the shear zone has a well-developed S-C fabric defined by chlorite and talc. A sample taken from the centre of the shear zone, (ZSZ-1) shows fabrics at a

Wattlebird mine

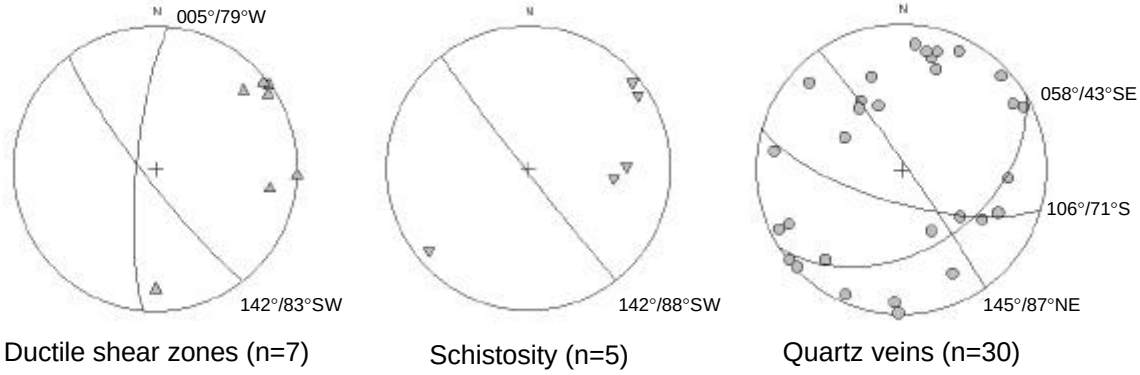

Figure 3.9 – Equal area stereograms of structural elements from Wattlebird mine. Orientations are for average great circles to the major clusters, with number of measurements (n). Data collected from diamond drill core and open pit mapping.

Bullant mine

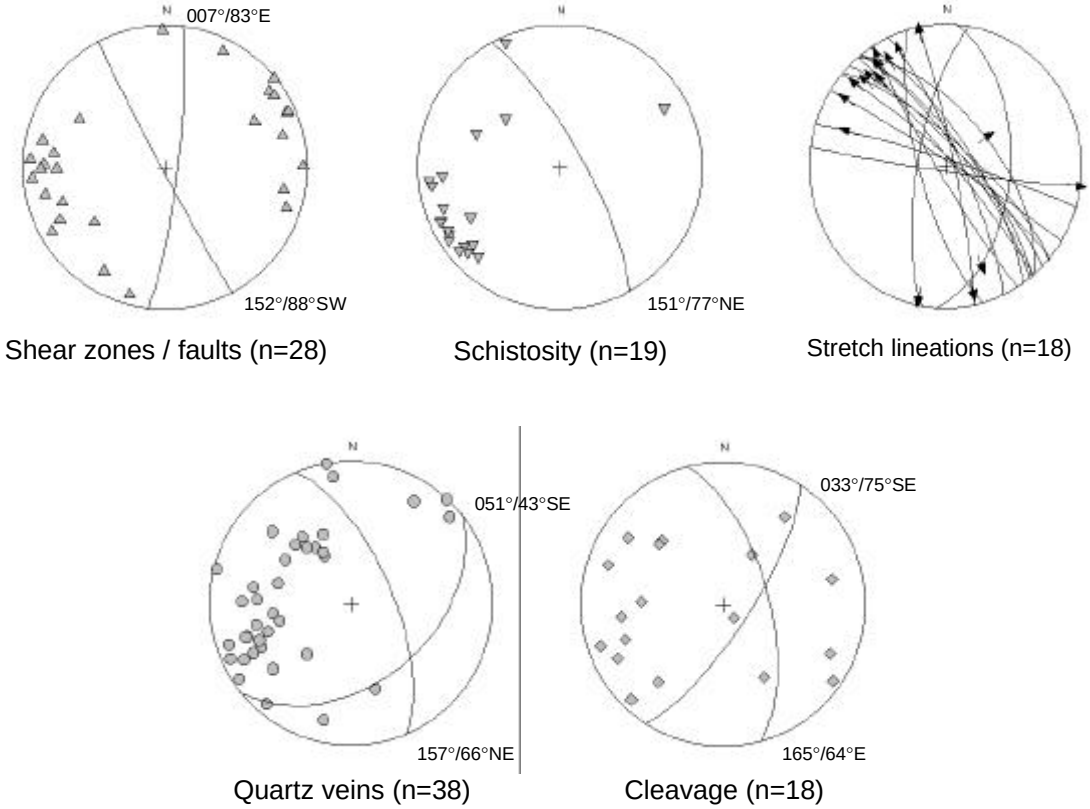

Figure 3.10 – Equal area stereograms of structural elements from Bullant mine. Orientations are for average great circles to the major clusters, with number of measurements (n). Data measured from diamond drill core and open pit mapping.

microscopic scale that emulate the interleaving of mafic and ultramafic rocks at the mesoscopic-scale (Figure 3.11c-d). The C planes of the shear zone are defined by chlorite with subordinate amounts of talc and calcite. S planes also are defined by chlorite, parallel to a weakly developed schistosity. C-plane cleavage domains account for about 40% volume of the rock and are smoothly anastomosing with a sharp transition to microlithon domains. Irregular-shaped clusters of talc overprint the chlorite C planes, but are optically continuous with them. Talc grains are poorly defined, yet individual grains are visible from divergent cleavage traces from grain to grain (Figure 3.12 p.49). Talc displays little or no intracrystalline deformation indicating almost total replacement post-dating deformation, and may indicate that this talc is a product of retrogression.

Microlithons are lens-shaped, up to 2mm long, composed of fine-grained quartz and chlorite (Figure 3.12 p.49). Quartz-rich microlithons are mostly strain-free with weak undulose extinction in about 30% of grains. The remainder is recrystallised with high-angle quartz grain boundaries pegged against chlorite in the surrounding cleavage domains. The microlithons are asymmetric, partially defining the left-lateral S-C fabric, and may be remnants of high magnesium basalt tectonically interleaved with ultramafic rocks. Calcite veins in the rock are up to 3mm-thick forming asymmetric porphyroclasts, or distended, isoclinal intrafolial folds with minor pinch-and-swell texture. The veins are composed of strain-free recrystallised calcite and ankerite, with 120° dihedral angles in highly deformed veins indicating significant post-deformation recovery. Nucleation microstructures of quartz growing at calcite triple-junctions, and irregular quartz grain-boundaries with 120° dihedral angles, indicate dynamic recrystallisation of the fabric. In most cases, the veins are parallel to the shear fabric, but also are disrupted by it. Syn to late-tectonic porphyry intrusion may have induced localised thermal recovery of the deformation fabrics.

Bullant mine

The Zuleika Shear Zone at Bullant open-pit is represented by a series of 0.5-20m wide zones of ductile shear developed within pillow basalt (Figure 3.5 p.38, Figure 3.6c-d p.40, Map 2 p.266). Ultramafic rocks are not present in the immediate mine area, but have been intersected in drill holes 100m west of the open pit. A series of shear zones spaced at 80-100m trends 152°/88°SW on average (Figure 3.10 p.45). Shallow-moderate plunging

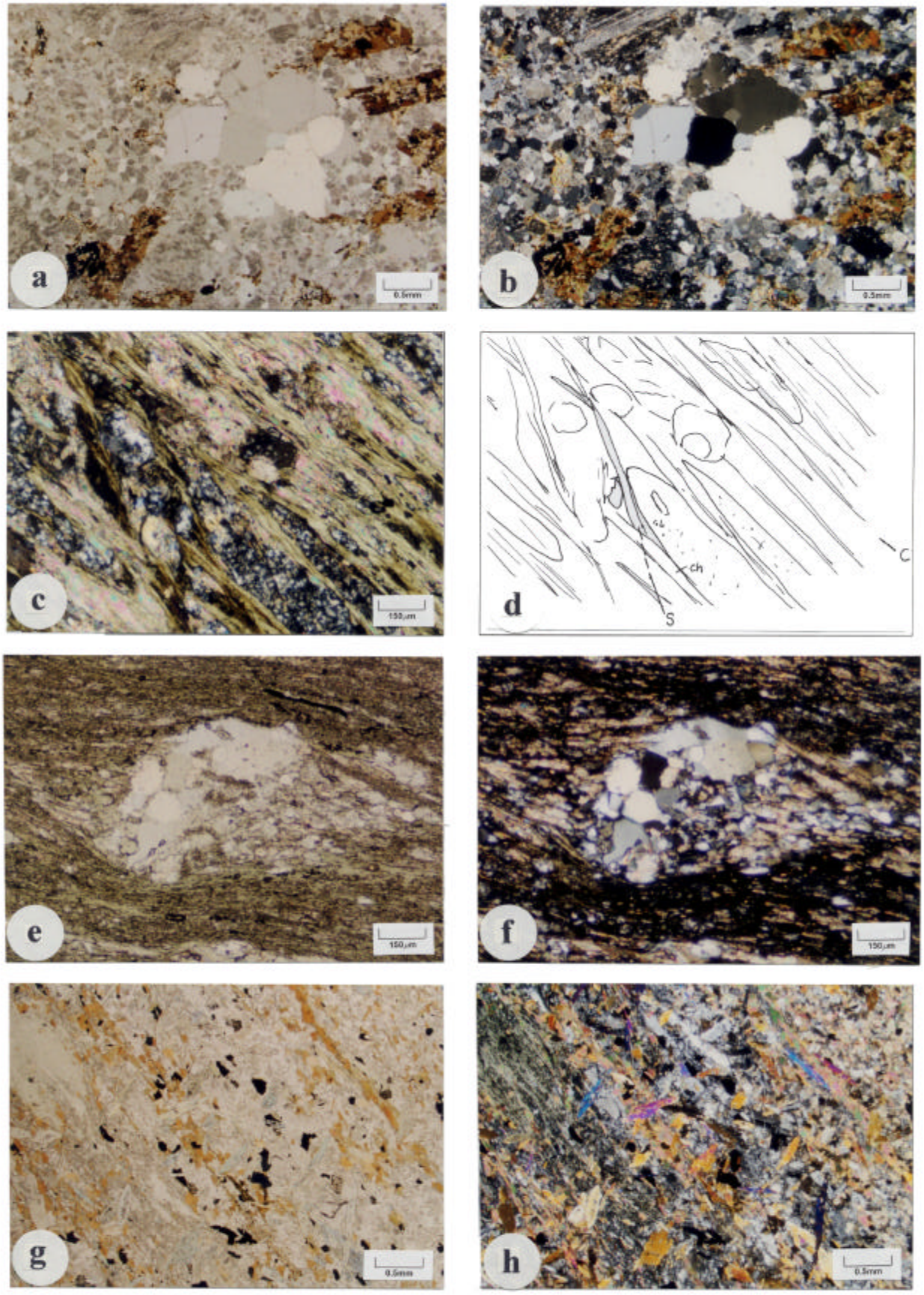

Figure 3.11 – Photomicrographs from the Zuleika shear zone. **a)** Felsic porphyry from the Porphyry mine, (PPL). **b)** Felsic porphyry from the Porphyry mine, (XPL). **c)** S-C fabric in talc-chlorite schist from the Wattlebird mine, (XPL). **d)** Line drawing of c). **e)** Assymetric porphyroclast showing dextral shear sense, from the Bullant mine, (PPL). **f)** Same as for Figure 3.11e), (XPL). **g)** Hydrothermal biotite forming the shear zone fabric, (PPL). **h)** Same as for Figure 3.11 g), (XPL). See text and over page for explanation.

Captions for figures on page 47

Figure 3.11a
Photomicrograph (PPL) of felsic porphyry from the Porphyry mine. Phenocrysts of rounded quartz and subhedral plagioclase are set in a fine-grained groundmass of saccaroidal textured quartz. Hydrothermal biotite pseudomorphs original hornblende. Sample is from 31.0m in diamond drill hole ZULD10.

Figure 3.11b
Sample as for Figure 3.11a), (XPL).

Figure 3.11c
Photomicrograph (XPL) showing S-C fabric in talc-chlorite ultramafic rock from the centre of the Zuleika Shear Zone. Films of chlorite and talc define both the S and C planes, and wrap microlithons of quartzofeldspathic material. The quartzofeldspathic material may be remnants of mafic rocks that are interleaved with ultramafic rocks in the shear zone. Sample trending 146°/84°NE is from the eastern wall of the Wattlebird south pit. ZSZ-1.

Figure 3.11d
Line drawing of the fabric relationships in Figure 3.11c).

Figure 3.11e
Photomicrograph (PPL) of an asymmetric porphyroclast in a N-S trending shear zone from the Bullant mine. The porphyroclast is a quartz vein fragment composed of strain-free recrystallised quartz grains. Quartz and calcite form pressure shadow beards around the vein fragment with asymmetry indicating dextral movement sense. Chlorite and calcite form a strong shear foliation that partially wraps the porphyroclast. Recrystallisation of the quartz indicates a degree of post-deformation recovery. A fire assay value of 0.05 g/T Au was returned for this sample. Sample trending 008°/68°E is from 209.3m in diamond drill hole ZULD9.

Figure 3.11f
Same view as for Figure 3.11e), (XPL).

Figure 3.11g
Photomicrograph (PPL) of ductile shear fabric in the Zuleika Shear Zone at the Bullant mine. Euhedral biotite forms a spaced cleavage parallel to the shear direction and smaller disseminated grains of biotite, feldspar and chlorite form the general fabric. The shear fabric is overprinted by randomly oriented actinolite indicating that peak metamorphism post-dates the shearing, and an earlier retrograde metamorphic event defined by chlorite. A fire assay value of 2.51 g/T Au was returned for this sample. Sample trending 138°/72°NE is from 202.4m in diamond drill hole ZULD9.

Figure 3.11h
Same view as for Figure 3.11g), (XPL).

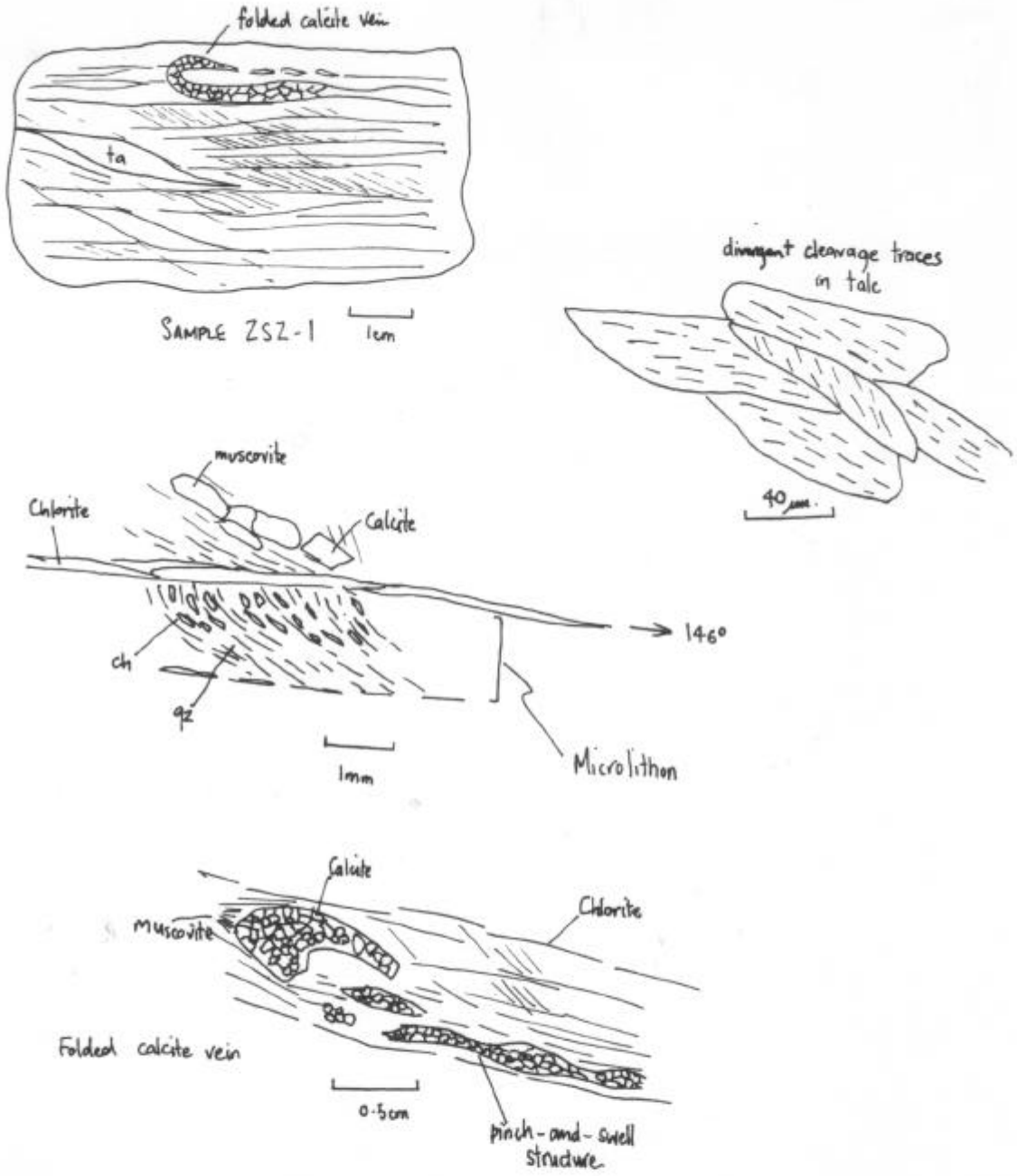

Figure 3.12 – Sketches of microfabrics from the Zuleika Shear Zone. Examples are from sample number ZSZ-1 from the Wattlebird mine.

stretching lineations in the C-plane of the shear zone indicate dominantly strike-slip movement (Figure 3.13a-b), with left-lateral offset displayed by S-C fabric asymmetry. Quartz veins are common in the plane of the shear zone trending 157°/66°NE, and cross-cutting the schistose fabric with an average trend of 051°/43°SE (Figure 3.10 p.45). Shearing-parallel quartz veins display pinch-and-swell morphology, whereas later veins are simple fracture-infill veins with non-directional controlled quartz addition textures (Vearncombe 1993) and triangular textures (Taylor 1992) displayed by hydrothermal biotite and chlorite.

An ENE-WSW trending brittle-ductile fault cross-cuts the Zuleika Shear Zone in the open-pit, with dextral offset trending sub-parallel to the S foliation. The fault bends into the main Zuleika Shear Zone, but the two may be developed as a conjugate pair (G. Adams, personal communication 1998). The later brittle-ductile fault is sub-parallel to a number of other mapped brittle-ductile faults trending 007°/83°E (Figure 3.10 p.45). Euhedral biotite defines a well-developed schistosity in the main shear zone trending 151°/77°NE (Figure 3.10 p.45) with a high proportion of silica recrystallisation of the groundmass (Figure 3.11g-h p.47). Mylonitisation is characteristic of the shear zone with flattened chlorite and white mica in poorly developed S-C fabrics.

In Bullant open-pit, the Zuleika Shear Zone is cross-cut by a late low-angle reverse fault with sub-parallel strike, that offsets the shear zone across the pit (Map 2 p.226). Spaced cleavage with about 5mm spacing defined by chloritic fractures, cross-cuts the schistose basalt with variable orientations that average 033°/75°SE (Figure 3.10 p.45).

A 4m-wide shear zone in the north wall, contains a series of fractures that may be brittle Riedel-type structures (Figures 3.6e-f p.40). The shear zone has sharp boundaries with weakly deformed basalt and the fractures appear to be contained within the shear zone, but do not extend into the wallrocks. The fractures have cross-cutting relationships with sequential development progressively approaching parallelism with the main shear zone orientation of 155°/83°W.

The detailed fabric of the shear zone in the area of strongest shearing in the pit, displays well-developed S-C fabrics and sharp planar boundaries with the wallrocks (Figure 3.6d

b

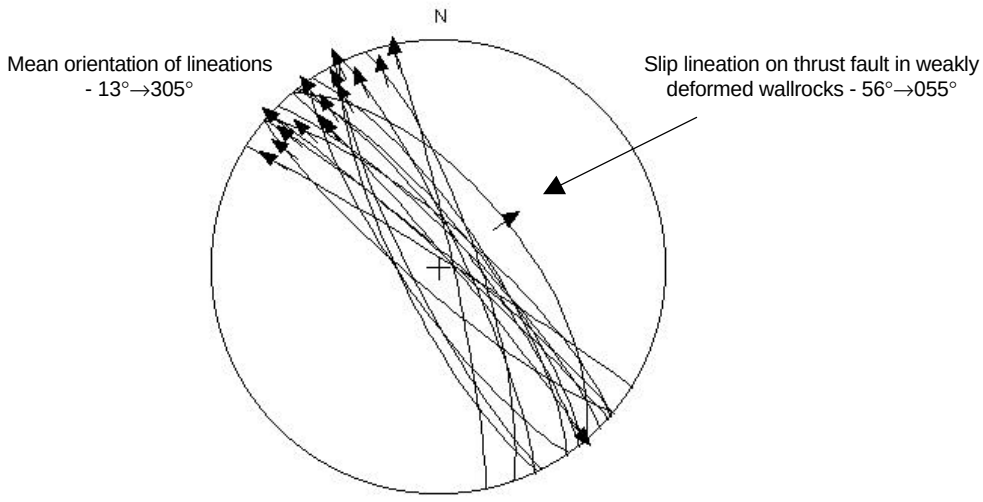

Figure 3.13- a) Photograph of stretching lineation in the plane of the Zuleika Shear Zone. The lineation trending 25°→320° is defined by aligned flakes of biotite and muscovite and quartz rods in the plane of the foliation trending 140°/86°E. **b)** Stereogram of lineations from the Zuleika Shear Zone from Anthill, Porphyry, Wattlebird and Bullant mines.

p.40). Pinch-and-swell quartz veins are common, and are developed parallel with the S-plane of the shear zone. A 20m band of schistosity in the northwest wall has discrete ductile shear zones with greater shearing-intensity spaced at about 5m.

In thin section (sample ZULD9 202.40), the shear fabric is defined by thin trails of hydrothermal biotite and calcite spaced at 1-5mm (Figure 3.11g-h p.47). Elongate flakes of brown biotite form smoothly anastomosing cleavage domains that overprint a fine-grained quartzofeldspathic matrix with up to 500*m*m long plagioclase (albite?) grains. Large un-oriented actinolite crystals up to 3mm long overprint the shear cleavage, indicating that peak metamorphism postdates the D3 shearing. The actinolite has weak undulose extinction in rare examples, but is mostly strain-free with ragged branching ends or euhedral terminations on acicular crystals.

Summary

The Zuleika Shear Zone consists of interlinked thin zones of mylonite that anastomose along strike. Strain is partitioned by rock contacts and anisotropies within basalt flow rocks including pillow margins. There is no evidence that major offset occurs across the shear zone and its location primarily at rock contacts suggests that the shearing may be a result of competency contrast between (previously) competent, olivine-rich ultramafic rocks and less competent basalt. The highly incompetent state of the ultramafic rocks seen today is a result of fluid movement through the shear zone and retrogression of the olivine during later shearing.

The shear zone was intruded by felsic porphyry bodies that appear to be mostly syn-late tectonic since cross-cutting relationships show both wrapping and truncation of the foliation. Felsic porphyries are most abundant in the Porphyry mine area where the ultramafic rock units are thickest indicating preferential intrusion into weak ultramafic schists. No logical source for the felsic porphyries is located in the vicinity of Zuleika, which is probably at depth. Randomly oriented actinolite overprinting the shear zone fabric indicates a post-D3 timing of peak metamorphism that may be related to the late porphyry intrusion.

A predominant sub-horizontal principal stretch direction is manifest as lineations, and elongate basalt pillows and ultramafic clasts, with no evidence of earlier dip-slip movement. S-C fabrics indicate left-lateral movement, but the amount of displacement may be negligible. The Zuleika Shear Zone is adequately exposed for analysis of its morphology and structural relationships, yet an appreciation of the broad structure and distribution of ductile deformation is hindered by poor surface exposure.

3.3.3 Brittle-ductile fault network (D4)

Late-tectonic brittle-ductile faults are ubiquitous throughout the Zuleika area and the Ora Banda Domain. The faults are interpreted from aeromagnetic imagery, ground-truthed in outcrop and drilling, and form a pervasive network that cross-cuts most other structures and all rock types (Fig 3.2 p.31, Chapter 4 p.86, Figure 4.1, p.87, Figure 4.6, p.100). Previous structural interpretations (Simpson *et al*. 1995; Swager *et al*. 1990) treat the faults as minor, locally developed features that do not persist through major geological and structural contacts, yet aeromagnetic images clearly show the structures extending through stratigraphic sequences over distances of tens to hundreds of kilometres.

The network of lineaments interpreted from aeromagnetic imagery (Figure 3.2 p.31) is divided into three principal structural orientations NE-SW, N-S and E-W (Figure 3.14). The number of NE-SW trending lineaments (n=374) is significantly greater than the other orientations, N-S (n=214), E-W (n=109) (Figure 3.15). A group of NW-SE trending lineaments (n=65) represents the D3 ductile shear zones

The lengths of the lineaments were analysed graphically to show the distribution of structures at a regional scale (Figure 3.15). Although some large features are interpreted (20 km, Zuleika Shear Zone) many lineaments in each of the principal structural orientations are less than 2000m long with most less than 1000m in length. In general, NE-SW and N-S trending lineaments have closer spacing than E-W trending lineaments.

These results indicate that the domain-wide fault network comprises brittle-ductile faults that individually are developed at the mesoscopic scale, but their widespread distribution indicates deformation of a regional extent. Veins, brittle-ductile faults and a poorly developed spaced cleavage cross-cut the Zuleika Shear Zone in most exposures. The late

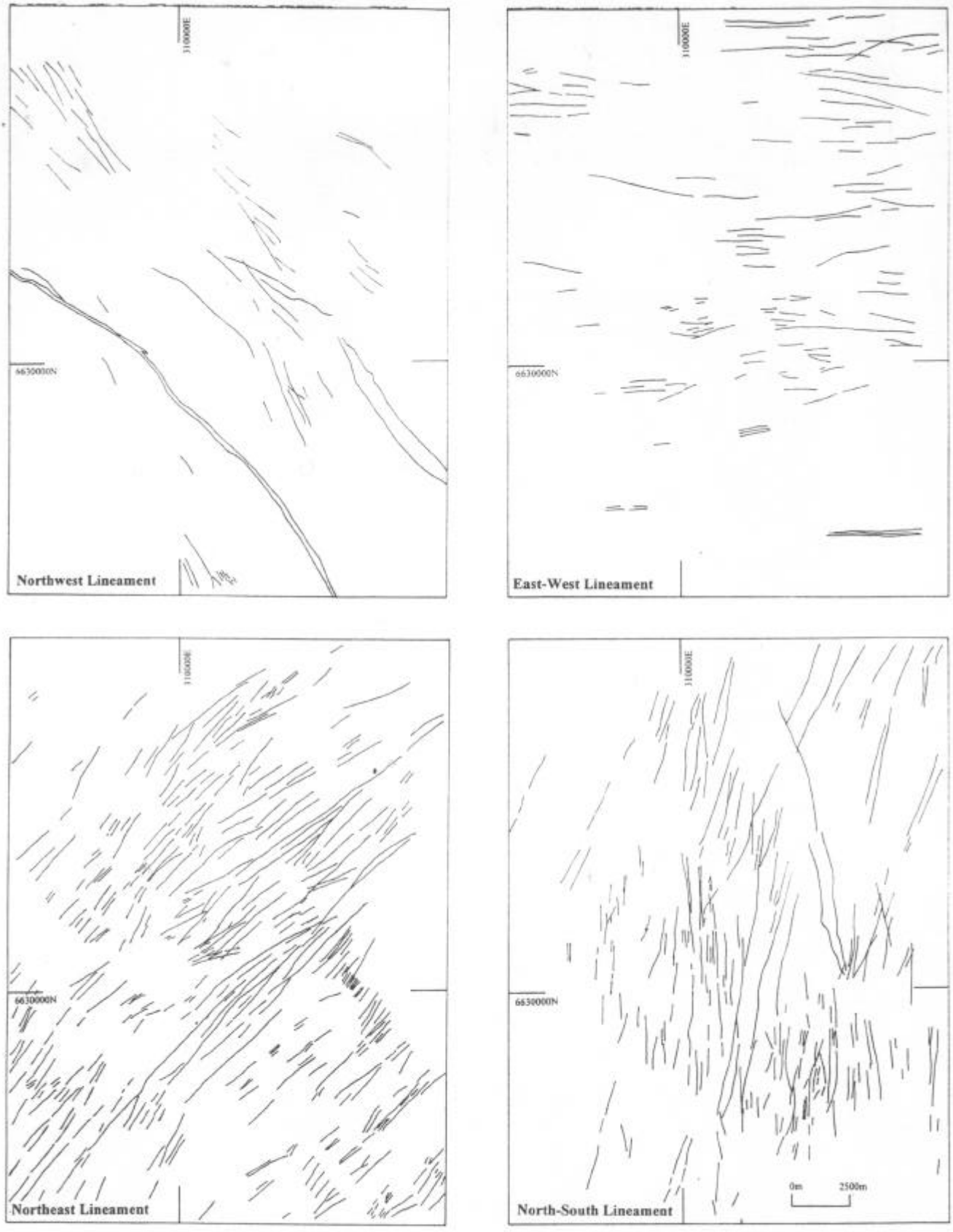

Figure 3.14 – Maps of individual lineaments from each of the four main groups interpreted from figure 3.1. Total lineaments in each group are 65 for NW-SE, 109 for E-W, 374 for NE-SW and 214 for N-S.

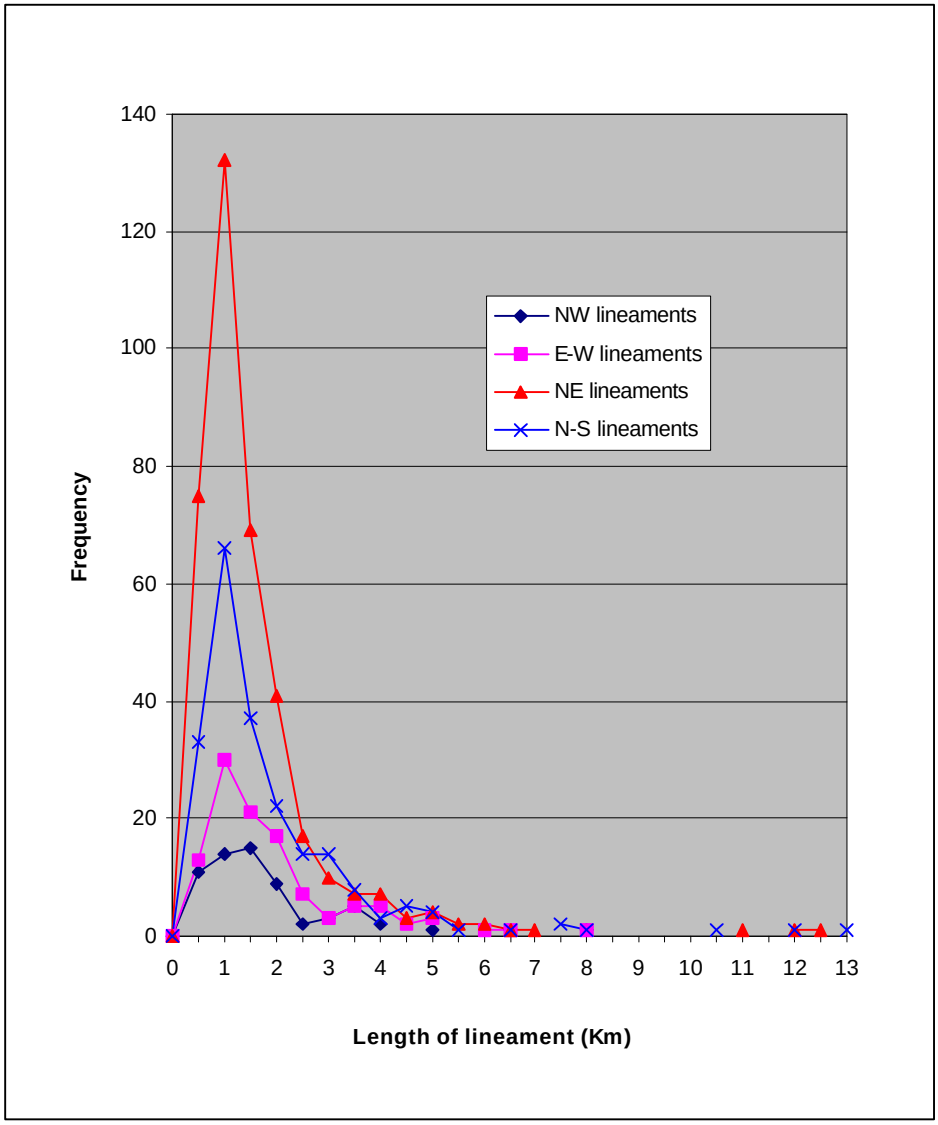

Figure 3.15– Graph of lineament lengths from maps in figure 3.14. The majority of lineaments are less than 2km long in each of the principal structural orientations.

structures have characteristic brittle-ductile textures and in some examples have either completely ductile or completely brittle fabrics.

Anthill mine

At the Anthill mine, brittle-ductile faults trending 134°/73°W cross-cut the main Zuleika Shear Zone with S-C fabrics indicating right-lateral offset (Figure 3.16c, Map 1 p.262). The late faults spaced at 0.5–1.0 metre, are up to 5cm wide and contain 10 to 20mm-thick lensoid quartz veins within parallel shear bands and fracture planes. Since sheared talc-chlorite ultramafic rocks are the dominant rock-type, the late structures developed in the ultramafic rocks have mostly ductile character. Thin lensoid quartz veins trending 067°/76°S cross-cut a weak foliation in felsic porphyry.

Porphyry mine

Structural analysis of diamond drill core from the Porphyry mine reveals three dominant structural orientations for stockwork quartz veins trending 033°/41°SE, 018°/67°NW, and 096°/45°NE (Map 3 p.271). Broadly scattered vein orientations from several drillholes have an average orientation of 057°/32°SE (Figure 3.7 p.43), and late brittle-ductile faults trend 172°/74°W and 044°/29°SE. Quartz veins at the Porphyry mine are usually thin (<5mm wide), simple fracture-sealing veins with displacement-controlled quartz addition textures. Quartz-pyrite is the dominant mineralogy with silica-albite alteration halos, but unmineralised quartz and quartz-calcite veins in fractures are also common. Fracturing of the porphyry body is more prominent in a 15-20m wide band on the western margin. The more fractured western margin may be a separate phase from the eastern part of the body (Map 3 p.271).

Bowerbird mine

Brittle-ductile features at the Bowerbird mine comprise mostly brittle-style comb-textured quartz veins that cross-cut the mylonitic shear fabric at a high angle. These veins are comb-textured with quartz fibres at a high angle to the vein walls or have recrystallised fabrics. Cataclastic textures are not observed.

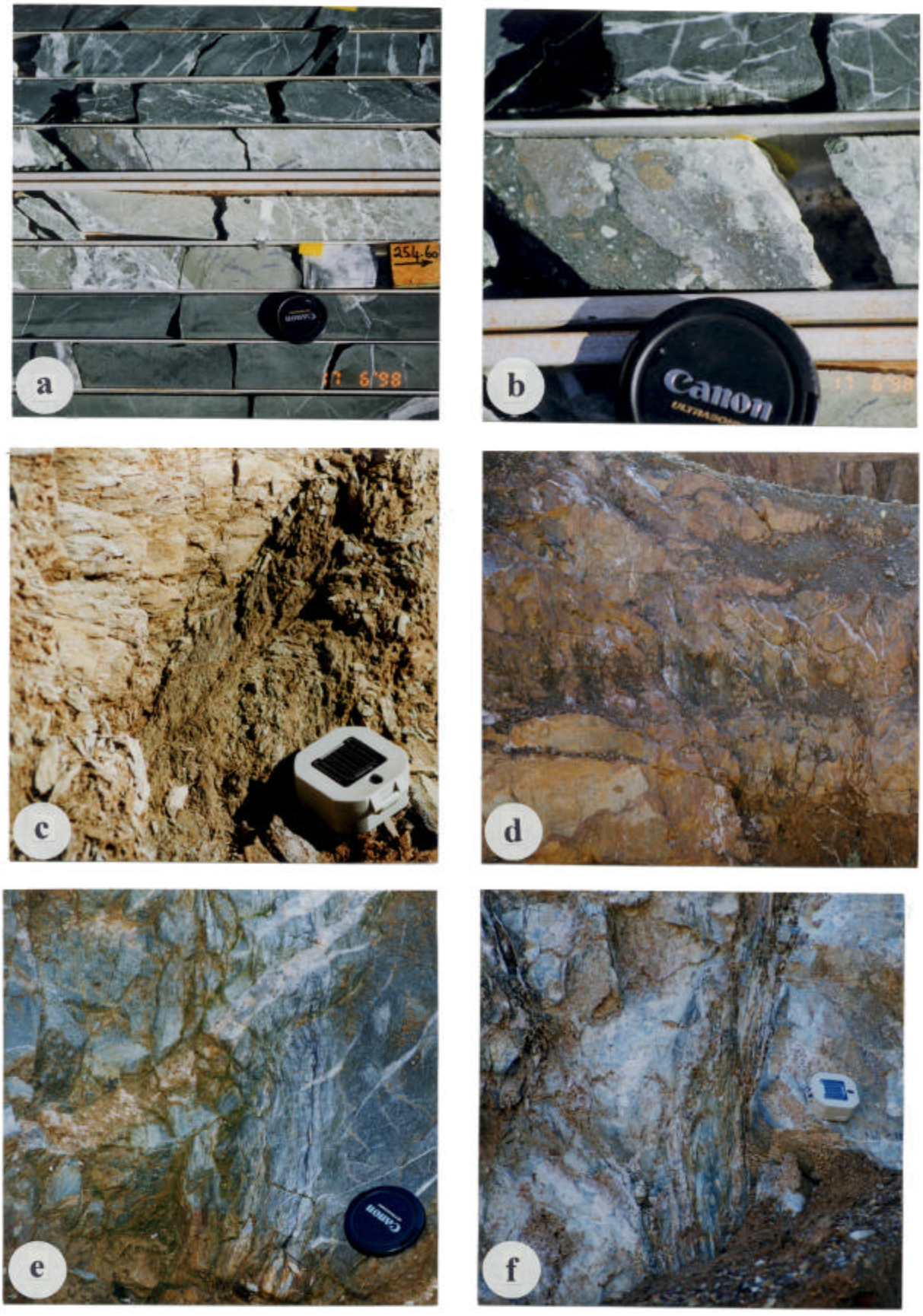

Figure 3.16 - a) Breccia zone with localised cataclasite and fault gouge crosscutting Zuleika Shear Zone, Bullant diamond drill core. **b)** Close-up of fault gouge from Figure 3.16a. **c)** Late ductile shear band cross-cutting Zuleika Shear Zone, Anthill open-pit. **d)** Quartz vein array, Wattlebird open-pit. **e)** Quartz vein array, Wattlebird open-pit. **f)** Oblique brittle-ductile shear zone on pillow margin, Bullant open-pit See text and over-page for explanation.

Captions for figures on page 57 – Brittle-ductile faults

Figure 3.16a
Brittle fault zone cross-cutting ductile fabrics related to the Zuleika Shear Zone. The fault zone is a markedly altered zone with intense muscovite-calcite alteration retrogressive after chlorite in high-magnesium basalt. Brittle fabrics include random fault breccia with cementation by hydrothermal precipitates, jigsaw puzzle textures with net-veined breccia morphology and random fault gouge with a high degree of milling of fragments and rolling of clasts. Large fragments of relatively undeformed but highly altered basalt separate zones displaying these textures. The fault trending 028°/70°SE is located at 252.30m in diamond drillhole ZULD18. Downhole direction is to the right, Lens cap is 55mm diameter.

Figure 3.16b
Close-up of fault gouge zone from 3.16a. The zone is 90mm wide and typified by cataclastic texture with several overprinting stages of cataclasis and brecciation followed by variable milling of the clasts. Zones of re-cementation of the breccia clasts occur around thin quartz-carbonate veins. Four types of clasts are present; angular to sub-rounded white-mica-altered schistose basalt, elongate rounded pyrite fragments up to 30mm long, clasts of several matrix generations (green chlorite-pyritic, dark grey pyritic and light grey pyritic), and chlorite-epidote? altered mafic. The variety of clasts of matrices to earlier failure events indicates a complex episodic movement history for the structure with several events related to mineralisation. Movement sense is undetermined at x10. A gold value of 0.21 ppm Au was returned for the fault, Lens cap is 55mm diameter.

Figure 3.16c
Photograph of an oblique brittle-ductile fault that cross-cuts penetrative schistosity in talc-chlorite ultramafic rock from Anthill open-pit. The late structure trends 134°/73°W, S-C fabric indicates right-lateral offset. The Zuleika Shear Zone trending 345°/89°W can be seen as a flat surface parallel to the plane of the photograph truncated against the C-plane of the late fault. Compass is 70mm square. View is looking west-southwest.

Figure 3.16d
Photograph of a late quartz vein array that cross-cuts the Zuleika Shear Zone from Wattlebird south-pit. The veins in the array trend parallel to the veins in Figure 5.3b but the array in total trends N-S. The quartz veins are less than 200mm thick and appear sigmoid in cross-section. Veins in the array do not have individual alteration halos but the wallrocks are pervasively altered to white-mica-carbonate in close vicinity of the Zuleika Shear Zone. The quartz vein array is 5-10m wide. View is looking NE-SW, long axis of the photograph is parallel to the Zuleika Shear Zone (north-west trend).

Figure 3.16e
Photograph of a quartz vein array that cross-cuts a discrete ductile shear zone from Wattlebird south-pit. The structures are developed in moderately schistose high-magnesium basalt. The ductile shear zone is a thin shear parallel to the main Zuleika Shear Zone to the east. Ductile fabrics include a strong shear foliation defined by slivers of chlorite interspersed with zones of highly schistose basalt and stretched elongated quartz veins. Parallel quartz veins form an array with average orientation 043°/45°S that cross-cuts the ductile shear zone. Dominantly brittle in character, the veins fill planar fractures with sharp boundaries against the fabric of the Zuleika Shear Zone. Lens cap is 55mm diameter. View is looking NW-SE.

Figure 3.16f
Photograph of an oblique brittle-ductile fault in strongly altered pillow basalt from Bullant open-pit. The shear zone 100mm wide, trends 010°/73°W with a well-developed slip-lineation plunging 9°→185° indicating dominantly strike-slip movement with a minor reverse component. The fabric of the fault is characterised by stretched elongate fragments of basalt and vein quartz, sharp boundaries and lack of a parallel planar fabric in the wallrocks, indicating strain partitioning into the plane of the shear zone. The brittle-ductile fault is localised along a pillow margin in high-magnesium basalt. Compass is 70mm square. View is looking north.

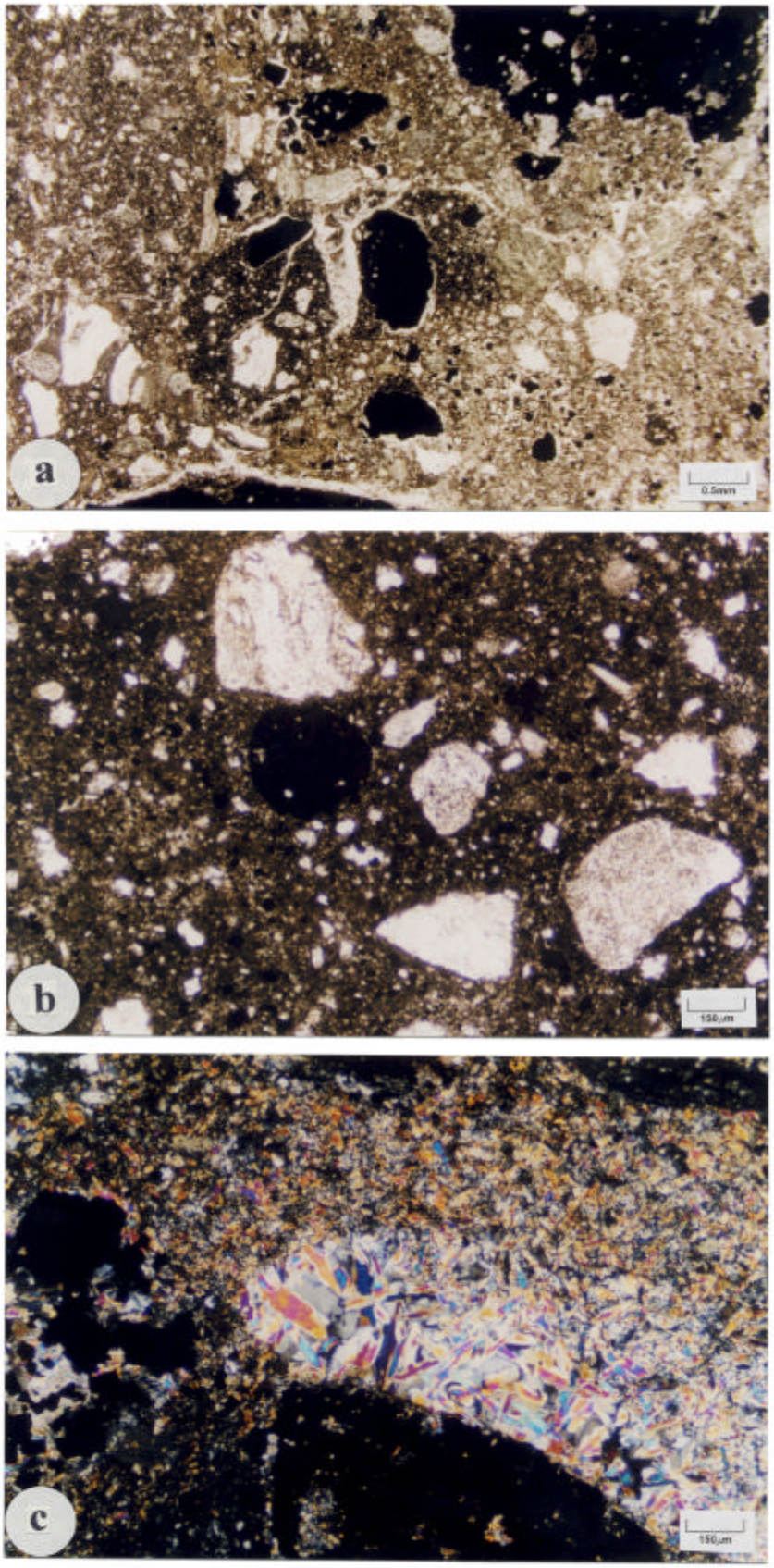

Figure 3.17 - a), b) Photomicrographs of polylithic, cataclastic breccia, from the fault in Figure 3.16b (PPL). Isotropic fragments are massive pyrite clasts. The fault shows a wide range of clast sizes and variable angularity of clasts in matrix supported breccia. **c)** Photomicrograph of a void in the rock, filled with euhedral prehnite (XPL). All photomicrographs from 252.3m in diamond drill hole ZULD18. See text for explanation.

faults group into three orientations with structural style and dimensions that are significantly different to the regional shear zones. Cross-cutting relationships indicate that the faults are later than the Zuleika Shear Zone with textural differences suggesting an increased strain rate or a crustal level different to that for the D3 shearing event.

3.4 REGIONAL MECHANICAL ANALYSIS

Three main episodes of shortening are evident in the Zuleika district. The following mechanical analysis is an attempt to assess the nature of the deformations that produced the strain fabrics and to assess possible orientations for the principal axes of strain for each deformation pulse. Mesoscopic data on the rock fabrics are from the Zuleika area only and these may be influenced by their location close to a regional-scale shear zone. Hence similar mechanical analyses are presented in Chapters 4 and 5 to compare principal shortening axes at several scales across the Ora Banda and Zuleika districts.

3.4.1 Regional folding

Folding in the Ora Banda and Zuleika districts is developed at the regional scale with only localised mesoscopic folding. The Kurrawang Syncline and Goongarrie – Mount Pleasant Anticline are close folds with 50° interlimb angles, and the fold geometry suggests a shortening of the crust in a direction orthogonal to the axial traces (Figure 3.18).

3.4.2 Ductile shearing

The Zuleika Shear Zone has been interpreted previously as a strike-slip deformation zone (Hunter 1993; Swager *et al*. 1990), however no significant mismatch of stratigraphic sequence is recorded across it. The location of the shear zone at a stratigraphic contact, and the geometry of wallrock strain markers implicate a deformation history dominated by shortening rather than one of non-coaxial strike-slip shearing.

Strain markers and flow partitioning

Strain is heterogeneously distributed in the Zuleika Shear Zone. The wallrocks of the shear zone contain markers that record a significant flattening component (pure shear) of the

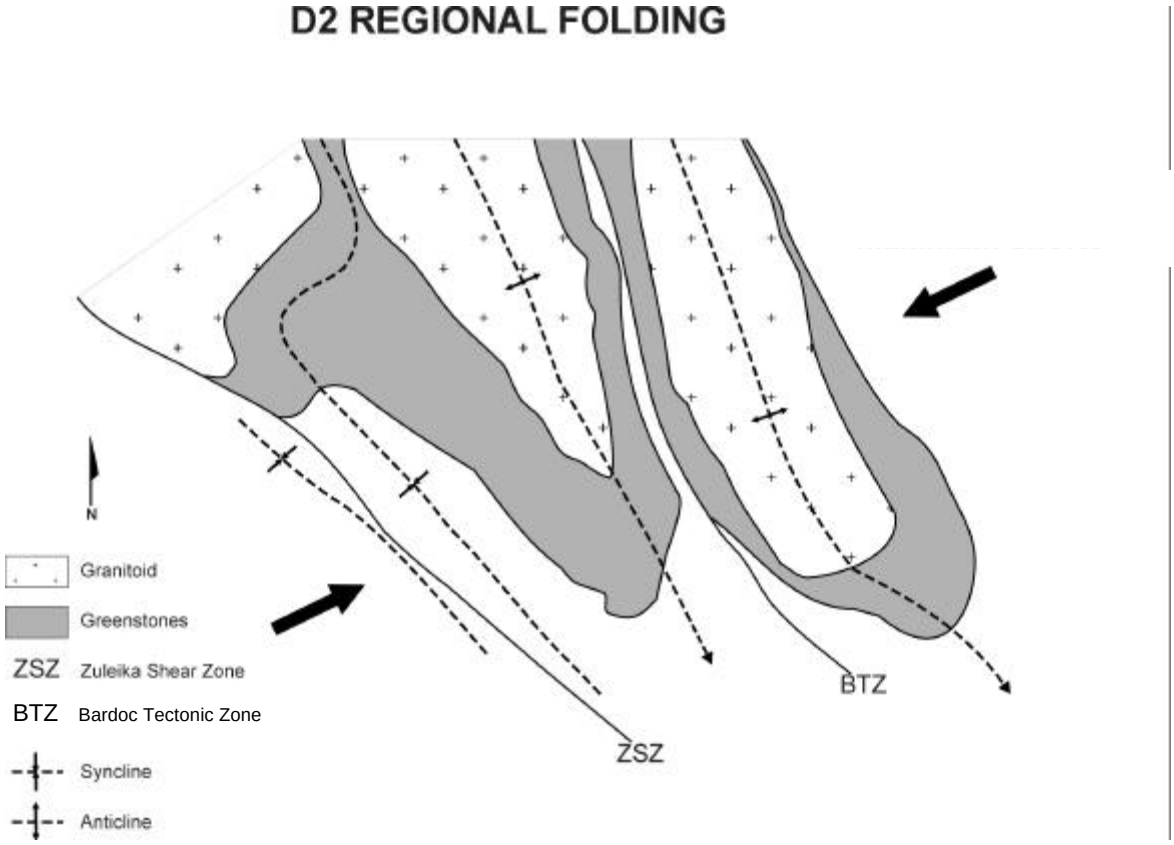

Figure 3.18 – Map of the regional folding pattern in the Ora Banda and Boorara Domains. NW-SE trending fold axes indicate that folding was produced by shortening orthogonal to the axial traces. NW-SE trending regional ductile shear zones trend sub-parallel to the fold axes, and in most cases are located in the synformal areas of the fold belt.

deformation, with the simple-shear component (non-coaxial) partitioned into discrete planar zones. Shear zones are localised mostly along rock unit boundaries but also are slightly transgressive of the contacts. Two types of strain marker at Zuleika, basalt pillow structures and varioles, are used to determine the nature of strain in the wallrocks of the shear zone (Figure 3.19).

Pillow structures in basalt are a primary depositional feature that usually form elongate tubes with long axes sub-parallel to the flow-direction (Compton 1985). Cross-sections perpendicular to the flow direction can have circular pillow shapes, but oblique cross-sections may have a variability of shapes from circular to flattened ellipsoids.

Basalt pillows at the Wattlebird mine display progressive flattening with proximity to the highest strain zone (Figures 3.20 b,c,d). Within 5-10m of the shear zone, previously round basalt pillow structures are ellipsoidal and are progressively flattened and elongated into long thin shapes as the strain increases. The cross-sectional orientation through the pillow structures may not be optimal for a quantitative strain analysis but qualitatively, the amount of flattening increases towards the zone of highest strain (simple shear). A sharp change in the axial ratios of the pillows occurs close to the shear zone indicating that although the immediate wallrock does not contain planar shear fabrics, a significant pure shear component is localised in the vicinity of the non-coaxial shear zone that decreases sharply with distance into the wallrock.

Variolitic texture (Figure 3.20a), is an igneous crystallisation phenomenon formed by spherical shaped clusters of radiating acicular amphibole or plagioclase crystals from mafic magma (Morris 1993). The spherical nature of the varioles means the structure is an excellent strain marker that records the shape of the finite strain ellipsoid, and may provide quanitative data on the component of flattening that accompanied non-coaxial simple shear. Variolitic texture is well-developed in basalt pillow margins, and groups of varioles show flattening strains developed with a common stretching axis orientation (Figure3.19a, 3.20a). Large elliptical centimetre-scale spots with elongate, flattened shapes, occur in the pillow margins of basalt in the Wattlebird north-pit (Figure 3.20e). The spots are interpreted as varioles or ocelli in the margin of the basalt pillows but they have an unusually large size and may be fragments of interpillow breccia.

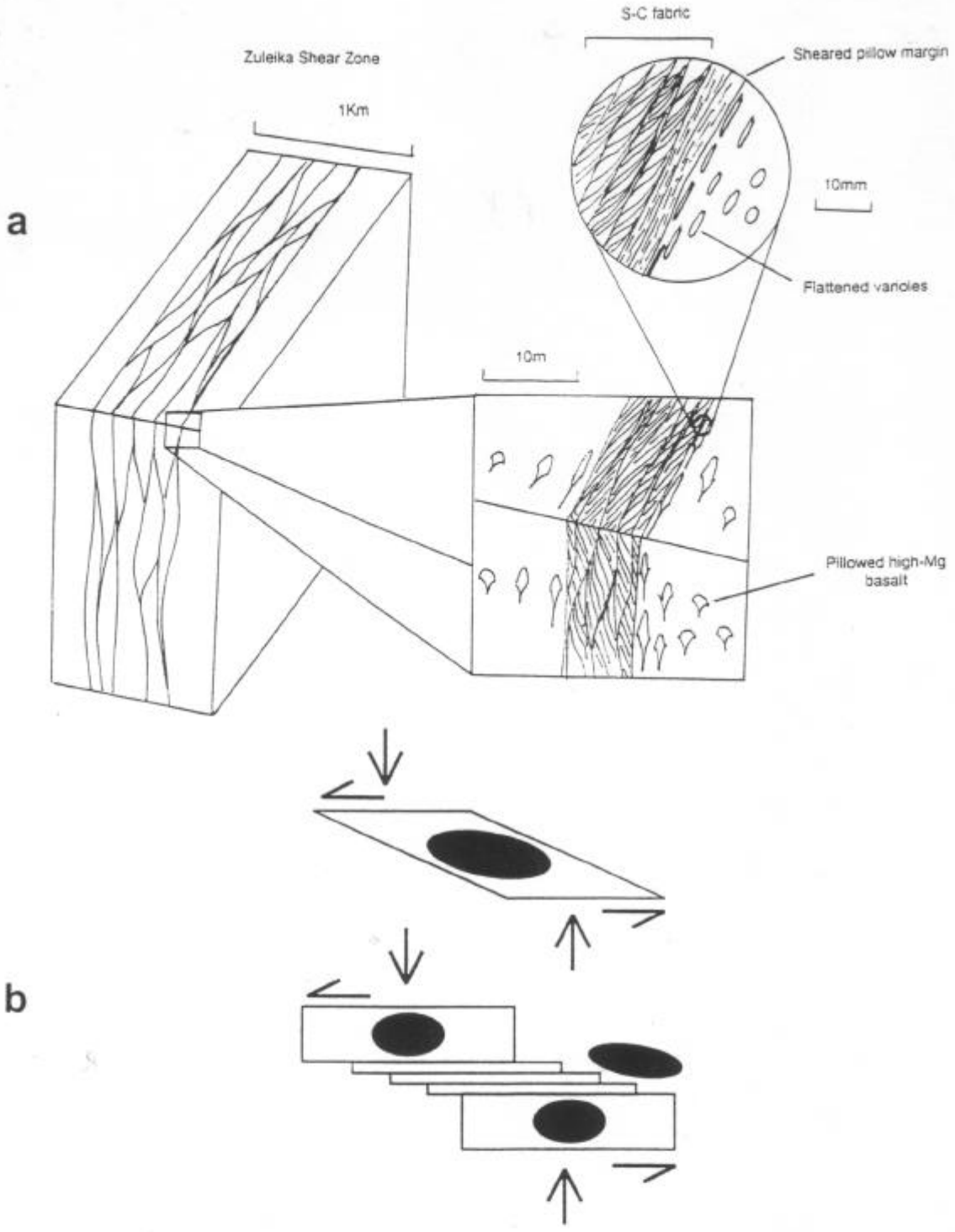

Figure 3.19 – a) Schematic diagram showing the distribution of strain markers in the Zuleika shear zone. A zone of thin shear zones enclosing lithons of weakly deformed rock consists of thin simple shear zones with flattening strains in the immediate wallrocks. b) During deformation the simple shear component of the flow was partitioned into discrete planar zones with flattening strains in the surrounding wallrocks. The relationship is typical of strain partitioning (modified from Hanmer and Passchier 1991).

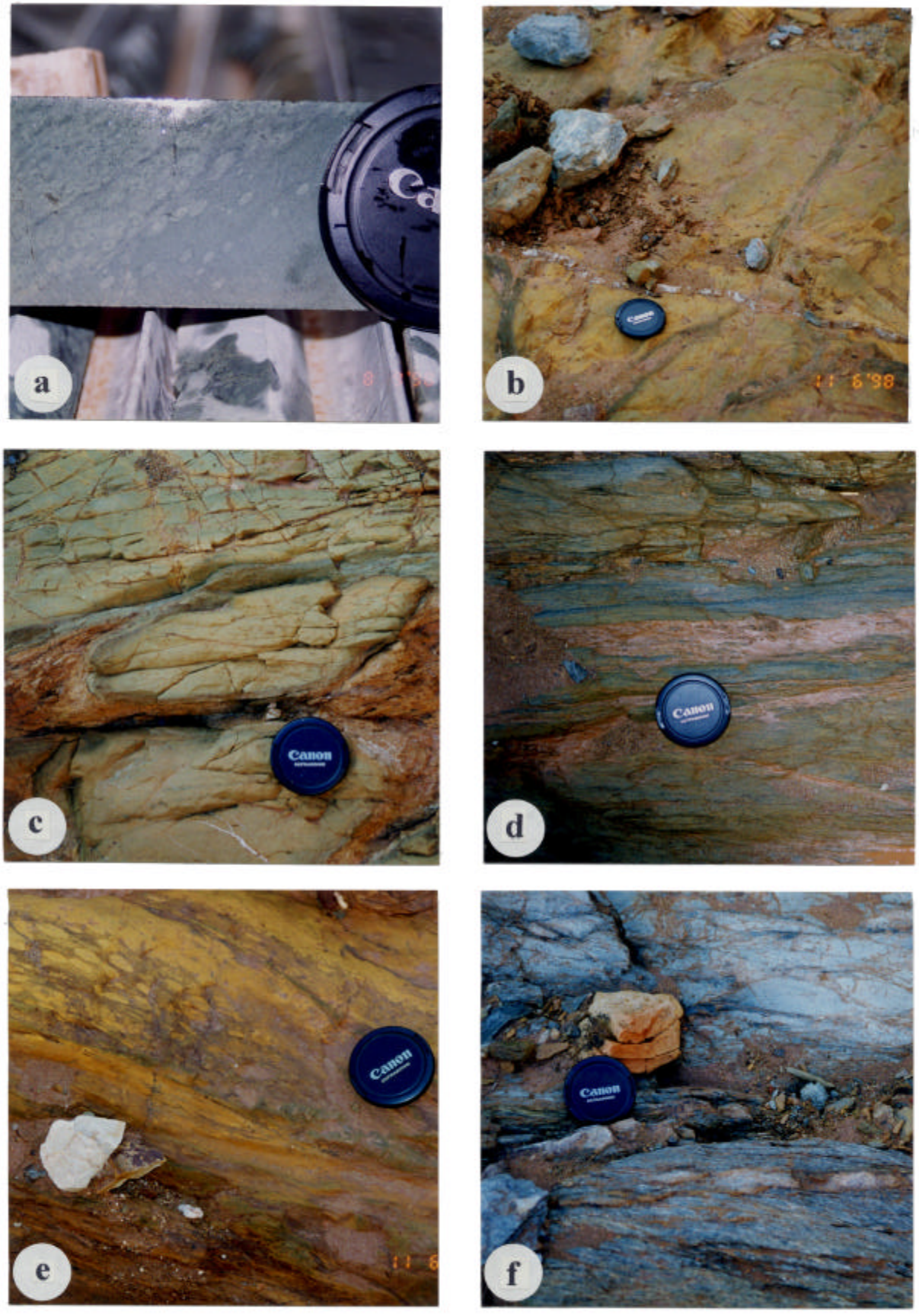

Figure 3.20 - a) Flattened varioles in high-magnesium basalt, Bullant. **b), c), d)** Basalt pillow margins from Wattlebird open-pit showing increasing degrees of flattening strain. **e)** Strained varioles / interpillow breccia material, Wattlebird north-pit. **f)** S-C mylonite / flattened ultramafic breccia contact, Wattlebird open-pit. See text and over-page for explanation.

Captions for figures on page 65 – Strain markers

Figure 3.20a

Flattened variolitic texture from a pillow margin in high-magnesium basalt, Bullant. The structure is a useful strain marker since varioles are spherical igneous crystallisation phenomena. Varioles when viewed in the correct orientation give the shape and orientation of the finite strain ellipsoid at the final stage of the deformation. The shapes of variolitic structures indicate a significant flattening component of the deformation orthogonal to the Zuleika Shear Zone. Sample is at 369.30m in diamond drillhole ZULD2.

Figure 3.20b, c and d

Series of photographs of pillow margins in high-magnesium basalt from Wattlebird south-pit. The pillow margins are zones of high chlorite concentration in strongly white mica-carbonate altered basalt. As the main Zuleika Shear Zone is approached the pillow structures are progressively flattened with aspect ratios decreasing markedly with decreasing distance from the shear zone. Within the shear zone the pillow structures are entrained parallel to the foliation. The dimensions of the basalt pillows are 800mm x 300mm, 300mm x 100mm and 900mm x 70mm for 5.2b,c and d respectively. The distance of the basalt pillows from the main shear zone is 7m, 2m and 0m for 5.2b,c,and d respectively. Long axes of the pillow margins trend sub-parallel to the weathered face in each photograph and pillow cross-sections in this plane are ellipsoidal, hence the exposure on the floor of the pit is not the optimum view for a quantitative strain analysis. The best section for viewing the pillows is a cross-section oriented at 90° to the foliation and the stretching lineation of the main shear zone. Optimum exposures were not available at Wattlebird. Lens cap is 55mm diameter. View in 5.2b is south-east, and in 5.2c and d top of photo points north-east

Figure 3.20e

Flattened varioles / interpillow breccia fragments in pillow basalt from Wattlebird north-pit. The fragments are unusually large for varioles but the weathered nature of the outcrop may mask the detailed texture of the structures. The fragments are located within a pillow margin of intensely sheared high-magnesium basalt and are flattened indicating a component of shortening orthogonal to the plane of the shear zone. Top of photo points NE-SW. Lens cap is 55mm diameter.

Figure 3.20f

Photograph of S-C fabric in sheared talc-chlorite ultramafic from Wattlebird open-pit. The outcrop demonstrates the inhomogeneous nature of the deformation on the Zuleika Shear Zone with the Lens cap at a sharp boundary of well developed S-C mylonite (below) and clast-supported breccia with coarse flattened clasts of talc-chlorite ultramafic (above). S-C fabrics indicate left-lateral offset on the Zuleika Shear Zone. A thin slightly stretched quartz vein occurs in a fracture sub-parallel to the C-plane of the shear zone. Lens cap is 55mm diameter. Top of photo points NE-SW.

An analysis of 13 varioles in a pillow margin from diamond drillhole ZULD2 – 369.3m at the Bullant mine, shows that the structures are deformed into triaxial ellipsoids with X>Y>Z where, X= axis of maximum elongation, Y=intermediate axis of elongation and Z=minimum axis of elongation. The samples plot on a Flinn diagram with K<1 (K=0.34), indicating an apparent flattening deformation. The axis of maximum elongation plunges in a direction parallel to the mineral elongation lineation defined by aligned micas in the plane of the shear zone (Figure 3.21). The mineral elongation contained within the C-plane is oriented at about 90° to the S-C intersection. Parallelism of the mineral elongation lineation (simple shear), and the axis of maximum elongation of varioles, may indicate that the two fabrics were produced during the same shortening event, and implies partitioning of the flow into rotational and irrotational components (Figure 3.19b p.64). Rotation of the variole long axes from some other angle into parallelism with the flow plane would be expected if the deformation was bulk non-coaxial, however the data are insufficient to determine this relationship.

This determination provides a general guide to the flattening component of the deformation based on relatively few samples, whereas a representative strain analysis requires a larger sample population that is not available from the current amount of exposure at Zuleika. Strain markers indicate a component of flattening approximately orthogonal to the Zuleika Shear Zone, and this combined with the development of obtuse conjugate shear zone pairs of NW-SE sinistral and NNW-SSE dextral shear zones, implies an ENE-WSW maximum shortening during the formation of the Zuleika Shear Zone (Figure 3.22).

3.4.3 Principal structural orientations of shear zones and brittle-ductile faults

Faults and shear zones in the study area cluster into four principal structural orientations: NW-SE, N-S, NE-SW and E-W trending structures (Figure 3.23, Table 3.1). These correspond to four groups of lineaments with similar orientations that have been interpreted from aeromagnetic imagery (Figure 3.2 p.31, Figure 3.14 p.54). The three principal orientations of brittle-ductile faults (N-S, NE-SW and E-W) are averages of structures with similar deformation styles that are interpreted as being formed synchronously.

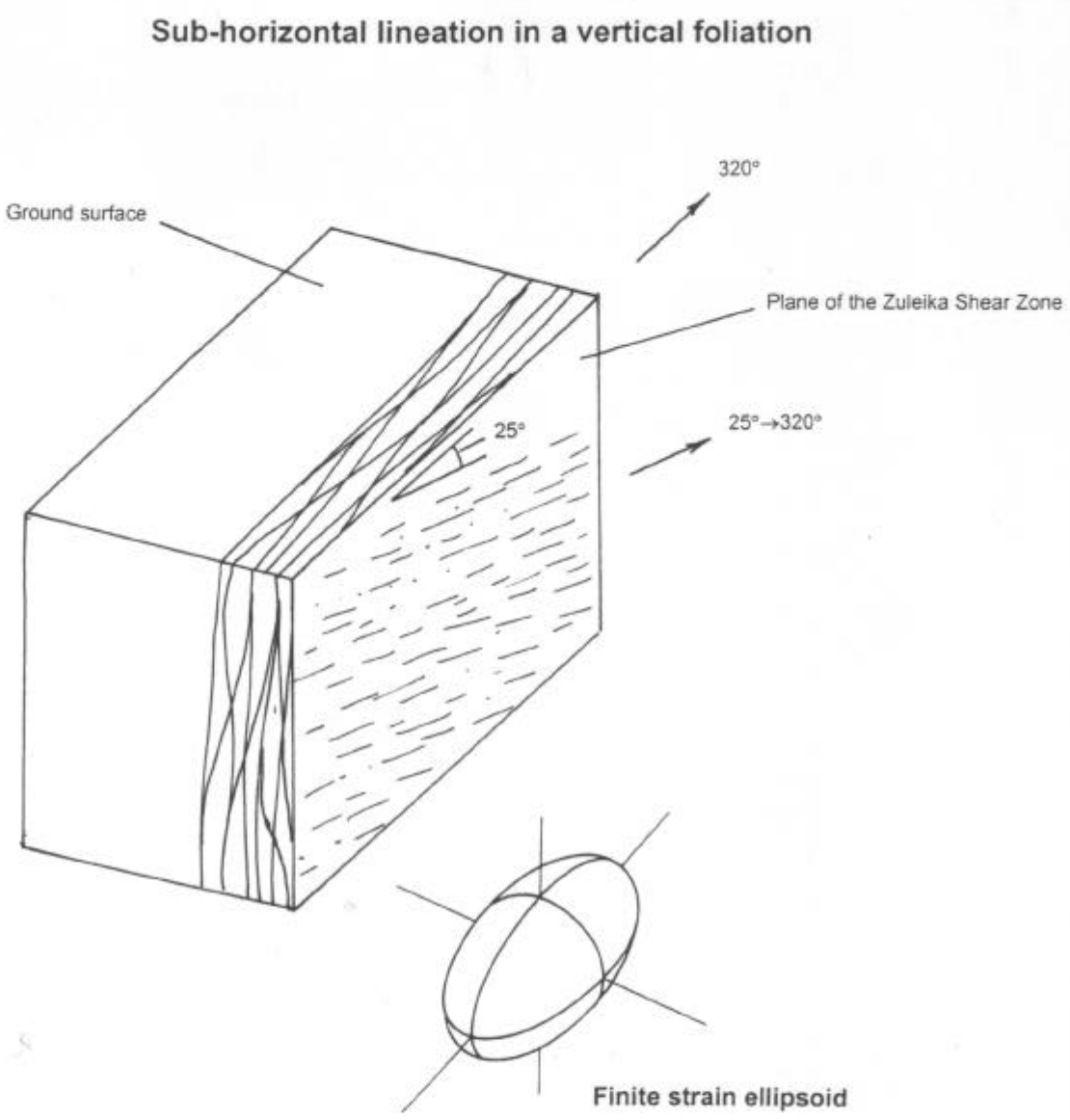

Figure 3.21 –Sketch of the slip / stretching lineation on the plane of the Zuleika Shear Zone in Bullant open pit. The geometry of varioles in high-magnesium basalt indicates that the slip lineation is sub-parallel to the local orientation of the maximum stretch axis of the finite strain ellipsoid.

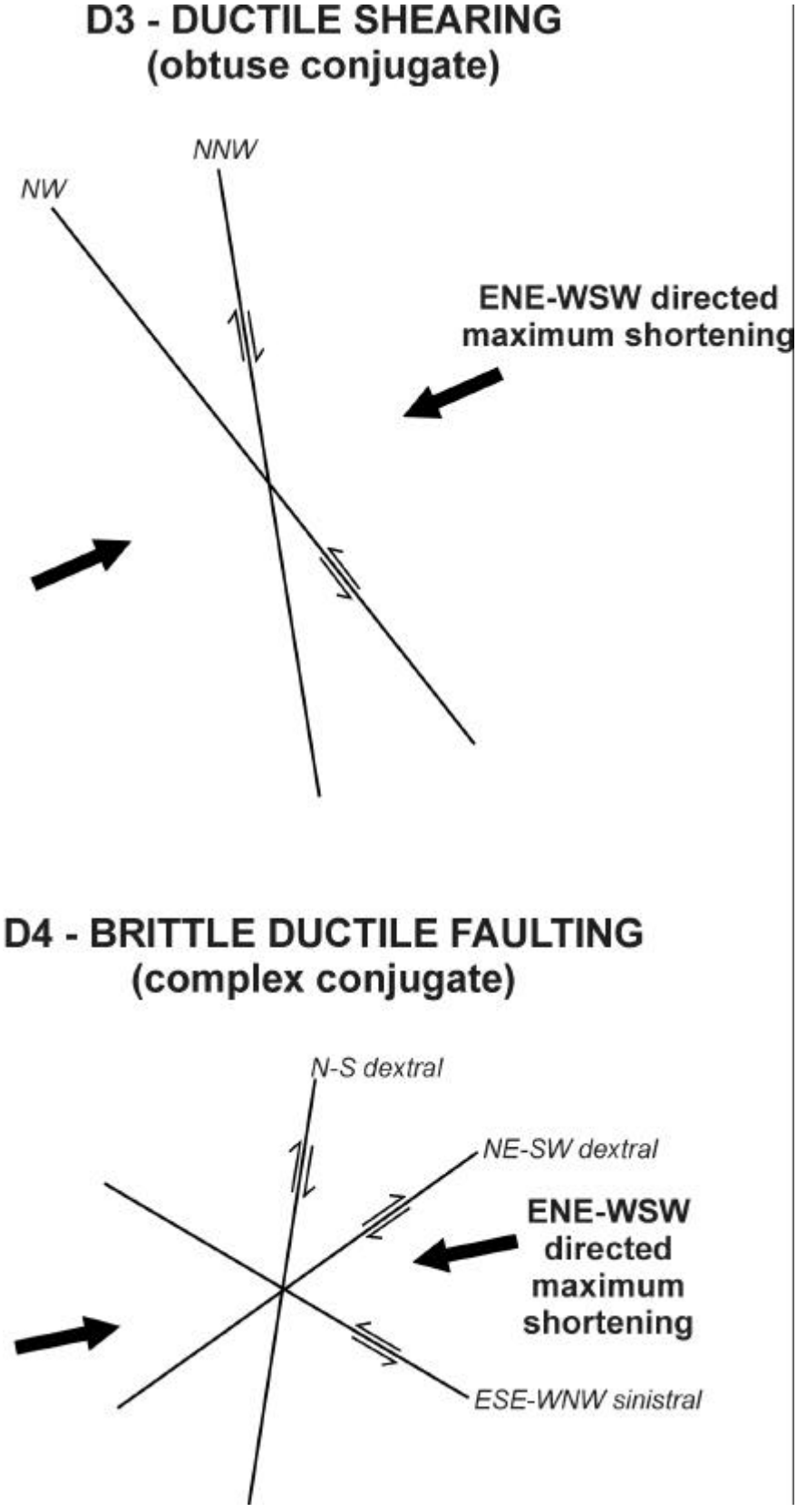

Figure 3.22 – Schematic diagrams showing the distribution and offset relationships of D3 ductile shear zones, and components of the D4 brittle-ductile fault network. Both events have orientations and sense of offset that indicate formation during ENE-WSW shortening.

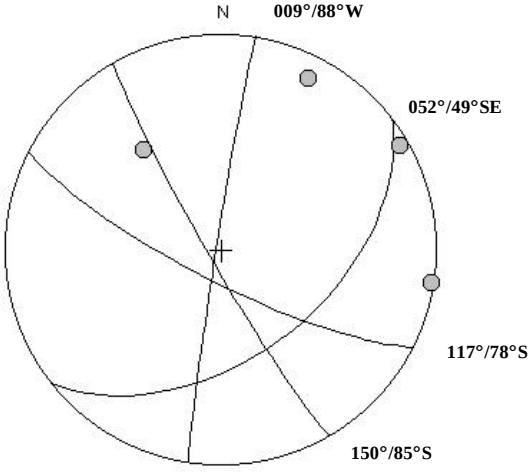

Figure 3.23 – Stereogram showing the four principal structural orientations at Zuleika. Great circles are for the average orientations listed in Table 3.1. The opposite-dipping variation for the NW-SE and N-S principal orientations are omitted for clarity.

Table 3.1 – Principal structural orientations in the Zuleika area compiled from drill-core and open pit observations, grouped by structural style. Orientations for each structural element are great circle orientations to the major clusters presented on stereograms for each prospect.

Principal Structural Orientations	NW-SE	N-S	NE-SW	E-W
Shear Zones				
Anthill	151°/68°W	015°/73°W	-	-
Porphyry	-	-	-	-
Bowerbird	157°/74°SW	-	-	-
Wattlebird	142°/83°SW	005°/79°W	-	-
Bullant	152°/88°SW	007°/83°E	-	-
Brittle Faults				
Anthill	-	-	-	-
Porphyry	-	-	057°/42°SE	-
Bowerbird	-	-	-	-
Wattlebird	-	-	-	-
Bullant	-	-	-	-
Veins				
Anthill	-	178°/72°W	067°/76°S	-
Porphyry	-	-	053°/38°SE	-
Bowerbird	151°/72°SW	021°/59°SE	-	-
Wattlebird	145°/87°NE	-	058°/43°SE	106°/71°S
Bullant	157°/66°NE	-	051°/43°SE	-
Schistosity and Cleavage				
Anthill	155°/66°W	-	-	-
Porphyry	-	-	044°/29°SE	-
Bowerbird	-	-	-	127°/85°SW
Wattlebird	142°/88°SW	-	-	-
Bullant	151°/77°NE	-	033°/75°SE	-
Average Orientations	**150°/85°SW**	**009°/88°W**	**052°/49°SE**	**117°/78°SW**

Relationships between deformation styles

Northwest-southeast trending structures have a mostly ductile character, typified by zones of schistosity and mylonite, and are represented by the Zuleika Shear Zone and conjugate shear zones. There is some evidence of minor brittle-ductile deformation related to the shear zones, such as subparallel shear veins with pinch-and-swell morphology. The other three principal orientations are brittle-ductile to brittle in character, ranging from breccia zones with localised cataclasite to fracture-fill quartz veins. A poorly developed spaced cleavage is also observed cross-cutting the earlier ductile fabrics.

Ductile features generally cluster tightly on a stereonet but brittle-ductile and brittle features may have up to 30° variability in strike with opposing dip directions. Additional scatter in orientations is produced by the anastomosing nature of foliations in shear zones especially when measured in diamond drill core. Not all of the structural styles are developed at each location, or in each of the principal orientations. Ductile shear zones trend in two main orientations; NW-SE and N-S. Some of these structures are brittle-ductile shear veins that overprint the NW-SE trending ductile shear zones, whereas others may be developed synchronously with the Zuleika Shear Zone forming an obtuse conjugate pair (eg. Ramsay 1980a). Brittle faults including rare cataclastic breccia and cataclasite seams mostly form in the NE-SW and E-W orientations. Quartz veins are ubiquitous in all of the principal structural orientations, whereas schistosity is sub-parallel to the NW-SE trending ductile shear zones. Spaced cleavage is developed sub-parallel to the NE-SW trending faults, the best examples of this being from the Bullant mine.

Overprinting relationships

Northwest-southeast trending ductile shear zones are overprinted by all other structures with rare exceptions. The other three principal orientations have mutual cross-cutting relationships that imply broadly synchronous development. Several examples were studied that demonstrate conjugate development of E-W and NE-SW trending brittle style quartz-pyrite and quartz-biotite-pyrite veins.

Offsets and displacements

The kinematic history of the Zuleika Shear Zone was predominantly left-lateral strike slip but similarities of lithological sequence across the shear zone indicate that there is not a large displacement of the wallrocks. Brittle-ductile faults in the N-S, NE-SW and E-W orientations have typically small apparent offsets from aeromagnetic imagery of the order of metres to a maximum of hundreds of metres. Mesoscopic data on offsets of the brittle-ductile fault network from Ora Banda (Chapter 4 p.86) show consistent offsets of N-S dextral, NE-SW dextral and E-W sinistral.

3.4.4 Kinematic interpretation

Regional folding produced fold structures with a geometry that suggests significant crustal shortening from an ENE-WSW orientation. The folds are the oldest deformation event in the Ora Banda Domain. Subsequent deformation events are shearing and faulting events that resulted in major disruptions to the folded sequence.

Fabrics in the Zuleika Shear Zone range from simple S-C mylonite to finely layered ultramylonite, characterised by grain size reduction and almost total destruction of primary rock fabrics with development of porphyroclastic texture. The fabric of the shear zone indicates predominantly ductile deformation which sets it apart from most other structures observed in the Zuleika area with brittle or brittle-ductile character.

The Zuleika Shear Zone has kinematic indicators with asymmetric geometry and a pronounced shallow stretching lineation in discrete high-strain zones, that indicate left-lateral strike-slip kinematics produced by inhomogeneous non-coaxial shear. Wallrock strain markers such as basalt pillows, breccia clasts in ultramafic rocks and centimetre-sized varioles from pillow margins at Wattlebird and Bullant show flattening strains that suggest part of the deformation was produced by inhomogeneous shortening (pure shear) normal to the plane of the Zuleika Shear Zone.

The two different types of strain indicate that bulk inhomogeneous shortening (Bell 1981) was an important component of the deformation coupled with inhomogeneous simple shear. A difference to the Bell (1981) model is that the Zuleika Shear Zone is a

predominantly NW-SE trending shear zone with a subordinate component of NNW-SSE trending conjugate dextral shear zones (Figure 3.22 p.69, Map 2 p.266). Sharp planar boundaries separate zones with non-coaxial strains from zones with co-axial strains (Figure 3.20f p.65). Boundaries between zones of co-axial deformation and undeformed rock are metre-scale tracts with a sharp change of strain intensity.

Various sets of mesoscopic-scale brittle-ductile faults and quartz veins that cross-cut the regional-scale Zuleika Shear Zone, support the aeromagnetic interpretation of a regional-scale network of late brittle-ductile faults, that cross-cuts both the rock sequences and earlier ductile shear zones. Late brittle-ductile faults also cross-cut the Zuleika Shear Zone to the south at the Broads Dam mine (Glasson *et al*. 1998).

Similar observations were made by Colvine *et al.* (1988) who concluded that deformation in the Ontario district produced a series of discrete tectonic structures of "regional and shield-wide extent". Early structures such as folds and major NNW-SSE trending shear zones at the Golden Mile, Kalgoorlie have also been cross-cut and offset by N-S trending oblique faults (Clout 1988).

Late faults can be grouped into three average orientations representing the strike directions of most structures, yet there is a moderate scatter of structural orientations in each group, and structures developed in a particular strike-group may display opposing dip directions. Cross-cutting relationships between the N-S, NE-SW and E-W groups are not obvious from aeromagnetic imagery since the majority of structures have small displacements of 50m or less, and timing relationships are therefore obtained only from mesoscopic observations.

The faults have varied morphologies that range from groups of small parallel faults making up a main fault zone, to single discrete fractures with or without quartz veins. Northerly trending faults are commonly developed as single discrete brittle-ductile faults with laminated quartz veins (Black Flag Fault / Quarters style), and may have a significant cataclastic component. Northeast-southwesterly and easterly trending faults may be both arrays of discrete fractures with quartz vein infill, and localised brittle-ductile faults. These late faults overprint the Zuleika Shear Zone and therefore represent a later deformation event.

Similar orientations for the resolved axes of maximum shortening for each of the deformation events may indicate a maintained regional crustal shortening from an ENE-WSW direction. Development of structural fabrics from ductile folding, cross-cut by ductile shearing and later brittle-ductile faulting may reflect a change in strain-rate, or alternatively, may be interpreted as progressive deformation during uplift and exhumation of the greenstone pile, with the structural styles recording translocation of the rocks from the lower-middle crust into the upper crustal seismogenic regime (Figure 3.24)

3.5 GOLD MINERALISATION – ZULEIKA SHEAR ZONE

The series of mines along the Zuleika Shear Zone have total gold endowment of 11 tonnes Au. Gold deposits occur in two lithological associations: those hosted by felsic porphyritic rocks and those in basalt.

3.5.1 Porphyry-hosted gold deposits

The main porphyry hosted gold deposits are at the Anthill and Porphyry mines, with other deposits at Hawkins Find, Porphyry West and in small lenticular bodies of felsic porphyry at Wattlebird. Gold mineralisation at the Porphyry mine is in a sheeted network of millimetre-scale fractures now filled with quartz-pyrite +/- chlorite. The veins trend 057°/32°SE on average (Figure 3.7 p.43) with a high vein-density in the economic envelope. Although the average orientation of the veins is NE-SW, there is wide variability in both strike and dip reflecting the complex nature of brittle fracturing and fracture-sealing processes. Silica-albite is the most common alteration assemblage with variable calcite alteration. Gold grades in quartz-pyrite veins are low (1-2ppm), however in areas of high fracture-density, the greater number of veins creates ore-grade zones. Intense ductile shear zones at the edges of the porphyry lenses also are well mineralised.

3.5.2 Basalt-hosted gold deposits

Several gold deposits in the Zuleika Shear Zone are hosted by high-magnesium basalt (eg. Bowerbird, Wattlebird and Bullant mines). The gold envelopes are elongate, trending parallel to the plane of the shear zone with high-grade zones localised in steep shoots that

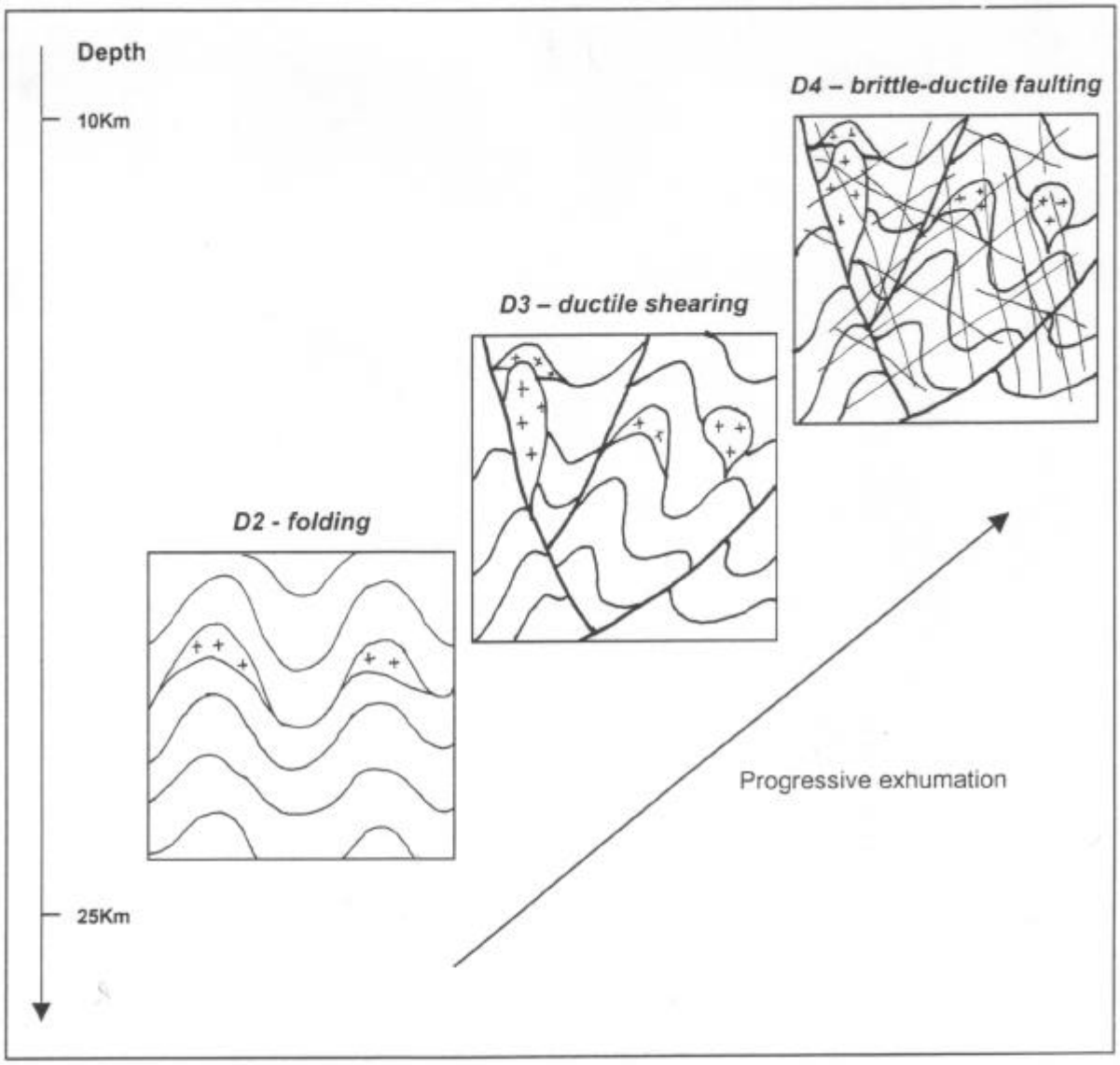

Figure 3.24 – Schematic diagram illustrating the structural development of the Ora Banda and Zuleika districts, during progressive exhumation of the Archaean supracrustal sequence. The three deformation events illustrated have finite strains specific to each episode, but form part of a progressive ENE-WSW regional shortening event.

plunge to the northwest and southeast. High-grade ore shoots occur at the intersection of the Zuleika Shear Zone with brittle-ductile faults in the three principal structural orientations. At Wattlebird, a ≈20m-wide quartz vein array with N-S trend cross-cuts the shear zone, with a high-grade shoot at the juncture of the two structures (Map 5 p.278). Gold grade is distributed away from the intersection point in the planes of both structures. Similar relationships occur at Bullant where a brittle-ductile fault trending 013°/77°E cross-cuts the main Zuleika Shear Zone. A large quartz vein in the plane of the Zuleika Shear Zone at Bullant that contains high-grade gold has associated galena, sphalerite and pyrrhotite with the vein, which is a significantly different mineralogy to the later cross-cutting structures (Figure 3.25h).

A sample of the ore zone at Bullant (sample ZULPIT-1) taken from the high-grade portion of the orebody, contains up to 14 g/T Au (G. Adams personal communication 1998). The sample displays relationships that constrain the timing of deformation, gold mineralisation and metamorphism. In thin section, the rock has a distinct domainal fabric with biotite-calcite rich domains interspersed with quartzofeldspathic (ultramylonite) domains. The mylonitised domains have undergone intense grain-size reduction during dynamic recrystallisation, with strong undulose extinction in equant to elongate quartz grains of 20*m*m average diameter. Very fine-grained ribbon texture is developed in long continuous bands. Biotite-calcite domains are mostly strain-free, have coarser grain-size and appear to overprint the ultramylonite. Pyrite (+/- marcasite) is present as elongate grains that trend parallel to the shear fabric and is assumed to represent the gold mineralisation event. The presence of marcasite indicates low-temperature alteration of the sulphides.

The shear fabric is overprinted by large, randomly oriented sheafs of actinolite that are strain free, cross-cutting both domain-types (Figure 3.25b-d). Actinolite crystals oriented at a high angle to the shear zone have very fine rims of pyrite up to 0.5*m*m thick (Figure 3.25d). The rims appear as coatings of pyrite that pseudomorph actinolite crystals on broken surfaces. Pyrite also occurs in large elongate grains closely associated with calcite, that cross-cut un-oriented actinolite sheafs (Figure 3.25g). These relationships displayed by pyrite indicate that mineralisation began with the ductile shearing, continued during metamorphism, and finally ceased after the peak of metamorphism. The elongate continuous form of the pyrite may indicate that pyrite is replacing pyrrhotite. Some secondary remobilisation of the sulphides is evident in the presence of minor marcasite.

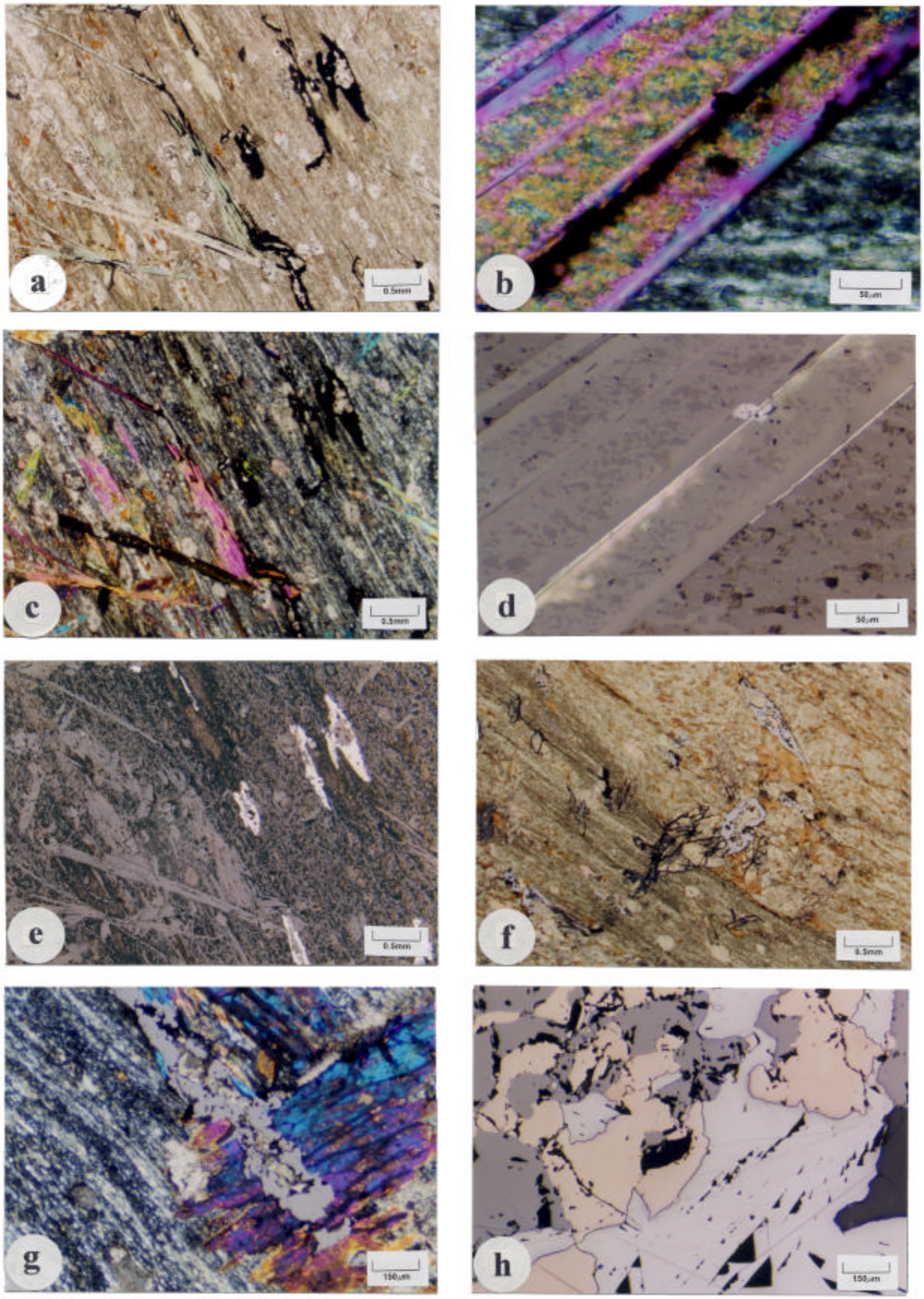

Figure 3.25 – Photomicrographs of mineralised basalt from the Bullant mine. Figures **a), c)** and **e)** are views of the same area - (PPL) in a), (XPL) in c), reflected light in e). **b)** Close up of actinolite overprinting the shear fabric at a high angle. **d)** Reflected light view of b) showing fine pyrite along actinolite margins. **f)** Pyrite overprinting biotite-calcite domains that appear to cross-cut the mylonitic fabric. **g)** Pyrite-calcite overprinting late actinolite, combined reflected and transmitted light (XPL). **h)** Massive sulphides in a mineralised quartz vein. See text and over page for explanation.

Captions for figures on page 77

Figure 3.25a, c, e,
Photomicrographs of the same area of sample ZULPIT1 (**a**-PPL, **c**-XPL, **e**-reflected light) from a high-grade ore zone in the Bullant open-pit. The samples show the relationships between deformation, metamorphism and mineralisation within the Zuleika Shear Zone. In all figures, the NW-SE trending shear fabric is clearly visible, defined by quartzofeldspathic material that has undergone intense grain-size reduction producing a mylonitic fabric. In Figure 3.25e pyrite is formed parallel to the shear zone and in some cases is stretched along it, or is replacing actinolite that is also parallel to the foliation. In Figure 3.25c actinolite is aligned along the foliation but mostly overprinting the shear fabric with random orientation.

These relationships indicate that metamorphism began late in the ductile shearing event but peak metamorphism overprints the D3 shear zone, and crystallisation of actinolite occurred in the absence of a significant stress. Pyrite in this sample is assumed to represent the gold mineralisation event and its form is significantly affected by the shearing indicating that gold mineralisation was synchronous with D3 ductile shearing. Additional evidence that supports this assertion includes the shear zone fabric being defined by hydrothermal biotite in Figure 3.11g and h.

Figure 3.25b, d
The shear zone is shown in close-up with detail of the overprinting relationships between metamorphic actinolite and the shear fabric. Dark isotropic edges of the actinolite in Figure 3.25b are revealed in Figure 3.25d as very fine films of pyrite (0.5*m*m-thick) pseudomorphing the actinolite, which indicates that the gold mineralisation event continued during peak metamorphism. Gold mineralisation also post-dates metamorphism as evinced by **Figure 3.25g** where pyrite overprints the randomly oriented actinolite. In all cases pyrite is closely associated with calcite. Pyrite also overprints biotite-calcite rich domains that appear to overprint the shear zone in **Figure 3.25f**.

Figure 3.25h
Photomicrograph of massive sulphides in a gold-bearing quartz vein from the Bullant mine. The vein is 3.3m wide and contains large inclusions of massive pyrrhotite-sphalerite and galena trending 146°/84°NE. This mineralogy is unusual for gold-bearing veins in the Zuleika Shear Zone, however the vein returned a fire assay value of 2.93 g/T Au. Sample is from 215.7m in diamond drill hole ZULD9.

3.5.3 Structural timing of gold mineralisation

Mineralogical studies by Vaughan (1988), demonstrate that gold is associated with both sulphides and silicates. Gold-related biotite and pyrite defining the Zuleika Shear Zone fabric implies that significant gold mineralisation occurred during movement on the structure. In comparison, the coincidence of significant gold at the intersection of late brittle-ductile faults with the Zuleika Shear Zone suggests a common timing of gold mineralisation and the late fault event. Hence the timing of gold mineralisation is constrained to a period during movement on the regional-scale Zuleika Shear Zone (D3), and continuing into the overprinting late fault event (D4).

3.6 DISCUSSION

Deformation in the Ora Banda Domain was heterogeneous in three distinct episodes represented by regional folding (D2), ductile shearing (D3) and brittle-ductile faulting (D4). This sequence is demonstrable from simple cross-cutting of the major structures visible in aeromagnetic imagery and outcrop. Early low-angle faults with stratigraphic repetition are not observed. Regional-scale upright folds (D2), with NNW-SSE trending axial planes suggest an ENE-WSW directed regional shortening event (Swager *et al.*1990). Ductile shearing (D3), possibly occurred along pre-existing structures that record several phases of movement and were interpreted as ancient extensional-normal-faults active during back-arc basin formation by Swager (1989).

Kinematic indicators in the D3 shear zones show that the last phase of movement was strike-slip with shallow to moderately north-plunging slip/stretch lineations, and left-lateral fabric asymmetry in S-C mylonites. Brittle and brittle-ductile fault structures (D4), in three principal structural orientations were formed synchronously, but post-dating movement on the regional ductile shear zones (D3). This relationship has resulted in four principal structural orientations that are identified at most outcrops in the north Kalgoorlie area. Finite strains indicate a deformation sequence that was ductile in the initial stages, progressing through brittle-ductile to brittle in the final stages of deformation. This sequence may indicate a change in strain-rate, or may be related to progressive uplift towards the final stages of orogenesis.

The heterogeneous distribution of strain in the Zuleika area with strong separation into high strain zones interspersed with relatively undeformed wallrocks, has contributed to the local tectonic fabric, and is analogous to the regional-scale geometry. In detail, the high strain zones have fabrics that suggest development due to bulk shortening at a high angle to the shear zones. This interpretation is significant for the Zuleika Shear Zone and the Kalgoorlie Terrane, since many regional-scale ductile shear zones are therefore implicitly low-displacement zones, with the amount of displacement unrelated to the intensity or thickness of the zones (eg. Walsh and Watterson 1988). With low displacements across major ductile shear zones, the interpretation of juxtaposed high and low strain domains requires revision. A strain gradient between the Coolgardie Domain and the Ora Banda Domain is evident if reference points are chosen well within each domain. However, the presence of a sharp strain gradient at the contact is not observed at Zuleika, which is the interpreted domain boundary between the Ora Banda and Coolgardie Domains (Swager *et al.* 1990). It is possible that the Zuleika Shear Zone is localised along a region of the crust that is both a strain and metamorphic gradient up to several kilometres wide, without the necessity for a sharp line of demarcation (however poor exposure hinders the resolution of the problem).

Although the Zuleika Shear Zone has been interpreted as coincident with a metamorphic isograd (Swager *et al.* 1990; Witt 1991; Witt 1993; Witt *et al*. 1997), data from geological mapping and drillcore logging do not support a significant change of metamorphic grade across the shear zone at Zuleika (Chapter 3 p.33-60, Tables A1.1–1.6 p.261-279). The shear zone was interpreted as a tectonic boundary between lower - middle greenschist facies rocks of the Ora Banda Domain and upper greenschist - lower amphibolite facies rocks of the Coolgardie Domain. The main indicator minerals of the change are biotite and actinolite, but these minerals are observed in exposures and drillholes on both sides of the shear zone. Furthermore, Hunter (1993) reported widespread development of metamorphic biotite in the Kurrawang Conglomerate, 3 km to the east of Zuleika. An alternative location for a metamorphic isograd juxtaposing tectonostratigraphic and metamorphic domains logically should be a shear zone or fault of regional compass, but there are no regional shear zones to the east of the Zuleika Shear Zone until the Bardoc Tectonic Zone (Figure 3.2 p.31). A previously recognised shear zone at the western contact of the Kurrawang formation (Hunter 1993) is interpreted as a significant truncating feature in the seismic image (Figure 3.4 p.36), and is a possible candidate for the metamorphic boundary, with seismic characteristics similar to the Zuleika Shear Zone. Alternatively, it is possible that

the change in metamorphic grade is a gradual one that accompanies a strain gradient with decreasing intensity towards the east.

The kinematic history of the Zuleika Shear Zone is complex, but there is at least one major phase of left-lateral movement. There is no evidence of early dip-slip events, although the fabrics of the shear zone may record only the latest movements. The later period of movement accommodated bulk shortening and was possibly related to oblique convergence during closure of the Kalgoorlie basin.

In a re-interpretation of regional-scale ductile shear zones in the central Norseman-Wiluna belt, Hammond and Nisbet (1992) identified early low-angle extensional shear zones (lags) on granite greenstone contacts. They considered that later shear zones with both vertical and horizontal stretch lineations were syn-regional folding thrust faults and upturned early thrusts, respectively. This model is important for the interpretation of fabric development in NW-SE trending structures like the Zuleika Shear Zone, since an original low-angle top-to-the-north thrust fault would display sinistral kinematics (as observed), when upturned by later E-W shortening. Conversely, most workers document kinematic indicators that lead to a strike-slip interpretation for that part of the deformation history.

The main point of contention is whether or not a regional sinistral wrenching event occurred (eg. Mueller and Harris 1987; Mueller *et al*. 1988), or the now sub-vertical structures were originally formed as basin-controlling normal faults during basin-development (Swager *et al*. 1990), and reactivated as reverse thrusts during subsequent basin closure. The problem is not easily resolved but if the model proposed by Hammond and Nisbet (1992) is correct, then an early (pre-folding) episode of gold mineralisation is implied for gold deposits hosted in regional ductile shear zones with gold-related alteration assemblages defining the shear zone fabric. The timing of gold mineralisation of the Zuleika Shear Zone is therefore dependent on the preferred interpretation, and timing of gold mineralisation becomes a major tool for resolving the tectonic history of the region. Four interpretations of the kinematic history of the Zuleika Shear Zone are possible:

1. *Early within-greenstone D^E extensional shear zone*. For an interpretation of the shear zone as an early within-greenstone D^E extensional (flat-lying) shear zone, an approximately vertical maximum shortening direction is implied, which would have

produced a top-to-the-SSE low angle shear zone (tectonic slide), and when upturned would display (apparent) dextral kinematics. Such an interpretation is inconsistent with observed field relations and strain marker geometry, and is therefore rejected.

2. *Upturned D1 thrust fault*. D1 thrusting was a north-directed shortening event that produced top-to-the-north low angle thrust faults, and resulted in widespread stratigraphic repetition. During the D1 event, the maximum shortening direction was horizontal in a direction which is at 90° to that interpreted from strain markers at Zuleika and therefore this model is also rejected. The apparent sinistral kinematics that would be produced by upturning a D1 thrust fault are however in agreement.

3. *Upturned syn-shortening D2 thrust fault*. An interpretation of the Zuleika Shear Zone as a syn-shortening D2 thrust fault is not plausible, since the observed stretching lineation is sub-horizontal whereas a steep to sub-vertical lineation would be expected. The option of the sub-horizontal stretch lineation overprinting an earlier formed sub-vertical lineation is possible, however there is no evidence of remnant early lineations, and all observed ductile fabrics and strain markers display a sub-horizontal maximum elongation direction. Furthermore, the seismic data show that the Zuleika Shear Zone is not listric at depth, and the contact with the mid crustal décollement is a sharp truncation instead of a smooth ‘soling-out’ against a sub-horizontal discontinuity, as would be expected from syn-shortening thrust faulting.

4. *Sinistral wrench fault*. Wrench tectonic interpretations have been proposed by many authors to explain the regional-scale ductile shear zones in the Eastern Goldfields Province (Swager 1989; Witt 1993b-c; Mueller and Harris 1987; Mueller *et al*. 1988). However, development of the Zuleika Shear Zone in a bulk shortening is preferred over a bulk non-coaxial wrench, since there is a lack of obvious displacement parallel to the shear zone and since there are no synchronous minor structures (Riedel structures, conjugate shears) as predicted for well-studied areas of wrench tectonism (Sylvester 1988; Mandl 1988). Strain fabrics require that the maximum shortening axis was at a high angle to the plane of the shear zone, which supports the interpretation of bulk shortening deformation with flow partitioning of non-coaxial deformation fabrics. Also, an obtuse conjugate system of ductile shear zones (320°/350°) is observed at the mesoscopic scale, interpreted at the regional-scale, and is reported for other areas in the

northern goldfields (eg. Vearncombe 1988a). In addition, the late tectonic fault network has timing and cross-cutting relationships that support a ENE-WSW directed maximum shortening. This relationship obviates the need for a major re-orientation of the stress field between ductile and brittle deformation events, but rather allows for deformation during progressive exhumation of the greenstones (or a period of increased strain rate), with a succession of overprinting structural styles from early ductile to later brittle.

The ductile shearing event as recognised at Zuleika displays cross-cutting relationships with later mesoscopic structures, that require a revised interpretation of the tectonic models applied to explain their development. Application of a model in which the far-field stress system is bulk non-coaxial in nature (wrench tectonics) is not consistent with the mesoscopic detail of structures in the Zuleika area.

The brittle-ductile fault network overprints within-greenstone-belt ductile shear zones (Zuleika Shear Zone) which is a new interpretation of the timing of development of these faults. Previously, the late faults were interpreted as second or third-order splays off 'first order' crustal deformation zones (Clarke *et al*. 1986; Mueller *et al*. 1988; Libby *et al*. 1990), or contemporaneous Riedel shears formed during strike slip deformation (Witt 1993b-c; Mueller and Harris 1987; Mueller *et al*. 1988). In some studies (Swager *et al*. 1990; Simpson *et al*. 1995) the brittle-ductile faults have been relegated to a minor role in the deformation history of the Kalgoorlie Terrane, but they are a prominent expression of strain at the outcrop, and a significant contributor to the regional fabric on aeromagnetic imagery. Problems with the interpretation of late brittle-ductile faults as low order splays off regional ductile shear zones include significant differences in magnitude, structural style and orientation. Furthermore, clear cross-cutting relations indicate that these structures postdate the regional ductile shear zones, and hence cannot have been formed during an event that they overprint.

The interpretation of the late brittle-ductile faults as Riedel structures has enjoyed popular status (Mueller *et al*. 1988; Mueller and Harris 1987; Eisenlohr 1987) but is also problematic considering the temporal evolution of structures as displayed in the original experiments by Riedel (1929) and Tchalenko (1970). Their work showed that a distinct sequence of fractures would develop at various angles to the shear direction, beginning with high-angle fractures progressively rotated to low-angle fractures and approaching sub-

parallelism with the shear direction with increasing displacement (Figure 3.26). To apply this model to the Ora Banda Domain, NW-SE trending regional ductile shear zones should overprint all other high-angle fractures, but this is not observed (see also Hagemann *et al.* 1992). Additionally, the Riedel experiment was applied to upper-crustal brittle deformation, designed to simulate the development of structures in sedimentary successions overlying deep basement faults, hence its applicability to rocks at the brittle-ductile transition is not proven (Vearncombe *et al*. 1989).

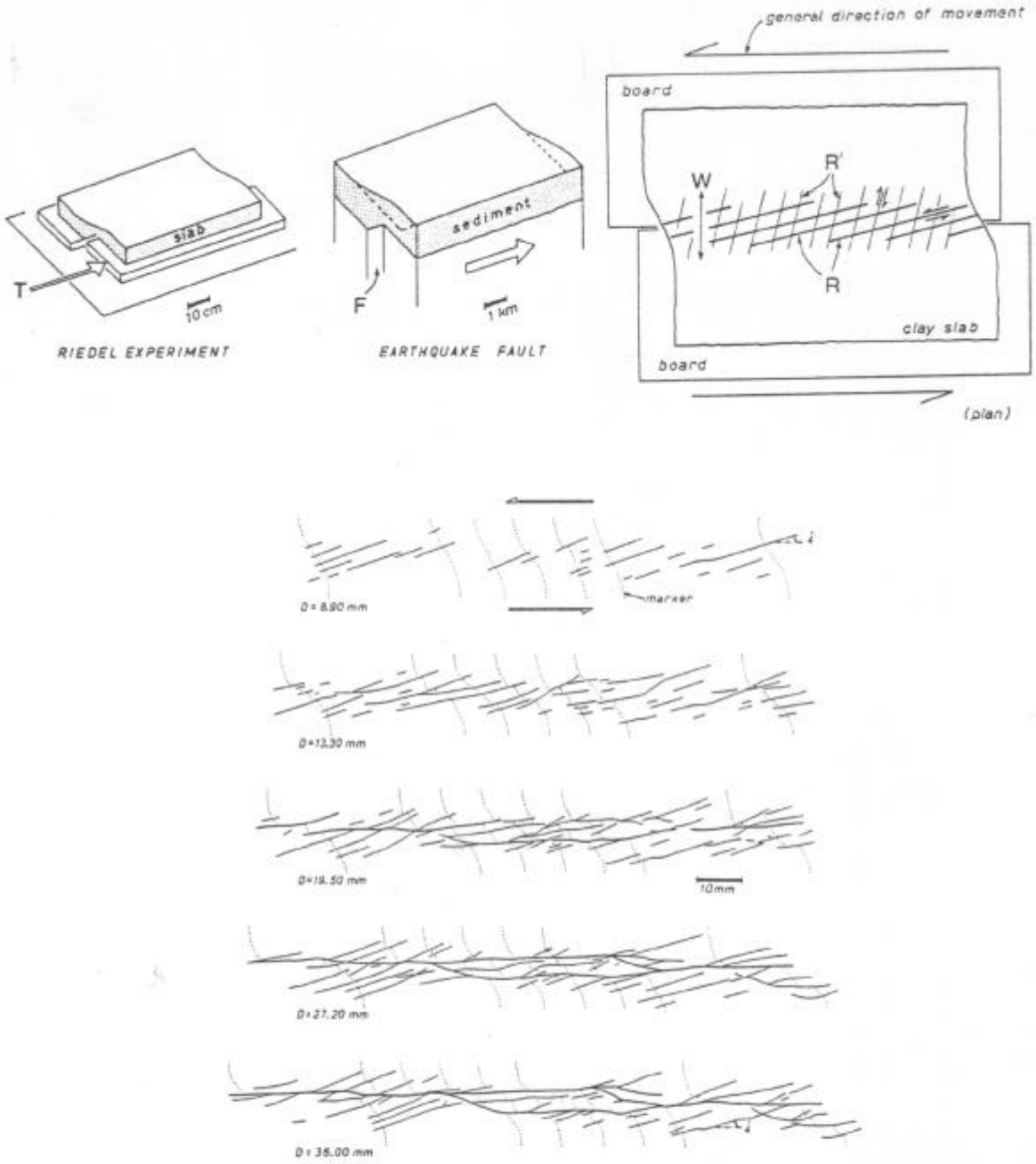

Figure 3.26 – Riedel experiment showing clay slab over movable boards to simulate a shear couple, and high angle fractures produced with the beginning of simple shear. The series of diagrams record the sequential development of fractures in clay produced with increasing displacement across the boards. High angle fractures form first followed by progressively shallower angles approaching parallelism with the direction of simple shear at maximum displacement. All diagrams reproduced from Tchalenko (1970).

4 ORA BANDA STRUCTURAL ZONE

4.1 INTRODUCTION

At a regional-scale, the brittle-ductile fault network (Chapter 3.3.3 p.53) is composed of sub-domains of faults, which intersect to form localised zones of high fracture-density. The zones have uniform relationships between sets of faults with different average orientations, and are therefore interpreted as structural zones. The term ‘structural zone’ is used to indicate that the areas are not simply chance intersections of randomly developed faults, but are considered to contain brittle-ductile faults that are related in space, time, origin and structural style.

The Ora Banda structural zone is discussed in detail in this chapter to document the D4 brittle-ductile fault network at a macroscopic scale. A group of faults intersect in the Ora Banda district and collectively form the ‘structural zone’. Geological relationships including structural style, geometry, structural orientation and cross-cutting relationships are assessed for the group of faults to test similarities, and to characterise the brittle-ductile fault network at a macroscopic scale.

The Ora Banda structural zone is a macroscopic zone of high-density faulting and shearing relative to adjacent areas (Figure 4.1). Strain distribution is heterogeneous, reflected by narrow, tabular high-strain zones (brittle-ductile faults) separating lithons of essentially undeformed rock. Faults and shear zones cross-cut the stratigraphic sequence and are also localised along rock-unit contacts especially interflow sedimentary rocks.

Two other structural zones at Grants Patch and Mount Pleasant are also coincident with gold mining centres, hence better exposure is available in these areas with well-developed fracturing. Local lithological factors control the spacing, size and geometry of the structural zones and some rock types appear particularly more sensitive to brittle-ductile deformation than others (eg. mafic versus ultramafic rocks).

Several major brittle-ductile faults make up the Ora Banda structural zone, including the Enterprise fault zone, the Gimlet South and Sleeping Beauty Faults (Harrison *et al.* 1990; Laing 1994; Bogacz 1995) and the Slippery Gimlet fault, which have good

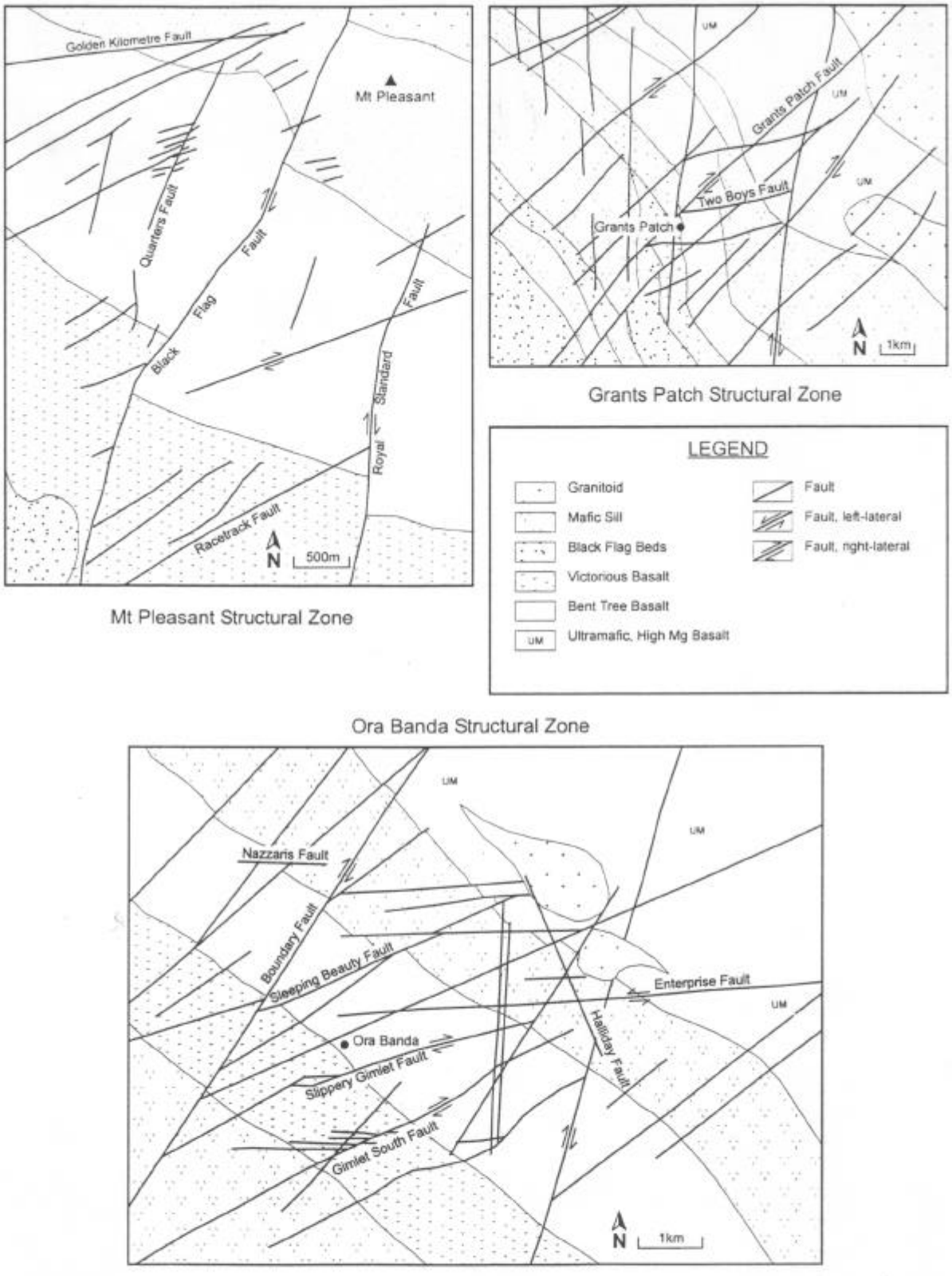

Figure 4.1 – Geological maps of structural zones at Mount Pleasant, Grants Patch and Ora Banda. The structural zones are localised zones of high fracture-density with respect to surrounding areas and contain brittle-ductile faults in similar orientations. Faults are interpreted from aeromagnetic and groundmagnetic imagery.

examples of mesoscopic structural elements developed in dolerite and basalt. Depth extensions at Nazzaris and Boundary are only recent discoveries and are at the initial stages of mine development. Bedding-parallel ductile shear zones, rarely host large gold deposits in the area and exposures are limited to chance drillhole intersections or open-pit exposures. Of these the Black shale shear zone, Cashmans Shear Zone and Enterprise-east shear zone are discussed in detail.

4.2 STRUCTURAL STYLES

Deformation in the Ora Banda structural zone is manifest in a variety of structural styles that range from ductile to brittle. The distribution of each is heterogeneous and most examples of deformed rocks exhibit a variety of fabrics. The following discussion focuses on examples of structural styles and their litho-stratigraphic relations. Fault rocks are grouped according to the classification of Passchier and Trouw (1996).

4.2.1 Brittle faults

Brittle faults occur as tabular breccia zones, cataclasite zones, discrete planar fault surfaces or wide rhomb shaped breccia ‘jogs’ in the dilatant parts of brittle-ductile shear zones. All brittle faults are cohesive types (Passchier and Trouw 1996) including breccia (c.f. Sibson 1977), with hydrothermal precipitates forming a matrix to the clasts. They have foliated and non-foliated fabrics, but most brittle structures fall into the non-foliated category. Non-foliated brittle faults are genetically related to movement on nearby shear zones, and form slip-transfer jogs where fault movement is accommodated by lateral transfer to a parallel fault or shear zone. In such transfer-jogs, dilation and brecciation was along pre-existing fractures with subsequent infill by vein material.

Brittle faults are developed primarily in basalt flows of the Grants Patch Group, which appear to fail by fracture more easily than the coarser grained intrusive dolerite/gabbro sills, that are commonly schistose. Contacts between fine-grained and coarse-grained rocks may control changes in the deformation style of high-angle faults that transect the contacts. Brittle fault textures in the Ora Banda structural zone can be grouped as; breccia, cataclasite, discrete fault planes and veins. Breccias are characterised by jigsaw textures without major comminution and rounding of the clasts.

Jigsaw breccia typically has a significant component of hydrothermal precipitates forming veins or infill matrices to large angular clasts (Figure 4.2a). The breccia zones are non-foliated tabular structures with dimensions in the order of several metres or tens of metres. Jigsaw breccia is developed at the margins of fault zones with random fabrics, closely associated with mesofracture arrays in the wallrocks. The development of jigsaw fabrics with inter-clast voids infilled by hydrothermal vein material may indicate a textural progression from incipient fracture propagation, to jigsaw breccia and finally random fragmental breccia/cataclasite towards the centre of a fault (Figures 4.2b and d). Mesofracture arrays are coincident with hydrothermal alteration of the wallrocks suggesting increased permeability facilitated by an interlinked network of fractures.

Cataclasites (Engelder 1974; Higgins 1971) are usually greater than 0.1m-wide, whereas some may be much less than 0.1m-wide (cataclasite seams). The cataclasite is characterised by 50-90% wear-abraded and rounded clasts in a weakly deformed matrix of hydrothermal precipitates. Cataclastic textures include poorly sorted conglomerate with sub-rounded to rounded fragments of quartz/carbonate veins, mafic host rocks, and variously mineralised and altered rock fragments (Figure 4.2b). Fine grained matrix materials of similar composition to the clasts are cemented in quartz and calcite and contain a variety of textures exhibited by alteration and sulphide minerals from early fracture and brecciation to post deformation infill. The zones display a greater degree of textural maturity than jigsaw breccia, with several generations of fracturing and fragmentation recorded in the clasts. Faults at Gimlet South mine contain re-brecciated breccia, and have clasts of altered basalt with parallel fractures infilled by quartz-sulphide veins (Figure 4.15c, p.114). The clasts are interspersed with fragments of re-cemented cataclasite matrices from several generations of fault movement. Such textures indicate a repetitive history of brecciation and cataclasis with subsequent healing by hydrothermal precipitates. The degree of textural maturity is displayed in the roundness of clasts and matrix/clast relationships.

Cataclasite zones usually do not have sharp boundaries but may grade into fractured wallrock adjacent to the fault. Non-foliated cataclasite typically has a higher proportion of hydrothermal precipitates than foliated types, and is probably produced by fluid assisted processes including overpressuring and wallrock implosion during fault movements. Textures indicate that the initial stages of faulting involved dilation along a series of

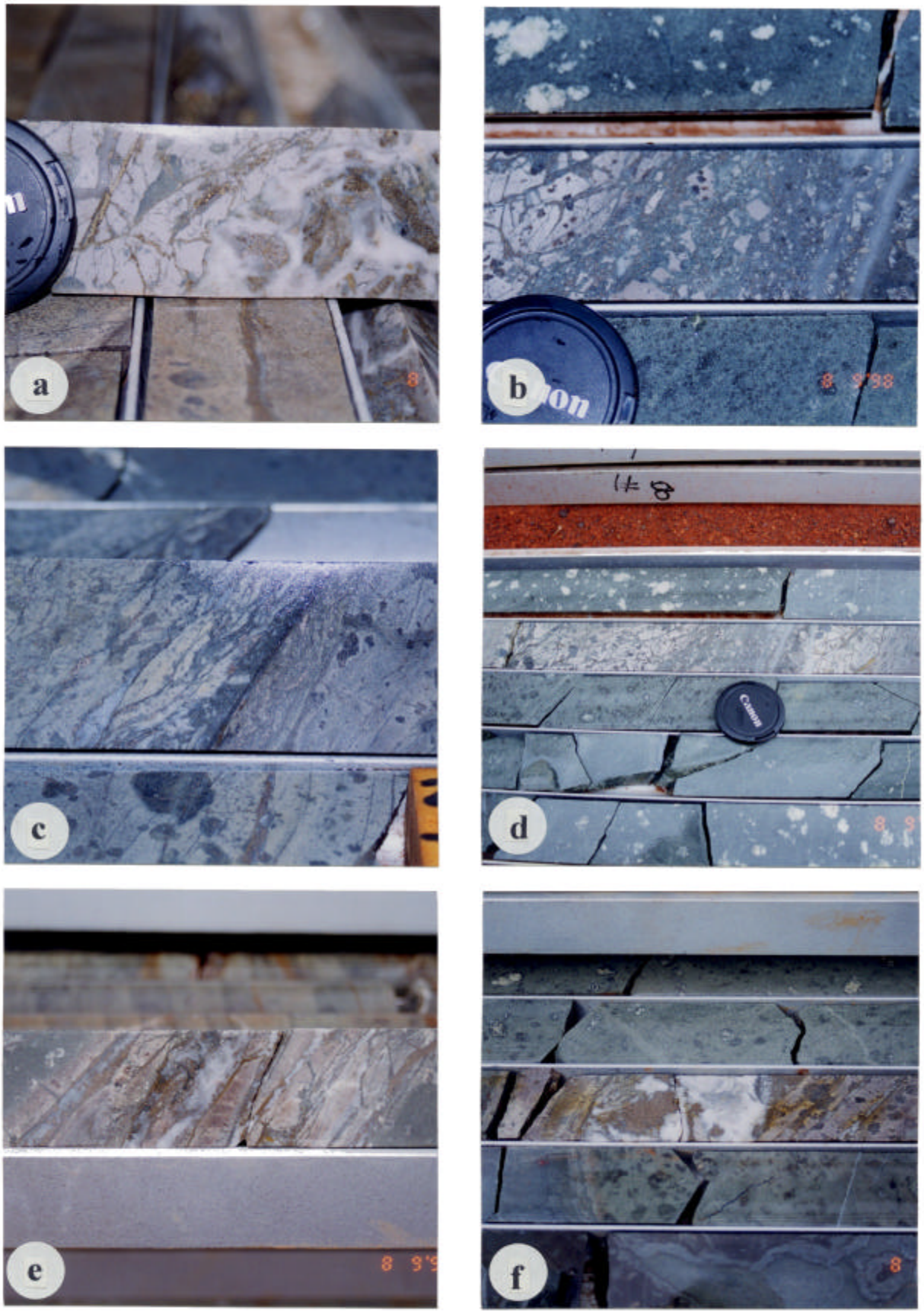

Figure 4.2 - a) Coarse-grained fragmental breccia zone from Slippery Gimlet. **b)** Cataclasite in the centre of a breccia zone, Slippery Gimlet. **c)** Ductile shear fabric at the margin of a breccia zone, Slippery Gimlet. **d)** Breccia zone in porphyritic basalt, Slippery Gimlet. **e)** Breccia zone with hydrothermal vein infill, Slippery Gimlet. **f)** Quartz-calcite vein with massive pyrrhotite, Slippery Gimlet. See text and over-page for explanation.

Captions for figures on Page 90

Figure 4.2a
Coarse-grained fragmental breccia zone from Slippery Gimlet. The zone is developed in grey muscovite-carbonate altered Victorious Basalt. Mesofracture arrays are visible in the wallrock of the zone with two orientations. The larger fractures trending parallel to the wall of the zone cross-cut an earlier fracture set trending top left to bottom right. Pyrite forms veins in the fractures, and fragments of wallrock with pyrite veins are clasts in the breccia, hence the timing of brecciation was later than fracture propagation in the wallrock. The clasts are sub-angular to rounded indicating rotation and moderate wear-abrasion. White quartz and calcite cement the breccia clasts. The breccia zone is at 222.00m in GIMD16, downhole direction is to the right. Lens cap is 55mm diameter.

Figure 4.2b
Cataclasite in the centre of a breccia zone from Slippery Gimlet. The photo is a close-up view of the breccia zone in 4.2d. Clasts comprise highly fragmented altered-basalt with a gradation of clast dimensions from <1mm to >20mm. The range of clast sizes contrasts with figure 4.2a where most clasts are up to several centimetres diameter. Clast size is distributed unevenly, decreasing towards the area of the zone marked by thin quartz veins. The quartz veins have diffuse boundaries, and with pyrrhotite and calcite appear to cement the breccia clasts. Clast morphology is mostly angular and may indicate dominance of fluid assisted brecciation over cataclasis and abrasion. The breccia zone is at 166.70m in diamond drillhole GIMD28, downhole direction is to the right. Lens cap is 55mm diameter.

Figures 4.2c
Ductile shear fabric at the edge of a breccia zone from Slippery Gimlet. Ductile deformation is evident from stretched plagioclase phenocrysts in the fine-grained basalt matrix, and from lens shaped pods of basalt separated by thin cleavage seams of chlorite and pyrrhotite. A thin cataclasite seam forms a sharp boundary with less altered basalt to the right, sub-parallel to the cleavage seams. Pyrrhotite forms veins along cleavage seams and grains disseminated throughout the rock. The shear zone oriented 043°/69°NW, is at 237.50m in diamond drillhole GIMD10. Downhole direction is to the right, base of photo is 112mm.

Figures 4.2d
Breccia zone in porphyritic basalt from Slippery Gimlet. The zone is 0.32m wide with intense muscovite-carbonate-pyrrhotite alteration in the vicinity of the structure, which grades sharply into carbonate-chlorite altered basalt in the wallrocks. Fractures in the wallrock of the fault with pyrrhotite-chlorite filled fractures at low angle to core axis, cross-cut high angle fractures. The two fracture sets are visible on both sides of the fault with constant orientation. Fracture propagation predates breccia with the pre-existing fractures forming planes of breakage during brecciation. Sample details as for figure 4.2b.

Figure 4.2e
Breccia zone in porphyritic basalt from Slippery Gimlet. Brecciation is characterised by thin slices of wallrock infilled by hydrothermal vein material. The slices have broken along fractures oriented parallel to the zone. Quartz-pyrrhotite infills previously fractured basalt with pyrrhotite veins in thin fractures. The breccia zone is at 298.00m in diamond drillhole GIMD22. Base of photo is 220mm.

Figure 4.2f
Quartz-calcite vein with massive pyrrhotite from Slippery Gimlet. The vein infills a weakly deformed zone with minor fracturing of the wallrock parallel to the vein. A large patch of pyrrhotite infills a void in the quartz-calcite vein. Few wallrock breccia fragments are present. Vein is at 253.50m in diamond drillhole GIMD22. Base of photo is 310mm.

fractures and parallel slices of wallrock in weakly deformed zones of breccia with vein infill (Figure 4.2e p.90). Subsequent dilation and brecciation produced jigsaw textures, with later significant differential displacement that resulted in cataclasis and milling of the wallrock fragments.

Cataclasite seams occur as thin restricted zones from 0.01-0.1m thick, or as fine sub-millimetre-scale seams. Most seams of cataclasite contain fragments of altered and mineralised rock. Cataclasite seams may occur in swarms defining a penetrative planar fabric or as individual zones either at the margins of large planar quartz veins or in the centre of brittle-ductile faults. The morphology of cataclasite seams is usually very fine-grained to microscopic gouge composed of sulphides (pyrrhotite and pyrite) and wallrock/vein fragments forming <1mm wide bands. Cataclasite seams are located in the centre of breccia zones (Figure 4.2b p.90), and thin bands of fine-grained fragmented sulphides and chlorite cross-cut angular breccia (Figure 4.3d). Cataclasite is also a common clast constituent in breccia zones indicating that in some examples cataclasis may be a precursor to later brecciation. The cataclasite appears to have formed channel ways for overpressurised hydrothermal fluids with subsequent implosion brecciation of the wallrocks, and there is evidence of cataclasite seams overprinting both coarse breccia zones (Figure 4.3d) and ductile shear fabrics (Figure 4.2c p.90).

Discrete fault surfaces are planar discontinuities that are usually less than 5mm wide. Slickenfibre growths, mineral lineations and stepping slickensides are characteristic of the faults, and permit determination of offset. Slickenfibres are composed of chlorite and calcite usually but may also contain quartz-carbonate veins. Cataclasite seams also form discrete fault surfaces with slickenfibre lineations of fine-grained gouge material.

Veins are relatively uncommon brittle textures in basalt hosted structural zones. The veins are usually simple fracture-fill types with thick bands of quartz or calcite/ankerite and minor amounts of pyrite, pyrrhotite, sphalerite, galena, tourmaline, chlorite, biotite, epidote and muscovite. Some veins show evidence of offset across the margins and, where movement has occurred, the vein margins have shallow-plunging slip lineations on stepping slickenfibres and variable deformation. Whereas veins are a subordinate deformation fabric, they occur in arrays or vein systems related to fault movements and are generally located in less deformed wallrocks.

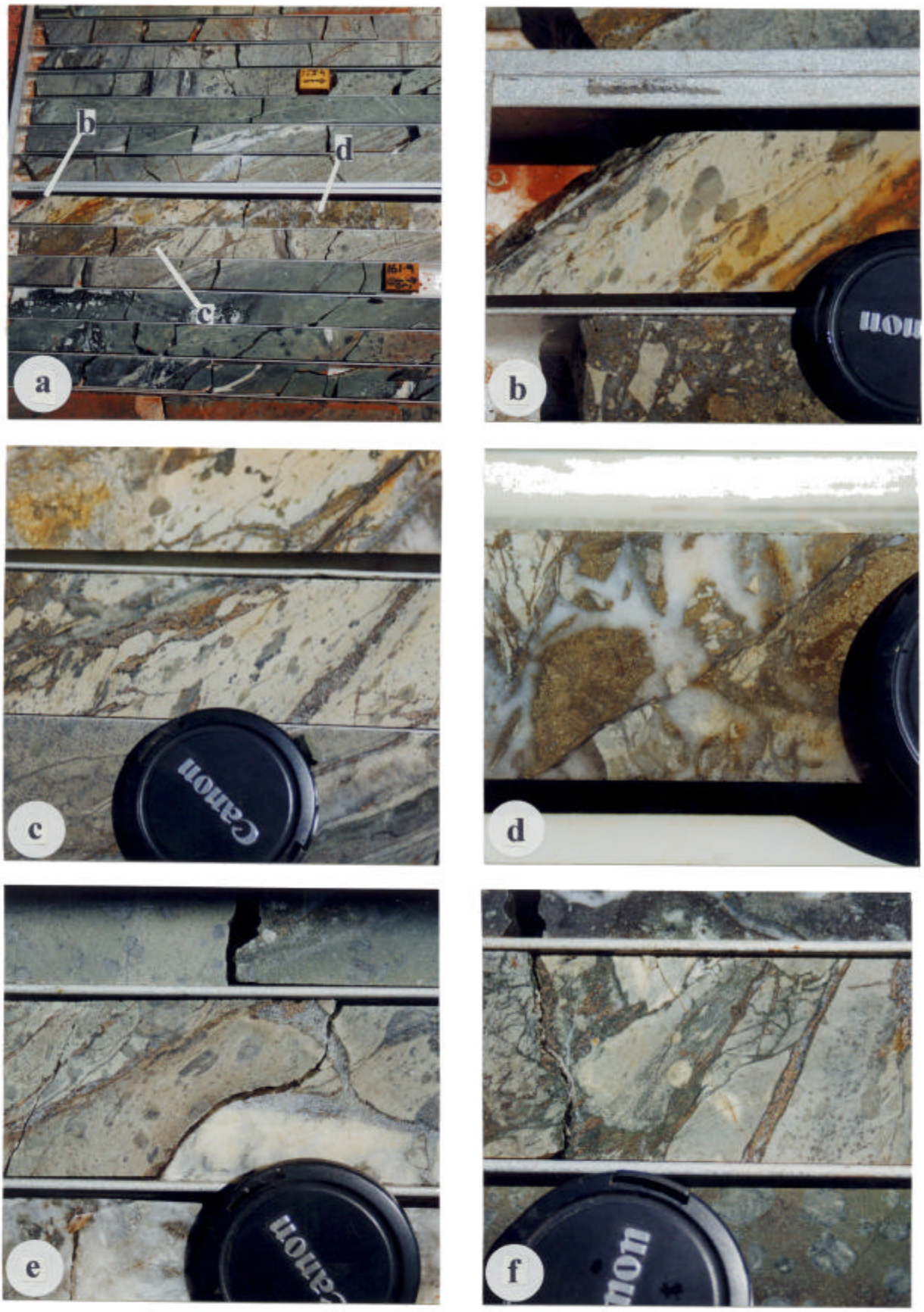

Figure 4.3 - a) Brittle-ductile fault zone, Slippery Gimlet. **b)** Ductile shear fabric at the edge of breccia zone, Slippery Gimlet. **c)** Ductile shear fabric from the edge of breccia zone, Slippery Gimlet. **d)** Central breccia zone crosscut by cataclasite seam, Slippery Gimlet. **e)** Ductile shear fabric in Victorious Basalt, Slippery Gimlet. **f)** Discrete ductile shear band in Victorious Basalt, Slippery Gimlet. See text and over-page for explanation.

Captions for figures on Page 93

Figure 4.3a
Brittle-ductile fault zone from Slippery Gimlet. The fault zone is 4m wide marked by light-grey coloured muscovite-carbonate alteration that grades into distal chlorite-carbonate alteration in porphyritic basalt. Ductile deformation manifest as aligned and stretched plagioclase phenocrysts (4.3b and c) is overprinted by brittle fault breccia and cataclasite (4.3d). Brittle fracture arrays at a shallow angle to the ductile shear fabrics extend into the wallrock of the zone. The brittle fractures cross-cut ductile fabric in 4.3b, c, e and f. This relationship was observed in many fault zones with ductile shearing usually located at the edges of fault zones implying brittle reactivation along pre-existing planes of weakness. Fragmental breccia forms the central part of the zone. The fault zone is at 159.30-160.60 in diamond drillhole GIMD29. Downhole direction is to the right, core block is 50mm wide.

Figure 4.3b
Ductile shear fabric from the area marked “b” in 4.3a. The fabric trending top to bottom is defined by aligned and stretched (flattened) plagioclase phenocrysts without development of fissile schistosity or cleavage. Quartz-calcite-pyrrhotite filled fractures oriented top-right to bottom-left overprint the ductile fabric. The ductile shear fabric trending 080°/85°S is at 159.30m in diamond drillhole GIMD29. Lens cap is 55mm diameter.

Figure 4.3c
Ductile shear fabric from the area marked “c” in 4.3a. The fabric is the same as in 4.3b and both are probably part of a pre-existing shear zone. Brittle fractures with quartz-calcite-pyrrhotite, +/- tourmaline cross-cut the ductile fabric. In contrast to 4.3b the ductile shear zone trends 086°/78°N suggesting either a small component of rotation across the fault zone or non-uniform extension during brecciation. The ductile shear fabric is at 160.60m in diamond drillhole GIMD29. Lens cap is 55mm diameter.

Figure 4.3d
Central breccia component of the fault zone marked “d” in 4.3a. Coarse clasts of fractured wallrock, massive pyrite/pyrrhotite and pre-existing breccia are cemented by hydrothermal quartz-calcite vein material. The breccia comprises angular and sub-rounded fragments of fractured/brecciated altered basalt and mineralised material indicating multiple episodes of faulting and mineralisation. A thin cataclasite seam traverses the specimen from top right to bottom left and cross-cuts the breccia fragments. Specimen is at 159.70m in diamond drillhole GIMD29. Lens cap at right of photo for scale.

Figure 4.3e
Ductile shear fabric in Victorious Basalt from Slippery Gimlet. The fabric is defined by aligned flattened phenocrysts of plagioclase with a weak planar anisotropy developed. Late white quartz with irregular morphology overprints the ductile fabric, and pyrite-pyrrhotite mineralisation is localised along thin quartz-calcite veins that also overprint the ductile shearing. The shear fabric trends 120°/84°SW at 266.80m in diamond drillhole GIMD31. Lens cap is 55mm diameter.

Figure 4.3f
Discrete ductile shear band in Victorious Basalt from Slippery Gimlet. A 5-10mm band of ductile deformation is defined by flattened plagioclase phenocrysts interspersed within a planar fabric of aligned and stretched chlorite slivers and thin flattened grains of pyrrhotite. The ductile fabric appears to overprint a small zone of fracturing to the right however some chloritic fractures cross-cut the ductile shear zone. A quartz-calcite-chlorite-pyrrhotite vein is parallel to the ductile shear zone. Pyrrhotite mineralisation occurs in veins, fractures and as part of the ductile fabric. The ductile shear band trends 092°/58°N in diamond drillhole GIMD9 at 244.65m. Lens cap is 55mm diameter.

4.2.2 Brittle-ductile faults

Brittle-ductile faults in the Ora Banda district have either mostly ductile or mostly brittle character with a subordinate component of the other. These relationships are expressed as ductile shear fabrics and schistosity cut by sub-parallel cataclasite seams (Figure 4.2c p.90) or conversely, thick breccia zones with thin ductile shear bands at the margins or centre of the breccia bodies (Figure 4.3 p.93). Shear veins are common brittle-ductile features with variably deformed quartz veins in schistose shear zones. In each case the subordinate component is an integral part of the structure, which suggests reactivation of these structures under different conditions to when the original fabric developed.

4.2.3 Ductile shear zones

A series of ductile shear zones is present in the Ora Banda structural zone developed both within and cross-cutting incompetent rocktypes such as interflow sedimentary rocks and ultramafic units. Type I S-C mylonite (Lister and Snoke 1984) is commonly developed in units with a pre-existing planar fabric or mineral composition dominated by weak minerals or phyllosilicates. S-C foliations are common in medium-grained doleritic sills but generally absent in ductile fabrics from basalt flow rocks where flattening strains dominate. The mylonite zones are discrete planar structures developed over several metres width and up to tens of kilometres long whereas ductile fabrics in basalt flows are usually restricted to zones of less than one metre width and tens of metres long. The localisation of ductile shear zones within interflow sedimentary rocks may be a factor of competence contrast as outlined by Robert *et al.* (1994), and a result of enforced shearing where strain is localised in the weaker rocks. Four of the ductile shear zones in the Ora Banda district (Black shale shear zone, Enterprise-east shear zone, Cashmans Shear Zone and Ora Banda shear zone), are discussed in Chapter 4.4 (p.99).

4.2.4 Schistosity and cleavage

Ductile deformation is accompanied by schistosity and cleavage development with heterogeneous distribution similar to high strain shear zones. The zones of foliation vary from spaced cleavage defined by thin seams of metamorphic chlorite and/or biotite less than 1mm wide, to continuous cleavage and schistosity defined by metamorphic chlorite, biotite

or muscovite penetrative over several metres. Ductile shear zones are spatially associated with zones of schistosity where the schistose zones may represent zones of preferential weakness and strain partitioning.

Schistosity and cleavage are localised primarily in doleritic parts of intrusive sills and are developed in massive basalt only at the boundaries of major shear zones. Intrusive sills have zones of cleavage and schistosity both parallel to, and overprinted by, later brittle-ductile faults and quartz veins. These relationships indicate a complex series of events that involved alternating brittle and ductile conditions with reactivation and localisation of brittle features along pre-existing ductile structures (eg. quartz veins emplaced parallel to zones of schistosity).

4.2.5 Discussion

Shear zones were classified as brittle, brittle-ductile or ductile by Ramsay (1980a), whereas Passchier and Trouw (1996) recognised only a two-fold subdivision into brittle zones (or faults), and ductile zones. The subdivision of Passchier and Trouw (1996) is based on the unique deformation processes that produce either totally brittle or totally ductile fabrics and is useful because it recognised that when exposed to stress, rock materials either flow or fail under given conditions.

In the classification of Ramsay (1980a), brittle shear zones have a clear discontinuity with unstrained or brecciated wallrocks whereas brittle-ductile shear zones have some ductile deformation in the walls of a discontinuity, and ductile shear zones have deformation and differential displacement but no visible discontinuities. He also recognised the possibility that in brittle-ductile shear zones the respective brittle and ductile parts of the deformation history may not be synchronous and that a critical limit to coherent flow may be reached after which brittle deformation proceeds. The reverse order of deformation is also possible where brittle deformation is overprinted by ductile flow. Brittle-ductile textures are therefore composite fabrics that combine elements of totally brittle and totally ductile deformation. The fabrics are characteristic of deformation at the brittle-ductile transition, an environment where brittle deformation processes and ductile deformation processes operate alternately but not synchronously, without large gaps in time, producing fabrics that show evidence of both kinds of deformation.

Since the transition between brittle and ductile deformation depends on many factors including strain rate, temperature, pressure, grain size, lithotype, fluid-pressure, pre-existing anisotropy and ambient stress conditions, the transitional environment can occur in a number of geological settings depending on conditions of deformation. This relationship means that the environment of brittle-ductile deformation is dependent on more than simply depth in the crust, hence a competent rock type that deforms in brittle fashion may be juxtaposed with a relatively incompetent rock type that flows under the same conditions. The presence of both brittle and ductile fabrics in the same lithotype where overprinting occurs in the same structure may indicate alternating conditions of deformation under a consistent prevailing stress field.

Brittle faults in the Ora Banda structural zone are developed in areas where pre-existing mesofracture arrays impart anisotropy to the rock from the intersection of two or more consistently oriented fracture sets (Figure 4.2 p.90). This process is analogous to tectonic comminution (Jebrak 1997), which includes the two processes of fracture propagation and wear abrasion (Figure 4.4). Fractures at Slippery Gimlet mine are commonly filled with pyrite or pyrrhotite with minor amounts of quartz-calcite and tourmaline with traces of sphalerite and arsenopyrite. Muscovite-calcite alteration and pyrite-pyrrhotite mineralisation in the wallrocks of the faults, show clear timing relationships between fracturing and brecciation, where breccia zones contain angular and rounded fragments of the fractured, mineralised wallrock. The jigsaw breccia / mill breccia distinction depends on the dominant clast type and the level of wear and abrasion. In the Ora Banda district, a full transition of clast morphology exists from angular blocks in jigsaw patterns with only minor infill components to poorly sorted breccia with rounded clasts and a higher matrix to clast ratio.

4.3 GEOMETRY OF THE ORA BANDA STRUCTURAL ZONE

Ora Banda structural zone has dimensions of about 6 km x 8 km, centered on Ora Banda (Figure 4.1 p.87). Felsic-intermediate sedimentary rocks to the southwest and ultramafic rocks to the northeast, flank the Ora Banda stratigraphic sequence of basalt flows and intrusive mafic sills. The structural zone is defined mostly within the mafic sequence on aeromagnetic imagery and in open-pit mines. The lower degree of brittle deformation

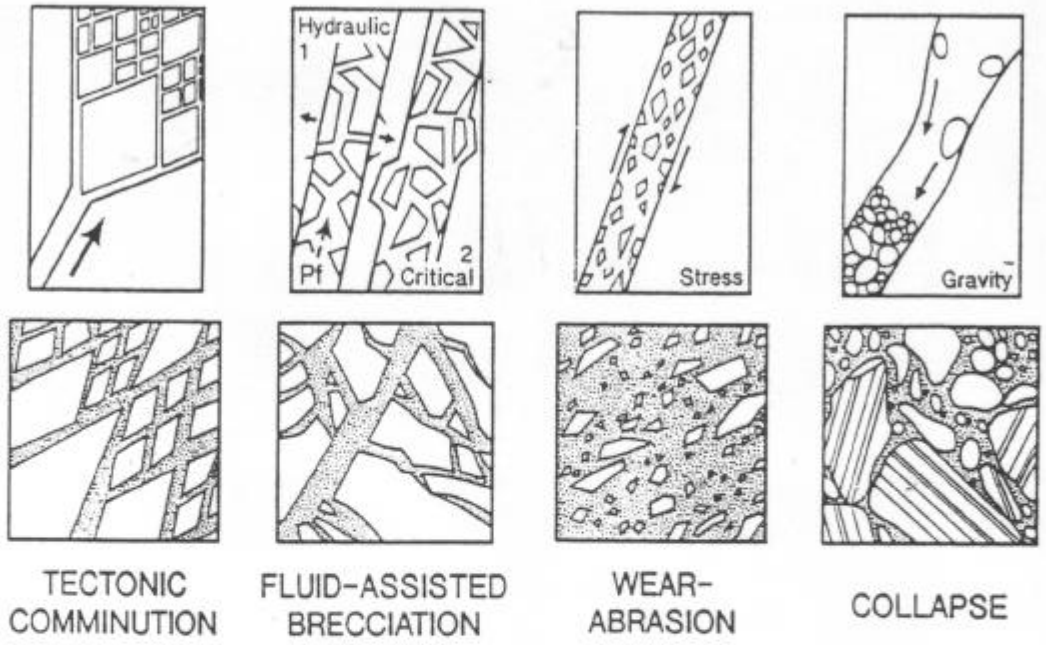

Figure 4.4 – Diagrams showing typical textures developed by various brecciation processes, modified from Jebrak (1997).

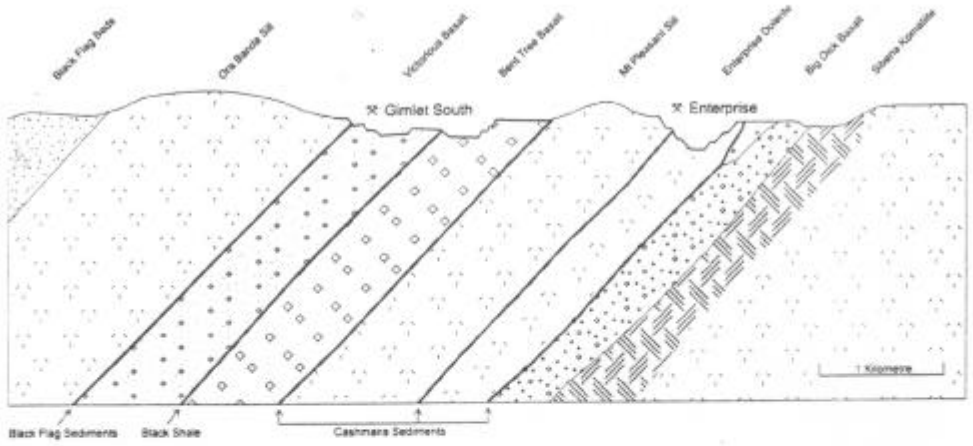

Figure 4.5 – Schematic geological cross-section through the Ora Banda structural zone

beyond the bounds of the mafic sequence may be an artifact of a lack of gold deposits in less chemically-favourable host units, and therefore fewer outcrops of critical structures always present with gold occurrences. However, remote sensing data suggest a higher density of fracturing in the mafic sequence that is diminished to the east and west. A series of brittle-ductile faults interpreted from ground magnetic imagery (Figure 4.1 p.87), extends into less competent rock types on both sides of the mafic package, but the density of faulting in these outer units appears markedly less than within the Ora Banda mafic sequence.

A schematic cross-section through the mafic sequence (Figure 4.5 p.98) shows moderately southwest dipping layers forming the limb of the Kurrawang Syncline. It is probable that the zone of high fracture-density represented at the surface as the structural zone, plunges parallel with the more brittle rocks in the layered sequence giving a pipe-like geometry to the structural zone with depth. Apparent fault offsets are determined from lateral breaks in the magnetic layers and fault slip lineations in most areas have shallow to moderate plunges indicating that much of the movement was strike-slip with subordinate oblique-slip components. Most brittle-ductile faults have offsets of less than 50m which is negligible at the scale of the map (Figure 4.1 p.87) and cross-section (Figure 4.5 p.98). A prominent feature of the Ora Banda structural zone is the array of parallel faults trending about 060° that are steeply dipping to sub-vertical with anastomosing geometry. Zones of schistosity and cleavage tend to be sub-parallel to most brittle-ductile faults and are present in restricted zones within the mafic sills. Poor distinction in magnetic imagery may be due to magnetite destruction in high strain shear zones. Several ductile shear zones trending NE-SW and NW-SE traverse the length of the structural zone and these can be traced in outcrop and drilling several tens of kilometres along strike.

4.4 Significant structures within the Ora Banda structural zone

4.4.1 Gimlet fault array (D4)

A series of five parallel faults locally known as the ‘Gimlet lodes’, dominates the structure of the Ora Banda district. These include the North Sandalwood, Gimlet South, Slippery Gimlet, Tom Allen and Sleeping Beauty faults (Figure 4.6). The faults are spaced at intervals of 500-800m trending ENE-WSW. Minor differences of size and structural

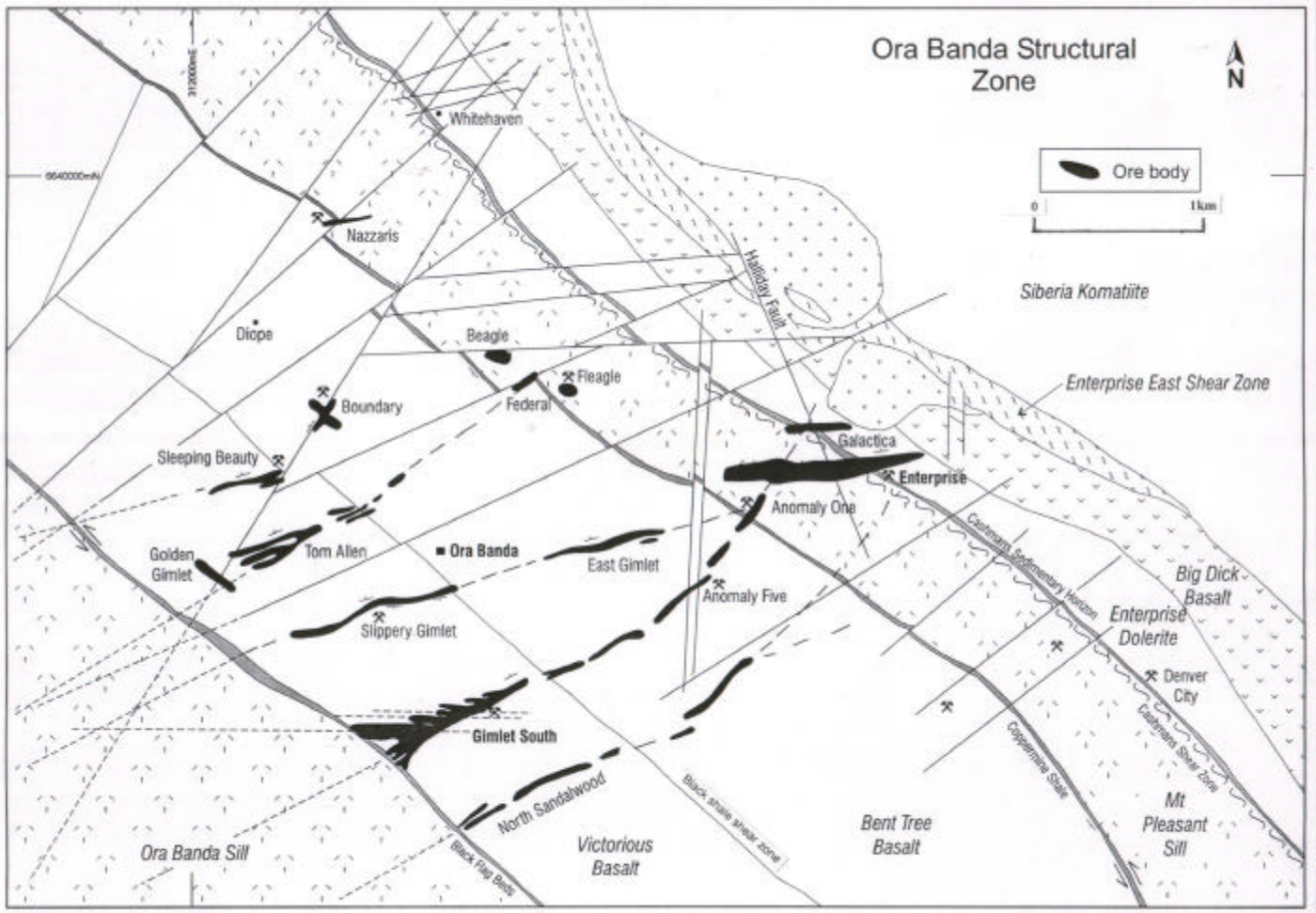

Figure 4.6 – Geological map of the Ora Banda structural zone, showing the interlinked network of brittle-ductile faults. Dip and strike symbols show general trends of igneous layering and structures.

setting distinguish the faults, however host rocks and timing are common to all five. Three of these five are discussed in some detail and are representative of the variation in style between the structures. The Black shale shear zone is also presented in detail since it provides important timing constraints on the structural development of the area.

Gimlet South and Sleeping Beauty faults (D4)

Gimlet South fault is the largest of the faults and includes a group of smaller historic prospects that are parts of the same structure (Figure 4.6 p.100). The group is collectively called "Gimlet South fault" and includes Victorious/east/deeps, Wilson's Lode, Gimlet South, Far East, Farther east, Old Mate, Corsair spur, Avenger and Hornet lodes. Full descriptions of the Gimlet South fault are given in Petersen (1987) and Harrison *et al*. (1990). Gimlet South fault and Sleeping Beauty fault have similar structural styles, but the main difference is the scale of development. Gimlet South fault is over 2 km long, up to 50m wide and known to extend to several hundred metres depth, whereas Sleeping Beauty fault is 300m long, 10m wide on average and known to about 150m depth (Figure 4.6 p.100, Map 8 p.353). The structures trend 060° and dip sub-vertical to 75° NW.

Kinematic indicators for the Gimlet South fault reported by several authors (Baxter 1989; Laing 1994; Oliver 1993), show right-lateral strike-slip offset with displacement of the basalt sequence in the order of several metres, which at the mine-corridor scale is negligible. Stereograms of structural elements compiled from underground mapping from the Gimlet South mine (Figure 4.7), show three dominant brittle-ductile fault sets striking 057°, 172° and 085°. The 057° cluster is the main trend of the structure with the weak 085° cluster representing the spur lodes. Cross-cutting brittle-ductile faults are subordinate features along the 172° trend.

Gimlet South fault and Sleeping Beauty fault are intersected by prominent E-W trending brittle-ductile faults locally known as spur lodes. The E-W faults have similar morphology to the main structures comprising fault and hydraulic breccia with components of ductile shear. Laing (1994) interpreted the E-W faults in terms of their intersection geometry with the main Gimlet South fault as either cross-cutting or asymptotic in contact with the 057° trending faults. In both cases the intersections form steeply northeast plunging, discrete shoot-style zones of high fracture-density (Figure 4.8). Slip lineations plotted on a

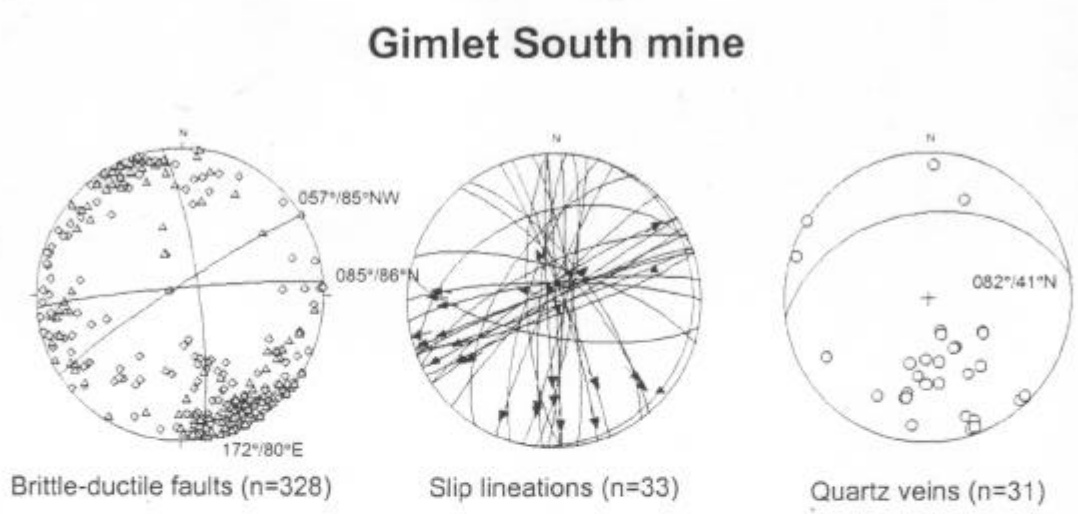

Figure 4.7 – Equal area stereograms of structural elements from the Gimlet South mine. Orientations are for average great circles to the major clusters. Squares represent faults, triangles represent shear zones. Data are compiled from several hundred underground face maps prepared by Ora Banda mine geologists. See text for explanation.

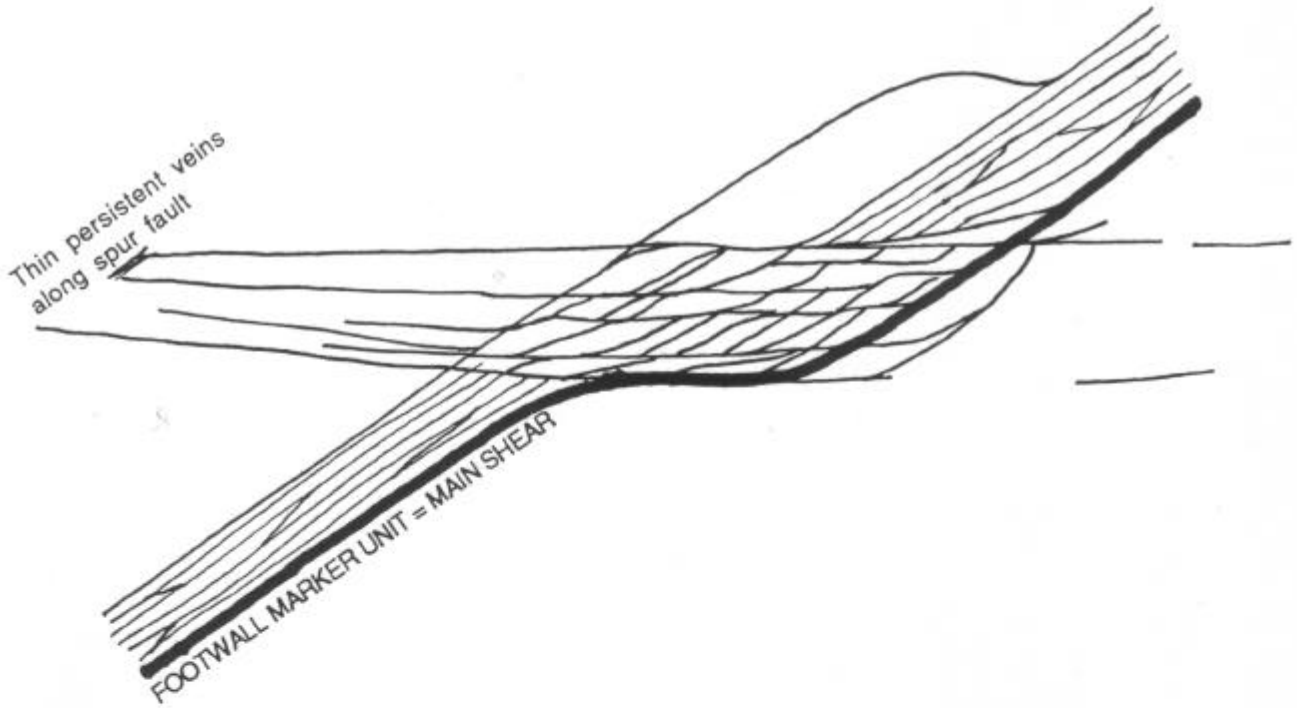

Figure 4.8 – Schematic plan view showing high fracture-density zones that form at the intersection of 057° and 085° shear zones (main lode, spur lode) from Gimlet South, and illustrating the two types of fault intersections at Gimlet South, asymptotic and cross-cutting. Modified from Laing (1994).

stereogram show one of the clusters plunging 73°→035° (Figure 4.7 p.102), indicating some fault movement parallel to ore-shoots that are developed in this orientation. Tabular quartz veins are common along sharp brittle fault planes located at the footwall boundary of the main structure, with thick breccia bodies in the hangingwall. The Gimlet South fault exhibits textures that indicate complex development of breccia lodes with a high degree of textural maturity (Figure 4.15c, p.114). Compared to the other four structures, the Gimlet South fault is the largest and most complex developed over 2 km of strike length, and probably represents a preferred locus of the most intense deformation, with the other structures decreasing in intensity away to the northwest and southeast. Gimlet South fault extends into the Mount Pleasant Sill, but changes orientation to 045° across a contact with coarse-grained gabbroic rocks in the base of the Bent Tree Basalt. The fault intersects the Enterprise fault zone in the Mount Pleasant Sill, but cross-cutting relations between the two faults have not been determined. A significant zone of faulting and fracturing is however, present at the point of intersection.

Slippery Gimlet fault (D4)

Slippery Gimlet fault is a brittle-ductile structure located 800m north of the Gimlet South fault (Figure 4.6 p.100). It is a good example of a dilational fault jog as described by Sibson (1987), with the 'jog' geometry mapped in the open-pit and interpreted from diamond drilling (Figure 4.9, Map 9 p.356). A NE-SW trending brittle-ductile fault is separated by a 35m wide jog zone. The location of the dilational jog may be controlled by a significant change in grainsize of the basalt sequence, at an intersection with the NE-SW trending fault.

The eastern segment of the NE-SW trending brittle-ductile fault oriented 067°/77°S, is a markedly deformed zone within relatively undeformed and unaltered porphyritic basalt (Figure 4.9, Map 9 p.356). The fault has a central section of intensely sheared fault gouge (0.8m wide) and outer sections of weakly to strongly sheared basalt with a total width of 1.9m. In the hanging wall of the structure (Figure 4.10) two sets of thin quartz-carbonate-chlorite filled fractures are parallel to the C and S planes of the main brittle-ductile fault. Two lineations are present on the C-plane. One is a product of the intersection between the C and S planes of the fault trending 25°→083°, and the other is a mineral elongation

Figure 4.9 – Geological map of the Slippery Gimlet open-pit. Coarse-grained units are integral parts of the basalt flow sequence.

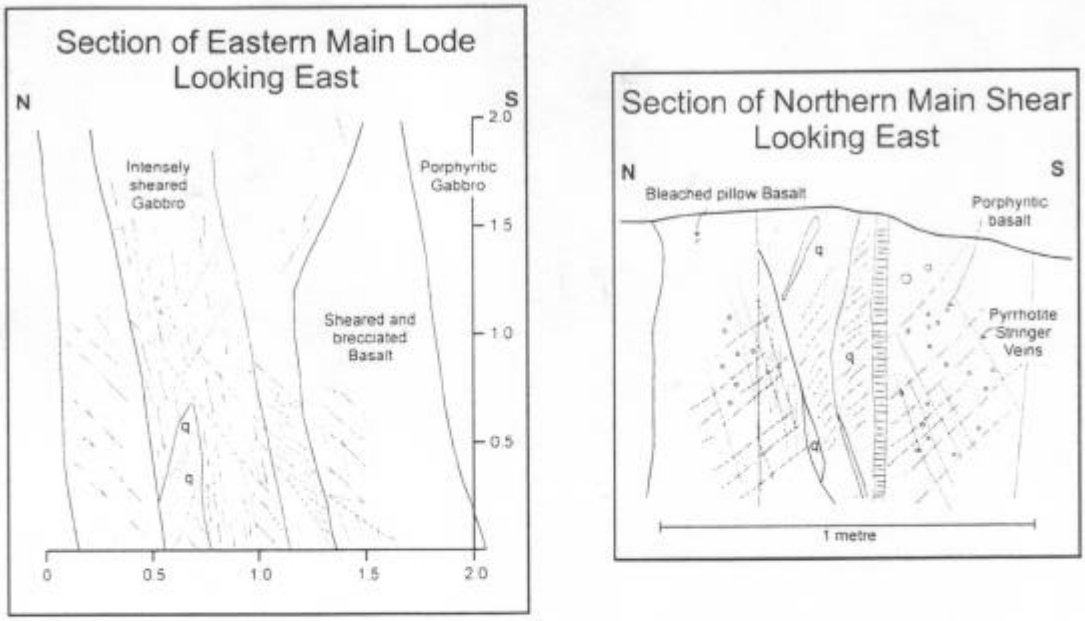

Figure 4.10 - Field sketches of cross-sections through the southern main shear zone and the northern main shear zone, Slippery Gimlet.

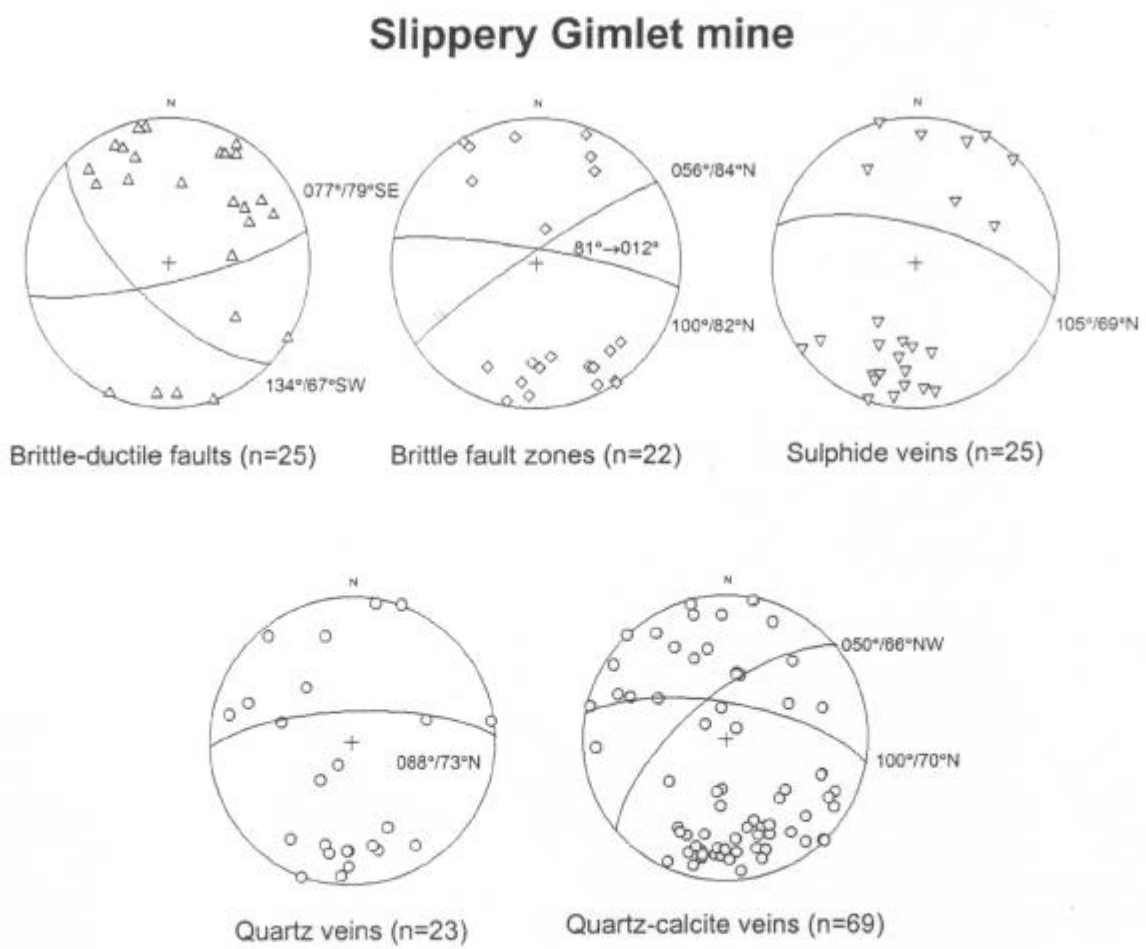

Figure 4.11 – Equal area stereograms of structural elements from Slippery Gimlet. Orientations are for average great circles to the major clusters, with number of measurements (n). Data collected from diamond drill core and open pit mapping. See text for explanation.

lineation defined by aligned micas trending 22°→245°. The S-C fabric geometry indicates right-lateral displacement, and the mineral elongation lineation confirms normal oblique-slip movement on the fault. Ferruginous quartz veins in the weathered fault are lens-shaped and appear to predate the shearing.

The western segment of the NE-SW trending brittle-ductile fault is oriented 056°/88°N and has mostly brittle textures with a higher degree of fracturing in the wallrock, but only a small <0.5m zone of schistosity and quartz veining. The structure is 1.1m wide with abundant pyrite-pyrrhotite veins and thin quartz veins. Deformation is in the form of pervasive fracturing with weakly developed jigsaw breccia. Interlinked mesofractures trend 099°/46°N and 062°/61°S.

A central rhomb shaped area (dilational jog) is enclosed by the eastern and western fault segments, which are linked by a layer-parallel brittle-ductile fault trending 122°/78°S on the northern boundary of the jog. The southern boundary is slightly sheared trending 115°/73°S (Figure 4.10 p.105). The northern boundary fault is 0.6m wide with a strong mineral elongation lineation developed in the C-plane. Strike-slip movement is indicated by this shallow NW-plunging lineation, but the sense of shear is unclear. In the central portion of the fault, the rock is intensely sheared and has sharp boundaries with outer portions of weakly foliated basalt. The fault contains abundant 5-10cm milky quartz veins and has a 0.2m wide alteration halo with carbonate-muscovite replacement of the wallrocks and intense bleaching. A greater proportion of quartz veins than the eastern segment of the NE-SW trending fault is present as thin veins with comb textured quartz growths at 90° to the vein walls, and iron oxide staining from the breakdown of pyrite. The predominance of quartz veins with open space growth textures suggests a component of dilation orthogonal to the fault. Some quartz veins are folded, indicating either that minor shearing postdated dilation, or the folded veins are an earlier generation. Quartz veins average about 088°/73°N (Figure 4.11 p.105). The western boundary of the jog area has a thin <0.1m zone with S-C fabrics that show left-lateral offset. Strong hematite-chlorite-muscovite alteration is confined to a few centimetres either side of the zone.

Within the dilational jog, a series of sub-parallel quartz veins and breccia zones are spaced at 2m intervals. Individual veins average 10mm-wide, with pyrite-pyrrhotite halos and wide calcite-muscovite-pyrrhotite alteration halos. The veins are sub-parallel to the northern

boundary fault defining a southwest plunging shoot 35m by 50m. Northeast-southwest and NW-SE trending quartz-breccia veins are not common in the open-pit but are observed in diamond drill core (Figure 4.2 p.90, Figure 4.3 p.93).

The Slippery Gimlet fault shows a wide range of brittle fault textures from weakly deformed zones with sub-parallel wallrock fragments (Figure 4.2e p.90), to complex mill breccia with rounding of clasts (Figure 4.2a p.90). Brittle-ductile faults form the boundaries to breccia zones in most instances (Figure 4.2c p.90, Figure 4.3 p.93) and the gross geometry of the structures is controlled by brittle-ductile faults that trend 077°/79°S and 134°/67°SW (Figure 4.11 p.105). A series of brittle fault zones trending 100°/82°N (Figure 4.11 p.105), are subparallel to sulphide veins trending 105°/69°N. Breccia lodes containing clasts of wallrock with sulphide filled fractures, clearly indicate that brecciation overprints an earlier phase of fracture development. However sulphidation and intense wallrock alteration also are widely developed with the formation of breccia, hence fracture propagation and subsequent brecciation are not widely separated in time. Areas of higher density fracture may become breccia loci, and breccia zones are closely associated with brittle-ductile faults. Quartz-carbonate veins are generally sub-parallel to breccia zones. A lack of hydrothermal alteration of the type associated with breccia zones indicates that the quartz carbonate veins overprint the brecciation event. The veins may have been emplaced under a similarly oriented but significantly diminished far-field stress, and localised by a pre-existing anisotropy.

4.4.2 Black shale shear zone (D2-D4?)

A thin, strike persistent interflow sedimentary shale layer separates the Victorious Basalt from the underlying Bent Tree Basalt (Figure 4.6 p.100). It is a critical structure in the Ora Banda district because pre-existing gold-bearing brittle-ductile faults are offset by the shear zone, and it therefore constrains the timing of gold mineralisation and deformation.

Morphology

The shale is generally 1m thick on average, but varies up to 5m. Along strike the unit is continuous with variable thickness and has been traced for 12km to Grants Patch, and further south at Mount Pleasant. Similar thin units of shale are mapped at various

stratigraphic levels between basalt flows, but these are generally discontinuous and irregular, some occurring as rip-up clasts within basalt. The shale has been described as carbonaceous, pyritic, chloritic, tuffaceous shale with banded pyrite horizons interpreted as exhalative in origin (Gilbert 1983).

The Black shale shear zone was investigated in the Gimlet South underground mine and diamond drill core at the Slippery Gimlet mine. An apparent 20m right-lateral offset of the main Gimlet South fault (20m) was mapped in underground development drives at the Gimlet South mine. The shear zone is an intense deformation zone with ductile fabrics characteristic of a thrust fault (Figure 4.12). Thrust-related textures and fabrics are exhibited mostly by quartz veins within the shale including boudinaged quartz veins with long axes of boudins parallel to a well developed stretching lineation, isoclinal drag folding with fold axes approximately parallel to the S-C intersection lineation, rootless intrafolial folds and ptygmatic folding. S-C relationships indicate west-over-east thrust movement (Figure 4.12). The S-plane is particularly well developed defined by slaty cleavage in graphitic shale. Isoclinal, rootless intrafolial folds are present in both the C and S planes.

Kinematics

Reverse dip-slip movement on the Black shale shear zone is confirmed by apparent right-lateral offset of the steeply north-dipping Gimlet South fault in plan view (Figure 4.6 p.100). This contrasts with an earlier interpretation of the Black shale layer as being offset by the Gimlet South fault (Gwatkin 1984; Harrison *et al*. 1990). Since known movement on the Black shale shear zone is dip-slip, determination of the true displacement (117m) and heave (83m) is possible using the throw (75m), looking orthogonal to strike. The shear zone overprints late brittle-ductile faults (Slippery Gimlet fault and Gimlet South fault) and is therefore one of the latest deformation fabrics in the Ora Banda structural zone.

The deformation is typical of bedding-parallel thrusting produced during flexural-slip folding (Tanner 1989) and may preserve evidence of continued tightening of regional D2 folds (Swager 1989; Witt 1993c). The ductile nature of the strain fabrics may reflect simply a relative strength contrast with surrounding basaltic rocks, however intense ductile

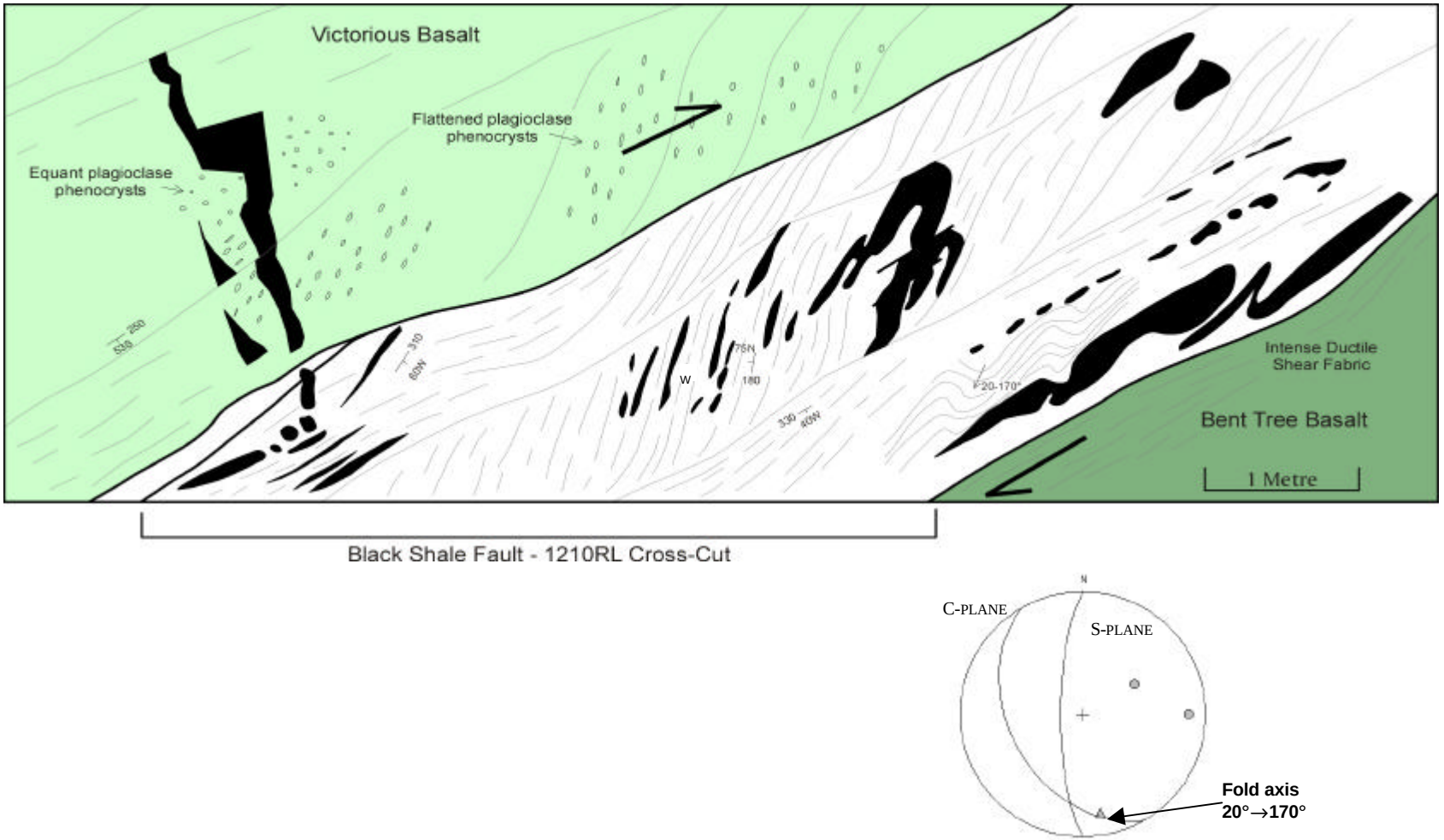

Figure 4.12 – Face map of the Black shale shear zone from an underground drive at the 1210 RL in the Gimlet South mine. Strong shearing in basalt in the immediate wallrocks of the shale, and ductile fabrics in the shale indicate west-over-east thrust movement. The stereogram shows the S-C fabric relationships, with the triangle symbol representing the fold axis orientation of bedding and folded quartz veins, approximately parallel to the S-C intersection lineation. A pre-shearing brittle quartz vein in the Victorious basalt is entrained parallel to the shear zone. View is looking towards 330°, for a plan view see Figure 4.6 (p.100).

shearing of the basalt wallrocks within 2m of the shear zone indicates significant ductile deformation. The thrust movements may have been initiated during the D2 regional folding event.

There is no evidence of strike slip movement during D3, however the Black shale shear zone is parallel to several other D3 shear zones within the Ora Banda structural zone. Kinematic analysis of the shear zone determines a direction for the maximum shortening axis at about E-W, which is similar to the ENE-WSW orientation interpreted for the Gimlet parallel-fault-array. This determination is supported by S-foliation fabrics within the shear zone and flattened plagioclase phenocrysts in the basalt wallrocks that are at angles of >45 to the shear plane, which suggests a horizontal E-W directed shortening axis. This later movement and offset of D4 faults may be a final effect of the regional ENE-WSW shortening, and may also indicate a marked decrease in strain-rate post-dating brittle-ductile faulting.

4.4.3 Enterprise fault zone (D4)

The Enterprise fault zone (Figure 4.6 p.100, Map 6 in pocket) is discussed in detail in Chapter 5 (p.145), but key features of the fault zone as they relate to the Ora Banda structural zone are presented here. The fault zone is a corridor of 080º-trending brittle-ductile faults, 1.3 km long and 50-100m wide. The Enterprise fault zone is somewhat different to most other structures as it is developed in a dolerite sill (Enterprise dolerite). Well-developed schistosity and cleavage in dolerite are typical of the fault zone, whereas breccia developed in fine-grained basalt, typical of the Gimlet parallel-fault-array, is relatively scarce.

East-west trending brittle-ductile faults that form the main structure, cross-cut the Big Dick Basalt, Enterprise dolerite and Mount Pleasant Sill, but the highest density of faulting occurs in the Enterprise dolerite. Differences in tensile strength of the rock units are displayed in the Enterprise open-pit where there is a large-scale sheeted vein system in the Enterprise dolerite, but the overlying Mount Pleasant Sill is only weakly veined. East-west trending brittle-ductile faults are cross-cut by a swarm of metre scale brittle faults and brittle-ductile faults that trend NE-SW and NW-SE on average. Localised zones of high fracture-density occur at intersections of major brittle-ductile faults and at the intersection

of major E-W faults with the Enterprise dolerite / Mount Pleasant Sill contact. The Enterprise fault zone extends west and may link up with the Sleeping Beauty fault.

4.4.4 Boundary fault (D4)

The Boundary fault is located 2.5 km north of Ora Banda and 500m east of the Sleeping Beauty fault (Figure 4.6 p.100). The structure is a brittle-ductile fault up to 5m wide with anastomosing geometry that bifurcates in several places producing a series of parallel shear planes. The main structure cross-cuts massive to pillowed chlorite-biotite altered Bent Tree Basalt and is characterised by quartz veining with intense shearing and breccia. Shear sense indicators (S-C fabrics) and stratigraphic offset show right-lateral displacement of 20-50m across the main fault trending 032°/67°NW (Figure 4.13). There is also a subsidiary set of brittle-ductile faults trending 002°/51°W but their offsets and displacements have not been determined.

Quartz veins at the Boundary mine are mostly simple crack-seal veins with laminations of chlorite parallel to the vein margins. The veins cluster about two main orientations, one parallel to NW-SE faults, which are poorly represented in the data-set, and one sub-parallel to the main brittle-ductile fault orientation at Boundary.

4.4.5 Nazzaris fault zone (D4)

The Nazzaris fault zone is a series of brittle-ductile faults located 1 km to the north of the Boundary mine (Figure 4.6 p.100, Map 7 p.347). The faults cross-cut the Mount Pleasant Sill and extend west into Bent Tree Basalt. This fault zone is typical of dolerite-hosted structures where the trend of the main zone of shearing is E-W, but also there are subsidiary faults oriented NE-SW to N-S. Similar relationships exist at Enterprise where a few large-scale brittle-ductile faults up to 1.3 km long control the main direction of gold mineralisation but at the mesoscopic scale, numerous oblique faults intersect the main brittle-ductile faults providing local structural controls.

Widely scattered fault measurements from Nazzaris have an average orientation of 003°/49°W which trends at about 90° to the main fault zone orientation (Figure 4.14). Schistosity measurements cluster tightly about 130° with moderate southwest dip,

Boundary mine

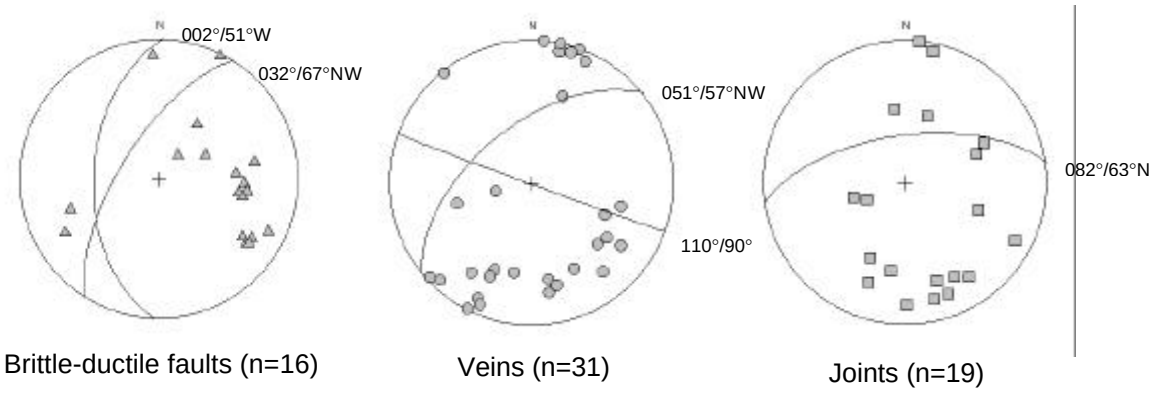

Figure 4.13 – Equal area stereograms of structural elements from diamond drill core at Boundary. Orientations are for average great circles to the major clusters with number of readings (n).

Nazzaris mine

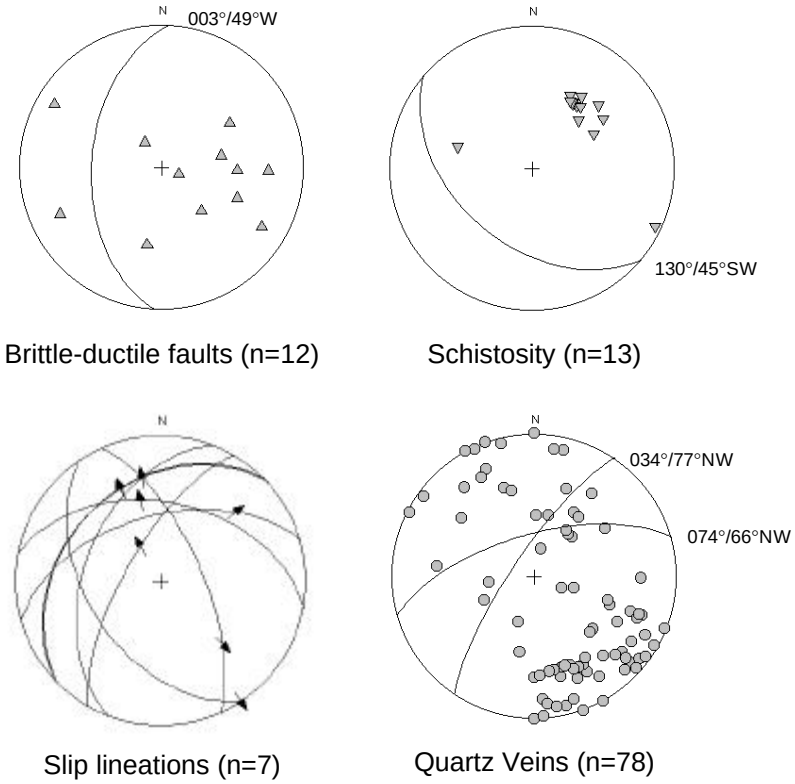

Figure 4.14 – Equal area stereograms of structural elements from diamond drill core at Nazzaris. Orientations are for average great circles to the major clusters with number of readings (n). Data compiled from diamond drill core structural logs (provided by G. Adams).

explained by the presence of bedding-parallel shearing in the Coppermine Shale at the Bent Tree Basalt / Mount Pleasant Sill contact. Two main orientations are observed for quartz veins averaging 034°/77°NW and 074°/66°NW.

4.4.6 Enterprise-east shear zone (D3)

Enterprise-east shear zone is an 80m-thick band of mylonite at the contact of Big Dick Basalt with Siberia Komatiite, with shearing of the lower units of Enterprise dolerite near the Lone Hand Monzogranite intrusion (Figure 4.6 p.100). The shear zone is at least 5 km long extending from Denver City-east to Whitehaven-north. Silicified outcrops of the shear zone are common along the length of the structure. A single diamond drillhole and several outcrops were studied in detail.

The shear zone is a significant feature in the area and is typified by intense ductile deformation. In the lower units of the Enterprise dolerite, coarse-grained dolerite is sheared with progressive flattening and development of schistosity towards the most intensely sheared parts. The mineralogy changes from epidote-chlorite altered dolerite, to biotite schist and ultramylonite with ribbon texture in quartz. Ultramylonite dominated by biotite-chlorite seams is interspersed with ribbons of quartz and rare asymmetric porphyroclasts of vein quartz that indicate left-lateral movement on the shear zone (Figure 4.15e).

Shearing appears to have been focussed within a thin zone of interflow sedimentary rock at the contact between Siberia Komatiite and Big Dick Basalt. This has resulted in localised total destruction of the primary rock fabric to muscovite-biotite schist with slaty cleavage. The protolith was probably black shale, as indicated by the presence of massive pyrite bands in dark chlorite-altered shale. The sedimentary unit exhibits complex shear fabrics with tight to isoclinal folding and microfaulting of quartz veins, and localised zones of ptygmatic folding and irregular distribution of quartz veins within the shear fabric (Figure 4.15f).

The underlying Siberia Komatiite is variably sheared with deformational intensity decreasing away from the contact into relatively undeformed komatiite with spinifex texture. Two stocks of the Lone Hand Monzogranite and associated quartz-porphyry dykes

Figure 4.15 - a) Mesofracture array with sulphide stringer veins, Slippery Gimlet. **b)** Mineralised pillow margin triple point, Slippery Gimlet. **c)** Multiple episode hydrothermal/fault breccia, Gimlet South. **d)** Cashmans Shear Zone exposure, Enterprise open-pit. **e)** Enterprise-east shear zone with multiple felsic intrusions, Enterprise. **f)** Mesoscopic folding in black shale, Enterprise-east shear zone. See text and over page for explanation.

Captions for figures on Page 114

Figure 4.15a
Mesofracture array in Victorious Basalt from Slippery Gimlet. The array comprises three regularly oriented fracture sets with apparent timing relationships. The poorly developed set trending subparallel to the core axis but from lower-left to upper-right is overprinted by the main set at a high angle. Fractures in the main set of several millimetres width are infilled with veins of pyrite that have thin halos of dark coloured tourmaline. The main set is overprinted by a late series of fractures with parallel quartz veins. The main fracture set trends 092°/71°N at 282.00m in diamond drillhole GIMD9, downhole direction is to the right. Lens cap is 55mm diameter.

Figure 4.15b
Pillow margin triple point in Victorious Basalt from Slippery Gimlet. White quartz vein material infills the central part of the structure with intense calcite-muscovite-pyrite alteration of the surrounding basalt. Small breccia fragments with a high proportion of chlorite are common primary features typical of interpillow breccia. Pyrite forms along fractures in the wallrock that show small displacements of plagioclase phenocrysts to the left of the pillow margin. Intense alteration and mineralisation indicates that the pillow margins are interlinked and impart a primary porosity to the massive basalt flows. Sample from the wallrock of a breccia zone at 235.30m in diamond drillhole GIMD16, downhole direction is to the right. Lens cap is 55mm diameter.

Figure 4.15c
Multiple episode hydrothermal/fault breccia from Gimlet South. Textural maturity in this specimen is indicated by rounded clasts of re-brecciated matrix to pre-existing hydrothermal breccia. The matrix clasts are interspersed with centimetre-scale angular fragments of altered and fractured basalt. Several pieces of matrix material with different composition to the large round clast in the photo (top right) were observed in the same fault zone. Numerous clast types and matrix compositions indicate a multi-stage history of brecciation and cementation followed by subsequent fault movements. White quartz material in subparallel bands cements a late fracture event that overprints all previous textures. Sample is from diamond drillhole DH54 at 188.5m. Lens cap for scale.

Figure 4.15d
Cashmans Shear Zone from Enterprise open-pit. Shearing is restricted to a 2.5-3.0m zone with S-C mylonite on boundaries. The wallrocks are strongly foliated but not sheared. Through going C-fabric trends bottom right to top left. S-C geometry and intersection lineation indicates left-lateral reverse oblique slip. The ductile shear zone is developed subparallel to bedding in talc-chlorite altered hornblende peridotite at about 30m above the base of the Mount Pleasant Sill. Talc alteration after serpentine and tremolite produced a layer of weak minerals that preferentially partitioned the deformation. View is to the southwest, hand lens for scale.

Figure 4.15e
Multiple felsic intrusions into Enterprise east shear zone. Ductile shearing textures vary from weakly foliated dolerite to ultramylonite at the base of the Enterprise dolerite. The ductile shear zone is a locus of felsic intrusion displayed mainly as dykes and sills of similar composition to the Lone Hand Monzogranite stock, but with a range of deformation textures that indicate syn to post tectonic intrusion. Intensely sheared muscovite altered quartz-feldspar porphyry in ultramylonite (bottom half of photo) contrasts sharply with relatively undeformed porphyry with large grey quartz veins intruded less than one metre away. Photo is at 151.00m in diamond drillhole ORD129. Lens cap is 55mm diameter.

Figure 4.15f
Mesoscopic folding in black shale from Enterprise dolerite / Big Dick Basalt contact. Close-up view of folded quartz veins with mesofaults and late extensional microvein arrays trending across the photo. The sediment is a complex fault plane at the base of the Enterprise east shear zone. An olivine rich Proterozoic dyke of 1m width intrudes the shale with local alteration effects in both rock types. Sample is from 190.00m in diamond drillhole ORD129. Lens cap is 55mm diameter.

intrude the shear zone. Outcrop patterns of the monzogranite indicate non-conformable intrusive relations as well as a large elongate fragment of mafic schist several hundred metres long stoped off the shear zone wallrocks and contained within the western margin of the northern monzogranite stock (Figure 4.6 p.100). Boundaries of the main stocks transgress the contacts of the shear zone, but porphyry dykes contained entirely within the shear zone show evidence of syn to post-tectonic intrusion. Quartz-feldspar porphyry dykes have intruded the same area of the shear zone displaying textures from undeformed porphyry with quartz veining to intensely sheared porphyry within ultramylonite (Figure 4.15e p.114). A small-undeformed Proterozoic mafic dyke in drillhole ORD129 (also identified on aeromagnetic imagery), intrudes the shear zone with reaction zones against the sheared sedimentary rock.

4.4.7 Cashmans Shear Zone (D3)

The Cashmans Shear Zone is a district-scale ductile shear zone sub-parallel to the stratigraphic sequence with a strike length of about 20 km. The shear zone is exposed in the Enterprise open-pit, as well as in over two hundred intersections in diamond and reverse-circulation drillholes, and numerous exposures in shafts and pits along the strike of the shear zone, which is a prominent host to gold mineralisation (Jutson 1914). The Cashmans Shear Zone is developed at 5-30m above the base of Mount Pleasant Sill, in a hornblende-peridotite unit within the sill. Alteration of pyroxene and olivine to serpentine, talc and chlorite within the unit has preferentially partitioned deformation (ductile shearing) at this position. Remarkably coherent layering and strike persistence of rock types in the 60 km long Mount Pleasant Sill are well documented (Witt *et al.* 1991), which resulted in the district-scale development of the Cashmans Shear Zone. Cashmans Shear Zone is similar to the Enterprise-east shear zone in terms of its style and structural controls. Witt (1990) reported both shear zones as actually being the Cashmans Shear Zone north of Enterprise. However, the two shear zones are subparallel, separated by the 150m thick Enterprise dolerite and are distinctly different in drillhole intersections.

Kinematics

The shear zone is developed as up-to 1.5m wide bands of S-C mylonite in strongly foliated coarse-grained ultramafic rock. An exposure of the shear zone in the Enterprise open-pit

shows S-C fabrics that indicate left lateral offset (Figure 4.15d p.114). Well developed C-foliations trending 142°/54°SW cross-cut an intense schistosity (S) trending 170°/66°W. The S-C intersection lineation plunges 50°→201°.

Stereographic analysis of the foliations and intersection lineation suggests reverse left-lateral oblique slip with a dominant strike-slip component. S-shaped drag folds in the Cashmans Sedimentary Horizon (Witt 1990) are consistent with left-lateral movement. Witt (1990) also considered the shear zone to be centered broadly on the sediment horizon, but many outcrops and drillhole intersections of the sediment display relatively undeformed bedding laminae.

Reactivation

An exposure in Enterprise open-pit shows the Cashmans Shear Zone cross-cutting minor brittle-ductile faults, which are normally observed to be late structures overprinting layer-parallel shear zones in most other exposures (Figure 4.6 p.100). Final movements on the Cashmans Shear Zone are interpreted as reactivation of the structure, which postdates the majority of 'later' brittle-ductile features. The 142° trend of the shear zone is unfavorably oriented for reactivation during ENE-WSW shortening (D4 late fault event) since the maximum shortening direction is about perpendicular to the shear zone.

Alternatively, shortening from about E-W is properly oriented to reactivate bedding-parallel shear zones, and movement across the Black shale shear zone at Gimlet South mine also offsets late faults and is interpreted as reactivation during an E-W directed shortening.

4.4.8 Minor structures within the corridor

Several structures at Ora Banda have minimal offsets, including North Sandalwood and Tom Allen faults. Golden Gimlet, Brace and Bit, and Ora Banda shear zones (Jutson 1914), are minor bedding-parallel shear zones located at or near the contact of Victorious Basalt with Ora Banda Sill. Witt (1990) interpreted the Ora Banda shear zone as extending several kilometres to the northeast and southwest of Ora Banda.

Bedding parallel shear zones

Bedding-parallel shear zones are located in the Ora Banda structural zone at interflow-sedimentary rock contacts (Coppermine Shale, Black shale, Back Flag Beds) and stratigraphically controlled zones of ductile shearing (Cashmans Shear Zone). Deep drillholes at Enterprise and underground workings at Gimlet South confirm depth extensions of these structures. Other ductile shear zones (Ora Banda shear zone, Enterprise-east shear zone) outcrop parallel to bedding contacts, yet deep drilling suggests steep to sub-vertical dips. In the case of the Ora Banda shear zone bedding is also steeper at the surface and shallows with depth.

4.5 MECHANICAL ANALYSIS

The following mechanical analysis is concerned with determination of the main structural events that affected the Ora Banda mafic sequence. Strain distribution in the Ora Banda Domain is heterogeneous which results in non-pervasive fabric elements and structures. With less than 1% outcrop, the non-pervasive nature of structural development makes determination of deformation events difficult. Other factors such as thick mafic sequences with sparse marker units, and stress fields that do not change markedly in orientation between deformation pulses further impair the recognition of separate folding and faulting events. Although six critical areas of detailed exposure have been examined in this study including a significant amount of diamond drill core, not all deformation events are recorded at each exposure hence observations from the group of exposures are combined in the analysis to determine the geological history of the area.

4.5.1 Principal structural orientations

Structural elements in the Ora Banda corridor are resolved into four principal structural orientations that represent the statistical averages of moderately scattered structural readings. Each principal orientation is defined by a group of factors including deformation-style, relative timing and sense of offset, that may be related to regional deformation events.

Relationships between deformation styles

Deformation features in the Ora Banda structural zone range from ductile to brittle. A full spectrum of brittle styles is developed, and a limited range of ductile features including zones of schistosity and cleavage. A wide range of structural styles in most orientations precludes the distinction of deformation events based on style alone, hence a method of grouping structures into 'principal structural orientations' was used, similar to that applied elsewhere in the Kalgoorlie region (Phillips 1986; Clout *et al.* 1990).

Observations from the six largest mines in the corridor have been grouped into ductile shear zones, brittle-ductile faults, veins and, schistosity and cleavage (Table 4.1). The average orientation for each structural style was compiled from the stereograms presented for each of the mines, and represents the entire data set of the particular structure at each mine. Four principal structural orientations (Figure 4.16) are determined as NW-SE, N-S, NE-SW and E-W. Brittle-ductile faults, schistosity and cleavage are developed in most of the principal orientations, but some directions are typified by a particular structural style (Table 4.1). Ductile features (shear zones, schistosity and cleavage) are developed in all orientations, whereas brittle-ductile faults are best-developed in N-S, NE-SW and E-W orientations. These distinctions show a possible separation of deformation events based on structural style.

Overprinting relationships

Overprinting between structures generally shows a clear sequence of timing, although there are inconsistencies. In most examples, NW-SE structures are overprinted by all other structures. Rare exceptions to the rule include NW-SE shear zones that overprint brittle structures at Enterprise, Slippery Gimlet and Boundary mines. North-south, NE-SW and E-W structures while texturally distinct, are commonly observed with mutual cross-cutting relationships. Northeast-southwest and E-W structures commonly overprint N-S brittle-ductile faults, but the reverse is also observed where the N-S features are large-scale (>1km).

Synchronous development of the three principal orientations over an extended time period is the most probable explanation for widespread mutual cross-cutting relationships.

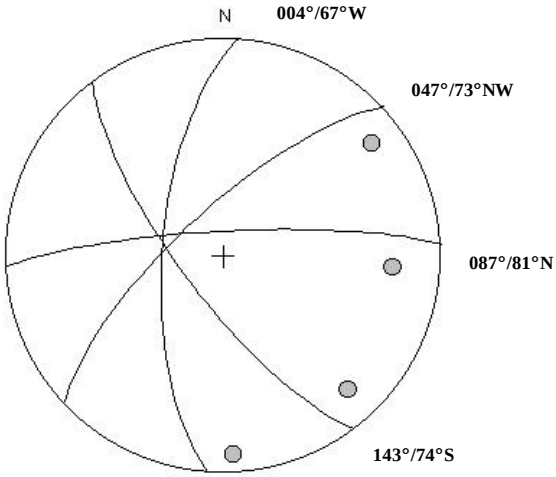

Figure 4.16 – Stereogram showing the four principal structural orientations at Ora Banda. Great circles are for the average orientations listed at the bottom of Table 4.1.

Table 4.1 – Principal structural orientations in the Ora Banda structural zone compiled from observations for the six major mines at Ora Banda, grouped by structural style. Orientations for each structural element are great circle orientations to the major clusters presented on stereograms for each prospect.

Principal Structural Orientations	NW-SE	N-S	NE-SW	E-W
Brittle-ductile faults				
Nazzaris	-	003°/49°W	-	-
Boundary	-	002°/51°W	032°/67°NW	-
Sleeping Beauty	147°/57°NE	-	-	-
Slippery Gimlet	134°/67°SW	-	-	077°/79°SE
Gimlet South	-	172°/80°E	057°/85°NW	085°/86°N
Enterprise	137°/60°SW	-	035°/78°NW	079°/79°NW
Brittle faults				
Nazzaris	-	-	-	-
Boundary	-	-	-	-
Sleeping Beauty	-	-	-	079°/86°NW
Slippery Gimlet	-	-	056°/84°NW	100°/82°N
Gimlet South	-	-	063°/82°NW	-
Enterprise	161°/81°SW		030°/59°NW	088°/69°N
Veins				
Nazzaris	-	-	034°/77°NW	074°/66°NW
Boundary	-	-	051°/57°NW	110°/90°
Sleeping Beauty	-	-	046°/68°NW	090°/70°N
Slippery Gimlet	-	-	050°/66°NW	088°/73°N
Gimlet South	-	-	-	082°/41°N
Enterprise	-	-	-	102°/47°SW
Schistosity and cleavage				
Nazzaris	130°/45°SW	-	-	-
Boundary	-	-	-	-
Sleeping Beauty	-	025°/61°NW	-	087°/80°N
Slippery Gimlet	-	-	-	-
Gimlet South	-	-	-	-
Enterprise		177°/54°W	058°/81°NW	-
Average Orientations	**143°/74°SW**	**004°/67°W**	**047°/73°NW**	**087°/81°N**

Alternatively, large-scale N-S structures with a more ductile style may have initiated early and as deformation proceeded, the style changed to a more brittle character. This may have been followed by NE-SW and E-W trending brittle-structures cross-cutting the N-S shear zones. The limited presence of ductile shear zones trending NE-SW and E-W, and schistose fabrics marginal to NE-SW and E-W structures suggests that the two orientations were initiated during a more brittle deformation event.

Offsets and displacements

Each of the principal structural orientations has a consistent sense of offset and comparably small displacements (Figure 4.17). Northwest-southeast shear zones and E-W brittle-ductile faults are left-lateral, whereas N-S and NE-SW brittle-ductile faults are right-lateral. Some kinematic data indicate the opposite of these relationships, but are a minority of the total data set. Displacements across NW-SE shear zones are generally undetermined (Chapter 3 p.29), depending on the scale of the shear zone. North-south brittle-ductile faults typically have displacements in the order of several hundred metres whereas NE-SW and E-W brittle-ductile faults have small displacements that rarely exceed 50m.

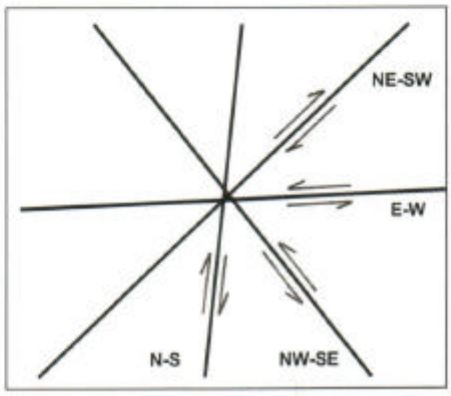

Figure 4.17 – Diagram showing offset relationships of the four principal structural orientations from the mines at Ora Banda.

4.5.2 Discussion

A complex series of structural styles with mutual cross-cutting relationships in the Ora Banda structural zone makes difficult the distinction of generations of structures, and implies broadly synchronous development. Orientation analysis of individual structural styles reveals systematic variation between the various brittle, brittle-ductile and ductile fabrics. Generally, most structural styles occur in all orientations, but some distinction is possible based on cross-cutting relationships of structures developed in each of the four principal orientations.

Ductile shear zones (D3) trending NW-SE on average are a prominent feature within interflow sedimentary rocks or in relatively incompetent rocks. Yet, examples of ductile fabrics are recorded in all principal orientations and commonly form thin zones at the margins of brittle fault structures indicating brittle-ductile conditions (D4). Brecciation caused by fracture propagation generally is developed in association with persisting stress, and for fluid–assisted brecciation, angular fragment morphology is produced by brecciation of rocks with pre-existing planes of discontinuity (Jebrak 1997). Re-brecciated breccias, ductile shear along discrete planes within cataclasites, and brecciated rock containing clasts with ductile shear fabrics and schistosity are all indicators of deformation in the brittle-ductile environment. Brittle fault zones are mostly aligned sub-parallel to the interpreted ENE-WSW maximum shortening direction. The orientation of these structures is favourable for extension orthogonal to the fault zone and may explain the predominance of brittle textures with volume increase and void infill by hydrothermal precipitates.

At Ora Banda, the Gimlet-parallel fault array is composed of breccia-style faults within a complex interlinked brittle-ductile fault network represented by simple shear-style faults (eg. Boundary, Nazzaris and Enterprise). The individual breccia zones and faults are themselves localised zones of high fracture-density *within* the corridor, the distribution of which is analogous to the distribution of structural zones regionally. Three principal structural orientations for brittle-ductile faults are observed at Ora Banda and are interpreted from regional aeromagnetic imagery (Chapter 3 p.29). The structural style and kinematics of each are determinable only at the mesoscopic scale, hence the next logical scale at which to assess high fracture-density zones is the mesoscopic scale. The following chapter (Chapter 5 p.145) treats the Enterprise fault zone in detail and demonstrates the

fractal nature of high fracture-density zones down to the hand specimen and microscopic scales that appear remarkably similar to larger-scale analogues.

4.6 Comparison of Ora Banda with Grants Patch and Mt Pleasant

Ora Banda structural zone is one of several high fracture-density zones in the Ora Banda Domain. Two other important structural zones located at Grants Patch and Mount Pleasant, to the southeast of Ora Banda (Figure 4.1 p.87), have comparable structural patterns.

4.6.1 Grants Patch

The Grants Patch structural zone as defined from aeromagnetic imagery, is dominated by the NE-SW trending Grants Patch Fault. The structure of the area is also controlled by two sub-parallel N-S trending faults that are cross-cut by a series of NE-SW trending structures parallel to the Grants Patch Fault (Figure 4.1 p.87). In terms of mining activity the Grants Patch area is markedly less developed than Ora Banda and Mount Pleasant however several significant structures have been exposed. Important faults include the Prince of Wales fault, Wentworth and Bent Tree faults. The Coppermine Shale at the Bent Tree Basalt / Mount Pleasant Sill contact, is a strongly sheared shale horizon with several mines located at intersections of NE-SW trending structures with the shear zone. Other bedding-parallel shear zones are common in mafic rocks near this contact.

North-south trending faults are poorly exposed at Grants Patch, hence the detailed fabric of these faults is not well known. Northeast-southwest trending structures are best exposed at the Prince of Wales mine where Witt (1993) has described 8m-wide anastomosing shear zones with quartz veins and brecciation, with relatively brittle character. Structural fabrics indicate left lateral movement on 100° striking shear zones but with mutual cross cutting relationships with 075° trending shear zones. There also are 160° trending ductile shear zones with drag folding that cross-cut E-W structures with west-side-up reverse movement. Slip lineations on faults indicate shortening from about E-W producing apparent right-lateral offset of the E-W lodes similar to the Black shale shear zone. All of these structural trends and relationships are similar to those identified at Ora Banda.

4.6.2 Mount Pleasant

The prominent Black Flag and Royal Standard faults control the geometry of the Mount Pleasant structural zone. The two N-S trending brittle-ductile faults cross cut the stratigraphic sequence with up to several hundred metres of right-lateral offset. An array of 060°-045° trending fault zones cross-cuts the sequence, including the Racetrack, Dog-Track, Golden Road, Southern Shoot and Tuart faults. Structural relationships at the Racetrack and Quarters mines show NE-SW faults cross-cutting N-S brittle-ductile faults, and cross-cut by the N-S faults indicating synchronous development. Major E-W trending fault zones include Golden Kilometre fault, and at the Racetrack mine a significant component of the fault zone is composed of E-W to 100° trending brittle-ductile faults. A number of 020° trending brittle-ductile faults also present at Racetrack are fractals of the nearby Black Flag and Royal Standard faults.

Brittle-ductile faults in the Grants Patch and Mount Pleasant structural zones have the same principal structural orientations as those observed at Ora Banda, with similar structural styles, offsets, displacements and overprinting relationships. Although N-S trending structures do not feature prominently in the aeromagnetic imagery at Ora Banda, several large N-S faults have been intersected by drilling and in open pits (eg. Enterprise, Chapter 5 p.145). Similarities between the three areas permit a structural framework to be devised with regards to timing and style of structural development.

4.7 SPACING OF HIGH FRACTURE-DENSITY ZONES

The non-uniform distribution of late-tectonic brittle-ductile faults in the Ora Banda Domain can be explained by the development of high fracture-density structural zones. Structural zones are areas of concentrated deformation, where a large number of brittle-ductile faults intersect in one particular area with higher density than in adjacent areas. The interlinked network of brittle-ductile faults at the mine-corridor scale is composed of three principal structural orientations, each of which represents the statistical average of a range orientations.

Minescale observations, and aeromagnetic interpretations provide evidence for the existence of high fracture-density networks. Observations at the regional-scale and Fry

analysis of the location of important gold mines (and structures) in Chapter 6 (p.213), demonstrates that zones of high fracture-density occur repetitively within the layered Ora Banda mafic sequence, and these are correlated with Ora Banda, Grants Patch and Mount Pleasant. A regular distribution of structural zones implies a common process of formation, and three mechanisms for producing these high fracture-density zones at regular-spaced intervals, are discussed below.

4.7.1 Pre-existing anisotropy due to regional folding

High fracture-density corridors may develop as a result of pre-existing anisotropy formed during the D2 regional folding event. Folding induced by regional deformation can produce fractures that cut through many different rocktypes with the formation of a-c joints orthogonal to the fold axis, and elongation of the rocks parallel to the hingeline (Hobbs *et al.* 1976). Although joints are entirely brittle phenomena, the weakness along which later fractures (joints) develop, may have been initiated during regional folding. The NE-SW trending structures (eg. Gimlet South fault) are orthogonal to the fold axis of the Goongarrie-Mount Pleasant Anticline, and whereas this may explain the NE-SW structures, N-S and E-W trending faults that were formed synchronous with those trending NE-SW can not be accounted for by fracture during regional folding.

Mason (1987) argued for a genetic model for the formation of the Gimlet South fault that involved regional folding. However, retrograde alteration assemblages in NE-SW faults that postdate regional metamorphism, cross-cutting relations of NE-SW faults with regional ductile shear zones (that clearly postdate folding), and synchronous faults in unfavorable orientations, preclude the formation of zones of high fracture-density as a by-product of regional folding.

4.7.2 Pre-existing anisotropy due to D4 brittle-ductile faulting

Regularly spaced corridors may form as a result of the intersection of N-S trending brittle-ductile faults, which have a spatial periodicity, with mafic host sequences. North-south trending structures may have formed early in D4 (Chapter 4.5.1. p.121), and it is possible that brittle-ductile faults up to tens of kilometres long (eg. Black Flag Fault) with spacing of about 5 km, intersected the mafic rocks resulting in fault zones spaced at about 10 km

along the trend of the mafic sequence. Slightly later (late D4) conjugate fracture in the corridor would then have resulted in high fracture-density controlled by the location of the N-S faults.

At Grants Patch and Mount Pleasant (Black Flag and Royal Standard faults), there are fault pairs spaced at about 2 km extending for tens of kilometres to the north and south. No significant N-S faults are known at Ora Banda or further to the west, except for weakly defined linears on aeromagnetic imagery. The N-S fault pairs coincide with zones of high fracture-density within the Ora Banda mafic sequence yet several other zones with dense fracturing identified on aeromagnetic imagery are not related to large-scale N-S faults.

4.7.3 Regional-scale pinch and swell structure

A preferred model to explain the location and regular spacing of the high fracture-density zones is broadly analogous to the process of pinch and swell of a series of layers of variable thickness and competence. Ora Banda structural zone is developed in the Grants Patch Group mafic sequence, with the layered stratigraphic sequence analogous to layers of variable competence. The Ora Banda mafic sequence may represent a competent layer surrounded by less-competent layers of the Linger and Die, and Black Flag Groups.

In describing natural and experimentally produced pinch and swell structures, Ramberg (1955) observed that when inter-layered rocks of different competence are exposed to compressive stress, ‘secondary’ tensile stresses affected the competent layers. Further, he observed that low-pressure regions between individual boudins in the competent layers strongly attracted chemically mobile material and acted as sinks for migrating fluids. The competent body does not necessarily deform by macroscopic fracturing or necking down, but the tensile stresses could affect the whole layer with nucleation of metasomatic materials at countless points throughout the competent body. Ramsay (1967) observed that if the competence contrast is great, initial failure of the most competent layers takes place on well defined cross fractures with small strains and without development of necking. Yet if the competence contrast is very slight, competent layers develop pinch and swell structures without separation into boudins.

Shortening normal to the layering on the east limb of the Kurrawang syncline under conditions of brittle-ductile behavior may have produced layer parallel extension of the sequence, evinced by the ubiquitous presence of quartz veins trending normal to the rock layers and about parallel to the shortening direction (Figure 4.18). Concentrated extension at regular spaced intervals of about 10 km in the layered mafic sequence may have developed zones of higher fracture/vein density relative to the surrounding areas. This process would have provided conditions conducive to the formation of tabular breccia zones normal to strike, such as the Gimlet South fault array, Grants Patch fault and Racetrack fault zone. In this model, the layer-parallel extension is arrested at the initial stages of development with localised zones of tensile fracture and only minor necking (eg. Grants Patch) (Figure 4.18). At the initial stages of extension, pinch and swell features develop followed by fracturing. The location and regular spacing of the high fracture-density zones may be controlled by structure, rock type, competency contrast with adjacent rock types, thickness of the mafic sequence, conditions of deformation or a combination of these.

Findlay (1994,1998) proposed boudinage as a structural process that controlled the emplacement of lodes in the Kalgoorlie goldfield, however he was concerned with boudinage of a layered sequence with pre-existing systematic fracture sets prior to the onset of flow in incompetent layers. Findlay's (1994, 1998) work in the Kalgoorlie area, was based on the geometric relations of rock units. Although he did not address the mesoscopic textural relationships of brittle-ductile faults that argue against structural preparation of the host rocks prior to mineralisation (eg. Clout *et al.*1990), the process is broadly similar to that proposed here. Indeed, mesoscopic textures associated with true boudinage are rare in the Kalgoorlie region, and only become prevalent in high strain domains.

In the Ora Banda and Zuleika districts, large-scale pinch and swell features are observed in northwest trending layered sequences and along within-greenstone-belt shear zones at marked competence contrasts between different rock types. However, in the Ora Banda mafic sequence areas that are considered extensional high fracture-density zones are located in mafic rocks of only slight competence contrast with the surrounding units. The Ora Banda mafic sequence displays weak pinch and swell structure with a major zone of thinning in the Grants Patch area, which may be related to the termination of the Ora

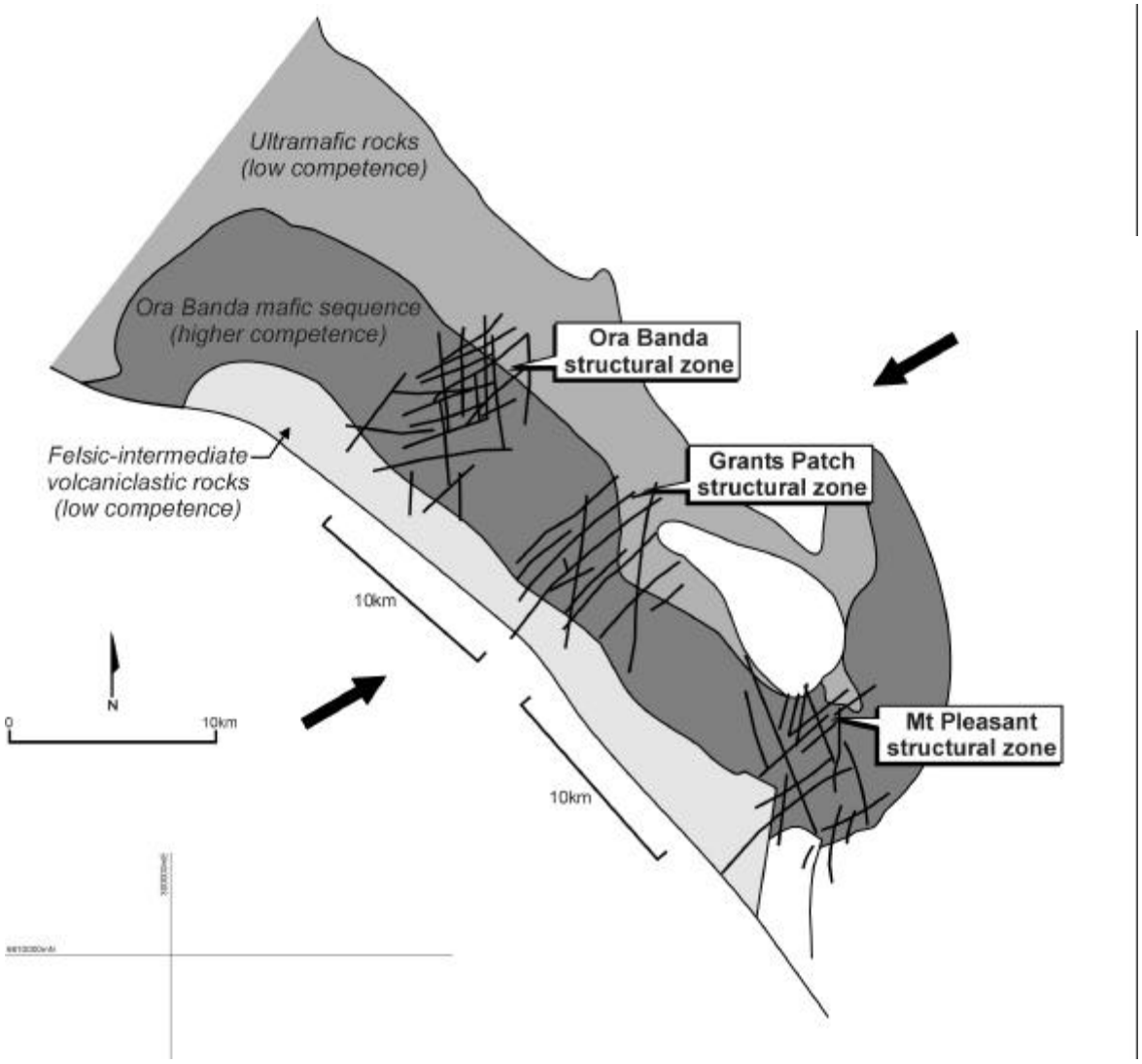

Figure 4.18 – Pinch and swell structure developed with variation in competence contrast in the layered Ora Banda mafic sequence. Competence contrast between the different rocks types is not significant enough to produce boudinage, but may have resulted in a higher density of tensile fracture in regular spaced zones.

Banda Sill. Comparison of Figure 4.18 (p.128) with Figure 3.2 (p.31) shows the higher density of fracture in equally spaced areas within the Ora Banda mafic sequence.

Ramberg (1955) treated competent and less competent rock layers as brittle and ductile respectively. In the model for the Ora Banda mafic sequence competent layers are treated as brittle, and incompetent layers as less brittle, such that the ductile features commonly associated with boudinage (i.e. flowage of incompetent units into extension zones and scar-folding) are not developed. As compressive stresses normal to layering produced only localised zones of high fracture-density, the 'secondary' tensile stresses resulting in the layer parallel extension were not conducive to separation of large-scale competent blocks into boudins.

The spatial distribution of high fracture-density zones at 10km intervals in the brittle layered Ora Banda mafic sequence is controlled by the thickness of the layers, relative competence contrast with surrounding rocks, tensile strength of the layers and local heterogeneities such as the presence of granitoid intrusions or pre-existing shear zones. Regional control on structural distribution suggests that a dominant influencing factor is related to the NW-SE trending mafic sequence. The spatial distribution of gold deposits in high fracture-density zones as discussed in Chapter 6 (p.213), supports this assertion, which may be an alternative to the correlation of gold deposits across strike (between separate mafic sequences) on the basis of lineament analysis (eg. Archibald 1998).

4.8 GOLD MINERALISATION - ORA BANDA

The coincidence of gold mineralisation with zones of high fracture-density at the regional-scale is also applicable at the mine corridor scale. The brittle-ductile faults previously described are also a locus for gold deposits at Ora Banda, which is demonstrated by a contoured plan of gold content from exploration drilling that shows the envelope of gold mapping out the fault distribution (Figure 4.19).

Two main deposit styles typify the Ora Banda gold deposits, Gimlet-style and Enterprise-style. Favourable host unit, structural orientation, structural style, wallrock alteration and ore mineralogy are investigated to distinguish between the two styles.

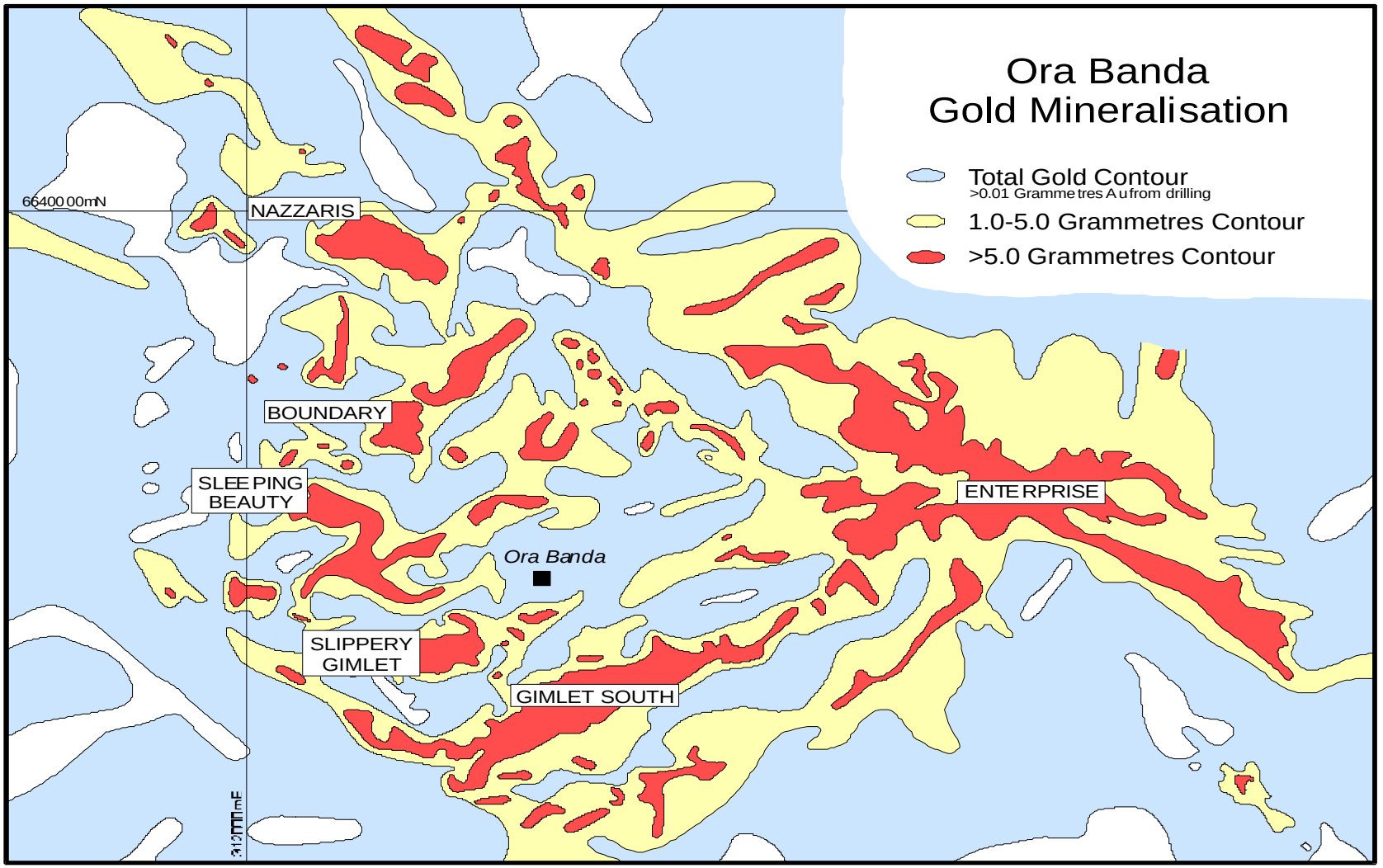

Figure 4.19 – Distribution of gold mineralisation in the Ora Banda structural zone. Gold distribution maps out the location of faults. The contours are determined by summing calculated grammetres (Au value x length of intersection) downhole in exploration drillholes.

4.8.1 Gimlet style mineralisation

Gimlet style mineralisation is represented by gold deposits at the Gimlet South, Slippery Gimlet, Sleeping Beauty, and North Sandalwood mines, and many other prospects and undeveloped deposits.

Lithological control

Gimlet style mineralisation occurred in 060°-trending brittle-ductile faults within the Victorious Basalt and Bent Tree Basalt. The location of the faults in the layered volcanic sequence produces textural relationships that are distinct from Enterprise-style. Both formations are multi-layered sequences with a well-defined volcanic stratigraphy (Harrison 1983; Harrison 1987). As host rocks to gold deposits, only specific layers within the flows are favourable for gold mineralisation. Each of the units consists of alternating pillowed, massive doleritic and coarse-grained layers (Chapter 2.3.1 p.17) with the pillowed and massive units hosting gold ore-shoots. The intersection of NE-SW trending structures with layering that dips SW, has produced southwest plunging ore shoots contained within the structures and in the plane of the favourable host rocks (Harrison *et al.* 1990) (Figure 4.20). Pillow basalt is a common component of the several flow-units that make up the basalt sequence and may be preferentially mineralised. Pillow margins in layered sequences form an interconnecting series of tubes and voids that impart an inherited primary porosity to the stratum. Pillow margins in the Victorious Basalt and Bent Tree Basalt are not vesicular but the triple points enclose voids that were sinks for migrating hydrothermal fluids and formed permeability pathways, evinced by strong gold-related wallrock alteration and ubiquitous calcite and chlorite infilling the voids (Figure 4.15b p.114). These characteristics combined with a possibly lower tensile strength due to the greater primary anisotropy (pillow margins), produce a low-order favourable host unit within the overall chemically-favourable basalt formation.

Structural control

Gimlet-style gold deposits are controlled by 060°-trending brittle-ductile faults with steep northwest dips. A secondary structural control is a result of the intersection of 090°-trending spur lodes with the 060° main structures. The intersection of these two structures

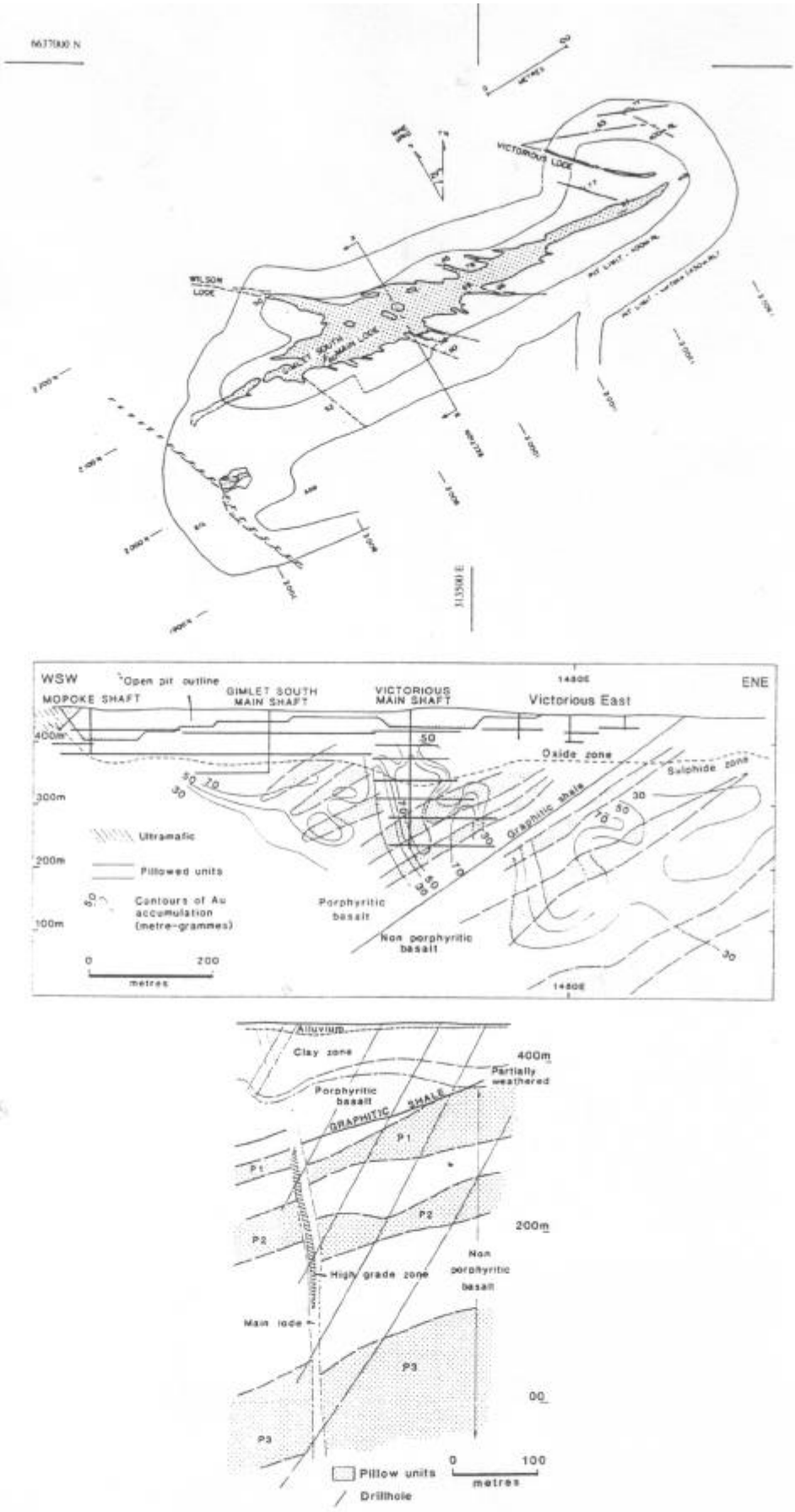

Figure 4.20 – Maps of the Gimlet South deposit showing structural control of gold distribution. Ore shoots plunge with the SW orientation of the basalt host rocks located at the intersection of the main Gimlet South fault with pillow basalt layers. Secondary high-grade shoots plunge to the east parallel to the intersection of the main fault with spur lode cross faults, shown as steeply east-plunging grade-thickness contours, from Harrison *et al.* (1990).

has produced zones of high fracture-density with coincident high-grade ore shoots located at the junctures. The gold orebodies typically blow out at the intersection of the brittle-ductile faults (Figure 4.20 p.132), demonstrating the increased efficiency of fluid infiltration and therefore fluid-wallrock interaction in the high fracture-density area.

At the Slippery Gimlet mine, dilation occurs where a NW-SE trending brittle-ductile fault cuts a rheologic boundary between fine-grained-pillowed and coarse-grained basalt units (Figure 4.9 p.104, Map9 p.356). Slippery Gimlet fault is an example of a dilational jog at the mine-scale, although numerous mesoscopic examples exist where quartz veins have dilated with simple-shear movement. The Slippery Gimlet mine is hosted by a NE-SW trending brittle-ductile fault with gold distributed irregularly along the structure, yet the best-mineralised area is in a southwest plunging jog. In long section, the structure exhibits similar characteristics to Gimlet South with lithologically controlled ore shoots plunging in the plane of the overall structure (Figure 4.21).

The brittle-ductile faults that are hosts to gold ores are zones of high fracture-density with respect to the surrounding wallrocks. Higher fracture-density provides pathways of enhanced permeability and fluid-flow during metamorphism. The episodic nature of deformation events resulted in transitory permeability and therefore cyclic processes of hydrothermal alteration and mineral precipitation. Such processes are reflected by mesoscopic examples of re-brecciated breccia, quartz veins and brittle-ductile faults that show evidence of complex movement histories (Figures 4.2 p.90, Figure 4.3 p.93, Figure 4.15 a-c p.114).

Ore mineralogy

The Gimlet-style ore is predominantly pyrite-pyrrhotite-gold with localised concentrations of arsenopyrite, sphalerite, galena and tellurides. Pyrite is the dominant ore mineral with arsenopyrite, sphalerite, marcasite, chalcopyrite and pyrrhotite occurring as inclusions within euhedral pyrite grains. Chalcopyrite and arsenopyrite are commonly attached to coarse pyrite grains that are aligned in trails along microfractures. Pyrrhotite is the dominant ore mineral at Slippery Gimlet. Gold occurs as specks in pyrite or in vein-like shapes closely associated with pyrite (Townend 1997b). Grains range from 1-15 microns

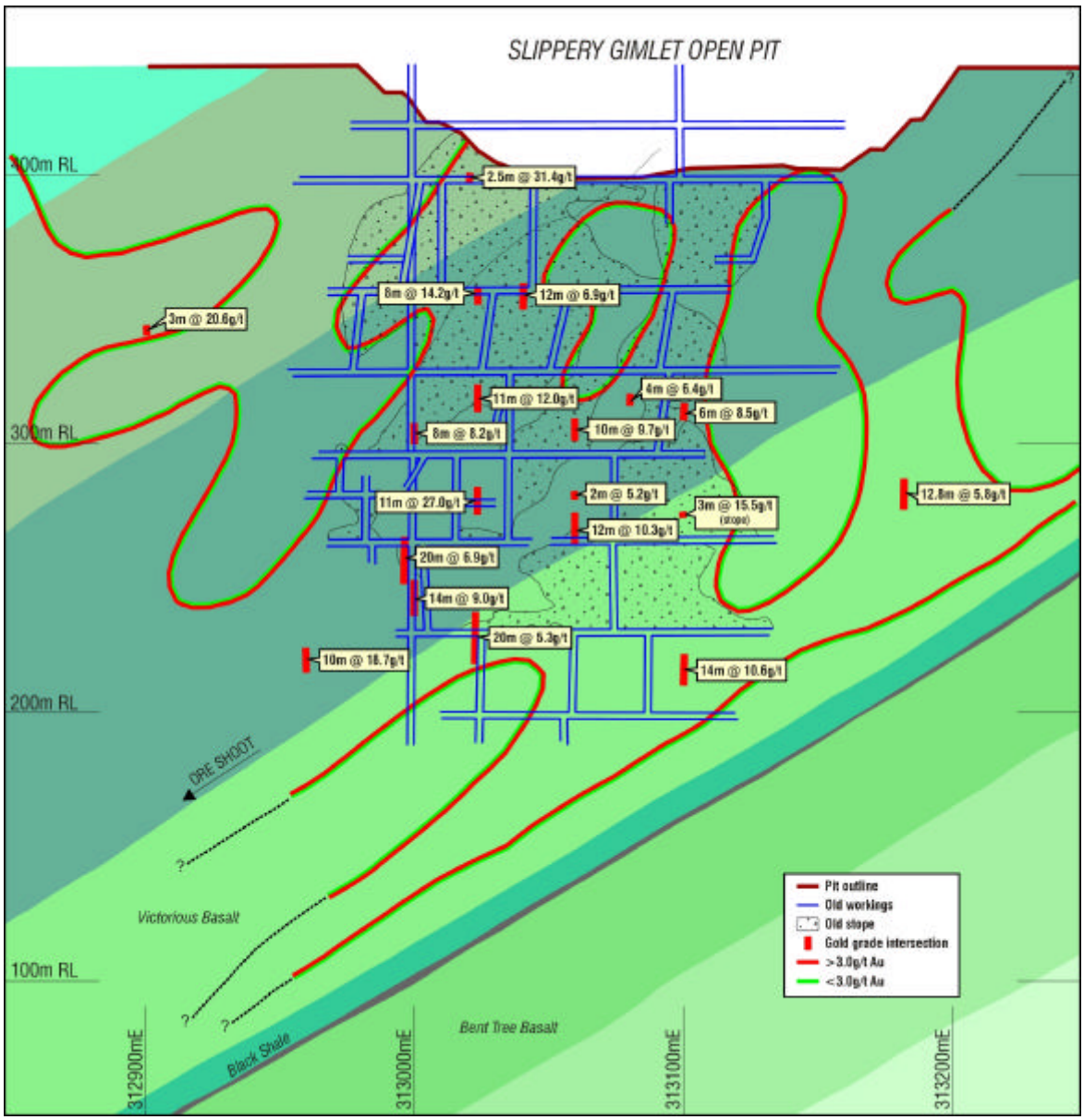

Figure 4.21 – Long section through the Slippery Gimlet gold deposit showing SW plunge of ore shoots in the dilational jog zone of the orebody, and preferential mineralisation controlled by lithological layering.

in pyrite at the margins of included chalcopyrite or pyrrhotite with trace amounts of gold tellurides including petzite (Ag_3AuTe_2) and calaverite ($AuTe_2$) (Townend 1997b).

Ore textures

Ore textures are similar to brittle-ductile fault textures that form the gold lodes. Brecciated basalt with intense alteration of the wallrocks, and clasts cemented in quartz-calcite veins form planar lodes. Sulphidic fragments with re-brecciation texture and angular to rounded morphology are the most common textures.

Wallrock alteration

The typical gold-related alteration assemblage for Gimlet-style mineralisation is muscovite-pyrite/pyrrhotite-calcite/ankerite, with minor zones of biotite and tourmaline. A distinct zonation is observed at Slippery Gimlet with chlorite-calcite, muscovite-calcite and muscovite-pyrite/pyrrhotite-quartz-gold assemblages, from the outer to inner margins of any given lode. At Slippery Gimlet, the alteration halo is much wider than the individual lode (Figure 4.22) with a ratio of about 3:1 for the alteration halo to structure width.

Most lodes at Slippery Gimlet have intense mesofracturing adjacent to the main fault or breccia structure with gold-related alteration in the wallrocks and sulphide/silicate mineral precipitates in the fractures (Figures 4.2 p.90, Figure 4.3 p.93). These relationships suggest that the rock fluid involved in cyclic overpressuring during brittle fracture and brecciation events was the same fluid responsible for gold precipitation.

Gold endowment

Gold deposits in the Ora Banda mining centre have a total gold endowment of 85 tonnes Au. A breakdown of the distribution of gold between the main deposits is given in Table A3.1 (p.371) (Appendix A3). The largest deposits are Gimlet South and Enterprise and several small to medium deposits make up the remainder of gold occurrences in the Ora Banda district.

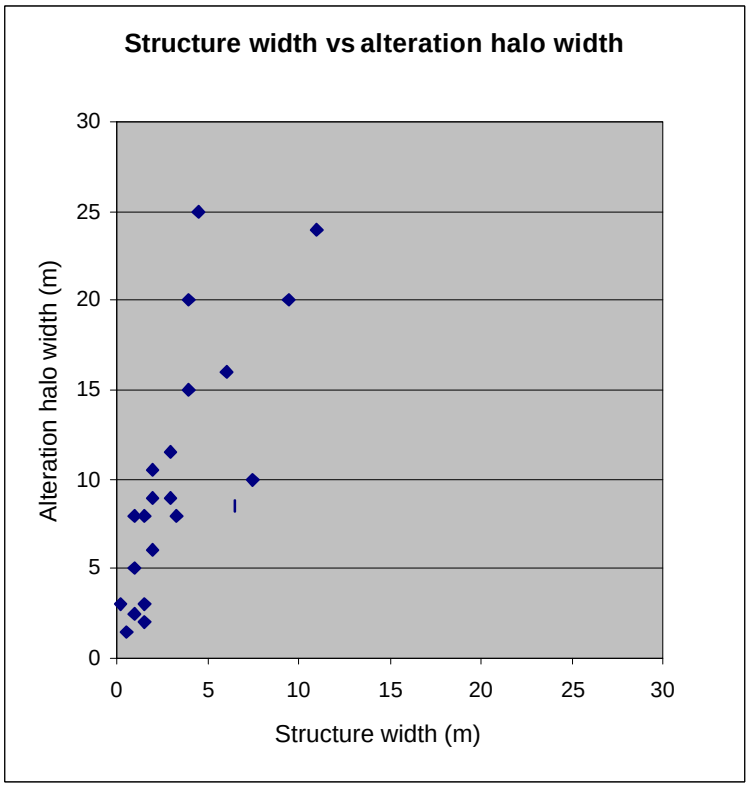

Figure 4.22 – Graph showing the true width of 22 brittle-ductile faults and their gold-related alteration halos from drillhole intersections at Slippery Gimlet. The graph shows that alteration widths are much greater than the width of individual brittle-ductile faults and implies that wallrock alteration around mesoscopic structures is an important process for localising economic gold. Alteration to structure width-ratios average about 3:1. The presence of the faults is co-incident with gold ore zones in most occurrences however in some cases brittle-ductile faulting and gold-related alteration assemblages are present without economic gold.

4.8.2 Enterprise-style

Enterprise-style mineralisation is controlled by several unique conditions that converge in a single location. The host rock is a differentiated tholeiitic intrusion with iron enrichment trends in the middle layers (Gregory 1998). The ore body dips beneath the Mount Pleasant Sill, with the intersection of an E-W trending fault zone and the chemically favourable Enterprise dolerite producing a plunging envelope of gold mineralisation that does not extend far into the overlying rocks. Detailed mesoscopic and microscopic structural control is discussed in later sections but the ore bearing structures are typically foliated in contrast to Gimlet-style deposits that display a predominance of breccia fabrics. The best mineralised parts of the Enterprise orebody are localised in fine-grained layers of the host rocks similar to the Gimlet-style. However, the ore mineralogy is significantly different dominated by pyrite with minor zones of pyrrhotite. Alteration also displays a lateral zonation, but the lode zone is predominantly biotite-pyrite in contrast to muscovite-calcite-

pyrite/pyrrhotite for Gimlet-style. The Enterprise deposit is of similar size to Gimlet South, approximately 40 tonnes Au endowment, but has significant differences that support the distinction of the deposit as a different style of mineralisation. Enterprise-style deposits also occur in the upper layers (unit 8) of the Mount Pleasant Sill at brittle-ductile fault intersections. Nazzaris is a typical example with similarities to Enterprise. An important difference however is the lack of a significant capping layer to provide a contrast in tensile strength and the low level of structural development.

4.8.3 Comparison of Ora Banda with Grants Patch and Mount Pleasant mining districts

Gold mining centres at Grants Patch and Mount Pleasant are located within the Ora Banda mafic sequence essentially with similar deposit styles to Ora Banda. The main differences between the mining centres are related to the principal controlling structures in each area. The Ora Banda district is dominated by 060° trending brittle-ductile fault arrays, whereas Mount Pleasant has significant N-S trending brittle-ductile faults that form an important component of most deposits in the area. Individual deposits may have fault controls in a specific structural orientation but all of these are part of the regional structural framework with movement sense, offset and structural style that accord with the relationships demonstrated for Ora Banda.

Deposit styles

At Grants Patch, the main gold deposits are Prince of Wales/Coronation, Bent Tree, Wentworth, and Dark Horse. Prince of Wales and Coronation were discussed in detail by Ransted (1990) and Witt (1993b). The two mines are located where an E-W trending fault intersects Victorious Basalt. The fault is typically brittle-ductile in character and was regarded as a splay fault to the NE-SW trending Grants Patch fault by Ransted (1990). He also recorded predominantly brittle deformation in the mineralised corridor, with gold lodes in 0.3m to 1.5m-wide breccia zones with pyrite-pyrrhotite, and locally arsenopyrite, chalcopyrite, sphalerite and galena. Alteration of the host rocks is intense in the vicinity of the lodes dominated by silica-muscovite with minor tourmaline. In the Grants Patch mine-corridor, many small gold deposits are located at fault intersections with the iron-rich granophyric layer of the Mount Pleasant Sill, however no significant examples are available for comparison.

Mount Pleasant gold mining centre is a major production area in the north Kalgoorlie region. The largest deposits are Quarters, Racetrack, Golden Kilometre and Henning. Additionally, many small to medium sized deposits are located within the corridor, distributed in a similar fashion to Ora Banda and Grants Patch where the distribution of gold deposits mimics the distribution of structure. The Quarters deposit is located at a right-handed kink in a N-S trending (020°) brittle ductile fault that may be an extension of the Black Flag Fault. The kink occurs at the intersection of a major 040° fault and a swarm of NE-SW trending (060°-080°) faults and veins with a broad zone of muscovite alteration at the intersection. The 020° trending structure typically is brittle-ductile with a 3-5m quartz vein that contains up to 30 g/T Au. A full assessment of Quarters gold deposit was presented by Forster *et al.* (1997).

Racetrack deposit is an interlinked brittle-ductile fault network dominantly composed of 060° trending breccia zones with 040° and 100° trending brittle-ductile faults. The mineralised envelope trends 060° on average and displays textural and structural similarities to Gimlet South and Slippery Gimlet. Intense arsenopyrite-pyrite-muscovite-carbonate alteration in the vicinity of the lodes grades outwards into chlorite-carbonate in the wallrocks.

Gold endowment

Gold deposits in the Grants Patch structural zone have 4 tonnes Au total endowment, which contrasts with Mount Pleasant 97 tonnes Au. The apparent lack of large gold deposits in the Grants Patch corridor may be due to a relatively lower level of exploration and mining activity compared to Ora Banda and Mount Pleasant. However, Grants Patch historically was a mining centre of equal significance to Ora Banda and of greater significance in the district than Mount Pleasant.

4.9 SUMMARY AND DISCUSSION

The Ora Banda district has a higher density of fracturing (shearing and faulting) than adjacent areas and forms a zone of anisotropy within the regional fault network. Ora Banda is of interest because it is located at least 7 km from the nearest regional-scale ductile shear

zone (Zuleika Shear Zone). This relationship contrasts with other major mining areas in the Kalgoorlie district that are much closer to or located on NNW-SSE trending deformation zones (Libby *et al.* 1990; Clarke *et al.* 1986). Previous interpretations of remote sensing data show the Ora Banda district as weakly deformed with few small-magnitude brittle-ductile faults (Witt 1990; Swager *et al.*1990), or even as devoid of structure altogether (Simpson *et al.* 1995).

The Ora Banda structural zone is one of a number of high fracture-density zones that are identified from aeromagnetic imagery (Figure 3.1 p.30), with structural relationships similar to those that are observed at Grants Patch and Mount Pleasant. The higher fracture-density is manifest as interlinked brittle-ductile faults within the corridor that are divided into three principal structural orientations, which is consistent with an interpretation of regional aeromagnetic imagery (Chapter 3 p.29). Regular structural style, offset and overprinting relations distinguish each of the principal orientations that were developed late in the tectonic history of the Ora Banda Domain.

Observations at Grants Patch (Witt 1993b) and at Mount Pleasant also demonstrate the existence of three principal structural orientations of brittle-ductile faults with similar structural relationships. At Ora Banda, NE-SW and E-W trending brittle-ductile faults are the most common, with N-S and NW-SE structures being relatively minor. The Mount Pleasant and Grants Patch areas show similar relationships.

The recognition of four principal structural orientations in the Kalgoorlie area is well documented. Although authors differ on the number of groupings of brittle-ductile faults and their mean attitudes (c.f. Woodall 1965; Phillips 1986; Mueller *et al.* 1988), components of the interlinked fault network can be resolved into N-S, NE-SW and E-W groupings. At Ora Banda, ENE-WSW extensional fault/breccia zones that were formed sub-parallel to the maximum shortening direction (Gimlet-parallel fault array) are included in the NE-SW subgroup.

All brittle-ductile faults overprint D2 regional folds however some bedding-parallel shear zones may have been initiated with the D2 event at lithological contacts (flexural slip folding), and in weak layers in differentiated mafic intrusions such as the Cashmans Shear

Zone (Witt 1990). Late N-S, E-W and NE-SW brittle-ductile faults overprint NW-SE trending regional ductile shear zones and smaller scale fractals of these structures.

Deformation styles at Ora Banda range from ductile to brittle, with individual structures displaying a combination of brittle and ductile deformation except for most early bedding-parallel ductile shear zones. This style of deformation has been correlated with crustal depths of 10-15 kilometres and is characteristic of deformation at or near the brittle-ductile transition (Sibson 1977). Brittle-ductile faults overprinting early bedding-parallel ductile shear zones indicates changing conditions of deformation that may be related to progressive uplift.

The combination of brittle and ductile deformation in most instances at Ora Banda reflects a brittle overprinting of ductile fabrics such as breccia clasts of altered foliated basalt cemented in hydrothermal quartz and calcite veins, and cataclasite and breccia overprinting ductile fabrics. Re-brecciated breccia and breccia clasts of mesofractured wallrocks, evince further brittle deformation that was episodic in nature and accompanied fluctuating fluid-pressures. In addition, many breccia zones at Ora Banda are faults with little or no displacement of the country rocks, and contain angular fragments in matrix-supported zones that do not show evidence of wear abrasion. Such textures in fault zones and hydrothermal veins indicate a close association between far-field stress and the mechanical effects of fluid-pressure. Examples of rounded clasts in deformed matrices display higher degrees of textural maturity than angular breccia, and may indicate that collapse has occurred within the fault zone resulting in further comminution of the particles. Possible scenarios for the formation of these structures include fluctuating fluid-pressures in a maintained far-field stress system, or a complex sequence that involves cyclic changes in the orientation of the stress system as well as fluid-pressures.

Brittle-ductile failure was characterised by Turner and Weiss (1963) as 5% cohesive flow preceding brittle failure. Textural evidence of brittle-ductile failure at Slippery Gimlet and Enterprise indicates that the onset of brittle failure accompanied the attainment of peak fluid-pressures, which may have provided a critical input to strain rate and initiated brittle failure. The importance of pore fluid-pressure during brittle fracturing was emphasised by Phillips (1972) where fracturing is related to the critical effective normal stress on a plane, which is equal to the difference between the normal stress and the fluid-pressure (σ_N - P_f).

The normal stress acts to close the fracture, but failure can occur in the presence of high fluid-pressures that exceed the normal stresses and the tensile rock strength (σ_N+T_0). At Ora Banda, $\sigma_N = \sigma_3$ locally for ENE-WSW trending breccia zones which are sub-parallel to σ_1. Planes parallel to this orientation are favourably oriented for extension orthogonal to the direction of maximum shortening (parallel to σ_3). Simple shear occurs along planes oriented at an angle (θ) to the maximum compressive stress but extension-fracturing and brecciation are more common as this angle tends to zero ($\theta \rightarrow 0°$).

The widespread development of conjugate-type brittle-ductile faults with variable orientations about statistical averages, suggests that the cyclic reorientation of σ_1 happened gradually within a bulk coaxial far-field-stress regime. In a regime of bulk coaxial deformation, conjugate fault pairs will form at regular orientation with respect to the principal axes of shortening (Anderson 1905). The orientations of conjugate fault pairs are determined by the Coulomb-Navier failure criterion, which predicts that shear fractures will form in planes parallel to the intermediate principal stress σ_2, and at $\theta \leq 45°$ to the maximum principal stress. Any shear fracture has two active forces σ_N (normal stress) and τ (shearing stress), between which a linear relationship is predicted by the Coulomb-Navier criterion. On a shear plane, the shear strength is increased by a constant (μ) x normal stress, where μ = coefficient of internal friction of the material.

The plane of maximum shear stress is located at 45° to σ_1 but there is some resistance to shearing because of the normal stress on the plane which leads to two possible planes of fracture equally inclined to σ_1. The coefficient of internal friction (μ) works to hinder rupture and fault development along planes across which there is maximum pressure, thus the directions of shear faulting instead of bisecting the directions of maximum and least compressive stress, will form at lower angles depending on the value of μ. Anderson (1905) proved mathematically that for $\mu = 0$, $\theta = 45°$ and for $\mu = 1$, $\theta = 22.5$. At Ora Banda, conjugate brittle-ductile faults show that $\theta \approx 22°$ for faults developed within the layered basalt and dolerite sequences.

The geometry and textures of brittle and brittle-ductile faults in the Ora Banda structural zone are very similar to dilational jogs described by Sibson (1987). Typical textures record incremental development in *en echelon* fault segments, fissure veins or hydrothermally cemented high-dilation wallrock breccia. The Slippery Gimlet fault is the most obvious

example of a dilational jog at Ora Banda, however dilational jogs are common along all brittle-ductile faults in areas of small changes in orientation. The type of change in orientation must be in a direction favourable for dilation, dictated by either left or right-lateral offset on the faults (Figure 4.23).

Although the dilational jogs described by Sibson (1987) are from epithermal environments, the structural style is typical of brittle-ductile faults in the northern Kalgoorlie area considered by most authors to reflect depths characteristic of mesothermal conditions (eg. Vearncombe *et al*. 1989). Dilational jogs are areas along a fault segment that simply have expanded for reasons that include change of orientation, intersection with
pre-existing faults, changes in rock type reflecting variance in tensile strength and fluid overpressuring.

At the Slippery Gimlet mine, a bedding-parallel brittle-ductile fault at a contact between fine-grained basalt and coarser-grained dolerite (Figure 4.9 p.104) is a rheological discontinuity that has formed a local anisotropy, and may have induced local fluid-pressure gradients conducive to overpressuring and dilation. Angular breccia in the jog zone (Figure 4.2 a,b,d, p.90, Figure 4.3d p.93), occurs almost entirely within fine-grained basalt at the point of intersection of the NE-SW trending Slippery Gimlet fault with a brittle-ductile fault located along a contact of a change in grainsize.

Right-lateral offset on the NE-SW trending Slippery Gimlet fault, and accompanying dilation, produced locally reduced fluid-pressures and induced suctions that oppose rapid slip-transfer across the jog (Sibson 1987). This was followed immediately by implosion of the wallrocks and hydraulic brecciation with focussed fluid-influx into the fissure. The scenario of void development at depth is unlikely since implosion and fluid-influx would be essentially synchronous with incremental fault movements. This method of fault development was termed suction-pump-mechanism by Sibson (1987).

The incremental nature of fault development is indicated by re-brecciated breccias that are common in the Ora Banda structural zone, implying an environment of widespread fault

NW 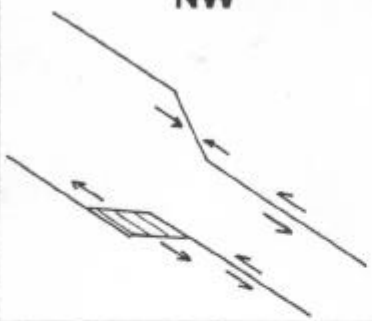	Northwest ductile shear zones are typically left-lateral, ductile-style structures that do not exhibit brittle-style fabrics characteristic of dilational jogs. Significant fault related dilation could be expected however in the vicinity of left-handed bends e.g. Zuleika Shear Zone north of Bowerbird.
N-S 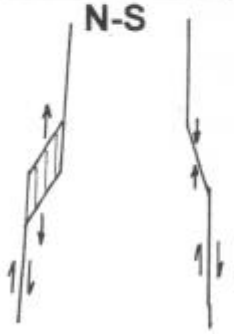	North-south brittle-ductile shear zones have right-lateral offset in schistose structures that usually contain quartz veins with minor breccia. Dilation occurs where right-handed bends trend towards 020° e.g. Black Flag Fault, Quarters Fault.
NE 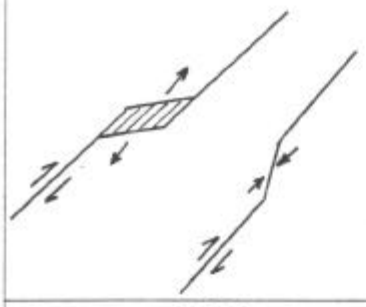	Northeast faults have right-lateral offset and are typically brittle-ductile with a predominance of brittle fabrics. Significant dilation occurs where right-handed bends trend towards 060° e.g. Slippery Gimlet, Gimlet South. Anti-dilation occurs where northeast faults have left-handed bends e.g. refraction of Gimlet South fault at Anomaly 1 (Mt Pleasant Sill interface).
E-W 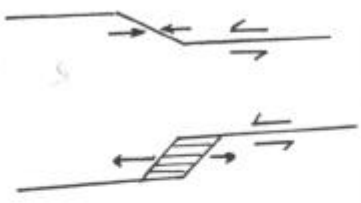	East-west faults and shear zones are left-lateral brittle-ductile structures with common cataclasite. Dilational jogs form at left-handed bends e.g. intersection of Enterprise fault zone with Gimlet south fault.

In general, LEFT lateral faults dilate at LEFT-handed bends
RIGHT lateral faults dilate at RIGHT-handed bends

Figure 4.23 – Fault bend-types favourably oriented for dilation applied to the four principal structural orientations in the Ora Banda Domain

reactivation. Drastic reductions in fluid-pressure (approaching P_f=0) and rapidly increased permeability occur in the vicinity of dilational jogs, and in the area of the fault plane with each sequential failure episode. As hydrothermal precipitates fill the void (fault self-sealing), mineral deposition should rapidly reduce the permeability of the conduit to zero, accompanied by increase and restoration of fluid-pressure to pre-failure conditions. Fluid-pressure cycling and transient permeability as a consequence of fault development are characteristics of mesothermal gold deposits at Ora Banda.

Abrupt fluid-pressure fluctuations associated with reverse-fault-hosted mesothermal gold-quartz deposits are described as fault-valve-behaviour (Sibson *et al.*1988). The model involves failure along high-angle reverse faults severely mis-oriented for reactivation, where fluid-pressure exceeds lithostatic pressures with cyclic fluctuations. Thick quartz veins are common in the planes of strike-slip faults in the Ora Banda district. The veins are usually composed of quartz bands deposited with incremental fault movements. The combined minimum principal stress and tensile rock strength ($\sigma_3 + T_0$) locally is exceeded by fluid-pressure producing ubiquitous quartz veins and dilational breccia zones parallel to the maximum compressive stress σ_1. Although the brittle-ductile faults mostly have oblique strike-slip movement (not reverse) the principal of fault-valve-behaviour may be applicable to the local balance between ($\sigma_3 + T_0$) and fluid-pressure.

At the district-scale, gold mineralisation was controlled by structure. Gold orebodies coincide with the largest faults in the structural zone, but particularly those oriented sub-parallel to the inferred maximum shortening direction. The coincidence of structure and gold is illustrated by Figure 4.19 (p.130). Most structures in the corridor are weakly mineralised at least, even though not all are hosts to large gold deposits, which reinforces the assertion that the brittle-ductile faults formed an interlinked network that facilitated fluid-flow during deformation and metamorphism. Lithological controls at the macroscopic scale are of secondary importance and usually result in the localisation of ore shoots within the plane of a structure.

5 STRUCTURAL GEOLOGY OF THE ENTERPRISE FAULT ZONE

5.1 INTRODUCTION

The Enterprise fault zone is discussed in detail in this chapter to document the D4 brittle-ductile fault network at mesoscopic and microscopic scales. At a macroscopic scale, the Enterprise fault zone is an east-west trending fault that is a single component of an interlinked brittle-ductile fault network (Ora Banda structural zone). Any of the faults within the Ora Banda structural zone could be documented to show the mesoscopic character of the regional fault network, but the major structures have been well-documented previously (eg. Harrison *et al*. 1990).

Investigation of the Enterprise fault zone for this study includes detailed structural mapping and analysis of the 85m deep Enterprise open-pit and 36 diamond drillholes (Figure A1.4 p.322). Although there is a relatively high degree of scatter in the data, some of this may be attributed to errors generated from the Alpha/Beta method of structural measurement of oriented core (Appendix A1.1 p.258). However, when the data collected from drillholes are compared with compass measurements of similar elements in the Enterprise open-pit there is only a slight variance between the major clusters. The high degree of scatter in the total data set is therefore considered a natural characteristic of a dominantly brittle-ductile style of deformation that is typical of the Enterprise fault zone.

5.2 GEOLOGICAL SETTING

Enterprise fault zone is located 2.5 km northeast of the Gimlet South mine at Ora Banda (Figure 4.6 p.100). The geological setting is unique in the Ora Banda district with the fault zone cross-cutting Big Dick Basalt, Enterprise dolerite, Mount Pleasant Sill and possibly Bent Tree Basalt. The host unit (Enterprise dolerite) is a differentiated layered mafic sill with tholeiitic bulk chemistry (Gregory 1998), that intruded the Cashmans Sedimentary Horizon (Figure 5.1, Figure 5.2). The Enterprise dolerite has an upper and lower chilled margin against the wallrocks with a crystallisation sequence that resulted in the most differentiated part of the sill (Fe-enriched quartz dolerite) being located in the centre of the intrusion (unit 4) (Figure 5.2). Rhythmic layering evident in upper units of the sill, indicates that the sill is the right way up. The sill is mostly concordant with surrounding

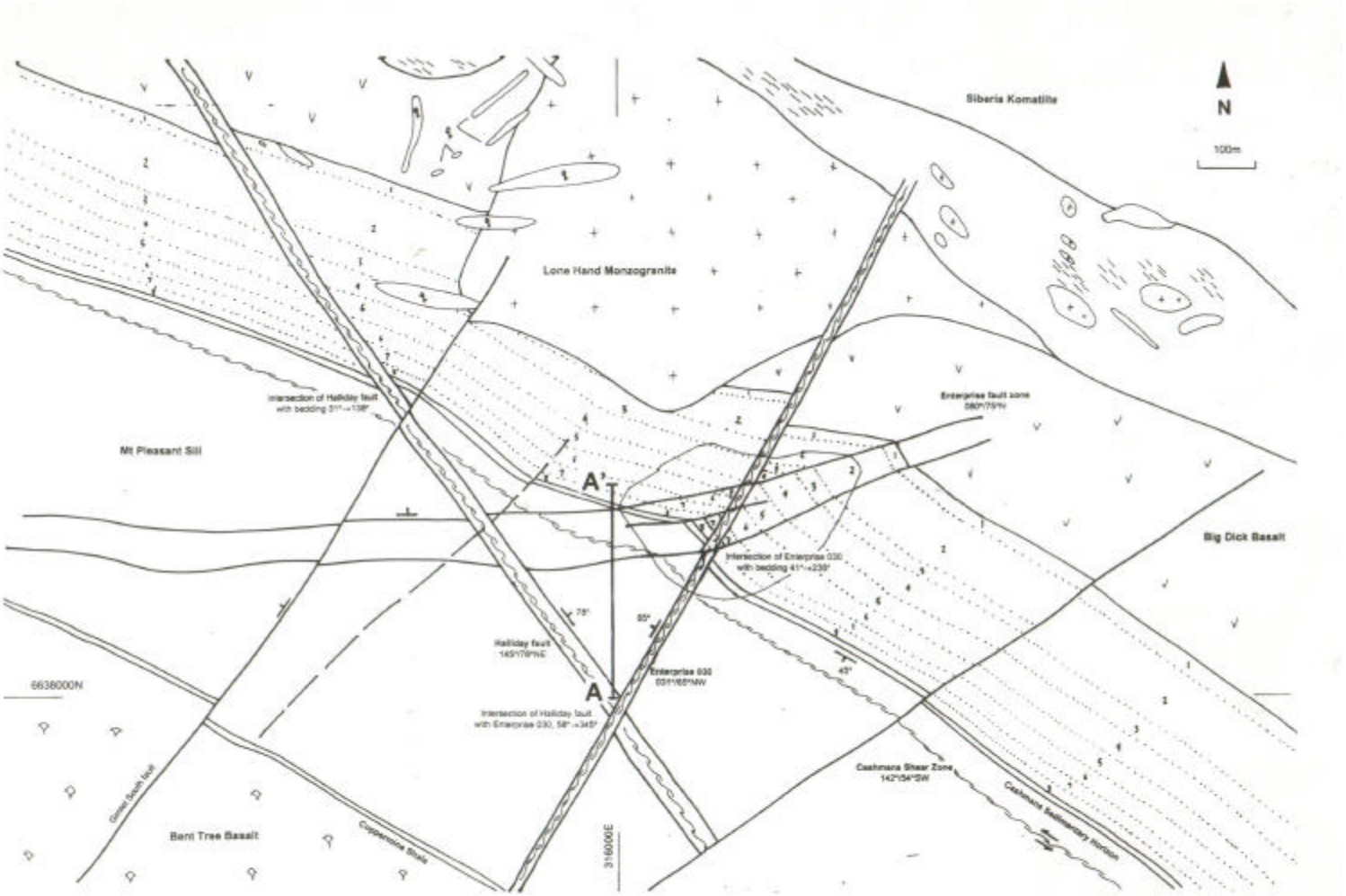

Figure 5.1 – Interpreted geological map of the Enterprise area. Enterprise open-pit is drawn as a thin line marking the pit crest. Layering in the Enterprise dolerite (units 1-8) is extrapolated from the type section from Gregory (1998). Line A-A' is for the cross-section in Figure 5.2. Rock unit boundaries are from surface mapping and interpreted from drilling with the exception of the Lone Hand Monzogranite contacts, which are from Smit (1984)

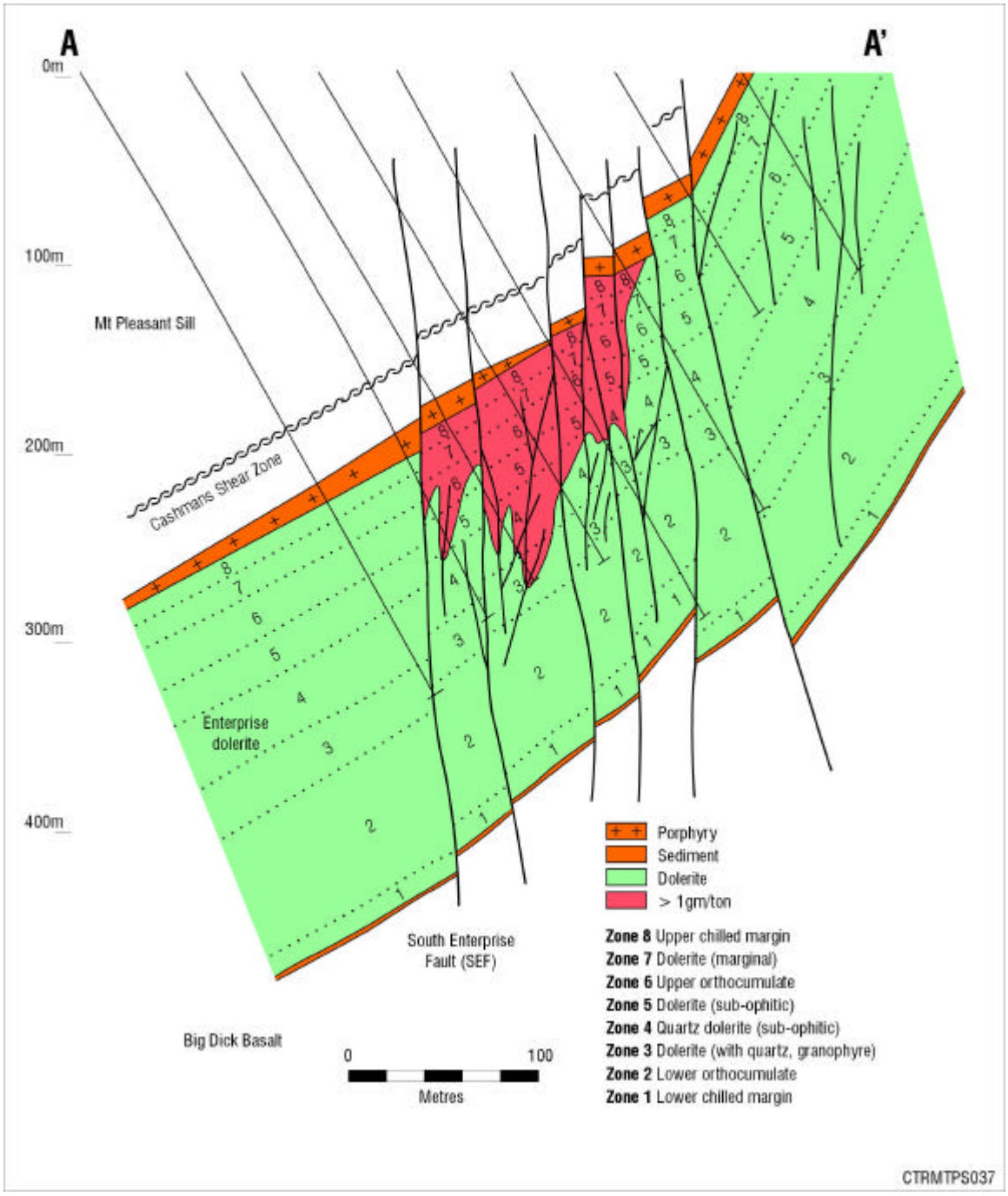

Figure 5.2 – Cross-section 315925E through the Enterprise fault zone showing the distribution of brittle-ductile faults and rocktypes. Layers are extrapolated from the type section from Gregory (1998), and interpreted from offsets of the Cashmans Sedimentary Horizon from drilling. Shaded area outlines the zone of intense meso/microfracturing, and is coincident with the > 1g/T Au contour of the Enterprise orebody.

country rocks, but drilling indicates that the intrusion is transgressive of layering at depth with some drillhole intersections of Big Dick Basalt stratigraphically overlying the sill.

Regionally, the Enterprise dolerite trends 120°/44°SW but its orientation changes to 147°/54°SW in the vicinity of the Enterprise fault zone, and to 109°/51°S further north (Figure 5.1 p.146). These changes in attitude may be attributed to offset on the fault zone, to a change in thickness of the Enterprise dolerite or one of the surrounding layers, or to intrusion of the Lone Hand Monzogranite stocks <100m north of the fault zone.

The intersection of 080° (E-W) trending brittle-ductile faults with the igneous layers produces an intersection lineation that plunges at about 30°→260°, which is the major structural control in the area and a common intersection direction of brittle-ductile faults, veins and cleavage. This plunge orientation is also an important structural control on ore-shoot development at the Gimlet South and Slippery Gimlet mines. The elongate geometry of granitoid intrusions to the north of the Enterprise fault zone is consistent with variation of layering to a more E-W trend (109°/51°S). Intrusive relations of the granitoids indicate late to post-tectonic intrusion (Chapter 4 p.86), which is also consistent with post-folding thickening of the sequence and local bending of the layering.

Ductile shear zones at the upper and lower contacts of the Enterprise dolerite (Cashmans Shear Zone) and Enterprise east shear zone, are approximately bedding-parallel hence the primary intrusive relations of the sill are preserved in exposures of its contact with Cashmans Sedimentary Horizon. The major structural controls in the area are the E-W trending Enterprise fault zone, NW-SE trending Halliday fault and NE-SW trending shear zones such as the Gimlet South fault and Enterprise 030° fault (Figure 5.1 p.146).

5.3 MESOSCOPIC STRUCTURES

At a mesoscopic scale, the Enterprise fault zone displays a wide variety of structural styles with complex timing and overprinting relations. Structural styles range from brittle to ductile but the presence of a range of styles in similar orientations indicates that deformation was predominantly brittle-ductile, and that the mechanical development of rock fabrics was significantly influenced by rock fluids. Ductile deformation is manifest as a continuous cleavage that is extensively overprinted by later deformation fabrics. Brittle-

ductile faults contain a combination of brittle and ductile fabrics that includes cataclasite, foliated cataclasite and various members of the mylonite series. Brittle deformation produced simple brittle faults with minimal displacements, and evidence of fluid-generated brittle deformation includes breccia and micro/mesofracture arrays. Other brittle structures include a range of quartz vein styles.

The spatial context of the structure of the Enterprise fault zone is determined from geological mapping of the open-pit (Map 6 in pocket). However, since the open-pit exposes weathered rock over much of its depth extent, the detailed mineralogy of the rock fabrics is determined from diamond drillholes that intersect the fault zone below the weathered zone. Thirty-six diamond drillholes were selected to give coverage of the fault zone over its entire strike length and to provide continuity with observations from the open-pit (Figure 5.3, Figure A1.3 p.287).

5.3.1 Continuous cleavage

Continuous cleavage in the Enterprise area is a pervasive planar fabric in several generations, but the earliest generation has a regular orientation throughout the area and may have been developed during ENE-WSW shortening (Figure 5.4). The cleavage is ascribed to S2, with implied formation during regional folding (D2), since it is commonly reactivated by later ductile shearing or brittle-ductile faults.

In the open-pit, the cleavage is a prominent plane of breakage with chlorite spotting on broken surfaces (Figure 5.5a). The chlorite spots are a retrogression product after actinolite and are flattened orthogonal to the cleavage plane. On broken surfaces, the spots form undulations that impart a crinkled appearance to the rock texture. Other generations of continuous cleavage are related to brittle-ductile fault events and have variable orientations. These later structures are more correctly associated with shearing rather than regional shortening.

Microfabric

The microfabric of the cleavage is dominated by a preferred alignment of chlorite flakes in

Mesoscopic structure - Enterprise open-pit

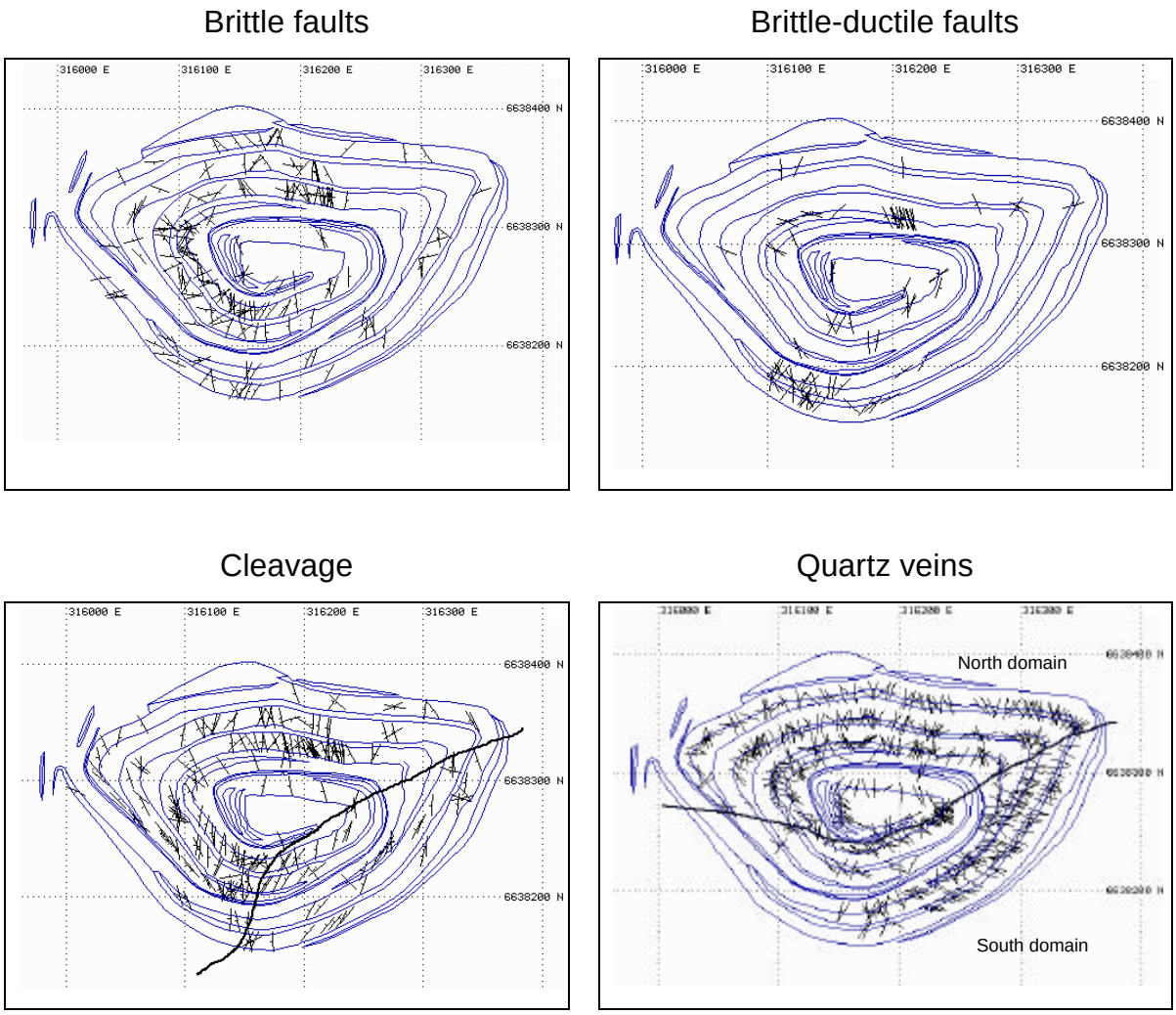

Figure 5.3 – Location maps with dip and strike symbols of elements measured from Enterprise open-pit. A significant change in strike of veins and cleavage occurs across a boundary marked by the thick black line. Broad scatter in the northern domain, coincides with the Enterprise fault zone and indicates that pre-existing veins and schistosity are disrupted by faulting. The black boundary line is an approximate trace of the south Enterprise shear zone. In the cleavage data, the boundary line bends to the south where the influence of the Enterprise 030° fault is significant. Dip values are removed for clarity (see Map1 for detail).

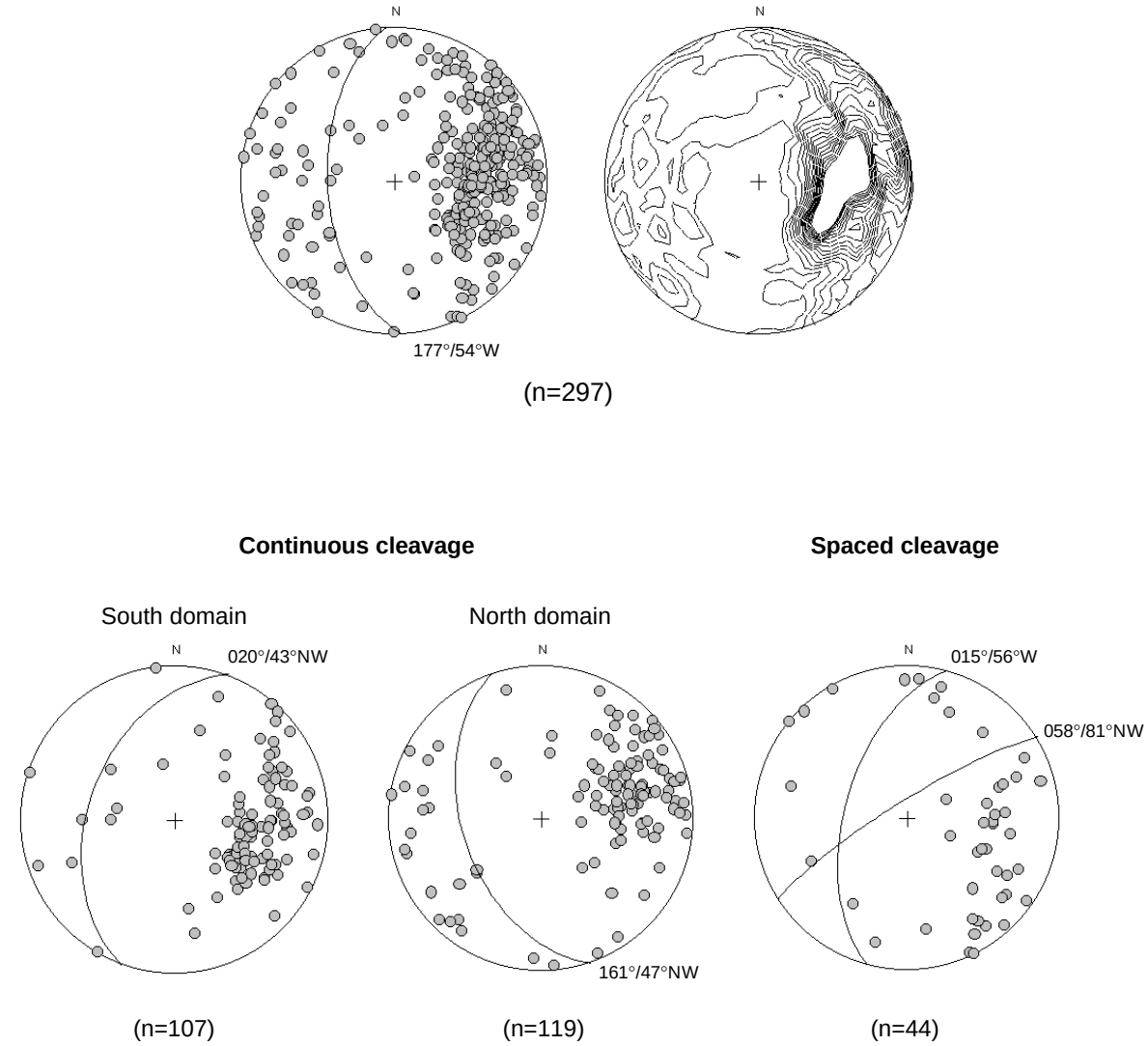

Figure 5.4 – Stereograms of cleavages measured in Enterprise open pit and diamond drill core. A significant change in strike of the cleavage occurs across the south-Enterprise fault in the pit. Continuous cleavages have tight clusters on both sides of the domain boundary. Spaced cleavages have greater scatter and make up a significantly-less proportion of foliations in the pit, but form parallel to the N-S and NE-SW principal structural orientations.

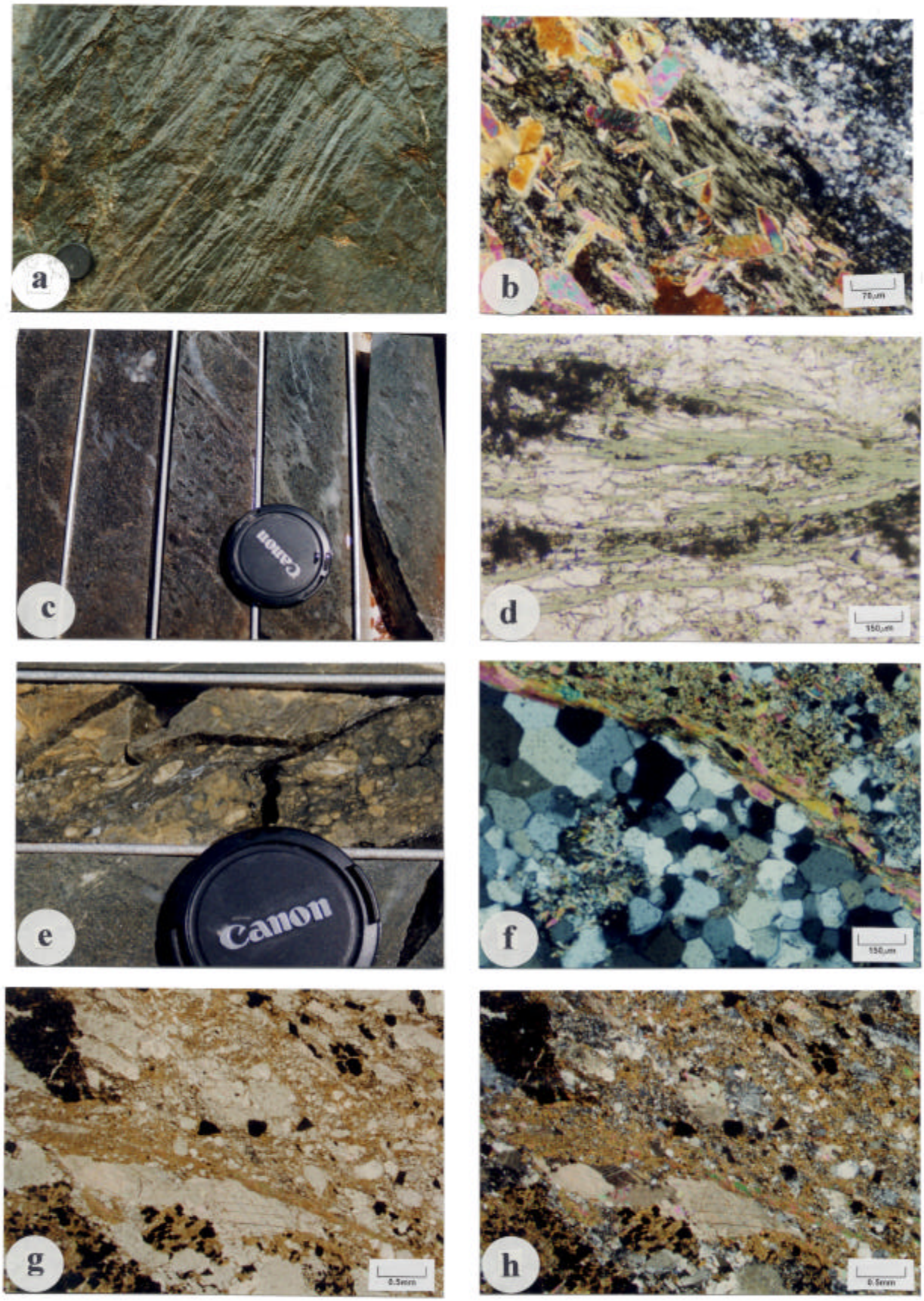

Figure 5.5 - a) Planes of breakage developed along cleavage from the Enterprise open-pit. **b)** Photomicrograph of randomly oriented biotite overprinting cleavage-domain chlorite, (XPL). **c)** Flattening fabric of continuous cleavage in dolerite. **d)** Photomicrograph showing chlorite-controlled growth of calcite, (XPL). **e)** Foliated cataclasite. **f)** Photomicrograph of biotite wrapping a recrystallised vein fragment in foliated cataclasite. **g)** Photomicrograph of foliated cataclasite, (XPL). **h)** Same view as in g), (XPL). See text and over page for explanation.

Captions for figures on page 152

Figure 5.5a
Planar fabric developed along pre-existing continuous cleavage in the Enterprise open-pit. The cleavage is formed in medium-grained chlorite-calcite altered dolerite. Late quartz-calcite veins have reactivated the cleavage producing a spaced fabric in the rock with minor offset on the vein margins, that appears similar to kink folding. The cleavage trends 165°/51°W, view is looking towards the north at 18m in Wall no. 4.

Figure 5.5b
Photomicrograph showing randomly oriented biotite overprinting E-W trending continuous cleavage in Unit 3 of the Enterprise dolerite. Flattened chlorite spots interspersed with wallrock domains of quartzofeldspathic material define the cleavage (continuous in hand specimen). Randomly oriented subhedral grains of biotite with high-order birefringence preferentially overprint the chlorite spots, with little or no alteration of the surrounding wallrocks. A fire assay result of 0.02 g/T Au was returned for this sample. The fabric trending 114°/74°SW is at 631.15m in diamond drill hole ORBD17.

Figure 5.5c
Continuous cleavage in diamond drillhole ORBD17, as for Figure 5.5b. The cleavage is a pervasive fabric with a high degree of flattening shown by clots of chlorite ,which is a retrograde product of actinolite. The E-W orientation of the cleavage indicates that it is related to local shearing rather than a direct expression of the regional shortening event. Lenscap is 55mm diameter.

Figure 5.5d
Photomicrograph (PPL) of a NW-SE trending spaced cleavage. Thin films of elongate chlorite interspersed with calcite define the cleavage, and significant mica-controlled calcite growth is evident in pegged calcite growth against the chlorite with 90° calcite-calcite grain boundaries. A fire assay value of 1.04 g/T Au was returned for the sample. Sample trending 148°/61°SW is from 240.0m in diamond drill hole ORD157.

Figure 5.5e
Foliated cataclasite. The shear zone is a typical cataclasite with angular to rounded fragments of wallrock that show significant comminution in a foliated matrix that contains the slip planes of the fault. Chlorite-calcite slickenfibres indicate right-lateral (north block up) offset across the zone which trends 053°/83°SE. Muscovite-ankerite alteration is most intense within the fault zone grading outwards into chlorite dominated alteration. A gold grade of 0.69ppm was returned for the fault. The fault is at 573.70m in diamond drillhole ORBD17, downhole direction is to the right. Lenscap is 55m diameter.

Figure 5.5f
Photomicrograph (XPL) of the boundary of a quartz vein clast in foliated cataclasite. The clast is sub-rounded and is wrapped by the foliation defined by fine-grained biotite. The internal microstructure of the clast is remarkably strain free, considering the sample is from a high strain zone. Quartz grains are free of intracrystalline deformation with 120° dihedral angles between straight to curved grain boundaries. The fault returned a fire assay value of 8.9 g/T Au. The sample trending 085°/84°N is from 264.5m in diamond drill hole ORBD12.

Figure 5.5g
Photomicrograph (PPL) of the typical microfabric of foliated cataclasite. The protolith is Unit 4 of the Enterprise dolerite, and shows intense biotite-calcite alteration within the fault. Biotite films wrap angular to rounded fragments of wall rock and vein material, with some larger calcite veins emplaced parallel to the foliation. A weak fabric asymmetry may indicate sinistral offset. Pyrite is disseminated in subhedral crystals. A fire assay value of 6.31 g/T Au was returned for the fault. The sample trending 153°/90° is from 170.2m in diamond drillhole ORD13.

Figure 5.5h
Same view as for Figure 5.5g), (XPL).

clusters surrounded by feldspar and quartz, which may have been part of an original ophitic texture in the dolerite host rock. The cleavage fabric is defined by chlorite, saussuritised plagioclase and quartz, which may be overprinted by hydrothermal biotite (Figure 5.5b p.152). The cleavage forms long continuous seams that are up to 100*m*m thick and more commonly, a preferred mineral alignment that is pervasive through the rock. The crinkled effect in hand specimen is due to planes of breakage that anastomose around chlorite clusters. In fine-grained portions, the cleavage is defined by 5mm x 2mm chlorite aggregates overprinted by fine muscovite. Quartzofeldspathic material between the cleavage domains has a very fine grainsize of 20-50*m*m of mostly strain-free grains with minor irregular grain boundaries and undulose extinction (evidence of dynamic recrystallisation).

Examples of continuous cleavage with biotite alteration are normally oriented at a high angle to the regional cleavage S2 (defined by chlorite), and are closely associated with brittle-ductile deformation and hydrothermal alteration (Figure 5.5c p.152). The foliation in these samples (eg. ORBD17 631.15) is defined by elongate chlorite clusters that are overprinted by fine-grained randomly oriented biotite, also with a high proportion of biotite overprinting the groundmass of the rock. Mineralisation is commonly associated with these structures and contributes to the planar fabric with trails of pyrite along foliation planes, or pyrrhotite in flattened grains, parallel to the foliation.

5.3.2 Spaced cleavage

Poorly-developed spaced cleavage at Enterprise is closely associated with brittle-ductile fault structures, and has an irregular distribution in the open-pit. The cleavage is defined by chlorite wisps spaced at about 10mm interspersed with lens-shaped vein fragments, forming well-defined cleavage domains with smooth anastomosing morphology. The cleavage domains contain highly flattened leucoxene, and a strong preferred alignment of biotite and calcite in altered specimens. Microstructures of calcite grain boundaries pegged against chlorite indicates significant mica-controlled calcite growth (Figure 5.5d p.152).

Cleavage zones trending towards 150° (ORD27 180.3), contain veins that are commonly boudinaged with unstrained recrystallised quartz grains in the highly deformed boudins.

Such textures are developed primarily in spaced cleavage seams of several millimetres thickness, and indicate some static recrystallisation post-dating the deformation.

5.3.3 Brittle-ductile faults

Brittle-ductile faults are prominent features in the Enterprise open-pit and form the major controlling structures. The classification of these structures (or portions thereof) as 'ductile shear zones' follows the definitions in the literature (eg. Sibson 1977; White *et al*. 1980; Wise *et al*. 1984) and by definition they are localised zones of 'ductile' deformation, but many are thin (<1m) and have an important brittle component or are overprinted by brittle fabrics. Ductile structures of this magnitude are insignificant in terms of the regional definition of 'ductile shear zones' adopted in this study (Chapter 1.5 p.9), and are considered to be a part of the late-tectonic brittle-ductile fault network. A range of fabric types may occur in any brittle-ductile fault with successive overprinting between brittle and ductile events.

Foliated cataclasite

Most brittle-ductile faults show evidence of a brittle overprinting of earlier ductile fabrics, however zones of foliated cataclasite have textures that suggest several phases of deformation alternating between brittle and ductile.

In zones of foliated cataclasite, the clasts may comprise foliated mafic rock, vein fragments of several generations, sheared vein fragments, or altered mafic rock fragments with variable alteration types. The clasts are rounded to sub-rounded and elongate, with a random distribution of fragments in a poorly sorted conglomerate, and variable size from 1mm to 30mm (Figure 5.5e p.152). Inter-clast foliation is predominantly formed by thin biotite bands in continuous seams that wrap the clasts. The foliation seams consist of elongate, moderately strained biotite flakes with preferred alignment.

Most samples of foliated cataclasite have several generations of biotite, with a coarse-grained biotite generation forming the foliation seams, and forming pressure-shadow beards on cataclased fragments. An earlier generation of fine-grained matted biotite forms a more pervasive alteration of the mafic fragments that originally were muscovite altered

(Figure 5.5f p.152). Pyrite has variable grain sizes up to 3mm and is not fractured, but overprints the cataclased fragments, and is wrapped by the biotite foliation with well-developed mica beards in pressure shadow positions. These textures indicate that the pyrite was crystallised after the cataclasis but is pre-tectonic with respect to the foliation.

At a high power, there is a marked contrast of strain intensity, with the highly deformed gross rock fabric composed of mostly strain-free mineral constituents. The biotite foliation overprints an original cataclastic fault rock with fracturing, cataclasis and milling of the clasts, which is then sheared with dynamic recrystallisation of quartz and calcite, and growth of biotite (Figure 5.5g-h p.152). Recovery postdates brecciation and grain-size reduction of the cataclasite, but a final brittle fracturing event is indicated by minor carbonate veins (post-cataclasis/foliation) emplaced in fractures along the foliation, broken and fragmented actinolite crystals, and slickenfibres of calcite on microfaults. Minor post-recovery intracrystalline strain is manifest as very weak undulose extinction in quartz vein fragments.

Cataclasite

Cataclasite is developed as discrete zones within larger faults, and commonly forms the brittle component of many brittle-ductile faults (Figure 5.6a). The zones are up to 20m wide and consist of intensely microfractured fragments of mafic wallrock and vein material, in a clast-supported arrangement with widely variable clast sizes. Most cataclasite has angular to highly rounded fragments in fault breccia zones up to several metres wide, or seams of finely milled rock fragments and sulphides in the order of millimetres wide (Figure 5.6b).

In thin section, cataclasite with an average clast size of < 2mm, has a high degree of brittle fracturing with healing of fractures by chlorite. Wallrock fragments may contain quartz and pyrite that are also significantly fractured (Figure 5.6c), and the cataclastic rock contains spaced microfaults defined by smoothly anastomosing seams of green chlorite (Figure 5.6d-e). The chlorite seams enclose lens-shaped pods of highly fractured, polycrystalline calcite veins with minor stretching of the pods. Significant chlorite-saussurite retrogression of biotite-calcite altered mafic wallrocks is common in the vicinity of the microfaults.

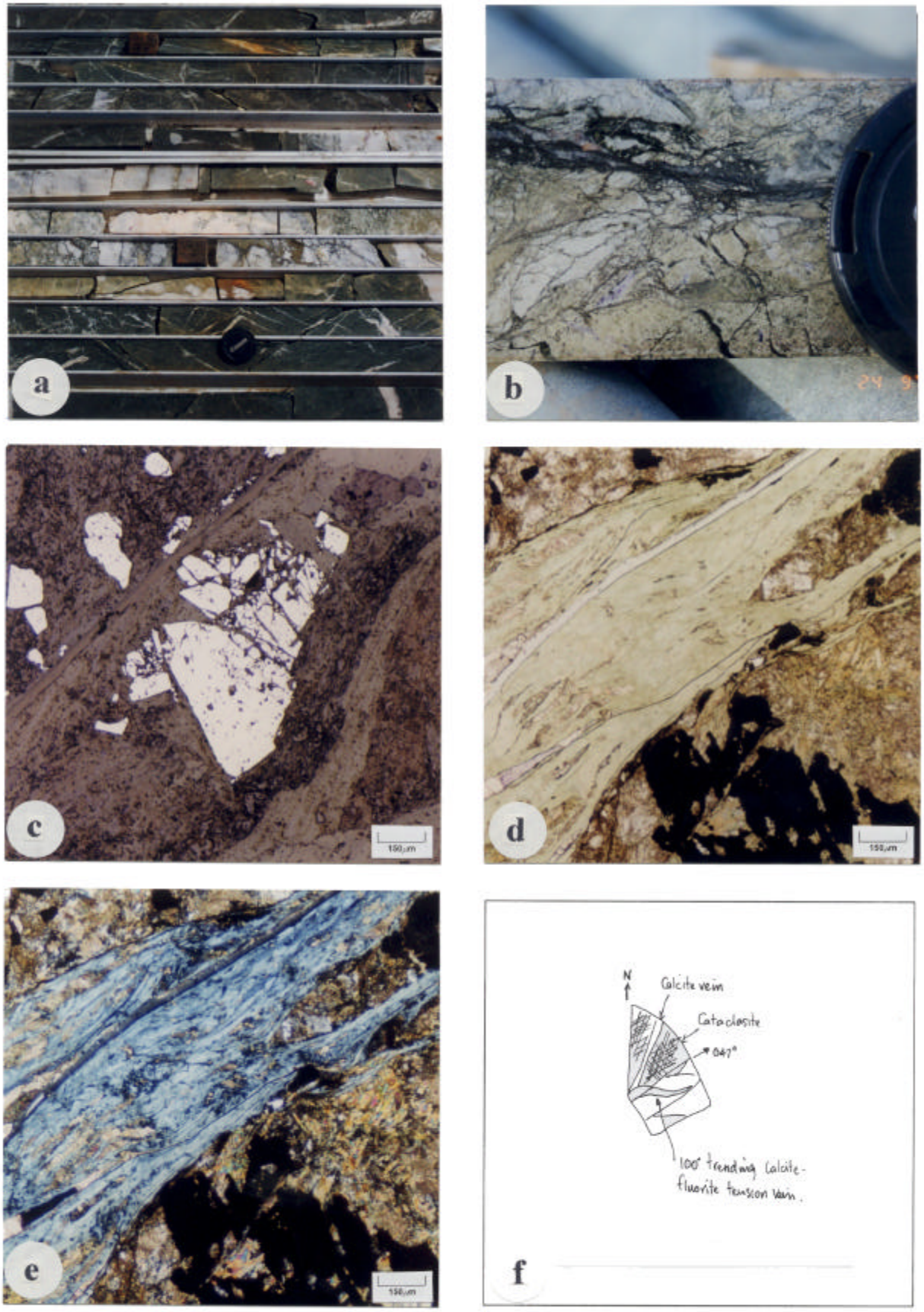

Figure 5.6 - a) Typical cataclastic fault zone in dolerite. **b)** Cataclastic texture in bleached dolerite **c)** Photomicrograph of cataclastic texture in pyrite, reflected light. **d)** Photomicrograph of chloritic microfault cross-cutting cataclasite, (XPL). **e)** Same view as in d), (XPL). **f)** Sketch of hand specimen showing microfaults and late granitoid related veins cross-cutting cataclasite. See text and over page for explanation.

Captions for figures on page 157

Figure 5.6a
Cataclastic fault zone in Enterprise dolerite. The fault has a major vein component with intense cataclasis of part of the vein, yet other parts are relatively undeformed. Pervasive muscovite-pyrite alteration of angular mafic fragments in the fault is typical of late granitoid-related overprinting of alteration that may have originally been biotite dominant. Mesofracturing in the wallrocks is defined by quartz-calcite veins in regular orientations. A composite fire assay for this fault returned a value of 3.87m @ 0.2 g/T Au. The fault is at 321.73m-325.60m in diamond drill hole ORD157.

Figure 5.6b
Cataclastic fault breccia with fine-grained gouge zones on the slip surfaces. The dark seam crossing the photograph is composed of very fine-grained pyrite and opaque material with fragments of wallrock. The wallrocks are intensely fractured and brecciated with interclast voids filled with chlorite and (?)glassy material. Thin calcite-fluorite veins crosscut the altered wallrocks but also are affected by the brecciation. Intense muscovite-calcite bleaching of the original doleritic rock resulted in the areas adjacent to the fault being light coloured in an overall dark green chloritic host. A fire assay value of 0.95 g/T Au. Sample is at 316.70m in diamond drillhole ORD157, downhole direction is to the right. Lenscap for scale.

Figure 5.6c
Photomicrograph (reflected light) of cataclastic texture in a pyrite crystal. The pyrite occurs within a NE-SW trending cataclasite zone (Figure 5.6d), and shows evidence that brittle fracturing was a dominant deformation mechanism. Sample is from 282.25m in diamond drillhole ORD157.

Figure 5.6d
Photomicrograph (PPL) of a NE-SW trending brittle fault plane in cataclasite. The fault is defined by a high degree of fracturing with green chlorite along the fracture surfaces. The chlorite seams enclose lens shaped fragments of cataclased wallrock that are totally replaced, with the exception of leucoxene visible in the bottom right corner of the figure. The most altered portions of the rock occur in areas of the highest fracture density. Thin calcite-fluorite veins occur parallel to the fault and in dilational jogs within the wallrock indicating right-lateral movement sense. A fire assay value of 1.78 g/T Au was returned for the fault. Sample trending 047°/61°NW is at 282.25m in diamond drillhole ORD157.

Figure 5.6e
Photomicrograph (XPL) of same area as in Figure 5.6d).

Figure 5.6f
Sketch of relationships between NE-SW trending cataclasite zone and E-W trending granitoid related veins. Hand specimen sample of Figure 5.6d).

Vein fragments in the cataclasite show a high degree of recovery with 120° dihedral angles in strain free quartz grains with a foam fabric arrangement, which indicates grain boundary area reduction during recovery. Primary quartz grains in a quartz-dolerite protolith are strain-free, but still show significant brittle fracturing. Sigmoid-shaped calcite-fluorite veins with 90° growth fibres overprint the cataclasite.

Highly angular cataclasite shows similar fabrics with pervasive microfracturing and a jigsaw arrangement of the fragments. Very little rotation of the fragments is common, with a transition from cataclasite to breccia.

Mylonite

Some mylonite fault rocks may lack obvious S-C fabrics but are dominated by the C-plane of the mylonite with a minor brittle component. These shear bands have a distinct banded appearance with alternating dark and light bands defined by millimetre-scale slivers of chlorite and biotite. Lens-shaped fragments of vein material and stretched leucoxene grains are common. A transition exists between these structures, and intensely developed continuous cleavage.

In thin section, the mylonites show intense grain-size reduction to 20*m*m or less in domainal fabrics with quartz-rich domains interspersed with cleavage domains, or vein domains. Flattening fabrics are common, and weak fabric asymmetry indicates the sense of movement. Vein domains contain distended vein fragments with lensoid shape, oriented parallel to the planar fabric of the structure. Strongly foliated wallrock segments against vein contacts may indicate that veins were emplaced into the zones of highest strain.

Quartz-rich domains contain equant to elongate grains overprinted by chlorite-calcite, which contrasts with pegging of quartz growth against quartz-quartz-chlorite grain boundaries commonly displayed in other faults. The quartz grains are mostly free of intracrystalline deformation with 120° dihedral angles. Cleavage domains may contain muscovite, which forms pressure shadow beards on pyrite grains within the shear cleavage. Muscovite cleavage domains have rough, parallel morphology spaced at about 2-3mm, with weak undulose extinction in muscovite grains. Randomly oriented biotite flakes overprint the mylonite fabrics.

S-C mylonite

S-C mylonite (Berthe *et al*. 1979) is the most common ductile component of brittle-ductile faults in the Enterprise fault zone (Figure 5.7a). In most examples the S-C mylonite shear zones have a significantly finer grainsize than the surrounding doleritic rocks. C planes form a spaced cleavage with 0.5-6.0mm spacing defined by a strong shape-preferred orientation in micaceous minerals (chlorite, biotite or muscovite). The C planes are localised bands of shearing with stretching fabrics exhibited by elongate pyrite grains (possibly replacing pyrrhotite) and stretched leucoxene grains, that otherwise behave in brittle fashion (Figure 5.7b-c). The C planes also appear to control retrogression with aligned birefringent chlorite forming an important component of the C foliation in biotite-rich rocks.

Asymmetric biotite aggregates and calcite vein fragments showing incipient development of porphyroclastic texture, commonly define the S planes. Some S fabrics are defined by segments of albitised mafic wallrocks wrapped with biotite films, and S foliations are parallel to continuous cleavage in the wallrocks indicating that the shearing may have entrained a pre-existing fabric.

The microfabric of the S-C mylonite zones is dominated by extensive recrystallisation of all mineral phases. Quartz in the recrystallised groundmass has an average grainsize of 30μm with foam fabric in grains lacking any intracrystalline deformation, whereas original quartz grain fragments (from quartz dolerite?) are highly strained with undulose extinction and well-developed deformation lamellae (Figure 5.7d). Quartz in quartz-calcite vein fragments entrained in the mylonite (with highly irregular morphology) is strain-free with straight grain boundaries intersecting in 120° dihedral angles.

Some calcite-quartz vein fragments in the mylonite have large grainsize (1-2mm) with strong intracrystalline deformation (undulose extinction, kinked and tapered deformation twins) and evidence of strain induced boundary migration with highly irregular grain boundaries.

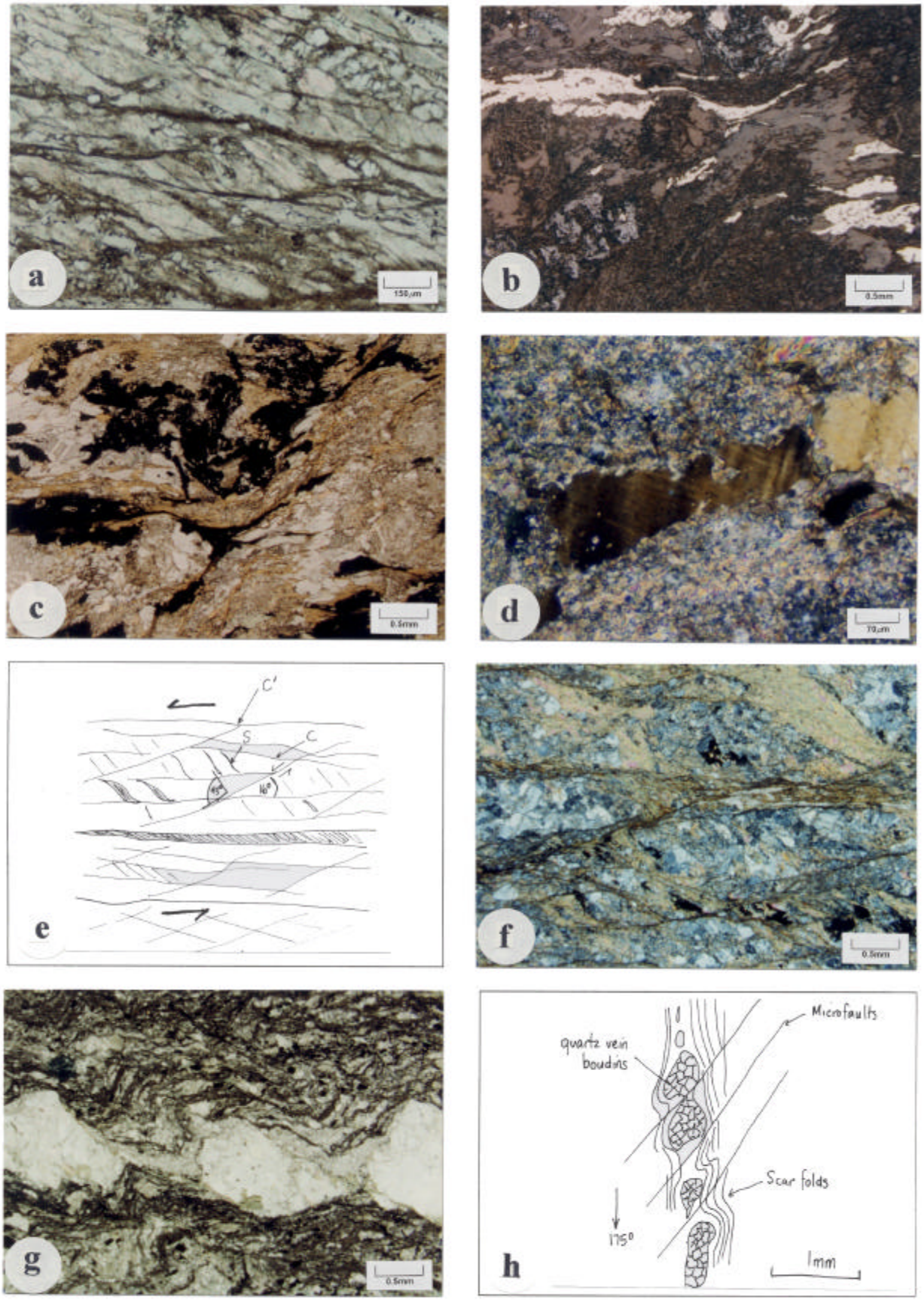

Figure 5.7 - a) Photomicrograph of S-C mylonite in a calcite vein, (XPL). **b)** Photomicrograph of stretched pyrite and leucoxene in the C-plane of a mylonite, reflected light. **c)** Same view as in b) transmitted light, (XPL). **d)** Photomicrograph showing deformation lamellae and subgrain development in quartz, (XPL). **e)** Sketch of foliation relationships in S-C-C' mylonite. **f)** Photomicrograph showing microlithon fabric in S-C-C' mylonite, (XPL). **g)** Photomicrograph of boudinaged quartz vein in banded mylonite, (XPL). **h)** Sketch of relationships in Figure 5.7g). See text and over page for explanation.

Captions for figures on page 161

Figure 5.7a
Photomicrograph (XPL) of S-C mylonite developed in a calcite vein. The C-planes are well developed as thoroughgoing shear planes defined by murky saussurite alteration. S-planes trend from bottom-right to top-left in lens-shaped domains bounded by the C-planes. The sample trending 046°/59°SE is from 525.6m in diamond drillhole ORBD21.

Figure 5.7b
Photomicrograph (reflected light) showing stretched pyrite crystallised along the C and S planes of a mylonite. The C-plane trends across the slide from left to right and the S-plane is trending up to the right. Elongate calcite and biotite from along the boundaries of a microlithon with stretched leucoxene in C and undeformed leucoxene in the microlithon. A fire assay value of 0.07 g/T Au was returned for the shear zone. Sample trending 176°/51°W is at 506.0m in diamond drillhole ORBD16.

Figure 5.7c
Photomicrograph (PPL) same view as for Figure 5.7b).

Figure 5.7d
Photomicrograph (XPL) showing intracrystalline deformation microstructures in quartz. The quartz is an elongate fragment within the wallrock of the shear zone in Figure 5.7b). Strong intracrystalline deformation is evident in the form of deformation lamellae trending down to the right, within the crystal. Minor evidence of recovery includes poorly developed low-angle subgrains shown as areas of common extinction within the crystal trending bottom-left to top-right.

Figure 5.7e
Sketch of foliation relationships in S-C-C' mylonite zone. A chloritic fault cross-cuts the fabric trending parallel to the C-plane. The C' plane is oriented at 16° to C and at 43° to S. C' has a shear sense synthetic with the reverse movement sense of the S-C fabric. The shear zone returned a fire assay value of 0.35 g/T Au. Sample trending 046°/59°SE is from 525.6m in diamond drill hole ORBD21.

Figure 5.7f
Photomicrograph (XPL) of the fault depicted in Figure 5.7e). S-planes are defined by thick bands of very fine-grained biotite, whereas C and C' have a high degree of retrograde overprinting of thin biotite bands by saussurite. Microlithons of quartzofeldspathic material appear recrystallised. The slide does not show good examples of C', which is a spaced fabric across the slide.

Figure 5.7g
Photomicrograph (PPL) of boudinaged quartz vein in a banded mylonite. The banding is defined by the dark seams across the slide. Scar folds are developed in the neck areas of boudins with some recrystallised vein material in the fold hinges. The veins fragments are totally recrystallised with no remnant intracrystalline strain, which indicates that significant recovery post-dates the high strain event that produced the shear zone. A fire assay value of 0.16 g/T Au was returned for the shear zone. Sample is from 360.65m in diamond drill hole ORBD12.

Figure 5.7h
Sketch of fabric relationships of the shear zone in Figure 5.7g).

Calcite in the vein fragments is strongly recrystallised with strain-free grains in stable 120° arrangements with an average diameter of 50*m*m. Calcite-chlorite aggregates show mica-controlled calcite growth in pegged grain boundaries with preferred orientation of calcite long axes.

Muscovite commonly overprints strain fabrics with unstrained muscovite crystals overprinting C planes. Muscovite oriented at 90° to the C foliation displays evidence of dislocation glide in microkinking of mica flakes with kink fold axes parallel to the foliation, and dilation fractures along the 001 cleavage direction in the mica, indicating shortening across the C plane.

Preferred orientation of mineral phases and strong shear fabrics indicate that the original structures were high strain zones. Remnant microstructural evidence of strain is abundant, however a significant degree of recovery has taken place. Recovery of deformation fabrics occurred via annealing recrystallisation, nucleation of new grains at quartz triple junctions and static recrystallisation with polygonisation and development of low-angle subgrains. The microstructures of the S-C mylonite zones indicate grain size reduction during dynamic recrystallisation and mylonite development, with a major thermally-driven phase of recovery that outlasted deformation.

S-C-C' mylonite

A variation of S-C mylonite zones includes shear band cleavages, which are minor shear zones that transect the mylonite, also termed extensional crenulation cleavage (Platt and Vissers 1980). An example of this structure in sample ORBD21 525.60m, shows well developed S-C mylonite with fine parallel shear bands overprinting the S-C fabric at a small angle (Figure 5.7e p.161). The shear zone is 1.9m wide trending 046°/59°SE, with a steep stretching lineation on the shear surface defined by muscovite-biotite-quartz-pyrite, and has S-C fabric asymmetry that indicates reverse movement sense.

C planes have smooth anastomosing morphology, spaced at 1-3mm, with good continuity and a variably spaced fabric with bifurcation of individual C planes. The C planes are up to 10*m*m thick defined by fine biotite flakes and stretched leucoxene, and sharply truncate the S planes with minor bending of S into C.

S planes are defined by sigmoid-shaped clusters of fine-grained biotite up to 600*m*m thick grown between and across poorly developed porphyroclast domains (microlithons) (Figure 5.7f p.161). Porphryroclast domains are lens-shaped (3 x 2mm), quartz-feldspar rich domains of albitised dolerite with strong biotite alteration. Biotite in the S planes is weakly strained with mild undulose extinction and sharp to irregular grain boundaries. Porphyroclast domains show strong undulose extinction with irregular grain boundaries in quartz and feldspar. Widespread fracturing in the porphyroclast domains indicates a phase of deformation that post-dates the shearing during which the microlithons behaved rigidly.

C' shear bands are not as well developed as S or C, but occur as either large shear bands or fine sub-parallel fractures and shear bands. The shear bands have synthetic shear sense with the reverse S-C fabric and clearly cross-cut S and C in all examples. C' is oriented at 16° to C and 43° to S with minor fracturing in surrounding microlithons parallel to the C' orientation.

The shear zone is a reverse S-C mylonite that has developed in response to a sub-horizontal shortening. C' shear bands develop late during shear zone activity after a strong mineral preferred orientation has already been established (Passchier and Trouw 1996). The structure is especially well-developed in stretching shear zones and is considered to facilitate an extension along the shear direction when the shear zone cannot accommodate any further shortening across its boundaries (Platt and Vissers 1980).

Banded mylonite

Banded mylonite (Figure 5.7g p.161), is a common shear fabric that appears to be developed early in the D4 event from a high degree of flattening and an extensive fluid history with widespread retrogression. In two samples (ORD14 224.20 and ORBD12 360.65), the fabric is typified by finely spaced banding with irregular wavy geometry. A strong planar alignment of all phases defines the banding, which is interspersed with large rounded vein fragments.

Under the microscope, the rock shows strong retrogression of the dark bands to saussurite. The fabric comprises elongate parallel mylonite bands with aligned green biotite seams in

between the bands, and weakly developed microlithon fabric. Mylonite bands may be up to 15mm wide composed of 80*m*m thick bands of very fine-grained saussurite, spaced at 200*m*m apart and interleaved with 200*m*m thick bands of quartz-feldspar-chlorite.

Fine-grained pyrite and minor chalcopyrite in the quartz-rich domains contrast with coarse-grained pyrite in the banded domains. Ductile shear domains and wallrock domains are truncated by high angle antithetic brittle microfaults (Figure 5.7h p.161) with significant separation of the fault blocks and infill with calcite vein material. There is some evidence of early cataclasis with a ductile overprint.

Vein fragments within the banded mylonite show significant microboudinage, which appears to be precursory to the development of porphyroclastic texture. The vein fragments have lensoid shape, and the surrounding mylonitic banding is compressed into the inter-boudin regions forming scar folds. Fold axes in the scar folds and edges of the boudins are sub-parallel to a weakly developed extensional crenulation cleavage oriented at 29° to the main shear fabric.

The extensional crenulation cleavage is a low-angle cross-cutting fabric that results in offsets of the vein fragments and mylonitic banding, with movement sense synthetic to that of the main shear zone. Wallrock domains are generally much coarser grained than the mylonitic banding with an interlocking mosaic of feldspar, quartz and calcite, and a higher proportion of coarse-grained pyrite along S-C planes.

The shear fabric is composed of very fine-grained quartz and feldspar with highly irregular grain boundaries and strong undulose extinction. Evidence of recovery includes polygonisation with sub-grain development producing low-angle subgrains in quartz, and nucleation of new grains along quartz-quartz grain boundaries. Dynamic recrystallisation was the major process resulting in grain size reduction of the shear zone, and porphyroclasts of wallrock material indicate a significantly coarser original grain size. However the recrystallisation leading to the present intracrystalline fabrics may have been mostly static and related to nearby granitoid intrusion.

Quartz vein fragments contain recrystallised equant strain-free grains of average 50*m*m diameter with slightly curved grain boundaries and 120° dihedral angles. Calcite veins

comprise fine-grained polygonal grains with straight to irregular shaped grain boundaries. The calcite is strain free but maintains a strong shape-preferred orientation parallel to the main shear fabric. Some nucleation of new grains and grain boundary migration recrystallisation is evident, but was terminated before the calcite could achieve a stable arrangement.

Calcite veins are clearly later than quartz, with a different degree of finite strain that can be explained by the earlier quartz being influenced by thermal-driven recovery for a longer period than the calcite. Crystallisation of the calcite appears to be constrained to a brittle fracturing event at the waning stages of deformation. The different modes of failure during a sustained thermal event may indicate an increase in strain rate that led to the brittle failure.

Ultramylonite

An example of ultramylonite (ORD16 492.65), shows well-developed ribbon texture that may be developed in a pre-existing quartz vein (Figure 5.8a). The shear zone (0.4m-wide), has a well-defined stretching lineation defined by elongate white mica clusters, which trends sub-horizontal to the north, indicating strike-slip offset. The shear zone is a low-angle structure trending 000°/32°W, and if produced as part of the D4 brittle-ductile faulting event during ENE-WSW shortening, the sub-horizontal slip lineation and strike-slip kinematics are unusual. Such a low-angle shear zone should display reverse movement during regional shortening. Although the shear zone is relatively minor (0.4m-wide), it is subparallel to several other brittle-ductile faults in the diamond drillhole developed for over 13m downhole.

In hand specimen the rock has a banded appearance with parallel muscovite seams (<1mm thick) and light coloured bands that contain leucoxene crystals. The banded fabric is distinct with recrystallisation of most phases. Ribbons of calcite (vein?) material up to 3mm thick are interspersed with ribbons of albitised (mafic?) rock predominantly composed of albite, white mica and leucoxene. Mica cleavage seams are spaced at 0.25-0.5mm defining the C-plane of the shear zone.

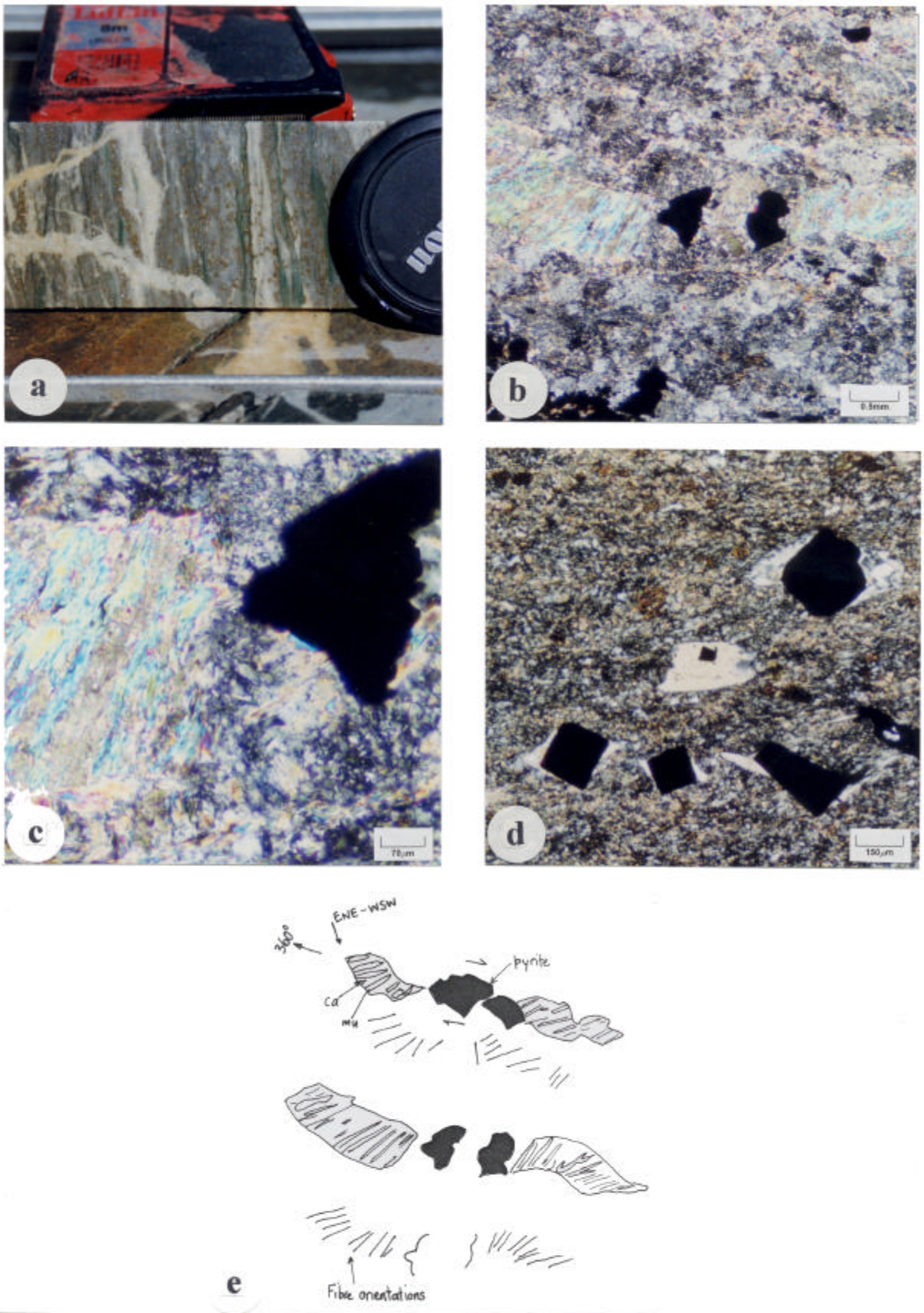

Figure 5.8 - a) Ultramylonite shear zone in dolerite. **b)** Photomicrograph of pressure shadow fringe structure around pyrite porphyroblast in ultramylonite, (XPL). **c)** Photomicrograph showing detail of pressure shadow fringe with anomalous growth orientation in mica, (XPL). **d)** Photomicrograph of pressure shadow fringes around pyrite porphyroblasts within continuous cleavage, (XPL). **e)** Sketches of anomalous fringe structure from Figure 5.8b). See text and over page for explanation.

Captions for figures on page 167

Figure 5.8a
Ultramylonite shear zone with ribbon texture. The shear zone is 0.4m wide and trends 000°/32°W with a shallow north plunging stretch lineation and strike-slip offset indicating right-lateral movement sense. Well-developed ribbon texture is displayed by quartz and thin quartz-calcite veins interspersed with stretched films of bright green chlorite. Fine-grained euhedral pyrite forms in trails parallel to the foliation. A gold grade of 0.65 g/T Au was returned for the structure. Shear zone is at 492.65m in diamond drillhole ORBD16, downhole direction is to the right. Lenscap is 55mm diameter.

Figure 5.8b
Photomicrograph (XPL) showing syn-tectonic strain fringes on a pyrite porphyroblast in the shear zone from Figure 5.8a). The porphyroblast has an unusual morphology occurring as two separate fragments. The fringes are composed of muscovite and calcite, and the fringe geometry indicates dextral offset on the N-S trending shear zone. The matrix of the ultramylonite is defined by recrystallised quartzofeldspathic material, but individual grains are not easily identified. Intense hydrothermal alteration of the shear zone masks the original mineralogy and the dominantly quartzofeldspathic mineralogy suggests that the shear zone may be developed in a vein, however the presence of leucoxene indicates a mafic protolith.

Figure 5.8c
Photomicrograph (XPL) showing detail of the left side of the pressure fringe in Figure 5.8b). The microstructure of the fringe is anomalous with the long axes of the muscovite and calcite oriented sub-parallel to the face of the porphyroblast. In most published examples, strain fringes are composed of fibrous minerals that are aligned parallel to the long axis of the fringe, and the bulk displacement path of the shear zone.

Figure 5.8d
Photomicrograph (XPL) of strain fringes around pyrite porphyroblasts. The strain fringes are poorly developed structures that indicate only minor rotation during simple shear, however the sense of shear is not clear in this specimen. Long axes of the fibres in the strain fringes have also grown sub-parallel to the face of the porphyroblast. Sample is from 225.6m in diamond drill hole ORD157.

Figure 5.8e
Photomicrograph (XPL) of similar relationships to those discussed for Figure 5.8c).

Figure 5.8f
Sketch of fibre relationships discussed in Figure 5.8 b) and c).

In thin section, calcite ribbons contain two main forms of calcite: Type-I remnant coarse-grained vein fragments, and Type-II dynamically recrystallised vein material. Type-I calcite is lens shaped and stretched along the ribbons tapering into Type-II calcite ribbons, which form the dominant component of the fabric. Type-I calcite has an interlocking mosaic texture composed of grains up to 0.5mm diameter, with weak undulose extinction and straight grain boundaries. Type-II calcite is murky in plane polarised light with grains up to 0.25mm diameter, straight to irregular grain boundaries and strong undulose extinction. Minor quartz-albite fragments in the ribbons have a larger grainsize and straight grain boundaries with weak undulose extinction. Deformation twins in albite indicate a component of intracrystalline deformation producing mechanical twinning via dislocation glide processes. The calcite ribbons originally may have been calcite-albite-quartz veins that were emplaced into the ductile shear zone.

The matrix of the mylonite comprises recrystallised feldspar (albite?) and quartz with a strong shape-preferred orientation. White mica cleavage seams are parallel to the fabric, with a common angle of extinction for any given cleavage seam over the length of the slide, indicating a crystallographic preferred orientation. The feldspar and quartz have <20*m*m diameter and display a strong dimensional elongation defining the fabric. White mica overprints feldspar especially along grain boundaries, but there is evidence of mica controlled quartz growth in pegged quartz-quartz-mica contacts. Feldspar-feldspar grain boundaries are irregular and at high angles to mica flakes. Most phases in the matrix have strong undulose extinction, and the grain boundary morphology indicates grainsize reduction by dynamic recrystallisation.

Calcite and pyrite are closely related in the rocks, with calcite-white mica pressure shadow fringes around syn-tectonic pyrite porphyroblasts. The fringes have a gross morphology that indicates dextral shear sense, however the internal morphology of the fringes is anomalous (Figure 5.8b p.167). The 001 cleavage direction in the mica is parallel to the pyrite face instead of being at a high angle (Figure 5.8c-e p.167), as documented widely in the literature (Durney and Ramsay 1973; Ramsay and Huber 1983; Barker 1990; Spencer 1991; Passchier and Trouw 1996). Micaceous minerals preferentially grow in the 001 direction, and rotation of the rigid porphyroblast during simple shear is indicated by a sequential change in the fringe orientation that approaches parallelism with the shear direction (Figure 5.8f p.167). This anomalous fringe morphology is common to nearly

every specimen of pressure shadow fringes observed in thin sections from the Enterprise fault zone, and is therefore formed by a common process at the Enterprise mine rather than being a rare variation (Figure 5.8d p.167).

Muscovite-calcite +/-albite in the fringes indicates the composition of the rock fluid at the time the shear zone was active. The geometry of these fringes depends upon the shape of the core object, the flow regime in the surrounding matrix, and whether fibre growth is face-controlled or displacement controlled (Passchier and Trouw 1996). Fringe fibres grow in geometrically recognisable patterns with their long axes parallel to the bulk displacement path (Spencer 1991). Pyrite-type fibres grow towards the grain, and crinoid-type fibres grow away from the grain towards the wallrocks. The fibres in this sample however, are not recognisable as either pyrite or crinoid type. The pyrite in the shear zone shows minor cataclastic texture and generally is euhedral with minor elongate forms.

The interpretation of these growth fibres is not simple, but possible interpretations include an overprinting origin where the muscovite and calcite is retrogressive after an earlier mineralogy. If this was the case, and the overprinting was mimetic, the original mineral fabric is anomalous. An alternative interpretation involves a progressive change in the orientation of the finite strain ellipsoid towards the rigid porphyroblast. The fibres at the ends of the fringe structures are at a high angle to the ENE-WSW shortening direction, and growth along 001 in the mica would be expected in this orientation. As the porphyroblast is approached, the local effects of the rigid structure on the flow field may rotate the local instantaneous stretching axes and control the growth of the white mica.

Summary

Brittle-ductile faults at the Enterprise mine may have a full spectrum of fabric styles in any given structure. It is important that the ductile parts of structures are not ascribed to earlier (D3) regional shearing events since the fault textures include ductile strains and brittle fabrics mutually overprinting. Intracrystalline strain is preserved in some faults as deformation lamellae and undulose extinction yet the majority of faults display evidence of recovery with recrystallised fabrics in quartz and calcite aggregates. Evidence of both dynamic recrystallisation in some faults and others with widespread nucleation and recrystallisation microstructures indicate that recovery outlasted deformation. The nature of

the fault fabrics shows that the deformation was predominantly brittle-ductile in an environment of fluid overpressure. Strong alteration of the structures with gold-related alteration mineralogy defining the fabrics implies that the rock fluid at the time of deformation was the same fluid responsible for major gold deposition.

5.3.4 Meso/microfracture arrays

Meso/microfracture arrays are distinctive structures closely related to brittle-ductile faults in the Enterprise fault zone. The distribution of the fabric is largely controlled by the Cashmans Sedimentary Horizon contact, with a 10-30m thick zone of intense meso/microfracturing of Enterprise dolerite in the vicinity of the contact. Well-developed mesofracturing is pervasive around brittle-ductile fault intersections and may be an expression of fluid pathways into the wallrocks (Figure 5.9a), analogous to the damage zone of Caine *et al*. (1996). In hand specimen, the texture appears to be defined by 1-3mm thick quartz-calcite-(pyrite) veins that separate angular fragments of intensely-altered dolerite.

Microfabric

In thin section the mesofractures are thin quartz-calcite veins that contain little or no alteration and for this reason probably overprint earlier deformation/mineralisation events. The mesofractures are in N-S / NE-SW conjugate sets that form an interlinked network through the rock. Individual fractures are straight to curved with fracture-fill morphology, and are spaced at 2-4mm lacking offset or oriented mineral growth. Some fractures are rhomb-shaped dilational jogs along shear fractures but these are relatively rare. A transition exists between regularly oriented fractures with straight morphology, to randomly oriented chaotic texture with distended vein segments throughout the rock. This transition may reflect the relative input of stress and fluid-pressure to the formation of the structures, with the effects of fluid pressure increasing in rocks with more of a random fabric.

Calcite in the fractures is equant with 120° dihedral grain-boundary angles in strain-free grains, or may be elongate with high angle calcite-calcite-biotite grain boundaries. The texture is almost totally recrystallised and indicates post-deformation recovery. Quartz in

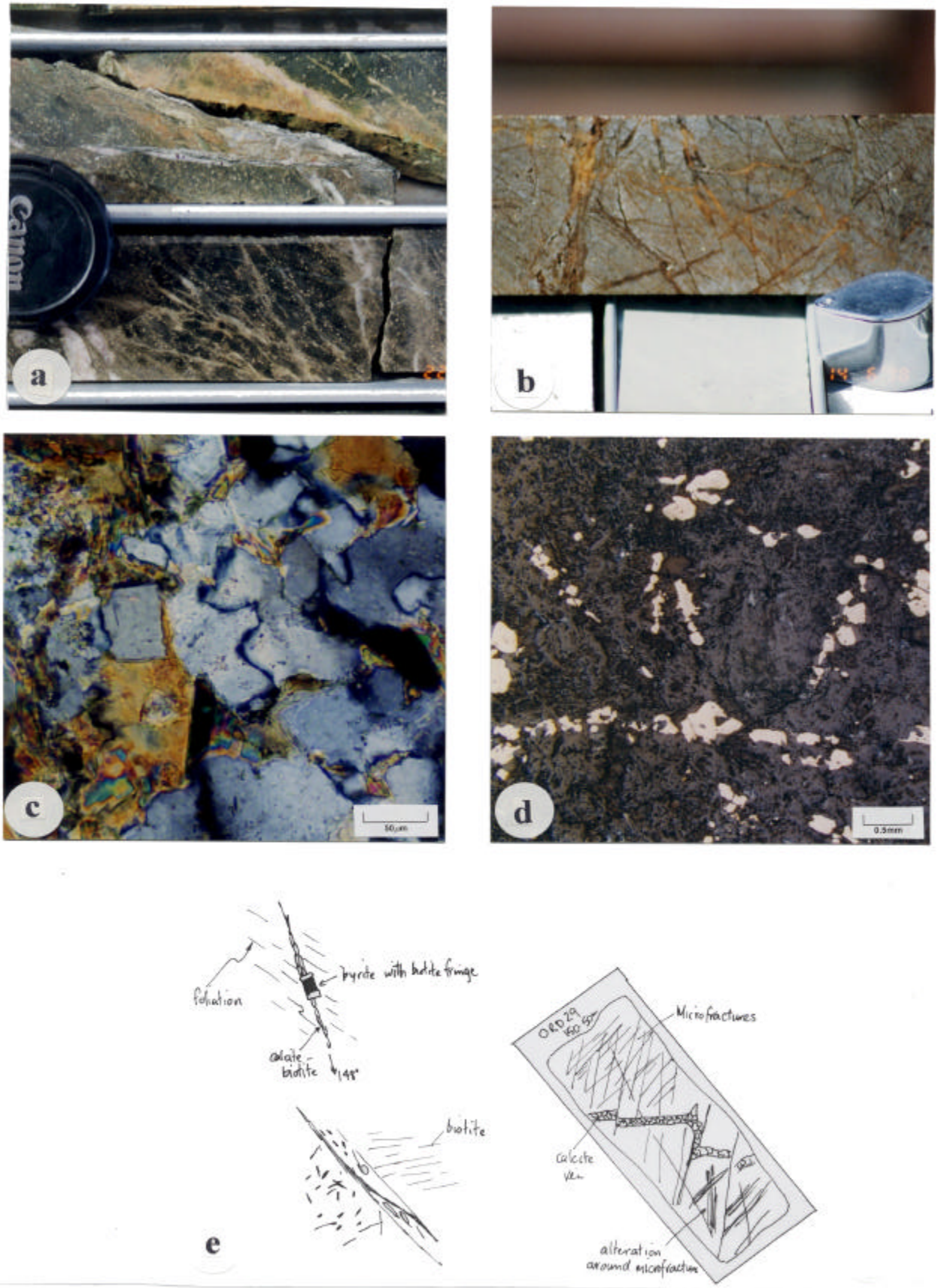

Figure 5.9 – a) Mesofracturing around cataclasite fault in dolerite. **b)** Jigsaw-style breccia effect produced by mesofracturing. **c)** Photomicrograph showing grain boundary bulging microstructures in quartz, (XPL). **d)** Photomicrograph showing microfracture control on pyrite distribution, reflected light. e) Sketches of detailed fabric of mesofractures. See text and over page for explanation.

Captions for figures on page 172

Figure 5.9a
Photograph of highly fractured dolerite in the vicinity of a cataclasite fault trending 047°/61°NW. Mesofractures trend 007°/47°W and intersect the fault in a point that plunges 40°→254° (subparallel to the mineralised envelope at Enterprise). Large 1-2mm fractures are spaced at about 5mm throughout, small localised areas have increased density of sub-millimetre microfractures. Chlorite-epidote alteration dominates the areas away from higher fracture-density zones with a progressive change to muscovite-carbonate alteration. Fine-grained pyrite occurs in clusters in the fractures and in the immediate wallrocks. The fracturing overprints poorly developed schistosity defined by wisps of chlorite. A direct relationship exists between intensity of alteration and density of meso/microfracturing. A fire assay value of 1.78 g/T Au was returned for the fault. The fault is at 282.25m in diamond drillhole ORD157, downhole direction is to the right. Lenscap is 55mm diameter.

Figure 5.9b
Photograph of mesofractured dolerite. A series of regularly oriented fractures produce a jigsaw breccia texture with only minor offsets and rotation of the "clasts". The rock is intensely muscovite-calcite altered with disseminated pyrite throughout. Veins have a high proportion of cavities and are slightly weathered. Inter-vein wallrock fragments have fine microfractures. A fire assay value of 1.8 g/T Au was returned for the sample. The sample is at 121.0m in diamond drillhole ORBD13, downhole direction is to the right. Handlens for scale.

Figure 5.9c
Photomicrograph (XPL) of microstructures in a quartz aggregate. The quartz grain boundaries are bulging into neighboring grains which is evidence of grain boundary migration recrystallisation, one of the two mechanisms of dynamic recrystallisation. A grain boundary will begin to bulge if the two grains have a different dislocation density. The boundary bulges into the grain with the highest density (Passchier and Trouw 1996) and eventually forms a new grain. The sample is from 150.5m in diamond drill hole ORD29.

Figure 5.9d
Photomicrograph (reflected light) showing control of pyrite distribution by microfractures in the rock. The microfractures are straight and almost exclusively contain the pyrite with no pyrite alteration in the intervening wallrock domains. A fire assay value of 1.8 g/T Au was returned for the sample. Sample is at 150.5m in diamond drill hole ORD29.

Figure 5.9e
Sketches of mesoscopic relationships in mesofractured rock.

the fractures is also strain-free with slightly irregular grain boundaries, but 120° dihedral angles may also indicate grain boundary area-reduction due to normal grain growth. Some shearing-reactivated fractures exhibit intracrystalline deformation with kinked deformation twins in calcite, strong undulose extinction in irregular-shaped quartz grains, and deformation twinning in albite. A moderate to high temperature and low strain-rate resulting in grain boundary migration-recrystallisation is evinced by minor grain-boundary bulging and nucleation microstructures (Figure 5.9c p.172).

Microfractures are ubiquitous in the fabric of the rocks developed along pre-existing foliation planes defined by trails of pyrite. Alteration intensity in the surrounding rocks increases with increased microfracture density with a close asscociation of pyrite-calcite and up to three generations of biotite near the fractures. Microfractures are defined by strained calcite grains and trails of pyrite that may be one crystal thick (20*m*m) or up to 100*m*m (Figure 5.9d p.172). The fractures have parallel to slightly anastomosing geometry and are rough shaped with sharp boundaries against the wallrocks, forming up to 10% volume of cleavage domains in the most altered areas. The fractures have been reactivated with saussurite retrogression along fractures and grain boundaries of calcite within the fractures. Biotite commonly forms a 0.25mm wide halo around the fractures with both biotite alteration and fracture density increasing towards major fluid channels such as quartz veins.

Stratigraphic control and genesis of meso/microfracture arrays

Strong development of meso/microfracturing in the vicinity of Cashmans Sedimentary Horizon may indicate the presence of major fluid barrier in this location (Dickie 1995). Shearing and fracturing are developed both in the sedimentary unit and the felsic porphyry sill that intruded it, with minor fracturing near faults that cross-cut the fine-grained basal chilled margin of the overlying Mt Pleasant Sill. A major change in grain-size from the lower coarse-grained norite / hornblende peridotite layers of the Mt Peasant Sill across the contact into the plagioclase-dominated Enterprise dolerite may produce significantly different tensile strengths between the units.

Hydrothermal alteration restricted to the hanging-wall side of the south Enterprise fault may indicate that fluids moved in an upward direction during deformation and

mineralisation. If this were the case, upwards moving fluids would have been restricted against the overlying fluid barrier of the Mt Pleasant Sill and leading to fluid overpressuring and subsequent hydraulic fracturing of the rocks (Figure 5.2 p.147).

5.3.5 Brittle faults

Brittle faults are planar to curviplanar surfaces that are generally expressed as discrete structures but may have zones of fracture and brecciation in the immediate wallrocks of the fault. Discrete planar breaks with well-developed slickenfibre lineations defined by chlorite, muscovite/biotite and calcite occur in a swarm of several tens of individual structures. The faults rarely have large offsets but show displacements of quartz veins of less than 1m. Rare examples display moderate ≈40°N plunging slickenfibre lineations overprinted by shallow <10° doubly-plunging lineations indicating a complex movement history. Minor development of curved slickenfibres of calcite and chlorite is observed.

In thin section, the faults are sharp planes with smooth slickenfibres of calcite, biotite and muscovite. Mesofracturing is common in the wallrocks with strong biotite-pyrite alteration. In sample ORBD18 617.6, the fault contains a 2-3mm wide zone of fine-grained euhedral biotite infilling the fault break, surrounded by thin chloritic fractures separating 200*m*m-thick lens-shaped wallrock fragments. The biotite is strain-free in anastomosing bands up to 100*m*m thick, with minor lenses of calcite-quartz vein material. The fault also contains irregular, stretched mafic clasts with internal cataclasis.

Brittle faults are the latest deformation structure to form and in all cases they offset pre-existing features such as quartz veins and brittle-ductile faults. The structures do not appear to have been major fluid conduits but instead are commonly formed on the margins of pre-existing quartz veins and thin quartz-calcite veins.

5.3.6 Veins

Veins are a major component of the brittle and brittle-ductile fabrics at Enterprise. Several overlapping generations of vein development with similar mineralogy and vein style, characterise the major vein event, with later veins associated with granitoid intrusion and retrogression.

Vein types

Eleven vein types are distinguished based on mineralogy (Table A1.2 p.283), but those most important to mineralisation can be further grouped into four main types as; Type-I quartz-calcite veins (V1), Type-II quartz veins (V2, V3, V6), Type-III granitoid related veins (V7, V8), and Type-IV other veins (V4, V5).

Of all the veins studied, Type-II are the most common (n=598), followed by Type-I veins (n=155), Type-III veins (n=18) and Type-IV veins (n=17). Quartz porphyry veins (V9) are more correctly classified as dykes or sills, and the quartz veins that are internal to porphyry dykes and sills (V10) do not cross the boundaries. These veins possibly were formed during intrusion of the dykes/sills, and are therefore unrelated to mineralisation. Sulphide stringer veins (SRpo, SRpy, SRcp), are minor veins not widely developed.

Type-I quartz-calcite veins, are simple fracture-fill veins composed of very fine-grained quartz and calcite. The veins are developed over a protracted period and may contain alteration minerals (biotite-pyrite-chlorite) or simply may overprint previously altered rocks. These veins are the dominant component of mesofracture arrays, and are commonly developed in the wallrocks of brittle-ductile faults. In one example (ORD157 225.60), the veins form three regularly oriented fracture sets that intersect in a point parallel to the slip lineation of the fault. Type-I veins have no significant aligned mineral growth on the margins, except where a pre-existing microfracture has been reactivated to form the vein. The veins are 2-3mm wide on average, and are commonly developed in conjugate sets.

Type-II quartz veins are predominantly composed of quartz and are emplaced either parallel to, or cross-cutting planar fabrics such as continuous cleavage or brittle-ductile faults, and in some cases foliations bend into vein margins (Figure 5.10a). Veins emplaced into faults are common, but faulting may have continued after vein emplacement, with shearing and boudinage fabrics developed in the vein, and well-developed stretching and mineral alignment lineations on vein surfaces (Figure 5.10b).

The veins vary in thickness from 5mm to 3m, but the majority are less than 150mm thick (Figure 5.11a). Type-II veins appear to predate most fault movement, but in some cases were emplaced at the time of the brittle-ductile fault event, and (rare) examples are

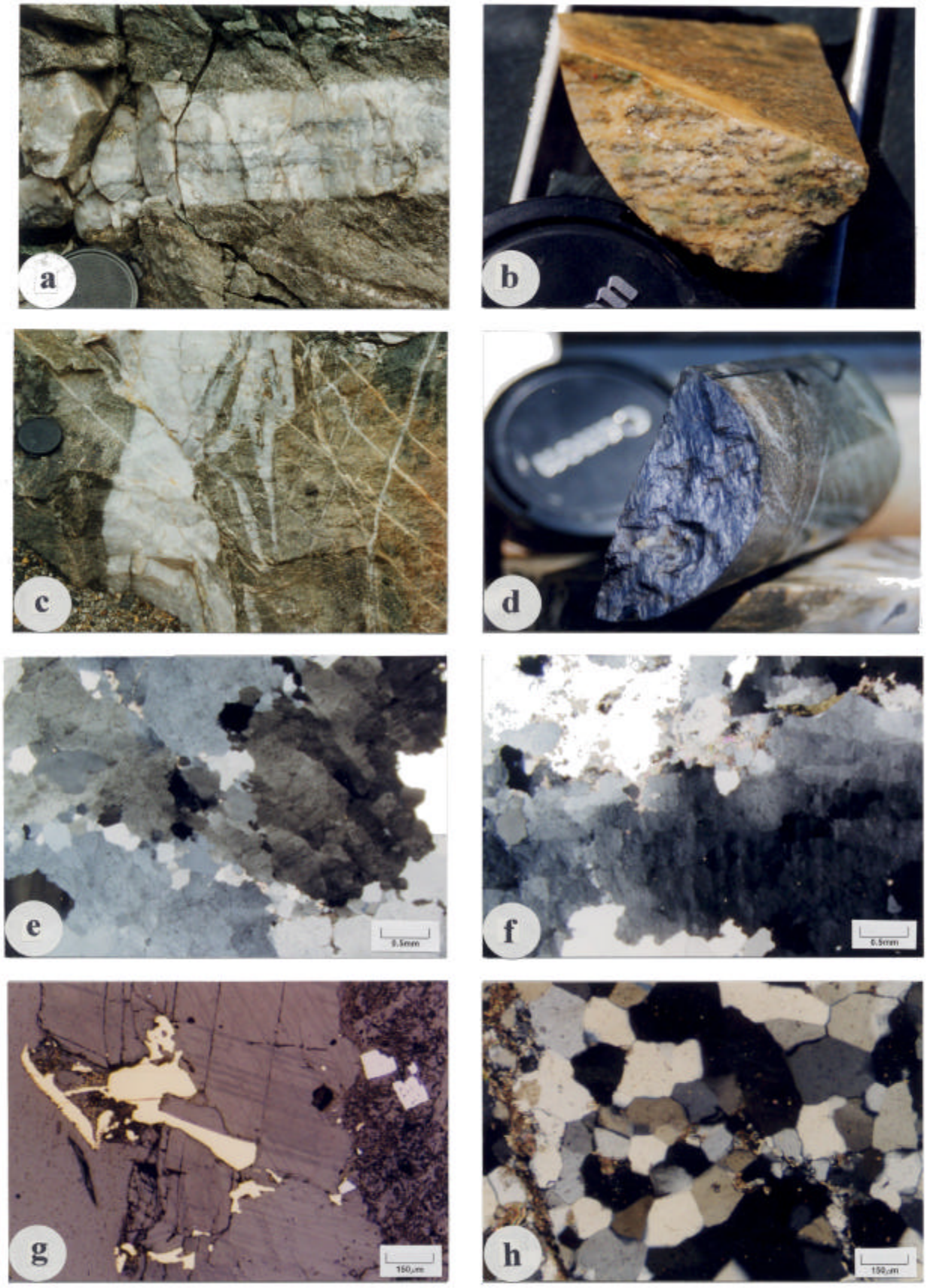

Figure 5.10 – a) Quartz vein with molybdenite seams cross-cutting foliation in wallrocks. **b)** Mineral stretching lineation on quartz-calcite vein surface. **c)** Intravein breccia showing initial stages of development. **d)** Molybdenite slickenfibres on wallrock/vein contact. **e)** Photomicrograph showing annealing recrystallisation texture in quartz with low-angle subgrains, (XPL). **f)** Photomicrograph of low-angle subgrains in quartz with deformation lamellae, (XPL). **g)** Photomicrograph of native gold in a calcite vein precipitated along a quartz vein boundary, reflected light. **h)** Photomicrograph showing totally recrystallised fabric in vein quartz. See text and over page for explanation.

Captions for figures on page 177

Figure 5.10a
Type-II quartz vein in Enterprise open-pit. The vein has thin stylolitic seams of molybdenite in the centre with bands of milky quartz, cross-cutting a pervasive cleavage in the wallrocks. Over 50 veins of this type occur in the southern wall of the open-pit and are continuous structures over 100-200 metres length. In many cases the veins maintain a constant thickness, but also bifurcate, thicken and converge with thicker veins. Lenscap is 55mm diameter.

Figure 5.10b
Mineral lineation in the plane of a sheared quartz-carbonate vein. The lineation is defined by stretched green chlorite clots with aligned trails of pyrite (+/-pyrrhotite), and defines the slip direction of the shearing. The vein occurs within a larger shear zone indicating that some vein emplacement occurred synchronous with the shearing event. A fire assay value of 0.16 g/T Au was returned for the shear zone. The sample trending 044°/59°SE is from 661.0m in diamond drill hole ORBD19. Lenscap for scale.

Figure 5.10c
Intravein breccia from Enterprise open-pit. The 16cm thick vein trends 138°/80°NE with thin quartz-filled mesofractures around the main vein. The mesofractures delineate blocks of altered wallrock that are stoped into the vein, which is at the initial stages of development. In other examples of intravein breccia the wallrock fragments may be significantly rounded and comminuted.

Figure 5.10d
Slickenfibre lineation defined by molybdenite selvedge at a vein contact. The contact has an irregular surface with stepping slickenfibres that clearly show movement sense. Sample is from 178.1m in diamond drill hole ORD29.

Figure 5.10e
Photomicrograph (XPL) showing recrystallisation texture in a quartz vein. The new quartz grains have nucleated along the grain boundaries of larger strained grains that show evidence of significant recovery, with well-developed low-angle subgrains in the dark grain on the right. The new grains are strain free with 120° dihedral angles and straight grain boundaries. The sample is from a vein cross-cutting a wallrock foliation, and trending 119°/38°SW at 269.9m in diamond drill hole ORBD12.

Figure 5.10f
Photomicrograph (XPL) of the same vein in Figure 5.10e), showing well-progressed subgrain development, with low-angle subgrains in quartz trending across the slide. The quartz still has significant intracrystalline strain with deformation lamellae trending top to bottom across the grain. Further recovery in this grain would see nucleation of new grains along the grain boundaries.

Figure 5.10g
Photomicrograph (reflected light) of gold grains in a calcite vein. The 2mm wide calcite vein is emplaced at the margin of a Type-II quartz vein and has intense white mica alteration associated. The gold is filling a void in the calcite and along microfractures, and clearly post-dates the Type-II vein event. The vein has a 7-10mm wide white mica alteration halo overprinting ophitic textured dolerite. A fire assay value of 5.7 g/T Au was returned for this vein. The vein trending 048°/89°NW is at 258.09m in diamond drill hole ORBD12.

Figure 5.10h
Photomicrograph (XPL) showing recrystallised texture in a quartz vein. The quartz is equigranular with 120° dihedral angles and irregular to straight grain boundaries. A fire assay value of 0.85 g/T Au was returned for this vein. The vein is at 194.36m in diamond drill hole ORD29.

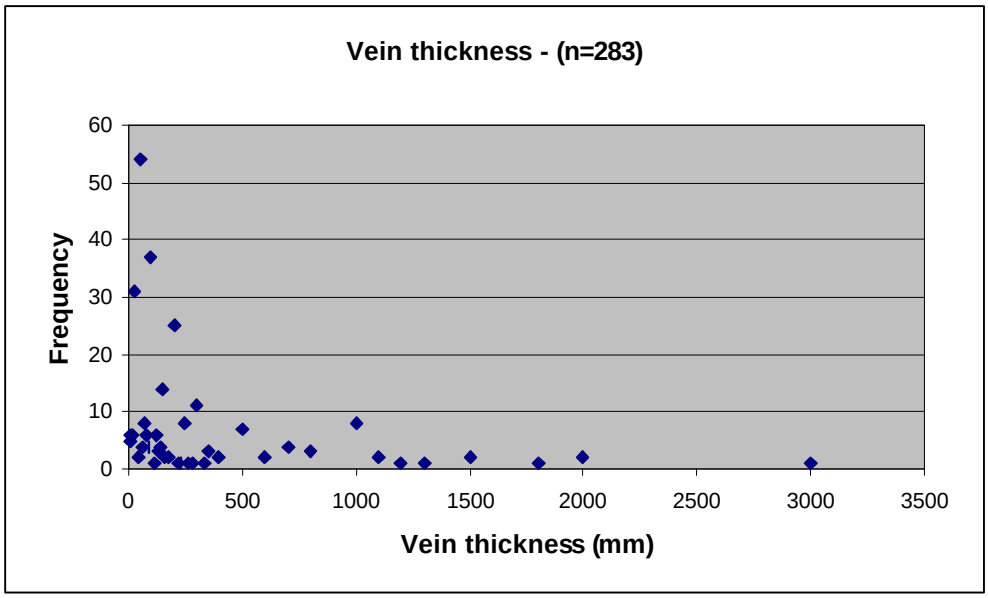

Figure 5.11a – Graph of vein thickness for 283 quartz veins measured in Enterprise open-pit. Veins are up to 3m thick but the majority are less than 150mm.

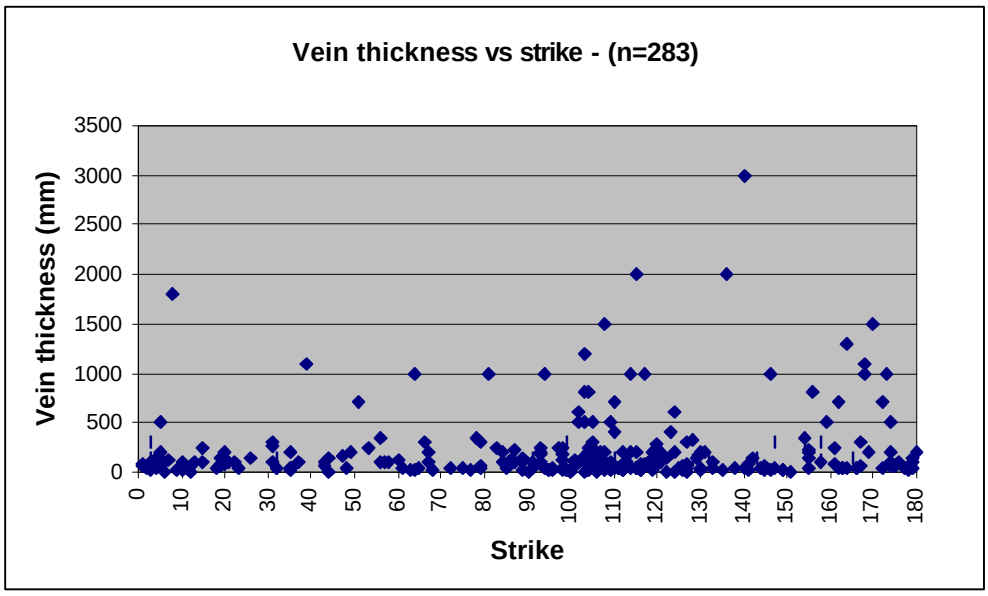

Figure 5.11b – Graph of vein thickness versus strike orientation. Thick veins (i.e. >0.5m) cluster around 110° (E-W) and 170° (N-S) orientations, however the thickest veins have a NW-SE orientation. Broad clusters of veins < 0.5m are spread over the compass, with slightly less in the NE-SW orientation.

observed of quartz veins cross-cutting brittle-ductile faults. The veins are developed in a broad scatter of orientations (Figure 5.11b p.179), but the thickest trend E-W and N-S. The veins consist of bands of quartz that may be either translucent or milky, variably with inclusions of wallrock material or sulphides. Vein textures are predominantly simple fracture-fill types with non-directional controlled quartz addition textures, that form thick bands of massive quartz. Type-II quartz veins have a minor component of cavities that are usually filled with calcite, chlorite and sulphides against euhedral quartz terminations that control the morphology of the infill phases.

Wallrock alteration in the vicinity of Type-II quartz veins is also variable with a range of relationships that includes no alteration, sharp alteration haloes of variable composition, to diffuse vein boundaries against altered wallrocks. A vein with no alteration halo implies emplacement before (or after) the alteration event, however significant fluid ingress with the intrusion of the Lone Hand Monzogranite, which postdates mineralisation, is not evident in these veins and they are therefore interpreted as earlier. The most common alteration assemblage is biotite-pyrite-calcite in thin uniform haloes sub-parallel to the vein margin, with minor development of hematite-epidote. Muscovite-ankerite is also a common assemblage, and in veins with diffuse boundaries, ankerite is particularly prevalent with minor calcite and pyrite.

A distinctive vein set termed ‘intravein breccia’ is observed in the open pit and in the diamond drilling (Figure 5.10c p.177). These structures are white quartz veins with large angular fragments of intensely altered mafic wallrocks, trending N-S on average with moderate to steep dips to the east or west.

Type-III granitoid-related veins are mostly calcite-fluorite (+/-ankerite) veins that occur in en-echelon arrays, whose geometry indicates formation during a sub-vertical directed shortening. The mineralogy includes minor scheelite and molybdenite, and is a distinctive vein generation commonly associated with muscovite-pyrite alteration around brittle-ductile faults. Molybdenite is more widespread than the other granitoid-related assemblages and may indicate a fluid event slightly earlier than the fluorite-calcite- muscovite alteration, since it is more closely associated with faults and Type-II quartz veins, and commonly forms slickenfibres on slip surfaces (Figure 5.10d p.177).

Calcite and fluorite in these veins is coarsely crystalline up to 0.5mm with strain-free grains and preserved rhombohedral cleavage in calcite. Isotropic fluorite appears to have filled cavities late in the crystallisation sequence, with its grain boundary shape controlled by calcite. The veins commonly contain scheelite and may have fluorite rims on chalcopyrite crystals. In thin section, small sigmoid tension gash veins mimic the morphology of mesoscopic veins in outcrop.

Microfabric

The microstructure of quartz-calcite veins is covered in Chapter 5.3.4 (p.171), since these veins are the dominant component of micro/mesofracture arrays. Type-II quartz veins were studied in thin section including quartz veins cross-cutting foliations, quartz veins emplaced within foliations, quartz veins cross-cutting brittle-ductile faults and quartz veins emplaced within brittle-ductile faults. The various quartz vein relationships were studied to determine if separate vein generations existed within this large group.

For veins cross-cutting wallrock foliation, the foliation is at ≈20° to the vein margin with chlorite-pyrite +/- biotite alteration halos up to 20mm-wide. The veins have a symmetrical banding of outer fine-grained quartz (5mm-wide) and inner bands of coarse-grained quartz (1.5mm-wide). Thin bands of highly strained albite in matted aggregates, and minor carbonates in microfractures, cross-cut the veins at a high angle.

The fine-grained outer bands are composed of strain-free quartz grains with straight to irregular grain boundaries, and small grains nucleated at grain boundary intersections in sutured grains (Figure 5.10e p.177). Coarse-grained quartz in the centre of the vein is highly strained with strong undulose extinction and deformation lamellae (Figure 5.10f p.177). Minor evidence of recovery includes polygonisation with well-developed low-angle subgrains.

Veins emplaced parallel to a foliation, have uniform quartz grain aggregates throughout. A selvedge of pyrite grains on the outer vein margin, and biotite-pyrite alteration halos, are evidence of alteration during vein emplacement. In hand specimen they contain laminated milky quartz, yet the laminations have no distinction in thin section. The veins have grains up to 200*m*m diameter at the junctures of larger grains with sutured boundaries.

In a vein cross-cutting a brittle-ductile fault (ORBD12 258.09), the 15mm-wide vein is composed of milky quartz with calcite filled cavities, and has a sharp margin against the wallrocks. The vein has an alteration halo of fine white mica 7-10mm wide, and outer bands of calcite-chlorite (2mm-wide) with crystalline calcite at 90° to the vein wall that contains coarse-grained visible gold (Figure 5.10g p.177). The calcite veins are strained with well-developed deformation twinning and fine muscovite alteration in the calcite. Pyrite occurs in a continuous band near the vein margin, but is elsewhere disseminated. The quartz vein contains coarse grains with undulose extinction and irregular grain boundaries, and evidence of annealing recrystallisation. At the vein centre there is a 2mm-wide band of very fine-grained recrystallised quartz with foam fabric.

Veins emplaced into brittle-ductile faults are usually termed ‘shear veins’ (Hodgson 1989; Colvine *et al.*1988). These veins at Enterprise have lensoid shape oriented parallel to the fault, and contain significant carbonate with fragments of quartz. The veins may postdate alteration in the wallrocks, and are emplaced along the C plane in S-C mylonite zones. The veins are mostly massive with little internal structure, composed of equigranular quartz grains of 60-200*m*m diameter, that are strain-free with 120° dihedral angles and straight grain boundaries (Figure 5.10h p.177). The vein margins may be sheared with ≈50*m*m thick calcite bands composed of equigranular strain-free calcite, but with long axes defining a preferred orientation.

Late vein generations include veins that do not have any alteration at the margin in chloritic wallrocks. These veins are mostly composed of milky quartz with highly strained quartz in thin section. Significant nucleation of new grains around large quartz grains indicates minor recovery, but the large grains have sutured boundaries, strong undulose extinction and well-developed deformation lamellae, and hence may postdate the late thermal recovery that has affected most other veins.

Vein generations

Vein generations are summarised in Figure 5.12, and show at least eight overlapping vein emplacement events. The consistent biotite-pyrite alteration associated with Type-II quartz veins that are emplaced in, and cross-cut by, brittle-ductile faults in the three principal

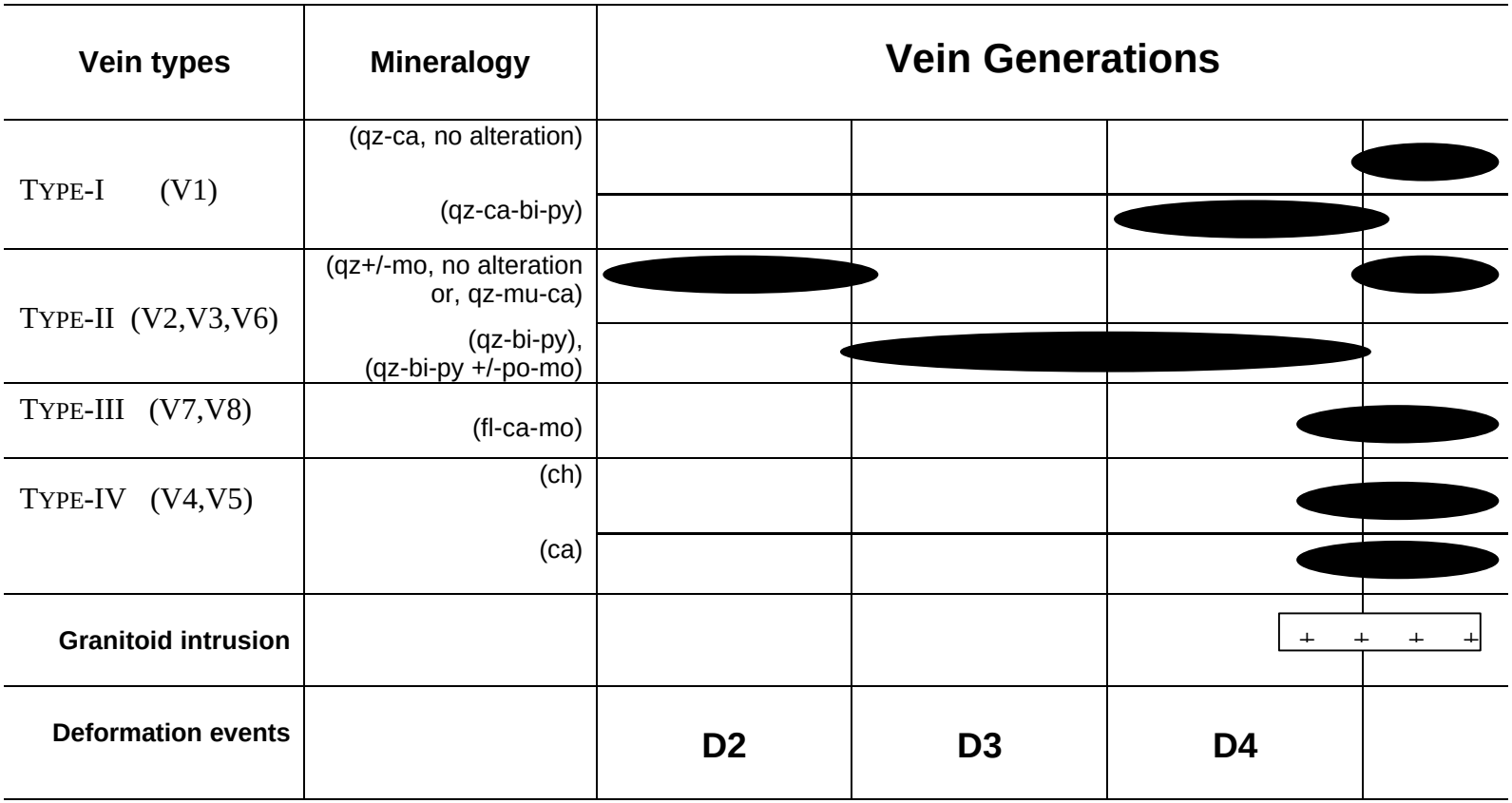

Figure 5.12 – Diagram showing the development of the four vein types at the Enterprise mine. Vein emplacement events for each generation are indicated by the black bulges corresponding to the relevant deformation event. At least eight vein generations are apparent including two generations of Type II veins without alteration. Type II veins with alteration may include several overlapping generations of vein emplacement within D3/D4. Granitoid intrusion is indicated for the Enterprise area only and does not include the regional granitoid emplacement event synchronous with D3. Mineral codes are listed in Table A1.7 (p. 283).

structural orientations, may be further evidence of synchronous development of the different fault orientations. At least two generations of Type-I and three generations of Type-II veins are developed over the three deformation events (D2-D4).

From the previous section, there is no significant difference between veins that cross-cut a foliation or veins emplaced into a foliation. Veins with both of these relationships have biotite-pyrite alteration, symmetric laminations of quartz and minor intracrystalline strain with evidence of recovery. However veins that cross-cut faults have significantly different mineralogy and may be a later fluid event with strong white mica and calcite alteration (+/- Au) around mostly recrystallised quartz. Some veins emplaced into faults are massive with little alteration associated with the vein and hence may be earlier structures that are reactivated by the faults. Three possible vein generations are determined within the Type-II vein set from these observations (Figure 5.12 p.183)

Folding in veins

Several large quartz veins in the north wall of the Enterprise open-pit are gently folded with uniform fold axis orientations. The veins are steeply south-dipping and strike sub-parallel to the north wall of the open-pit giving the appearance of a ‘wall of quartz’. However vein / wallrock contacts at the base of the wall are folded into steeply south plunging open forms with average orientation of 40°→197°. Shearing on the surrounding Cashmans and Enterprise east shear zones may have produced this folding (Chapter 5.4.6 p.190).

Vein timing and interpretation

Vein timing can generally be determined by cross-cutting relationships with early ductile and later brittle ductile structures, and whereas the major groups have variable mineralogy, the Type-II quartz veins are a long lived vein emplacement event with some change in mineralogy. In a similar fashion, Type-I quartz-calcite veins are closely related to the brittle-ductile faulting event, and are in part generated by a combination of fault movement and fluid overpressure. A late carbonate vein event extensively overprints microfractures in the rocks forming thin calcite veins with no alteration. The distinction of generations within these two groups is therefore based on the presence or lack of alteration. Fluorite-calcite veins postdate most other structures and constrain the timing of granitoid intrusion as late

to post-tectonic. Disruption of these veins in brittle-ductile faults and undeformed veins cross-cutting the faults is evidence of this timing.

A significant problem for the interpretation of veins is qualifying the origin of the quartz. In chlorite-rich rocks with little or no alteration of the wallrocks and sharp vein contacts, the silica may be introduced from a distant source and precipitated into a fracture. However, disequilibrium can result if a fluid that is equilibrated with one rock type enters another, also implying a more distant source. Alternatively, a locally derived fluid in equilibrium with the wallrocks may cause no reaction between the two. Yet in other situations such as veins with strong wallrock alteration and darkening of the margins from silica loss, and particularly in cases where the vein has diffuse boundaries, the source of the silica may also be much closer to the vein or even from the immediate wallrocks.

Summary

Veins at the Enterprise mine are grouped into four types with at least eight generations of vein emplacement. The veins have complex relationships with the brittle-ductile faults that range from veins that pre-date fault movements, to vein systems produced as a result of faulting and veins that overprint fault movements. Each generation is characterised by alteration and timing relationships. As for the brittle-ductile faults, microstructures indicate significant recovery of intracrystalline strain. This recovery in the veins is expressed mostly as static recrystallisation with polygonal foam fabrics in quartz bands, whereas remnant strains may be restricted to early vein precipitation events.

5.3.7 Summary of mesoscopic fabrics

The mesoscopic structure of the Enterprise fault zone is complex with a wide range of fabric types in faults and veins. Cataclasite, foliated cataclasite, various types of mylonite, brittle faults, mesofracture arrays and vein systems overprint early cleavages. These later structures are difficult to separate in time with mutual cross-cutting that indicates synchronous development. The brittle-ductile and brittle faults are synchronous events with mesofracture arrays and some vein generations produced by fault movements. Some vein generations may pre-date the faults, whereas others post-date the faulting.

Granite-related structures mostly post-date the faults and veins but in some areas are also offset indicating a late timing of emplacement for the nearby Lone Hand Monzogranite. This late timing accords with widespread recovery of intracrystalline strains in the faults and veins at the Enterprise mine. Deformation mechanisms; polygonisation, dynamic recrystallisation, sub-grain development and grain boundary migration, are all produced in a low-temperature / low-moderate strain-rate environment.

5.4 ENTERPRISE FAULT ZONE

The gross geometry of the Enterprise fault zone is controlled by the E-W trending, south Enterprise fault and north Enterprise fault zone (SEF, and NEFZ). Other major faults that intersect these are the Halliday and Enterprise 030° faults. In all cases the character of the faults changes where they intersect different host rocks. For example, the degree of schistosity in the faults increases in the talc schist layers near the base of the Mount Pleasant Sill, but is less where the faults cross-cut the underlying Enterprise dolerite. The four brittle-ductile faults have variable development of the fabrics types as discussed in Chapter 5.3.3 (p.155), and are part of a group of faults with variable orientations about poorly defined averages (Figure 5.14 p.188). Additional major structural elements include ubiquitous brittle faults and a large sheeted vein system.

5.4.1 South Enterprise fault

The SEF is a strike-persistent brittle-ductile structure with left lateral metre-scale offset. In the open-pit the structure trends 053°/88°NW, but tends to a more E-W orientation to the west of the open-pit. The fault is 2.5-3.0m wide with a 0.5m-thick, strongly brecciated quartz vein in the centre that contains abundant fragments of intensely altered mafic wallrocks (Figure 5.13a). The outer zone comprises mostly muscovite-pyrite altered dolerite, and weakly foliated chloritic rocks. The SEF has intense muscovite-pyrite alteration in the vicinity of the structure with well-developed shear foliations that bend into the fault plane. Quartz tension veins within the fault trend 034°/18°NW, but do not cross-cut the boundaries. The geometry of these veins indicates sinistral displacement. In the western area of the open-pit the orientation of the SEF changes to 085°/78°N with shallow plunging quartz-calcite slickenfibre lineations trending 9°→273°, that indicate

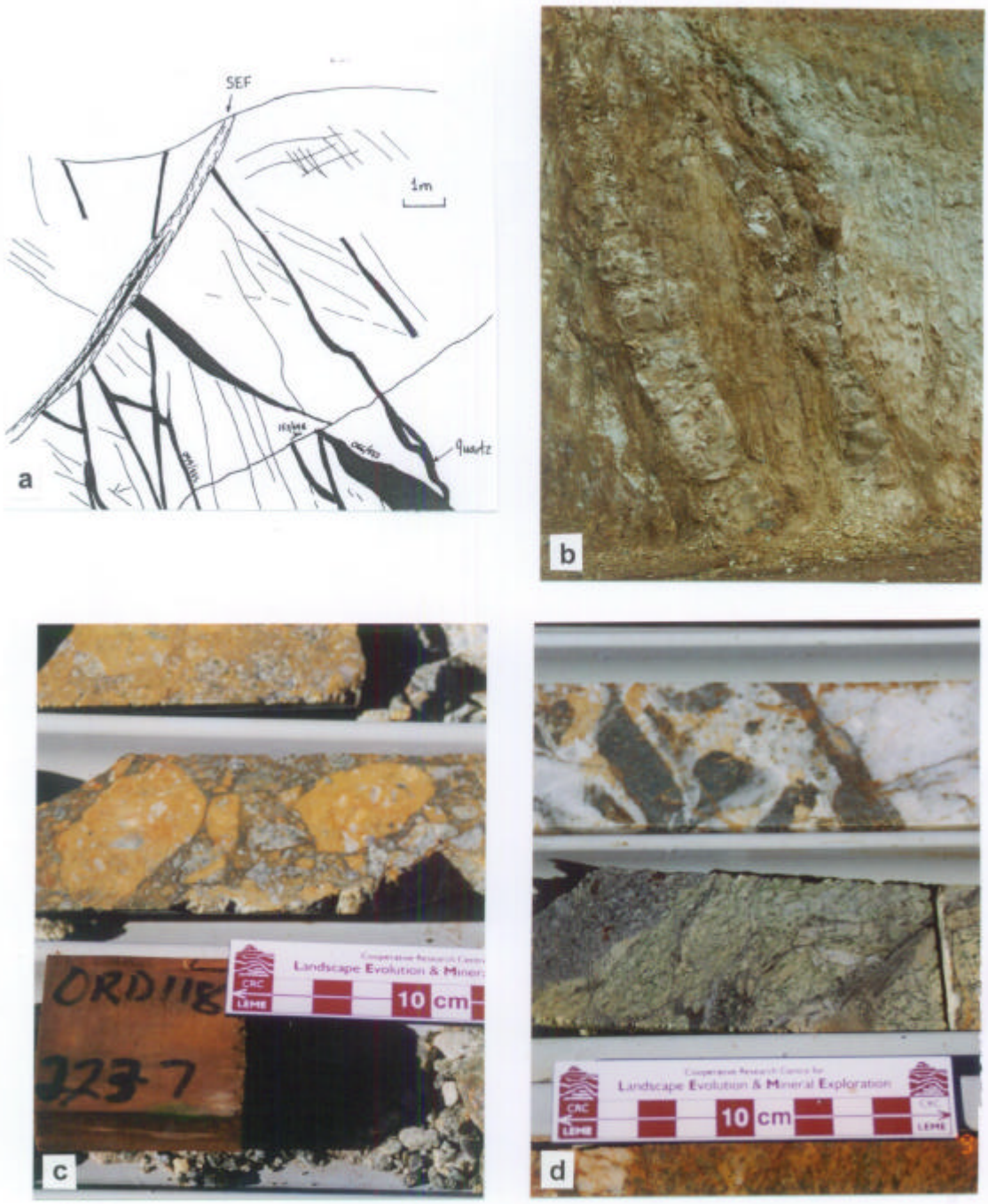

Figure 5.13 – Mesoscopic-scale detail of brittle-ductile faults in the Enterprise fault zone. **a)** Face map of the south Enterprise fault from Wall no. 4 in the open-pit, view looking east. **b)** Enterprise 030 fault in the south wall of the open-pit. **c)** Angular polylithic fault breccia from the north Enterprise fault, in diamond drill hole ORD118 at 223.6m. **d)** Ductile shear fabric in mafic wallrocks of intravein breccia, at 211.6m in diamond drill hole ORD118.

187

Brittle-ductile faults

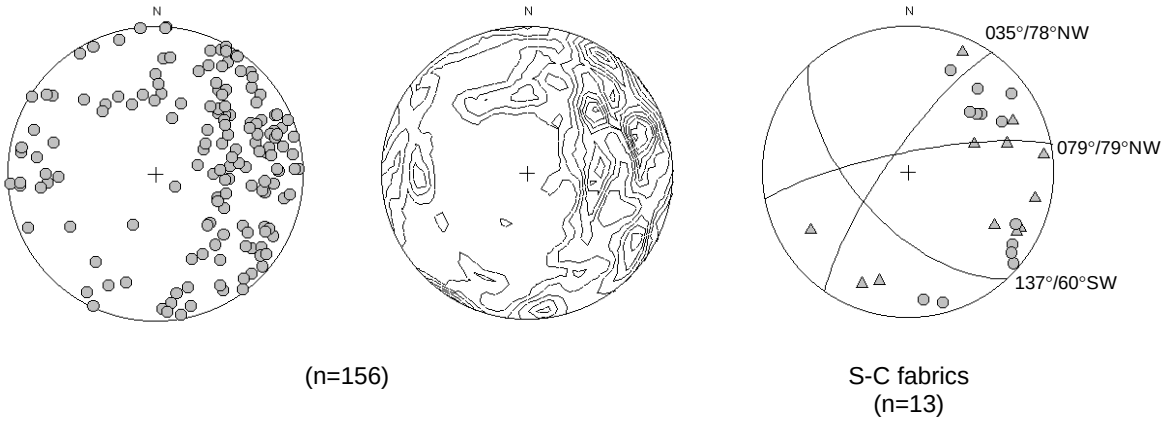

Figure 5.14 – Stereograms of brittle-ductile faults from Enterprise open-pit and diamond drill core. Northwest trending ductile structures (eg. Cashmans Shear Zone) are included with the brittle-ductile faults. Brittle-ductile faults with S-C fabrics cluster into three principal orientations with regular offset relationships NW-SE sinistral, E-W sinistral and NE-SW dextral.

Brittle faults

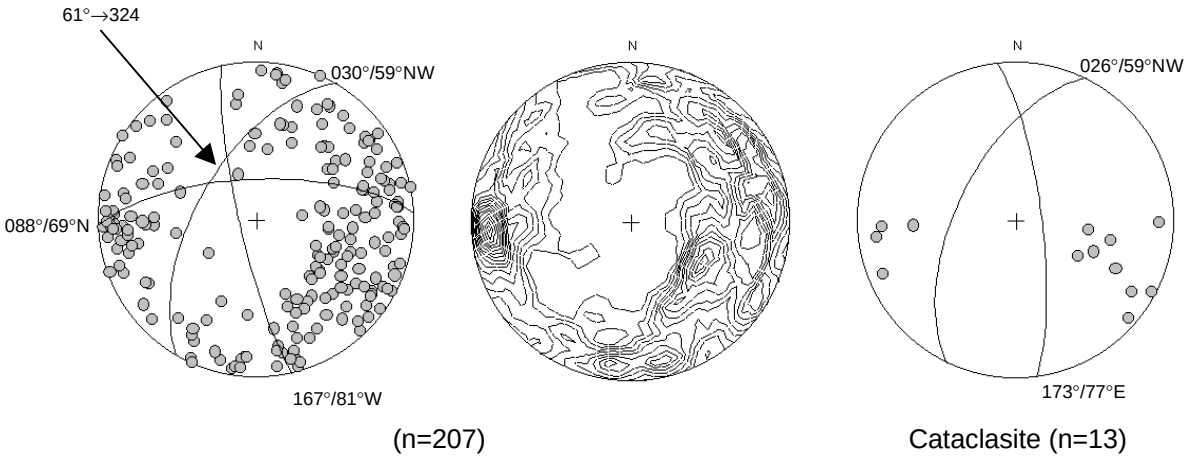

Figure 5.15 – Stereograms of brittle faults measured in Enterprise open pit and diamond drill core. Brittle faults cluster into three main orientations that coincide with the N-S, NE-SW and E-W principal structural orientations. The NE-SW subset has a high degree of scatter in both strike and dip of the brittle faults. A unique intersection point for the brittle faults may indicate synchronous development. Cataclasite zones cluster into two main orientations.

left-lateral strike-slip offset on the fault. In the upper southern wall of the open-pit, the SEF cross-cuts the Cashmans Sedimentary Horizon with drag-folding and offset that indicates right-lateral offset in plan, but may contain a significant dip-slip component.

5.4.2 North Enterprise fault zone

The NEFZ is a broad fault zone developed over 30-40m wide in the northern area of Enterprise open-pit composed of several fault planes of average 2-3m thickness, with zones of cataclasite and fault breccia up to 20m thick. The fault zone trends 080°/87°NW with quartz veins emplaced in the plane of the fault, and significantly disrupted by the fault. Some veins are folded into isoclines within the plane of the fault with pinch-and-swell texture and detached boudins. The wallrocks of the fault are intensely silicified and altered, and contain quartz veins that bend into the fault with north-block-up movement sense. A well-developed S-C fabric in the NEFZ indicates sinistral displacement with the C-plane trending 083°/77°N and the S-plane trending 105°/65°NE. Marked changes in fault style along strike are evident from the map of the open-pit (Map 6 in pocket), with the fault changing from a simple fault plane, to a ductile shear zone, to a fault containing a major quartz vein, to a zone of angular breccia, at major changes in the orientation of the structure. In diamond drill hole ORD118 200m-230m, the NEFZ shows typical brittle-ductile fabrics with a major component of milled fault breccia (Figure 5.13c-d p.187). The rock is intensely altered and indicates a protracted fluid movement history with the most prominent alteration being related to granitoid intrusion, with intense muscovite-ankerite alteration and abundant fluorite-calcite veins. Fragments of rocks with ductile shear fabrics are rounded and interspersed with angular to rounded breccia fragments of mafic rocks and re-brecciated matrix clasts from previous failure episodes. The fault zone is up to 20m wide and contains zones of cataclasite with fine gouge zones defining planes of slip.

5.4.3 Enterprise 030° fault

A major cross-cutting fault in the open-pit is the Enterprise 030° fault. The structure is a typical brittle-ductile fault, of 5m average thickness, but varies from 1m thick in the Enterprise dolerite, to 10m thick in the lower units of the Mount Pleasant Sill (Figure 5.13b p.187). The fault trends 031°/65°NW with a well-developed schistosity in the wallrocks trending 010°/64°NW. S-C fabrics indicate dextral offset, and large 1-2m-thick quartz veins

are emplaced parallel to the C-plane. The veins are composed of translucent buck quartz with variable deformation on their margins. In the open-pit, the Enterprise 030° fault appears to be cross-cut by the SEF, but the continuation of the fault on the northern block of the SEF is unclear. A strong development of brittle faults and cleavage in the northern fault block may indicate a continuation of the structure, but if this is the case the character of the fault is markedly different in this area.

5.4.4 Halliday fault

The Halliday fault is a northwest trending brittle-ductile structure that cross-cuts the Enterprise fault zone 200m to the west of the open-pit. There are few exposures of the fault in diamond drill core and its detailed fabric is unknown, however the trend of the structure is 145°/78°NE, and it may be developed for over 30-40m. A significant down-throw of about 30m of the western block across the fault indicates a major component of oblique slip.

5.4.5 Brittle fault arrays

Brittle faults are ubiquitous in the Enterprise open-pit, forming large smooth planar discontinuities that cross-cut most other structures. The faults show a broad scatter of orientations on the stereonet but group into three poorly defined clusters trending 167°/81°W, 030°/59°NW and 088°/69°N (Figure 5.15 p.188). These three orientations intersect in a single point trending 61°→324°. The intersection of the three orientations and similar fabrics in each may indicate synchronous development. The faults occur in arrays of ten or more faults or as single fractures.

5.4.6 Sheeted vein system

In the open-pit quartz veins show a remarkably constant average orientation of 102°/47°SW south of the south Enterprise fault, but to the north of this boundary they have highly variable orientations with a change of 56° between the major clusters (Figure 5.16) that may be related to disruption by faulting. A small cluster of veins trending

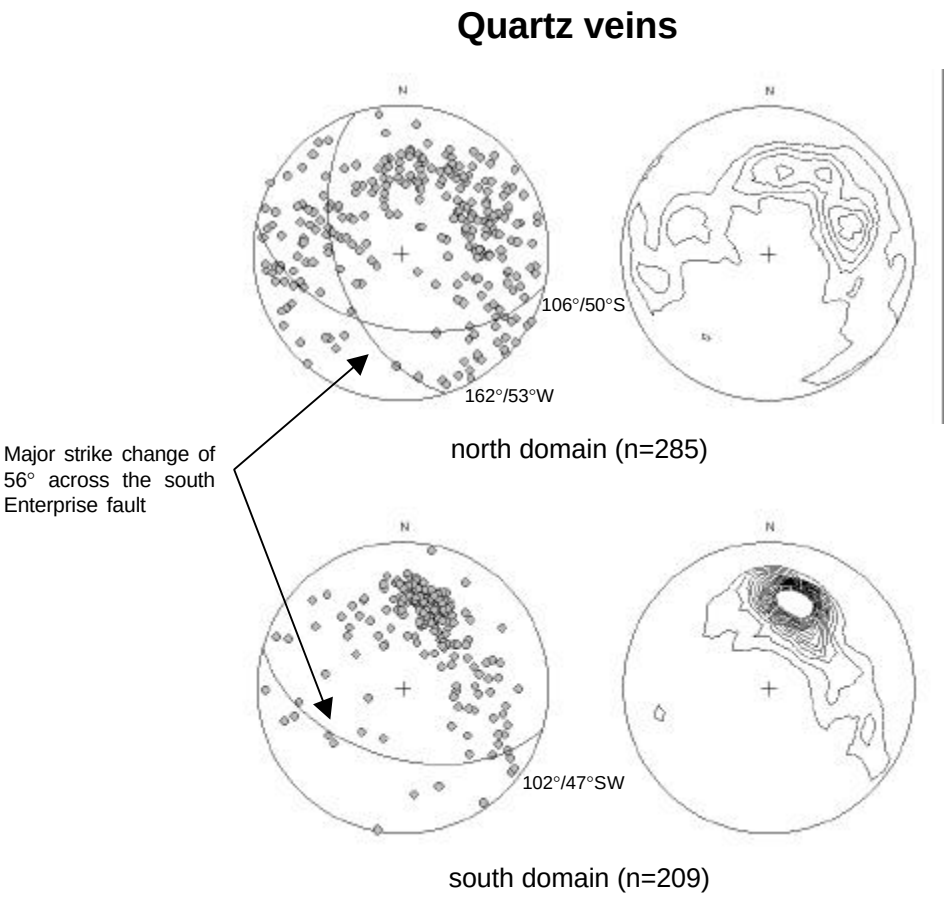

Figure 5.16 – Stereograms of orientations of Type-II quartz veins from Enterprise open-pit. Veins in this group are the most commonly recorded of the four vein types.

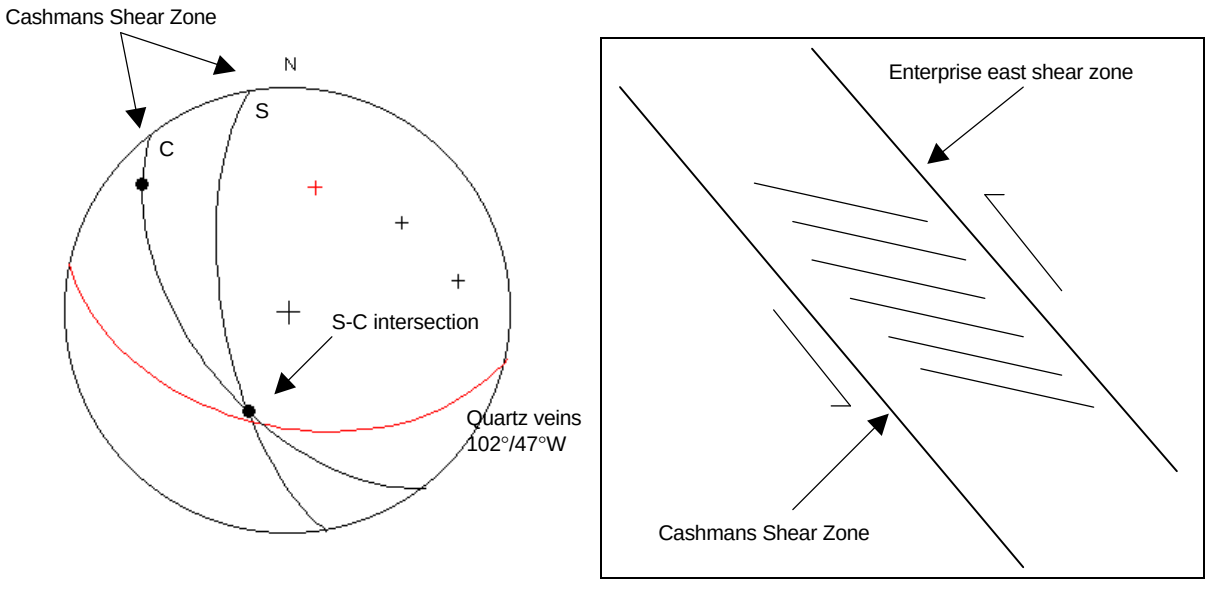

Figure 5.17 - Stereogram and diagram of structural relationships between the quartz vein system at the Enterprise mine and the Cashmans Shear Zone. The average vein orientation intersects the shear zone in a line parallel to the S-C intersection lineation, and may indicate that the two are coeval. Sinistral movement on the Enterprise-east and Cashmans Shear Zones may have influenced the development of the vein system.

106°/50°SW in the northern domain of the open-pit, may indicate that the veins are undisrupted remnants of an earlier vein generation, that preceded the brittle-ductile faulting event.

This large system of sheeted veins is the most striking group of structures in the Enterprise open pit, with strike persistent veins that are sub-parallel in the southern wall. The veins appear sheeted or 'stacked' similar to a geometry described by Peters (1993) and were previously described as 'bedding parallel' (Dickie 1995). However, the average orientation of quartz veins in the southern area of the open-pit is at a moderate angle to the layering in the dolerite and bedding in the Cashmans Sedimentary Horizon, and individual vein orientations may vary up to 40°. Certainly some of the veins have used the layering in the Enterprise dolerite to facilitate their emplacement. Strong vein development in the Enterprise dolerite that does not extend far into the overlying Mount Pleasant Sill, may indicate that the vein system was formed during shearing on the surrounding Cashmans and Enterprise east shear zones (Figure 5.17 p.191). A genetic relationship is also suggested by the average vein orientation intersecting the Cashmans Shear Zone parallel to the S-C intersection lineation. Further shearing after vein emplacement may have induced folding in the veins trending 40°→197° (Section 5.3.6 p.175).

5.5 DISTRIBUTION OF HIGH FRACTURE-DENSITY ZONES

Several areas of high fracture density are evident in the open-pit, most notably at fault intersections but also in the vicinity of the Cashmans Sedimentary Horizon. A zone of intense mesofracturing occurs in this area composed of regularly oriented fracture sets in three average orientations that intersect in a point that plunges shallow westward. Another major zone of high fracture-density is located in the eastern area of the northern wall, where the projected extension of the Enterprise 030° fault intersects the NEFZ. This area is typified by intense fracturing and cleavage development with a high degree of wallrock alteration.

5.6 STRUCTURAL CONTROLS ON PORPHYRY INTRUSION

The Lone Hand Monzogranite (LHM) intrusion at Enterprise is a significant influence on the structural development of the area. The intrusion forms two small stocks up to 1.5km

long with abundant thin porphyry dykes at the periphery and is located less than 100m north of the Enterprise fault zone. The granitoid stocks are enveloped by the Enterprise-east shear zone to the south but the northern stock cross-cuts the shear zone into the wallrocks. A large enclave of the NW trending mylonitic shear zone is contained within and parallel to the western margin of the northern LHM stock which is clear evidence of intrusion postdating the major shear zone movements with stoping of the wallrocks.

The LHM is massive to porphyritic and locally quartz or plagioclase phyric. Lack of foliation in the LHM indicates post-tectonic intrusion, yet foliated and sheared porphyry dykes within the Enterprise-east shear zone, and brittle-ductile faulting in the granitoid body evince minor post-intrusion shearing. Large white quartz veins with an average trend of 100° are extensively exposed in the vicinity of the southern margin of the LHM and within the body indicating high rock-fluid pressures in the area post-dating the intrusion.

A distinct suite of minerals is associated with the intrusion including extensive green-muscovite alteration, carbonate-fluorite, molybdenite and minor scheelite, pyrite, chalcopyrite and chalcocite. These granite-related minerals overprint gold-bearing structures indicating post-gold intrusion. Relationships include stylolitic molybdenite seams within and as selvedges to mineralised quartz veins, steeply-dipping extensional fluorite-calcite filled tension gash arrays that cross-cut all other structures, and extensive muscovite alteration and ankerite bleaching of gold-bearing brittle-ductile shear zones. No known gold deposits are hosted within the LHM.

The geometry of the LHM and related structures (formed very late in the deformation) indicate significant variations to the regional stress field at the time of intrusion. Most 100° trending quartz veins have shallow to moderate SW dips and are simple extension veins with thick bands of quartz, indicating formation by extension orthogonal to the vein wall. However, the formation of stylolitic molybdenite seams in the middle of these veins suggests *shortening* orthogonal to the vein wall after the vein was formed. Calcite-fluorite extension vein arrays trend at about 100° with steep northward dips, but individual veins in the arrays cluster around 060°/70°NW The array geometry indicates sub-horizontal extension perpendicular to the trend of the arrays, which may have formed by shortening from a steep to sub-vertical direction (Figure 5.18).

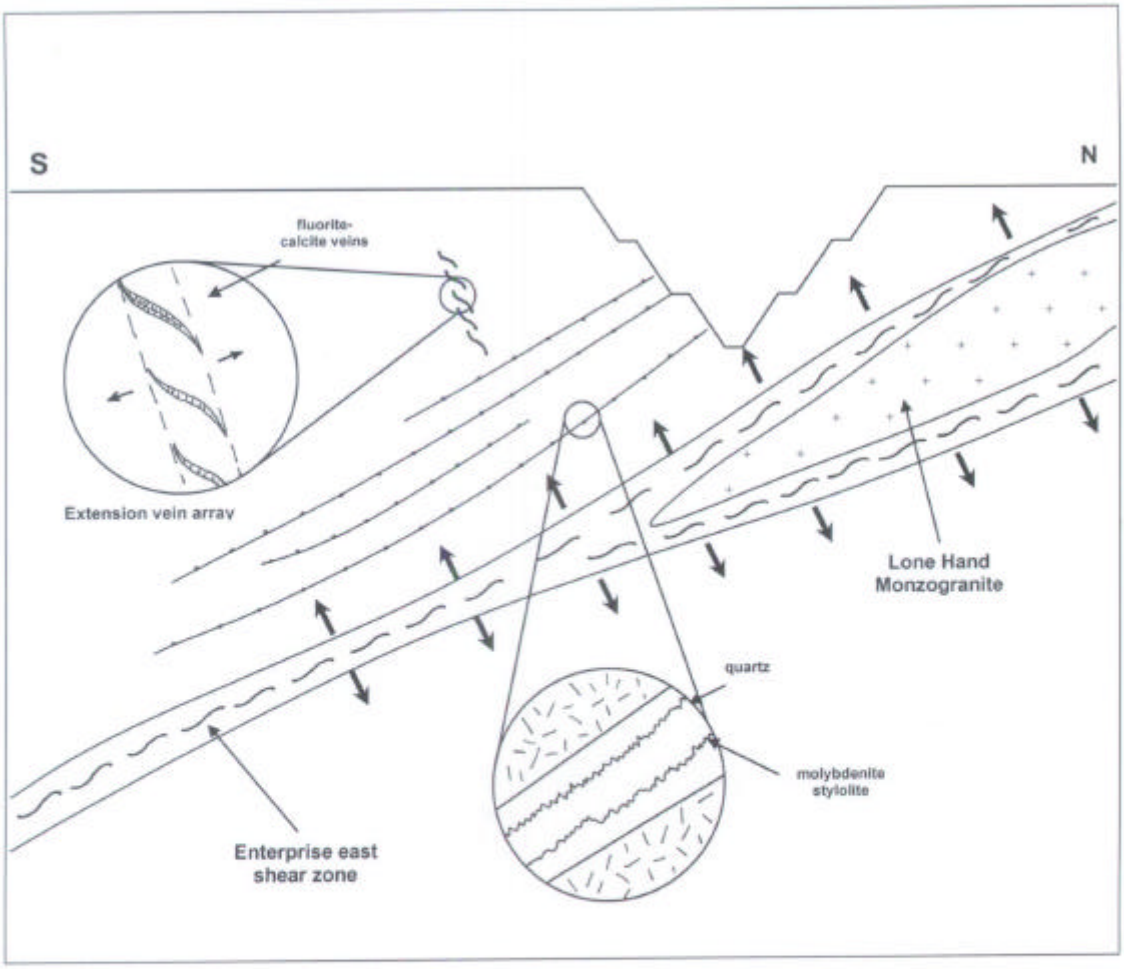

Figure 5.18 – Schematic cross-section showing structural controls on intrusion of the Lone Hand Monzogranite. The granitoid was emplaced into the Enterprise east shear zone and may have re-oriented the local stress field with a sub-vertical principal shortening axis during emplacement. Cross section is looking west.

Intrusion of the LHM into the bedding-parallel Enterprise-east shear zone would have had some forceful effects on the wallrocks and reorientation of bedding to 109°/51°S in the area is evidence of this. This orientation of bedding is sub-parallel to the orientation of quartz veins and calcite fluorite vein arrays and hence the intrusion of the LHM is a likely cause for the formation of stylolitic structures and extension vein arrays with granite-related mineralogy, produced by a local reorientation of the maximum compressive stress.

5.7 MECHANICAL ANALYSIS

The Enterprise fault zone provides information on the nature of the brittle-ductile fault network at a mesoscopic scale. In Chapter 3.4 (p.61) and Chapter 4.5 (p.118), mechanical analyses of regional-scale and macroscopic-scale data sets, were augmented with mesoscopic data from the mines at Zuleika and Ora Banda to assess the kinematics of the major deformation events. Similar relationships of NW-SE trending ductile shear zones and brittle-ductile faults are observed across these two scales. The following mechanical analysis treats brittle-ductile faults specifically at a mesoscopic scale, to compare relationships with the brittle-ductile fault network at macroscopic and regional scales.

5.7.1 Principal structural orientations

As with regional and macroscopic scales, structural data from the Enterprise mine cluster into four principal structural orientations (Figure 5.19). The data show wide scatter for brittle and brittle-ductile faults especially, however tight clusters appear in the cleavage and vein data. In contrast to regional and macroscopic scales, NW-SE trending structures mostly have brittle or brittle-ductile character. The N-S principal orientation is defined by continuous cleavage, and a strong component of brittle and brittle-ductile faults is prominent in this orientation. Northeast-southwest and E-W principal orientations are represented by brittle-ductile faults, with veins forming the most important component of the E-W cluster.

Overprinting relationships

Northwest-southeast trending structures are overprinted by later faults in most exposures (eg. Cashmans Shear Zone), yet the reverse of this relationship is indicated by minor

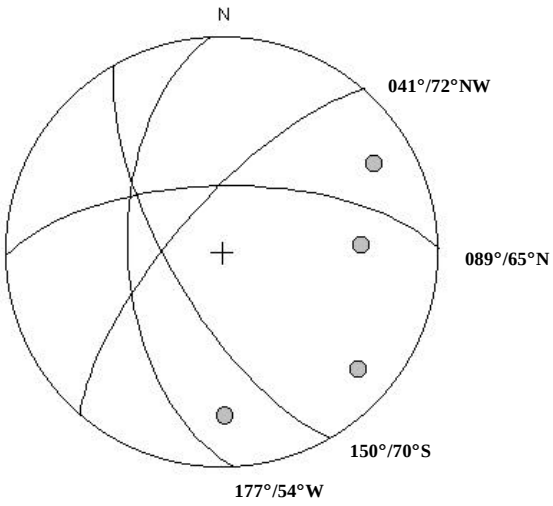

Figure 5.19 – Stereogram showing the four principal structural orientations at the Enterprise mine. Great circles are for the average orientations listed at the bottom of Table 5.1.

Table 5.1 – Principal structural orientations from the Enterprise fault zone, grouped by structural style. Orientations for each structural element are great circle orientations to the major clusters presented on stereograms for each fabric element.

Principal Structural Orientations	**NW-SE**	**N-S**	**NE-SW**	**E-W**
Brittle-ductile faults	137°/60°SW	-	035°/78°NW	079°/79°NW
Brittle faults	161°/81°SW	-	030°/59°NW	088°/69°N
Veins	-	-	-	102°/47°SW
Cleavage	-	177°/54°W	058°/81°NW	-
Average Orientations	**150°/70°SW**	**177°/54°W**	**041°/72°NW**	**089°/65°N**

reactivation. The remaining three principal structural orientations show mutual overprinting in over 100 exposures of cross-cutting relationships recorded from the open-pit. In general N-S structures are slightly earlier than NE-SW and E-W, with the latter orientations forming conjugate structures in most examples. Brittle-ductile faults with a strong ductile component tend to be extensively cross-cut by later brittle-ductile faults with a dominant brittle component. The timing of development in the brittle-ductile fault network therefore appears to favour a progression from early ductile to later brittle.

Fault kinematics from offset and slip lineation data

Fault kinematics were resolved using offset data and fault slip-vector analysis. The majority of brittle-ductile faults at Enterprise are strike-slip faults: from a population of 32 faults studied, the mean plunge of slip vectors is 18° with 88% of readings less than 30°. A test of the consistency of movement-sense in each of the principal structural orientations was conducted on a data set of 55 brittle-ductile faults with about equal numbers of faults studied from each of the four principal structural orientations. Microstructural analysis was used to verify the sense of movement in faults using kinematic indicators, and for determination of S-C fabric relationships (Passchier and Trouw 1996). From these analyses the following general rules apply; N-S and NE-SW faults are right lateral, E-W and NW-SE faults are left-lateral. Displacements are rarely greater than a few metres with a majority of faults having decimetre-scale displacements.

An abundance of brittle faults with well-developed slip lineations in the Enterprise open-pit, provides an opportunity to gain quantitative data on the orientations of the principal shortening directions during the D4 brittle-ductile faulting event. Fault orientation and slip vector data were collected from 32 brittle faults for analysis using the method of Marret and Allmendinger (1990) (Figure 5.20). The method assumes that for a fault produced by brittle failure, a great circle containing the pole to the fault and the slip vector of the fault (the movement plane), also contains the kinematic P and T (shortening and extension) axes of the deformation that produced the fault. One of these axes is located along the great circle halfway between the pole to the fault and the slip vector, and the other at 90° to this axis. The determination of the respective shortening and extension axes requires additional offset and displacement data. Contouring the kinematic axes of a population of faults provides average orientations for the principal incremental strain axes.

The group of 32 brittle faults from Enterprise shows average orientations of P axes at 2°→235°, and 8°→138° for T axes (Figure 5.20). These results suggest an 055° or ENE-WSW directed maximum shortening axis during brittle-faulting.

5.7.2 Summary

The Enterprise fault zone comprises several major brittle-ductile faults in three principal orientations. Earlier NW-SE trending shear zones may have been reactivated during the faulting event. A major sheeted vein system predates the faulting but some vein arrays were emplaced as a result of fault movements. Early veins appear to have acted as preferentially brittle domains since many are highly disrupted by later faults producing cataclasite and breccia. Whereas the E-W trending faults are the most prominent features in the open pit (Map 6, in pocket), N-S trending faults make up the majority of field measurements. The fault groups are similar to those recognised at macroscopic and regional scales, their cross-cutting relationships indicate broadly synchronous development and kinematic analysis implies formation by an ENE-WSW shortening.

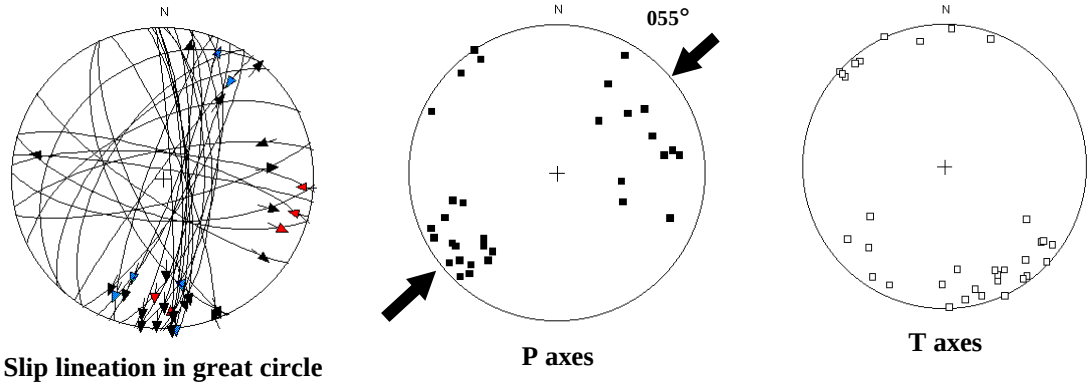

Figure 5.20 – Equal area stereograms of 32 brittle fault planes from Enterprise pit. Kinematic PT (shortening and extension) axes measured from slip lineation data using the method of Marret and Allmendinger (1990). The average orientation of the main clusters for shortening axes is 2°→235° and for the extension axes is 8°→148°. The smaller secondary populations of P and T axes are for NW trending faults and for N-S trending faults with sinistral movement sense. The two populations imply that two separate shortening events have affected the rocks one from 235°/055° and one from 126°/306°. North-south faults have dextral offset in the majority of exposures hence the sinistral offset in the second population is interpreted as reactivation. See text for further explanation.

5.8 GOLD MINERALISATION – ENTERPRISE DEPOSIT

Enterprise gold deposit is a recent discovery in the Ora Banda district with a total resource of 40 tonnes Au. The deposit has characteristics that set it apart from most other Archaean lode gold deposits including stratigraphic control on the geometry of the orebody and complex structural control by a system of interlinked brittle-ductile faults.

5.8.1 Geometry of the mineralised envelope

Total envelope of gold mineralisation

Data on the total envelope of gold mineralisation at Enterprise are derived from diamond and reverse circulation drilling. The detection limit of gold assays is about 0.01 g/T (grams per tonne) Au and the presence of 'gold mineralisation' therefore indicates assays greater than this amount. Gold mineralisation at Enterprise occurred within a tightly constrained, 1.3 km elongate zone that plunges 30° towards 260° and dips steeply north to sub-vertical (Figure 5.21). At the surface the mineralised envelope is 150-200m wide and narrows to 50-60m wide at depth in fresh rock. The width of the envelope at the surface is due to the mobility and subsequent dispersion of gold in the oxidised portion of the weathering profile around brittle-ductile faults that trend towards 260°. The orebody plunges under the Mount Pleasant Sill within a favourable host unit constrained to the south by the SEF and to the north by the NEFZ. A shallow to moderate plunge of the mineralised envelope is produced by the intersection of 080° trending faults within the southwest dipping Enterprise dolerite sill.

Economic envelope of gold mineralisation

For mining purposes, the economic envelope of gold mineralisation is classified as greater than 1.0 g/T Au. Gold is concentrated in linear zones that coincide with brittle-ductile faults (Figure 5.2 p.147, Figure 5.22), hence the economic envelope trends with the controlling structures and host rocks, but with the envelope more tightly constrained adjacent to the faults. Large areas of low-grade gold fill the gaps between the faults, and these areas form part of the total envelope (Figure 5.2 p.147).

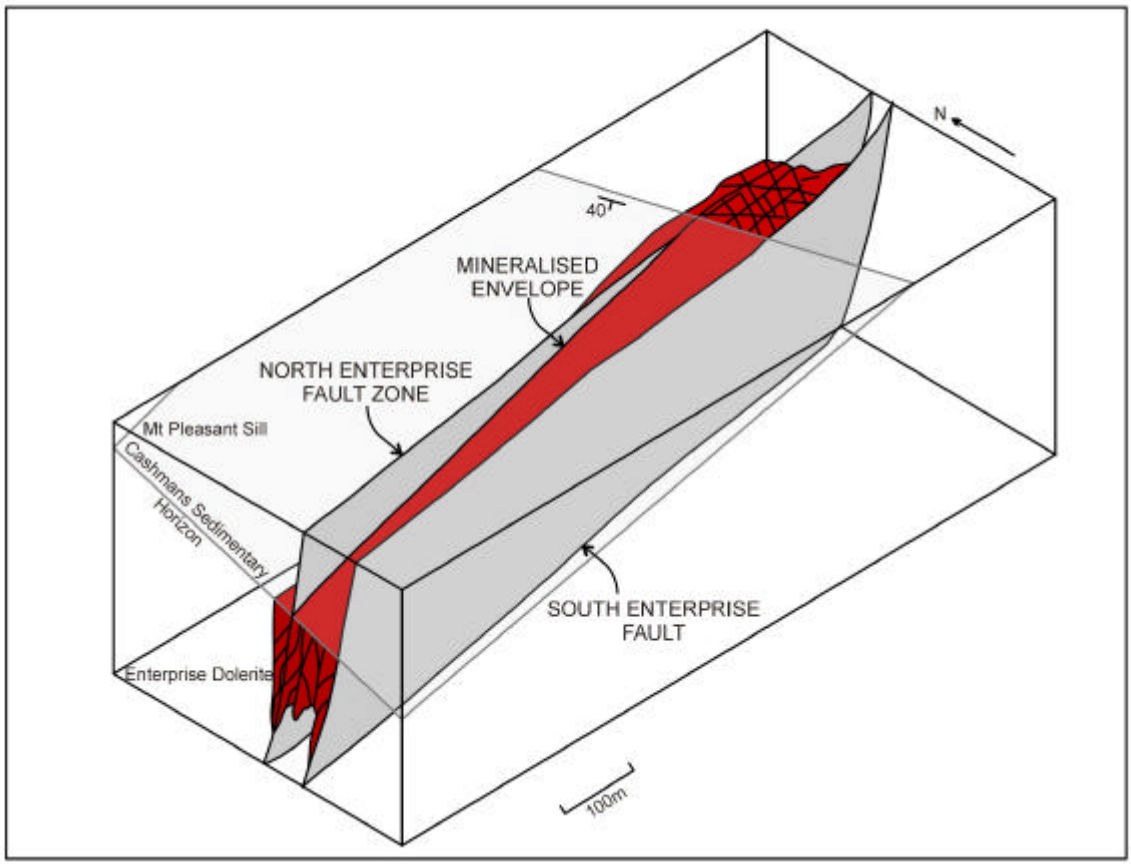

Figure 5.21 – Schematic block diagram illustrating the geometry of the mineralised envelope of the Enterprise deposit. The gold envelope plunges under the Mount Pleasant Sill with the intersection of E-W trending brittle-ductile faults and the base of the Cashmans Sedimentary Horizon. The south Enterprise fault is a boundary to the mineralisation.

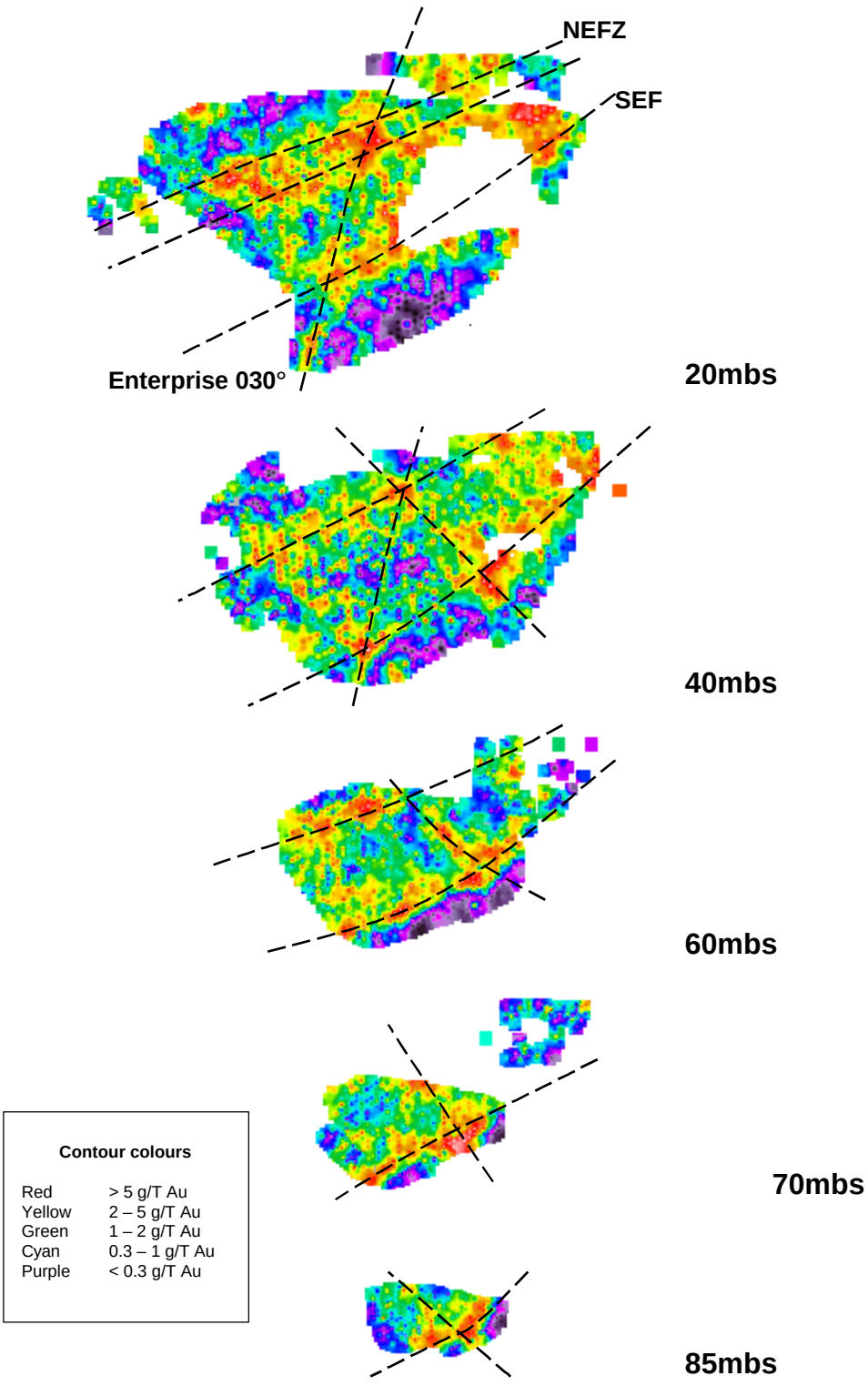

Figure 5.22 – Stacked level plans of contour-imaged grade control assay data from Enterprise open-pit. The data-sets are from 20, 40, 60, 70 and 85 metres below surface (mbs) from top to bottom. Each image is a level plan view that displays strong fault control on grade distribution and illustrates the discontinuous nature of grade distribution along strike but reasonable continuity down-dip in most structures. Colours represent grade ranges. North is up the page

The principal controlling structures are part of a network of fractures that pervades the mineralised envelope and appear to be the main fluid conduit system evinced by the high degree of wallrock alteration in the vicinity of the fractures. Fault planes are significantly smaller than the width of altered rock around them and many zones of the highest strain host lower grade gold than the surrounding halo. Vein control on gold is unclear with many veins yielding sporadic high-grade gold values. Low-grade haloes in the deposit may reflect the weaker influence of veins in relatively undeformed areas.

High-grade ore shoots

High-grade ore shoots at Enterprise are localised in steeply plunging zones that coincide with the intersection lineations of brittle-ductile faults and veins. Intersections of geological structures have long been recognised as zones of structural complexity and sites of preferential mineral deposition. Enhanced gold-grade and structural development occurs at the intersections of different structures with depth continuity. Although planar structures are the primary control on gold, the distribution within any given brittle-ductile fault is variable along strike and at depth (compare southern zone at 420RL with levels above and below from Figure 5.22 p.201). However, the intersection zones with other structures are traceable through the levels of the mine reinforcing the close relationship of gold ore and localised zones of high fracture-density.

5.8.2 Gold mineralisation

Lithological control

Stratigraphically controlled zones of high fracture-density (and high-grade ore shoots) occur at the intersection of E-W trending brittle-ductile faults with the Cashmans Sedimentary Horizon. Although some disruption of the contact sedimentary rocks is common, fracturing and development of high-grade gold ore in the overlying Mount Pleasant Sill is rare with only limited mineralisation of a restricted layer of fine-grained hornblende microgabbro (chilled zone) near the base. The top 20-30m of the Enterprise dolerite is intensely fractured and brecciated around the intersection points of the brittle-ductile faults and the upper contact, forming the main lode of the Enterprise orebody. Coarse-grained lower units of the Enterprise dolerite have a lower density of rock fracture

and hence reduced gold content. However, the Enterprise fault zone extends through the lower units as thin discrete brittle-ductile faults mineralised along the depth of the structures including rare mineralised intersections of the faults in Big Dick Basalt.

Structural control

Brittle-ductile faults, veins and mesofracture arrays are the principal structures that controlled gold mineralisation at Enterprise. The contribution of each structural style to the orebody is variable in different areas but the major control is a series of E-W trending brittle-ductile faults developed over the length of the mineralised envelope. Lithological layering that constrained the upward movement of hydrothermal fluids produced intense mesofracturing of the upper layers of the host unit adjacent to the E-W shear zones which enhanced the permeability of the rock mass and led to focussed flow of gold fluids.

Gold-related alteration zones are located in the wallrocks of many brittle-ductile fault structures. Quartz veins at Enterprise form a system of sheeted subparallel arrays that pervade the mineralised envelope and the areas adjacent to the orebody. Other deposits distant from Enterprise (eg. Whitehaven, Denver City) show similar development of large quartz vein systems in the Enterprise dolerite that may imply a lithological control on the development of these veins. The contribution of quartz veins to the Enterprise orebody is difficult to determine since individual veins are sporadically mineralised, and mineralised quartz veins occur in most orientations further obscuring the vein control on gold (Figure 5.23). Undeformed quartz veins with well-defined alteration haloes are common in the lower units of Enterprise dolerite and appear to have a slightly higher density than in upper zones. However, the total destruction of rock fabric in the most deformed upper parts of the orebody may mask early quartz veins. Spaced cleavages planes defined by films of chlorite or biotite are normally located in mineralised zones with thin quartz-calcite-pyrite veins that abound in areas of strong cleavage development.

Enterprise "feeder zones" and boundary faults

East-west trending ductile and brittle-ductile shear zones at the Enterprise deposit have been described previously as "feeder zones" to hydrothermal alteration and gold mineralisation (Dickie 1995), and ductile fabrics (schistosity, mineral stretch lineations,

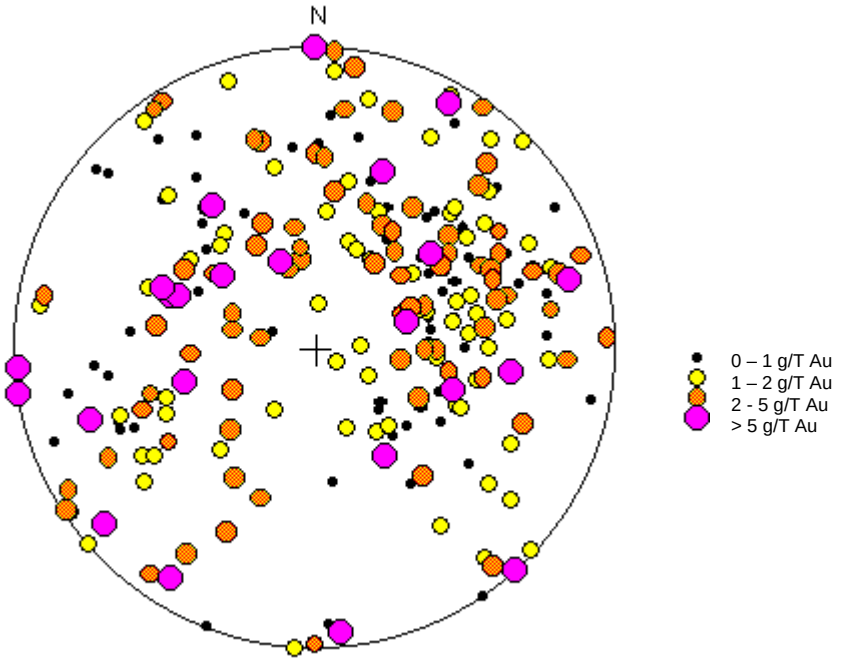

a

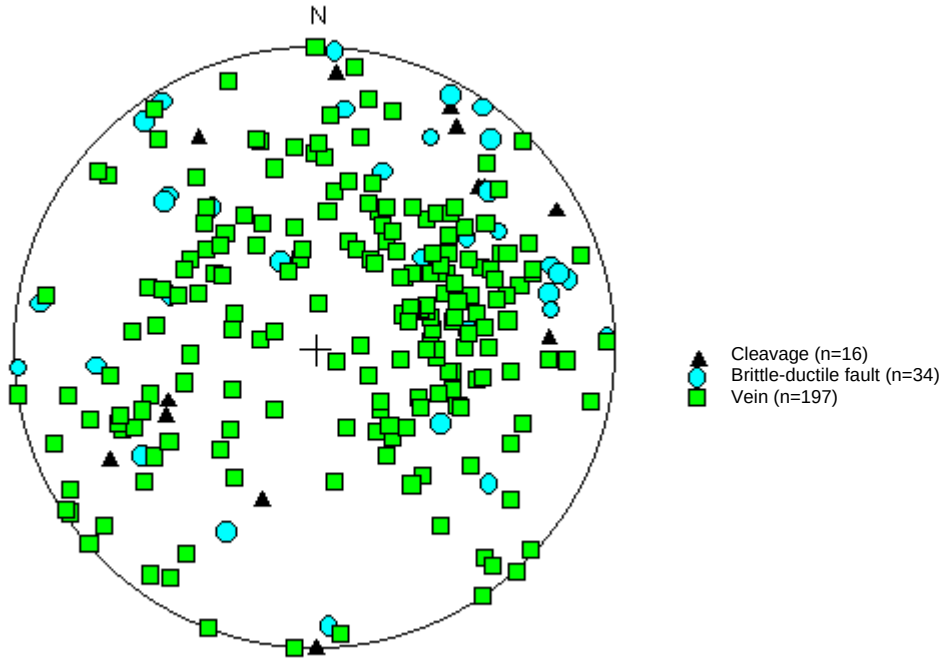

b

Figure 5.23 - **a)** Stereogram showing structural orientation and gold grade for a population of 247 measurements of cleavage, brittle-ductile faults and quartz veins from Enterprise mine. **b)** Stereogram showing distribution of structure types for same data set in (a), includes 107 measurements of quartz veins in Enterprise Stage-1 open-pit from Schiemer (1995). The stereograms do not show conclusive relationships between individual structural orientations and gold grade.

S-C mylonite) were interpreted as “streaming textures” implying development by mechanical flow of fluids (and gases) from the nearby Lone Hand Monzogranite (Dickie 1995). The SEF and NEFZ are clearly the major controls on the geometry of the orebody but the idea that they ‘tap’ a deep source and ‘feed’ an orebody at a shallower level is ambiguous considering the overprinting nature of the granite-related mineralogy.

The brittle-ductile faults are integral parts of the orebod*y* and are at least conduits of fluid-flow during gold mineralisation. The structures display intense metasomatism both within the sheared zone and in the immediate wallrocks indicating a high-degree of fluid-interaction, but are a small subset of the total number of shear zones and may not be the only (or even primary) channels of fluid-flow during gold mineralisation. Shear zones with N-S, NE-SW and NW-SE strikes (Enterprise 030°, Halliday fault, Gimlet structure) were also major fluid channels and are important controls on high-grade ore shoot locations.

The influence from the Lone Hand Monzogranite is manifest in the form of a strong retrograde overprint during which hydrothermal fluids used the brittle-ductile faults as channels during flow. Many of the major faults (NEF, SEF, Halliday Fault, Enterprise 030°) and smaller cross-faults have intense bleaching with muscovite-calcite-fluorite-molybdenite alteration, indicating a granitoid-related fluid source. This alteration overprints the biotite-pyrite gold-related alteration in the faults and slightly lower gold-grades indicate possible remobilisation of gold during the late event.

An interpretation of the SEF and NEFZ as bounding features is unproven, with the exception of the SEF, which appears from drilling to constrain lateral hydrothermal fluid-flow to the hangingwall side of the structure. The NEFZ marks a zone of broad low-grade gold alteration that extends into fractured wallrocks for several tens of metres to the north of that structure.

Ore mineralogy

The dominant ore mineralogy at Enterprise is pyrite and gold with traces of chalcopyrite, pyrrhotite, galena and molybdenite. Pyrite occurs as fine euhedra (0.1-0.5mm) with gangue inclusions and/or coarse-grains lacking internal structure. The coarse grained pyrite varies

from anhedral to euhedral, is usually associated with quartz veins and may be an early phase. Fine-grained pyrite is ubiquitous in gold ore zones and occurs as disseminated crystals, as trails along microfractures or in rare thin veins. Leucoxene has replaced ilmenite or titanomagnetite in ore zones and usually forms complex intergrowths with pyrite. Other sulphide minerals form inclusions in pyrite with the exception of molybdenite, which commonly forms halos on vein margins and stylolitic cleavage within quartz veins. Gold occurs as fine speck inclusions in, or as attachments to, pyrite and leucoxene. Vein-like strips are recorded in chalcopyrite up to 80 *m*m long however most occurrences of gold are associated with pyrite or in silicates close to pyrite grains (Townend 1997a).

Ore Textures

Gold ore at Enterprise has three main textural associations; mesofracture arrays (breccia), brittle-ductile faults and quartz veins. The distribution of the three is variable throughout the deposit depending on depth in the host unit (distance from Cashmans Sedimentary Horizon) and distances from the nearest major fault or shear zone.

Mesofracture arrays (breccias) form the dominant ore texture, which appears as weakly developed jigsaw-style crackle breccia with inter-clast voids defined by quartz-calcite veins. The veins (<5mm thick) have variable geometry from well-defined sets to irregularly distributed lensoid fragments. Mesofracturing has produced a stockwork of veins crossing at a moderate to high angle with relatively little movement or rotation of the rock fragments. Mesofracture veins have infill texture, vuggy interiors and films of chlorite-biotite at the margins. Fine-grained pyrite (<20%) forms halos up to 10mm wide grading into weak disseminations away from the fluid channel whereas biotite alteration is concentrated close to the veins. The veins have boundaries that grade from sharp (fracture-fill) to diffuse where there is significant replacement of the wallrock. Mesofractured ore is best developed in a 10-30m thick fine-grained chilled zone at the top of the Enterprise dolerite (Figure 5.24). Some of the zones have small areas of ≈10% pyrite that are chlorite-dominated with only weak biotite alteration in an overall zone of intensely mineralised rock. Pervasive biotite alteration and disseminated-pyrite (up to 40%) occur in the surrounding rock over 40-50m. Intense breccia zones in the quartz dolerite unit of Enterprise dolerite are typified by small eyelets of blue strained quartz in zones of markedly higher silicification and intense shearing. Relict ophitic texture may be well

Enterprise - diamond drillhole ORBD12

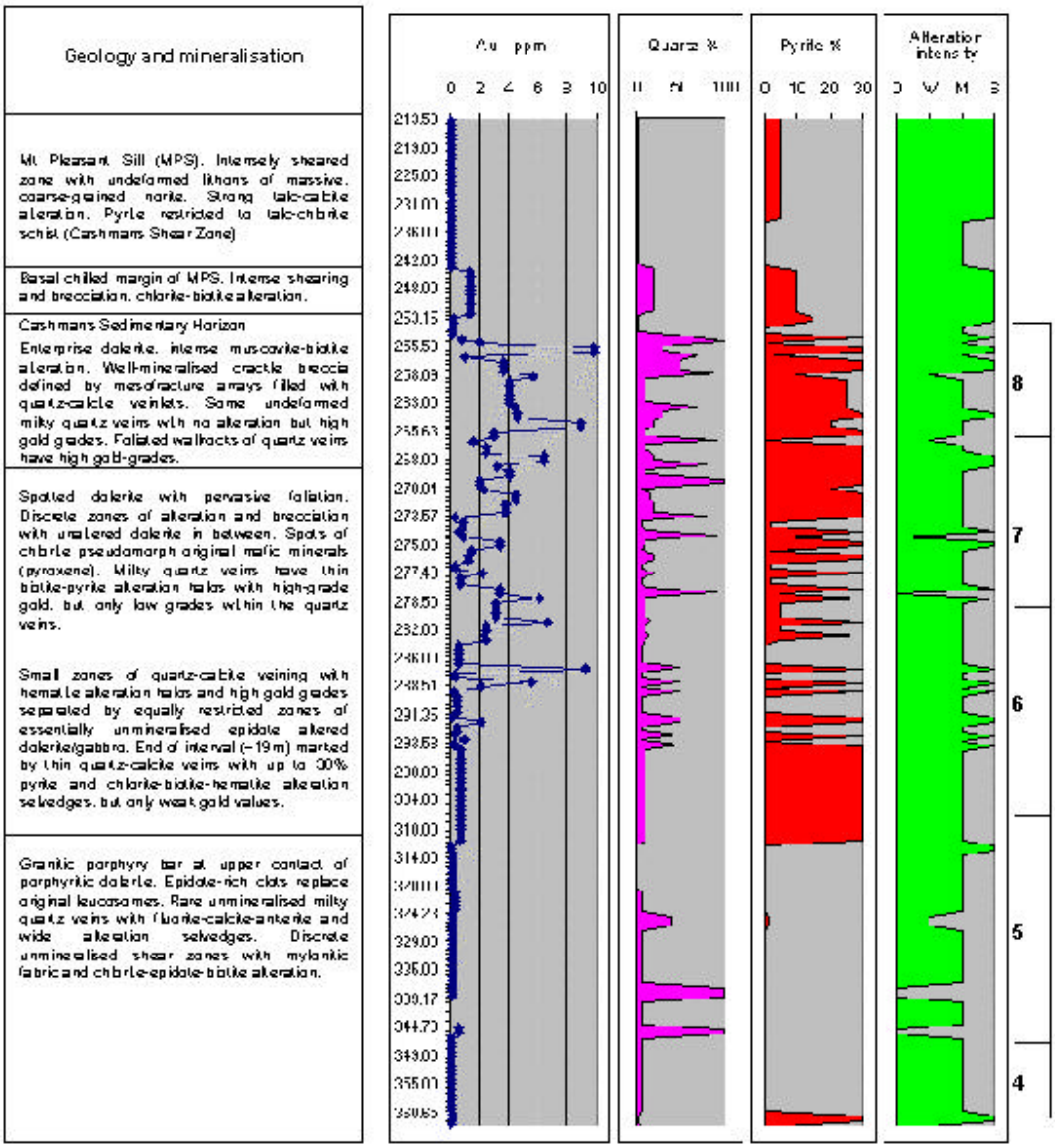

Figure 5.24 - Graphic presentation of diamond drillhole ORBD12 showing geology, Au (ppm), %quartz veining, % pyrite and alteration intensity. Depth downhole in metres at the vertical margin of the Au graph. ORBD12 was drilled at –60° towards 360° and intersects the Enterprise dolerite at approximately 90 degrees, hence downhole widths are greater than true widths. Numbers against the right-hand margin indicate units in the Enterprise dolerite sill.

preserved with biotite or chlorite intergrown with quartz. Most zones of mesofracturing are in the vicinity of a fault or shear zone, and in the upper contact area of the host unit.

In brittle-ductile faults, localised ore zones occur in and around the faults along strike and down-dip, and most fault-related lodes are intensely bleached with brittle-ductile deformation fabrics and variable quartz vein textures. Mill breccia is common in the largest faults with clasts of siliceous altered dolerite and patches of finely crystalline quartz containing large (up to 10cm) angular to rounded fragments of milky quartz. Breccia clasts are of two types; siliceous, light green-grey coloured containing a shear foliation defined by aligned bright green chlorite and pyrite trails, and dark green clasts with intense chlorite alteration. Brittle-ductile faults may have a high proportion of very fine-grained biotite in the groundmass and wallrocks with bright green chlorite stretched and aligned defining a pervasive foliation. Pyrite occurs as veins and disseminations throughout. Slivers of bright green and dark green chlorite contrast with light grey coloured siliceous groundmass minerals that are totally replaced by white-mica (muscovite), calcite and albite. In zones with preserved igneous textures, leucoxene appears buff to pink coloured in the most altered zones but usually retains skeletal forms except near ductile shear zones where it is stretched into parallelism with the foliation. Interlocking chlorite and biotite +/-albite? display rare preservation of original ophitic textures after actinolite-plagioclase.

The deeper parts of the deposit are quartz vein dominated with markedly less faulting and fracturing indicating a transition into the coarse-grained parts of the host unit. The upper ore zones grade downward into variably silicified epidote altered dolerite and gabbro. Epidote alteration is patch-textured with spots of epidote in some cases replacing original leucosomes of quartzo-feldspathic material. Epidote patches are affected by brecciation and shearing, and some of these may be hydrothermal in origin. The quartz veins are typically simple crack-seal veins with thick (≈20mm) bands of crystalline quartz and thin alteration haloes of biotite-pyrite-calcite. Localised gold-ore zones occur where large quartz veins have been emplaced into zones of schistosity in the wallrocks. Shearing is most intense close to the quartz vein with biotite and fine-grained pyrite trails defining the planar fabric. Further into the wall of the vein the rocks are intensely mesofractured with cross-cutting thin quartz-calcite veins. Original crystals of pyroxene were regionally metamorphosed to actinolite and are now hydrothermally altered to chlorite with patchy texture. Large chlorite

spots are commonly stretched (flattened) in the plane of the foliation with cores of actinolite.

Wallrock alteration

A distinct series of alteration zones is developed at Enterprise that extends into the wallrocks past the limits of the gold envelope. The alteration zonation from distal to proximal is chlorite-calcite, biotite-pyrite, mica-pyrite-carbonate and mica-pyrite-gold (Figure 5.25). Mica may be either muscovite or biotite, however muscovite is more restricted in distribution compared to biotite, occurring closer to the host structures. Chlorite-calcite forms a 400m x 1500m envelope parallel to the main shear zones, however the alteration zone is poorly constrained laterally and may be significantly wider than depicted in Figure 5.25. A wide envelope of biotite-pyrite alteration is overprinted by muscovite-ankerite and mica-pyrite-gold haloes that are restricted to the host shear zones. Large areas of low grade gold within the orebody are typical in chlorite-epidote rich areas. Epidote-hematite forms a distal envelope with some epidote predating the gold mineralising event. Samples of gold ore are typically intensely muscovite altered with total replacement of the rock fabric.

Quartz veins are ubiquitous in the Enterprise deposit, but the width of vein alteration haloes demonstrates the subordinate nature of these structures as a control on gold with restricted infiltration of fluids into the surrounding rocks (Figure 5.26). Assessment of the veins in Enterprise open pit and diamond drill core (Chapter 5.3.6 p.175) illustrates the common occurrence of quartz veins sub-parallel to zones of foliation and schistosity and the relative paucity of veins that cross-cut schistosity. Layers of minerals parallel to the wall of a vein may inhibit the infiltration of fluids into the surrounding wallrocks and this may account for the low ratio of alteration halo-width to vein-width.

5.8.3 Summary

Ore textures indicate that the structures hosting gold were formed during the mineralising event, in which case gold mineralisation is epigenetic and was synchronous with deformation. The number of economically mineralised structures at Enterprise is a small subset of the total number of faults that are mapped in the open-pit. Factors that led to gold

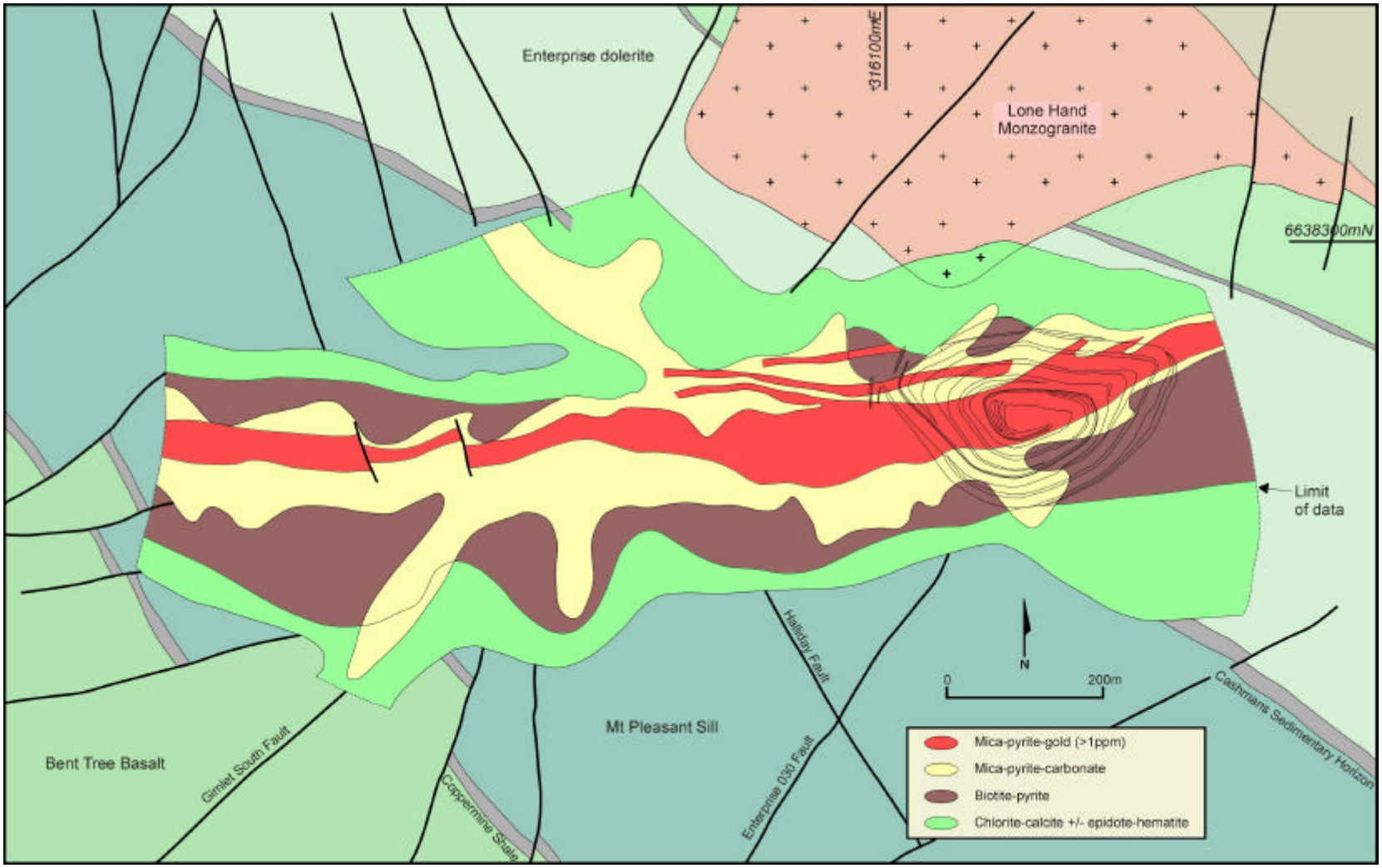

Figure 5.25 – Alteration zonation of the Enterprise deposit. The gold alteration zones map out the distribution of faults and show the dominant E-W control with subsidiary NW-SE and NE-SW faults.

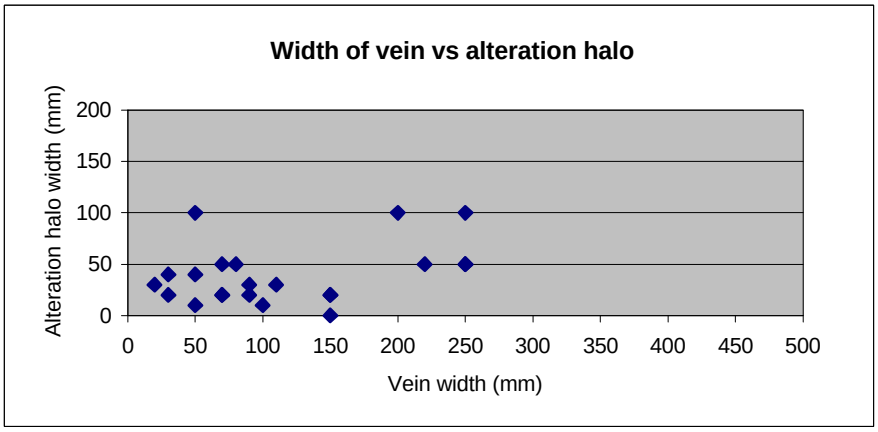

Figure 5.26 – Graph of 25 veins with alteration haloes measured from Enterprise open pit. Alteration zones consist of mostly biotite or chlorite with varying amounts of pyrite. The graph shows a distinct trend of alteration haloes being significantly thinner than the host structure. Width ratios of alteration halo to vein average 0.5 : 1. This relationship contrasts with that observed for shear / breccia zones at Slippery Gimlet (Figure 4.22).

deposition in some structures and not others include chemical affinity of the host rocks, contrasts in tensile strength, orientation of the fracture with respect to the regional stress field and local anisotropy in the form of rheologic layering and brittle-ductile fault bends and terminations.

5.9 DISCUSSION

The Enterprise fault zone shows the nature of the brittle-ductile fault network at a mesoscopic scale. A wide diversity of structural styles from brittle to ductile is common, with most structures displaying a combination of brittle and ductile fabrics. These styles may include textures that are more commonly associated with ductile shear zones (mylonite series) but their scale of development and orientations preclude these structures from being related to major regional ductile deformation events. Some features of the Enterprise fault zone may not be representative of the regional brittle-ductile fault network since the Enterprise area is significantly influenced by the intrusion of the Lone Hand Monzogranite. Well progressed recovery of deformation fabrics and granitoid-related mineralogy are characteristics that are exclusive to fault zones developed in proximity to late granitoids. However, the development of ductile and brittle fabrics intimately associated in the same fault is a characteristic of the brittle-ductile fault network, and in areas distant from

granitoids, the preservation of strong intracrystalline deformation fabrics with a lesser degree of recovery might be expected.

The detailed fabrics of mesoscopic structures from the Enterprise fault zone show principal structural orientations on mesoscopic and microscopic scales similar to those recognised on macroscopic and regional scales. This factor indicates that the rock fabrics at the outcrop reveal information about regional deformation events and not simply local variations in the regional stress field.

Gold distribution is primarily controlled by brittle-ductile faults at a mesoscopic scale. The faults at the Enterprise mine were the main conduits of the mineralising fluids. Enhanced fluid-flow occurred through local areas of high density fracturing to produce high-grade ore shoots. This relationship between high-density fracturing and gold distribution is similar to that observed on regional and macroscopic scales. The system of sheeted quartz veins may have been generated with early ductile shearing on the Cashmans and Enterprise east shear zones, but gold-related alteration halos around many veins indicate that these veins were formed during gold mineralisation. Brittle-ductile fault movements mostly appear to postdate vein formation, however that part of the Type-II vein generation with biotite-pyrite alteration haloes was synchronous with faulting and therefore an integral part of the fault network.

The location of the gross envelope of mineralisation at a lithological contact may be related to significant differences in tensile rock strength and therefore fracture density. A similar mechanism for gold mineralisation has been proposed at a regional scale (Walshe 1998), with lithological layering (Black Flag Group) acting as a regional fluid-pressure seal. The Enterprise deposit may be a mesoscopic-scale analogue of this model, with the Cashmans Sedimentary Horizon / Mount Pleasant Sill acting as a local seal with overpressuring at this contact.

6 STRUCTURAL CONTROLS ON GOLD MINERALISATION

6.1 INTRODUCTION

Gold deposits with greater than 2kg recorded production from the Siberia, Ora Banda, Grants Patch and Mount Pleasant mining districts (Figure 6.1) have a total gold endowment (mined, plus resource) of 203 tonnes which represents about 11% of total gold production of the Menzies-Kambalda belt. The gold deposits are concentrated in mining centres at Siberia, Ora Banda, Grants Patch and Mount Pleasant.

Recent studies have shown that gold deposits in the southern Eastern Goldfields Province are structurally controlled (eg. Vearncombe *et al.* 1989; Witt 1993c), and the close association between gold mineralisation and structure has been recognised since the early part of this century. In this chapter, the relationships between structure and gold mineralisation in the Ora Banda and Zuleika districts are investigated with special emphasis on the geometry of gold distribution.

6.2 REGIONAL CONTROLS ON GOLD MINERALISATION

6.2.1 Introduction

In the north Kalgoorlie region each mining centre has one or two large gold deposits with many peripheral ‘satellite’ deposits that mostly have small tonnages and shallow workings. Mining centres include Siberia, Ora Banda, Grants Patch, Mount Pleasant, Zuleika, Carbine, Broad Arrow, Bardoc and Menzies.

In the Ora Banda and Mount Pleasant centres, there are several large gold deposits (>30 tonnes) and many medium-size deposits (>8 tonnes) in each area with abundant peripheral deposits in between, evident from shafts and old workings. The gold deposits from Ora Banda to Mount Pleasant have similar host units (Ora Banda mafic sequence), structural style, mineralisation style and alteration and as such can be studied in further detail as a group of related deposits.

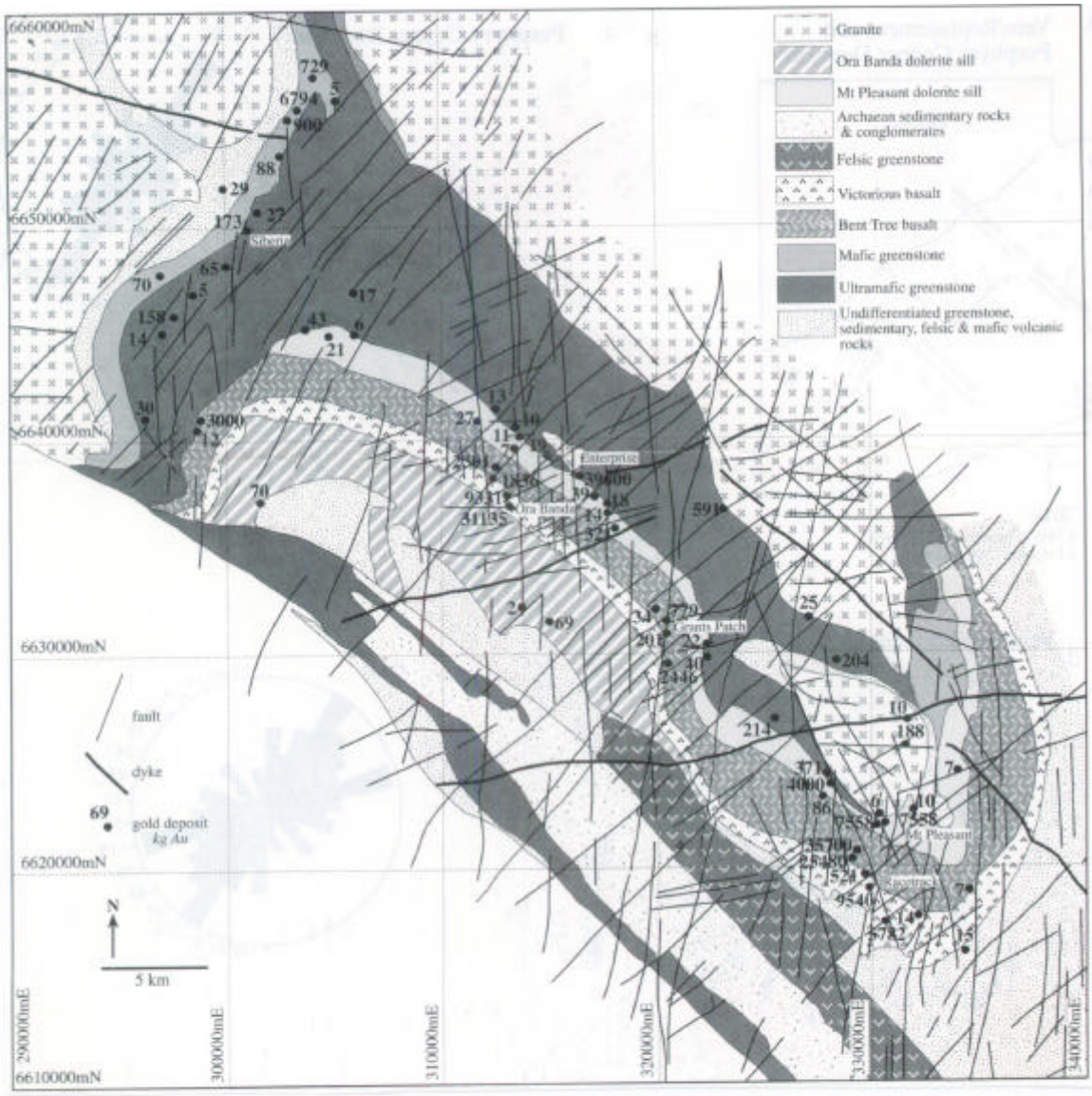

Figure 6.1 – Map of the geology and location of 66 gold mines in the Siberia – Mount Pleasant mining district with greater than 2kg recorded production (from Vearncombe and Vearncombe 1999).

6.2.2 Gold mineralisation – Zuleika Shear Zone

In the Zuleika area, gold orebodies trend NW-SE controlled by the location of the Zuleika Shear Zone. High-grade ore shoots and minor ore-bearing structures are controlled by the intersection of ductile shear zones and brittle-ductile faults with the shear zone. Analysis of individual faults, shear zones and quartz veins indicates that NE-SW and N-S trending cross structures are important orientations, yet the trends of mineralised envelopes at each of the deposits are largely sub-parallel to the NW-SE trend of the shear zone.

Layer-parallel ductile shear zones are not major hosts for gold deposits in the north Kalgoorlie region yet significant deposits are located at Zuleika (Figure 3.5 p.38). Problems exist for the mechanical formation of these deposits in that most gold deposits in the region are hosted in late tectonic brittle-ductile faults that formed with an ENE-WSW maximum shortening direction. Under such conditions NW-SE trending ductile shear zones are mis-oriented for reactivation and since oriented at a high angle to the shortening direction, are unlikely to dilate unless P_f is high.

Similar problems were discussed for the main lodes at the Golden Mile deposit, Kalgoorlie by Scott (1997), who inferred maintenance of high fluid pressures to keep the structures active during gold mineralisation. This alternative suits gold lodes that are texturally consistent with formation by a component of high fluid-pressure (breccia, vein deposits), but the ductile shear zones at Zuleika contain gold-related alteration mineralogy and gross orebody geometry that formed primarily during ductile shearing (see also Craw *et al*. 1999).

Possible solutions to this problem include two-stage gold deposition, or a protracted period of gold mineralisation that persisted through the deformation. A significant complicating factor for the Zuleika deposits is that late brittle-ductile structures contain retrograde metamorphic assemblages in the alteration halos of gold lodes (Figure 3.16a-b p.57), whereas in the NW-SE ductile shear zones, gold-related biotite alteration defines the fabric of the shear zone (Figure 3.11g p.47). An explanation involving overprinting is tenable if gold mineralisation is maintained during the early ductile shearing and continued through later brittle-ductile faulting events synchronous with late-orogenic uplift and metamorphism as described by Witt *et al*. (1997).

6.2.3 Gold mineralisation – Ora Banda mafic sequence

Spatial distribution analysis of gold deposits from Siberia to Mt Pleasant

The spatial distribution of 66 mines with greater than 2kg production in the Siberia to Mount Pleasant area was assessed in terms of deposit location and gold endowment by Vearncombe and Vearncombe (1999), who used historic production data and current mining resource/reserves statistics compiled for this study (Figure 6.1 p.214). The technique of assessment is termed Fry Analysis and is based on autocorrelation. The spatial distribution of a random series of point data was originally used to determine strain in deformed rocks (Fry 1979). Application of this technique to the location of gold deposits (or any point data eg. grade control assays) allows anisotropy to be distinguished from data that may appear to be randomly distributed.

A list of the gold deposits and their gold endowment values is given in Appendix A3 (p.370) and the spatial distribution is shown in Figure 6.2. Gold deposits are located in the mining districts that are about 10 km apart geographically. Fry analysis has been used to assess the deposits in three endowment categories >50kg, >400kg and >900kg of gold. The total data set displays a dominant NW-SE trend and indicates the regional bias controlled by deposit location within the NW-SE trending stratigraphic sequence. For deposits of >50kg Au, wide bands of anisotropy appear in the data at roughly 10 km spacing (Figure 6.2). As higher values for endowment are assessed the anisotropy shows clustering in 10 km spaced bands. An interesting feature of the distribution of the data points is the strong N-S trend of larger gold deposits indicating that in the mine corridors gold deposits stack in a N-S orientation primarily in NE-SW trending faults (Figure 6.2).

The geometry of gold distribution is coincident with the spacing of structural zones demonstrated in Chapter 4.7 (p.124), and illustrates a positive correlation between the location of zones of high fracture-density and gold mineralisation, at a regional-scale. A regular distribution of structure implies regional-scale deformation processes, and when coupled with coincident gold mineralisation, suggests that deformation and gold mineralisation are closely associated genetically. The belt of gold deposits in the Ora Banda Domain is located at least 7 km from the nearest major ductile shear zone which has negative implications for the interpretation of linked regional ductile shear zones as a

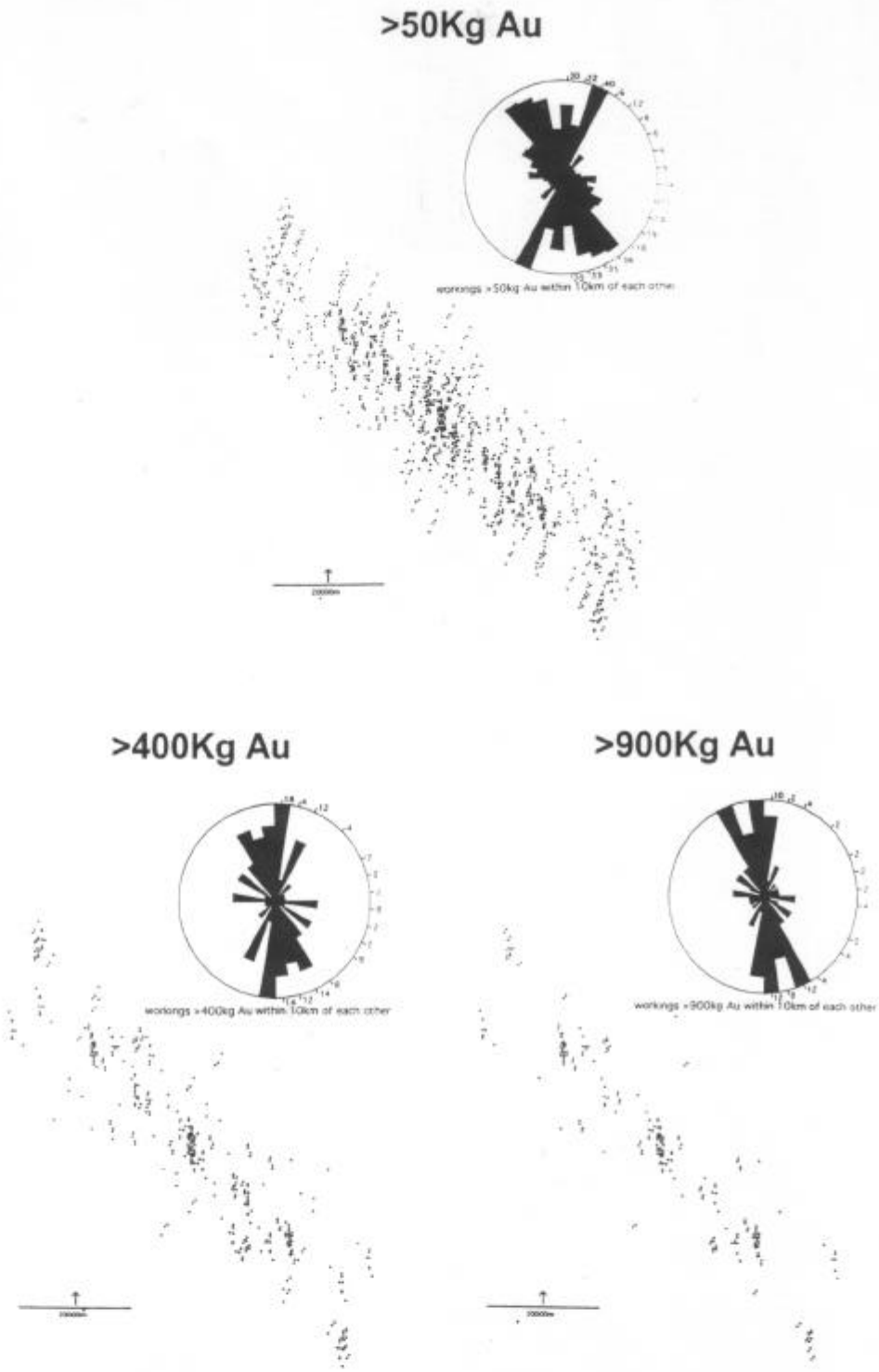

Figure 6.2 – Diagrams showing results of Fry analysis of the location of 66 gold deposits in the Siberia – Mt Pleasant belt, from Vearncombe (1988b). Analysis of deposits with >50Kg, >400kg and >900kg Au, was done using SpaDis spatial analysis software.

first order crustal-scale gold mineralising system (Libby *et al*. 1990; Vearncombe *et al*. 1989).

The interpretation of within-greenstone-belt ductile shear zones as crustal or terrane-scale boundary features is equivocal, as are suggestions that the shear zones form crustal-scale fluid pathways for gold mineralising fluids (Vearncombe 1998a). Regional ductile shear zones of interpreted crustal-scale (Goleby *et al.* 1993) are located at granite-greenstone contacts (eg. Ida Fault) but reach the mid-lower crust only and are not proven as crustal-scale. These shear zones are characterised by a lack of large gold deposits compared to intervening areas (with the exception of the Paddington mine in the Bardoc Tectonic Zone) and hence their role as possible deeply tapping fluid conduits during gold mineralisation is unlikely. In the Ora Banda Domain, gold mineralisation is controlled by mesoscopic (mine-corridor) scale structures that occur in groups with regular regional distribution (Chapter 3.3.3 p.53).

The distance of Ora Banda from the nearest within-greenstone ductile shear zone precludes comment about the relationships of specific faults with regional shear zones, but mesoscopic brittle-ductile faults in the Zuleika area that form part of the domain-wide fault network clearly cross-cut the shear zone. They are not subsidiary shear zones or lower order structures related to the ductile shear zone movements and hence models that propose fluid transfer from first order shear zones to lower order structures with subsequent gold mineralisation may be invalidated.

Relationships between structural orientation and gold

The data set of 66 mines between Siberia and Mount Pleasant includes measurements of the orientation of the main ore-bearing structures at each deposit (Table A1.1 p.371). Although several structural orientations are commonly developed in any one deposit, the gross trend of the mineralised envelope generally is controlled by one dominant structure with minor structures producing local complexities in the orebody.

Analysis of the structural orientation of gold deposits in a region is another method for determining the regional-scale structural controls on gold mineralisation and for identifying common trends between gold deposits that are apparently unrelated spatially.

The trends of the major controlling structures of the gold deposits, plotted together with gold endowment (Figure 6.3) shows a distinct cluster of medium to large gold deposits (i.e. > 8 tonnes Au) at about 060° and 090°. Smaller gold deposits are scattered around the stereogram forming broad clusters in each of the four principal structural orientations identified previously (Figure 3.23 p.70, Figure 4.16 p.120 and Figure 5.19 p.196), which confirms the coincidence of structure and gold mineralisation. A regular orientation of medium to large gold deposits has important implications for related processes of gold mineralisation and structural development in the Ora Banda Domain.

An assessment of the subsidiary structures indicates that 020° trending structures are the most common subsidiary control on gold mineralisation in the largest deposits (eg. Quarters deposit 020°, Forster *et al.*1997). East-west and ENE-WSW trending mineralised envelopes with subsidiary NNE-SSW structures are directly correlated with large gold deposits in the Siberia - Mount Pleasant area. The total endowment figures for deposits in each of the four principal structural orientations confirm the same relationship;

ENE-WSW	- 136 tonnes Au,	or 67% of total gold endowment
E-W	- 49 tonnes Au,	or 24% of total gold endowment
NW-SE	- 12 tonnes Au,	or 6% of total gold endowment
N-S	- 5 tonnes Au,	or 3% of total gold endowment

Of the 66 mines in the Siberia - Mount Pleasant area, ENE-WSW and E-W trending brittle-ductile faults account for 91% of the total gold endowment. This relationship implies that fluid-flow and subsequent fluid-wallrock interaction, were enhanced in brittle-ductile structures developed in ENE-WSW and E-W orientations due to structurally induced permeability. Aeromagnetic interpretation (Figure 3.2 p.31) and field observations confirm a high frequency of fractures developed in these orientations.

Discussion

The development of the largest gold deposits in two closely related orientations is significant. The gold deposits are from mining centres that are widely separated with no obvious physical links, and the presence of similarly oriented large and small gold deposits is strong evidence of regional structural controls during gold mineralisation. Gold deposits in the Siberia to Mount Pleasant district can be viewed as components of the same

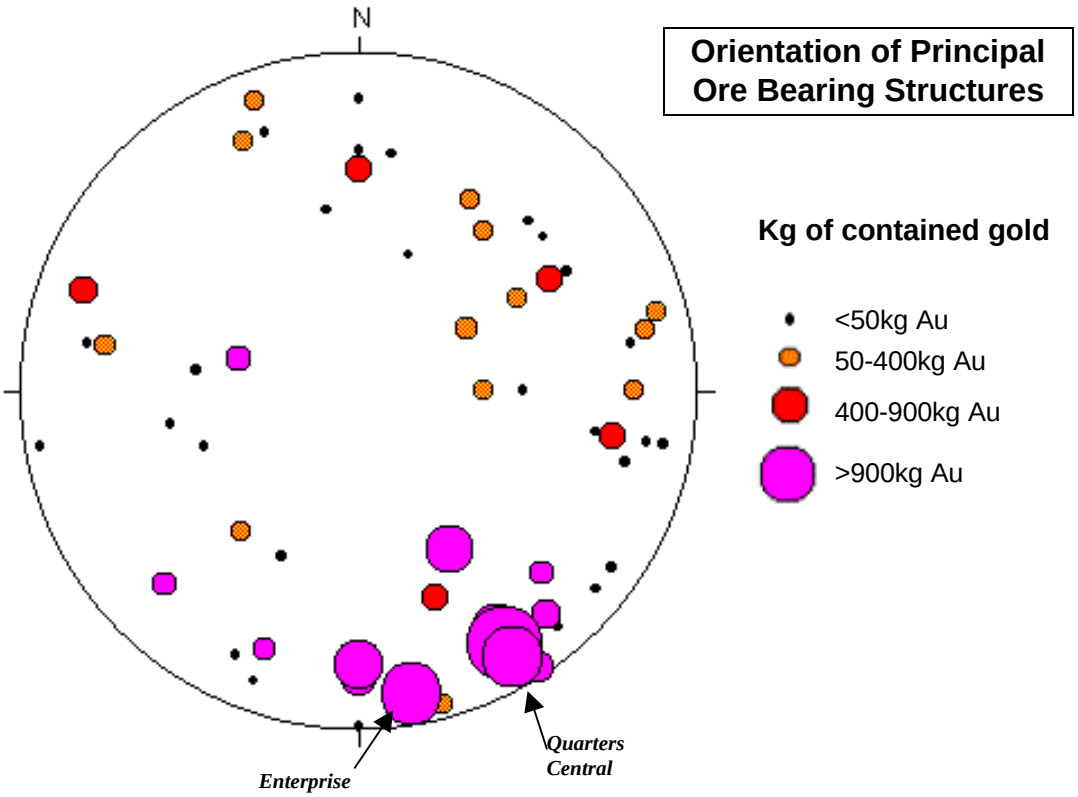

Figure 6.3 – Schematic stereogram showing orientation of the principal ore-bearing structures and gold endowment (kg) for 66 mines in the Siberia – Mount Pleasant region. The largest gold deposits are hosted in NE and EW trending structures. Colored circles represent poles to planes, the size of each deposit is indicated by the colour and size of pole.

gold mineralising system active during the development of the interlinked brittle-ductile fault network.

A model for structural development that involves shortening at a high angle to bedding accompanied by secondary tensile layer-parallel stress in Chapter 4.7.3 (p.126), predicts widespread fracturing orthogonal to layering and attraction of chemically mobile material into the fractures, in spatially-periodic high fracture-density zones. A mean strike of 330° for layering in the Ora Banda Domain with layer-perpendicular fractures at about 060°, is consistent with dominant orientations at 060° to 090° for medium to large gold deposits, and provides a predictive tool for exploration.

6.3 FRACTAL GEOMETRY OF STRUCTURE AND GOLD MINERALISATION

Fractal geometry is similar to a concept in structural geology where the study of minor structures in rocks allows determination of the geometry and orientation of major structures, familiarly known as ‘Pumpelly’s rule’ after Pumpelly *et al.* (1894). Although many applications of fractals are purely mathematical, the idea emphasises a fundamental aspect of natural geological features. The concept of fractals was proposed by Mandelbrot (1983) as a way of explaining problems of scale in nature. A fractal (short for fractional dimension) is a rough or fragmented geometric shape that can be subdivided in parts, each of which is approximately a reduced-size copy of the whole. Alternatively, a fractal is any curve or surface whose geometry is independent of scale. The term ‘fractal’ as used in this study refers to the geometry and distribution of structure and gold mineralisation and implies that both of these geological features are similar across several scales of observation.

6.3.1 Structure

Ductile shear zones

At a regional-scale, ductile shear zones are NNW-SSE trending greenstone-belt wide features that may be hundreds of kilometres long and several kilometres wide (Chapter 3.3 p.32). Although regional-scale ductile shear zones are widely spaced in the Ora Banda Domain, many parallel features are developed with greater frequency at the minescale and

mesoscopic scale. Mesoscopic ductile shear zones are developed primarily at lithological contacts between layers of variable grain-size or within metasedimentary rocks at major rock unit contacts, the positions of which usually represent sharp changes in rock competence.

The Zuleika Shear Zone trends sub-parallel to rock contacts generally, but cross-cuts some contacts to the northwest of Ora Banda mostly as a result of the shear zone overprinting a pre-existing macroscopic structure (Kurrawang Syncline). Strain in the Zuleika Shear Zone is distributed in a markedly heterogeneous fashion with thin anastomosing zones of intense non-coaxial ductile shear separated by lens-shaped lithons of rock exhibiting flattening strains at the margins and a gradual decrease of strain towards the interior of these bodies. This heterogeneous distribution of strain results in a characteristic geometry that exists on several scales (Figure 6.4):

Regional scale - regional maps of the Kalgoorlie Terrane (eg. Swager *et al.* 1990) show the distribution of terrane and domain boundary shear zones as anastomosing structures that enclose lens-shaped pods of greenstone sequences (tectonostratigraphic domains). The ductile shear zones are localised at greenstone contacts with regional-scale granitoids that are analogous to rigid porphyroblasts on a grand scale, with areas like the weakly deformed Ora Banda Domain occupying a zone that may be regional-scale strain-shadow
Macroscopic scale - pit mapping and drilling along the Zuleika Shear Zone show that high-magnesium basalt is distributed as lens-shaped boudins of several hundred metres length. Similar lens-shape geometry of late-tectonic felsic porphyry is recorded in the Porphyry and Anthill open-pits.
Mesoscale - individual shear zones anastomose around less-deformed lens-shaped pods of wallrock (eg. Bullant and Wattlebird mines).
Micro-scale - thin section studies of sheared rock from the Zuleika Shear Zone show mica films forming anastomosing foliations that surround aggregates of feldspar and quartz.

Interlinked brittle-ductile fault networks

A regional-scale brittle-ductile fault network of at least domain-wide influence is identified from aeromagnetic imagery (Chapter 3.3.3 p.53). Three of the four principal structural orientations that make up the fault network are interpreted as synchronous on

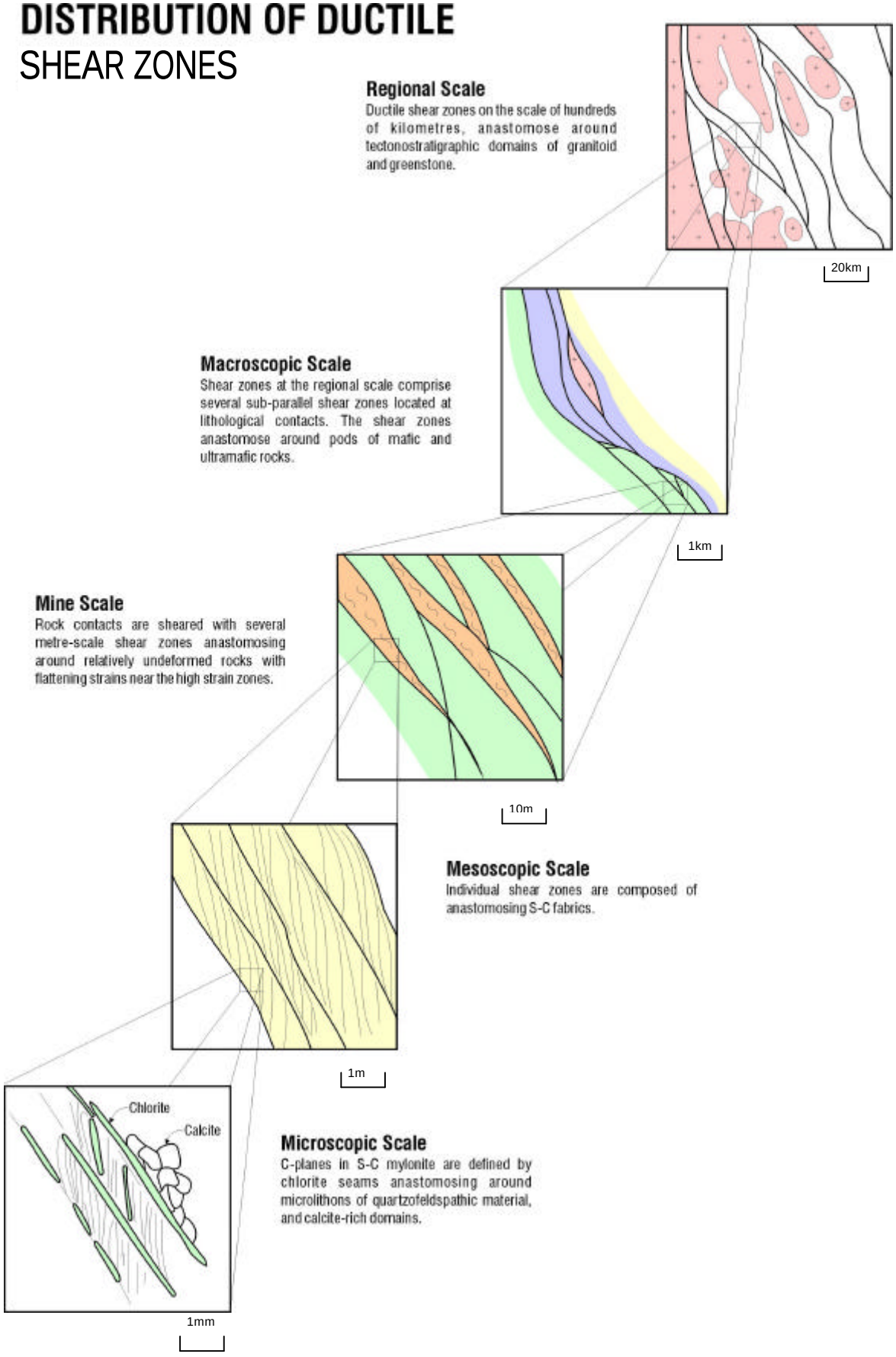

Figure 6.4 – Fractal distribution of ductile shear zones in the Ora Banda Domain. Maps at each scale are reproduced from published regional maps, open-pit mapping and hand specimen / thin section sketches. In each map north is up the page.

macroscopic and mesoscopic scales (Chapter 4 p.86, Chapter 5 p.145) with a similar geometry and distribution across several scales of observation (Figure 6.5). Brittle-ductile faults that make up the network are rarely single structures, but are zones of sub-parallel brittle-ductile faults, or in some cases small network structures on the scale of hundreds of metres (eg. Enterprise, Slippery Gimlet, Racetrack). Although these examples are from structural zones, other brittle-ductile faults in the intervening areas are aligned along the principal structural orientations with local complexities at fault intersections in the other orientations but with less intensity of development. At the scale of a local fault zone individual structures enclose pods of relatively undeformed rock. Mesoscopic exposures of the brittle-ductile faults also display thin zones of simple shear in one or more of the three principal orientations surrounding lithons of weakly deformed rock. Alternatively, in areas where brittle deformation is dominant (dilational jogs, quartz vein arrays), hand specimen samples display pervasive mesofracturing as interlinked networks of millimetre scale fractures with quartz-calcite infill. The fracture network surrounds undeformed slices of rock usually with a high degree of alteration in the wallrocks of the fractures.

High fracture-density zones

In the regional brittle-ductile fault network, high fracture-density zones occur at the intersection of brittle-ductile faults in one or more of the principal structural orientations. The high fracture-density zones at the regional-scale are structural zones as described in Chapter 4 (p.86). Within the structural zones individual fault zones and shear zones also are high fracture-density zones with respect to the surrounding wallrocks (eg. Gimlet South to Slippery Gimlet). Areas of localised high fracture-density occur in individual brittle-ductile faults at intersections with cross-cutting structures producing steeply plunging zones of sheared rock with a significant increase in volume. At a mesoscopic scale, high fracture-density zones are usually manifest as mesofracture arrays at the intersection of two differently oriented structures or in the wallrocks of major brittle-ductile faults.

Structural orientation

A less obvious geometric relationship is displayed by structural orientation whereby the average orientations identified at the regional-scale are present at all scales of observation.

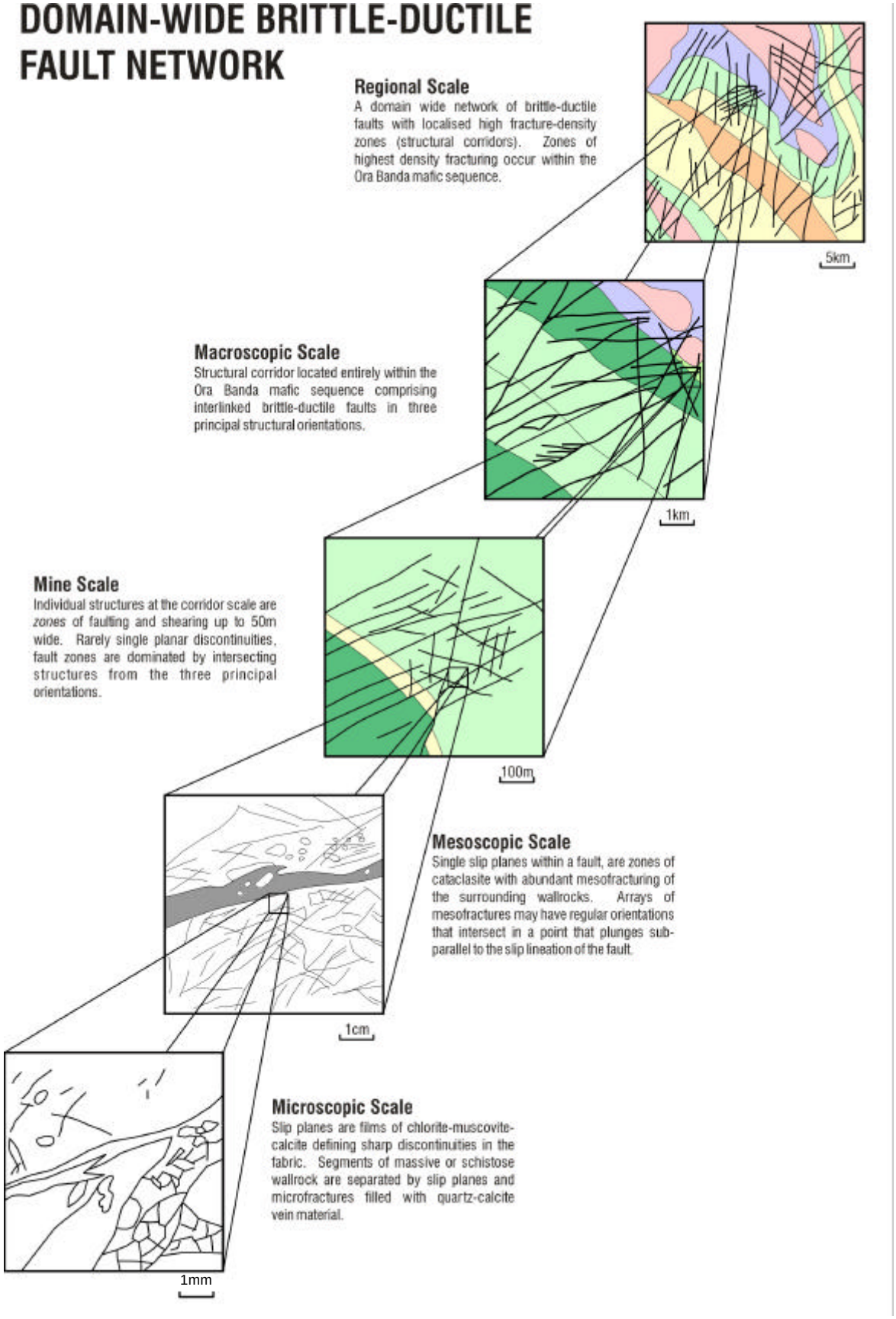

Figure 6.5 – Maps showing the fractal geometry of the brittle-ductile fault network at all scales. Fault distributions at regional, macroscopic and mine scales are taken from aeromagnetic interpretation, and at mesoscopic and microscopic are sketched from hand specimen and thin section photographs. In each map north is up the page.

Structural style and orientation remain the same at all scales whereas the apparent level of deformation may change. For example, a single fault at the regional-scale such as the Enterprise fault zone, is actually a 50-100m wide zone of parallel features with the same orientation at a mesoscopic scale.

6.3.2 Gold mineralisation

Gold mining centres, gold deposits, high grade ore-shoots

Structures in the Ora Banda Domain display an anisotropy that is repeatable at all scales. Gold mineralisation mimics this distribution but with a slightly broader geometry due to the interaction of hydrothermal fluids with the wallrocks of a host structure. The geometry and distribution of structures and their equivalent gold occurrences at each scale are listed in Table 6.1. Gold mining centres are coincident with structural zones and within each mining centre, gold deposits are coincident with brittle-ductile fault zones.

Gold deposits do not have a uniform distribution of gold in any given deposit but have high-grade shoots developed apparently at regular intervals that coincide with zones of high fracture-density. Individual gold lodes display widespread meso/microfracturing in the highest-grade areas. Similar correlation of gold grade and fracture density is documented in the highly mineralised Witwatersrand Basin, South Africa (Jolley *et al*. 1999). The coincidence of high fracture-density zones and gold within a deposit is analogous to the location of both high fracture-density zones and gold mining centres at the regional-scale.

6.3.3 Host rocks

At a regional-scale Fe-rich mafic volcanic rocks are the most favourable host rocks (Table A3.4 p.375, Appendix 3) and are distributed in NNW-SSE trending linear belts (eg. Ora Banda mafic sequence). Areas between the favourable host units are composed of granitoid, ultramafic and sedimentary rocks. This distribution produces a characteristic ‘striped’ geometry to the host rocks when grouped as favourable and less-favourable for gold mineralisation (Figure 6.6). Basaltic flow rocks in the Ora Banda Domain have layering with alternating pillowed, massive and coarse-grained layers (Chapter 2.3 p.17)

Table 6.1 - Fractal distribution of structure and gold mineralisation at all scales in the Ora Banda Domain.

Fractal geometry and distribution of fault networks and gold mineralisation

Scale	Structural element	Gold equivalent	Description
Regional	Fault network	Gold province	Comprises a domain-scale network of fractures that cross-cuts the entire sequence, but contains packets of high fracture density (structural zones)
Macroscopic	Structural zone	Gold mining district	A kilometre-scale network of individual faults with small concentrated areas of high fracture density
Mine scale	Zone of faulting	Gold deposit	Ore deposits usually occur with a single principal orientation, but structures in many other orientations contribute to the overall geometry. The intersection zones are areas of high-fracture density
Mesoscopic	Fault / shear zone	Gold lode	Millimetres-scale mesofracture networks form high fracture-density zones at the intersections of individual faults and shear zones. One or more fabric elements or principal structural orientations may dominate the rock fabric.
Microscopic	Microfracture array	Gold ore	At the grain scale, fractures in pyrite and silicates, and discontinuities defined by new mineral growth are the equivalent of larger scale high fracture density zones with respect to adjacent mineral material, and are sites of gold precipitation.

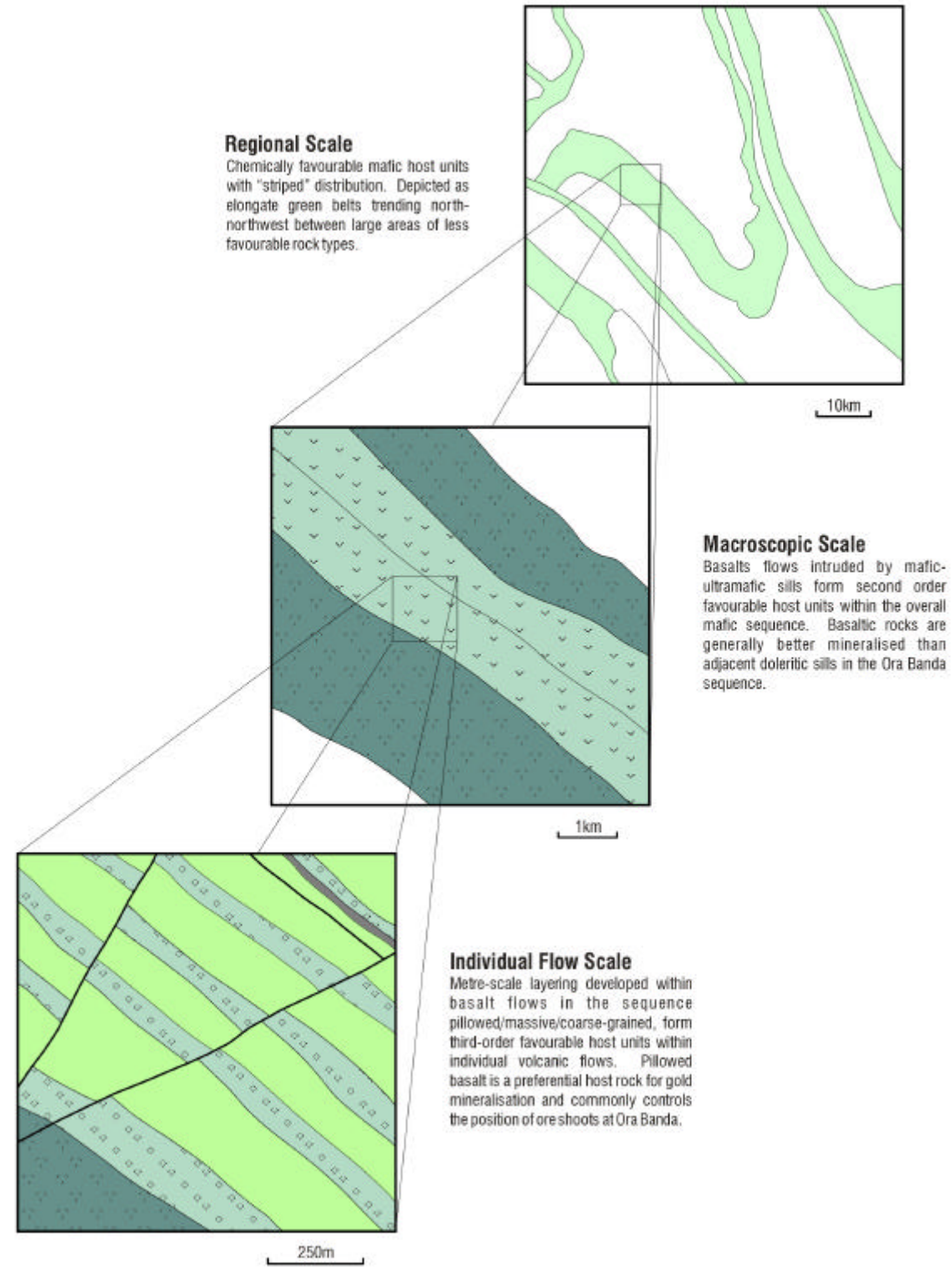

Figure 6.6 – Maps showing the fractal distribution of layered mafic host rocks in the Ora Banda Domain, north is up the page.

and comparable layering exists in mafic sills (Witt 1995; Witt *et al*. 1991; Gregory 1998). Gold deposits are distributed in clusters at the intersection of brittle-ductile faults with pillowed units in basalt flows and in iron-enriched granophyric zones of intrusive sills. A third type of favourable host occurs at significant rheologic gradients between layers of markedly different tensile strength (eg. Enterprise deposit at the contact of the Enterprise dolerite and the Mount Pleasant Sill). The regional distribution of favourable host units is mimicked at the corridor scale within a mafic sequence, where pillowed layers in basalt flows and iron-enriched zones in layered sills produce a second order distribution of more chemically favourable rock types. This geometric relationship breaks down at the mesoscopic scale since layered anisotropy is not recognised within any single pillowed unit or granophyric zone.

6.4 DISCUSSION

Gold deposits in the Siberia to Mount Pleasant area have similar geometry and distribution from the regional-scale to hand specimen scale, and previous petrologic studies illustrate a close relationship between gold related alteration and grain-scale microfractures (Collins 1995; Townend 1997a). The structural orientation and gold endowment data of gold deposits in the Siberia to Mount Pleasant area show that the largest gold deposits are in brittle-ductile faults striking between 060° and 090°. This orientation is subparallel to the inferred regional maximum shortening direction, which has implications for structural development and ore deposit formation, and confirms regular variation of structural style and gold mineralisation with orientation. In high fracture-density structural zones, most brittle-ductile faults display evidence of hydrothermal alteration and gold anomalism but most of the large gold deposits are hosted by only three or four main structures.

At a regional scale, spatial distribution analysis shows that gold deposits cluster in structural zones at about 10 km spacing which coincide with historic mining centres at Ora Banda, Grants Patch and Mount Pleasant. The gold mining centres are located in the vicinity of zones of high-density brittle-ductile faulting interpreted from aeromagnetic imagery and field mapping. The close relationship between structure and gold mineralisation is evident at the structural zone scale and at the individual deposit scale with the gold halo mapping out the brittle-ductile faults. Individual deposits occur at the intersection of structures with chemically favourable host rocks or other structures. At the

mining district scale, gold deposits are larger scale analogues of high-grade shoots within a deposit.

Most gold deposits in the north Kalgoorlie region occur in three main structural styles; brittle-ductile faults, cataclastic/hydraulic breccia and fault/fracture networks. The three styles have distinct differences but each has the capacity to host large gold deposits. Fault-hosted deposits are brittle-ductile structures with a quartz vein (system) emplaced in a brittle-ductile fault. Deposits of this type are usually low-tonnage / low-volume high-grade gold systems, and these include the Quarters deposit (Forster *et al.* 1997) and numerous deposits along the Black Flag Fault at Mount Pleasant. Cataclastic/hydraulic breccia style deposits such as the Gimlet South deposit (Harrison *et al.*1990) Slippery Gimlet deposit and Racetrack deposit (Gebre-Mariam *et al.* 1993), are brittle-ductile faults that failed by dominantly brittle processes with the onset of fluctuating fluid-pressure conditions. Fault/fracture networks also host gold deposits where a large fracture system that is in part fluid-generated (Sibson 1996) enables a high degree of fluid – wallrock interaction and results in large tonnage / large volume deposits such as at the Enterprise deposit.

An important characteristic of these deposits is that components of the three styles are found in each. For example the Enterprise deposit is a large system of millimetre scale fractures localised in the wallrocks of kilometre scale E-W trending brittle-ductile faults, with cross-cutting cataclastic and hydraulic breccia zones. The Gimlet South, Slippery Gimlet and Racetrack deposits are predominantly breccia lodes with sharp brittle-ductile fault planes along the footwall contacts and spaced fracture systems in the wallrocks. Quarters deposit has a dominant 020° shear vein control with a large system of intersecting 040° and 060° trending fracture veins (Forster *et al.* 1997).

Local structural controls and lithological heterogeneities determine the dominant structural style that forms in any given location but the brittle-ductile faults that host gold deposits are a part of the regional structural framework of three principal structural orientations. Dominant structures in any deposit will be in one of these orientations with the complexity of the system resulting from intersecting structures from the other orientations. For example E-W trending brittle-ductile faults at Enterprise are the main control on the mineralised envelope with high-grade zones produced at the intersection of NW-SE, N-S and NE-SW trending brittle-ductile faults.

Ore shoots in vein deposits were described by Peters (1993) as discrete hypogene masses usually hosted within a planar channel, surface lode or conduit, which may be either a shear zone, fissure, fault zone or lithological unit or contact. Ore shoots in lode gold deposits are by their nature structurally controlled but in some instances geological features converge to produce high-grade ore shoots. Three main types of high-grade ore shoot are recognised in this study as structurally controlled, lithologically controlled and rheologically controlled.

Structurally controlled high-grade ore shoots are high fracture-density zones produced by the intersection of brittle-ductile faults or at changes in the orientation of a fault segment. The dominantly steep dips of structures in the region are reflected in high-grade ore shoots that plunge steeply in most cases. A higher degree of fluid – wallrock interaction is a result of the increased fracture-density at these intersections.

Lithologically controlled high-grade ore shoots are localised where zones of fracturing and shearing intersect chemically favourable Fe-rich host rocks. The structure may have allowed the ore fluid to interact with a more chemically reactive host rock and therefore enhanced gold precipitation in the region of intersection. An example of this is pillowed basalt units within composite flow sequences (Harrison *et al.* 1990) or layered differentiated doleritic intrusions within a mafic / ultramafic sequence (Phillips 1986).

Rheologically-controlled high-grade ore shoots are localised at the intersection of brittle-ductile faults with contacts between rocks of markedly different tensile strength, and a higher degree of fracturing is possible in the weaker units in the vicinity of the contacts, by cyclic fluid pressure fluctuations in adjacent fault zones. After each sequential failure event the fluid pressure gradually returns to pre-failure conditions and may overpressure with healing of the fault by hydrothermal precipitation. Overpressuring can induce fluid-generated fracturing at the layer interface in the method envisaged by Sibson (1996). The contribution of the relative tensile rock-strength is indeterminate without rigorous experimental testwork on the rock properties and yield strengths of the materials. However, the presence of variable high-density tensile fracture across a bedding contact (eg. sheeted veining in the Enterprise open-pit), makes appreciation of the different tensile strengths of each rock type intuitive.

7 SUMMARY AND DISCUSSION

Regional folding, ductile shearing and brittle-ductile faulting are the dominant strains in the Ora Banda and Zuleika districts. The absence of early low-angle faults and stratigraphic repetition is an intriguing aspect of the structural geology that indicates partitioning of the early low-angle extensional and shortening deformations outside of the Ora Banda Domain. Inferred thrust movement on granite-greenstone contacts by Witt (1990) is a plausible but un-testable hypothesis from current exposure, as is the interpretation of D1 structures in the seismic data of Goleby *et al*. (1993) and Drummond *et al*. (1997). The Ora Banda Domain may have acted as a rigid block since the stratigraphic succession is one of the largest intact rock packages in the Norseman-Wiluna greenstone belt. The interpreted direction of D1 thrusting (Swager and Griffin 1990) is at about 90° to the regional ENE-WSW shortening and therefore a significant change in orientation of the principal axes of shortening occurred between these two tectonic events.

Progressive structural development during uplift is typical of convergent tectonic environments, and accords with the deformation sequence in the Ora Banda and Zuleika districts. Ductile shear zones (i.e. Zuleika Shear Zone) exhibit finite strains similar to those reported in transpressive shear zones worldwide (eg. Harland 1971; Coward 1980; Goodwin and Williams 1996; Tikoff and Greene 1997). Shallow-plunging stretching lineations along the Zuleika Shear Zone may indicate dominantly strike-slip movement, whereas other major shear zones in the Eastern Goldfields Province have kinematic indicators that display strike-slip movement, dip-slip movement or both (Eisenlohr *et al*. 1989; Skwarnecki 1987; Vearncombe 1992; Vearncombe 1998a). These studies also report significant flattening at a high angle to the shear zones, which is typical of transpressional/transtensional shear zones, defined by Dewey *et al*. (1999) as “strike-slip deformations that deviate from simple shear because of a component of, respectively, shortening or extension orthogonal to the deformation zone”. The strike-slip part of the definition is used loosely to accommodate some component of oblique-slip, common in strike-slip fault zones (Dewey *et al*. 1999).

In transpressional deformation zones, flow (deformation-path) partitioning (Hanmer and Passchier 1993; Goodwin and Williams 1996) is also common with the simple shear component localised within the high strain zone, and the pure shear component more

widely distributed. Simple shear fabrics usually have shallow-plunging stretching lineations whereas pure shear fabrics indicate a steep to sub-vertical axis of maximum elongation (Goodwin and Williams 1996; Tikoff and Greene 1997). Another type of partitioning is 'slip-partitioning' (Molnar 1992), where strike-slip deformation is partitioned into strike-slip orogen-parallel shear zones at the margins of less deformed blocks that contain dip-slip orogen-parallel shear zones. This partitioning is a possible explanation for the distribution of strike-slip and dip-slip shear zones within orogenic belts in the Eastern Goldfields Province. The shallow lineations at Zuleika for both pure and simple shear components indicate that the Zuleika Shear Zone is a partitioned zone of dominantly strike-slip deformation in an overall bulk shortening. Coincident orientations of pure shear and simple shear components may indicate a rotation of the maximum principal stretch axis into parallelism with the flow direction, in the vicinity of the high strain partition. This relationship is similar to the distribution of lineations near high-strain zones in areas of modern transpression such as the Alpine Fault, New Zealand (Little and Holcombe 1999).

An assessment of foliation – lineation relationships in transpressional environments by Teyssier and Tikoff (1999) found that the combination of a vertical foliation and horizontal lineation is typical of shear zones that transect most continents. When considering the angle of convergence in transpression, this combination is stable for convergence angles of <20º, which approximates to a pure wrenching as the convergence angle tends to 0º. This combination of a horizontal lineation in a vertical foliation is the same as that for the Zuleika Shear Zone, but wrenching has been ruled out for the reasons discussed in Chapter 3.6 (p.79), and the inferred maximum shortening direction is at a high angle to the Zuleika Shear Zone (i.e. >20º). Teyssier and Tikoff (1999) considered alternative possibilities where the vertical foliation – horizontal lineation combination is induced by a lateral extrusion along the shear direction instead of a vertical extrusion (c.f. Sanderson and Marchini 1984) to eliminate space problems during transpression. A relationship exists between the accumulation of finite strain and the convergence angles whereby horizontal lineations can remain stable at high angles of convergence, provided the finite strains are relatively small (i.e. axial ratio of the horizontal strain ellipsoid < 11).

Regionally, brittle-ductile faults (D4) occur in high fracture-density structural zones that are sited at evenly-spaced locations within the Ora Banda layered mafic sequence. The distribution of these structural zones displays spatial periodicity as defined by Cobbold and

Ferguson (1979). A model analogous to pinch-and-swell at a regional-scale may explain the regional distribution of structure in the Ora Banda and Zuleika districts, and may account for the spatial periodicity of high fracture-density zones, but some areas (eg. Mount Pleasant) may be controlled by major N-S trending brittle-ductile faults. As discussed by Ramberg (1955), the low-pressure neck areas in attenuated layers are sinks for migrating hydrothermal fluids, a fact that is confirmed by the mineralogy and textural relationships of veins and brittle-ductile faults at Ora Banda, Grants Patch and Mount Pleasant. The secondary tensile stresses that promote layer-parallel extension during regional shortening would have enhanced fluid-flow by the development of regional gradients in fluid-pressure, thereby providing focussed conduits for mineralising hydrothermal fluids. These secondary tensile stresses probably acted against σ_3 locally and resulted in fluid-overpressuring at a significantly reduced critical value, further enhancing the structural development of the region.

Fault networks have received much attention in the recent literature and are recognised from the Archaean to present day (Hill 1977; Sibson 1996; Sibson and Scott 1998; Witt *et al.* 1997; Vearncombe 1998a; Cox 1999; Cox *et al.* 1999). The model proposed by Hill (1977) involves an interlinked network of shear fractures, extensional fractures and extensional shear fractures that are developed in a triaxial stress field. Several types of fault-shear zone network are recognised as developed under either bulk coaxial or bulk non-coaxial stress fields (Sibson 1996) with internal variation in the presence of pre-existing anisotropy such as lithological layering. The bulk coaxial type of fault-shear zone network with internal layer anisotropy is in accord with the pattern of brittle-ductile fault development in the Ora Banda district (Figure 7.1).

The fault networks are typically developed with fluctuating fluid pressures in the presence of a far-field stress system. The intersections of brittle-ductile faults form high fracture-density zones that enhance rock permeability by adding a tabular component in the σ_2 direction, orthogonal to fault slip vectors (Sibson 1996). Micro and meso extension fracturing becomes more pronounced as fluid pressure approaches ($\sigma_3 + T_0$). At Ora Banda, brittle-ductile faults have shallow plunging slip lineations indicating dominantly strike slip movement, and intersections between the principal structural orientations locally produce steeply plunging linear zones of high fracture-density (eg. Gimlet South).

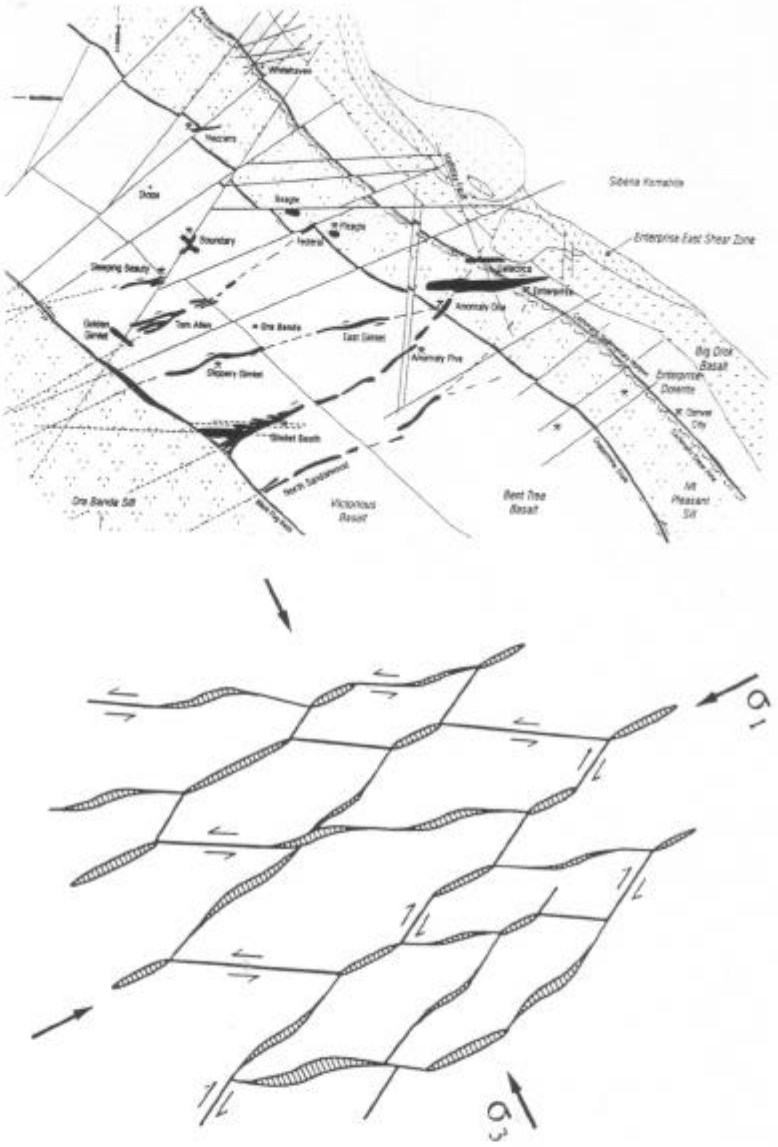

Figure 7.1 – Fault fracture network after Hill (1977) reoriented to the fault geometry of the Ora Banda structural zone. The fault network developed at Ora Banda has a similar series of interlinked simple shear style faults and extensional breccia zones. At Ora Banda, NE-SW trending faults are dextral, E-W trending faults are sinistral and 060 trending faults have a major component of extensional breccia. North is up the page.

Many fault networks are considered as being primarily fluid-driven (Sibson 1996) since they occur in uniform rock masses and are commonly associated with hydrothermal veins and alteration (Figure 4.2 p.90, Figure 4.3 p.93). Evidence of this at Ora Banda includes remarkably little offset across relatively wide deformation zones. However, post-failure mineral precipitation necessitates ongoing deformation for the structures to remain high-permeability fluid conduits (Sibson 1996), hence the type of brittle failure that occurs from fluid overpressuring depends on the balance between differential stress and local tensile strength of the rocks.

Layered sequences are considered favourable for network development with layer thickness controlling the size of the network. Layered basalt flows and dolerite sills make up the entire sequence at Ora Banda and may explain the high level of fault network development. Layering on the scale of the corridor is mimicked by 'layering-within-layering' such that a single basalt flow has individual pillowed layers that may be more susceptible to tensile fracture than coarse-grained doleritic or gabbroic layers. Furthermore, pillow basalts have inherited primary-porosity in the form of a linked system of interpillow voids commonly filled with hydrothermal veins and hyaloclastic fragments of chloritic basalt (Figure 4.15b p.114). In doleritic sills, fine grained zones appear to have relatively lower tensile strength than coarse grained zones and, if flanked by coarse-grained units, stratigraphically controlled zones of high fracture-density and fault networks will develop. Widespread development of micro/mesofracture arrays occurs along brittle-ductile faults at the Enterprise and Slippery Gimlet mines (Figure 4.2b-d p.90, Figure 4.15a p.114).

Gold mineralisation occurs as a result of destabilisation of a fluid that transports gold. This destabilisation may occur by changing any combination of a number of variables that work to reduce the solubility of gold in a fluid. Variation in temperature, pressure, pH, oxygen fugacity (fO_2), sulphur fugacity (fS_2) and mole fraction of CO_2 (XCO_2) results in precipitation of gold through fluid-wallrock interaction, mixing of two or more fluid species or phase separation in fluids associated with rapid loss of confining pressure during faulting (Witt 1993). Studies of fluid composition and gold transport (Phillips and Groves 1983; Phillips 1986; Kerrich 1989; Witt 1993a), have shown that gold precipitation occurs through the reaction of gold complexes with Fe-rich wallrocks to precipitate iron sulphides and gold in mafic and ultramafic rocks.

Deposits in mafic rocks commonly display sulphide-rich alteration halos around the gold orebodies. In contrast, gold deposition in Fe-poor granitic rocks and felsic porphyry may be related to oxidation of the ore fluids by reduction of Fe^{3+} in magnetite and mafic minerals (c.f. Phillips and Zhou 1999). In sulphidic metasedimentary rocks it may be related to reduction of the fluids by interaction with carbonaceous material (Witt 1993a).

Tholeiitic mafic rocks that host gold deposits in the Kalgoorlie Terrane are inherently low potassium rocks (Morris 1993), and the introduction of potassium can be assumed in any mafic volcanic rocks with biotite or muscovite. High-potassium/sulphur alteration around fractures and brittle-ductile faults in the vicinity of gold deposits, presents strong evidence of fluid-wallrock interaction as the destabilising process that led to gold precipitation. Structures that do not display a high degree of wallrock alteration, yet host large gold deposits, may have involved a fluid precipitation mechanism different to that for nearby deposits, or may indicate a different timing of structural development with evolution of the composition of the gold-bearing fluid.

Gold mineralisation of the regional-scale Zuleika Shear Zone was synchronous with the D3 deformation event but continued into the D4 event, during which gold mineralisation was a more widely distributed process facilitated by the development of the regional-scale brittle-ductile fault network (Figure 7.2). Metamorphism peaked during D1 with the intrusion of pre-regional folding granitoids (Witt and Davy 1997), and a second (slightly lower temperature) metamorphic event was the result of post-regional folding / syn-post D3 granitoid intrusion. Systematic variation of gold alteration isograds with metamorphic isograds related to post-regional folding granitoids (Witt 1991), indicates that the beginning of the gold mineralisation event was synchronous with metamorphism. Gold mineralisation was most prominently developed with the late tectonic brittle-ductile faulting event (D4), which shows mostly retrograde alteration assemblages.

The clear cross-cutting relationships between the D4 fault network and D3 ductile shear zones indicates that the D3 shear zones were not primary ore-fluid conduits focussing gold into lower-order brittle-ductile faults (Hagemann 1997), (c.f. Groves 1993; Eisenlohr *et al*.1989). The fault network is a regionally developed deformation fabric, and in the Ora Banda Domain, large gold deposits are located in areas significantly distant from the D3 shear zones. Hence, models for gold mineralisation that involve widespread metamorphic-

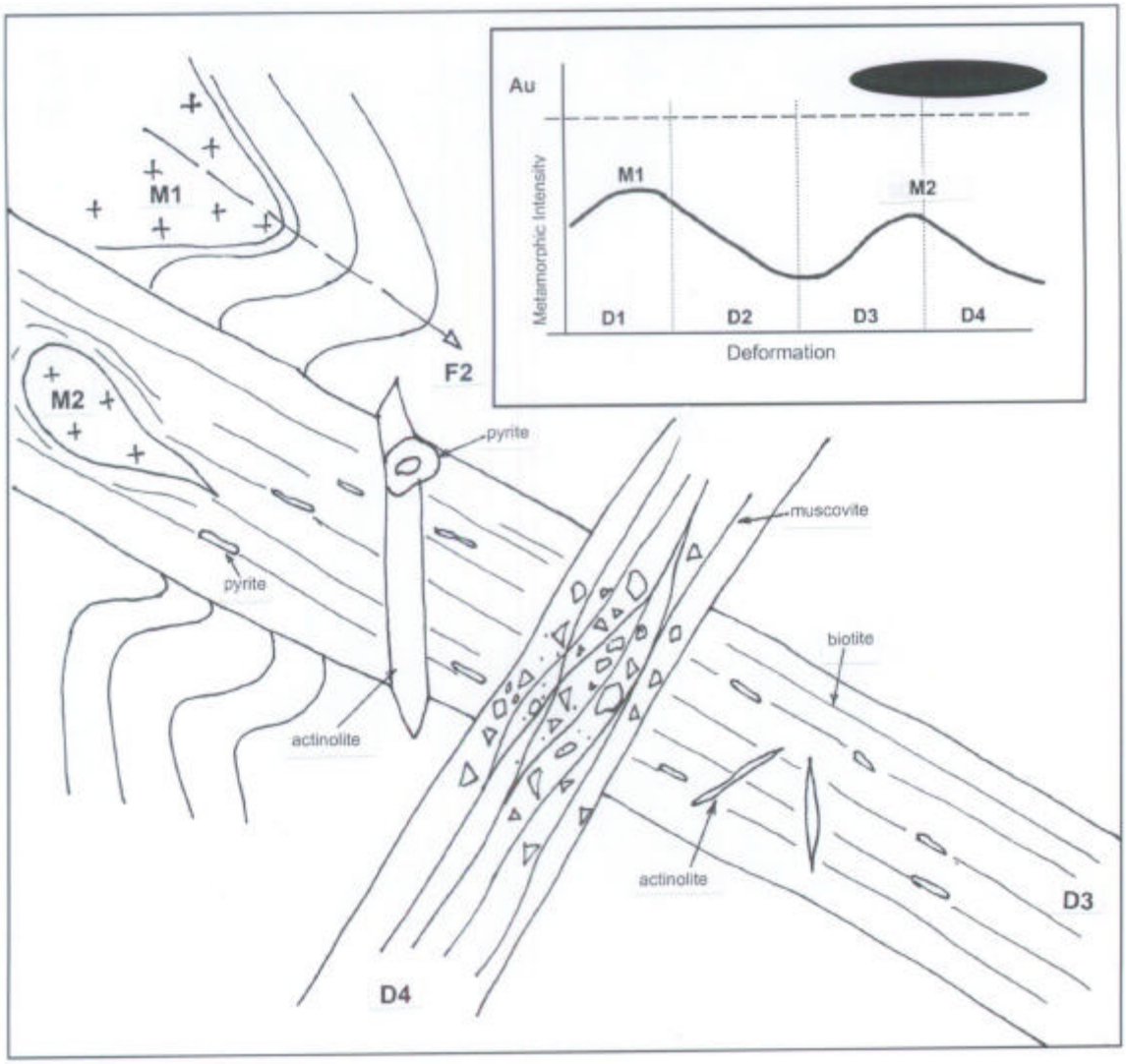

Figure 7.2 – Schematic diagram illustrating the relationships between gold mineralisation, deformation and metamorphism. Gold is developed in D3 and D4 structures that cross-cut early D2 folds. D3 – ductile shearing terminated just before the peak of metamorphism (M2), however gold mineralisation and deformation continued with D4 brittle-ductile faulting, and accompanying retrogression.

fluid generation and focussing, in the middle and upper crust (eg. Groves and Phillips 1987; Witt *et al*. 1997), better explain the distribution of mineralisation in the region.

Textural relationships of mesoscopic brittle-ductile structures show evidence of fluid-assisted failure during the formation of the gold lodes with both mechanical and hydraulic components. Cyclic overpressuring during metamorphic devolatilisation, in the presence of an active far-field-stress system, initiated mechanical brittle failure on deforming brittle-ductile faults over a protracted period, with significantly increased strain rates. The fluids were not in equilibrium with the wallrocks of the structures and reacted with mafic and felsic rocks to produce distinct potassic and sulphur-rich alteration assemblages that constrain the timing of structural development and (gold-related) wallrock alteration as synchronous. Gold mineralisation occurred via syn-tectonic mass transfer of material in solution, with migration of the fluid to precipitation sites (Vearncombe *et al*. 1989; Boulter *et al*. 1987; Cox *et al*. 1986).

Fluid-flow during metamorphism may be either pervasive or focussed (Oliver *et al.* 1998). Models that propose metamorphic devolatilisation of greenstones as the source of the gold fluids (eg. Groves and Phillips 1987; Phillips *et al.*1987; Powell *et al.* 1991; Witt *et al.* 1997), require large scale fluid-flow at depth in the crust (Norris and Henley 1976). Pervasive fluid-flow is suggested as the most efficient regional process for extraction of ore fluid components under greenschist-amphibolite facies conditions (Oliver *et al.* 1998), and occurs via an interconnected grain-scale network across large regions driven by thermal or deformation induced regional fluid pressure gradients. The interconnected grain-scale network may be either a microcrack network produced during deformation resulting in broad evenly distributed low strains (Oliver 1996), or an intergranular film localised along grain boundaries (eg. Fyfe *et al.* 1978).

Channelised (focussed) flow is a possible mechanism of metal extraction from the crust. The channels must reactivate repeatedly during deformation and metamorphism (eg. crack-seal veins, polylithic hydrothermal breccia), yet the brittle-ductile faults that facilitate channelised flow are usually pressure and temperature sinks that are more suited to precipitation than dissolution (Oliver *et al.* 1998). Furthermore, the fluid that reacts with the rock must be chemically favourable for reactions that dissolve the components of gold alteration, and leave the rock with a changed mineralogy typical of greenschist-amphibolite

facies assemblages. Retrograde assemblages with potassium and sulphur addition and net volume increase in gold lodes in the Ora Banda district (Harrison 1984), indicate that this is not the case.

Channelised flow is more likely to operate in the focussing and precipitation phase of fluid-flow. Brittle-ductile faults are the conduits that localise gold fluids during deformation, whereas the grain-scale network is a pervasive system that does not provide conditions favourable to ore formation. A fundamental characteristic of the gold mining corridors in the Ora Banda Domain is the spread of the total gold content throughout 30 or more deposits in each. This distribution has important implications for gold mining and exploration, and reveals the nature of gold mineralisation at the macroscopic scale and the efficiency of fluid-flow dictated by structural development and interconnectivity of fluid conduits (Cox *et al.* 1999). The domain-wide brittle-ductile fault network is analogous to a regional-scale structurally induced porosity that enabled the focussed flow of gold fluids.

An important implication of these observations is that all of the gold deposits in the Ora Banda and Zuleika districts are related by regional deformation events, which formed the domain-wide brittle-ductile fault network. Differences between individual gold deposits therefore reflect local variables of structural setting, rock-type and fluid chemistry, and are not due to significantly different mineralising (or deformation) events. Formation of the three principal structural orientations in the brittle-ductile fault network formation was essentially synchronous, but a time sequence within the event is implied due to the mutual cross-cutting of structures and variable mineralogy between deposits with proximity.

8 CONCLUSIONS

The Zuleika Shear Zone is a major NW-SE trending, within-greenstone-belt shear zone of significance only to the greenstone sequence. Finite strains indicate that the shear zone developed in response to a regional transpression with a ENE-WSW bulk shortening direction. The shear zone is truncated at an upper-crustal décollement at the base of the greenstone sequence and therefore is not of a crustal-scale. Smaller-scale brittle-ductile faults that cross-cut the Zuleika Shear Zone indicate a later deformation event, and these smaller-scale faults are not lower-order structures (Riedel shears) related to movement on the major shear zone.

The Ora Banda structural zone is composed of brittle-ductile faults with similar geometry and distribution to the interpreted regional brittle-ductile fault network. At a macroscopic scale, several brittle-ductile faults are interlinked to form a localised zone of high fracture-density. Synchronous development of the numerous faults is implicated by the mutual cross-cutting and similarities of style and mineralogy in structures of markedly different orientation.

The Enterprise fault zone is a zone of high fracture-density within the Ora Banda structural zone in which brittle-ductile structures are developed in the same three principal structural orientations to those recognised regionally. A diverse array of structural styles is typical of the D4 brittle-ductile fault network reflecting alternating conditions of deformation at the brittle-ductile transition during dewatering of the metamorphic pile. In the Enterprise fault zone fabrics range from ductile shear zones to cataclastic fault breccia and sheeted vein systems. The gross fabrics of the faults indicate that they were zones of high strain yet microfabrics show evidence that the intracrystalline strain is erased by recovery processes related to static recrystallisation. This recrystallisation may be attributed to thermal effects during intrusion of the late to post-tectonic Lone Hand Monzogranite.

A changing deformation style with similar maximum shortening axes for successive deformation events (D2, D3 and D4) may indicate that deformation was synchronous with progressive uplift of the Archaean supracrustal sequence. NW-SE trending D3 structures predominantly have ductile (mylonitic) character with flattening fabrics, well-developed stretch lineations and left-lateral movement sense in partitioned zones of simple shear. D4

(brittle-ductile and brittle) structures are developed across all scales in three principal structural orientations N-S dextral, E-W sinistral and NE-SW dextral. Deformation style changed from early ductile to later brittle-ductile which accords with upward transport of the rocks through the brittle-ductile transition from the middle to upper crust. The local development of gold deposits in ductile shear zones at Zuleika, and the widespread occurrence of brittle-ductile fabrics in gold bearing structures regionally, demonstrates that gold mineralisation was also synchronous with uplift of the crust during orogenesis.

Gold mineralisation in the Ora Banda and Zuleika districts was a protracted event that spanned at least two regional deformation events with gold deposits hosted in ductile shear zones at Zuleika, and in brittle-ductile faults across the region. Gold mineralisation resulted from regional fluid-focussing though the mid-upper crustal network of brittle-ductile faults and into zones of highest fracture-density. Gold mineralised zones are also coincident with spatially-periodic high fracture-density structural zones in the Ora Banda mafic sequence. The largest gold deposits in the Ora Banda mafic sequence are hosted in brittle-ductile faults that trend 060°-090°. Since the faults crosscut early ductile shear zones, interpretations of gold mineralising fluids being focussed from first-order crustal-scale shear zones into second or third-order synchronous structures may be invalid. Regional and local fluid focussing was influenced by the development of high fracture-density zones and by the presence of fluid pressure seals such as the upper contact of the Enterprise dolerite.

Zones of high fracture-density have analogues at regional, macroscopic, mesoscopic and microscopic scales, and these are coincident with areas of high gold concentration. The geometry and the distribution of geological structures and gold deposits in the Ora Banda and Zuleika districts are remarkably similar across several scales of observation from regional-scale to microscopic-scale. Such a relationship indicates a fractal distribution with scale invariant structural characterisitics.

9 REFERENCES

ANDERSON, E.M., 1905, The dynamics of faulting: *Edinburgh Geological Society Transactions*, v.8, p. 393-402.

ANNHAEUSSER, C.R., 1971, Cyclic volcanicity and sedimentation in the evolutionary development of Archaean greenstone belts of shield areas, *in* Symposium on Archaean Rocks, *edited by* J.E. GLOVER, Geological Society of Australia, Special Publication no. 3, p. 57-70.

ARCHIBALD, N.J., BETTENAY, L.F., BINNS, R.A., GROVES, D.I., and GUNTHORPE, R.J., 1978, The evolution of Archaean greenstone terrains, Eastern Goldfields Province, Western Australia, *Precambrian Research*, v. 6, p. 103-131.

ARCHIBALD, N.J., BETTENAY, L.F., BICKLE, M.J., and GROVES, D.I., 1981, Evolution of Archaean crust in the Eastern Goldfields Province of the Yilgarn Block, Western Australia, *in* Archaean Geology *edited by* J.E.Glover and D.I Groves: International Archaean Symposium, 2nd, Perth, W.A., 1980, Proceedings: Geological Society of Australia, Special Publication no. 7, p 491-504.

ARCHIBALD, N.J., 1998, 3D geology and tectonic synthesis of the Kalgoorlie Terrane, *in* Geodynamics and Gold Exploration in the Yilgarn, Australian Geodynamics Cooperative Research Centre workshop abstracts, p. 17-22.

BARKER, A.J., 1990, Introduction to metamorphic textures and microstructures, Blackie, USA, 162p.

BARLEY, M.E., and GROVES, D.I., 1988, Geological setting of gold mineralisation in the Norseman-Wiluna Belt, Eastern Goldfields Province, Western Australia, *in* Western Australian gold deposits, Bicentennial Gold 88 Excursion Guide Book *edited by* D.I. GROVES, M.E. BARLEY, S.E. HO, G.M.F. HOPKINS: University of Western Australia and Extension Service, Publication no. 14, p 17-46

BARLEY, M.E., EISENLOHR, B.N., GROVES, D.I., PERRING, C.S., and VEARNCOMBE, J.R, 1989, Late Archaean convergent margin tectonics and gold mineralisation: a new look at the Norseman-Wiluna Belt: *Geology*, v. 17, p. 826-829

BARRON, B.J., 1995, Petrological and mineragraphic examination of twenty five drill core samples from units in the Archaean greenstone belt north of Kalgoorlie, Western Australia, Newcrest Mining (WA) Ltd. unpublished report, no. OB394.

BAVINTON, O.A., 1979, The nature of sulphidic metasediments at Kambalda and their broad relationship with associated ultramafic rocks and nickel ores: *Economic Geology*, v. 76, p. 1606-1628.

BAXTER, J.L., 1989, Ora Banda mine district a review of the structural setting based on mapping and geometric analysis, unpublished report to BHP Gold, Hermitage Holdings report no. WA89/066 (OB221).

BELL, T.H., 1981, Foliation development – the contribution, geometry and significance of progressive, bulk, inhomogeneous shortening, *Tectonophysics*, v. 75, p. 273-296.

BERTHÉ, D., CHOUKROUNE, P., and JEGOUZO, P., 1979, Orthogneiss, mylonite, and non coaxial deformation of granites: the example of the South Armorican shear zone, *Journal of Structural Geology*, v. 1, p. 31-42.

BOGACZ, V., 1995, Enterprise gold mineralised system structural geometry and exploration potential, kinematic and tectogenetic explanation, Archon Resource Technologies Pty. Ltd: Newcrest Mining (WA) Ltd. unpublished report, no. OB395.

BOULTER, C.A., FOTIOS, M.G., and PHILLIPS, G.N., 1987, The Golden Mile, Kalgoorlie a giant gold deposit localised in ductile shear zones by structurally induced infiltration of an auriferous metamorphic fluid, *Economic Geology*, v. 82 p. 1661-1678.

CAINE, J.S., EVANS, J.P., and FORSTER, C.B., 1996, Fault zone architecture and permeability structure, *Geology*, v., 24, p. 1025-1028.

CLARKE, M.E., ARCHIBALD, N.J., and HODGSON, C.J., 1986, The structural and metamorphic setting of the Victory gold mine, Kambalda, Western Australia, *in* Proceedings of Gold ’86, and international symposium on the geology of gold, *edited by* A.J. MacDonald: Toronto, 1986, p. 243-254.

CLOUT, J.M.F., 1988, The tectonic setting and plumbing system of the Golden Mile, Kalgoorlie, Western Australia, *in* Bicentennial Gold 88, Extended Abstracts Poster Programme, *compiled by* A.D.T.GOODE, E.L.SMYTHE, W.D.BIRCH and L.I.BOSMA, Geological Society of Australia Abstracts no. 23, p. 65-67.

CLOUT, J.M.F, CLEGHORN, J.H., and EATON, P.C., 1990, Geology of the Kalgoorlie Goldfield, *in* Geology of the mineral deposits of Australia and Papua New Guinea, *edited by* F.HUGHES: Australasian Institute of Mining and Metallurgy, Monograph 14, p. 411-431.

COBBOLD, P.R., and FERGUSON, C.C., 1979, Description and origin of spatial periodicity in tectonic structures: report on a Tectonic Studies Group conference held at Nottingham University, 8 November 1978, *Journal of Structural Geology*, v. 1, no. 1, p. 93-97.

COLVINE, A.C., FYON, J.A., HEATHER, K.B., MARMONT, S., SMITH, P.M., and TROOP, D.G., 1988, Archaean lode gold deposits in Ontario, Part I a depositional model Part II a genetic model, Ontario Geological Survey, Miscellaneous Paper 139.

COLLINS, P.L.F., 1995, Petrology and mineragraphy of the ore at the Enterprise deposit, Ora Banda, Newcrest Mining (WA) Ltd., petrographic report CR95/3, (unpublished) 96p.

COMPTON, R.R., 1985, Geology in the field, Wiley and Sons, 398 p.

COX, S.F., ETHERIDGE, M.A., and WALL, V.J., 1986, The role of fluids in syntectonic mass transport and the localisation of metamorphic vein-type ore deposits, *Ore Geology Reviews*, v. 2, p. 65-86.

COX, S.F., KNACKSTEDT, M.A., and BRAUN, J., 1999, Percolation theory approaches to fluid flow in fracture-controlled hydrothermal systems, *in* The Specialist Group in

Tectonics and Structural Geology Field Conference, Halls Gap Victoria, Australia, *edited by* M. JESSELL, Geological Society of Australia Abstracts Series, no. 53, p. 37-38.

COX S.F., 1999, Deformational controls on the dynamics of fluid flow in mesothermal gold systems, *in* Fractures, Fluid Flow and Mineralisation, *edited by*, K. McCAFFREY, L. LONERGAN and J. WILKINSON, Geological Society of London, Special Publications, no. 155, p. 123-139.

COWARD, M.P., 1980, Shear zones in the Precambrian crust of southern Africa, *Journal of Structural Geology*, v. 2, no. 1/2, p. 19-27.

CRAW, D., WINDLE, S.J., and ANGUS, P.V., 1999, Gold mineralisation without quartz veins in a ductile-brittle shear zone, Macraes mine, Otago Schist, New Zealand, *Mineralium Deposita*, v. 34, p. 382-394.

DEWEY, J.F., HOLDSWORTH, R.E., and STRACHAN, R.A., 1999, Discussion on transpression and transtension zones: reply, *Journal of the Geological Society, London*, v. 156, p. 1048-1050.

DICKIE, M, 1995, Enterprise: progress report and observations, Newcrest Mining WA Ltd., unpublished report, no. OB324, 36 p.

DRUMMOND, B.J., GOLEBY, B.R., and SWAGER, C.P., 1997, Crustal signature of the major tectonic episodes in the Yilgarn Block, Western Australia: Evidence from deep seismic sounding, *in* Kalgoorlie '97: An International Conference on Crustal Evolution, Metallogeny and Exploration of the Yilgarn Craton – An Update, *compiled by* K.F.CASSIDY, A.J.WHITAKER and S.F. LIU, Australian Geological Survey Organisation, Extended Abstracts, Record 1997/41. p. 15-20.

DURNEY, D.W., and RAMSAY, J.G., 1973, Incremental strains measured by syn-tectonic crystal growth, *in* Gravity and Tectonics *edited by* K.A.DEJONG, Wiley, New York, p. 67-96

EISENLOHR, B.N., 1987 Structural geology of the Kathleen Valley-Lawlers region, Western Australia, and some implication for Archaean gold mineralisation, *in* Recent advances in understanding Precambrian gold deposits, *edited by* S.E.HO and D.I.GROVES: University of Western Australia, Department of Geology and Extension Service, Publication no. 11, p. 85-96.

EISENLOHR, B.N., GROVES, D., PARTINGTON, G.A., 1989, Crustal-scale shear zones and their significance to Archaean gold mineralisation in Western Australia, *Mineralium Deposita*, v. 24, p. 1-8.

ENGELDER, J.T., 1974, Cataclasis and the generation of fault gouge, *Geological Society of America Bulletin*, v. 85, p1515-1522.

FINDLAY, D., 1994, Boudinage emplacement of lodes of the Kalgoorlie goldfield, *Australian Journal of Earth Sciences*, v. 41, p. 105-113.

FINDLAY, D., 1998, Boudinage – a key to an organizing principle for the formation of ore deposits, *Economic Geology*, v. 93, p 671-682.

FYFE, W.S., PRICE, N.J., and THOMPSON, A.B., 1978, Fluids in the Earth's crust, (Developments in Geochemistry, 1), Elsevier, Amsterdam, 383p.

FORSTER, P., HELLSTEN, K., RADONJIC, A., and TOMS, B., 1997, Discovery and evaluation of the Quarters deposit, Mt Pleasant, *in* New Generation Gold Mines, Case Histories of Discovery, Australian Mineral Foundation, p.

FRY, N., 1979, Random point distributions and strain measurement in rocks, *Tectonophysics*, v. 60, p. 89-105.

GEE, R.D., BAXTER, J.L., WILDE, S.A., and WILLIAMS, I.R., 1981, Crustal development in the Archaean Yilgarn Block, Western Australia, Geological Society of Australia, *in* Archaean Geology *edited by* J.E.GLOVER and D.I.GROVES: International Archaean Symposium, 2nd, Perth, W.A., 1980, Proceedings: Geological Society of Australia, Special Publication no. 7, p 43-56.

GEBRE-MARIAM, M., GROVES, D.I., MCNAUGHTON, N.J., MIKUCKI, E.J., and VEARNCOMBE, J.R., 1993, Archaean Au-Ag mineralisation at Racetrack, near Kalgoorlie, Western Australia: a high crustal-level expression of the Archaean composite lode-gold system, *Mineralium Deposita*, v. 28, p. 375-387.

GILBERT, D.J., 1983, Comparative petrology, alteration mineralogy, geochemistry and sulphide-telluride-gold mineralisation within lodes in basalt, BHP Minerals Division Exploration Department, unpublished report, no. OB168.

GLASSON, M.J., HENDERSON, R.G., and TIN, M., 1998, Broads Dam gold deposits, *in* Geology and Mineralisation of Australian and Papua New Guinean mineral deposits, edited by D.A. BERKMAN and D.H. MACKENZIE, Australasian Institute of Mining and Metallurgy, Monograph 22 p. 197-200.

GOLEBY, B.R., RATTENBURY, M.S., SWAGER, C.P., DRUMMOND, B.J., WILLIAMS, P.R., SHERATON, J.W., and HEINRICH, C.A., 1993, Archaean crustal structure from seismic reflection profiling, Eastern Goldfields: results from the Kalgoorlie seismic transect: Australian Geological Survey Organisation, Record 1993/15, 54p.

GOODWIN, L.B., and WILLIAMS, P.F., 1996, Deformation path partitioning within a transpressive shear zone, Marble Cove, Newfoundland, *Journal of Structural Geology*, v. 18, no. 8, p. 975-990.

GREGORY, M.J., 1998,. The geochemistry and petrology of the Enterprise dolerite, Ora Banda, Western Australia, University of Melbourne BSc. Thesis (unpublished), 146p.

GROVES, D.I., 1993, The crustal continuum model for late-Archaean lode-gold deposits of the Yilgarn Block, Western Australia, *Mineralium Deposita,* v. 28, p. 366-374.

GROVES, D.I., and BATT, W.D., 1984, Spatial and temporal variations of Archaean metallogenic associations in terms of evolution of granitoid-greenstone terrains with particular emphasis on Western Australia, in Archaean Geochemistry edited by A.KRONER, G.N. HANSON and A.M. GOODWIN: Berlin, Springer-Verlag, p. 73-98.

GROVES, D.I., and PHILLIPS, G.N., 1987, The genesis and tectonic control on Archaean gold deposits of the Western Australian shield – a metamorphic replacement model, Ore Geology Reviews, v. 2, p. 287-322.

GWATKIN, C.C., 1984, Report on the Black shale at Ora Banda, BHP Minerals Division Exploration Department, unpublished report, no. OB54.

HAGEMANN, S.G., 1997, Structural and hydrothermal architecture of craton-scale deformation zones: the example of the Wiluna Greenstone Belt, Western Australia, *in* Kalgoorlie '97: An International Conference on Crustal Evolution, Metallogeny and Exploration of the Yilgarn Craton – An Update, *compiled by* K.F.CASSIDY, A.J.WHITAKER and S.F. LIU, Australian Geological Survey Organisation, Extended Abstracts, Record 1997/41. p. 137-139.

HAGEMANN, S.G., GROVES, D.I., RIDLEY, J.R., and VEARNCOMBE, J.R., 1992, The Archaean lode gold deposits at Wiluna, Western Australia: high-level brittle-style mineralisation in a strike-slip regime, *Economic Geology*, v. 87, p. 1022-1053.

HALL, G., 1998, Autochthonous model for gold metallogenesis and exploration in the Yilgarn, *in* Geodynamics and Gold Exploration in the Yilgarn, Australian Geodynamics Cooperative Research Centre workshop abstracts, p. 32-35.

HAMMOND, R.L., and NISBET, B.W., 1992, Towards a structural and tectonic framework for the central Norseman-Wiluna greenstone belt, Western Australia, *in* The Archaean: terranes, processes and metallogeny, *edited by* J.E. GLOVER and S.E.HO, Geology Department (Key Centre) and University Extension, University of Western Australia, Publication 22, p. 39-50.

HANMER, S., and PASSCHIER, C., 1991, Shear-sense indicators: a review, Geological Survey of Canada Paper, 90-17, 72 p.

HARLAND, W.B., 1971, Tectonic transpression in the Caledonian Spitsbergen, *Geological Magazine*, v. 108, no. 1, p27-42.

HARRISON, N.M., 1982, Geology and gold mineralisation of the Ora Banda region, Eastern Goldfields Western Australia, BHP Minerals Division Exploration Department, unpublished report, no. OB8.

HARRISON, N.M., 1983, Geochemistry of the basaltic greenstones and lodes, Gimlet South and Victorious mine areas, Ora Banda Western Australia, BHP Minerals Division Exploration Department, unpublished report, no. OB17.

HARRISON, N.M., 1984, The influence of volcanic stratigraphy and chemistry on the development of lodes in the basalts and porphyritic basalts at Ora Banda, Western Australia, BHP Minerals Division Exploration Department, unpublished report, no. OB52.

HARRISON, N.M., 1987, Structural observations on mines and projects in the Ora Banda region and interpretation of the regional controls of gold mineralisation, BHP Minerals Division Exploration Department, unpublished report, no. OB146.

HARRISON, N.M., 1984, Composition – volume relationships in the formation of the Ora Banda lodes, BHP Minerals Division Exploration Department, unpublished internal report, no. OB24.

HARRISON, N., BAILEY, A., SHAW, J.D., PETERSEN, G.N., and ALLEN, C.A., 1990, Ora Banda gold deposits, *in* Geology and mineral deposits of Australia and Papua New Guinea, *edited by* F.E.HUGHES, Australasian Institute of Mining and Metallurgy, Monograph 14, p. 389-394.

HIGGINS, M.W., 1971, Cataclastic rocks, US Geological Survey professional paper 687, 97 p.

HILL, D.P., 1977, A model for earthquake swarms, *Journal of Geophysical Research*, v. 82, p. 347-352.

HILL, R.E.T, BARNES, S.J., GOLE, M.J., and DOWLING, S.E., 1987, Physical volcanology of Komatiites: a field guide to komatiites between Kalgoorlie and Wiluna, Eastern Goldfields Province, Yilgarn Block, Western Australia: Geological Society of Australia (Western Australian Division), Excursion Guide no. 1.

HOBBS, B.E., MEANS, W.D., and WILLIAMS, P.F., 1976, An outline of structural geology, Wiley, New York, 571p.

HODGSON, C.J., 1989, The structure of shear-related, vein-type gold deposits: a review, *Ore Geology Reviews*, v. 4 p. 231-273.

HUNTER, W.M., 1993, Geology of the granite-greenstone terrane of the Kalgoorlie and Yilmia 1:100,000 sheets, Western Australia, Western Australia Geological Survey, Report 35, 80p.

IRVINE, R.J., 1979, IP surveys at Ora Banda Western Australia, BHP Minerals Division Exploration Department, unpublished report, no. OB29.

JÉBRAK, M., 1997, Hydrothermal breccias in vein-type ore deposits: a review of mechanisms, morphology and size distribution, *Ore Geology Reviews*, v. 12, p. 111-134.

JOLLEY, S.J., HENDERSON, I.H.C., BARNICOAT, A.C., and FOX, N.P.C., 1999, Thrust fracture network and hydrothermal gold mineralisation: Witswatersrand Basin, South Africa, *in* Fractures, Fluid Flow and Mineralisation, *edited by*, K. McCAFFREY, L. LONERGAN and J. WILKINSON, Geological Society of London, Special Publications, no. 155, p. 153-165.

JUTSON, J.T., 1914, The mining geology of Ora Banda, Broad Arrow Goldfield, Western Australia Geological Survey, Bulletin 54.

KERRICH, R., 1989, Geochemical evidence on the sources of fluids and solutes for shear zone-hosted mesothermal gold deposits: Geochemical Association of Canada, Short Course Notes, v. 6, p. 129-197.

KNIPE, R.J., Deformation mechanisms – recognition from natural tectonites, *Journal of Structural Geology*, v. 11, no. 1/2, p. 127-146.

KONECNY, S., 1988, Zuleika annual report 1-1-87 to 31-12-87, BHP Minerals Division Exploration Department, unpublished report, no. OB179.

LABEL, A., 1984, Ora Banda area, downhole induced polarisation surveys, BHP Minerals Division Exploration Department, unpublished report, no. OB23.

LAING, W.P., 1994, Ore systems at New Celebration and Ora Banda and a comparison with the Kalgoorlie system, Newcrest Mining (WA) Ltd. unpublished report, no. OB364.

LIBBY, J.W., BARLEY, M.E., EISENLOHR, B.N., GROVES, D.I., HRONSKY, J.M.A., and VEARNCOMBE, J.R., 1990, Craton-scale deformation zones, *in* Gold deposits of the Archaean Yilgarn Block, Western Australia,

LISTER, G.S., and SNOKE, A.W., 1984, S-C mylonites, *Journal of Structural Geology*, v. 6, p. 617-638.

LITTLE, T.A., and HOLCOMBE, R.J., 1999, Microstructural evolution and flow of rocks in a zone of active transpressional deformation near the Alpine Fault, New Zealand, *in* The Specialist Group in Tectonics and Structural Geology Field Conference, Halls Gap Victoria, Australia, *edited by* M. JESSELL, Geological Society of Australia Abstracts Series, no. 53, p.151-152.

MARRETT, R., and ALLMENDINGER, R.W., 1990, Kinematic analysis of fault slip data, *Journal of Structural Geology*, v. 12, no. 8, p. 973-986.

MASON, J.C., 1987, The structure and geochemistry of gold-bearing lodes at Ora Banda, Western Australia, University of London BSc thesis, (unpublished).

MANDELBROT, B.B., 1983, The fractal geometry of nature, Freeman, San Francisco.

MANDL, G. 1988, Mechanics of tectonic faulting – models and basic concepts, Developments in structural geology, *edited by* H.J.ZWART, Elsevier, 407p.

MOLNAR, P., 1992, Brace-Goetz strength profiles, the partitioning of strike-slip and thrust faulting at zones of oblique convergence, and the stress-heat flow paradox of the San Andreas Fault, *in* Fault Mechanics and Transport Properties of Rocks, *edited by* B. EVANS and T. WONG, Academic Press, p. 434-459.

MORRIS, P.A., 1993, Archaean mafic and ultramafic volcanic rocks, Menzies to Norseman, Western Australia, Western Australia Geological Survey, Report 36, 107p.

MUELLER, A.G., and HARRIS, L.B., 1987, An application of wrench tectonic models to mineralised structures in the Golden Mile district, Kalgoorlie, Western Australia, *in* Recent Advances in Understanding Precambrian Gold Deposits, *edited by* S.E. HO and D.I.GROVES, University of Western Australia Department of Geology and University Extension Service, Publication 11, p. 97-107.

MUELLER, A.G., HARRIS, L.B., and LUNGAN, A. 1988, Structural control of greenstone-hosted gold mineralisation by transcurrent shearing: a new interpretation of

the Kalgoorlie mining district, Western Australia, *Ore Geology Reviews*, v. 3, p. 359-387.

MUHLING, J.R., 1980, Report on thirty-two thin sections from DDH 5 at Ora Banda, BHP Minerals Division Exploration Department, unpublished report, no. OB30.

MUHLING, J.R., 1982, Petrographic report on 31 samples from Ora Banda and 7 samples from Zuleika, BHP Minerals Division Exploration Department, unpublished report, no. OB230.

NORRIS, R.J., and HENLEY, R.W., 1976, Dewatering of a metamorphic pile, *Geology* v. 4, p. 333-336.

OLIVER, N.H.S., RUBENACH, M.R.J., and VALENTA, R.K., 1998, Precambrian metamorphism, fluid-flow and metallogeny of Australia, *AGSO Journal of Australian Geology and Geophysics*, v. 17, p. 31-53.

OLIVER, N.H.S., 1996, Review and classification of structural controls on fluid flow during metamorphism, *Journal of Metamorphic Geology*, v. 14, p. 477-492.

OLIVER, R., 1993, Underground operations – Ora Banda, a structural, mineralogical, petrological and geochemical study of the main lode and spur lodes, Newcrest Mining (WA) Ltd. unpublished report, no. OB301.

PASSCHIER, C.W., and TROUW, R.A.J., 1996, Microtectonics, Springer-Verlag, Berlin Heidelberg, 289p.

PETERS, S.G., 1993, Nomenclature, concepts and classification of oreshoots in vein deposits, *Ore Geology Reviews*, v. 8, p. 3-22.

PETERSEN, G., 1987, Gold mineralisation at Gimlet South, Ora Banda, W.A., *in* The Second Eastern Goldfields Geological Field Conference, Abstracts and Excursion Guide, 1987 *edited by* W.K. WITT and C.P. SWAGER: Geological Society of Australia (Western Australian Division), p.78-85.

PHILLIPS, G.N., 1986, Geology and alteration in the Golden Mile, *Economic Geology*, v. 81, p. 779-808.

PHILLIPS, G.N., and GROVES, D.I., 1983, The nature of Archaean gold-bearing fluids as deduced from gold deposits of Western Australia, *Journal of the Geological Society of Australia*, v. 30, p. 25-39.

PHILLIPS, G.N., GROVES, D.I., and BROWN, I.J., 1987, Source requirements for the Golden Mile, Kalgoorlie: significance to the metamorphic replacement model for Archaean gold deposits, *Canadian Journal of Earth Sciences*, v. 24, p. 1643-1651.

PHILLIPS, G.N., and ZHOU, T., 1999, Gold-only deposits and Archaean granite, SEG Newsletter, Society of Economic Geologists, no. 37, p. 1, 8-13.

PHILLIPS, W.J., 1972, Hydraulic fracturing and mineralisation, *Journal of the Geological Society of London*, v. 128, p. 337-359.

PLATT, J.P., and VISSERS, R.L.M., 1980, Extensional structures in anisotropic rocks, *Journal of Structural Geology*, v. 2, p. 397-410.

POWELL, R., WILL, T.M., and PHILLIPS, G.N., 1991, Metamorphism of Archaean greenstone belts: Calculated fluid compositions and implications for gold mineralisation, *Journal of Metamorphic Geology*, v. 9, p. 141-150.

PUMPELLY, R., WOLFF, J.E., and DALE, T.N., 1894, Geology of the Green Mountains, U.S. Geological Survey Memoir 23, p 1-157.

RAMBERG, H., 1955, Natural and experimental boudinage and pinch-and-swell structures, *Journal of Geology*, v. 63, p.512-526.

RAMSAY, J.G., 1967, Folding and fracturing of rocks, McGraw-Hill, New York, 568p.

RAMSAY, J.G., 1980a, Shear zone geometry: a review, *Journal of Structural Geology*, v. 2, p. 83-101.

RAMSAY, J.G., 1980b, The crack-seal mechanism of rock deformation, *Nature*, v. 284, p.135-139.

RAMSAY, J.G., and HUBER, M.I., 1983, The techniques of modern structural geology, 1: Strain Analysis, Academic Press, London.

RANSTED, T.W., 1990, Grants Patch gold deposits, *in* Geology and mineral deposits of Australia and Papua New Guinea, *edited by* F.E.HUGHES, Australasian Institute of Mining and Metallurgy, Monograph 14, p. 373-375.

RIEDEL, W., 1929, Zur Mechanik geologischer Brucherscheinungen: Centralbl. f. Mineral. Geol. u. Pal., v. 1929 B, p. 354-368.

ROBERT, F., and BROWN, A.C., Archaean gold-bearing quartz veins at the Sigma mine, Abitibi greenstone belt, Quebec: part I. geologic relations and formation of the vein system, *Economic Geology*, v. 81, p 578-592.

ROBERT, F., POULSEN, K.H., and DUBÉ, B., 1994, Structural analysis of lode gold deposits in deformed terranes, Geological Survey of Canada, open file 2850, 140p.

SANDERSON, D.J., and MARCHINI, W.R.D., 1984, Transpression, *Journal of Structural Geology*, v., 6, no. 5, p. 449-458.

SCHIEMER, P., 1995, Ora Banda gold mine resource report: Enterprise oxides, Newcrest Mining (WA) Ltd. unpublished report, no. OB369.

SCOTT, R.J., 1997, Fault control on fluid-flow and mineralisation at Mount Charlotte and the Golden Mile, *in* Kalgoorlie ’97: An International Conference on Crustal Evolution, Metallogeny and Exploration of the Yilgarn Craton – An Update, *compiled by* K.F.CASSIDY, A.J.WHITAKER and S.F. LIU, Australian Geological Survey Organisation, Extended Abstracts, Record 1997/41. p. 145-150.

SHERIFF, R.E., 1982, Structural interpretation of seismic data, American Association of Petroleum Geologists, Short course notes: continuing education course for the Dallas Geological Society, 73p..

SIBSON, R.H., 1977, Fault rocks and fault mechanisms, *Journal of the Geological Society of London*, v. 133, p. 191-213.

SIBSON, R.H., 1987, Earthquake rupturing as a mineralizing agent in hydrothermal systems, *Geology*, v. 15, p. 701-704.

SIBSON, R.H., ROBERT, F., and POULSEN, K.H., 1988, High-angle reverse faults, fluid-pressure cycling and mesothermal gold-quartz deposits, *Geology*, v. 16, p. 551-555.

SIBSON, R.H., 1996, Structural permeability of fluid-driven fault-fracture meshes, *Journal of Structural Geology*, v. 18, p. 1031-1042.

SIBSON, R.H., and SCOTT, J., 1998, Stress/fault controls on the containment and release of overpressured fluids: examples from gold-quartz vein systems in Juneau, Alaska; Victoria, Australia and Otago, New Zealand, *Ore Geology Reviews*, v.13, p.293-306.

SIMPSON, C., 1986, Determination of movement sense in mylonites, *Journal of Geological Education*, v. 34, p. 246.

SIMPSON, G., WILLIAMS, P., HARRIS, D., and HAMER, K., 1995, Interpretation of Menzies – Kalgoorlie – Norseman region Yilgarn Craton, Western Australia: Bardoc-3137 1:100,000 sheet, Etheridge Henley Williams and World Geoscience Corporation Limited.

SKWARNECKI, M.S., 1987, Controls on Archaean gold mineralisation in the Leonora district, Western Australia, *in* Recent advances in understanding Precambrian gold deposits, *edited by* S.E.HO and D.I.GROVES: University of Western Australia, Department of Geology and Extension Service, Publication no. 11, p.109-135.

SMIT, R., 1984, Orban joint venture Western Australia: report for the period 1st September to 31st December 1983 text, figures, appendices 1 and 2, BHP Minerals Division Exploration Department, unpublished report, no. OB238.

SPENCER, S., 1991, The use of syntectonic fibres to determine strain estimates and deformation paths: an appraisal, *Tectonophysics*, v. 194, p. 13-34.

SWAGER, C.P., 1989, Structure of the Kalgoorlie greenstones – regional deformation history and implications for the structural setting of the Golden Mile gold deposits, Western Australia Geological Survey, Report 25, Professional Papers, p. 59-84.

SWAGER, C.P., 1994, Geology of the Dunnsville 1:100,000 sheet, Western Australia Geological Survey, Record no. 1990/2, 35p.

SWAGER, C.P., 1995, Geology of the greenstone terranes in the Kurnalpi-Edjudina region, Southeastern Yilgarn Craton: Western Australia Geological Survey, Report 47, 31p.

SWAGER, C.P., 1997, Structural evolution of greenstone terranes in the southern Eastern Goldfields, Western Australia *in* Kalgoorlie '97: An International Conference on Crustal Evolution, Metallogeny and Exploration of the Yilgarn Craton – An Update, *compiled by* K.F.CASSIDY, A.J.WHITAKER and S.F. LIU, Australian Geological Survey Organisation, Extended Abstracts, Record 1997/41. p. 49-53.

SWAGER, C., and GRIFFIN, T.J., 1990, An early thrust duplex in the Kalgoorlie-Kambalda greenstone belt, Eastern Goldfields Province, Western Australia, *Precambrian Research*, v. 48, p. 63-73.

SWAGER, C.P., GRIFFIN, T.J., WITT, W.K., WYCHE, S., AHMAT, A.L., HUNTER, W.M., and MCGOLDRICK, P.J., 1990, Geology of the Archaean Kalgoorlie Terrane – an explanatory note: Western Australia Geological Survey, Report 48, 26p.

SWAGER, N., 1993, Review of gold mineralisation at Ora Banda, Newcrest Mining (WA) Ltd. unpublished report.

SYLVESTER, A.G., 1988, Strike-Slip faults, *Geological Society of America Bulletin*, v. 100, p. 1666-1703.

TANNER, P.W.G., 1989, The flexural-slip mechanism, *Journal of Structural Geology*, v. 11, p. 635-655.

TAYLOR, R.G., 1992, Ore textures – volume 1: infill textures: Key Centre in Economic Geology and Economic Geology Research Unit, James Cook University, Townsville, 24p.

TCHALENKO, J.S., 1970, Similarities between shear zones of different magnitudes, *Geological Society of America Bulletin*, v. 81, p. 1625-1640.

TEYSSIER, C., and TIKOFF, B., 1999, Fabric stability in oblique convergence and divergence, *Journal of Structural Geology*, v. 21, p. 969-974.

TIKOFF, B., and GREENE, D., 1997, Stretching lineations in transpressional shear zones: an example from the Sierra Nevada Batholith, California, *Journal of Structural Geology*, v. 19, no. 1, p. 29-39.

TOWNEND, R., 1997a, Preparation of 41 polished sections of 41 cores and mineragraphic examination (Enterprise diamond drill sulphide samples), Centaur Mining and Exploration, unpublished report, no. OB396.

TOWNEND, R., 1997b, Preparation of 26 polished sections of 26 cores, mineragraphic / SEM examination with reference to gold and tellurides, Gimlet South, Centaur Mining and Exploration, unpublished report, no. OB397.

TURNER, F.J., and WEISS, L.E., 1963, Structural analysis of metamorphic tectonites, McGraw-Hill, New York, 1963.

VAUGHAN, J.P., 1988, Gold mineralogy of selected Bullant samples, Centaur Mining and Exploration Limited, unpublished report, no. OB400.

VEARNCOMBE, J.R., 1992, Archaean gold mineralisation in a normal-motion shear zone at Harbour Lights, Leonora, Western Australia, *Mineralium Deposita*, v. 27, p. 182-191.

VEARNCOMBE, J.R., 1993, Quartz vein morphology and implications for formation depth and classification of Archaean gold-vein deposits, *Ore Geology Reviews*, v. 8, p. 407-424.

VEARNCOMBE, J.R., 1998a, Shear zones, fault networks, and Archaean gold, *Geology*, v.26, no. 9, p. 855-858.

VEARNCOMBE, J.R., 1998b, Aeromagnetic interpretation of the Mt Pleasant – Ora Banda area with comments on the spatial distribution of gold deposits, report to Centaur Mining and Exploration Ltd., unpublished, 25 p.

VEARNCOMBE, J.R., and VEARNCOMBE, S., 1998c, Structural data from drillcore, *in* More Meaningful Sampling in the Mining Industry, *edited by* B. DAVIS and S.E. HO, Australian Institute of Geoscientists, Bulletin No. 22, p. 67-82.

VEARNCOMBE, J.R., and VEARNCOMBE, S. 1999, The spatial distribution of mineralisation: Application of Fry Analysis, *Economic Geology* v. 94, p. 475-486.

VEARNCOMBE, J.R., BARLEY, M.E., EISENLOHR, B.N., GROVES, D.I., HOUSTOUN, S.M., SKWARNECKI, M.S., GRIGSON, M.W., and PARTINGTON, G.A., 1989, Structural controls on mesothermal gold mineralisation: examples from the Archaean terranes of southern Africa and Western Australia, *Economic Geology*, Monograph 6, p. 124-134.

WALSH, J.J., and WATTERSON, J., 1988, Analysis of the relationship between displacements and dimensions of faults, *Journal of Structural Geology*, v.10, no. 3, p. 239-247.

WALSHE, J., 1998, Kalgoorlie exploration model, Australian Geodynamics Cooperative Research Centre, AGCRC Project No: 3067CO, www.agcrc.csiro.au/projects/3067CO/kem1/

WHITE, S.H., BURROWS, S.E., CARRERAS, J., SHAW, N.D., and HUMPHREYS, F.J., 1980, On mylonites in ductile shear zones, *Journal of Structural Geology*, v. 2, no. 1/2, p. 175-187.

WILLIAMS, I.R., 1974, Structural subdivision of the Eastern Goldfields Province, Yilgarn Block: Western Australia Geological Survey, Annual Report 1973, p. 53-59.

WILLIAMS, D.A.C, and HALLBERG, J.A., 1973, Archaean layered intrusions of the Eastern Goldfields region, Western Australia, *Contributions to Mineralogy and Petrology*, v. 38, p. 45-70.

WILLIAMS, P.R., and WHITAKER, A.J., 1993, Gneiss domes and extensional deformation in the highly mineralised Archaean Eastern Goldfields Province, Western Australia, *Ore Geology Reviews*, v. 8, p. 141-162.

WINER, N., 1980, Results and interpretation of a slimline geophysical logging survey carried out by GEOEX Pty. Ltd. Ora Banda, BHP Minerals Division Exploration Department, unpublished report, no. OB40.

WISE, D.U., DUNN, D.E., ENGELDER, J.T., GEISER, P.A., HATCHER, R.D., KISH, S.A., ODOM, A.L., and SCHAMEL, S., 1984, Fault-related rocks: suggestions for terminology, *Geology*, v. 12, p. 391-394.

WITT, W.K., 1987, Stratigraphy and layered mafic/ultramafic intrusions of the Ora Banda sequence, Bardoc 1:100,000 sheet, Eastern Goldfields: and excursion guide, *in* The Second Eastern Goldfields Geological Field Conference, Abstracts and Excursion Guide, 1987 *edited by* W.K. WITT and C.P. SWAGER: Geological Society of Australia (Western Australian Division), p.49-63.

WITT, W.K., 1990, Geology of the Bardoc 1:100,000 sheet, Western Australia Geological Survey, Record 1990/14. 50p.

WITT, W.K., 1991, Regional metamorphic controls on alteration associated with gold mineralisation in the Eastern Goldfields Province, Western Australia: implications for the timing and origin of Archaean lode-gold deposits, *Geology* v. 19, p. 982-985.

WITT, W.K., 1992, Porphyry intrusions and albitites in the Bardoc-Kalgoorlie area, Western Australia, and their role in Archaean epigenetic gold mineralisation, *Canadian Journal of Earth Sciences*, v. 29, p 1609-1622.

WITT, W.K., 1993a, Gold mineralisation in the Menzies-Kambalda region, Eastern Goldfields, Western Australia, Geological Survey of Western Australia, Report 39, 165p.

WITT, W.K., 1993b, Gold deposits of the Mount Pleasant – Ora Banda areas, Western Australia – Part 2 of a systematic study of the gold mines of the Menzies-Kambalda region: Western Australia Geological Survey, Record 1992/14.

WITT, W.K., 1993c, Lithological and structural controls on gold mineralisation in the Archaean Menzies-Kambalda area, Western Australia, *Australian Journal of Earth Sciences*, v. 40, p. 65-86.

WITT, W.K., 1995, Tholeiitic and high-Mg mafic/ultramafic sills in the Eastern Goldfields Province, Western Australia: implications for tectonic settings, *Australian Journal of Earth Sciences*, v. 42, p. 407-422.

WITT, W.K., and DAVY, R., 1997, Geology and geochemistry of granitoid rocks in the southwest Eastern Goldfields Province: Western Australia Geological Survey, Report 49, 137p.

WITT, W.K., DAVY, R., and CHAPMAN, D., 1991, The Mount Pleasant Sill Eastern Goldfields, Western Australia – iron-rich granophyre in a layered high-Mg intrusion, Western Australia Geological Survey, Report 30, p. 73-92.

WITT, W.K., KNIGHT, J.T., and MIKUCKI, E.J., 1997, A synmetamorphic lateral fluid-flow model for gold mineralisation in the Archaean southern Kalgoorlie and Norseman terranes, Western Australia, *Economic Geology*, v. 92, p. 407-437.

WOODALL, R.W., 1965, Structure of the Kalgoorlie Goldfield, *in* Geology of Australian ore deposits (2nd edition) *edited by* J. McANDREW: Commonwealth Mining and Metallurgical Congress, 8th, Australia and New Zealand, 1965, Publications v. 1, p. 71-79.

WYNNE, A., and ISLES, D., 1986, Lady Evelyn prospect Ora Banda Western Australia, PL's 24/1136 – 11452: Geology, geochemical sampling and aeromagnetic interpretation, BHP Minerals Division Exploration Department, unpublished report, no. OB107.

APPENDICES

A1 STRUCTURAL DATA

Structural data from diamond drillholes and open-pit mines are presented in this section in tabular format. The data are grouped according to location in either the Zuleika district (Figure A1.1 p.260), or the Ora Banda district (Figure A1.2 p.282). Geological maps of the open-pits are included with the structural data in each section. Slight differences in structural styles led to different mapping schemes between the two main areas, and these differences are detailed in 'explanation of codes' listed at the beginning of each group of tables.

A1.1 Data collection methods

All open-pit mapping was carried out using a compass-and-tape method. Data were plotted in the field, onto open-pit maps that show the pit topography as a string. Locations were determined by tape measurement from known points within the pits.

Mapping of diamond drill core employed the Alpha/Beta method for the measurement of geological structures. The Alpha/Beta method entails measurement of two angles, 1. the angle between the structure and the core axis (Alpha), and 2. the angle between the top of core orientation mark and the bottom-most part of the ellipse that a planar structure makes with the core. Beta is measured in a clockwise direction, around the core, looking downhole.

This method treats the core as being in a temporary vertical reference frame, hence Alpha is a 'local' dip and Beta is a 'local' dip direction. The measurements were then rotated back to the true drillhole orientation using DIPS 3.1 structural analysis software. The same operation can be done by simple rotations on a stereonet.

Of the several methods available for core measurement, Alpha/Beta can produce quite accurate results, but the error in the Beta measurement increases dramatically as Alpha approaches 90º. Several other sources of error in this method are outlined in Vearncombe and Vearncombe (1998c). The amount of error can be minimised with a strong focus on quality control during drilling, core orientation and mapping.

A1.2 Zuleika district

Geological mapping was conducted at five open pit mines in the Zuleika district including Anthill, Porphyry, Bowerbird, Wattlebird and Bullant mines. None of these mines are currently operating and in the case of the Bowerbird mine, a small trial mining pit is the only area of exposure.

At the Anthill mine, exposures were limited hence only few observations are made here. The Wattlebird mine comprises two open-pit exposures and most of the observations were made from the southern pit, which exposes unweathered rocks in the bottom of the pit. At the time of mapping the Bullant mine was not operating and the majority of the data were collected during this time, but subsequent mining has exposed the Zuleika Shear Zone to greater depth and some of the data and samples were collected from these exposures.

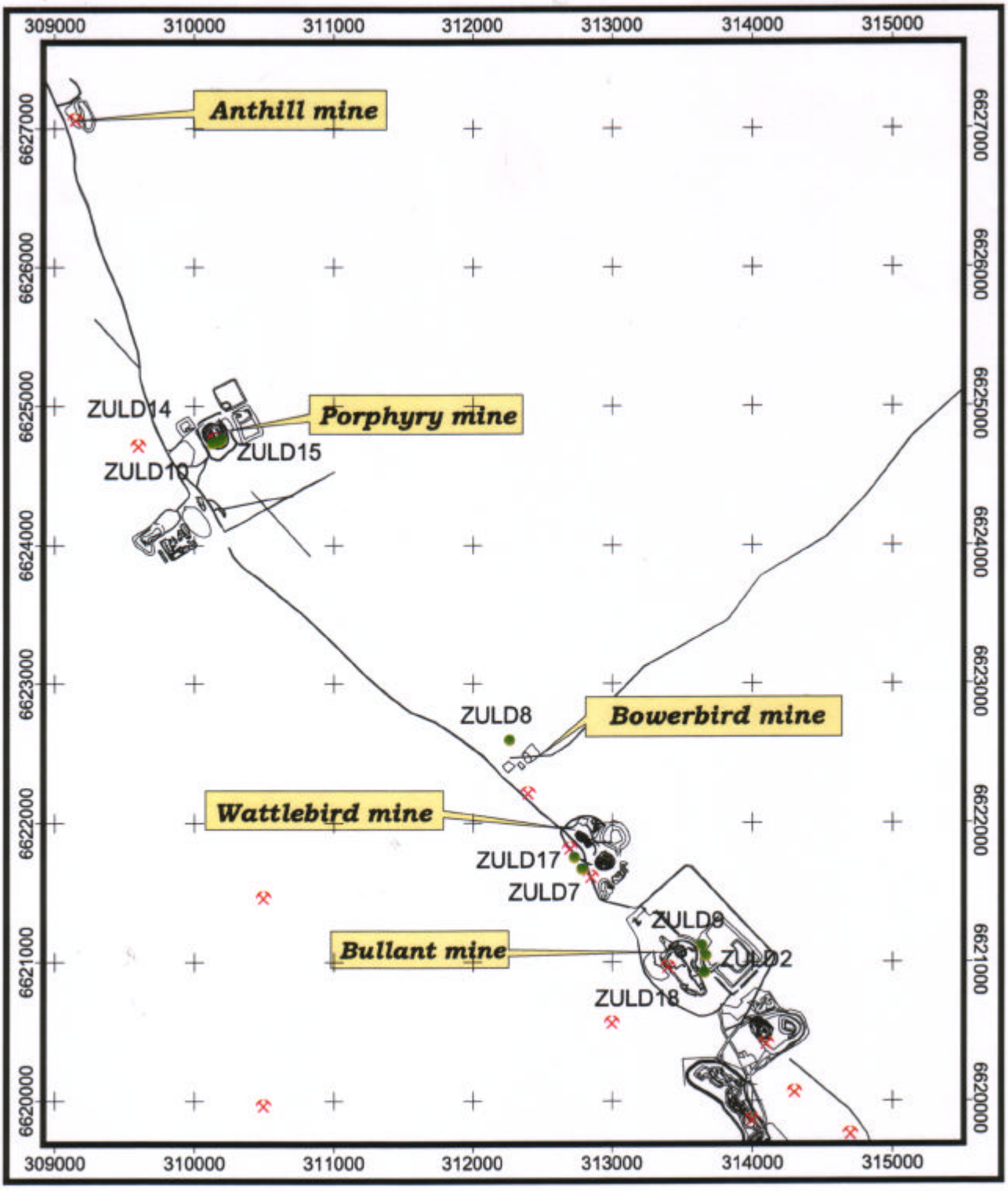

Figure A1.5 - Location plan of drillholes sampled in the Zuleika district

Table A1.1 – Explanation of codes used for drill hole logging in the Zuleika district

VEINS

V1	-	Minor quartz / quartz-carbonate vein
V2	-	Sugary quartz vein
V3	-	Vuggy quartz vein
V4	-	Shear / breccia vein
V5	-	Vein cross-cutting foliations / shear zones
V6	-	Vein cross-cutting all other features
V7	-	Milky buck quartz vein
V8	-	Translucent grey quartz vein
V9	-	Translucent clear vein
V10	-	Vein of material other than quartz (eg chlorite)
SRpy	-	Pyrite stringer vein
SRpo	-	Pyrrhotite stringer vein
SRcp	-	Chalcopyrite stringer vein

SHEAR ZONES

SH1	-	Shear zone undefined
SH2	-	Breccia zone
SH3	-	Fault surface
SH4	-	Cataclasite zone
SH5	-	Mylonitic shear zone

FOLIATIONS

FL1	-	Foliation undefined
FL2	-	Spaced foliation/Cleavage
FL3	-	Joint
FL4	-	Fracture foliation
FL5	-	Continuous foliation/Cleavage

BEDDING

BED1	-	Undefined bedding contact

MINERAL CODES

ab - albite	**py** - pyrite	**bi** - biotite	**ep** - epidote
cb - carbonate	**po** - pyrrhotite	**mu** - muscovite	**si** - silica
ch - chlorite	**cp** - chalcopyrite	**ca** - calcite	**qT** – translucent quartz
ac - actinolite	**sph** - sphalerite	**fl** - flourite	**qM** – milky quartz
ta - talc	**asp** - arsenopyrite	**qz** - quartz	**fu** - fuchsite
fd - feldspar	**mo** - molybdenite	**ka** - kaolinite	**hm** - hematite
to - tourmaline			

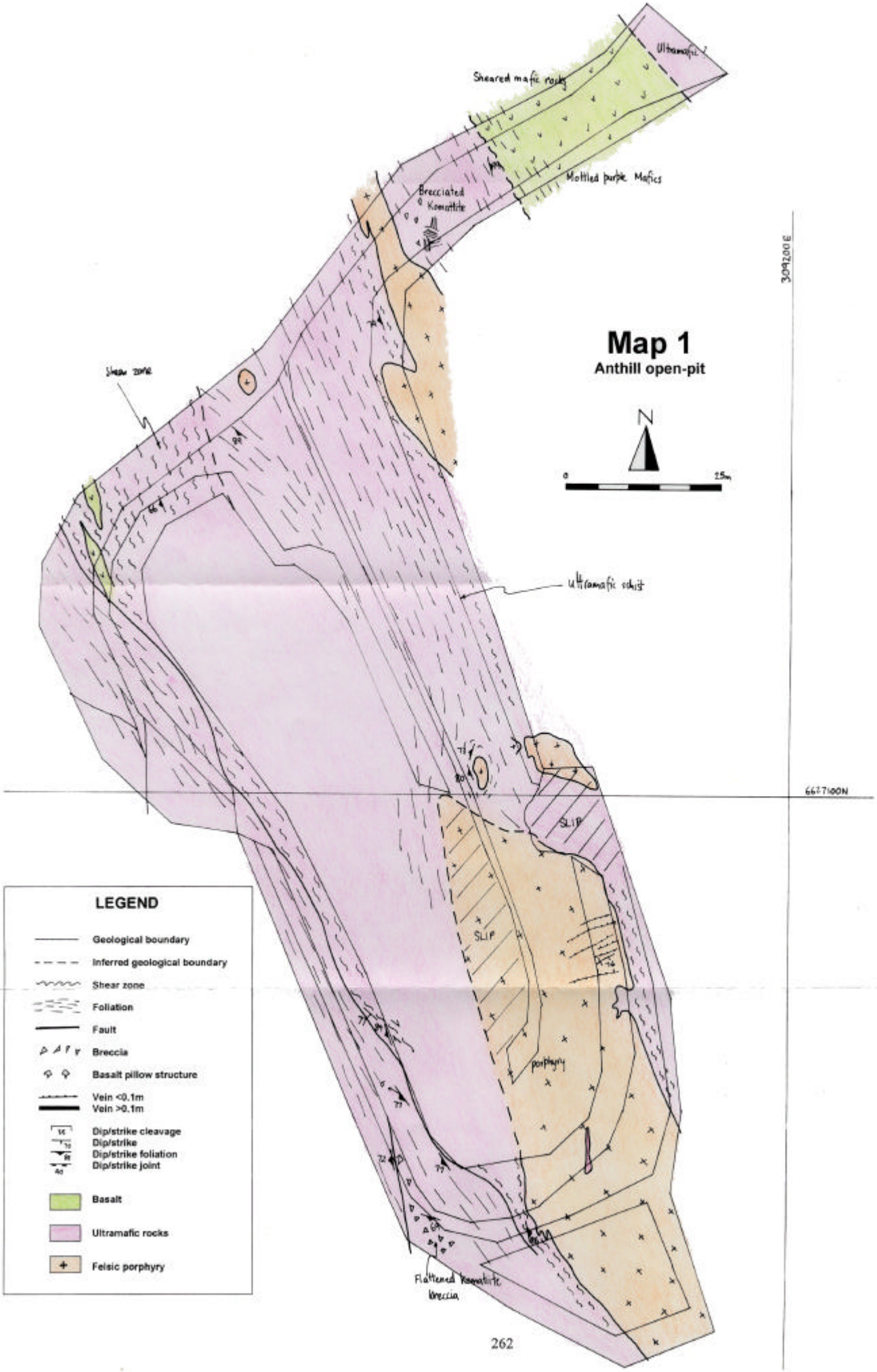
Map 1
Anthill open-pit
N
0
25m
Sheared mafic rocks
Ultramafic ?
Mottled purple Mafics
Brecciated Komatiite
Shear zone
Ultramafic schist
SLIP
SLIP
porphyry
Flattened Komatiite breccia
3092000E
6627100N
LEGEND
Geological boundary
Inferred geological boundary
Shear zone
Foliation
Fault
Breccia
Basalt pillow structure
Vein <0.1m
Vein >0.1m
Dip/strike cleavage
Dip/strike
Dip/strike foliation
Dip/strike joint
Basalt
Ultramafic rocks
Felsic porphyry

Table A1.2 - Anthill Deposit, structural data from open-pit mapping

HOLE NO	DEPTH	STRUCTURE	ALPHA	BETA	STRIKE	DIP	DIP DIRECTION	MINERALOGY	ALTERATION	GROUP	OVERPRINTING	HOLE DIP	HOLE AZIM	Au VALUE	COMMENTS
Pit	-	schistosity	-	-	336	80	66	-	-	Lmin	-	-	-	-	Pervasive schistosity in weathered mafics
Pit	-	schistosity	-	-	15	73	285	-	-	Lmin	-	-	-	-	Schistosity orientation deflected around porphyry body
Pit	-	quartz vein	-	-	67	76	157	-	-	Lmin	-	-	-	-	50mm quartz vein cross-cutting porphyry
Pit	-	shear zone	-	-	345	89	255	-	-	Lmin	-	-	-	-	Ductile shear zone
Pit	-	shear zone	-	-	314	73	224	-	-	Lmin	xprev	-	-	-	Dextral shear zone with lensoid quartz veins cross-cutting main shear
Pit	-	quartz vein	-	-	358	72	268	-	-	Lmin	-	-	-	-	Ferruginous, folded quartz vein
Pit	-	schistosity	-	-	335	66	265	-	-	Lmin	-	-	-	-	Main schistosity in north wall of pit
Pit	-	shear zone	-	-	325	77	235	-	-	Lmin	-	-	-	-	Shear zone
Pit	-	lineation	-	-	-	5	327	-	-	Lmin	-	-	-	-	Stretching lineation in the plane of previous shear zone

Table A1.3 - Bowerbird Deposit - structural data from diamond drill core

HOLE NO	DEPTH	STRUCTURE	ALPHA	BETA	STRIKE	DIP	DIP DIRECTION	MINERALOGY	ALTERATION	GROUP	OVERPRINTING	HOLE DIP	HOLE AZIM	Au VALUE	COMMENTS
ZULD8	177.10	shear zone	43	147	106	88	196	qz,cb,wr	-	SH1	-	39	220	-	5cm shear zone with wallrock breccia fragments
ZULD8	177.10	qcb vein	26	177	127	66	217	qz,cb	-	V1	-	39	220	-	2mm quartz carbonate vein
ZULD8	177.10	qcb vein	26	283	26	65	116	qz,cb	-	V1	-	39	220	-	1mm quartz carbonate vein
ZULD8	177.50	foliation	39	153	109	82	199	ch?,si	-	FL1	-	39	220	-	Intense schistosity
ZULD8	177.60	foliation	48	156	114	90	204	ch?,si	-	FL1	-	39	220	-	Intense schistosity
ZULD8	191.30	mylonite	43	175	126	83	216	si,ch,mu	-	FL1	-	39	220	-	Mylonitic foliation
ZULD8	191.40	fracture	52	54	77	40	347	qz	-	V1	-	39	220	-	Quartz filled joint plane
ZULD8	191.85	foliation	52	171	124	89	34	wr	-	BED1	-	39	220	-	Distinct lithologic contact with transposed foliation
ZULD8	192.10	qcb vein	25	203	152	68	242	qz	-	V5	x-cuts fol	39	220	-	1mm quartz filled fracture cross-cuts foliation
ZULD8	192.60	quartz vein	33	274	15	68	105	qz	-	V6	x-cuts all	39	220	-	5mm quartz vein
ZULD8	192.60	foliation	63	161	121	77	31	qz,mu	-	BED1	-	39	220	-	Lithologic contact x-cut by foliation
ZULD8	192.60	quartz vein	33	198	145	74	235	qz	-	V5	x-cuts fol	39	220	-	1mm quartz vein cross-cuts foliation
ZULD8	194.00	mylonite	61	167	123	80	33	qz,mu	-	FL1	-	39	220	-	Mylonitic foliation
ZULD8	194.60	quartz vein	30	284	23	62	113	qz	-	V1	-	39	220	-	2mm recrystallised quartz vein
ZULD8	195.40	mylonite	53	166	121	88	31	mu,qz ribbons	-	FL1	-	39	220	0.05	Mylonitic foliation
ZULD8	195.80	quartz vein	55	162	119	85	29	rxt qz	-	V1	-	39	220	0.05	Recrystallised 1mm quartz vein parallel to foliation
ZULD8	195.80	quartz vein	23	264	18	81	108	qz	-	V6	x-cuts all	39	220	0.05	5mm recrystallised quartz vein x-cuts all
ZULD8	196.20	ultramylonite	53	181	130	88	40	mu,qz ribbons	-	FL1	-	39	220	0.28	Intense mylonite - sub gneissic?
ZULD8	196.80	quartz vein	5	262	31	87	301	qz	-	V1	-	39	220	0.28	10mm recrystallised quartz vein
ZULD8	197.75	mylonite	53	182	131	88	41	qz ribbons	-	FL1	-	39	220	0.01	Intense mylonite
ZULD8	198.55	quartz vein	33	287	21	58	111	qz	-	V1	-	39	220	0.22	2mm quartz vein
ZULD8	198.60	mylonite	50	186	133	90	223	qz ribbons	-	FL1	-	39	220	0.22	Ultramylonite foliation with gneissic segregation?
ZULD8	200.00	quartz vein	27	342	73	20	163	qz	-	V1	-	39	220	0.09	2mm recrystallised quartz vein
ZULD8	200.50	quartz vein	40	344	30	13	120	qzT	-	V1	-	39	220	0.09	6mm recrystallised quartz vein
ZULD8	201.15	mylonite	37	207	151	80	241	mu,bi	-	FL1	-	39	220	0.06	Mylonitic foliation
ZULD8	201.30	quartz vein	53	326	177	28	87	qzT	-	V5	-	39	220	0.06	3cm recrystallised comb textured quartz vein
ZULD8	201.50	mylonite	40	196	142	81	232	qz ribbons	-	FL1	-	39	220	0.06	Mylonitic foliation
ZULD8	208.85	mylonite	46	170	123	86	213	qz,mu,bi,ch	-	FL1	-	39	220	0.01	Mylonitic foliation
ZULD8	209.25	quartz vein	34	169	120	74	210	qz	ch,bi	V4	-	39	220	0.02	3mm sheared quartz vein
ZULD8	209.40	mylonite	45	168	121	85	211	si,mu	-	FL1	-	39	220	0.02	Mylonitic foliation
ZULD8	212.00	quartz vein	18	285	34	68	124	qzT	-	V1	-	39	220	0.01	Recrystallised quartz vein
ZULD8	213.75	quartz vein	30	269	15	73	105	qzT,cb	-	V5	-	39	220	0.01	5mm crack-seal quartz vein
ZULD8	228.70	quartz vein	84	93	122	52	32	qzT	-	V6	x-cuts all	39	220	-	8mm crack-seal quartz vein

HOLE NO	DEPTH	STRUCTURE	ALPHA	BETA	STRIKE	DIP	DIP DIRECTION	MINERALOGY	ALTERATION	GROUP	OVERPRINTING	HOLE DIP	HOLE AZIM	Au VALUE	COMMENTS
ZULD8	177.10	shear zone	43	147	106	88	196	qz,cb,wr	-	SH1	-	39	220	-	5cm shear zone with wallrock breccia fragments
ZULD8	228.85	quartz vein	52	150	112	86	22	qzT,qzM	-	V6	x-cuts all	39	220	-	3mm comb textured crack-seal quartz vein
ZULD8	229.60	quartz vein	32	213	158	78	248	qzM	-	V1	-	39	220	-	3mm quartz vein parallel to foliation
ZULD8	232.65	quartz vein	27	200	149	69	239	qzM,fu	-	V2	-	39	220	-	5mm boudinaged milky quartz vein
ZULD8	233.45	quartz vein	45	213	152	90	242	qz,cb	-	V1	-	39	220	-	2mm quartz vein parallel to foliation
ZULD8	233.45	foliation	50	183	131	90	221	bi,ch,qz	-	FL1	-	39	220	-	Intense schistosity
ZULD8	233.45	quartz vein	78	107	116	56	26	qzT	-	V1	-	39	220	-	2mm translucent recrystallised quartz vein
ZULD8	233.75	quartz vein	16	303	48	55	138	qzT	-	V6	x-cuts all	39	220	-	10mm recrystallised quartz vein
ZULD8	259.00	shear zone	35	137	95	84	185	qz,cb,ch	-	FL1	-	39	220	-	Intense shear foliation with wallrock fragments
ZULD8	260.80	quartz vein	45	217	155	90	65	qzT	-	V5	-	39	220	0.01	2cm translucent comb texured quartz vein
ZULD8	263.80	quartz vein	42	287	11	54	101	qzT	-	V6	x-cuts all	39	220	0.01	2cm translucent comb texured quartz vein
ZULD8	264.20	quartz vein	17	151	98	63	188	qz,fu	-	V5	x-cuts fol	39	220	0.85	Recrystallised quartz vein
ZULD8	264.30	quartz vein	40	299	18	47	108	qzT	-	V5	-	39	220	0.85	5cm crack-seal translucent quartz vein
ZULD8	264.50	quartz vein	19	334	74	31	164	qzT	-	V1	-	39	220	0.85	10mm recrystallised quartz vein
ZULD8	265.00	shear zone	39	187	135	79	225	qz,ch,bi	-	FL1	-	39	220	1.96	Intense schistosity
ZULD8	265.00	quartz vein	58	282	171	52	81	rxt qz	-	V1	-	39	220	1.96	1mm recrystallised quartz vein
ZULD8	265.15	quartz vein	49	181	130	89	220	rxt qz	ch	V5	x-cuts fol	39	220	1.96	1mm fine grained recrystallised quartz vein
ZULD8	265.20	foliation	30	190	139	70	229	ch	-	FL2	-	39	220	1.96	Spaced foliation cross-cuts dominant schistosity
ZULD8	272.65	shear zone	57	34	360	29	360	mu,si,qz	-	SH1	-	39	220	0.36	Intensely sheared and brecciated felsic porphyry
ZULD8	274.70	quartz vein	52	15	96	17	6	qzT	-	V6	x-cuts all	39	220	0.22	5mm translucent quartz vein
ZULD8	274.95	quartz vein	3	269	37	89	127	qz,cb	-	V5	-	39	220	0.22	2cm recrystallised crack-seal folded quartz vein
ZULD8	275.45	foliation	31	187	136	71	226	bi,ch	-	FL2	-	39	220	7.08	Thin interbreccia biotite sutures
ZULD8	276.15	quartz vein	34	317	34	35	124	qzT	-	V5	-	39	220	0.07	4cm quartz vein
ZULD8	290.00	shear zone	34	197	144	75	234	ta,ch	-	SH1	-	39	220	0.01	Intensely sheared breccia
ZULD8	315.00	shear zone	20	206	157	64	247	ta,ch	-	SH1	-	39	220	-	Intense shear zone
ZULD8	323.85	shear zone	30	229	171	83	261	ta,ch	-	SH1	-	39	220	-	Intense shear zone with breccia wallrock fragments

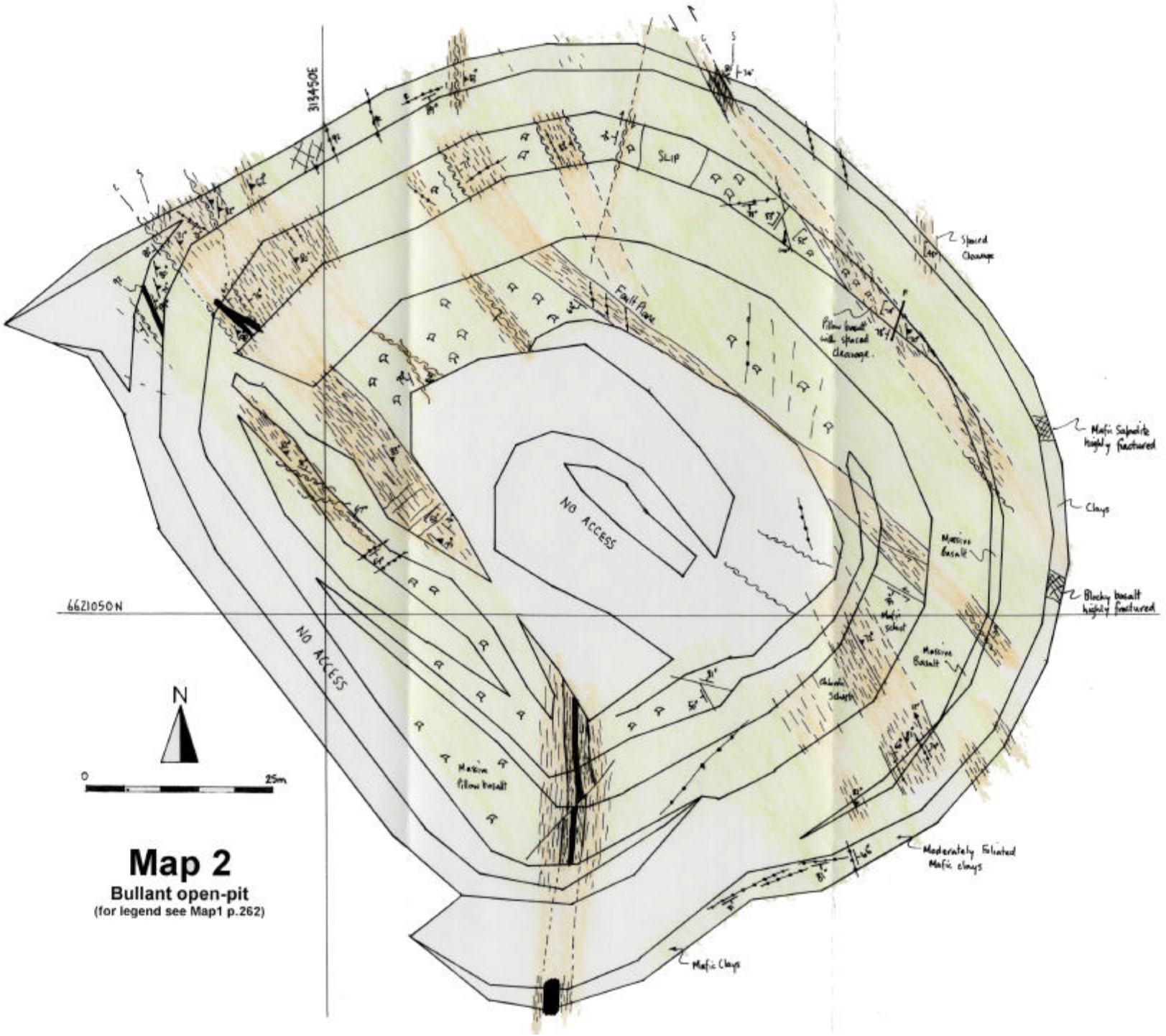

Map 2

Bullant open-pit

(for legend see Map1 p.262)

Table A1.4 - Bullant Deposit - structural data from pit mapping and diamond drill core

HOLE NO	DEPTH	STRUCTURE	ALPHA	BETA	STRIKE	DIP	DIP DIRECTION	MINERALOGY	ALTERATION	GROUP	OVERPRINTING	HOLE DIP	HOLE AZIM	Au VALUE	COMMENTS
ZULD9	154.75	shear zone	45	218	168	75	78	ch,cb	-	SH1	-	56	232	0.01	Thin shear zone at contact of folded quartz carbonate vein
ZULD9	155.00	breccia zone	61	228	167	58	77	qz,cb,ep	-	V4	-	56	232	0.01	10mm crack-seal breccia vein
ZULD9	155.40	qz ab vein	24	177	139	81	229	qz,ab,cb	-	V1	-	56	232	0.01	3mm irregular quartz albite vein
ZULD9	155.40	qz cb vein	30	311	63	43	158	qz,cb,ep	-	V6	xprev	56	232	0.01	5mm comb textured vein "late"
ZULD9	155.80	shear zone	49	150	121	73	31	ch,cb,mu	-	SH1	-	56	232	0.01	20mm intense shear zone with quartz veining
ZULD9	155.10	joint	55	16	52	10	322	qz,cb,ep	-	FL3	-	56	232	0.01	1mm late pervasive microfracturing
ZULD9	157.40	qz ab vein	42	165	130	82	40	qz,ab,cb	-	V1	-	56	232	0.01	10mm variably albitised quartz vein
ZULD9	158.00	shear zone	17	124	89	87	179	ch,ep,qz,cb	-	SH1	-	56	232	0.01	10mm intense mylonitic shear zone with clear quartz veins
ZULD9	158.90	qz ep vein	73	252	166	43	76	qz,ep,ab	-	V1	-	56	232	0.01	2mm quartz muscovite (epidote?) vein, pervasive microfracturing
ZULD9	159.75	qz cb fract	56	233	173	61	83	qz,cb,cp	-	FL2	-	56	232	0.01	<1mm pervasive microfracturing
ZULD9	159.75	qz cb vein	41	316	61	33	151	qz,cb	-	V1	xprev	56	232	0.01	2mm irregular crack-seal quartz carbonate vein
ZULD9	160.55	qz cb ab vein	49	253	9	59	99	qz,cb,ab	-	V4	-	56	232	0.05	5-20mm vein with wallrock breccia
ZULD9	160.55	shear joint	38	70	61	49	331	qz,cb,ab	-	FL3	xprev	56	232	0.05	Shear joint with qz cb ab fill
ZULD9	160.60	qz cb ab vein	68	224	161	52	71	qz,cb,ab	-	V1	-	56	232	0.05	5mm quartz carbonate +/- albite vein
ZULD9	162.00	qz cb shear vn	32	170	133	89	223	qz,cb,ch,ep	-	V4	-	56	232	0.02	Shear zone with quartz carbonate + axinite
ZULD9	165.40	qz ab vein	42	127	103	73	13	qz,cb,ab	-	V1	-	56	232	0.02	5mm quartz albite vein with wallrock fragments
ZULD9	168.80	qz cb ab vein	42	83	74	53	344	qz,cb,axinite	-	V4	-	56	232	0.01	10mm shear joint with wallrock breccia + axinite
ZULD9	180.80	qz cb sh joint	69	250	172	46	82	qz,cb	-	V4	-	56	234	0.02	5mm shear joint with brecciated wallrock fragments
ZULD9	184.40	shear vein	24	237	14	87	104	qz,cb,ch,ep	bi	V4	-	56	234	0.02	10mm laminated quartz carbonate shear vein with euhedral quartz
ZULD9	186.50	foliation	27	267	35	70	125	ch,bi,ep	-	FL2	-	56	234	0.2	Spaced foliation
ZULD9	188.40	shear fol	48	269	21	53	111	ch,bi,qz,cb	-	FL1	-	56	234	0.23	Intense shear foliation
ZULD9	189.00	shear fol	45	295	41	42	131	ch,bi,qz,cb	bi	FL1	-	56	234	0.24	Pervasive spaced shear foliation
ZULD9	189.20	qz vein	39	293	46	47	136	qz,cb	-	V1	-	56	234	0.24	5mm euhedral quartz vein with carbonate infill
ZULD9	189.75	shear vein	34	297	53	48	143	qz,cb	-	V4	-	56	234	0.24	30mm shear vein with slivers of wallrock boudins
ZULD9	193.30	qz cb vein	81	118	131	39	41	qz,cb,mu	si	V1	-	56	234	0.01	10mm euhedral quartz vein with carbonate muscovite infill
ZULD9	200.40	shear fol	46	171	137	78	47	qz,ch,bi	-	FL1	-	56	234	1.93	Intense pervasive shear foliation with chlorite slivers
ZULD9	202.00	qz bi vein	46	285	33	46	123	qz,bi,po	-	V5	xprev	56	234	2.51	Late crosscutting quartz biotite pyrrhotite vein
ZULD9	202.10	shear fol	52	171	138	72	48	bi,ch,qz	-	FL1	-	56	234	2.51	Intense continuous shear foliation
ZULD9	203.25	qz vein	57	275	15	44	105	qz,cb,bi,py,po	cb	V5	xprev	56	234	2.45	25mm late crosscutting coarse-grained biotite vein
ZULD9	204.25	biotite vein	40	302	131	41	141	bi,po	-	V10	-	56	234	4.83	25mmbiotite vein with open space growth textures
ZULD9	204.65	foliation	42	204	161	80	71	bi,ch,cb	-	FL2	-	56	234	4.83	Intense domainal shear foliation
ZULD9	205.15	qz vein	38	309	57	38	147	qz,cb,bi,py,po	-	V5	xprev	55	233	0.83	25mm crosscutting crack-seal quartz carbonate vein with biotite infill
ZULD9	207.20	shear zone	40	231	360	76	90	ch,si,ep	-	SH1	-	55	233	4.12	Intense orthomylonite

HOLE NO	DEPTH	STRUCTURE	ALPHA	BETA	STRIKE	DIP	DIP DIRECTION	MINERALOGY	ALTERATION	GROUP	OVERPRINTING	HOLE DIP	HOLE AZIM	Au VALUE	COMMENTS
ZULD9	208.25	qz vein	48	239	1	66	91	qz,cb	-	V5	xprev	55	233	0.51	10mm euhedral quartz vein with carbonate infill
ZULD9	208.55	qz vein	56	250	2	56	92	qz,cb	-	V6	xall	55	233	0.51	20mm euhedral quartz vein with chlorite infill
ZULD9	209.30	shear fol	43	245	8	68	98	qz,si	-	SH1	-	55	233	0.05	Intense continous mylonitic foliation with chlorite spots
ZULD9	214.40	shear fol	31	230	4	84	94	ch,si,ep	-	SH1	xnxt	55	233	0.22	Contact parallel to foliation with veined zone also foliated
ZULD9	214.45	fol parall qz vn	55	212	162	67	72	qz,cb	-	V1	-	55	233	0.22	2mm quartz carbonate vein parallel to foliation
ZULD9	214.80	qz cb vein	41	197	155	83	65	qz,cb	-	V6	xnxt	55	233	0.22	10mm quartz carbonate infill vein
ZULD9	214.85	qz cb vein	58	199	153	66	63	qz,cb	-	V5	-	55	233	0.22	1mm quartz carbonate veins crosscut foliation
ZULD9	215.70	qz po vein	41	184	146	84	56	qz,mu,po	sp,ga	V4	-	55	233	2.93	3200mm quartz vein with extensive wallrock fragments and base metal sulphides
ZULD9	220.15	shear zn ct	50	239	360	65	90	-	-	SH1	-	55	233	2.26	Intense sheared rock in contact with undeformed basalt
Pit	-	shear zone	-	-	10	73	280	-	-		-	-	-	-	Shear zone in highly altered basalt, intense ductile fabric
Pit	-	stretching lin	-	-	-	9	185	-	-	-	-	-	-	-	Stretching lineation in previous shear plane
Pit	-	shear zone	-	-	155	84	245	-	-	-	-	-	-	-	Main Zuleika shear zone
Pit	-	shear zone	-	-	179	86	269	-	-	-	-	-	-	-	10cm shear zone discrete S-C fabric
Pit	-	shear vein	-	-	13	77	103	qz	-	-	-	-	-	-	3000mm vein in southwest wall of pit
Ramp	3	quartz vein	-	-	61	31	151	-	-	-	-	-	-	-	10-15m long quartz vein with schistose chloritic fragments
Top Bench	10	quartz vein	-	-	80	89	170	-	-	-	-	-	-	-	Subvertical quartz vein
Top Bench	14	shear vein	-	-	162	66	72	-	-	-	-	-	-	-	60mm foliation parallel shear vein
Top Bench	109	cleavage	-	-	2	48	92	-	-	-	-	-	-	-	5mm spaced cleavage in schistose basalt
Top Bench	143	C-plane	-	-	151	80	61	-	-	-	-	-	-	-	C-plane of left lateral shear zone
Top Bench	143	S-plane	-	-	182	74	92	-	-	-	-	-	-	-	S-plane of left lateral shear zone
Top Bench	143	lineation	-	-	-	59	120	-	-	-	-	-	-	-	S-C intersection lineation strike-slip movement with minor normal component
Top Bench	176	shear zone	-	-	176	83	86	-	-	-	-	-	-	-	Intense shear zone
Top Bench	182	quartz vein	-	-	66	84	156	-	-	-	-	-	-	-	50mm quartz vein highly fractured
Top Bench	210	cleavage	-	-	160	62	70	-	-	-	-	-	-	-	Spaced cleavage
Top Bench	215	schistosity	-	-	173	82	83	-	-	-	-	-	-	-	-
Top Bench	215	shear zone	-	-	150	62	60	-	-	-	-	-	-	-	-
Top Bench	217	quartz vein	-	-	122	73	212	-	-	-	-	-	-	-	-
Top Bench	217	schistosity	-	-	148	81	58	-	-	-	-	-	-	-	-
Top Bench	223	shear zone	-	-	143	80	233	-	-	-	-	-	-	-	-
Top Bench	227	schistosity	-	-	160	76	70	-	-	-	-	-	-	-	-
Top Bench	227	schistosity	-	-	171	80	81	-	-	-	-	-	-	-	-
Top Bench	229	quartz vein	-	-	158	59	68	-	-	-	-	-	-	-	-
Top Bench	230	shear zone	-	-	146	81	236	-	-	-	-	-	-	-	-
Ramp	8	schistosity	-	-	155	82	65	-	-	-	-	-	-	-	Strong schistosity in mottled basalt
Ramp	17	quartz vein	-	-	154	60	64	-	-	-	-	-	-	-	Highly fratured schistosity parallel quartz vein

HOLE NO	DEPTH	STRUCTURE	ALPHA	BETA	STRIKE	DIP	DIP DIRECTION	MINERALOGY	ALTERATION	GROUP	OVERPRINTING	HOLE DIP	HOLE AZIM	Au VALUE	COMMENTS
Ramp	21	quartz vein	-	-	152	74	62	-	-	-	-	-	-	-	Intense shear zone with large quartz vein with pinch and swell structure
Ramp	21	schistosity	-	-	155	81	65	-	-	-	-	-	-	-	Pervasive schistosity, S-C fabric shows left-lateral movement
Ramp	21	stretching lin	-	-	-	12	344	-	-	-	-	-	-	-	Stretching lineation defined by aligned micas
Ramp	39	fault	-	-	140	77	50	-	-	-	-	-	-	-	Fault plane with intense schistosity
Ramp	58	C-plane	-	-	143	52	53	-	-	-	-	-	-	-	Thin quartz veins parallel to C-plane of shear zone
Ramp	79	schistosity	-	-	175	72	85	-	-	-	-	-	-	-	Schistosity in basalt
Ramp	79	fault	-	-	18	78	288	-	-	-	-	-	-	-	Late fault
Ramp	79	cleavage	-	-	18	74	108	-	-	-	xprev2	-	-	-	Crosscutting spaced cleavage
Ramp	98	cleavage	-	-	46	52	136	-	-	-	-	-	-	-	Cleavage in pillow basalt
Ramp	100	fault	-	-	164	74	254	-	-	-	-	-	-	-	Smooth fault plane
Ramp	100	stretching lin	-	-	-	10	173	-	-	-	-	-	-	-	Left lateral slickensides
Ramp	100	cleavage	-	-	35	83	305	-	-	-	xprev2	-	-	-	Spaced cleavage cuts previous fault
Ramp	109	quartz vein	-	-	82	78	172	-	-	-	-	-	-	-	10mm quartz vein in pillow basalt
Ramp	125	shear zone	-	-	10	73	280	-	-	-	-	-	-	-	Poorly defined S-C fabric shows left lateral movement
Ramp	129	shear zone	-	-	155	83	245	-	-	-	-	-	-	-	4m wide ductile shear zone
Ramp	129	Riedel fracture	-	-	134	82	44	-	-	-	-	-	-	-	Riedel? Fractures within the shear zone
Ramp	129	Riedel fracture	-	-	167	67	257	-	-	-	-	-	-	-	Riedel? Fractures within the shear zone
Ramp	129	Riedel fracture	-	-	25	71	295	-	-	-	-	-	-	-	Riedel? Fractures within the shear zone
Ramp	146	shear zone	-	-	154	71	64	-	-	-	-	-	-	-	-
Ramp	171	schistosity	-	-	150	80	60	-	-	-	-	-	-	-	-
Ramp	175	quartz vein	-	-	140	61	50	-	-	-	xnxt	-	-	-	-
Ramp	175	schistosity	-	-	161	80	71	-	-	-	-	-	-	-	-
W-Ramp	20	shear band	-	-	116	81	26	-	-	-	-	-	-	-	Thin shear band overprints main shear zone
W-Ramp	32	quartz vein	-	-	52	64	142	-	-	-	-	-	-	-	50mm quartz vein with minor foliation at the edge
W-Ramp	63	shear zone	-	-	162	65	72	-	-	-	-	-	-	-	-
W-Ramp	63	quartz vein	-	-	161	80	71	-	-	-	-	-	-	-	-
W-Ramp	63	schistosity	-	-	153	72	63	-	-	-	-	-	-	-	Intense chlorite schist
W-Ramp	63	fault	-	-	120	33	210	-	-	-	-	-	-	-	Low angle crosscutting fault
Base	17	quartz vein	-	-	130	76	40	-	-	-	-	-	-	-	Quarzt vein in intensely cleaved mafic
Base	17	cleavage	-	-	43	52	133	-	-	-	-	-	-	-	Crosscutting cleavage
Base	17	schistosity	-	-	132	75	42	-	-	-	-	-	-	-	Main schistosity
Base	39	schistosity	-	-	146	83	56	-	-	-	-	-	-	-	Chlorite schist
Base	39	C-plane	-	-	96	35	186	-	-	-	-	-	-	-	-
Base	39	S-plane	-	-	110	51	200	-	-	-	-	-	-	-	-
Base	41	shear band	-	-	151	72	61	-	-	-	-	-	-	-	Thin ductile shear band

HOLE NO	DEPTH	STRUCTURE	ALPHA	BETA	STRIKE	DIP	DIP DIRECTION	MINERALOGY	ALTERATION	GROUP	OVERPRINTING	HOLE DIP	HOLE AZIM	Au VALUE	COMMENTS
Base	46	shear zone	-	-	120	85	210	-	-	-	xprev	-	-	-	0.5m wide ductile shear zone
Base	58	shear zone	-	-	140	90	-	-	-	-	-	-	-	-	1.5m wide shear zone
Base	70	fault	-	-	125	64	215	-	-	-	-	-	-	-	Large fault plane at east wall
Pit (1999)	-	shear zone	-	-	146	74	56	-	-	-	-	-	-	-	Shear zone
Pit (1999)	-	lineation	-	-	-	16	331	-	-	-	-	-	-	-	Lineations in previous shear zone
Pit (1999)	-	cross fault	-	-	104	86	194	-	-	-	-	-	-	-	Large cross fault
Pit (1999)	-	lineation	-	-	-	25	296	-	-	-	-	-	-	-	Lineations in previous shear zone
Pit (1999)	-	shear zone	-	-	302	87	32	-	-	-	-	-	-	-	Shear zone
Pit (1999)	-	lineation	-	-	-	14	314	-	-	-	-	-	-	-	Lineations in previous shear zone
Pit (1999)	-	shear zone	-	-	131	76	41	-	-	-	-	-	-	-	Shear zone
Pit (1999)	-	lineation	-	-	-	16	321	-	-	-	-	-	-	-	Lineations in previous shear zone
Pit (1999)	-	shear zone	-	-	130	85	40	-	-	-	-	-	-	-	Shear zone
Pit (1999)	-	lineation	-	-	-	14	313	-	-	-	-	-	-	-	Lineations in previous shear zone
Pit (1999)	-	shear zone	-	-	135	79	45	-	-	-	-	-	-	-	Shear zone
Pit (1999)	-	lineation	-	-	-	19	312	-	-	-	-	-	-	-	Lineations in previous shear zone
Pit (1999)	-	shear zone	-	-	168	85	78	-	-	-	-	-	-	-	Cross lode
Pit (1999)	-	shear zone	-	-	174	78	84	-	-	-	-	-	-	-	Cross lode
Pit (1999)	-	lineation	-	-	-	6	332	-	-	-	-	-	-	-	Lineations in previous shear zone
Pit (1999)	-	lineation	-	-	-	6	142	-	-	-	-	-	-	-	Lineations in western main lode
Pit (1999)	-	shear zone	-	-	141	76	51	-	-	-	-	-	-	-	Shear zone
Pit (1999)	-	lineation	-	-	-	16	321	-	-	-	-	-	-	-	Lineations in previous shear zone
Pit (1999)	-	shear zone	-	-	142	79	52	-	-	-	-	-	-	-	Shear zone
Pit (1999)	-	lineation	-	-	-	17	321	-	-	-	-	-	-	-	Lineations in previous shear zone
Pit (1999)	-	thrust fault	-	-	140	61	50	-	-	-	-	-	-	-	Thrust fault in undeformed wasllrocks, 0.5m wide
Pit (1999)	-	lineation	-	-	-	56	55	-	-	-	-	-	-	-	Lineations in previous shear zone

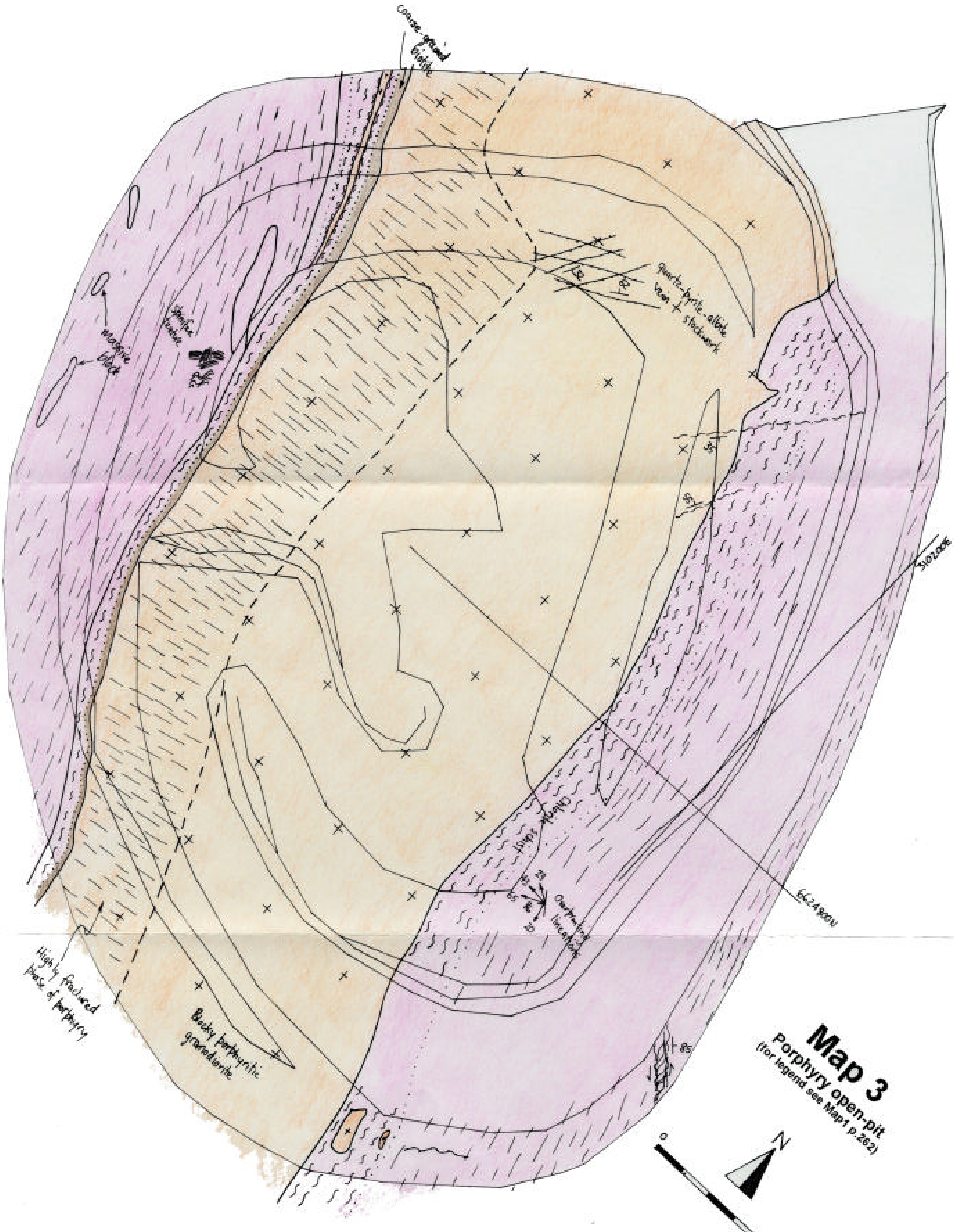

Map 3
Porphyry open-pit
(for legend see Map1 p.262)

Table A1.5 - Porphyry Deposit - structural data from diamond drill core

HOLE NO	DEPTH	STRUCTURE	ALPHA	BETA	STRIKE	DIP	DIP DIRECTION	MINERALOGY	ALTERATION	GROUP	OVERPRINTING	HOLE DIP	HOLE AZIM	Au VALUE	COMMENTS
ZULD10	35.10	fracture	29	305	65	48	335	py,ch,mu	si,ab	FL4	-	60	50	0.09	Thin <1mm fracture plane
ZULD10	40.50	quartz vein	23	335	103	41	13	ch,py,qT	si,ab	V1	xnxt2	60	50	0.08	Thin 2mm quartz chlorite pyrite vein
ZULD10	40.70	py stringer	9	107	69	90	339	py,cb,bi	-	SRPY	xnxt	60	50	0.08	<1mm pyrite stringer vein
ZULD10	40.70	quartz vein	39	65	52	45	142	qz,mu	si,ab	V1	-	60	50	0.08	2mm quartz vein
ZULD10	40.60	foliation	60	252	179	48	269	bi,qz,fd	-	FL5	-	60	50	0.08	Pervasive foliation
ZULD10	40.85	quartz vein	28	85	60	64	150	qz,cb,ch	si,ab	V1	-	60	50	0.08	5mm quartz vein
ZULD10	41.27	contact	34	299	55	47	325	si,bi	-	BED1	-	60	50	0.15	Sharp contact with microgranitic dyke
ZULD10	42.55	py stringer	55	71	74	37	164	py,cb,bi	-	SRPY	xnxt	60	50	0.52	<1mm pyrite stringer vein
ZULD10	42.55	qz,ch vein	23	178	138	84	48	qz,fd,ch	-	V1	-	60	50	0.52	5mm vein with sharp margins
ZULD10	42.90	foliation	53	235	175	59	265	qz,bi,py	-	FL2	-	60	50	0.52	Pervasive spaced foliation
ZULD10	43.00	qz,ch,cb vein	84	225	147	35	237	qz,ch,cb	-	V1	-	60	50	0.48	2mm quartz chlorite carbonate vein
ZULD10	43.00	qz,py cb vein	49	70	66	41	156	qz,py,cb	-	V1	xnxt	60	50	0.48	<1mm quartz carbonate pyrite vein
ZULD10	44.50	qz,ch vein	39	91	72	58	162	qz,cb,ch,py	cb,mu,ab	V3	-	60	50	0.38	5mm coarse-grained vuggy quartz vein
ZULD10	45.65	quartz vein	36	49	34	40	124	qz,cb,py	mu,ab,FeO	V1	-	60	50	0.3	2mm quartz vein with 5mm alteration zone
ZULD10	46.20	qz,ab vein	27	85	60	65	150	qz,ab	si,ab	V1	-	60	50	0.65	5mm quartz albite vein chlorite on fracture planes
ZULD10	46.30	qz vein	69	129	117	46	207	qz,ch,cb	si,ab	V1	xprev	60	50	0.65	1mm quartz vein
ZULD10	48.30	qz,cb,py vein	28	59	38	51	128	qz,cb,bi,py	si,ab	V1	-	60	50	0.27	1mm quartz vein
ZULD10	48.60	quartz vein	42	39	30	30	120	qz,cb	bi,cb,ch,py	V9	-	60	50	0.27	6mm crack-seal recrystallised quartz vein
ZULD10	59.80	quartz vein	41	133	104	72	194	qz,ch,cb	si,ab	V9	-	60	50	0.23	4mm coarse-grained euhdral crack-seal quartz vein
ZULD10	60.75	quartz vein	50	317	53	27	323	qT	py,bi	V9	-	60	50	0.49	<1mm quartz vein with alteration selvedge
ZULD10	63.65	qz,py vein	17	311	78	56	348	qz,py	bi,si	V1	-	60	50	1.04	1mm quartz vein
ZULD10	64.65	quartz vein	30	70	49	55	139	qz,py	bi,si,ab	V1	-	60	50	1.02	1mm crack-seal quartz vein with pyrite slivers
ZULD10	65.70	quartz vein	22	322	87	47	357	qT	si	V9	-	60	50	0.2	5mm coarse-grained euhedral quartz vein
ZULD10	69.30	quartz vein	25	5	147	36	57	qz,cb,ch,py	si	V1	-	60	50	0.18	5mm crack-seal laminated quartz vein
ZULD10	70.50	quartz vein	39	33	19	30	109	qz	si,ab	V1	-	60	50	1.04	5mm crack-seal comb textured quartz vein
ZULD10	77.50	quartz vein	32	250	17	72	287	qz,ch,cb	-	V1	-	60	50	0.78	15mm crack-seal quartz vein
ZULD10	77.60	quartz vein	41	195	151	79	241	qz	bi,ch	V1	-	60	50	0.78	1mm quartz vein with biotite chlorite selvedge
ZULD10	80.10	quartz vein	49	236	178	62	268	qz,ch,py	si,mu	V1	-	60	50	1.26	10mm crack-seal quartz vein with pyrite slivers and wallrock fragments
ZULD10	84.00	quartz vein	52	191	149	68	239	qz,py	si,mu,bi	V1	-	60	52	1.74	5mm crack-seal quartz vein
ZULD10	96.90	foliation	35	226	179	78	269	bi,qz,fd	-	FL5	-	60	52	0.17	Pervasive foliation
ZULD10	175.35	shear zone	50	35	38	23	128	ch,si	-	SH5	-	61	52	0.02	Intense pervasive mylonitic foliation
ZULD10	176.30	shear zone	40	31	18	29	108	ch,ci,cb	-	SH5	-	61	52	0.23	Intense pervasive mylonitic foliation

HOLE NO	DEPTH	STRUCTURE	ALPHA	BETA	STRIKE	DIP	DIP DIRECTION	MINERALOGY	ALTERATION	GROUP	OVERPRINTING	HOLE DIP	HOLE AZIM	Au VALUE	COMMENTS
ZULD10	176.40	quartz vein	54	271	18	45	288	qz,cb,bi,to	-	V9	xprev	61	52	0.23	10mm coarse grained euhedral crosscutting vein
ZULD10	177.00	qz,cb vein	29	40	20	42	110	qz,cb	-	V10	-	61	52	0.01	15mm vein with quartz and coarse-grained carbonate
ZULD10	178.70	qz,cb vein	47	113	95	60	185	qz,cb	qcb	V9	-	61	52	0.02	15mm coarse-grained crack-seal comb textured vein
ZULD10	180.90	shear zone	49	70	67	40	157	ch,si	-	SH5	-	61	52	0.09	Pervasive continuous shear foliation
ZULD10	181.90	qz,cb vein	51	72	71	40	161	qz,cb	-	V5	-	61	52	0.06	3mm boudinaged quartz-carbonate vein parallel to shear zone
ZULD10	187.80	quartz vein	22	225	3	90	273	qz	-	V2	-	61	53	0.05	30mm fine-grained crystalline sugary quartz vein with irregular contacts
ZULD10	188.50	qz,cb vein	22	347	124	41	34	qz,cb	-	V1	-	61	53	0.01	5mm parallel quartz carbonate veins and fractures
ZULD10	194.25	quartz vein	11	92	60	82	150	qz,cb	-	V9	-	61	53	0.04	Coarse-grained euhedral comb textured quartz vein
ZULD10	197.10	qz,cb vein	19	97	68	77	158	qz,cb,bi	-	V1	xnxt	61	53	0.04	10mm sheared quartz carbonate vein
ZULD10	197.15	qz,cb vein	41	348	117	22	27	qz,cb	-	V1	-	61	53	0.04	10mm crack-seal quartz carbonate vein
ZULD10	197.20	foliation	66	291	13	30	283	ch,si	-	FL1	-	61	53	0.01	Pervasive foliation
ZULD10	215.10	shear zone	30	212	170	86	260	qz,cb,ch	bi	SH1	-	61	53	0.01	Intense shear zone with 5-10 cm coarse grained biotite alteration selvedge
ZULD10	215.20	qz,cb vein	46	130	107	66	197	qz,cb	-	V1	-	61	53	0.01	10mm crack-seal carbonate vein
ZULD10	218.55	quartz vein	40	256	20	62	290	qz,cb,bi	-	V1	-	61	53	-	5mm laminated crack-seal quartz vein
ZULD14	36.00	quartz vein	42	321	45	28	135	qz	ab,si	V1	-	51	222	0.86	1mm quartz vein with albite selvedge
ZULD14	36.60	qz,bi vein	21	339	95	35	185	qz,bi	ab,si	V1	-	51	222	0.86	1mm quartz vein with euhedral biotite
ZULD14	40.60	quartz vein	38	319	50	32	140	qz,py	ab,si	V11	-	51	222	0.72	3mm crystalline quartz vein with 8mm selvedge
ZULD14	40.60	quartz vein	33	94	66	68	336	qT	ch	V9	xprev	51	222	0.72	9mm crack-seal quartz vein
ZULD14	40.90	qz,py vein	38	329	60	26	150	qz,bi,py	asi,ab	V11	-	51	222	0.72	2mm quartz-pyrite vein
ZULD14	42.60	qz,py vein	26	326	73	36	163	qT,py	si,ab	V11	-	51	222	1.15	3mm quartz-pyrite vein with 20mm albite-silica selvedge
ZULD14	42.60	qz,py vein	59	319	6	25	96	qz,ab,py	si,ab,hm	V11	xprev	51	222	1.15	2mm quartz vein with 100mm hematite selvedge
ZULD14	48.15	fracture py	59	229	157	64	67	py	-	SRPY	-	51	222	0.53	Thin <1mm pyritic fracture
ZULD14	48.75	foliation	38	226	166	83	76	qz,bi	-	FL1	-	51	222	0.07	Fine grained pervasive foliation in granite
ZULD14	49.25	qcb vein	22	347	107	31	197	qz,cb	-	V3	-	51	222	0.07	Vuggy 3mm quartz carbonate vein
ZULD14	49.25	fracture ch	68	57	95	32	5	ch	-	V10	xprev	51	222	0.07	Chlorite filled fracture
ZULD14	49.90	quartz vein	24	337	90	33	180	qT,py,bi	si,ab	V11	-	51	222	0.77	3mm crack-seal laminated vein, very fine grained pyrite
ZULD14	50.00	qcb vein	60	140	111	65	21	qcb,py	-	V11	-	51	222	0.77	<1mm quartz carbonate vein
ZULD14	50.85	qz,py vein	60	113	98	57	8	qz,bi,py	si,ab	V11	-	51	222	0.75	2mm quartz -pyrite vein , very fine-grained pyrite
ZULD14	51.80	quartz vein	73	82	105	40	15	qT,py	-	V11	-	51	222	0.1	2mm crack-seal quartz vein
ZULD14	52.85	quartz vein	44	339	60	16	150	qz,ch,bi,py	si	V11	-	51	222	0.69	3mm translucent quartz vein with triangular textured biotite, chlorite +/-pyrite
ZULD14	58.60	quartz vein	20	293	46	61	136	qz,py	-	V11	-	51	222	0.49	1mm quartz vein with pyrite in late fractures
ZULD14	58.90	quartz vein	66	271	167	45	77	qz,py	si,ab	V11	-	51	222	0.49	1mm quartz vein with pyrite in late fractures
ZULD14	59.30	quartz vein	17	305	59	56	149	qT,py	-	V11	-	51	222	0.49	5mm laminated quartz vein with 3mm pyrite vein at centre
ZULD14	59.65	quartz vein	18	112	70	90	340	qT,py	si,ab	V11	-	51	222	0.34	2mm comb textured quartz vein

HOLE NO	DEPTH	STRUCTURE	ALPHA	BETA	STRIKE	DIP	DIP DIRECTION	MINERALOGY	ALTERATION	GROUP	OVERPRINTING	HOLE DIP	HOLE AZIM	Au VALUE	COMMENTS
ZULD14	60.60	quartz vein	33	329	68	29	158	qT	si,ab	V11	-	51	222	0.39	2mm quartz vein with triangular textured pyrite in late infill
ZULD14	60.90	quartz vein	36	310	45	39	135	qT,ab	si,ab	V9	-	51	222	0.39	3mm quartz vein with pyrite on fractures
ZULD14	60.95	quartz vein	45	10	3	9	273	qz	si,ab	V1	-	51	222	0.39	<1mm quartz vein
ZULD14	61.00	quartz vein	18	111	69	89	339	qz	si,ab	V1	-	51	222	0.39	1mm crack-seal quartz vein with pyrite on fractures
ZULD14	62.00	quartz vein	25	333	83	34	173	qT,py	si	V11	-	51	222	0.62	10mm translucant quartz vein
ZULD14	62.25	quartz vein	37	291	30	50	120	qz,py	si	V11	-	51	222	0.4	1mm quartz pyrite vein
ZULD14	63.80	qz,ca vein	27	323	68	37	158	qz,bi,ch,ca	-	V1	-	51	222	0.29	10mm crack-seal vein with coarse-grained euhedral calcite
ZULD14	68.30	quartz vein	30	112	77	80	347	qT+/-py	si	V11	-	51	222	0.31	20mm comb textured translucent quartz vein
ZULD14	69.20	qcb vein	48	316	30	29	120	qz,cb,py	si,ab	V11	-	51	222	0.26	20mm coarse-grained vuggy carbonate vein with pyrite
ZULD14	82.35	qz,py vein	23	289	41	61	131	qz,py	si,ab	V11	-	51	222	0.43	5mm quartz vein with pyrite on fractures
ZULD14	83.50	quartz vein	34	358	126	18	216	qT	py,bi	V11	-	51	222	0.78	2mm translucent quartz vein with thin pyrite selvedge
ZULD14	83.30	qz,py vein	49	359	113	3	203	qz,bi,py	-	V11	-	51	222	0.78	2mm translucent quartz vein with 1mm thin pyrite selvedge
ZULD14	83.70	quartz vein	36	7	153	16	243	qz,py,ak	si,ab	V3	xnext	51	222	0.93	10mm vuggy quartz vein with broad alteration halo
ZULD14	83.70	quartz vein	50	113	360	65	360	qz,bi,py	si,ab	V11		51	222	0.93	1mm quartz vein with broad alteration halo
ZULD14	85.00	qz bx vein	53	9	65	6	335	qT	si,ab	V9	-	51	222	0.69	Sharp contact of breccia zone with translucent infill quartz vein
ZULD14	85.20	py stringer	4	107	57	83	147	py,bi	bi	V11	-	52	222	0.69	<1mm pyrite stringer vein with thin selvedge
ZULD14	85.50	quartz vein	15	127	80	82	170	qz,bi	si,ab	V1	-	52	222	0.69	2mm crack-seal quartz vein with 10mm selvedge
ZULD14	86.50	qz,py vein	35	105	75	72	345	qz,py	si,ab	V11	xnext	52	222	0.71	2mm crack-seal quartz vein with 10mm selvedge
ZULD14	86.50	qz,py vein	65	341	161	17	71	qz,py	si,ab	V11	-	52	222	0.71	2mm crack-seal quartz vein with 10mm selvedge
ZULD14	86.82	dyke contact	55	21	63	13	333		-	BED3	-	52	222	0.63	Sharp veined contact with fine-grained felsic dyke
ZULD14	88.35	py stringer	47	45	50	30	320	py	py,bi	SRPY	-	52	222	0.12	2mm pyrite stringer vein
ZULD14	90.75	quartz vein	28	24	178	30	268	qz,cb	qz,cb	V3	-	52	222	0.06	3mm vuggy quartz carbonate vein crosscuts felsic dyke
ZULD14	96.00	quartz vein	39	13	171	16	261	qT,ch,py	si	V11	-	52	224	0.07	90mm translucent quartz vein with wallrock fragments
ZULD14	114.30	quartz vein	38	342	84	19	174	qz,bi,py	bi	V11	-	52	224	0.34	5mm quartz biotite pyrite vein
ZULD14	118.35	quartz vein	21	277	35	70	125	qz,ch+/-py	-	V1	-	52	224	0.09	2mm quartz chlorite vein
ZULD14	127.15	quartz vein	38	343	86	19	176	qzG,py	-	V11	-	52	224	0.09	40mm laminated grey quartz vein with 3mm pyrite selvedge
ZULD14	131.00	py,bi stringer	6	98	53	90	143	py,bi	si,ab	SRPY	-	52	224	0.09	<1mm pyrite biotite stringer vein with 10mm alteration selvedge
ZULD14	140.00	UM contact	31	233	177	86	87		ch,si	BED3	-	52	224	0.13	Diffuse contact with ultramafic
ZULD15	30.50	quartz vein	28	30	14	31	284	qz,ak,py	-	V11	-	47	223	0.37	2mm quartz vein with ankerite pyrite infill
ZULD15	31.00	quartz vein	42	289	21	50	111	qz,py,bi	-	V11	-	47	223	0.27	1mm thin quartz vein
ZULD15	31.35	quartz vein	52	51	70	33	340	qz	ch	V1	-	47	223	0.27	10mm crack-seal quartz vein
ZULD15	33.35	quartz vein	54	11	92	10	2	qz,bi,py	sich	V11	-	47	223	0.17	1mm quartz vein
ZULD15	34.60	quartz vein	27	74	51	61	321	qz,ak,py	-	V1	-	47	223	0.73	8mm crack-seal quartz vein
ZULD15	36.25	quartz vein	39	315	40	34	130	qz	si,ab,ch	V3	-	47	223	0.41	5mm vuggy quartz vein

HOLE NO	DEPTH	STRUCTURE	ALPHA	BETA	STRIKE	DIP	DIP DIRECTION	MINERALOGY	ALTERATION	GROUP	OVERPRINTING	HOLE DIP	HOLE AZIM	Au VALUE	COMMENTS
ZULD15	38.10	quartz vein	19	314	63	47	153	qz,ak,ch	si,ab	V1	-	47	223	0.1	5m shear vein with chlorite slivers
ZULD15	39.00	shear foliation	41	65	60	46	330	qz,ch	-	SH1	-	47	223	0.1	2mm chloritic shear vein
ZULD15	39.30	quartz vein	63	325	170	26	80	qz,ak,ab,ch	si,ab	V1	-	47	223	0.1	5mm crack-seal quartz vein with 20mm alteration selvedge
ZULD15	40.40	quartz vein	8	295	56	68	146	qz,ch	-	V1	-	47	223	0.21	5mm crack-seal comb textured quartz vein
ZULD15	40.90	quartz vein	34	199	148	83	238	qz,ch	-	V1	-	47	223	0.21	1mm crack-seal quartz chlorite vein
ZULD15	41.10	quartz vein	30	323	60	34	150	qz,ch	-	V1	-	47	223	0.28	8mm vuggy quartz vein with chlorite
ZULD15	42.20	quartz vein	18	76	45	68	315	qz,ch,py	si,ab	V11	-	47	223	0.19	5mm crack-seal quartz vein
ZULD15	42.80	contact	77	151	125	55	35	-	-	BED3	-	47	223	0.05	Sharp granite / dyke contact
ZULD15	42.80	quartz vein	48	91	80	58	350	qT	-	V9	xprev	47	223	0.05	15mm sigmoidal quartz vein
ZULD15	42.80	quartz vein	62	321	174	27	84	qz	-	V1	xprev2	47	223	0.05	<1mm crack-seal quartz vein
ZULD15	47.10	contact	45	211	154	85	64	-	-	BED3	-	47	223	0.27	Sharp lower granite / dyke contact
ZULD15	47.35	quartz vein	83	335	137	37	47	qz,ch,py	si,ab	V1	-	47	223	0.27	8mm infill crack-seal quartz chlorite vein
ZULD15	48.40	quartz vein	17	31	3	40	273	qz,ch	si,ab	V1	-	47	223	0.53	Fracture with quartz chlorite infill
ZULD15	50.20	fracture	62	345	157	18	67	ch	si,ab	V10	-	47	223	0.18	<1mm fracture with chlorite slivers
ZULD15	50.80	quartz vein	50	59	69	39	339	qz,py	si,ab	V11	-	47	223	0.18	5mm crack-seal quartz pyrite vein
ZULD15	50.95	qz,ch vein	47	10	46	7	316	qz,ch	si,ab	V1	-	47	223	0.18	1mm quartz chlorite vein
ZULD15	55.20	quartz vein	43	10	17	9	287	qz,py,bi	si,ab	V11	-	47	223	0.32	2mm crack-seal quartz vein
ZULD15	55.30	quartz vein	16	305	58	55	148	qz,py	si	V11	xprev	47	223	0.32	8mm crack-seal quartz vein
ZULD15	56.05	quartz vein	41	311	34	36	124	qz,py	si	V11	-	47	223	0.11	5mm crack-seal quartz pyrite vein
ZULD15	56.10	ch fracture	18	330	82	39	172	qz,ch,py	-	FL4	-	47	223	0.11	1mm fracture with chlorite and pyrite
ZULD15	56.40	quartz vein	63	44	92	30	2	qz,py,bi	-	V11	xnxt	47	223	0.11	5mm crack-seal quartz vein
ZULD15	56.55	quartz vein	8	137	85	67	175	qz,py,bi	-	V11	xprev,nxt	47	223	0.11	5mm comb textured crack-seal vein
ZULD15	56.55	quartz vein	32	329	64	28	154	qz,py,bi	-	V11	-	47	223	0.11	2mm crack-seal vein cut by previous
ZULD15	58.45	quartz vein	12	112	67	85	157	qz,py,bi	-	V11	-	47	223	1.14	5mm crack-seal quartz pyrite vein
ZULD15	59.90	quartz vein	21	307	55	50	145	qz,py,bi,ab,cb	si,ab	V11	-	47	223	1.32	15mm crack-seal quartz carbonate vein
ZULD15	60.10	quartz vein	20	325	74	40	164	qz,ab,ch	py	V11	-	47	223	1.32	5mm crack-seal comb textured quartz pyrite vein
ZULD15	60.10	quartz vein	31	331	68	28	158	qz,py	-	V11	-	47	223	1.32	Fractured 5mm quartz pyrite vein
ZULD15	60.35	qcb vein	53	25	72	18	342	qz,cb,py	si	V11	-	47	223	0.14	2mm vein with chlorite and pyrite
ZULD15	60.85	qcb vein	55	29	77	20	347	qz,ab,ch	-	V1	-	47	223	0.14	15mm crack-seal vein with chlorite infill
ZULD15	61.30	quartz vein	46	3	18	3	288	qz,ab,ch	-	V1	-	47	223	0.06	20mm crack-seal vein with wallrock fragments
ZULD15	63.10	quartz vein	12	191	145	60	235	qz,py	si	V11	-	47	223	0.56	Folded crack-seal vein with fracture fill pyrite about parallel to core axis
ZULD15	63.75	quartz vein	10	321	78	50	168	qz,py,ch	-	V11	-	47	223	0.56	2mm quartz chlorite pyrite vein
ZULD15	64.00	quartz vein	21	5	143	27	233	qz,py,bi	-	V4	-	47	223	0.44	2mm shear vein
ZULD15	64.10	quartz vein	37	13	1	14	271	qz,py,bi	py	V11	-	47	223	0.44	2mm crack-seal vein with pyrite stringers
ZULD15	65.95	quartz vein	37	27	26	23	296	qz,py,bi	py	V11	-	47	223	0.74	2mm crack-seal vein with pyrite stringers

HOLE NO	DEPTH	STRUCTURE	ALPHA	BETA	STRIKE	DIP	DIP DIRECTION	MINERALOGY	ALTERATION	GROUP	OVERPRINTING	HOLE DIP	HOLE AZIM	Au VALUE	COMMENTS
ZULD15	66.60	qz,py vein	7	265	34	89	124	qz,py	si,ab	V11	-	47	223	0.08	1mm quartz pyrite vein with pyrite in fractured quartz
ZULD15	70.50	quartz vein	42	315	35	33	125	qz,ak,ch,py	si	V3	-	47	223	1.03	10mm vuggy crack-seal quartz vein
ZULD15	71.40	quartz vein	24	328	73	35	163	qG,py	-	V8	-	47	223	0.4	10mm grey quartz vein
ZULD15	75.80	quartz vein	30	350	104	19	194	qG,py	pycb	V8	-	47	223	0.01	15mm grey quartz vein
ZULD15	76.30	quartz vein	32	34	25	30	295	qG,py,ch	-	V8	-	47	223	0..62	25mm grey quartz vein
ZULD15	76.85	qz,py stringer	5	97	51	89	141	qz,cb,bi,py	-	SRPY	-	47	223	0.72	2mm quartz carbonate vein with pyrite stringer vein
ZULD15	77.40	quartz vein	33	4	146	15	236	qG,py	-	V8	-	47	223	0.72	15mm grey quartz vein
ZULD15	78.00	qz,py vein	33	344	86	19	176	qz,py	-	V11	-	47	223	1.3	5mm quartz pyrite vein
ZULD15	80.00	quartz vein	46	338	38	16	128	qz,py	si,ab	V11	-	47	223	0.45	15mm euhedral quartz vein
ZULD15	82.90	quartz vein	44	339	46	15	136	qz,ab,py	si,ab	V11	-	47	223	0.45	10mm quartz vein with wallrock parallel slivers
ZULD15	84.90	quartz vein	25	315	58	42	148	qz,cb,py	-	V11	-	47	223	0.56	5mm crack-seal chlorite pyrite vein
ZULD15	85.10	fracture	12	89	48	81	318	qz,ch,py	si	V11	-	47	221	0.27	<1mm chlorite pyrite fracture
ZULD15	85.25	quartz vein	46	33	50	23	320	qT	ch	V9	xnxt	47	221	0.27	25mm quartz vein
ZULD15	85.35	quartz vein	35	313	42	37	132	qz,py	-	V11	-	47	221	0.25	15mm quartz vein with pyrite on subgrain boundaries
ZULD15	86.30	py stringer	34	308	40	41	130	pyl,ch,bi	-	SRPY	-	47	221	0.06	1mm pyrite stringer vein
ZULD15	86.65	contact	33	183	133	81	223	-	-	BED3	-	47	221	0.06	Sharp contact with ultramafic
ZULD15	89.00	shear zone	47	209	150	83	60	ch,ta,bi	-	SH4	-	47	221	0.07	Talc chlorite shear / cataclasite zone
ZULD15	89.15	quartz vein	63	187	134	70	44	qz,ab	-	V4	-	47	221	0.07	Sheared quartz vein
ZULD15	90.05	shear vein	59	271	172	51	82	qz,ab	-	V4	-	47	221	0.14	Crack-seal shear vein with chloritic wallrock slivers
Pit	-	lineation	-	-	-	19	145		-	-	-	-	-	-	Chloritic slip planes
Pit	-	shear zone	-	-	180	89	270		-	-	-	-	-	-	Shear Zone
Pit	-	lineation	-	-	-	15	N		-	-	-	-	-	-	Elongate pyritic fragments
Pit	-	late fault	-	-	145	86	235		-	-	-	-	-	-	Late fault parallel to shear zone with multiple lineations
Pit	-	lineation	-	-	-	20	S		-	-	-	-	-	-	Slickenfibre lineations
Pit	-	lineation	-	-	-	23	N		-	-	-	-	-	-	Slickenfibre lineations
Pit	-	lineation	-	-	-	43	N		-	-	-	-	-	-	Slickenfibre lineations
Pit	-	lineation	-	-	-	65	N		-	-	-	-	-	-	Slickenfibre lineations
Pit	-	shear zone	-	-	180	73	270		-	-	-	-	-	-	Shear zone
Pit	-	lineation	-	-	-	11	185		-	-	-	-	-	-	Stretching lineation

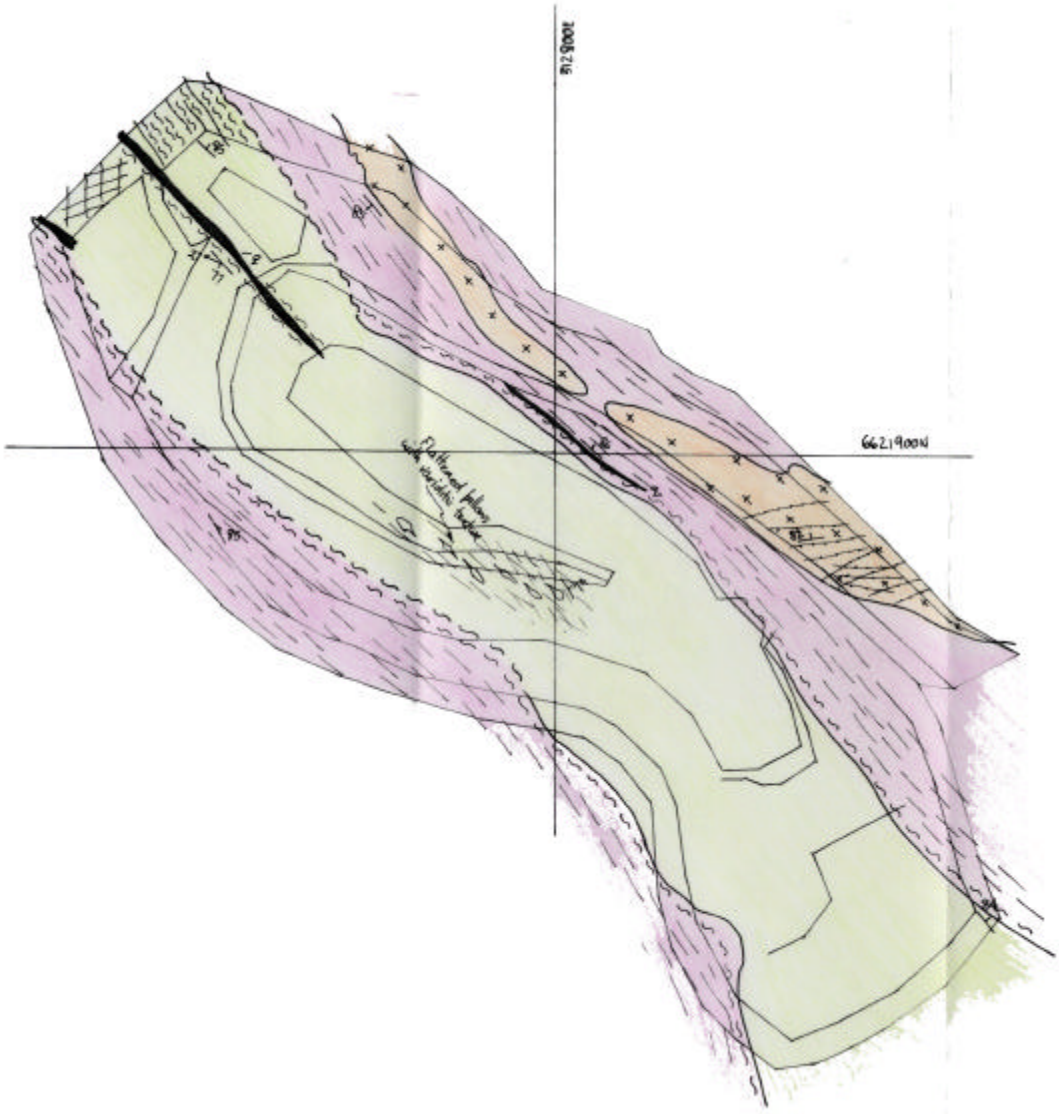

Map 4
Wattlebird north open-pit
(for legend see Map1 p.262)

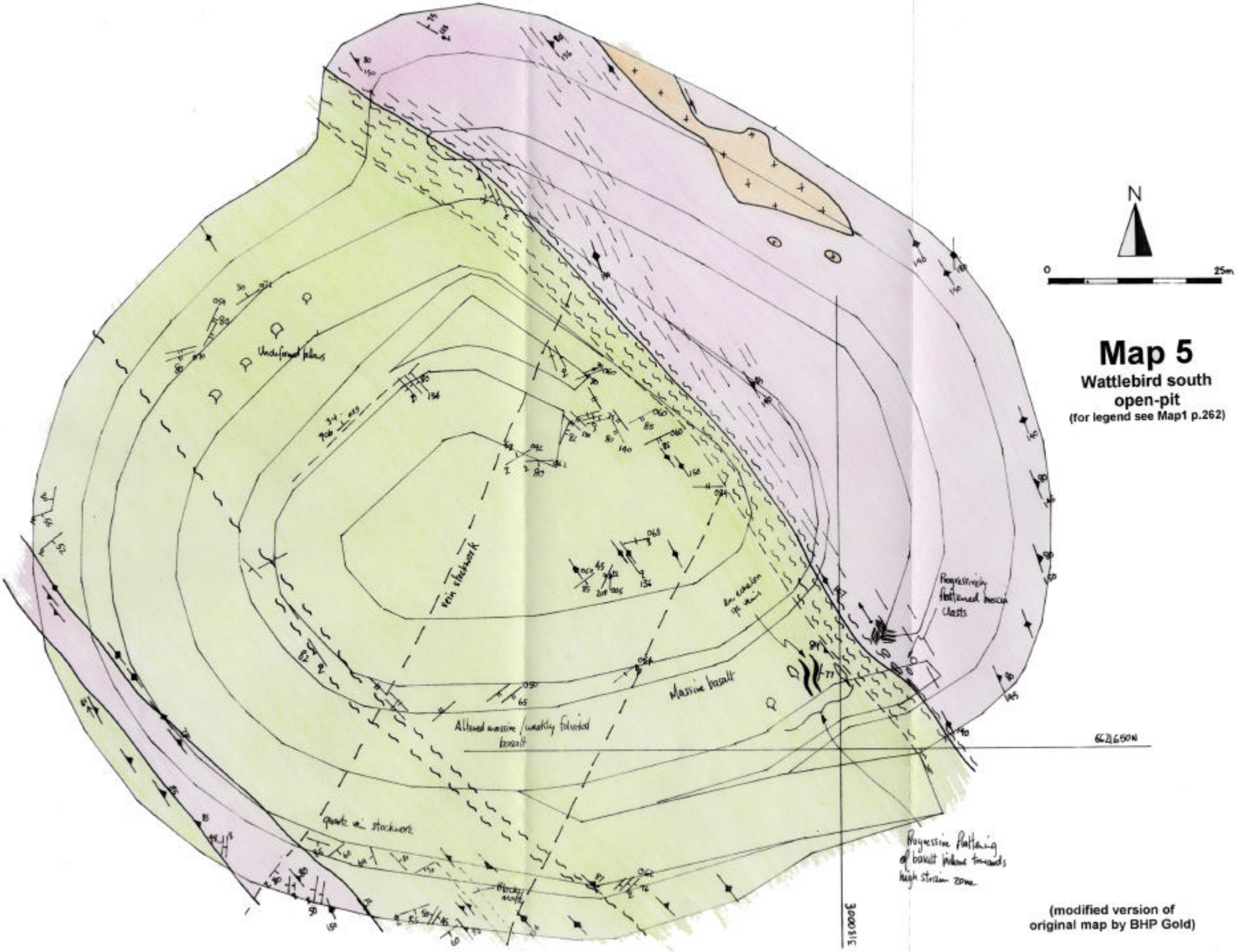

Map 5

Wattlebird south open-pit

(for legend see Map1 p.262)

(modified version of original map by BHP Gold)

Table A1.6 - Wattlebird Deposit - structural data from pit mapping and diamond drill core

HOLE NO	DEPTH	STRUCTURE	ALPHA	BETA	STRIKE	DIP	DIP DIRECTION	MINERALOGY	ALTERATION	GROUP	OVERPRINTING	HOLE DIP	HOLE AZIM	Au VALUE	COMMENTS
ZULD7	145.90	quartz vein	45	113	105	68	195	qz	-	V1	-	52	60	0.01	10mm crack seal quartz vein with comb texture
ZULD7	146.10	quartz vein	42	120	107	73	197	qz	-	V1	-	52	60	0.01	1mm quartz vein, joint fill?
ZULD7	146.65	quartz vein	52	113	109	62	199	qz	-	V4	-	52	60	0.01	6mm quartz vein with some wallrock breccia fragments
ZULD7	146.85	quartz vein	15	161	130	70	40	qz	-	V1	x-cuts prev	52	60	0.01	2mm quartz vein, west block down offset
ZULD7	147.75	shear zone	41	169	141	87	31	qz,ch,bi	-	SH1	-	52	60	0.01	Intense shear zone
ZULD7	148.00	quartz vein	34	75	72	56	162	qz	-	V3	x-cuts prev	52	60	0.01	10mm vuggy quartz vein, breccia infill
ZULD7	177.60	foliation	45	165	141	83	231	ch,bi	-	FL1	-	52	62	0.01	Intense pervasive foliation, close spaced
ZULD7	178.20	quartz vein	36	167	141	89	51	qz	-	V2	-	52	62	0.08	5mm sugary quartz vein in dilation fracture
ZULD7	190.80	rxt quartz vein	11	121	93	81	3	qz	-	V1	x-cuts next	52	62	-	1mm recrystallised vein in dilatent fracture
ZULD7	190.90	quartz vein	26	34	29	37	119	qz	-	V1	-	52	62	-	1mm quartz vein
ZULD7	191.70	quartz vein	40	111	102	71	192	qz,wr	-	V4	-	52	62	-	4cm quartz vein with wallrock breccia fragments
ZULD7	191.90	rxt quartz vein	55	238	5	63	275	qz	-	V1	-	52	62	-	5mm recrytallised quartz vein
ZULD7	192.55	rxt quartz vein	45	259	24	62	294	qz	-	V1	-	52	62	-	4mm recystallised quartz vein
ZULD7	193.00	shear vein	33	109	96	75	186	qz,wr	-	V4	-	52	62	-	6mm quartz vein with brecciated wallrock fragments
ZULD7	193.70	quartz vein	23	139	114	84	24	qz,ch,bi	-	V1	-	52	62	-	1mm quartz vein cross-cuts foliation
ZULD7	193.90	quartz vein	33	56	59	45	149	qz	-	V1	-	52	62	-	5mm comb textured recrystallised quartz vein
ZULD7	207.80	foliation	28	167	140	81	50	ch,bi	-	FL1	-	52	62	-	Intense pervasive foliation
ZULD7	207.85	foliation	47	173	147	81	237	ch,bi	-	FL1	-	52	62	-	Intense pervasive foliation
ZULD7	232.00	rxt quartz vein	30	183	154	83	64	qz	ch,bi	V1	-	52	62	0.01	5mm clear recrystallised quartz vein
ZULD7	257.00	quartz vein	34	53	55	42	145	qz	-	V1	-	52	62	0.06	5mm translucent recrystallised quartz vein in intensely foliated sediment
ZULD7	286.30	quartz vein	44	163	137	83	227	qz,ab?	ch,bi	V4	-	52	60	0.01	4cm intensely sheared and brecciated quartz vein
ZULD7	287.30	shear zone	45	182	153	84	243	mu,bi,qz	ch,bi	V4	-	51	62	0.09	Intense shear zone with quartz veining
ZULD7	302.80	quartz vein	42	55	70	38	160	qz sugary	-	V2	-	51	62	0.02	Recrystallised sugary quartz vein in shear zone
ZULD7	333.35	quartz vein	41	132	116	79	206	qz,tr,ac	-	V1	-	51	61	-	3mm recrystallised quartz vein
ZULD7	333.35	quartz vein	23	184	154	75	64	qzM	-	V1	-	51	61	-	3mm white quartz vein
ZULD7	345.60	quartz vein	16	113	91	90	1		-	V4	-	52	64	-	1mm shear vein
ZULD7	346.40	quartz vein	38	308	64	39	334	qz	-	V1	-	52	64	-	3mm recystallised quartz vein
ZULD7	375.65	shear vein	33	162	137	88	47	qz sugary	-	V2	-	53	63	-	2cm sugary quartz vein parallel to shearing
ZULD7	379.60	shear foliation	63	258	8	50	278	qz	-	FL1	-	53	63	-	Dominant shear foliation cross-cuts breccia
ZULD7	390.30	shear foliation	61	235	0	58	270	qz,tr,ac	-	FL1	-	53	63	-	Dominant shear foliation cross-cuts breccia
ZULD17	288.60	shear foliation	33	211	2	89	272	qz,ac,ch	-	SH1	-	54	67	0.13	Spaced shear foliation
ZULD17	291.50	shear bx zone	52	151	138	72	228	ch,qz,WR	-	SH1	-	54	67	0.04	15cm shear / breccia zone
ZULD17	295.20	qz ab vein	19	281	64	69	334	qT,ab	-	V2	-	54	67	0.2	10mm crack-seal quartz-albite vein with 90 degree comb textured qz

HOLE NO	DEPTH	STRUCTURE	ALPHA	BETA	STRIKE	DIP	DIP DIRECTION	MINERALOGY	ALTERATION	GROUP	OVERPRINTING	HOLE DIP	HOLE AZIM	Au VALUE	COMMENTS
ZULD17	101.30	quartz vein	47	290	39	43	309	qT	-	V2	-	56	58	0.02	Thin 3mm quartz vein crosscuts low angle veins
Pit	-	shear zone	-	-	143	89	233	ch,ep	-	SH1	-	-	-	-	Sheared pillow basalts very stretched and hard to recognise close to ZSZ
Pit	-	qz vein	-	-	8	77	98	qz	-	V9	-	-	-	-	En echelon veins in the Zuleika shear zone
Pit	-	stockwork vein	-	-	43	45	133	qz	-	V9	-	-	-	-	Stockwork veining within sheared pillow basalt
Pit	-	stockwork vein	-	-	32	55	122	qz	-	V9	-	-	-	-	Stockwork veining within sheared pillow basalt
Pit	-	stockwork vein	-	-	150	78	240	qz	-	V9	-	-	-	-	Stockwork veining within sheared pillow basalt
Pit	-	shear zone	-	-	146	84	236	ta,ch	-	SH5	-	-	-	-	Talc chlorite ultramafic mylonite
Pit	-	cren foliation	-	-	90	72	360	ta,ch	-	FL2	xprev	-	-	-	Spaced foliation crenulates Zuleika shear zone fabric
Pit	-	shear zone	-	-	9	70	279	ta,ch	-	SH5	xprev2	-	-	-	Late crosscutting shear zone
Pit	-	shear zone	-	-	153	80	243	-	-	-	-	-	-	-	Shear zone
Pit	-	lineation	-	-	-	11	343	-	-	-	-	-	-	-	Stretching lineation
Pit	-	shear zone	-	-	154	76	244	-	-	-	-	-	-	-	Shear zone
Pit	-	lineation	-	-	-	1	334	-	-	-	-	-	-	-	Stretching lineation
Pit	-	shear zone	-	-	132	86	42	-	-	-	-	-	-	-	Shear zone
Pit	-	lineation	-	-	-	3	316	-	-	-	-	-	-	-	Stretching lineation

A1.3 Ora Banda district

Structural data were collected from six mines in the Ora Banda district: Boundary, Enterprise, Gimlet South, Nazzaris, Sleeping Beauty and Slippery Gimlet mines. The locations of open-pits and associated diamond drillholes is shown in Figure A1.2. For Enterprise and Slippery Gimlet mines, a greater number of drillholes were logged in these areas and detailed maps of drillhole locations are located at the beginning of the tables for each of these areas.

All structural data were collected during this study with the exception of data from the Nazzaris and Gimlet South mines. Structural data from the Nazzaris mine were provided by Garry Adams (Centaur). Data from the Gimlet South mine were compiled from maps of underground development drive faces. These data were collected by mine geologists from BHP Gold, Newcrest Mining, and Centaur Mining and Exploration that worked in the Gimlet South mine from the early 1990's to 1997.

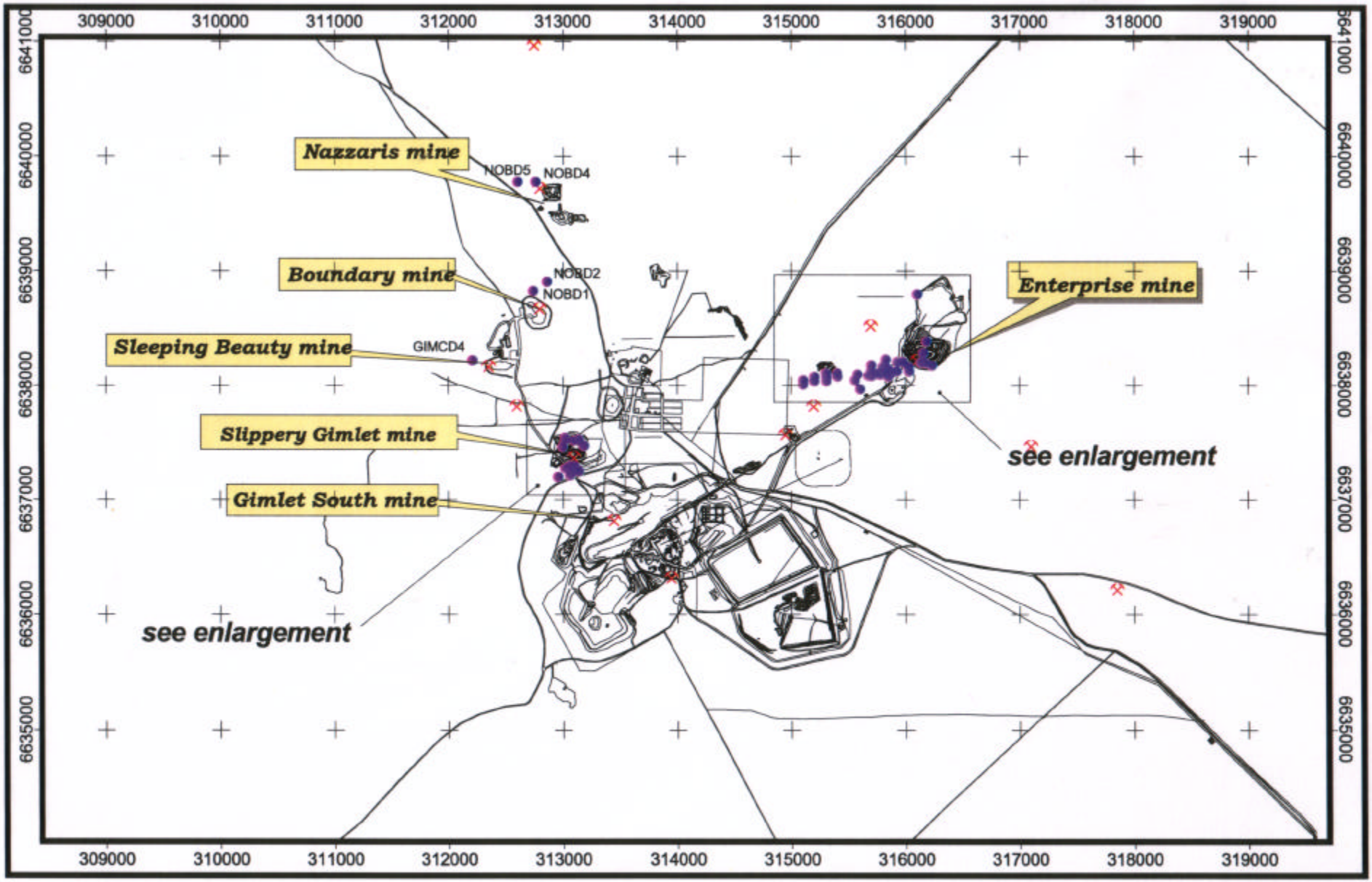

Figure A1.1 - Location plan of drillholes sampled from the Ora Banda area

Table A1.7 – Explanation of codes used for drill hole logging

VEINS

V1	-	Minor quartz / quartz-carbonate vein
V2	-	Translucent quartz vein
V3	-	Milky quartz vein
V4	-	Coarse-grained recrystallised carbonate vein
V5	-	Vein of material other than quartz e.g. chlorite, talc
V6	-	Vein (undefined)
V7	-	Vein with fluorite
V8	-	Extension vein
V9	-	Quartz porphyry vein
V10	-	Vein within porphyry dyke
SRpy	-	Pyrite stringer vein
SRpo	-	Pyrrhotite stringer vein
SRcp	-	Chalcopyrite stringer vein

BRITTLE-DUCTILE FAULTS

SH1	-	Mylonitic shear zone
SH2	-	Talc schist shear zone
SH3	-	Cataclasite zone
SH4	-	Crackle breccia zone with definable boundary
SH5	-	Mill breccia zone
SH6		Shear zone (undefined)
SH7		Discrete fault plane with slickenfibres

FOLIATIONS

CC	-	Continuous cleavage
CS1	-	Spaced foliation/Cleavage
CS2	-	Crenulation cleavage
J1	-	NE trending extension joint
J2	**-**	Extension joint

BEDDING

BED1	-	Compositional layering in the Mount Pleasant Sill
BED2	**-**	Cashmans Sedimentary Horizon
BED6	**-**	Interflow sedimentary bedding

LINEATIONS

Lslk	**-**	Slickenfibre lineation
Lmin	**-**	Mineral lineation
F1	**-**	Fold axis
VL	**-**	Limb of folded vein

MOVEMENT SENSE DESCRIPTORS

SS – sinistral, **DX** – dextral, **NblkW** – north block west

CROSS-CUTTING

xprev	current structure cross-cuts previous structure
xnxt	current structure cross-cuts next structure
xnxt2	current structure cross-cuts next two structures

MINERAL CODES

ab - albite	**py** - pyrite	**bi** - biotite	**ep** - epidote
cb - carbonate	**po** - pyrrhotite	**mu** - muscovite	**si** - silica
ch - chlorite	**cp** - chalcopyrite	**ca** - calcite	**qT** – translucent quartz
ac - actinolite	**sph** - sphalerite	**fl** - flourite	**qM** – milky quartz
ta - talc	**asp** - arsenopyrite	**qz** - quartz	**fu** - fuchsite
fd - feldspar	**mo** - molybdenite	**ka** - kaolinite	**hm** - hematite
to - tourmaline			

Table A1.8 - Boundary Deposit, structural data from diamond drill core

HOLE NO	DEPTH	STRUCTURE	ALPHA	BETA	STRIKE	DIP	DIP DIRECTION	MINERALOGY	ALTERATION	GROUP	OVERPRINTING	HOLE DIP	HOLE AZIM	Au VALUE	COMMENTS
NOBD1	139.60	joint	61	312	156	24	66	qz,cb	-	J2	xnxt	60	180	-	1mm thick quartz carbonate filled joint
NOBD1	139.60	joint	30	49	159	45	249	qz,cb	-	J2	-	60	180	-	1mm thick quartz carbonate filled joint
NOBD1	139.60	joint	55	302	163	31	73	qz,cb	-	J2	-	60	180	-	1mm thick quartz carbonate filled joint
NOBD1	139.90	joint	18	355	82	43	172	qz,cb	-	J2	-	60	180	-	0.5mm quartz carbonate filled fracture
NOBD1	155.30	quartz vein	26	203	110	89	200	qz,cb,ch	-	V1	-	60	180	0.23	10mm recrystallised quartz carbonate vein
NOBD1	155.55	quartz-cb vein	23	195	103	84	193	qz,cb	-	V1	-	60	180	0.23	2mm recrystallised quartz carbonate vein
NOBD1	155.70	quartz-cb vein	39	213	115	78	25	qz,cb,ch	bi,ch	V1	-	60	180	0.23	10mm recrystallised quartz carbonate vein with wallrock slivers
NOBD1	156.45	quartz-cb vein	19	206	114	82	204	qz,cb,ch	bi,ch	V1	-	60	180	0.05	5mm recrystallised quartz carbonate vein
NOBD1	196.00	quartz-cb vein	45	166	76	74	346	qz,cb	-	J2	-	61	177	-	1mm quartz carbonate joint infill
NOBD1	196.50	quartz-cb vein	22	202	107	85	197	qz,cb	-	V1	-	61	177	-	3mm quartz carbonate vein
NOBD1	196.60	quartz-cb vein	56	157	72	62	342	qz,cb	-	J2	-	61	177	-	1mm quartz carbonate joint fill
NOBD1	197.75	quartz-cb vein	45	138	56	69	326	qz,cb	-	J2	-	61	177	-	1mm quartz carbonate joint fill
NOBD1	197.75	quartz-cb vein	17	181	87	79	177	qz,cb	-	SH6	xprev	61	177	-	3mm quartz carbonate shear vein, north block up
NOBD1	198.20	quartz-cb vein	22	202	107	85	197	qz,cb,ch	-	V1	-	61	177	-	20mm quartz carbonate vein south block down
NOBD1	199.50	quartz-cb vein	21	197	102	83	192	qz,cb	-	V1	-	61	177	-	5mm vein
NOBD1	201.40	quartz-cb vein	8	19	110	54	200	ch,si	-	V1	-	61	177	-	2mm vein with dark halo
NOBD1	208.10	quartz-cb vein	22	236	137	87	47	cb,ep,si,po	po,ch	V1	-	61	177	-	10mm laminated quartz carbonate vein
NOBD1	212.65	quartz-cb vein	65	236	115	49	25	-	-	J2	-	61	177	-	1mm quartz carbonate joint infill
NOBD1	250.10	shear zone	39	65	175	46	265	ch,qz,cb	-	SH6	-	62	176	-	0.1m shear zone and quartz vein
NOBD1	250.30	quartz-cb vein	44	287	164	45	74	qz,cb,ch	-	V1	xall	62	176	0.40	10mm irregular quartz carbonate vein
NOBD1	250.40	quartz-cb vein	40	88	15	55	285	qz,cb	cb,ep	V1	-	62	176	0.40	1mm pervasive fracture veining with alteration
NOBD1	250.60	quartz-cb vein	59	319	166	21	76	qz,cb	ch,ep,cb	V1	xall	62	176	0.40	1mm quartz carbonate vein with wallrock slivers
NOBD1	250.70	quartz-cb vein	40	114	35	66	305	qz,cb	-	V1	-	62	176	0.40	3mm quartz carbonate vein
NOBD1	250.90	quartz-cb vein	27	113	28	77	298	qz,cb	-	J2	-	62	176	0.40	1mm quartz carbonate vein with wallrock slivers
NOBD1	251.70	shear zone	36	277	162	56	72	qz,cb	-	SH6	-	62	176	0.02	5mm shear zone with quartz carbonate vein
NOBD2	154.85	shear vein	27	233	133	83	43	qz,cb,ch	ch	V1	-	61	178	-	10mm shear vein parallel to layers of chlorite and quartz carbonate
NOBD2	156.50	quartz vein	21	141	51	88	141	qz	-	V1	-	61	178	-	3mm comb textured quartz vein
NOBD2	160.20	qcb joint	52	214	110	64	20	qz,cb,ch	-	J2	-	61	178	-	1mm quartz carbonate joint infill
NOBD2	160.45	qcb vein	47	232	124	65	34	qz,cb	-	V1	-	61	178	-	5mm recrystallised quartz carbonate vein
NOBD2	160.50	fault	34	259	151	66	61	ch	-	SH6	xprev	61	178	-	<1mm wide fault plane WBlk down
NOBD2	161.75	qcb vein	59	223	113	56	23	qz,cb,ch	-	V1	-	61	178	-	20mm recrystallised quartz carbonate vein with abundant chlorite
NOBD2	175.20	qcb vein	54	219	114	61	24	qz,cb,ch	-	V1	-	61	179	0.04	10mm shear vein

HOLE NO	DEPTH	STRUCTURE	ALPHA	BETA	STRIKE	DIP	DIP DIRECTION	MINERALOGY	ALTERATION	GROUP	OVERPRINTING	HOLE DIP	HOLE AZIM	Au VALUE	COMMENTS
NOBD2	175.45	qcb joint	44	181	89	75	359	qz,cb	-	J2	-	61	179	0.04	3mm qcb joint
NOBD2	175.25	qcb joint	44	154	69	73	339	qz,cb	-	J1	-	61	179	0.04	3mm qcb joint
NOBD2	177.55	qcb joint	28	189	96	90	186	qz,cb	-	J1	-	61	179	0.08	1mm quartz carbonate joint infill
NOBD2	178.00	qcb joint	66	200	99	53	9	qz,cb	-	J2	-	61	179	0.04	<1mm quartz carbonate joint infill
NOBD2	178.10	qcb joint	21	194	102	83	192	qz,cb	-	J2	-	61	179	0.04	<1mm quartz carbonate joint infill
NOBD2	178.10	qcb joint	23	14	109	40	199	qz,cb	-	J2	-	61	179	0.04	<1mm quartz carbonate joint infill
NOBD2	182.50	shear zone	39	111	36	66	306	ch,bi	si,ch	SH6	xnxt	61	179	0.36	Intense shear zone
NOBD2	182.50	foliation	23	50	154	52	244	ch,si	-	CC	-	61	179	0.36	Pervasive foliation
NOBD2	193.40	shear zone	36	76	7	53	277	ch,qz,cb	-	SH3	-	61	179	0.54	Sharp upper contact of shear zone
NOBD2	194.25	shear zone	43	106	34	61	304	qz,py,po	lx,si,ch	SH3	-	61	179	0.72	Intense shear zone dextral NBLKE
NOBD2	194.65	shear zone	26	106	25	75	295	qz,cb,ch	py,lx,mu	SH3	-	61	179	0.72	Intense shear zone 1-2m wide
NOBD2	195.00	shear zone	46	15	126	18	216	ch	-	SH3	-	61	179	0.08	Cross-cutting shear zone
NOBD2	205.35	qcb vein	49	105	36	55	306	-	-	V1	-	62	178	0.07	10mm quartz carbonate vein
NOBD2	207.00	qcb vein	54	111	43	53	313	qz,cb,ch	ch	V1	-	62	178	0.03	8mm quartz carbonate vein
NOBD2	209.38	shear zone	24	211	116	90	206	ch,bi	-	SH6	-	62	178	0.03	5mm shear zone
NOBD2	209.40	qcb vein	26	196	102	89	192	qz,cb	-	V1	-	62	178	0.03	5mm quartz carbonate vein
NOBD2	213.55	qcb vein	26	213	117	89	27	qz,cb,si	py,po	V1	-	62	178	0.03	25mm quartz carbonate vein
NOBD2	224.10	qcbv ein	42	131	51	69	321	qz,cb	-	V1	-	62	178	0.04	5mm recrystallised quartz carbonate vein
NOBD2	224.60	shear zone	38	113	35	67	305	ch,bi	py,po	SH6	-	62	178	0.40	Intense shear foliation
NOBD2	225.65	qcb vein	58	141	64	57	334	-	-	V1	-	62	178	0.02	5mm quartz carbonate vein
NOBD2	229.00	qcb shear vein	63	204	101	54	11	qz,cb,ch,po	bi,ch,ac	V1	-	62	178	0.03	15mm quartz carbonate shear vein
NOBD2	241.00	qcb shear vein	33	212	113	82	23	qz,cb,ch	py	V1	-	62	177	0.03	10mm shear vein
NOBD2	244.90	qcb vein	27	189	95	90	185	qz,cb	bi,ch	V1	-	62	177	0.11	20mm vein with sulphides
NOBD2	253.15	qcb joint	51	144	62	64	332	qz,cb	-	J1	-	62	177	0.58	2mm quartz carbonate filled joint plane
NOBD2	254.30	fault contact	42	77	9	48	279	qz,cb	si	SH4	-	62	177	0.96	Sharp contact of breccia zone and foliated wallrock
NOBD2	254.55	quartz vein	60	169	80	58	350	qT	bi	V2	-	62	177	0.16	10mm translucent quartz vein with carbonate at the contact
NOBD2	255.10	shear vein	50	87	24	47	294	qT	-	V2	-	62	177	0.16	Sharp vein boundary within the shear zone
NOBD2	255.30	shear zone	41	80	11	51	281	qz,cb,ch	-	SH6	-	62	177	0.16	Sharp lower contact of shear zone
NOBD2	255.60	qcb joint	49	84	21	46	291	qz,cb	-	J1	-	62	177	0.16	2mm recrystallised quartz carbonate joint fill
NOBD2	268.20	fault	26	26	124	40	214	qz,cb,ch,py,po	-	SH4	-	62	177	0.02	Flow top breccia?, intense zone of shearing
NOBD2	278.45	qcb vein	55	163	76	63	346	qz,cb,ch,py,po	-	V5	-	62	177	-	10mm chlorite vein
NOBD2	278.80	qcb vein	51	172	81	67	351	qz,cb	-	V1	-	62	177	-	5mm recrystallised quartz carbonate vein

Enterprise Deposit – pit mapping scheme

Mapping in Enterprise open-pit was conducted during July 1997. Access was available to almost every wall in the pit, and therefore a systematic approach was necessary to cover all areas. Each berm was separately mapped at 1:100 scale in 30m segments (walls), for the majority, for a total of 88 walls covering the entire pit (Figure A1.3). Walls were marked out from known points in the pit (beginning of the berm) and mapped from left-to-right, facing the wall, in all cases. Structural data in the tables are listed according to wall number and metres distance along the wall, hence the attached wall-location plan should be referred to for the location of specific features. Locations of diamond drillholes logged are shown in Figure A1.4 (p.322).

In the following table, “Vein Inc” refers to vein inclusions and “Pos” refers to the position of the structure either north (N) or south (S) of the south Enterprise fault.

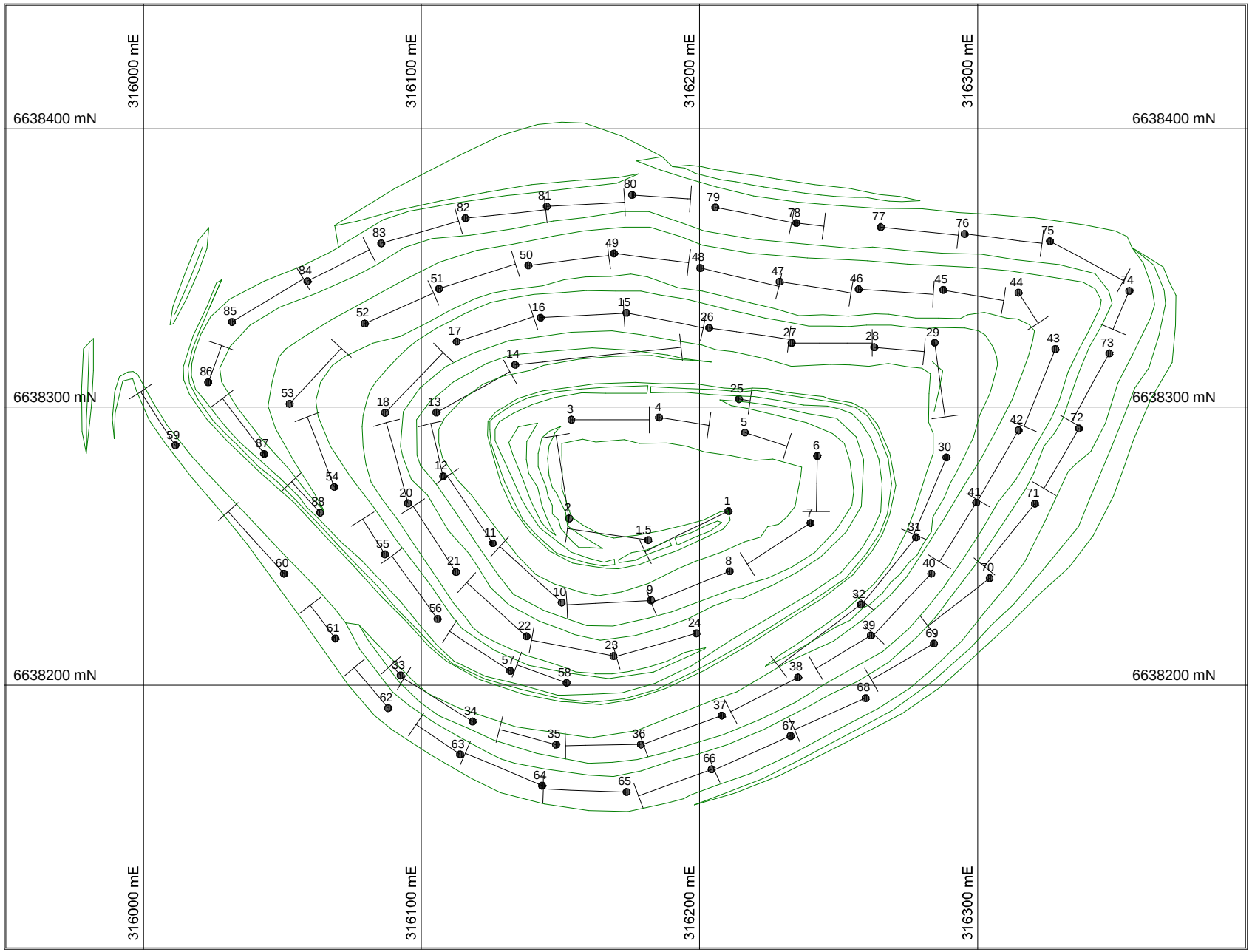

Figure A1.3 - Mapping plan of Enterprise open pit showing 1:100 scale wall mapping locations. To locate structural data from the tables, the black dots mark the beginning of each wall and the location in metres for each reading should be measured from the beginning of the wall. 5mm = 10metres on the plan.

Table A1.9 - Enterprise Deposit, structural data from open-pit mapping

LOCATION		Structural	Orientation					Defining Mineralogy					Alteration					Group	X-cut	Vein	Vein	Vein	Halo	Pos	DESCRIPTION
WALL	Metres	Element	Strike	Dip	Dip/Dir	Plunge	Dir	1	2	3	4	5	1	2	3	4	5		Rel.	Width	Style	Inc	Width		
1	0	sh fol	21	37	291	-	-	ka	ch	-	-	-	-	-	-	-	-	SH1	-	-	-	-	-	N	Intense shear foliation at angle to main breccia zone
1	0	qz vein	65	81	335	-	-	qM	-	-	-	-	py	mu	ka	-	-	V3	xnxt	3000	bx	wr	2000	N	3m wide quartz vein in shear/breccia zone
1	15	qz vein	43	78	313	-	-	qM	mo	-	-	-		-	-	-	-	V3	-	100	-	-	-	N	Vein with oxidised molybdenite coatings
1	19	slicks	-	-	-	23	198	si	ch	-	-	-	si	cb	-	-	-	LSLK	-	-	-	-	-	N	Slickenfibres on plane of previous fault
1	19	fault plane	21	83	111	-	-	si	ch	-	-	-	-	-	-	-	-	SH7	-	-	-	-	-	N	Spaced fault planes at 80cm
1	19	qz vein	123	58	213	-	-	qT	qM	ab	-	-	-	-	-	-	-	V2	-	100	-	-	-	N	Crack-seal quartz vein qT infills qM + ab
1	19	qz vein	176	42	266	-	-	qT	qM	-	-	-	bi	si	py	-	-	V2	-	100	-	-	-	N	Minor po mo in qM py only in qT
1	29	qz vein	178	59	88	-	-	qT	-	-	-	-	py	mo	bi	-	-	V2	-	-	-	-	30	N	Fracture fill lineation blocky qT
1.5	33	foliation	85	86	355	-	-	-	-	-	-	-	-	-	-	-	-	CC	-	-	-	-	-	N	Intense foliation at angle to previous vein
1.5	33	fault plane	105	76	15	-	-	-	-	-	-	-	-	-	-	-	-	SH7	xall	-	-	-	-	N	Prominent fault plane x-cuts all veins
1.5	33	qz vein	126	17	216	-	-	qT	-	-	-	-	si	mu	py	ca	-	V2	-	250	-	-	100	N	
1.5	33	qz vein	163	38	253	-	-	qT	-	-	-	-	mo	py	ca	-	-	V2	-	-	mcs	-	-	N	Crack-seal qT veins with thin mo selvedges
1.5	42	slicks	-	-	-	6	40	ch	mu	-	-	-	-	-	-	-	-	LSLK	-	-	-	-	-	N	Slickensides on previous fault
1.5	42	fault plane	34	57	304	-	-	-	-	-	-	-	-	-	-	-	-	SH7	-	-	-	-	-	N	Arcuate fault plane
1.5	42	qz vein	106	37	196	-	-	qz	-	-	-	-	-	-	-	-	-	V2	-	1100	-	-	30	N	Quartz vein extends into base of pit
1.5	57	qz vein	103	59	193	-	-	qz	fl	-	-	-	mo	py	si	-	-	V7	-	200	-	-	100	N	
1.5	59	qz vein	90	40	180	-	-	qT	qM	-	-	-	py	si	bi	-	-	V2	-	500	-	-	30	N	Spaced quartz veins milky quartz infill translucent
1.5	59	qz vein	40	41	310	-	-	qz	-	-	-	-	-	-	-	-	-	V6	-	-	-	-	-	N	
1.5	59	qz vein	4	41	94	-	-	qz	-	-	-	-	si	py	-	-	-	V6	-	30	-	-	-	N	
1.5	59	qz vein	17	54	107	-	-	qz	-	-	-	-	py	si	bi	-	-	V6	-	-	-	-	-	N	Vein x-cut by later tension veins
1.5	59	tension vein	93	56	3	-	-	qz	ab	py	fl	ca	-	-	-	-	-	V7	xprv	-	-	-	-	N	Thin shear tension veins
2	0	slicks	-	-	-	29	71	-	-	-	-	-	-	-	-	-	-	LSLK	-	-	-	-	-	N	Slickensides in splay fault
2	0	slicks	-	-	-	3	177	-	-	-	-	-	-	-	-	-	-	LSLK	-	-	-	-	-	N	Slickensides in main fault
2	0	fault plane	79	75	349	-	-	qz	ca	fl	-	-	-	-	-	-	-	SH7	-	-	-	-	-	N	3cm splay off next fault with parallel recrystallised qcb vein
2	0	fault plane	177	86	87	-	-	-	-	-	-	-	-	-	-	-	-	SH7	-	-	-	-	-	N	1.2m spaced fault planes
2	1	cataclasite	30	37	300	-	-	-	-	-	-	-	-	-	-	-	-	SH3	xnxt2	-	-	-	-	N	Pervasive dip slip cat zone + vein infill
2	1	qz vein	108	43	198	-	-	qz	cl	-	-	-	bi	si	py	-	-	V2	-	300	-	ch	-	N	Recrystallised vein with ch slivers
2	4	qz vein	104	40	194	-	-	qz	mo	-	-	-	py	-	-	-	-	V6	-	800	mcs	-	-	N	Laminated quartz vein
2	7	qz vein	138	80	48	-	-	qT	fl	-	-	-	si	mu	py	fu	-	V2	-	160	-	-	-	N	Fu spots in wallrock breccia
2	8	qz vein	131	59	221	-	-	qT	-	-	-	-	-	-	-	-	-	V2	-	20	-	-	-	N	Vein parallel to moderate foliation
2	12	qz vein	120	54	210	-	-	-	-	-	-	-	-	-	-	-	-	V6	-	-	-	-	-	N	
2	12	qz vein	179	57	269	-	-	qz	ca	-	-	-	-	-	-	-	-	V6	-	5	-	-	-	N	
2	12	qz vein	35	61	305	-	-	qz	ca	fl	-	-	-	-	-	-	-	V7	xprv	5	-	-	-	N	Vein has sheared margins
2	12	qz vein	74	84	344	-	-	qz	ca	fl	-	-	-	-	-	-	-	V7	xall	-	scs	-	-	N	Subvert tension vein recrystallised comb txt ca+fl

LOCATION		Structural	Orientation					Defining Mineralogy					Alteration					Group	X-cut	Vein	Vein	Vein	Halo	Pos	DESCRIPTION
WALL	Metres	Element	Strike	Dip	Dip/Dir	Plunge	Dir	1	2	3	4	5	1	2	3	4	5		Rel.	Width	Style	Inc	Width		
2	15	shear fol	179	72	269	-	-	bi	mu	fu	-	-	-	-	-	-	-	SH1	-	-	-	-	-	N	Shear foliation in wall of previous vein+breccia
2	15	qz vein	122	53	212	-	-	qM	-	-	-	-	bi	mu	fu	py	-	V3	xnxt	1100	mcs	-	-	N	Sheared halo
2	18	slicks	-	-	-	12	178	-	-	-	-	-	-	-	-	-	-	LSLK	-	-	-	-	-	N	Slickensides in previous fault plane
2	18	shear plane	11	81	101	-	-	-	-	-	-	-	-	-	-	-	-	SH6	-	-	-	-	-	N	
2	18	qz vein	144	39	234	-	-	qT	-	-	-	-	-	-	-	-	-	V2	-	-	-	WR	-	N	Thin vein between main veins
2	20	qz vein	120	47	210	-	-	qM	-	-	-	-	-	-	-	-	-	V3	-	500	mcs	-	-	N	Several events of vein intrusion
2	30	cataclasite	130	79	40	-	-	bi	ch	-	-	-	-	-	-	-	-	SH3	xprv	-	-	-	-	N	**Cataclasite Eblock down, DX strk slip~1m offset**
2	30	qz vein	22	49	112	-	-	qT	-	-	-	-	bi	si	py	-	-	V2	-	50	-	-	100	N	
3.1	3	qz vein	34	67	304	-	-	qz	ca	fu	-	-	mu	hm	py	-	-	V6	-	-	-	vu	-	N	Int altered dolerite with vuggy infill vein
3.1	6	foliation	175	69	85	-	-	-	-	-	-	-	cp	-	-	-	-	CS1	-	-	-	-	-	N	Intense foliation/microfracture with cu carbonate preciptate
3.1	11	qz vein	17	54	107	-	-	-	-	-	-	-	bi	si	-	-	-	V6	-	-	-	-	50	N	Foliated margins
3.1	13	foliation	93	81	3	-	-	-	-	-	-	-	-	-	-	-	-	CC	-	-	-	-	-	N	Foliation in Aod
3.1	13	joint	24	81	294	-	-	-	-	-	-	-	-	-	-	-	-	J1	-	-	-	-	-	N	Pervasive joint perp to hingeline + ax surf
3.1	13	joint	35	31	305	-	-	-	-	-	-	-	-	-	-	-	-	J2	-	-	-	-	-	N	Prominent joint plane
3.1	20	qz vein	160	56	250	-	-	qz	-	-	-	-	si	mu	ca	-	-	V6	-	-	-	WR	-	N	Vein with intense breccia wallrock fragments
3.1	28	qz vein	175	68	265	-	-	qz	-	-	-	-	si	bi	py	mu	-	V6	-	-	-	-	30	N	Thin recrystallised comb txt vein, parallel to foliation schist
4	3	foliation	129	59	219	-	-	-	-	-	-	-	-	-	-	-	-	BED2	-	-	-	-	-	N	Smooth plane contains sev lineation Bedding?
4	3	foliation	173	78	263	-	-	-	-	-	-	-	-	-	-	-	-	CC	-	-	-	-	-	N	Close spaced foliation alteration along seams
4	3	slicks	-	-	-	32	85	si	ca	fl	-	-	-	-	-	-	-	LSLK	-	-	-	-	-	N	Slickensides in previous fault plane
4	3	qz vein	74	22	164	-	-	qT	-	-	-	-	-	-	-	-	-	V2	-	-	-	-	-	N	Several quartz veins no selvedge
4	3	fault plane	76	77	166	-	-	si	ch	fl	ca	-	-	-	-	-	-	V7	-	-	-	-	-	N	Fault plane with slicks
4	15	joint	120	61	210	-	-	-	-	-	-	-	-	-	-	-	-	J2	-	-	-	-	-	N	Lineation on joint plane at intersection of cataclasite+kinks
4	18	fold axis	-	-	-	50	263	-	-	-	-	-	-	-	-	-	-	F1	-	-	-	-	-	N	Fold axis in quartz vein
4	18	qz vein	172	81	82	-	-	qT	-	-	-	-	si	mu	py	fu	-	V2	-	500	-	WR	-	N	Vein with intense breccia wallrock fragments
5	0	foliation	167	62	257	-	-	si	mu	fu	-	-	-	-	-	-	-	CC	-	-	-	-	-	N	Int shear foliation in wallrock of previous vein
5	0	qz vein	155	81	245	-	-	qT	-	-	-	-	-	-	-	-	-	V2	-	1800	-	vu	-	N	Vuggy vein with euhedral quartz terminations
5	2	cbx plane	31	58	301	-	-	-	-	-	-	-	-	-	-	-	-	CS1	-	-	-	-	-	N	Foliation plane defining crackle breccia
5	2	cbx plane	144	30	54	-	-	-	-	-	-	-	-	-	-	-	-	SH4	-	-	-	-	-	N	Foliation plane defining crackle breccia
5	2	cbx plane	166	83	256	-	-	-	-	-	-	-	-	-	-	-	-	SH4	-	-	-	-	-	N	Foliation plane defining crackle breccia
5	6	qz vein	165	35	75	-	-	qz	-	-	-	-	-	-	-	-	-	V6	-	-	-	-	-	N	
5	16	qz vein	154	51	64	-	-	qz	fd	-	-	-	py	mo	cp	-	-	V6	-	-	-	-	-	N	Quartz feldspar pegmatite vein
6	0	foliation	18	88	108	-	-	ch	bi	-	-	-	-	-	-	-	-	CC	-	-	-	-	-	S	Prominent foliation
6	0	joint	6	37	276	-	-	-	-	-	-	-	-	-	-	-	-	J2	-	-	-	-	-	S	Well developed joint plane
6	0	joint	124	71	214	-	-	-	-	-	-	-	-	-	-	-	-	J2	-	-	-	-	-	S	Well developed joint plane
6	0	joint	134	38	224	-	-	-	-	-	-	-	-	-	-	-	-	J2	-	-	-	-	-	S	Well developed joint plane
6	2	qz vein	84	21	174	-	-	-	-	-	-	-	-	-	-	-	-	VL	-	200	-	-	-	S	Foliated quartz vein this orientation for single limb only
6	3	slicks	-	-	-	29	105	-	-	-	-	-	-	-	-	-	-	LSLK	-	-	-	-	-	S	Slickensides on vein surface

LOCATION		Structural	Orientation					Defining Mineralogy					Alteration					Group	X-cut	Vein	Vein	Vein	Halo	Pos	DESCRIPTION
WALL	Metres	Element	Strike	Dip	Dip/Dir	Plunge	Dir	1	2	3	4	5	1	2	3	4	5		Rel.	Width	Style	Inc	Width		
6	3	qz vein	92	67	182	-	-	qz	-	-	-	-	mu	si	py	ka	-	V6	-	-	-	-	-	S	
6	4	foliation	44	79	314	-	-	-	-	-	-	-	-	-	-	-	-	CC	-	-	-	-	-	S	Intense shear foliation bending into fault
6	4	fault plane	53	88	323	-	-	-	-	-	-	-	mu	py	ka	si	-	SEF	-	-	-	-	-	S	3m wide SEF fault plane
6	4	alt zone ct	60	53	330	-	-	-	-	-	-	-	-	-	-	-	-	SEF	-	-	-	-	-	S	Contact of chAod and SEF alteration zone
6	4	tension vein	34	18	304	-	-	qT	-	-	-	-	-	-	-	-	-	V8	-	-	-	-	-	S	Tension vein does not cut fault
6	4	tension vein	78	54	348	-	-	qT	-	-	-	-	-	-	-	-	-	V8	-	-	-	-	-	S	Upper boundary of main tension vein
6	5	foliation	174	35	264	-	-	ch	bi	-	-	-	-	-	-	-	-	CC	-	-	-	-	-	S	Well developed spaced foliation/joint
6	5	foliation	35	85	305	-	-	-	-	-	-	-	-	-	-	-	-	CS1	-	-	-	-	-	S	Well developed spaced foliation/joint
6	5	foliation	54	77	324	-	-	ch	bi	-	-	-	-	-	-	-	-	CS1	-	-	-	-	-	S	Well developed spaced foliation/joint
6	5	foliation	162	53	252	-	-	ch	bi	-	-	-	-	-	-	-	-	CS1	-	-	-	-	-	S	Well developed spaced foliation/joint
6	5	foliation	170	44	260	-	-	-	-	-	-	-	-	-	-	-	-	CS1	-	-	-	-	-	S	Well developed spaced foliation/joint
6	5	lineation	-	-	-	0	35	-	-	-	-	-	-	-	-	-	-	LSLK	xprv	-	-	-	-	S	Horizontal lineation in previous plane
6	7	qz vein	35	32	125	-	-	qT	qM	mo	py	-	mo	py	-	-	-	V2	xprfol	-	mcs	-	-	S	New orientation of previous vein
6	7	qz vein	104	53	194	-	-	qT	qM	mo	py	-	mo	py	-	-	-	V2	xprfol	-	mcs	-	-	S	Complex crack-seal vein
6	7	qz vein	104	52	194	-	-	qM	-	-	-	-	mo	bi	py	si	-	V3	-	80	scs	-	50	S	1-2cm mo sl, 3-5 cm py sl
6	9	qz vein	96	60	186	-	-	qz	-	-	-	-	bi	si	-	-	-	V6	-	150	-	-	20	S	Recrystallised cs quartz
6	9	qz vein	104	38	194	-	-	qz	-	-	-	-	-	-	-	-	-	V6	-	150	mcs	-	0	S	Vein with no selvedge
6	9	qz vein	104	51	194	-	-	qz	-	-	-	-	si	-	-	-	-	V6	x284vn	70	-	-	50	S	
6	11	qz vein	94	53	184	-	-	qz	-	-	-	-	bi	si	py	-	-	V6	-	30	scs	-	20	S	
6	11	qz vein	114	40	204	-	-	qz	ca	-	-	-	-	-	-	-	-	V6	-	50	-	-	-	S	
6	14	shear zone	17	61	107	-	-	-	-	-	-	-	-	-	-	-	-	SH6	xprv3	-	-	-	-	S	**Quartz infill of shear DX strk slip slicks plng S**
6	14	qz vein	93	56	183	-	-	qT	ab	-	-	-	bi	py	si	-	-	V2	-	50	-	-	10	S	Thin albite infill
6	14	qz vein	10	45	100	-	-	qM	-	-	-	-	bi	si	py	-	-	V3	-	-	-	-	20	S	Thin boudinaged vein
6	14	qz vein	110	56	200	-	-	qM	-	-	-	-	mo	-	-	-	-	V3	-	50	scs	-	-	S	
6	14	qz vein	115	53	205	-	-	qM	py	-	-	-	mo	bi	si	py	-	V3	-	50	scs	-	-	S	mo selvedge on cs planes
6	17	qz vein	99	56	189	-	-	qM	-	-	-	-	mo	bi	py	si	-	V3	xprv	100	-	-	-	S	
6	17	qz vein	116	47	206	-	-	qM	py	-	-	-	mo	bi	py	si	-	V3	-	100	mcs	WR	-	S	
6	17	qz vein	115	61	205	-	-	-	-	-	-	-	-	-	-	-	-	V6	-	-	-	-	-	S	Thin veins intrude foliation parallel cleavage
6	20	qz vein	66	55	156	-	-	qM	py	-	-	-	bi	si	py	-	-	V3	-	1200	-	WR	-	S	Buck vein x-cuts other veins int shear foliation margins
7	0	slicks	-	-	-	22	130	-	-	-	-	-	-	-	-	-	-	LSLK	-	-	-	-	-	S	Slickensides in plane of fault
7	0	fault plane	178	78	88	-	-	-	-	-	-	-	-	-	-	-	-	SH7	-	-	-	-	-	S	**WBLk up DX fault x-cuts veins**
7	0	qz vein	108	48	198	-	-	qM	mo	-	-	-	mo	-	-	-	-	V3	-	-	-	-	-	S	Mo stylolites on vein margin
7	0	tension vein	13	42	283	-	-	-	-	-	-	-	-	-	-	-	-	V8	-	-	-	-	-	S	
7	5	foliation	15	36	285	-	-	-	-	-	-	-	-	-	-	-	-	CC	-	-	-	-	-	S	Foliation in wallrock
7	5	foliation	24	61	294	-	-	-	-	-	-	-	-	-	-	-	-	CC	-	-	-	-	-	S	Foliation in wallrock
7	5	qz vein	64	42	154	-	-	qz	-	-	-	-	py	bi	si	-	-	V6	-	-	-	-	20	S	
7	8	qz vein	94	54	184	-	-	qM	-	-	-	-	bi	si	py	-	-	V3	xnxt	70	scs	wr	20	S	Fractured buck vein

LOCATION		Structural	Orientation					Defining Mineralogy					Alteration					Group	X-cut	Vein	Vein	Vein	Halo	Pos	DESCRIPTION
WALL	Metres	Element	Strike	Dip	Dip/Dir	Plunge	Dir	1	2	3	4	5	1	2	3	4	5		Rel.	Width	Style	Inc	Width		
7	8	qz vein	117	43	207	-	-	qz	-	-	-	-	-	-	-	-	-	V6	-	50	mcs	bimoch	-	S	Thin vein intruded by previous
7	10	qz vein	107	46	197	-	-	qz	mo	-	-	-	bi	si	py	-	-	V6	-	100	mcs	-	10	S	Composite vein with thin vein intruded @ margin
7	12	qz vein	111	55	201	-	-	qM	mo	-	-	-	bi	si	py	-	-	V3	xnxt	80	-	-	-	S	Foliated vein bends into previous vein
7	15	slicks	-	-	-	20	202	qz	cb	-	-	-	-	-	-	-	-	LSLK		-	-	-	-	S	**Slickensides DX Wblock north movement**
7	15	fault plane	19	81	289	-	-	qz	cb	-	-	-	-	-	-	-	-	SH7	-	-	-	-	-	S	Undulating plane terminates against veins
7	18	foliation	11	31	101	-	-	-	-	-	-	-	-	-	-	-	-	CC	-	-	-	-	-	S	Pervasive foliation
7	18	fault plane	176	46	266	-	-	-	-	-	-	-	-	-	-	-	-	SH7	xbyprv	-	-	-	-	S	Fault surfaces bend into veins with foliated mgn
7	18	qz vein	129	39	219	-	-	qM	-	-	-	-	-	-	-	-	-	V3	xfaultpln	30	scs	-	-	S	Vein with no selvedge
7	19	qz vein	131	34	221	-		qz	-	-	-	-	hm	-	-	-	-	V6	-	-	scs	-	-	S	Intense hm alteration halo in foliated wallrock
7	19	qz vein	179	41	269	-	-	qz	-	-	-	-	-	-	-	-	-	V6	-	-	mcs	-	-	S	Intense foliated wallrock
7	20	fault plane	18	59	288	-	-	-	-	-	-	-	-	-	-	-	-	SH7	xall	-	-	-	-	S	Fault planes undulate between previous vein S+C style
7	23	qz vein	106	53	196	-	-	qM	-	-	-	-	bi	si	py	-	-	V3	-	110	mcs	-	30	S	Well dev crack seal fabric with foliated wallrock
7	24	foliation	16	41	286	-	-	-	-	-	-	-	-	-	-	-	-	SH1	-	-	-	-	-	S	SEF parallel foliation
7	27	SEF	38	71	308	-	-	-	-	-	-	-	ch	si	mu	bi	py	SEF	-	-	-	-	3500	S	SEF fragmental breccia shear zone ptygmatic foliated veins
7	27	foliation	0	63	90	-	-	-	-	-	-	-	-	-	-	-	-	SH1	-	-	-	-	-	S	Subsidiary foliation S-plane to SEF?
8	0	foliation	6	38	276	-	-	-	-	-	-	-	-	-	-	-	-	CC	-	-	-	-	-	S	Dominant foliation
8	0	fract fol	38	71	308	-	-	-	-	-	-	-	-	-	-	-	-	CS1	-	-	-	-	-	S	Prominent fracture foliation
8	0	joint	132	47	42	-	-	-	-	-	-	-	-	-	-	-	-	J2	-	-	-	-	-	S	Prominent joint plane
8	3	qz vein	141	38	231	-	-	qM	-	-	-	-	-	-	-	-	-	V3	-	140	mcs	mosty	-	S	Alteration selvedge indicates post-vein-intrusion shear of wallrock
8	4	qz vein	43	43	133	-	-	qM	ch	-	-	-	-	-	-	-	-	V3	-	-	-	-	-	S	Variable width vein thin halo
8	6	ca fl vein	49	88	319	-	-	ca	ab	fl	-	-	-	-	-	-	-	V7	-	-	tens	-	-	S	Recrystallised vein
8	8	qz vein	133	32	223	-	-	qz	mo	-	-	-	si	mu	fu	-	-	V6	-	100	mcs	-	-	S	Foliated margin
8	11	qz vein	107	36	197	-	-	qT	-	-	-	-	-	-	-	-	-	V2	-	70	-	-	-	S	Thin alteration selvedge
8	15	joint	36	40	306	-	-	-	-	-	-	-	-	-	-	-	-	J2	xprv	-	-	-	-	S	Poorly developed joint plane
8	15	fault plane	172	36	262	-	-	-	-	-	-	-	-	-	-	-	-	SH7	-	-	-	-	-	S	Prominent fault surface
8	19	foliation	38	43	128	-	-	ch	-	-	-	-	-	-	-	-	-	CC	-	-	-	-	-	S	Dominant foliation
8	19	foliation	171	57	261	-	-	ch	-	-	-	-	-	-	-	-	-	CC	-	-	-	-	-	S	Dominant foliation
8	19	qz vein	105	50	195	-	-	qT	-	-	-	-	-	-	-	-	-	V2	xnxt2	50	mcs	-	-	S	Thin fractured vein very thin halo
8	21	qz vein	136	35	226	-	-	qM	qT	-	-	-	ch	si	ka	-	-	V3	-	-	-	-	-	S	Very foliated wallrock
8	23	qz vein	102	52	192	-	-	qT	qM	mo	py	-	-	-	-	-	-	V2		200	mcs	-	-	S	Vuggy quartz vein mo stylolites
8	24	foliation	22	44	292	-	-	ch	-	-	-	-	-	-	-	-	-	SH3	-	-	-	-	-	S	Chlorite seams give sheen to surfaces
8	25	qz vein	58	55	148	-	-	qM	qT	cp	py	-	mu	ab	fu	-	-	V3	-	260	mcs	-	-	S	Foliated vein with broad alteration halo
8	26	fault plane	36	86	306	-	-	-	-	-	-	-	-	-	-	-	-	SH7	-	-	-	-	-	S	**Well developed fault plane DX W block N**
8	27	slicks	-	-	-	21	34	-	-	-	-	-	-	-	-	-	-	LSLK	-	-	-	-	-	S	Slickensides in previous fault plane
8	60	foliation	29	39	299	-	-	ch	hm	-	-	-	-	-	-	-	-	CC	-	-	-	-	-	S	Intense foliation on W side of fault
8	60	foliation	31	40	301	-	-	-	-	-	-	-	-	-	-	-	-	CC	-	-	-	-	-	S	Main foliation abundant vuggy quartz vein + hm conc
8	60	foliation	156	53	246	-	-	-	-	-	-	-	-	-	-	-	-	CC	-	-	-	-	-	S	Main foliation abun vuggy quartz vein + hm conc

LOCATION		Structural	Orientation					Defining Mineralogy					Alteration					Group	X-cut	Vein	Vein	Vein	Halo	Pos	DESCRIPTION
WALL	Metres	Element	Strike	Dip	Dip/Dir	Plunge	Dir	1	2	3	4	5	1	2	3	4	5		Rel.	Width	Style	Inc	Width		
8	60	joint	80	86	350	-	-	-	-	-	-	-	-	-	-	-	-	J1	-	-	-	-	-	S	Joint plane with trace of previous foliation
8	60	joint	159	72	69	-	-	-	-	-	-	-	-	-	-	-	-	J2	-	-	-	-	-	S	Joint plane with trace of previous foliation
9	1	vein fract	46	86	136	-	-	-	-	-	-	-	-	-	-	-	-	CS1	-	-	-	-	-	S	Prominent fracture within previous vein
9	4	qz vein	156	30	246	-	-	qM	hm	-	-	-	-	-	-	-	-	V3	-	230	scs	-	-	S	Vein with foliated wallrock
9	5	qz vein	124	45	214	-	-	qM	mu	hm	-	-	mu	ka	-	-	-	V3	-	90	scs	-	30	S	Fractured quartz vein
9	6	vein fract	60	77	330	-	-	-	-	-	-	-	-	-	-	-	-	CS1	-	-	-	-	-	S	Prominent fracture within previous vein
9	6	vein fract	65	87	335	-	-	-	-	-	-	-	-	-	-	-	-	CS1	-	-	-	-	-	S	Prominent fracture within previous vein
9	6	cataclasite	41	83	311	-	-	-	-	-	-	-	-	-	-	-	-	SH3	xprv	-	-	-	-	S	**Thin zones with W block down dip slip**
9	6	qz vein	136	32	226	-	-	qM	-	-	-	-	-	-	-	-	-	V3	-	1000	-	WR	-	S	Large vein up to 2m wide 5cm int sheared margin
9	10	vein fract	48	84	318	-	-	-	-	-	-	-	-	-	-	-	-	CS1	-	-	-	-	-	S	Mesofracturing of vein at angle to vein walls
9	10	qz vein	93	65	183	-	-	qT	-	-	-	-	-	-	-	-	-	V2	-	40	scs	-	-	S	Simple crack seal vein
9	14	foliation	167	35	257	-	-	ch	hm	-	-	-	-	-	-	-	-	CC	-	-	-	-	-	S	Foliation in wallrock
9	14	sh foliation	169	24	259	-	-	ch	hm	-	-	-	-	-	-	-	-	SH1	-	-	-	-	-	S	Intense shear foliation between last two veins
9	14	fault plane	32	75	302	-	-	-	-	-	-	-	hm	lm	-	-	-	SH3	-	-	-	-	100	S	**E Block up cataclasite fault zone + breccia vein mat**
9	14	qz vein	108	52	198	-	-	qM	-	-	-	-	-	-	-	-	-	V3	-	130	scs	-	-	S	Vuggy cs vein int shear foliation wallrock between vein
9	14	qz vein	120	52	210	-	-	-	-	-	-	-	-	-	-	-	-	V6	-	50	scs	-	-	S	Vuggy cs vein int shear foliation wallrock between vein
9	18	fault plane	38	77	308	-	-	-	-	-	-	-	-	-	-	-	-	SH7	-	-	-	-	-	S	**E block UP fault plane only minor offset**
9	20	foliation	40	28	310	-	-	-	-	-	-	-	-	-	-	-	-	CC	-	-	-	-	-	S	Foliation in wallrock
9	20	foliation	50	34	320	-	-	-	-	-	-	-	-	-	-	-	-	CC	-	-	-	-	-	S	Foliation in wallrock
9	20	foliation	129	44	219	-	-	-	-	-	-	-	-	-	-	-	-	CC	-	-	-	-	-	S	Foliation in wallrock
9	20	minlin	-	-	-	14	11	ch	hm	-	-	-	-	-	-	-	-	LMIN	-	-	-	-	-	S	Mineral preferred orientation in previous plane
9	20	cataclasite	177	73	87	-	-	-	-	-	-	-	-	-	-	-	-	SH3	-	-	-	-	-	S	**Cataclasite fault zone with app W block up**
9	21	qz vein	105	49	195	-	-	qT	-	-	-	-	py	mu	-	-	-	V2	-	70	mcs	mosty	20	S	Vuggy crack-seal vein intense alt halo vughs developed at margin
9	22	qz vein	114	50	204	-	-	qT	-	-	-	-	py	mu	-	-	-	V2	-	-	mcs	mosty	-	S	Veins converge along strike foliation bends into mgn
9	23	fault plane	28	79	298	-	-	-	-	-	-	-	-	-	-	-	-	SH1	-	-	-	-	-	S	**W block up dom strike slip S+C surfaces?**
9	24	slicks	-	-	-	3	175	-	-	-	-	-	-	-	-	-	-	LSLK	-	-	-	-	-	S	Slickensides in previous fault
9	24	fault plane	176	77	86	-	-	-	-	-	-	-	-	-	-	-	-	SH7	xall	-	-	-	-	S	Fault plane x-cuts all
9	26	foliation	32	35	302	-	-	-	-	-	-	-	-	-	-	-	-	CC	-	-	-	-	-	S	
9	26	foliation	36	44	306	-	-	-	-	-	-	-	-	-	-	-	-	CC	-	-	-	-	-	S	
9	26	foliation	83	88	173	-	-	-	-	-	-	-	-	-	-	-	-	CC	-	-	-	-	-	S	
9	26	joint	141	89	231	-	-	-	-	-	-	-	-	-	-	-	-	J2	-	-	-	-	-	S	
9	28	fault plane	54	50	324	-	-	-	-	-	-	-	-	-	-	-	-	SH7	-	-	-	-	-	S	Fault plane at angle to foliation several over 3m
9	28	fault plane	58	51	328	-	-	-	-	-	-	-	-	-	-	-	-	SH7	-	-	-	-	-	S	Fault plane at angle to foliation several over 3m
9	28	fault plane	3	79	93	-	-	-	-	-	-	-	-	-	-	-	-	SH7	xprv	-	-	-	-	S	Fault plane x-cuts both previous faults
9	30	intlin	-	-	-	47	266	-	-	-	-	-	-	-	-	-	-	LINT	-	-	-	-	-	S	Intersection direction of previous S+C
9	30	c-plane	26	71	296	-	-	-	-	-	-	-	-	-	-	-	-	SH1	-	-	-	-	-	S	Wallrock shear foliation DX Wblock N+ down
9	30	s-plane	156	41	246	-	-	-	-	-	-	-	-	-	-	-	-	SH1	-	-	-	-	-	S	Wallrock shear foliation

LOCATION		Structural	Orientation					Defining Mineralogy					Alteration					Group	X-cut	Vein	Vein	Vein	Halo	Pos	DESCRIPTION
WALL	Metres	Element	Strike	Dip	Dip/Dir	Plunge	Dir	1	2	3	4	5	1	2	3	4	5		Rel.	Width	Style	Inc	Width		
9	30	fault plane	81	59	351	-	-	-	-	-	-	-	-	-	-	-	-	SH7	-	-	-	-	-	S	Fault gently undulating foliation int in wallrock
10	0	fault plane	3	82	273	-	-	-	-	-	-	-	-	-	-	-	-	SH7	-	-	-	-	-	S	Shear fault planes x-cut main fault without offset
10	3	foliation	3	28	273	-	-	-	-	-	-	-	si	mu	py	-	-	CC	-	-	-	-	-	S	Foliated wallrock around major fault plane
10	3	foliation	14	82	284	-	-	-	-	-	-	-	si	mu	py	-	-	CC	-	-	-	-	-	S	Foliated wallrock around major fault plane
10	3	foliation	81	49	351	-	-	-	-	-	-	-	si	mu	py	-	-	CC	-	-	-	-	-	S	Foliated wallrock around major fault plane
10	7	fault plane	47	43	317	-	-	-	-	-	-	-	-	-	-	-	-	SH7	-	-	-	-	-	S	Fault plane
10	7	fault plane	0	82	90	-	-	-	-	-	-	-	-	-	-	-	-	SH7	-	-	-	-	-	S	Fault plane
10	9	foliation	4	62	274	-	-	-	-	-	-	-	-	-	-	-	-	CC	-	-	-	-	-	S	Foliation
10	9	fault plane	165	72	75	-	-	-	-	-	-	-	-	-	-	-	-	SH7	xnxt	-	-	-	-	S	Fault plane
10	10	slicks	-	-	-	10	177	-	-	-	-	-	-	-	-	-	-	LSLK	-	-	-	-	-	S	Slickensides in previous fault
10	10	fault plane	14	73	284	-	-	-	-	-	-	-	-	-	-	-	-	SH7	-	-	-	-	-	S	Fault plane x-cut by both previous veins
10	10	fault plane	1	68	91	-	-	-	-	-	-	-	-	-	-	-	-	SH7	-	-	-	-	-	S	**Fault plane SS E block up movement**
10	10	qz vein	79	34	169	-	-	qT	qM	ab	-	-	-	-	-	-	-	V2	-	200	scs	-	-	S	Crack seal vein
10	10	qz vein	162	20	72	-	-	-	-	-	-	-	-	-	-	-	-	V6	-	-	-	-	-	S	Thin quartz vein
10	12	foliation	161	55	251	-	-	-	-	-	-	-	-	-	-	-	-	CC	-	-	-	-	-	S	
10	14	foliation	13	42	283	-	-	-	-	-	-	-	-	-	-	-	-	CC	xprv	-	-	-	-	S	Foliation on fault plane
10	14	joint	73	77	343	-	-	-	-	-	-	-	-	-	-	-	-	J1	-	-	-	-	-	S	
10	14	fault plane	161	80	71	-	-	-	-	-	-	-	-	-	-	-	-	SH7	xnxt	-	-	-	-	S	Fault plane offsets quartz veins
10	16	QP vein	128	46	218	-	-	-	-	-	-	-	-	-	-	-	-	V10	-	60	-	-	-	S	Crack-seal qT vein in middle of QP
10	17	qz vein	4	30	274	-	-	qT	-	-	-	-	ch	-	-	-	-	V2	xall	150	-	WR	-	S	Late vuggy vein foliation wallrock parallel to vein dip slip
10	21	fault plane	39	42	309	-	-	-	-	-	-	-	-	-	-	-	-	SH7	-	-	-	-	-	S	Fault offsets porphyry marker
10	21	fault plane	62	54	332	-	-	-	-	-	-	-	-	-	-	-	-	SH7	-	-	-	-	-	S	Fault offsets porphyry marker
10	21	fault plane	168	89	258	-	-	-	-	-	-	-	-	-	-	-	-	SH7	-	-	-	-	-	S	Fault offsets porphyry marker
10	21	QP vein	99	38	189	-	-	-	-	-	-	-	-	-	-	-	-	V9	-	-	-	-	-	S	Porphyry marker
10	24	foliation	1	53	271	-	-	-	-	-	-	-	-	-	-	-	-	CC	-	-	-	-	-	S	Foliation in wallrock
10	26	foliation	13	39	283	-	-	-	-	-	-	-	-	-	-	-	-	CC	-	-	-	-	-	S	Foliation in wallrock parallel to that in porphyry
10	26	qz vein	5	43	275	-	-	-	-	-	-	-	-	-	-	-	-	V6	xprv	-	-	WR	-	S	Vein with inclusions of ch schist
10	26	QP vein	103	50	193	-	-	qz	fd	-	-	-	si	mu	-	-	-	V9	-	50	-	-	-	S	Quartz porphyry bar
10	30	qz vein	174	55	264	-	-	qT	-	-	-	-	si	mu	fu	py	cp	V2	-	700	mcs	-	-	S	Fol in w'rock parallel to vein margin, elongate wallrock inclusions
11	2	foliation	5	37	275	-	-	-	-	-	-	-	-	-	-	-	-	CC	-	-	-	-	-	S	Foliation wallrock near margins of main vein
11	3	slicks	-	-	-	9	105	qz	-	-	-	-	-	-	-	-	-	LSLK	-	-	-	-	-	S	Slickensides on previous fault
11	3	slicks	-	-	-	19	281	-	-	-	-	-	-	-	-	-	-	LSLK	-	-	-	-	-	S	Slickensides in previous fault plane
11	3	foliation	67	54	337	-	-	-	-	-	-	-	-	-	-	-	-	SH7	-	-	-	-	-	S	Foliation within fault zone bends into boundaries
11	3	fault plane	99	85	9	-	-	-	-	-	-	-	-	-	-	-	-	SH7	-	-	-	-	-	S	Northern fault plane
11	3	fault plane	107	76	17	-	-	-	-	-	-	-	-	-	-	-	-	SH7	xprv	-	-	-	-	S	**Prom fault pln strike slip Nblock up move**
11	5	foliation	177	59	267	-	-	mu	si	ka	py	-	-	-	-	-	-	CC	-	-	-	-	-	S	Intense foliation in altered mafic
11	5	qz vein	64	32	154	-	-	qT	-	-	-	-	-	-	-	-	-	V2	xprv	5	-	-	-	S	Thin vein x-cuts foliation

LOCATION		Structural	Orientation					Defining Mineralogy					Alteration					Group	X-cut	Vein	Vein	Vein	Halo	Pos	DESCRIPTION
WALL	Metres	Element	Strike	Dip	Dip/Dir	Plunge	Dir	1	2	3	4	5	1	2	3	4	5		Rel.	Width	Style	Inc	Width		
11	6	qz vein	3	50	273	-	-	qT	-	-	-	-	si	mu	fu	py	cp	V2	-	700	mcs	-	-	S	Continuation of main vein
11	9	joint	135	50	45	-	-	-	-	-	-	-	-	-	-	-	-	J2	-	-	-	-	-	S	Joint in chloritic spotted mafic
11	9	joint	172	88	82	-	-	-	-	-	-	-	-	-	-	-	-	J2	-	-	-	-	-	S	Joint in chloritic spotted mafic
11	9	joint	126	89	216	-	-	-	-	-	-	-	-	-	-	-	-	J2	-	-	-	-	-	S	Joint in chloritic spotted mafic
11	9	joint	174	56	264	-	-	-	-	-	-	-	-	-	-	-	-	J2	-	-	-	-	-	S	Joint in chloritic spotted mafic
11	11	qz vein	115	49	205	-	-	qT	ab	-	-	-	-	-	-	-	-	V2	-	120	-	-	-	S	Vein with late albite infill
11	12	fault plane	63	47	333	-	-	qz	fl	-	-	-	-	-	-	-	-	SH7	xprv	-	-	-	-	S	Fault with open space cavities cg quartz+fl
11	12	fault plane	168	78	78	-	-	-	-	-	-	-	-	-	-	-	-	SH7	-	-	-	-	-	S	Fault plane
11	15	foliation	13	36	283	-	-	-	-	-	-	-	-	-	-	-	-	CC	-	-	-	-	-	S	Intense foliation in cg spotted gabbro
11	15	qz vein	102	45	192	-	-	-	-	-	-	-	-	-	-	-	-	V6	-	-	-	-	-	S	Foliated quartz vein thin slivers of GP on margins + spch
11	21	fault plane	1	54	91	-	-	-	-	-	-	-	-	-	-	-	-	SH7	-	-	-	-	-	S	**Undulating fault apparent E block up slicks plunge S**
11	24	foliation	9	42	279	-	-	-	-	-	-	-	-	-	-	-	-	CC	-	-	-	-	-	S	Well developed foliation
11	29	fault plane	128	68	38	-	-	-	-	-	-	-	-	-	-	-	-	SH7	-	-	-	-	-	S	Well developed fault plane prominent in face
11	29	qz vein	114	46	204	-	-	qT	-	-	-	-	-	-	-	-	-	V2	-	80	scs	-	-	S	Simple crack seal vein
12	0	qz vein	8	56	98	-	-	qT	-	-	-	-	-	-	-	-	-	V2	-	100	scs	-	-	N	Quartz vein intruding fault plane
12	1	fault plane	117	75	27	-	-	-	-	-	-	-	-	-	-	-	-	SH7	xprv	-	-	-	-	N	Fault set x-cuts last
12	4	foliation	47	53	317	-	-	-	-	-	-	-	-	-	-	-	-	CS1	-	-	-	-	-	N	Spaced foliation in spotted chloritic dolerite
12	4	fault plane	101	76	191	-	-	-	-	-	-	-	-	-	-	-	-	SH7	xprv	-	-	-	-	N	**Fault plane with N block up movement**
12	4	fault plane	114	89	204	-	-	-	-	-	-	-	-	-	-	-	-	SH7	-	-	-	-	-	N	Dominant fault set parallel to fractures in quartz vein
12	4	qz vein	98	42	188	-	-	qT	-	-	-	-	-	-	-	-	-	V2	-	120	scs	-	-	N	Single phase intrusion halo obscured by weathering
12	4	qz vein	127	52	217	-	-	qT	-	-	-	-	-	-	-	-	-	V2	-	50	scs	-	-	N	Vein with minor vughs
12	5	cren fol	95	80	185	-	-	-	-	-	-	-	-	-	-	-	-	CS2	-	-	-	-	-	N	Crenulation cleavage 1-3cm spacing
12	7	fractures	60	86	150	-	-	-	-	-	-	-	-	-	-	-	-	CS1	-	-	-	-	-	N	Fractures in previous fault plane
12	7	fractures	89	79	179	-	-	-	-	-	-	-	-	-	-	-	-	CS1	-	-	-	-	-	N	Fractures in previous fault plane
12	7	fault plane	119	72	29	-	-	-	-	-	-	-	-	-	-	-	-	SH7	-	-	-	-	-	N	Fault plane with open space fractures
12	9	slicks	-	-	-	25	184	-	-	-	-	-	-	-	-	-	-	LSLK	-	-	-	-	-	N	Slickensides in previous fault plane
12	9	fault plane	17	64	107	-	-	-	-	-	-	-	-	-	-	-	-	SH7	-	-	-	-	-	N	**Prominent fault plane sinistral movement**
12	11	fault plane	48	73	138	-	-	-	-	-	-	-	-	-	-	-	-	SH7	-	-	-	-	-	N	Well developed fault plane
12	11	qz vein	127	54	217	-	-	qT	-	-	-	-	-	-	-	-	-	V2	-	200	scs	vu	-	N	Vein with intrusive porphyry bar + fracturing @ 90 to wall
12	11	QP vein	104	42	194	-	-	qz	fd	-	-	-	-	-	-	-	-	V9	xprv	330	-	-	-	N	GP bar intrusive to vein, fracture parallel to next
12	16	foliation	150	62	240	-	-	-	-	-	-	-	-	-	-	-	-	CC	-	-	-	-	-	N	Intense foliation produces lineations
12	16	cren fol	104	73	14	-	-	-	-	-	-	-	-	-	-	-	-	CS2	xprv	-	-	-	-	N	Crenulation cleavage x-cuts previous fault plane
12	16	fault plane	30	54	120	-	-	-	-	-	-	-	-	-	-	-	-	SH7	-	-	-	-	-	N	Well developed fault plane
12	18	fault plane	98	82	188	-	-	-	-	-	-	-	-	-	-	-	-	SH7	-	-	-	-	-	N	Thin fault plane with quartz vein infill
12	19	c-plane	113	64	203	-	-	-	-	-	-	-	-	-	-	-	-	SH1	-	-	-	-	-	N	Intense anastomosing fault zone
12	19	c-plane	130	63	220	-	-	-	-	-	-	-	-	-	-	-	-	SH1	-	-	-	-	-	N	Intense anastomosing fault zone
12	19	foliation	32	89	122	-	-	-	-	-	-	-	-	-	-	-	-	SH7	-	-	-	-	-	N	Foliation bending into fault zone

LOCATION		Structural	Orientation					Defining Mineralogy					Alteration					Group	X-cut	Vein	Vein	Vein	Halo	Pos	DESCRIPTION
WALL	Metres	Element	Strike	Dip	Dip/Dir	Plunge	Dir	1	2	3	4	5	1	2	3	4	5		Rel.	Width	Style	Inc	Width		
12	19	qz vein	109	31	199	-	-	-	-	-	-	-	-	-	-	-	-	V6	-	-	-	-	-	N	Large quartz vein fragment
12	19	qz vein	152	46	242	-	-	-	-	-	-	-	-	-	-	-	-	V6	-	-	-	-	-	N	Quartz vein within zone
13	1	foliation	160	65	250	-	-	-	-	-	-	-	-	-	-	-	-	CS1	-	-	-	-	-	N	Spaced foliation <1mm with parall quartz veins
13	1	fault plane	80	63	170	-	-	-	-	-	-	-	-	-	-	-	-	SH7	-	-	-	-	-	N	Fault plane x-cuts altered mafic
13	3	fault plane	120	69	30	-	-	-	-	-	-	-	-	-	-	-	-	SH7	xprv2	-	-	-	-	N	Late fault plane x-cuts both previous structures
13	3	fault plane	150	69	60	-	-	-	-	-	-	-	-	-	-	-	-	SH7	-	-	-	-	-	N	Fault plane conjugate? with fault at 1m
13	4	foliation	124	55	214	-	-	-	-	-	-	-	-	-	-	-	-	CC		-	-	-	-	N	Main foliation
13	4	foliation	174	83	264	-	-	-	-	-	-	-	-	-	-	-	-	CC	-	-	-	-	-	N	Main foliation conjugate with next
13	4	foliation	9	58	279	-	-	-	-	-	-	-	-	-	-	-	-	CS1	xprv2	-	-	-	-	N	Wider spaced foliation x-cuts both previous struct
13	6	fault plane	71	68	341	-	-	-	-	-	-	-	-	-	-	-	-	SH7	-	-	-	-	-	N	Fault plane x-cuts intensely altered rock
13	6	fault plane	135	54	225	-	-	-	-	-	-	-	-	-	-	-	-	SH7	-	-	-	-	-	N	Fault plane x-cuts intensely altered rock
13	6	qz vein	133	49	223	-	-	qT	-	-	-	-	-	-	-	-	-	V2	-	350	-	-	-	N	Large buck quartz vein
13	11	foliation	154	70	244	-	-	-	-	-	-	-	-	-	-	-	-	CC	-	-	-	-	-	N	Foliation at moderate angle to quartz vein dip
13	11	qz vein	124	67	34	-	-	-	-	-	-	-	-	-	-	-	-	V6	-	-	-	-	-	N	Quartz vein not foliated
13	11	qz vein	14	36	104	-	-	-	-	-	-	-	-	-	-	-	-	V6	-	-	-	-	-	N	Veins dipping out of face
13	11	qz vein	158	60	248	-	-	-	-	-	-	-	-	-	-	-	-	V6	-	5	-	-	-	N	**Fe stained qz veins Z fold looking N, ->E verging**
13	14	sh zone	154	80	244	-	-	-	-	-	-	-	-	-	-	-	-	SH6	xprv	-	-	-	-	N	Prominent shear plane
13	14	qz vein	3	23	93	-	-	-	-	-	-	-	-	-	-	-	-	V6	-	150	-	-	-	N	Quartz vein dipping out of face
13	18	qz vein	72	31	162	-	-	-	-	-	-	-	-	-	-	-	-	V6	-	350	-	-	-	N	Buck quartz vein dipping out of face
13	22	sh foliation	130	74	220	-	-	-	-	-	-	-	-	-	-	-	-	SH7	-	-	-	-	-	N	Close spaced shear foliation near major fault plane
13	26	fault plane	23	85	113	-	-	-	-	-	-	-	-	-	-	-	-	SH7	xprv	-	-	-	-	N	Fault plane x-cuts foliation
13	27	fault plane	80	87	350	-	-	-	-	-	-	-	-	-	-	-	-	NEF	-	-	-	-	-	N	NEF major fault plane ka alteration + ptygmatic folding?
13	30	foliation	146	75	56	-	-	-	-	-	-	-	-	-	-	-	-	CC	-	-	-	-	-	N	Foliation in mafic
13	30	qz vein	30	79	300	-	-	-	-	-	-	-	-	-	-	-	-	V6	-	-	-	-	-	N	Thin vein
13	30	qz vein	72	80	342	-	-	-	-	-	-	-	-	-	-	-	-	V6	-	-	-	-	-	N	SW dipping quartz vein
13	30	qz vein	148	73	238	-	-	-	-	-	-	-	-	-	-	-	-	V6	-	-	-	-	-	N	Quartz veins isoclinal folding and pinch/swell
14	6	fault plane	75	83	165	-	-	-	-	-	-	-	-	-	-	-	-	NEF	-	-	-	-	-	N	NEF fault plane stockwork fracturing int si'd breccia
14	7	fault plane	60	80	330	-	-	-	-	-	-	-	-	-	-	-	-	NEF	-	-	-	-	-	N	NEF
14	10	fract fol	64	89	334	-	-	-	-	-	-	-	-	-	-	-	-	CS1	-	-	-	-	-	N	Fracture foliation in at 90 degrees to hingeline
14	10	qz vn fold	-	-	-	31	159	-	-	-	-	-	-	-	-	-	-	F1	-	-	-	-	-	N	E verging Z folds in ferruginous quartz vein
14	22	qz vein	115	66	205	-	-	-	-	-	-	-	-	-	-	-	-	V6	-	30	-	-	-	N	Gently undulating quartz vein
14	28	foliation	163	77	253	-	-	-	-	-	-	-	-	-	-	-	-	CC	-	-	-	-	-	N	Foliation in hematite stained mafic
14	40	joint	61	82	331	-	-	-	-	-	-	-	-	-	-	-	-	J1	-	-	-	-	-	N	Joint in mu,ka,fu,py altered mafic
14	43	joint	178	79	88	-	-	-	-	-	-	-	-	-	-	-	-	J2	-	-	-	-	-	N	Joint in mu,ka,fu,py altered mafic
14	49	foliation	9	88	99	-	-	-	-	-	-	-	-	-	-	-	-	CC	-	-	-	-	-	N	Foliation in weathered and altered mafic
14	49	qz vein	39	80	309	-	-	-	-	-	-	-	-	-	-	-	-	V6	-	-	-	-	-	N	Veins in weathered and altered mafic
14	54	foliation	173	74	83	-	-	-	-	-	-	-	-	-	-	-	-	CC	-	-	-	-	-	N	

LOCATION		Structural	Orientation					Defining Mineralogy					Alteration					Group	X-cut	Vein	Vein	Vein	Halo	Pos	DESCRIPTION
WALL	Metres	Element	Strike	Dip	Dip/Dir	Plunge	Dir	1	2	3	4	5	1	2	3	4	5		Rel.	Width	Style	Inc	Width		
15	0	qz vein	54	77	324	-	-	-	-	-	-	-	-	-	-	-	-	V6	-	-	bx	-	-	N	Int breccia vein large angular wallrock fragments
15	0	qz vein	61	87	331	-	-	-	-	-	-	-	-	-	-	-	-	V6	-	50	-	-	-	N	Thin quartz vein
15	1	foliation	35	70	125	-	-	-	-	-	-	-	-	-	-	-	-	CC	-	-	-	-	-	N	Foliation between veins
15	1	qz vein	44	88	314	-	-	-	-	-	-	-	-	-	-	-	-	V6	-	-	-	-	-	N	Thin ferruginous quartz veins
15	4	foliation	158	73	248	-	-	-	-	-	-	-	-	-	-	-	-	CC	-	-	-	-	-	N	Wallrock foliation
15	10	foliation	168	74	258	-	-	-	-	-	-	-	-	-	-	-	-	CC	-	-	-	-	-	N	Foliation in weathered mafic
15	10	fold axis	-	-	-	31	135	-	-	-	-	-	-	-	-	-	-	F1	-	-	-	-	-	N	Fold axis in quartz vein
15	12	foliation	165	79	75	-	-	-	-	-	-	-	-	-	-	-	-	CC	-	-	-	-	-	N	
15	14	qz vein	167	76	77	-	-	-	-	-	-	-	-	-	-	-	-	V6	-	30	-	-	-	N	Thin quartz vein
15	15	fault plane	106	52	196	-	-	-	-	-	-	-	-	-	-	-	-	SH7	-	-	-	-	-	N	Fault plane between int-mod foliated mafic
15	16	foliation	172	53	262	-	-	-	-	-	-	-	-	-	-	-	-	CC	-	-	-	-	-	N	
15	16	foliation	173	40	263	-	-	-	-	-	-	-	-	-	-	-	-	CC	-	-	-	-	-	N	Gently undulating foliation
15	16	cataclasite	1	79	271	-	-	-	-	-	-	-	-	-	-	-	-	SH3	xprv	-	-	-	-	N	Cataclasite zone x-cuts foliations
15	16	foliation	175	24	265	-	-	-	-	-	-	-	-	-	-	-	-	SH7	xprv	-	-	-	-	N	X-cutting foliation bends into fault plane
15	19	foliation	51	38	141	-	-	-	-	-	-	-	-	-	-	-	-	CC	-	-	-	-	-	N	Foliation pervasive over 1-2m
15	19	cataclasite	28	86	298	-	-	-	-	-	-	-	-	-	-	-	-	SH3	xall	-	-	-	-	N	Thin cataclasite fault plane x-cuts all foliation
15	20	stock vein	19	69	289	-	-	-	-	-	-	-	-	-	-	-	-	V6	-	-	-	-	-	N	stockwork vein
15	20	stock vein	130	65	40	-	-	-	-	-	-	-	-	-	-	-	-	V6	-	-	-	-	-	N	stockwork vein
15	20	stock vein	158	55	248	-	-	-	-	-	-	-	-	-	-	-	-	V6	-	-	-	-	-	N	stockwork vein
15	22	foliation	172	43	262	-	-	-	-	-	-	-	-	-	-	-	-	CC	-	-	-	-	-	N	
15	22	foliation	154	79	244	-	-	-	-	-	-	-	-	-	-	-	-	SH1	-	-	-	-	-	N	Shear foliation in fault
15	22	cataclasite	8	38	278	-	-	-	-	-	-	-	-	-	-	-	-	SH3	-	-	-	-	-	N	Cataclasite zone x-cut by fault
15	22	fault plane	28	80	298	-	-	-	-	-	-	-	ch	-	-	-	-	SH7	-	-	-	-	-	N	Fault plane cuts entire face int ch alteration
15	23	foliation	112	63	202	-	-	-	-	-	-	-	-	-	-	-	-	CS2	-	-	-	-	-	N	Plane contains crenulation lineation
15	23	cren fol	153	75	243	-	-	-	-	-	-	-	-	-	-	-	-	CS2	-	-	-	-	-	N	"
15	23	cren fol	156	23	246	-	-	-	-	-	-	-	-	-	-	-	-	CS2	-	-	-	-	-	N	Intersection with previous foliation to produce crenulation lineation
15	23	cren fol	178	48	268	-	-	-	-	-	-	-	-	-	-	-	-	CS2	-	-	-	-	-	N	"
15	25	foliation	138	40	228	-	-	-	-	-	-	-	-	-	-	-	-	CC	-	-	-	-	-	N	Close spaced foliation
15	27	foliation	160	51	250	-	-	-	-	-	-	-	-	-	-	-	-	CC	-	-	-	-	-	N	Intense foliation
15	27	qz vein	8	71	98	-	-	-	-	-	-	-	-	-	-	-	-	V6	xprv	-	-	-	-	N	Thin ferruginous quartz vein cuts foliation
15	28	foliation	160	80	250	-	-	-	-	-	-	-	-	-	-	-	-	SH1	-	-	-	-	-	N	Shear foliation on west side of fault
15	28	foliation	163	47	253	-	-	-	-	-	-	-	-	-	-	-	-	SH1	-	-	-	-	-	N	Shear foliation on east side of fault
15	28	fault plane	145	83	235	-	-	-	-	-	-	-	-	-	-	-	-	SH7	-	-	-	-	-	N	Fault plane cuts entire face
16	0	foliation	47	57	317	-	-	-	-	-	-	-	-	-	-	-	-	CC	-	-	-	-	-	N	Intensely altered ferruginous dolerite
16	1	fold limb	160	53	250	-	-	-	-	-	-	-	-	-	-	-	-	VL	-	-	-	-	-	N	West limb of fold in quartz vein E verge Z folds
16	3	sr vein	30	46	300	-	-	-	-	-	-	-	-	-	-	-	-	SRPY	-	-	-	-	-	N	Ferruginous stringer vein
16	3	sr vein	32	64	302	-	-	-	-	-	-	-	-	-	-	-	-	SRPY	-	-	-	-	-	N	Ferruginous stringer vein

LOCATION		Structural	Orientation					Defining Mineralogy					Alteration					Group	X-cut	Vein	Vein	Vein	Halo	Pos	DESCRIPTION
WALL	Metres	Element	Strike	Dip	Dip/Dir	Plunge	Dir	1	2	3	4	5	1	2	3	4	5		Rel.	Width	Style	Inc	Width		
16	3	sr vein	27	80	117	-	-	-	-	-	-	-	-	-	-	-	-	SRPY	-	-	-	-	-	N	Ferruginous stringer vein
16	4	qz vein	115	62	205	-	-	qT	-	-	-	-	-	-	-	-	-	V2	-	600	-	chpy		N	Foliated vein
16	8	foliation	156	43	246	-	-	-	-	-	-	-	-	-	-	-	-	CC	-	-	-	-	-	N	
16	10	fault plane	158	77	248	-	-	-	-	-	-	-	-	-	-	-	-	SH7	-	-	-	-	-	N	Fault plane with 10cm quartz vein intruding
16	10	foliation	165	60	255	-	-	-	-	-	-	-	-	-	-	-	-	SH7	-	-	-	-	-	N	Wall rock foliation bends into fault plane
16	11	qz vein	145	61	235	-	-	-	-	-	-	-	-	-	-	-	-	V6	-	100	-	-	-	N	Buck quartz vein
16	12	foliation	147	51	237	-	-	-	-	-	-	-	-	-	-	-	-	CC	-	-	-	-	-	N	Intense shear foliation
16	12	fold axis	-	-	-	40	300	-	-	-	-	-	-	-	-	-	-	F1	-	-	-	-	-	N	Z folds in previous vein 90:1 limb-hinge ratio
16	12	foliation	42	41	312	-	-	-	-	-	-	-	-	-	-	-	-	SH1	-	-	-	-	-	N	Intense shear foliation
16	12	fault plane	145	72	235	-	-	-	-	-	-	-	-	-	-	-	-	SH7	-	-	-	-	-	N	Abundant euhedral py stringers
16	12	qz vein	101	50	191	-	-	-	-	-	-	-	-	-	-	-	-	V6	-	20	-	-	-	N	Quartz vein within fault plane
16	12	qz vein	159	50	249	-	-	-	-	-	-	-	-	-	-	-	-	V6	-	50	-	-	-	N	Foliated quartz vein
16	14	qz vein	143	44	233	-	-	-	-	-	-	-	-	-	-	-	-	V6	-	30	-	-	-	N	Thin quartz vein foliation parallel
16	14	qz vein	144	85	234	-	-	-	-	-	-	-	-	-	-	-	-	V6	xprv	-	-	-	-	N	**X-cuts previous with apparent E Block down**
16	17	foliation	165	51	255	-	-	-	-	-	-	-	-	-	-	-	-	CC	-	-	-	-	-	N	Intense close spaced foliation
16	17	fault plane	136	71	226	-	-	-	-	-	-	-	-	-	-	-	-	SH7	-	-	-	-	-	N	Fault plane, previous foliation bends into
16	20	qz vein	94	38	184	-	-	-	-	-	-	-	-	-	-	-	-	V6	-	-	-	-	-	N	Gently foliated quartz vein dipping out of face
16	24	foliation	3	56	273	-	-	-	-	-	-	-	-	-	-	-	-	CC	-	-	-	-	-	N	Intense wallrock foliation
16	24	foliation	165	83	255	-	-	-	-	-	-	-	-	-	-	-	-	CC	-	-	-	-	-	N	Intense wallrock foliation
16	24	qz vein	71	27	161	-	-	-	-	-	-	-	-	-	-	-	-	V6	-	-	-	-	-	N	Thin quartz vein
16	27	fault plane	64	85	154	-	-	-	-	-	-	-	-	-	-	-	-	NEF	-	-	-	-	-	N	NEF? cuts entire face with parallel quartz vein
16	27	qz vein	45	29	135	-	-	-	-	-	-	-	-	-	-	-	-	V6	-	-	-	-	-	N	**Vein bends into NEF with N Block up**
16	30	qz vein	53	80	323	-	-	-	-	-	-	-	-	-	-	-	-	V6	-	-	-	-	-	N	Lensoidal attenuated quartz vein parallel to fault
17	1	c-plane	75	82	345	-	-	-	-	-	-	-	-	-	-	-	-	SH1	-	-	-	-	-	N	Mylonitic foliation
17	1	s-plane	113	71	23	-	-	-	-	-	-	-	-	-	-	-	-	SH1	-	-	-	-	-	N	Mylonitic foliation
17	6	fault plane	115	44	205	-	-	-	-	-	-	-	-	-	-	-	-	SH7	-	-	-	-	-	N	Prominent fault plane
17	11	qz vein	95	59	185	-	-	-	-	-	-	-	py	bi	ka	-	-	V6	-	150	-	-	-	N	
17	11	qz vein	97	44	187	-	-	-	-	-	-	-	-	-	-	-	-	V6	-	-	-	-	-	N	Quartz vein fragments in quartz/mafic breccia
17	14	fault plane	74	82	344	-	-	-	-	-	-	-	-	-	-	-	-	SH7	-	-	-	-	-	N	
17	15	qz vein	81	84	171	-	-	-	-	-	-	-	-	-	-	-	-	V6	xnxt	-	-	-	-	N	Quartz vein on N side of fault
17	15	qz vein	167	50	257	-	-	-	-	-	-	-	-	-	-	-	-	V6	-	150	-	-	-	N	Vein x-cut by previous
17	19	qz vein	179	42	269	-	-	-	-	-	-	-	-	-	-	-	-	V6	-	30	-	-	-	N	Thin vein within fault zone
17	21	c-plane	83	77	353	-	-	-	-	-	-	-	-	-	-	-	-	SH1	-	-	-	-	-	N	C fabric in quartz crush zone
17	21	s-plane	105	65	15	-	-	-	-	-	-	-	-	-	-	-	-	SH1	-	-	-	-	-	N	S fabric in quartz crush zone
17	21	fault plane	43	80	133	-	-	-	-	-	-	-	-	-	-	-	-	SH7	-	-	-	-	-	N	Prominent fault plane cut by NEF
17	23	qz vein	34	82	124	-	-	-	-	-	-	-	-	-	-	-	-	V6	-	-	-	-	-	N	Ka altered qab veinlets
17	27	qz vein	13	34	103	-	-	-	-	-	-	-	-	-	-	-	-	V6	xprv	-	-	-	-	N	**Vein with SS N Block W (apparent) movement**

LOCATION		Structural	Orientation					Defining Mineralogy					Alteration					Group	X-cut	Vein	Vein	Vein	Halo	Pos	DESCRIPTION
WALL	Metres	Element	Strike	Dip	Dip/Dir	Plunge	Dir	1	2	3	4	5	1	2	3	4	5		Rel.	Width	Style	Inc	Width		
17	27	qz vein	151	68	241	-	-	-	-	-	-	-	-	-	-	-	-	V6	-	-	-	-	-	N	Faulted quartz vein
17	29	foliation	176	76	266	-	-	-	-	-	-	-	-	-	-	-	-	CC	-	-	-	-	-	N	Intense foliation in hm,lm stained dolerite
18	0	fault plane	82	68	172	-	-	-	-	-	-	-	-	-	-	-	-	SH7	-	-	-	-	-	N	Fault plane in intensely altered fine grained mafic
18	4	fault plane	92	83	182	-	-	-	-	-	-	-	-	-	-	-	-	SH7	-	-	-	-	-	N	**Fault plane foliation bends in with Nblock up m'ment**
18	5	qz vein	1	44	271	-	-	qM	qT	-	-	-	-	-	-	-	-	V3	-	500	-	-	-	N	Foliated vein
18	7	fault plane	122	74	212	-	-	-	-	-	-	-	-	-	-	-	-	SH7	-	-	-	-	-	N	
18	7	qz vein	90	56	180	-	-	-	-	-	-	-	-	-	-	-	-	V6	-	-	-	-	-	N	Quartz vein fragment
18	7	qz vein	163	42	253	-	-	-	-	-	-	-	-	-	-	-	-	V6	-	-	-	-	-	N	Foliated quartz vein
18	9	foliation	145	76	235	-	-	fu	ka	mu	-	-	-	-	-	-	-	SH7	-	-	-	-	-	N	Intense foliation near major fault plane
18	12	qz vein	83	70	173	-	-	-	-	-	-	-	-	-	-	-	-	V6	-	-	-	-	-	N	Fault with quartz vein , veins on W side terminate
18	20	foliation	129	74	39	-	-	-	-	-	-	-	-	-	-	-	-	CC	-	-	-	-	-	N	
18	20	qz vein	82	74	352	-	-	-	-	-	-	-	-	-	-	-	-	V6	xnxt	-	-	-	-	N	Foliation bends into quartz veins
18	22	fract fol	30	65	300	-	-	-	-	-	-	-	-	-	-	-	-	CS1	-	-	-	-	-	N	
18	22	qz vein	170	63	80	-	-	-	-	-	-	-	-	-	-	-	-	V6	-	-	-	-	-	N	**Foliated quartz vein W verging S-folds**
18	22	qz vein	162	52	252	-	-	-	-	-	-	-	-	-	-	-	-	V6	-	-	-	-	-	N	Vein traverses entire face
18	26	qz vein	132	66	42	-	-	-	-	-	-	-	-	-	-	-	-	V6	-	30	-	-	-	N	Vein x-cut by shallow NW dipping veins
18	28	slicks	-	-	-	35	197	-	-	-	-	-	-	-	-	-	-	LSLK	-	-	-	-	-	N	**Slickensides DX W BLK N**
18	28	fault plane	26	77	116	-	-	-	-	-	-	-	-	-	-	-	-	SH7	-	-	-	-	-	N	Prominent fault plane
18	29	foliation	158	44	248	-	-	-	-	-	-	-	-	-	-	-	-	CC	-	-	-	-	-	N	
18	30	fract fol	4	47	274	-	-	-	-	-	-	-	-	-	-	-	-	CS1	-	-	-	-	-	N	Prominent microfracture direction in crackle breccia mafic
18	30	fract fol	80	63	350	-	-	-	-	-	-	-	-	-	-	-	-	CS1	-	-	-	-	-	N	Fracture foliation with open space cavities
19	0	foliation	50	35	320	-	-	-	-	-	-	-	ch	-	-	-	-	CC	-	-	-	-	-	N	Intense foliation in near vicinity of vein
19	0	qz vein	30	36	300	-	-	qT	-	-	-	-	ch	hm	-	-	-	V2	-	-	-	-	-	N	Quartz vein
19	2	joint	58	78	328	-	-	-	-	-	-	-	-	-	-	-	-	J1	-	-	-	-	-	N	
19	2	joint	168	81	258	-	-	-	-	-	-	-	-	-	-	-	-	J2	-	-	-	-	-	N	Dilatent fracture with crystal growth
19	2	fault plane	11	65	281	-	-	-	-	-	-	-	-	-	-	-	-	SH7	-	-	-	-	-	N	
19	7	foliation	139	46	49	-	-	-	-	-	-	-	-	-	-	-	-	CC	-	-	-	-	-	N	Prominent foliation with large slip
19	12	joint	23	45	293	-	-	-	-	-	-	-	-	-	-	-	-	J2	-	-	-	-	-	N	
19	13	qz vein	101	41	191	-	-	qT	-	-	-	-	-	-	-	-	-	V2	-	200	scs	-	-	N	Thin veins of GP intrude vein in vcg spotted porphyritic, ophitic Aog
20	0	foliation	6	22	276	-	-	-	-	-	-	-	-	-	-	-	-	CC	-	-	-	-	-	N	Dominant fine foliation
20	0	foliation	98	35	188	-	-	-	-	-	-	-	-	-	-	-	-	CC	-	-	-	-	-	N	Secondary foliation
20	0	foliation	56	71	326	-	-	-	-	-	-	-	-	-	-	-	-	CS1	-	-	-	-	-	N	Secondary foliation
20	2	fault plane	66	71	336	-	-	-	-	-	-	-	-	-	-	-	-	SH7	-	-	-	-	-	N	
20	5	foliation	8	57	278	-	-	-	-	-	-	-	-	-	-	-	-	CC	-	-	-	-	-	N	
20	5	foliation	141	45	51	-	-	-	-	-	-	-	-	-	-	-	-	CC	-	-	-	-	-	N	
20	5	foliation	123	72	213	-	-	-	-	-	-	-	-	-	-	-	-	CC	-	-	-	-	-	N	
20	5	foliation	137	73	227	-	-	-	-	-	-	-	-	-	-	-	-	CC	-	-	-	-	-	N	

LOCATION		Structural	Orientation					Defining Mineralogy					Alteration					Group	X-cut	Vein	Vein	Vein	Halo	Pos	DESCRIPTION
WALL	Metres	Element	Strike	Dip	Dip/Dir	Plunge	Dir	1	2	3	4	5	1	2	3	4	5		Rel.	Width	Style	Inc	Width		
20	5	qz vein	120	44	210	-	-	qT	-	-	-	-	-	-	-	-	-	V2	-	30	-	-	-	N	
20	9	foliation	129	66	219	-	-	-	-	-	-	-	-	-	-	-	-	CC	-	-	-	-	-	N	
20	9	foliation	162	59	252	-	-	-	-	-	-	-	-	-	-	-	-	CC	xnxt	-	-	-	-	N	Dominant foliation
20	9	foliation	171	72	261	-	-	-	-	-	-	-	-	-	-	-	-	CC	xnxt	-	-	-	-	N	
20	11	slicks	-	-	-	6	93	-	-	-	-	-	-	-	-	-	-	LSLK	-	-	-	-	-	N	**Slickensides show SS Nblock W movement**
20	11	fault plane	95	76	5	-	-	-	-	-	-	-	-	-	-	-	-	SH7	xprv	-	-	-	-	N	Fault plane x-cuts vein
20	11	qz vein	158	59	248	-	-	qM	qT	-	-	-	-	-	-	-	-	V3	-	700	mcs	shWR	-	N	Foliation parallel to vein at margins
20	13	foliation	19	43	289	-	-	-	-	-	-	-	-	-	-	-	-	CC	-	-	-	-	-	N	
20	13	fract fol	155	58	65	-	-	-	-	-	-	-	-	-	-	-	-	CS1	-	-	-	-	-	N	
20	16	foliation	141	58	51	-	-	-	-	-	-	-	-	-	-	-	-	CC	-	-	-	-	-	N	Intense foliation in fg basalt
20	16	qz vein	163	60	73	-	-	-	-	-	-	-	-	-	-	-	-	V2	-	-	-	-	-	N	
20	20	qz vein	3	45	273	-	-	-	-	-	-	-	-	-	-	-	-	V6	xnxt	50	scs	-	-	N	
20	20	qz vein	103	48	193	-	-	-	-	-	-	-	-	-	-	-	-	V6	-	20	-	-	-	N	Foliation parallel veins
20	23	foliation	167	66	257	-	-	-	-	-	-	-	-	-	-	-	-	CC	-	-	-	-	-	N	Foliation in highly weathered fg pyritic basalt
20	23	joint	70	66	340	-	-	-	-	-	-	-	-	-	-	-	-	J1	-	-	-	-	-	N	Joint plane in highly weathered fg pyritic basalt
20	25	stock vein	1	50	271	-	-	-	-	-	-	-	-	-	-	-	-	V6	xnxt	-	-	-	-	N	stockwork pyritic vein 30% diss py+kach
20	25	stock vein	53	75	323	-	-	-	-	-	-	-	-	-	-	-	-	V6	xnxt	-	-	-	-	N	stockwork pyritic vein 30% diss py+kach
20	25	stock vein	102	55	192	-	-	-	-	-	-	-	-	-	-	-	-	V6	xnxt	-	-	-	-	N	stockwork pyritic vein 30% diss py+kach
20	25	qz vein	170	57	260		-	-	-	-	-	-	-	-	-	-	-	V6	-	-	-	-	-	N	
20	26	fault plane	146	57	236	-	-	-	-	-	-	-	-	-	-	-	-	SH7	xprv	-	-	-	-	N	Fault plane with intense foliation in wall rock
20	26	qz vein	103	55	193	-	-	-	-	-	-	-	-	-	-	-	-	V6	-	70	-	-	-	N	Several veins terminate against next fault
20	30	fault plane	102	79	192	-	-	-	-	-	-	-	-	-	-	-	-	SH7	-	-	-	-	-	N	Splay fault off previous
21	0	foliation	2	34	272	-	-	-	-	-	-	-	-	-	-	-	-	CC	-	-	-	-	-	S	Intense foliation in si'd pyritic basalt
21	0	tension vein	60	69	330	-	-	-	-	-	-	-	-	-	-	-	-	V8	-	-	-	-	-	S	Open space tension vein with hm alteration
21	2	fault plane	70	49	340	-	-	-	-	-	-	-	-	-	-	-	-	SH7	xprv	-	-	-	-	S	
21	3	foliation	157	61	67	-	-	-	-	-	-	-	-	-	-	-	-	CC	-	-	-	-	-	S	
21	3	fault plane	96	78	6	-	-	-	-	-	-	-	-	-	-	-	-	SH7	-	-	-	-	-	S	
21	7	foliation	5	47	275	-	-	-	-	-	-	-	-	-	-	-	-	CC	-	-	-	-	-	S	Intense foliation in blocky basalt
21	7	qz vein	108	26	198	-	-	-	-	-	-	-	-	-	-	-	-	V6	xprv	50	-	-	-	S	Quartz vein x-cuts previous foliation
21	10	qz vein	67	26	157	-	-	-	-	-	-	-	-	-	-	-	-	V6	-	400	-	-	-	S	
21	11	cleavage	4	42	274	-	-	-	-	-	-	-	-	-	-	-	-	CS2	-	-	-	-	-	S	Well developed cleavage x-cut by thin veins
21	11	vein	84	63	354	-	-	-	-	-	-	-	-	-	-	-	-	V6	-	-	-	-	-	S	
21	13	fault plane	28	51	298	-	-	-	-	-	-	-	-	-	-	-	-	SH7	-	-	-	-	-	S	Shallow fault plane
21	13	qz vein	65	26	155	-	-	-	-	-	-	-	-	-	-	-	-	V6	xprv	-	-	-	-	S	Quartz vein cuts previous fault with reverse movement
21	14	joint	67	26	157	-	-	-	-	-	-	-	-	-	-	-	-	J2	-	-	-	-	-	S	Prominent joint plane
21	16	fault plane	168	65	78	-	-	-	-	-	-	-	-	-	-	-	-	SH7	-	-	-	-	-	S	**Prominent fault plane DX Strike slip N Block down**
21	18	fract fol	3	47	273	-	-	-	-	-	-	-	-	-	-	-	-	CS1	-	-	-	-	-	S	Well developed fracture cleavage

LOCATION		Structural	Orientation					Defining Mineralogy					Alteration					Group	X-cut	Vein	Vein	Vein	Halo	Pos	DESCRIPTION
WALL	Metres	Element	Strike	Dip	Dip/Dir	Plunge	Dir	1	2	3	4	5	1	2	3	4	5		Rel.	Width	Style	Inc	Width		
21	19	fault plane	3	84	93	-	-	-	-	-	-	-	-	-	-	-	-	SH7	xnxt	-	-	-	-	S	Main quartz vein
21	19	qz vein	166	58	256	-	-	-	-	-	-	-	-	-	-	-	-	V6	-	-	-	-	-	S	Fault plane developed every 1m for 25m. Offset as for fault at 16m
21	25	fault plane	171	75	81	-	-	-	-	-	-	-	-	-	-	-	-	SH7	-	-	-	-	-	S	Fault as for previous
21	28	tension vein	55	64	325	-	-	-	-	-	-	-	-	-	-	-	-	V8	-	-	-	-	-	S	Tension veins in basalt x-cut foliation
21	28	tension vein	90	77	0	-	-	-	-	-	-	-	-	-	-	-	-	V8	-	-	-	-	-	S	Tension veins in basalt x-cut foliation
21	28	tension vein	98	41	188	-	-	-	-	-	-	-	-	-	-	-	-	V8	-	-	-	-	-	S	Tension veins in basalt x-cut foliation
22	0	foliation	80	64	350	-	-	-	-	-	-	-	-	-	-	-	-	CC	-	-	-	-	-	S	Intensely foliated grey green basalt
22	2	qz vein	152	24	242	-	-	qM	-	-	-	-	-	-	-	-	-	V3	-	-	-	-	-	S	Milky quartz veins weakly foliated
22	5	fault plane	74	86	344	-	-	-	-	-	-	-	-	-	-	-	-	SH7	-	-	-	-	-	S	Fault plane offsets large blocky quartz veins
22	11	fault plane	54	64	324	-	-	-	-	-	-	-	-	-	-	-	-	SH7	-	-	-	-	-	S	**N blK up vein offset parallel to tension cavity**
22	14	foliation	26	46	296	-	-	-	-	-	-	-	ka	mu	-	-	-	CC	-	-	-	-	-	S	Foliation basalt with ka mu and light green stain near py quartz
22	15	foliation	20	66	290	-	-	-	-	-	-	-	-	-	-	-	-	CC	-	-	-	-	-	S	Intense foliation in chloritic, pyritic basalt
22	15	fault plane	173	70	83	-	-	-	-	-	-	-	-	-	-	-	-	SH7	-	-	-	-	-	S	Undulating fault plane N Block down offset
22	19	foliation	165	79	255	-	-	py	qz	-	-	-	-	-	-	-	-	CS1	-	-	-	-	-	S	Fine stockwork of microfractures with py infill
22	22	fault plane	98	81	188	-	-	-	-	-	-	-	-	-	-	-	-	SH7	-	-	-	-	-	S	**Main fault stratigraphic offset Nblock up**
22	22	GP vein	173	68	263	-	-	-	-	-	-	-	mu	-	-	-	-	V9	-	-	-	-	-	S	Altered porphyry x-cuts foliation in S wall
22	29	foliation	0	50	90	-	-	-	-	-	-	-	-	-	-	-	-	CC	-	-	-	-	-	S	Intense foliation in basalt
23	0	foliation	32	37	302	-	-	-	-	-	-	-	-	-	-	-	-	CC	-	-	-	-	-	S	Intensely foliated ferruginous dolerite
23	1	qz vein	128	34	218	-	-	qT	-	-	-	-	-	-	-	-	-	V2	-	-	-	-	-	S	Vein x-cuts foliated dolerite
23	3	foliation	33	40	303	-	-	ch	-	-	-	-	-	-	-	-	-	CC	-	-	-	-	-	S	Flat ch spots define foliation
23	3	qz vein	24	82	114	-	-	qz	py	-	-	-	-	-	-	-	-	SRPY	xprv	-	-	-	-	S	Quartz py stringers x-cut foliation
23	5	joint	176	81	266	-	-	-	-	-	-	-	-	-	-	-	-	J2	-	-	-	-	-	S	
23	6	fault plane	11	44	281	-	-	-	-	-	-	-	-	-	-	-	-	SH7	-	-	-	-	-	S	Fault plane with 30cm quartz veins intruding shear wallrock
23	8	joint	67	83	337	-	-	-	-	-	-	-	-	-	-	-	-	J1	-	-	-	-	-	S	
23	8	joint	133	53	43	-	-	-	-	-	-	-	-	-	-	-	-	J2	-	-	-	-	-	S	
23	8	qz vein	19	55	289	-	-	-	-	-	-	-	-	-	-	-	-	V6	-	-	-	-	-	S	Quartz vein with marked alteration halo
23	13	joint	70	40	340	-	-	-	-	-	-	-	-	-	-	-	-	J1	-	-	-	-	-	S	
23	13	joint	4	67	274	-	-	-	-	-	-	-	-	-	-	-	-	J2	-	-	-	-	-	S	
23	13	joint	154	84	244	-	-	-	-	-	-	-	-	-	-	-	-	J2	-	-	-	-	-	S	
23	16	foliation	163	64	253	-	-	-	-	-	-	-	-	-	-	-	-	CC	-	-	-	-	-	S	Intense foliation in chlorite spotted gabbro
23	16	fault plane	49	56	319	-	-	-	-	-	-	-	-	-	-	-	-	SH7	-	-	-	-	-	S	**Nblock down fault with 30 cm quartz vein intruding**
23	17	foliation	2	61	272	-	-	-	-	-	-	-	-	-	-	-	-	CC	-	-	-	-	-	S	Foliation in mafic breccia fragments
23	17	foliation	160	88	70	-	-	-	-	-	-	-	-	-	-	-	-	SH7	-	-	-	-	-	S	Foliation in wallrock of major fault
23	17	qz vein	31	73	301	-	-	-	-	-	-	-	-	-	-	-	-	V6	xnxt	2000	-	-	-	S	Main vein in fault zone
23	17	qz vein	133	34	43	-	-	-	-	-	-	-	-	-	-	-	-	V6	-	-	-	-	-	S	Vein trending out of face
23	17	qz vein	144	46	234	-	-	-	-	-	-	-	-	-	-	-	-	V6	-	-	-	-	-	S	
23	26	foliation	8	61	278	-	-	-	-	-	-	-	-	-	-	-	-	CC	-	-	-	-	-	S	Foliation in northern wallrock of major fault

LOCATION		Structural	Orientation					Defining Mineralogy					Alteration					Group	X-cut	Vein	Vein	Vein	Halo	Pos	DESCRIPTION
WALL	Metres	Element	Strike	Dip	Dip/Dir	Plunge	Dir	1	2	3	4	5	1	2	3	4	5		Rel.	Width	Style	Inc	Width		
23	26	qz vein	140	38	230	-	-	-	-	-	-	-	-	-	-	-	-	V6	-	-	-	-	-	S	Quartz vein offset by fault
23	30	fault plane	21	43	291	-	-	-	-	-	-	-	-	-	-	-	-	SH7	-	-	-	-	-	S	**Prominent fault plane Nblock down movement**
24	0	foliation	36	35	306	-	-	-	-	-	-	-	-	-	-	-	-	CC	-	-	-	-	-	S	Prominent foliation plane
24	4	qz vein	109	37	199	-	-	qT	-	-	-	-	hm	-	-	-	-	V2	-	150	-	-	-	S	Thin vein with hm staining
24	7	foliation	22	46	292	-	-	-	-	-	-	-	-	-	-	-	-	CS1	-	-	-	-	-	S	High fracture and joint density
24	9	fault plane	179	58	269	-	-	-	-	-	-	-	-	-	-	-	-	SH7	-	-	-	-	-	S	**Fault x-cuts vein with app Wblock down**
24	11	sh zone	11	77	281	-	-	-	-	-	-	-	-	-	-	-	-	SH1	-	-	-	-	-	S	**GP intruded shear with apparent Wblock down**
24	17	foliation	35	51	305	-	-	-	-	-	-	-	-	-	-	-	-	CC	-	-	-	-	-	S	Intense foliation in spotty ch gabbro
24	17	sh zone	178	83	268	-	-	-	-	-	-	-	-	-	-	-	-	SH6	-	-	-	-	-	S	**Shear pln with subvert quartz vein Wblock down**
24	28	foliation	28	43	298	-	-	-	-	-	-	-	-	-	-	-	-	CC	-	-	-	-	-	S	Foliation rock with irregular GP veins intruded near quartz veins
24	29	fault plane	178	81	88	-	-	-	-	-	-	-	-	-	-	-	-	SH7	xnxt	-	-	-	-	S	**Thin GP vein intrudes fault WBLk down**
24	29	qz vein	104	50	194	-	-	-	-	-	-	-	-	-	-	-	-	V6	-	-	-	-	-	S	Vein intruded by GP on E side of fault only
25	1	joint	69	81	339	-	-	-	-	-	-	-	-	-	-	-	-	J1	-	-	-	-	-	N	Prominent joint plane
25	4	qz vein	9	81	279	-	-	qz	py	-	-	-	-	-	-	-	-	V6	-	-	-	-	-	N	mm scale pyritic quartz veinlets
25	4	qz vein	26	63	116	-	-	qz	py	-	-	-	-	-	-	-	-	V6	-	-	-	-	-	N	mm scale pyritic quartz veinlets
26	0	foliation	152	56	242	-	-	bi	hm	-	-	-	-	-	-	-	-	CC	-	-	-	-	-	N	Foliation defined by elongate slivers of bi+hm
26	0	cren fol	103	69	193	-	-	-	-	-	-	-	-	-	-	-	-	CS2	-	-	-	-	-	N	Plane crenulates previous foliation
26	1	c-plane	143	78	233	-	-	-	-	-	-	-	-	-	-	-	-	SH1	-	-	-	-	-	N	Sheared zone with 2cm undeformed qT intruding
26	1	s-plane	172	83	262	-	-	-	-	-	-	-	-	-	-	-	-	SH1	-	-	-	-	-	N	S-plane of S-C fabric
26	1	fault plane	163	73	253	-	-	-	-	-	-	-	-	-	-	-	-	SH7	-	-	-	-	-	N	Splay fault off previous fault
26	1	qz vein	43	85	313	-	-	hm	-	-	-	-	-	-	-	-	-	V6	-	-	-	-	-	N	Plane cutting foliation 2mm open cavity
26	2	foliation	139	86	229	-	-	-	-	-	-	-	-	-	-	-	-	CC	-	-	-	-	-	N	
26	2	foliation	160	43	250	-	-	-	-	-	-	-	-	-	-	-	-	CC	xnxt	-	-	-	-	N	Foliation offsets next in silicified chloritic dolerite
26	3	fault plane	168	69	78	-	-	-	-	-	-	-	-	-	-	-	-	SH7	-	-	-	-	-	N	Fault x-cuts all structures cataclasites bend in
26	4	foliation	145	83	235	-	-	-	-	-	-	-	-	-	-	-	-	CC	-	-	-	-	-	N	
26	4	foliation	166	59	256	-	-	-	-	-	-	-	-	-	-	-	-	CC	-	-	-	-	-	N	
26	4	shear band	175	81	85	-	-	-	-	-	-	-	-	-	-	-	-	SH1	xprv2	-	-	-	-	N	**Bending in sense of foliations Eblock up**
26	5	foliation	50	29	140	-	-	-	-	-	-	-	-	-	-	-	-	CC	-	-	-	-	-	N	
26	5	foliation	142	65	232	-	-	-	-	-	-	-	-	-	-	-	-	CC	-	-	-	-	-	N	
26	5	foliation	152	60	242	-	-	-	-	-	-	-	-	-	-	-	-	CC	-	-	-	-	-	N	
26	5	foliation	163	58	253	-	-	-	-	-	-	-	-	-	-	-	-	CC	xprv3	-	-	-	-	N	Prominent foliation x-cuts previous 3
26	5	fault plane	85	38	175	-	-	-	-	-	-	-	-	-	-	-	-	SH7	-	-	-	-	-	N	Prominent fault surface
26	7	shear fol	168	77	258	-	-	ch	-	-	-	-	-	-	-	-	-	SH1	-	-	-	-	-	N	Shear foliation in f-mg chlorite schist
26	7	shear fol	154	60	244	-	-	ch	-	-	-	-	-	-	-	-	-	SH6	-	-	-	-	-	N	Shear foliation in f-mg chlorite schist
26	9	qz vein	38	88	308	-	-	-	-	-	-	-	-	-	-	-	-	V6	-	-	-	-	-	N	Late x-cutting ferruginous quartz vein
26	10	foliation	26	43	296	-	-	-	-	-	-	-	-	-	-	-	-	CS1	-	-	-	-	-	N	Moderately developed x-cutting foliation
26	10	shear fol	160	74	250	-	-	-	-	-	-	-	-	-	-	-	-	SH1	-	-	-	-	-	N	Intense shear foliation

LOCATION		Structural	Orientation					Defining Mineralogy					Alteration					Group	X-cut	Vein	Vein	Vein	Halo	Pos	DESCRIPTION
WALL	Metres	Element	Strike	Dip	Dip/Dir	Plunge	Dir	1	2	3	4	5	1	2	3	4	5		Rel.	Width	Style	Inc	Width		
26	10	cataclasite	12	51	282	-	-	-	-	-	-	-	-	-	-	-	-	SH3	xprv	-	-	-	-	N	**Cataclasite seams with WoverE movement**
26	10	qz vein	38	70	308	-	-	qz	-	-	-	-	-	-	-	-	-	V6	-	-	-	-	-	N	Gently foliated sigmoidal quartz veins
26	11	shear fol	162	75	252	-	-	-	-	-	-	-	-	-	-	-	-	SH6	-	-	-	-	-	N	
26	11	stock vein	16	64	286	-	-	-	-	-	-	-	-	-	-	-	-	V6	-	-	-	-	-	N	Ferruginous vein in stockwork arrngmt
26	11	stock vein	174	50	84	-	-	-	-	-	-	-	-	-	-	-	-	V6	-	-	-	-	-	N	Ferruginous vein in stockwork arrngmt
26	13	shear fol	165	86	255	-	-	-	-	-	-	-	-	-	-	-	-	SH6	-	-	-	-	-	N	
26	13	shear fol	178	71	268	-	-	-	-	-	-	-	-	-	-	-	-	SH6	-	-	-	-	-	N	
26	13	fault plane	173	83	83	-	-	-	-	-	-	-	-	-	-	-	-	SH7	-	-	-	-	-	N	X-cutting fault plane
26	13	qz vein	154	75	64	-	-	-	-	-	-	-	-	-	-	-	-	V6	-	-	-	-	-	N	Thin ferruginous vein
26	13	qz vein	85	21	175	-	-	qz	-	-	-	-	-	-	-	-	-	V6	xprv2	30	-	-	-	N	Thin vein dipping out of face
26	14	foliation	159	75	249	-	-	-	-	-	-	-	-	-	-	-	-	CC	-	-	-	-	-	N	
26	15	qz vein	15	31	105	-	-	-	-	-	-	-	-	-	-	-	-	V6	-	50	-	-	-	N	**Gently foliated quartz vein Sfolds verge west**
26	16	foliation	6	85	276	-	-	-	-	-	-	-	-	-	-	-	-	CC	-	-	-	-	-	N	
26	16	fault plane	172	66	262	-	-	-	-	-	-	-	-	-	-	-	-	SH7	-	-	-	-	-	N	
26	17	foliation	173	34	263	-	-	-	-	-	-	-	-	-	-	-	-	CC	xprv	-	-	-	-	N	
26	17	foliation	179	84	269	-	-	-	-	-	-	-	-	-	-	-	-	CC	-	-	-	-	-	N	
26	17	fault plane	99	37	189	-	-	-	-	-	-	-	-	-	-	-	-	SH7	-	-	-	-	-	N	Prominent fault plane dipping out of face
26	18	fault plane	19	53	289	-	-	-	-	-	-	-	-	-	-	-	-	SH7	xall	-	-	-	-	N	**Sharp fault plane x-cuts all Wover E**
26	21	foliation	5	62	95	-	-	-	-	-	-	-	-	-	-	-	-	CC	-	-	-	-	-	N	
26	21	foliation	151	80	241	-	-	-	-	-	-	-	-	-	-	-	-	CC	-	-	-	-	-	N	
26	21	fault plane	179	61	89	-	-	-	-	-	-	-	-	-	-	-	-	SH7	-	-	-	-	-	N	Weakly foliated fault plane
26	21	fault plane	20	55	110	-	-	-	-	-	-	-	-	-	-	-	-	SH7	-	-	-	-	-	N	Anastomosing fault planes A bends into B
26	21	fault plane	162	72	252	-	-	-	-	-	-	-	-	-	-	-	-	SH7	-	-	-	-	-	N	Prev bends into this one
26	21	fault plane	175	79	265	-	-	-	-	-	-	-	-	-	-	-	-	SH7	-	-	-	-	-	N	Undulating fault plane
26	23	foliation	160	52	250	-	-	-	-	-	-	-	-	-	-	-	-	CC	-	-	-	-	-	N	
26	23	fault plane	175	70	85	-	-	-	-	-	-	-	-	-	-	-	-	SH7	-	-	-	-	-	N	
26	23	py sr vein	18	74	108	-	-	qz	py	-	-	-	-	-	-	-	-	SRPY	-	-	-	-	-	N	Thin ferruginous quartz py sr veins in py Aod
26	23	stock vein	71	84	341	-	-	-	-	-	-	-	-	-	-	-	-	V6	xnxt	-	-	-	-	N	Thin x-cutting quartz vein stockwork
26	23	qz vein	124	57	34	-	-	qz	-	-	-	-	-	-	-	-	-	V6	-	-	-	-	-	N	Thin vein traverses entire face
26	23	stock vein	18	78	108	-	-	-	-	-	-	-	-	-	-	-	-	V6	-	-	-	-	-	N	
26	23	qz vein	75	34	165	-	-	-	-	-	-	-	-	-	-	-	-	V6	-	-	-	-	-	N	Gently foliated quartz vein W verging S folds
26	24	foliation	167	80	77	-	-	-	-	-	-	-	-	-	-	-	-	CC	-	-	-	-	-	N	
26	24	foliation	172	53	262	-	-	-	-	-	-	-	-	-	-	-	-	CC	xnxt	-	-	-	-	N	Intense foliation
26	27	foliation	172	51	262	-	-	-	-	-	-	-	-	-	-	-	-	CC	-	-	-	-	-	N	
26	27	joint	131	53	221	-	-	-	-	-	-	-	-	-	-	-	-	J2	-	-	-	-	-	N	
26	27	qz vein	165	50	255	-	-	qz	-	-	-	-	-	-	-	-	-	V6	-	30	-	-	-	N	Boudinaged quartz vein
26	29	foliation	173	42	263	-	-	-	-	-	-	-	-	-	-	-	-	CC	-	-	-	-	-	N	Intense foliation

LOCATION		Structural	Orientation					Defining Mineralogy					Alteration					Group	X-cut	Vein	Vein	Vein	Halo	Pos	DESCRIPTION
WALL	Metres	Element	Strike	Dip	Dip/Dir	Plunge	Dir	1	2	3	4	5	1	2	3	4	5		Rel.	Width	Style	Inc	Width		
26	29	joint	61	80	331	-	-	-	-	-	-	-	-	-	-	-	-	J1	-	-	-	-	-	N	Prominent joint surface
27	0	foliation	176	50	266	-	-	ch	-	-	-	-	-	-	-	-	-	CC	-	-	-	-	-	N	Intensely foliated chlorite schist
27	3	qz vein	64	37	154	-	-	-	-	-	-	-	-	-	-	-	-	V6	-	100	-	-	-	N	Gentle S-fold kinks in quartz vein
27	4	py sr vein	31	73	301	-	-	-	-	-	-	-	-	-	-	-	-	SRPY	-	-	-	-	-	N	Fine grained pyritic quartz veinlets
27	5	fault plane	11	74	101	-	-	-	-	-	-	-	-	-	-	-	-	SH7	-	-	-	-	-	N	Thin fault plane cut by foliated quartz vein
27	6	foliation	154	52	244	-	-	-	-	-	-	-	-	-	-	-	-	CC	-	-	-	-	-	N	
27	6	joint	52	63	322	-	-	-	-	-	-	-	-	-	-	-	-	J1	-	-	-	-	-	N	Prominent joint plane
27	6	qz vein	77	43	167	-	-	qM	-	-	-	-	-	-	-	-	-	V3	-	350	-	foWR	-	N	Foliated vein bi ch altered clasts of wallrock
27	14	qz vein	28	52	298	-	-	-	-	-	-	-	-	-	-	-	-	V6	-	-	-	-	-	N	Pyritic ferr quartz veinlets in stngly weath foliated mafic
27	19	qz vein	92	66	2	-	-	-	-	-	-	-	-	-	-	-	-	V6	-	-	-	-	-	N	Ferruginous quartz vein
27	24	foliation	4	66	94	-	-	-	-	-	-	-	-	-	-	-	-	CC	-	-	-	-	-	N	
27	24	fold axis	-	-	-	23	247	-	-	-	-	-	-	-	-	-	-	F1	-	-	-	-	-	N	Fold axis in quartz vein
27	24	qz vein	32	71	302	-	-	-	-	-	-	-	-	-	-	-	-	V6	-	2000	-	-	-	N	Irregular E boundary, thin fault breccia on W boundary
27	24	e-limb	98	40	188	-	-	-	-	-	-	-	-	-	-	-	-	VL	-	-	-	-	-	N	Eastern limb of foliated vein
27	24	w-limb	163	23	253	-	-	-	-	-	-	-	-	-	-	-	-	VL	-	-	-	-	-	N	Western limb of foliated vein
27	29	foliation	27	71	117	-	-	-	-	-	-	-	-	-	-	-	-	CC	-	-	-	-	-	N	Foliation in wallrock of vein
28	1	qz vein	30	89	300	-	-	qz	-	-	-	-	-	-	-	-	-	V6	-	-	-	-	-	N	Thin ferruginous quartz veinlets
28	5	fold axis	-	-	-	60	328	-	-	-	-	-	-	-	-	-	-	F1	-	-	-	-	-	N	Hingeline to folds in quartz vein
28	5	qz vein	60	74	330	-	-	qT	-	-	-	-	-	-	-	-	-	V2	-	50	scs	-	-	N	Foliated quartz vein in foliated limonitic mafic
28	5	foliation	165	85	255	-	-	-	-	-	-	-	-	-	-	-	-	V6	-	-	-	-	-	N	
28	8	qz vein	10	63	280	-	-	-	-	-	-	-	-	-	-	-	-	V6	-	-	-	-	-	N	Ferruginous quartz veins parallel to foliation
28	8	qz vein	157	68	247	-	-	-	-	-	-	-	-	-	-	-	-	V6	-	-	-	-	-	N	Ferruginous quartz veins parallel to foliation
28	18	qz vein	130	43	40	-	-	qT	-	-	-	-	-	-	-	-	-	V2	-	100	-	-	-	N	
29	10	qz vein	6	81	276	-	-	qT	-	-	-	-	-	-	-	-	-	V2	-	10	-	-	-	N	
29	10	qz vein	13	43	103	-	-	qT	-	-	-	-	-	-	-	-	-	V2	-	30	-	-	-	N	Vein in wkly foliation pallid limonitic mafic
29	10	qz vein	48	78	138	-	-	qT	-	-	-	-	-	-	-	-	-	V2	-	10	-	-	-	N	
29	25	qz vein	55	86	325	-	-	-	-	-	-	-	-	-	-	-	-	V6	-	-	-	bxWR	-	S	Sheared fupysimu altered mafic
29	27	qz vein	117	44	207	-	-	-	-	-	-	-	-	-	-	-	-	V6	-	-	-	-	-	S	Thin south dipping quartz veins
30	3	qz vein	174	49	264	-	-	qT	-	-	-	-	-	-	-	-	-	V2	-	1500	-	-	-	S	Quartz vein with intensely sheared wallrock
30	9	qz vein	120	44	210	-	-	-	-	-	-	-	-	-	-	-	-	V6	-	-	-	-	-	S	White ka altered rock with 20% py relicts
30	10	joint	178	44	268	-	-	-	-	-	-	-	-	-	-	-	-	J2	-	-	-	-	-	S	Prominent joint plane
30	10	qz vein	179	84	89	-	-	qT	-	-	-	-	-	-	-	-	-	V2	xnxt	50	-	-	-	S	**Apparent W Block N offset across vein**
30	15	qz vein	86	61	176	-	-	qz	-	-	-	-	-	-	-	-	-	V6	-	50	-	-	-	S	
30	21	qz vein	79	58	169	-	-	qT	-	-	-	-	-	-	-	-	-	V2	-	90	-	-	-	S	
30	23	qz vein	112	56	202	-	-	qT	-	-	-	-	-	-	-	-	-	V2	-	200	-	-	-	S	
30	25	qz vein	119	56	209	-	-	qT	-	-	-	-	-	-	-	-	-	V2	-	80	-	-	-	S	Buck quartz vein with intensely foliated wallrock
30	28	qz vein	49	54	139	-	-	qT	-	-	-	-	-	-	-	-	-	V2	-	50	-	-	-	S	Sheared quartz vein dipping into wall

LOCATION		Structural	Orientation					Defining Mineralogy					Alteration					Group	X-cut	Vein	Vein	Vein	Halo	Pos	DESCRIPTION
WALL	Metres	Element	Strike	Dip	Dip/Dir	Plunge	Dir	1	2	3	4	5	1	2	3	4	5		Rel.	Width	Style	Inc	Width		
30	30	qz vein	78	45	168	-	-	qT	-	-	-	-	-	-	-	-	-	V2	-	50	-	-	-	S	Sheared quartz vein dipping into wall
31	2	qz vein	141	51	51	-	-	qT	-	-	-	-	-	-	-	-	-	V2	-	50	-	-	-	S	Vein in weakly foliated purple mafic
31	6	qz vein	112	55	202	-	-	-	-	-	-	-	-	-	-	-	-	V6	-	-	-	-	-	S	**Several thin vein offset by previous Eblock N**
31	8	foliation	0	34	90	-	-	-	-	-	-	-	-	-	-	-	-	CC	-	-	-	-	-	S	Prominant foliation forms slip surface
31	12	foliation	24	52	294	-	-	-	-	-	-	-	-	-	-	-	-	CC	-	-	-	-	-	S	
31	17	foliation	45	47	315	-	-	-	-	-	-	-	-	-	-	-	-	CC	-	-	-	-	-	S	Foliated med grained weathered mafic
31	22	foliation	29	38	299	-	-	-	-	-	-	-	-	-	-	-	-	CC	-	-	-	-	-	S	
31	22	joint	85	89	355	-	-	-	-	-	-	-	-	-	-	-	-	J1	-	-	-	-	-	S	Prominent joint set
31	26	joint	15	48	285	-	-	-	-	-	-	-	-	-	-	-	-	J2	-	-	-	-	-	S	Weathered slickensided joint plane
31	30	foliation	23	39	293	-	-	-	-	-	-	-	-	-	-	-	-	CC	-	-	-	-	-	S	Intensely weathered m-cg chloritic gabbro
32	3	qz vein	127	42	217	-	-	qT	qM	-	-	-	ch	py	fu	-	-	V2	-	250	-	-	50	S	Sheared chloritic halo, relict py and fu
32	5	qz vein	38	35	308	-	-	-	-	-	-	-	-	-	-	-	-	V6	-	-	-	-	-	S	Fe rich quartz on slickensided foliation surface
32	7	qz vein	125	50	215	-	-	qz	-	-	-	-	mu	-	-	-	-	V6	-	180	scs	-	-	S	Intense foliation wallrock, high angle fracture in quartz
32	8	fault plane	9	72	99	-	-		-	-	-	-	-	-	-	-	-	SH7	xprv	-	-	-		S	**Thin vein intrudes fault, app W Block up movement**
32	13	foliation	24	37	294	-	-	-	-	-	-	-	-	-	-	-	-	CC	-	-	-	-	-	S	Int foliation in heavily weathered chspAod
32	16	qz vein	121	72	211	-	-	qz	-	-	-	-	-	-	-	-	-	V6	-	1000	-	-	-	S	Int sheared margins+thin intruding veins
32	22	qz vein	106	59	196	-	-	qz	-	-	-	-	-	-	-	-	-	V6	-	50	-	vu	-	S	Fe indurated margins
32	30	foliation	137	65	227	-	-	-	-	-	-	-	-	-	-	-	-	CC	-	-	-	-	-	S	Prominent foliation in mg strongly weathered ch Aod
32	37	qz vein	10	29	280	-	-	qz	-	-	-	-	-	-	-	-	-	V6	-	120	-	-	-	S	Quartz vein with fe indurated margins
33	2	qz vein	100	87	10	-	-	qz	ca	-	-	-	-	-	-	-	-	V1	xprv3	-	-	-	-	S	Quartz carbonate veins
33	2	qz vein	165	72	75	-	-	qz	ca	-	-	-	-	-	-	-	-	V1	-	-	-	-	-	S	Quartz carbonate veins
33	2	qz vein	125	84	215	-	-	qz	ca	-	-	-	-	-	-	-	-	V1	-	-	-	-	-	S	Quartz carbonate veins
33	2	qz vein	140	82	230	-	-	qz	ca	-	-	-	-	-	-	-	-	V1	-	-	-	-	-	S	Quartz carbonate veins
33	5	fault plane	116	60	26	-	-	-	-	-	-	-	-	-	-	-	-	SH7	-	-	-	-	-	S	Ferruginous plane
34	0	c-plane	142	54	232	-	-	-	-	-	-	-	-	-	-	-	-	SH1	xnxt2	-	-	-	-	S	C-plane of Cashmans Shear Zone S-C
34	0	s-plane	170	66	260	-	-	-	-	-	-	-	-	-	-	-	-	SH2	-	-	-	-	-	S	S-plane of Cashmans Shear Zone S-C
34	0	fault plane	61	68	331	-	-	-	-	-	-	-	-	-	-	-	-	SH7	-	-	-	-	-	S	**Dilatent fault plane cut by CSZ EBlockN SS**
34	4	fault plane	82	83	352	-	-	-	-	-	-	-	-	-	-	-	-	SH7	-	-	-	-	-	S	**Fault pln bending into CSZ with E Block N**
34	6	joint	98	35	8	-	-	-	-	-	-	-	-	-	-	-	-	J2	-	-	-	-	-	S	Weathered joint surface
34	8	joint	27	77	297	-	-	-	-	-	-	-	-	-	-	-	-	J2	-	-	-	-	-	S	Dilatent joint plane with cavities
34	11	joint	78	62	348	-	-	-	-	-	-	-	-	-	-	-	-	J1	-	-	-	-	-	S	Dilatent plane congugate with previous
34	11	joint	176	52	86	-	-	-	-	-	-	-	-	-	-	-	-	J2	-	-	-	-	-	S	Dilatent joint plane
34	11	shear zone	39	67	309	-	-	-	-	-	-	-	-	-	-	-	-	SH6	-	-	-	-	-	S	Dilatent shear plane x-cut by previous
34	11	shear zone	145	48	235	-	-	-	-	-	-	-	-	-	-	-	-	SH6	xp+nx	-	-	-	-	S	**Shear plane with Eblock N offset**
34	17	s-plane	26	74	296	-	-	-	-	-	-	-	-	-	-	-	-	SH1	-	-	-	-	-	S	**Nblock down S-C mylonite**
34	17	c-plane	35	76	305	-	-	-	-	-	-	-	-	-	-	-	-	SH1	-	-	-	-	-	S	**Nblock down S-C mylonite**
34	21	foliation	157	68	247	-	-	-	-	-	-	-	-	-	-	-	-	CC	-	-	-	-	-	S	Int foliated clay weathered ultramafic

LOCATION		Structural	Orientation					Defining Mineralogy					Alteration					Group	X-cut	Vein	Vein	Vein	Halo	Pos	DESCRIPTION
WALL	Metres	Element	Strike	Dip	Dip/Dir	Plunge	Dir	1	2	3	4	5	1	2	3	4	5		Rel.	Width	Style	Inc	Width		
34	25	foliation	120	89	30	-	-	-	-	-	-	-	-	-	-	-	-	CC	-	-	-	-	-	S	Prominent foliation in mg strong wth chAod
34	25	fault plane	158	85	248	-	-	-	-	-	-	-	-	-	-	-	-	SH7	xnxt	-	-	-	-	S	tacbsi altered rock at fault plane
34	29	foliation	164	68	254	-	-	-	-	-	-	-	-	-	-	-	-	CC	-	-	-	-	-	S	Intense foliation
35	0	shear fol	5	69	275	-	-	-	-	-	-	-	-	-	-	-	-	SH2	-	-	-	-	-	S	Intensely foliated near major shear/fault zone ta schist
35	9	foliation	169	53	259	-	-	-	-	-	-	-	-	-	-	-	-	CC	-	-	-	-	-	S	
35	12	foliation	2	82	272	-	-	-	-	-	-	-	-	-	-	-	-	CC	-	-	-	-	-	S	Foliation bending into sheared ct
35	12	shear ct	168	44	258	-	-	-	-	-	-	-	-	-	-	-	-	SH6	-	-	-	-	-	S	Sheared lith contact in um
35	19	fault plane	46	83	316	-	-	-	-	-	-	-	-	-	-	-	-	SH1	-	-	-	-	-	S	**Thin fault plane S+C shows Nblock down**
35	21	s-plane	28	73	298	-	-	-	-	-	-	-	-	-	-	-	-	SH1	-	-	-	-	-	S	S-C mylonite fault
35	21	c-plane	41	85	311	-	-	-	-	-	-	-	-	-	-	-	-	SH1	-	-	-	-	-	S	**S-C mylonite fault Nblock down**
36	0	qz vein	127	36	217	-	-	-	-	-	-	-	-	-	-	-	-	V10	-	10	-	-	-	S	Vein in QF porphyry intruding CSH
36	0	qz vein	100	89	10	-	-	qG	-	-	-	-	-	-	-	-	-	V6	-	250	-	-	-	S	Vein in QF porphyry intruding CSH
36	3	stock vein	23	74	113	-	-	-	-	-	-	-	-	-	-	-	-	V6	-	10	-	-	-	S	stockwork of thin veins
36	3	stock vein	130	56	220	-	-	-	-	-	-	-	-	-	-	-	-	V6	-	10	-	-	-	S	stockwork of thin veins
36	6	qz vein	172	61	82	-	-	-	-	-	-	-	-	-	-	-	-	V6	-	200	-	-	-	S	Fragmented quartz vein
36	11	lith ct	143	42	233	-	-	-	-	-	-	-	-	-	-	-	-	BED2	-	-	-	-	-	S	Contact between felsic porphyry and lam SE
36	14	lith ct	130	38	220	-	-	-	-	-	-	-	-	-	-	-	-	BED2	-	-	-	-	-	S	Finely sheared contact between SE and mafic
36	18	fault plane	38	40	308	-	-	-	-	-	-	-	-	-	-	-	-	SH7	-	-	-	-	-	S	Thin ferruginous pyritic fault plane
36	20	foliation	45	41	315	-	-	-	-	-	-	-	-	-	-	-	-	SH1	-	-	-	-	-	S	Intensely foliated mafic in vicinity of shear zone
36	23	foliation	177	54	87	-	-	-	-	-	-	-	-	-	-	-	-	SH3	-	-	-	-	-	S	Intensely sheared brecciated basalt
36	23	shear zone	22	52	292	-	-	-	-	-	-	-	-	-	-	-	-	SH7	-	-	-	-	-	S	Shear zone with int silicified wallrock
36	25	qz vein	31	65	301	-	-	qM	qT	cp	-	-	-	-	-	-	-	V3	-	1000	scs	-	-	S	Green Cu? staining near wallrock clasts
36	26	shear fol	10	64	280	-	-	-	-	-	-	-	-	-	-	-	-	SH1	-	-	-	-	-	S	Shear foliation in mafic/UM
36	27	foliation	6	65	276	-	-	-	-	-	-	-	-	-	-	-	-	CC	-	-	-	-	-	S	Intensely foliated wallrock
36	27	qz vein	15	60	285		-	qT	-	-	-	-	-	-	-	-	-	V2	-	800	-	-	-	S	Fractured breccia at vein margin
37	3	foliation	28	65	298	-	-	-	-	-	-	-	-	-	-	-	-	CC	-	-	-	-	-	S	Foliation bending into fault plane
37	3	fault plane	22	83	292	-	-	-	-	-	-	-	-	-	-	-	-	SH7	-	-	-	-	-	S	**West Block down fault plane**
37	5	qz vein	70	61	340	-	-	-	-	-	-	-	-	-	-	-	-	V6	-	-	-	-	-	S	Quartz vein parallel to face
37	6	qz vein	156	40	246	-	-	-	-	-	-	-	-	-	-	-	-	V6	-	-	-	-	-	S	Intense qcb microfracture stockwork in wallrock
37	11	qz vein	122	37	212	-	-	qM	-	-	-	-	-	-	-	-	-	V3	-	300	-	-	-	S	Buck quartz vein with foliated margin
37	15	foliation	23	44	293	-	-	-	-	-	-	-	-	-	-	-	-	CS1	-	-	-	-	-	S	Variably developed foliation
37	21	bedding	18	50	288	-	-	py	-	-	-	-	-	-	-	-	-	BED2	-	-	-	-	-	S	Bedding laminations in ferruginous pyritic sed
37	21	qz vein	10	61	280	-	-	qM	-	-	-	-	-	-	-	-	-	V3	-	100	-	-	-	S	Quartz vein at contact between sediment and basalt
37	21	qz vein	35	62	125	-	-	qz	-	-	-	-	-	-	-	-	-	V6	xnxt	30	-	-	-	S	Ferruginous quartz vein
37	21	qz vein	146	43	236	-	-	qz	-	-	-	-	-	-	-	-	-	V6	-	30	-	-	-	S	Ferruginous quartz vein
37	23	fold axis	-	-	-	50	194	-	-	-	-	-	-	-	-	-	-	F1	-	30	-	-	-	S	Foliated ferruginous quartz vein
37	23	qz vein	163	54	253	-	-	qT	-	-	-	-	-	-	-	-	-	V2	xprv	100	-	-	-	S	Quartz vein x-cuts previous foliated vein

LOCATION		Structural	Orientation					Defining Mineralogy					Alteration					Group	X-cut	Vein	Vein	Vein	Halo	Pos	DESCRIPTION
WALL	Metres	Element	Strike	Dip	Dip/Dir	Plunge	Dir	1	2	3	4	5	1	2	3	4	5		Rel.	Width	Style	Inc	Width		
37	24	bedding	156	42	246	-	-	-	-	-	-	-	-	-	-	-	-	BED2	-	-	-	-	-	S	Sedimentary laminations
37	25	qz vein	14	57	104	-	-	-	-	-	-	-	-	-	-	-	-	V10	-	-	-	-	-	S	Quartz vein in porphyry not x-cutting contact
37	25	qz vein	48	32	138	-	-	-	-	-	-	-	-	-	-	-	-	V10	-	-	-	-	-	S	Quartz vein in porphyry not x-cutting contact
37	25	qz vein	144	53	234	-	-	-	-	-	-	-	-	-	-	-	-	V10	-	-	-	-	-	S	Quartz vein in porphyry not x-cutting contact
37	27	qz vein	37	46	307	-	-	qT	-	-	-	-	-	-	-	-	-	V2	-	100	-	-	-	S	
37	30	joint	179	61	89	-	-	-	-	-	-	-	-	-	-	-	-	J2	-	-	-	-	-	S	Dilatent fracture plane developed each 2.5m
38	0	qz vein	90	41	180	-	-	-	-	-	-	-	-	-	-	-	-	V6	-	-	-	-	-	S	Quartz vein in chhm alteration op gabbro
38	5	qz vein	121	54	211	-	-	qT	-	-	-	-	-	-	-	-	-	V2	-	150	-	-	-	S	Thin quartz vein
38	7	qz vein	116	53	206	-	-	qM	-	-	-	-	-	-	-	-	-	V3	-	300	-	-	-	S	Buck quartz vein
38	11	foliation	27	43	297	-	-	-	-	-	-	-	-	-	-	-	-	SH1	-	-	-	-	-	S	Foliation, fault plane?
38	17	qz vein	112	54	202	-	-	-	-	-	-	-	-	-	-	-	-	V6	-	-	-	-	-	S	
38	18	qz vein	111	59	201	-	-	qT	-	-	-	-	ch	-	-	-	-	V2	-	20	-	-	30	S	Vein with chloritic halo
38	22	qz vein	102	57	192	-	-	qT	-	-	-	-	-	-	-	-	-	V2	-	30	-	-	-	S	
38	23	qz vein	113	60	203	-	-	-	-	-	-	-	-	-	-	-	-	V6	-	50	-	-	-	S	Ferruginous quartz vein
38	25	foliation	38	42	308	-	-	-	-	-	-	-	-	-	-	-	-	CC	-	-	-	-	-	S	Moderately to heavily foliated mg dolerite
38	26	qz vein	105	47	195	-	-	qM	-	-	-	-	-	-	-	-	-	V3	-	100	-	-	-	S	Ferruginous quartz vein
38	27	fault plane	53	62	323	-	-	-	-	-	-	-	-	-	-	-	-	SEF	-	-	-	-	3000	S	Large fault plane SEF? intense alteration - ka rock
38	27	foliation	19	44	289	-	-	-	-	-	-	-	-	-	-	-	-	SH7	-	-	-	-	-	S	Foliation on north side of fault plane
38	27	qz vein	37	66	307	-	-	-	-	-	-	-	-	-	-	-	-	V6	-	-	-	-	-	S	Internal quartz veins in fault zone
39	0	qz vein	44	75	134	-	-	qT	-	-	-	-	-	-	-	-	-	V2	-	70	-	-	-	S	
39	0	qz vein	112	52	202	-	-	qM	-	-	-	-	-	-	-	-	-	V3	xprv	200	-	-	-	S	Vein with sheared margin x-cuts previous vein
39	2	fault plane	177	64	267	-	-	-	-	-	-	-	-	-	-	-	-	SH7	xprv	-	-	-	-	S	**W Block down displacement of previous vein**
39	3	fault plane	164	59	254	-	-	-	-	-	-	-	-	-	-	-	-	SH7	-	-	-	-	-	S	Thin splay fault off previous
39	8	fault plane	4	83	274	-	-	-	-	-	-	-	-	-	-	-	-	SH7	-	-	-	-	-	S	**Splay fault offsets vein with W Block down**
39	8	qz vein	1	68	271	-	-	-	-	-	-	-	-	-	-	-	-	V2	-	100	-	-	-	S	Quartz vein in fault plane
39	10	fault plane	40	44	310	-	-	-	-	-	-	-	-	-	-	-	-	SH7	-	-	-	-	-	S	Fault plane in spotty ch hm alteration gabbro
39	13	qz vein	19	33	289	-	-	-	-	-	-	-	-	-	-	-	-	V6	-	-	-	-	-	S	Thin quartz vein intruding fault plane
39	14	foliation	21	54	291	-	-	-	-	-	-	-	-	-	-	-	-	CC	-	-	-	-	-	S	Foliation in wallrock
39	16	qz vein	91	59	181	-	-	qM	-	-	-	-	ch	-	-	-	-	V3	-	220	-	-	50	S	
39	20	qz vein	142	39	232	-	-	qz	-	-	-	-	-	-	-	-	-	V6	-	30	-	-	-	S	Quartz vein intruding 1m wide fault plane
39	23	qz vein	102	85	192	-	-	-	-	-	-	-	-	-	-	-	-	V6	-	-	-	-	-	S	Quartz vein intruding 1m wide fault plane
40	0	qz vein	98	50	188	-	-	-	-	-	-	-	-	-	-	-	-	V6	-	10	-	-	-	S	Ferruginous quartz vein
40	5	qz vein	99	58	189	-	-	-	-	-	-	-	-	-	-	-	-	V6	-	50	-	-	-	S	Ferruginous quartz vein
40	8	qz vein	96	60	186	-	-	qM	-	-	-	-	ch	hm	-	-	-	V3	-	250	-	-	-	S	Quartz vein with foliated margin
40	12	qz vein	97	50	187	-	-	-	-	-	-	-	-	-	-	-	-	V6	-	-	-	-	-	S	Ferruginous quartz veins foliation parallel
40	13	qz vein	45	54	315	-	-	-	-	-	-	-	-	-	-	-	-	V6	-	-	-	-	-	S	
40	20	qz vein	149	34	239	-	-	qG	-	-	-	-	-	-	-	-	-	V2	-	50	-	-	-	S	Translucent grey quartz vein

LOCATION		Structural	Orientation					Defining Mineralogy					Alteration					Group	X-cut	Vein	Vein	Vein	Halo	Pos	DESCRIPTION
WALL	Metres	Element	Strike	Dip	Dip/Dir	Plunge	Dir	1	2	3	4	5	1	2	3	4	5		Rel.	Width	Style	Inc	Width		
40	22	qz vein	106	37	196	-	-	qM	-	-	-	-	ch	hm	-	-	-	V3	-	120	-	-	-	S	Vein with foliated chloritic halo
40	23	qz vein	127	36	217	-	-	qT	-	-	-	-	hm	-	-	-	-	V2	-	90	-	-	20	S	
40	26	qz vein	114	47	204	-	-	qM	-	-	-	-	-	-	-	-	-	V3	xall	-	-	-	-	S	30cm intensely sheared/foliated wallrock
40	26	qz vein	149	68	239	-	-	-	-	-	-	-	-	-	-	-	-	V6	-	-	-	-	-	S	Quartz vein with breccia in pressure shadow
40	28	qz vein	79	61	169	-	-	qT	-	-	-	-	-	-	-	-	-	V2	-	200	-	-	-	S	Vein x cut by previous main vein
40	30	qz vein	105	55	195	-	-	qT	-	-	-	-	-	-	-	-	-	V2	-	120	mcs	-	-	S	
41	0	fault plane	169	34	259	-	-	-	-	-	-	-	-	-	-	-	-	SH7	-	-	-	-	-	S	Thin fault plane fe oxide stained wallrock mg Aod
41	1	qz vein	108	54	198	-	-	qT	-	-	-	-	-	-	-	-	-	V2	-	200	-	vu	-	S	Vuggy quartz vein
41	4	foliation	21	40	291	-	-	-	-	-	-	-	-	-	-	-	-	CC	-	-	-	-	-	S	Prominent foliation/slip plane
41	6	qz vein	82	66	172	-	-	qM	-	-	-	-	-	-	-	-	-	V3	-	-	-	-	-	S	Vein with thin foliated wallrock margin
41	6	tension vein	76	74	346	-	-	ka	-	-	-	-	-	-	-	-	-	V8	-	-	-	-	-	S	Thin tension fractures ka filled
41	6	tension vein	121	73	31	-	-	ka	-	-	-	-	-	-	-	-	-	V8	-	-	-	-	-	S	Second set intersect first assymptotically
41	8	qz vein	93	59	183	-	-	-	-	-	-	-	-	-	-	-	-	V6	-	50	-	-	-	S	Quartz vein with dilational rhombs
41	8	qz vein	110	58	200	-	-	-	-	-	-	-	-	-	-	-	-	V6	-	50	-	-	-	S	Quartz vein with dilational rhombs
41	10	foliation	26	42	296	-	-	-	-	-	-	-	-	-	-	-	-	CC	-	-	-	-	-	S	Large prominent foliation/slip plane
41	10	foliation	57	68	327	-	-	-	-	-	-	-	-	-	-	-	-	CS1	-	-	-	-	-	S	Large prominent foliation/slip plane
41	14	qz vein	97	65	187	-	-	qT	-	-	-	-	-	-	-	-	-	V2	xnxt	90	-	-	-	S	
41	14	qz vein	38	84	308	-	-	-	-	-	-	-	-	-	-	-	-	V6	-	-	mcs	vu	-	S	
41	25	qz vein	147	51	57	-	-	qM	-	-	-	-	-	-	-	-	-	V3	-	200	-	-	-	S	Quartz vein in med-coarse grained dolerite
42	0	qz vein	104	47	194	-	-	qM	-	-	-	-	-	-	-	-	-	V3	-	60	-	-	-	S	Fe oxide margin on quartz vein
42	1	fault plane	174	77	264	-	-	-	-	-	-	-	-	-	-	-	-	SH7	-	-	-	-	-	S	
42	2	qz vein	108	54	198	-	-	-	-	-	-	-	-	-	-	-	-	V6	-	20	-	-	-	S	
42	3	fault plane	73	84	343	-	-	-	-	-	-	-	-	-	-	-	-	SH7	-	-	-	-	-	S	
42	5	qz vein	105	53	195	-	-	qM	-	-	-	-	-	-	-	-	-	V3	-	130	-	-	-	S	Fe rich foliated wallrock margin
42	8	qz vein	170	44	260	-	-	qT	-	-	-	-	-	-	-	-	-	V2	-	300	-	-	-	S	Intensely foliated wallrock margin
42	12	qz vein	98	59	188	-	-	qT	-	-	-	-	-	-	-	-	-	V2	-	70	-	-	-	S	
42	12	qz vein	67	56	157	-	-	-	-	-	-	-	-	-	-	-	-	V6	-	50	-	-	-	S	Vein co-intruding with last vein
42	14	qz vein	101	55	191	-	-	qT	-	-	-	-	-	-	-	-	-	V2	-	70	-	-	-	S	Vein traverses entire face
42	15	foliation	4	38	274	-	-	-	-	-	-	-	-	-	-	-	-	CC	-	-	-	-	-	S	Foliation in wallrock of previous vein
42	15	qz vein	103	58	193	-	-	qT	-	-	-	-	-	-	-	-	-	V2	-	130	mcs	WR	-	S	Vein with foliated margins
42	17	qz vein	128	47	218	-	-	-	-	-	-	-	-	-	-	-	-	V6	-	50	-	-	-	S	Ferruginous quartz vein
42	20	fault plane	76	80	346	-	-	-	-	-	-	-	-	-	-	-	-	SH7	-	-	-	-	-	S	Thin fault plane x-cutting entire face
42	20	qz vein	120	45	210	-	-	qT	-	-	-	-	-	-	-	-	-	V2	-	140	-	-	-	S	Coarsely pyritic wallrock
42	23	qz vein	114	50	204	-	-	qT	-	-	-	-	-	-	-	-	-	V2	-	50	-	-	-	S	Irregular quartz vein
42	24	qz vein	87	51	177	-	-	qT	-	-	-	-	-	-	-	-	-	V2	-	50	-	-	-	S	Vein with 2 or more generations co intr
42	26	qz vein	113	51	203	-	-	qT	-	-	-	-	-	-	-	-	-	V2	-	50	-	-	-	S	
42	27	qz vein	98	49	188	-	-	-	-	-	-	-	-	-	-	-	-	V6	-	40	-	-	-	S	Brecciated quartz vein with dilational rhombs

LOCATION		Structural	Orientation					Defining Mineralogy					Alteration					Group	X-cut	Vein	Vein	Vein	Halo	Pos	DESCRIPTION
WALL	Metres	Element	Strike	Dip	Dip/Dir	Plunge	Dir	1	2	3	4	5	1	2	3	4	5		Rel.	Width	Style	Inc	Width		
42	28	tension vein	73	70	343	-	-	ka	ca	-	-	-	-	-	-	-	-	V8	-	-	-	-	-	S	Tension veins
42	29	fault plane	5	51	275	-	-	-	-	-	-	-	-	-	-	-	-	SH7	-	-	-	-	-	S	
43	5	foliation	177	42	267	-	-	-	-	-	-	-	-	-	-	-	-	CC	-	-	-	-	-	S	Foliated ferruginous ka py alteration mafic
43	5	py sr vein	124	57	34	-	-	-	-	-	-	-	-	-	-	-	-	SRPY	-	-	-	-	-	S	
43	5	py sr vein	156	62	246	-	-	-	-	-	-	-	-	-	-	-	-	SRPY	-	-	-	-	-	S	
43	9	qz vein	95	29	185	-	-	qT	-	-	-	-	-	-	-	-	-	V2	-	100	-	-	-	S	
43	10	foliation	1	52	271	-	-	-	-	-	-	-	-	-	-	-	-	CC	-	-	-	-	-	S	
43	15	foliation	106	50	196	-	-	-	-	-	-	-	-	-	-	-	-	CC	-	-	-	-	-	S	Foliation defined by pyritic foliation surface
43	17	qz vein	112	52	202	-	-	qT	mo	-	-	-	fu	ka	si	py	-	V2	-	250	-	-	50	S	Intensely sheared halo
43	20	qz vein	86	44	176	-	-	qT	-	-	-	-	-	-	-	-	-	V2	-	300	mcs	-	-	S	Variable width vein with large dilation rhomb
43	21	GP vein	89	60	179	-	-	qz	fd	-	-	-	mu	fu	-	-	-	V9	-	1000	-	-	-	S	Several vein directions contained in GP
43	25	qz vein	111	31	21	-	-	qG	-	-	-	-	-	-	-	-	-	V2	-	-	-	-	-	S	Vein with no alteration selvedge
43	25	GP vein	106	54	196	-	-	qz	fd	-	-	-	ka	mu	-	-	-	V9	-	1300	-	-	-	S	Abundant translucent quartz vein with no alteration selvedge
43	28	fault plane	125	62	215	-	-	-	-	-	-	-	-	-	-	-	-	SH7	xnxt	-	-	vu	-	S	**Thin fault plane with vuggy quartz apparent Wblock up**
43	29	qz vein	22	82	112	-	-	-	-	-	-	-	-	-	-	-	-	V6	-	-	-	-	-	S	
44	0	qz vein	41	77	131	-	-	-	-	-	-	-	-	-	-	-	-	V6	-	-	-	WR	-	N	Quartz vein breccia with large fragments of wallrock
44	5	slicks	-	-	-	14	24	-	-	-	-	-	-	-	-	-	-	LSLK	-	-	-	-	-	N	Slickensides on quartz vein
44	5	qz vein	60	82	330	-	-	qT	-	-	-	-	-	-	-	-	-	V2	-	-	-	-	-	N	Quartz vein within lm mu altered porphyry
44	5	qz vein	32	59	302	-	-	-	-	-	-	-	-	-	-	-	-	V6	-	1000	-	-	-	N	Quartz vein on boundary of porphyry bar
44	7	qz vein	147	35	237	-	-	-	-	-	-	-	ka	mu	-	-	-	V6	-	50	-	-	-	N	Ferruginous quartz vein
44	9	qz vein	83	54	173	-	-	-	-	-	-	-	-	-	-	-	-	V6	-	500	-	-	-	N	Foliated quartz vein
44	13	qz vein	47	58	317	-	-	-	-	-	-	-	-	-	-	-	-	V6	-	-	-	-	-	N	Quartz vein in plane of major fault
45	8	qz vein	119	55	209	-	-	qM	-	-	-	-	-	-	-	-	-	V3	-	-	-	-	-	N	Quartz mafic contact limb of fold
45	9	qz vein	78	38	168	-	-	-	-	-	-	-	-	-	-	-	-	V6	-	-	-	-	-	N	Quartz mafic contact limb of fold
45	13	shear ct	36	80	126	-	-	-	-	-	-	-	-	-	-	-	-	SH6	-	-	-	-	-	N	Contact of major vein with intensely sheared mafic
45	13	shear zone	120	85	210	-	-	-	-	-	-	-	-	-	-	-	-	SH6	-	-	-	-	-	N	Intense shear fracture zones within quartz vein
45	14	qz vein	150	73	240	-	-	-	-	-	-	-	-	-	-	-	-	V6	-	-	-	-	-	N	Intensely fractured quartz vein intruding ferruginous fault plane
45	17	qz vein	9	27	99	-	-	qT	-	-	-	-	-	-	-	-	-	V2	-	100	-	-	-	N	Ferruginous quartz vein
45	19	qz vein	14	20	104	-	-	-	-	-	-	-	-	-	-	-	-	V6	-	-	-	-	-	N	
45	19	qz vein	45	62	135	-	-	-	-	-	-	-	-	-	-	-	-	V6	xnxt	-	-	-	-	N	**E block up disp of nxt vein**
45	22	qz vein	176	78	266	-	-	-	-	-	-	-	-	-	-	-	-	V6	-	280	bx	-	-	N	Brecciated quartz vein
46	0	qz vein	68	39	158	-	-	-	-	-	-	-	py	-	-	-	-	V6	-	-	-	-	-	N	Wall parallel vein foliated int alteration wallrock
46	9	qz vein	95	58	185	-	-	-	-	-	-	-	mu	-	-	-	-	V6	-	-	-	-	-	N	Extensively recrystallised vein mm scale
46	10	foliation	158	86	248	-	-	-	-	-	-	-	-	-	-	-	-	SH1	-	-	-	-	-	N	Intensely sheared and altered mafic
46	10	qz vein	155	55	245	-	-	-	-	-	-	-	-	-	-	-	-	V6	-	100	-	-	-	N	
46	11	foliation	165	79	255	-	-	-	-	-	-	-	-	-	-	-	-	CC	-	-	-	-	-	N	
46	11	qz vein	120	59	210	-	-	-	-	-	-	-	-	-	-	-	-	V6	-	-	-	-	-	N	

LOCATION		Structural	Orientation					Defining Mineralogy					Alteration					Group	X-cut	Vein	Vein	Vein	Halo	Pos	DESCRIPTION
WALL	Metres	Element	Strike	Dip	Dip/Dir	Plunge	Dir	1	2	3	4	5	1	2	3	4	5		Rel.	Width	Style	Inc	Width		
46	16	fold axis	-	-	-	67	50	-	-	-	-	-	-	-	-	-	-	F1	-	-	-	-	-	N	Fold axis in quartz vein
46	16	qz vein	68	43	158	-	-	-	-	-	-	-	-	-	-	-	-	V6	-	200	-	-	-	N	Quartz vein within large mafic block
46	16	qz/mafic ct	40	86	310	-	-	-	-	-	-	-	-	-	-	-	-	VL	-	-	-	-	-	N	Contact of mafic with foliated quartz vein to W
46	19	foliation	57	82	327	-	-	-	-	-	-	-	-	-	-	-	-	CC	-	-	-	-	-	N	
46	19	foliation	167	57	257	-	-	-	-	-	-	-	-	-	-	-	-	CC	xnxt	-	-	-	-	N	Foliation within mafic block
46	20	fold axis	-	-	-	66	158	-	-	-	-	-	-	-	-	-	-	F1	-	-	-	-	-	N	Fold axis in quartz vein
46	20	qz vein	14	76	284	-	-	-	-	-	-	-	-	-	-	-	-	VL	-	-	-	-	-	N	Wallrock/vein contact
46	21	qz vein	54	84	144	-	-	-	-	-	-	-	-	-	-	-	-	VL	-	-	-	-	-	N	Vein/wallrock contact
46	22	fold axis	-	-	-	64	156	-	-	-	-	-	-	-	-	-	-	F1	-	-	-	-	-	N	Fold axis in quartz vein
46	22	qz vein	64	64	154	-	-	-	-	-	-	-	-	-	-	-	-	VL	-	-	-	-	-	N	Wallrock/vein contact
46	27	qz vein	110	50	200	-	-	-	-	-	-	-	-	-	-	-	-	VL	-	-	-	-	-	N	Fold nose in quartz
47	0	stock vein	4	43	274	-	-	-	-	-	-	-	-	-	-	-	-	V6	-	-	-	-	-	N	Quartz stockwork in int foliated purple mafic
47	0	stock vein	37	44	127	-	-	-	-	-	-	-	-	-	-	-	-	V6	-	-	-	-	-	N	Quartz stockwork in int foliated purple mafic
47	0	stock vein	134	80	224	-	-	-	-	-	-	-	-	-	-	-	-	V6	-	-	-	-	-	N	Quartz stockwork in intensely foliated purple mafic
47	3	qz vein	53	42	143	-	-	qT	-	-	-	-	-	-	-	-	-	V2	-	200	-	-	-	N	
47	4	qz vein	31	48	121	-	-	-	-	-	-	-	-	-	-	-	-	V6	-	300	-	-	-	N	Sigmoid quartz vein minor GP on contact
47	5	qz vein	81	53	171	-	-	-	-	-	-	-	-	-	-	-	-	V6	-	-	-	-	-	N	Quartz vein in ch py bi alteration rock
47	9	qz vein	114	55	204	-	-	-	-	-	-	-	-	-	-	-	-	VL	-	-	-	-	-	N	Foliated vein undulating in and out of face
47	12	fold axis	-	259	-	-	-	-	-	-	-	-	-	-	-	-	-	F1	-	-	-	-	-	N	Fold axis in quartz vein
47	12	qz vein	102	41	192	-	-	-	-	-	-	-	-	-	-	-	-	VL	-	-	-	-	-	N	Foliated vein undulating in and out of face
47	15	fold axis	-	283	-	-	-	-	-	-	-	-	-	-	-	-	-	F1	-	-	-	-	-	N	Fold axis in quartz vein
47	15	qz vein	74	45	164	-	-	-	-	-	-	-	-	-	-	-	-	VL	-	-	-	-	-	N	Foliated vein undulating in and out of face
47	18	fold axis	-	340	-	-	-	-	-	-	-	-	-	-	-	-	-	F1	-	-	-	-	-	N	Fold axis in quartz vein
47	18	qz vein	161	75	251	-	-	-	-	-	-	-	-	-	-	-	-	VL	-	-	-	-	-	N	Foliated vein undulating in and out of face
47	19	fold axis	-	178	-	-	-	-	-	-	-	-	-	-	-	-	-	F1	-	-	-	-	-	N	Fold axis in quartz vein
47	19	qz vein	68	48	158	-	-	-	-	-	-	-	-	-	-	-	-	VL	-	-	-	-	-	N	Foliated vein undulating in and out of face
47	21	fold axis	-	188	-	-	-	-	-	-	-	-	-	-	-	-	-	F1	-	-	-	-	-	N	Fold axis in quartz vein
47	21	qz vein	106	44	196	-	-	-	-	-	-	-	-	-	-	-	-	VL	-	-	-	-	-	N	Foliated vein undulating in and out of face
47	23	fold axis	-	178	-	-	-	-	-	-	-	-	-	-	-	-	-	F1	-	-	-	-	-	N	Fold axis in quartz vein
47	23	qz vein	87	43	177	-	-	-	-	-	-	-	-	-	-	-	-	VL	-	-	-	-	-	N	Foliated vein undulating in and out of face
47	26	fold axis	-	212	-	-	-	-	-	-	-	-	-	-	-	-	-	F1	-	-	-	-	-	N	Fold axis in quartz vein
47	26	qz vein	100	39	190	-	-	-	-	-	-	-	-	-	-	-	-	VL	-	-	-	-	-	N	Foliated vein undulating in and out of face
48	0	foliation	125	79	35	-	-	-	-	-	-	-	-	-	-	-	-	CC	-	-	-	-	-	N	Strongly foliated limonitic mafic
48	3	fault plane	39	58	309	-	-	-	-	-	-	-	-	-	-	-	-	SH7	-	-	-	-	-	N	Thin ferruginous fault plane
48	6	stock vein	28	90	298	-	-	-	-	-	-	-	-	-	-	-	-	V6	-	-	-	-	-	N	Stockwork of thin ferruginous quartz veins
48	6	stock vein	66	50	336	-	-	-	-	-	-	-	-	-	-	-	-	V6	-	-	-	-	-	N	Stockwork of thin ferruginous quartz veins
48	6	stock vein	17	60	107	-	-	-	-	-	-	-	-	-	-	-	-	V6	-	-	-	-	-	N	Stockwork of thin ferruginous quartz veins

LOCATION		Structural	Orientation					Defining Mineralogy					Alteration					Group	X-cut	Vein	Vein	Vein	Halo	Pos	DESCRIPTION
WALL	Metres	Element	Strike	Dip	Dip/Dir	Plunge	Dir	1	2	3	4	5	1	2	3	4	5		Rel.	Width	Style	Inc	Width		
48	8	foliation	4	55	274	-	-	-	-	-	-	-	-	-	-	-	-	CC	-	-	-	-	-	N	Purple ferruginous mafic with qcb veining
48	12	shear zone	2	78	92	-	-	-	-	-	-	-	-	-	-	-	-	SH4	-	-	scs	-	-	N	Intense shear breccia zone with several thin quartz veins
48	13	foliation	5	66	275	-	-	-	-	-	-	-	-	-	-	-	-	CC	-	-	-	-	-	N	Intense foliation
48	13	fault plane	168	75	258	-	-	-	-	-	-	-	-	-	-	-	-	SH7	-	-	-	-	-	N	Fault plane withthin quartz veins
48	13	fault plane	175	78	265	-	-	-	-	-	-	-	-	-	-	-	-	SH7	-	-	xprv	-	-	N	Thin fault plane
48	13	qz vein	157	47	247	-	-	-	-	-	-	-	-	-	-	-	-	V6	xall	-	-	-	-	N	x-cutting quartz vein
48	15	fault plane	167	65	257	-	-	-	-	-	-	-	-	-	-	-	-	SH7	-	-	-	-	-	N	
48	18	fold axis	-	-	-	36	147	-	-	-	-	-	-	-	-	-	-	F1	-	-	-	-	-	N	Fold axis in quartz vein
48	18	qz vein	93	42	183	-	-	-	-	-	-	-	-	-	-	-	-	VL	-	30	-	-	-	N	Foliated vein undulating in and out of face
48	19	fold axis	-	-	-	35	169	-	-	-	-	-	-	-	-	-	-	F1	-	-	-	-	-	N	Fold axis in quartz vein
48	19	qz vein	65	36	155	-	-	-	-	-	-	-	-	-	-	-	-	VL	-	-	-	-	-	N	Foliated vein undulating in and out of face
48	19	qz vein	125	45	215	-	-	-	-	-	-	-	-	-	-	-	-	VL	-	-	-	-	-	N	Foliated vein undulating in and out of face
48	21	foliation	2	59	272	-	-	-	-	-	-	-	-	-	-	-	-	CC	-	-	-	-	-	N	Blocky foliated purple dolerite
48	23	foliation	5	41	275	-	-	-	-	-	-	-	-	-	-	-	-	CC	-	-	-	-	-	N	
48	23	fault plane	150	77	240	-	-	-	-	-	-	-	-	-	-	-	-	SH7	-	-	-	-	-	N	
48	23	qz vein	174	71	84	-	-	-	-	-	-	-	-	-	-	-	-	V6	-	30	-	-	-	N	Vein traverses entire face
48	26	qz vein	130	73	220	-	-	-	-	-	-	-	-	-	-	-	-	V6	-	200	-	-	-	N	Vein dipping out of face
48	27	qz vein	79	48	169	-	-	-	-	-	-	-	-	-	-	-	-	V6	-	-	-	-	-	N	Same vein as previous
48	29	qz vein	108	37	198	-	-	-	-	-	-	-	-	-	-	-	-	V6	-	-	-	-	-	N	
49	0	qz vein	25	58	115	-	-	-	-	-	-	-	-	-	-	-	-	V6	xnxt	-	-	-	-	N	Thin ferruginous vein in ka lm alteration mafic
49	2	foliation	13	80	103	-	-	-	-	-	-	-	-	-	-	-	-	CC	xprv	-	-	-	-	N	Secondary x-cutting foliation
49	2	foliation	149	58	239	-	-	-	-	-	-	-	-	-	-	-	-	CC	-	-	-	-	-	N	
49	3	fault plane	143	75	233	-	-	-	-	-	-	-	-	-	-	-	-	SH7	-	-	-	-	-	N	Thin fault zone foliation bends in
49	4	qz vein	161	38	251	-	-	-	-	-	-	-	-	-	-	-	-	V6	-	200	-	-	-	N	Variable width quartz vein
49	5	foliation	168	42	258	-	-	-	-	-	-	-	-	-	-	-	-	CC	-	-	-	-	-	N	
49	9	qz vein	178	45	268	-	-	qT	-	-	-	-	-	-	-	-	-	V2	-	160	-	vu	-	N	Vein parallel to foliation
49	9	qz vein	178	44	268	-	-	-	-	-	-	-	-	-	-	-	-	V6	-	50	mcs	-	-	N	Ferruginous vein
49	12	foliation	168	30	258	-	-	-	-	-	-	-	-	-	-	-	-	CC	-	-	-	-	-	N	Intense foliation in limonitic mafic
49	12	qz vein	144	40	234	-	-	qT	-	-	-	-	mu	ka	-	-	-	V2	-	150	-	-	-	N	Vein diverges and converges through face
49	14	cleavage	15	67	105	-	-	-	-	-	-	-	-	-	-	-	-	CS2	-	-	-	-	-	N	Wide spaced cleavage
49	14	qz vein	32	77	302	-	-	-	-	-	-	-	-	-	-	-	-	V6	-	-	-	-	-	N	Thin ferruginous stringer veins
49	16	qz vein	95	55	185	-	-	-	-	-	-	-	-	-	-	-	-	V6	-	-	-	-	-	N	
49	19	foliation	75	75	165	-	-	-	-	-	-	-	-	-	-	-	-	CC	-	-	-	-	-	N	
49	19	foliation	141	47	51	-	-	-	-	-	-	-	-	-	-	-	-	FL6	-	-	-	-	-	N	
49	22	cleavage	40	70	310	-	-	-	-	-	-	-	-	-	-	-	-	CS2	-	-	-	-	-	N	
49	25	fault plane	95	51	5	-	-	-	-	-	-	-	-	-	-	-	-	SH7	-	-	-	-	-	N	**Thin ferruginous veined fault plane NBlockE**
49	25	tension vein	30	82	300	-	-	qz	-	-	-	-	-	-	-	-	-	V8	-	-	-	-	-	N	

LOCATION		Structural	Orientation					Defining Mineralogy					Alteration					Group	X-cut	Vein	Vein	Vein	Halo	Pos	DESCRIPTION
WALL	Metres	Element	Strike	Dip	Dip/Dir	Plunge	Dir	1	2	3	4	5	1	2	3	4	5		Rel.	Width	Style	Inc	Width		
49	26	qz vein	53	82	143	-	-	qz	-	-	-	-	-	-	-	-	-	V6	xbbyfault	-	-	-	-	N	Intensely foliated margins 0.5m offset by previous fault
49	27	fault plane	145	75	235	-	-	-	-	-	-	-	-	-	-	-	-	SH7	xprv	-	-	-	-	N	Thin fault plane ~2m offset+folding by fault
49	27	qz vein	7	77	277	-	-	qz	-	-	-	-	-	-	-	-	-	V6	-	100	-	-	-	N	Ferruginous vein offset by fault
50	0	foliation	40	38	310	-	-	-	-	-	-	-	-	-	-	-	-	CC	-	-	-	-	-	N	Weakly foliated pylmka weathered mafic
50	6	foliation	8	44	278	-	-	-	-	-	-	-	-	-	-	-	-	CC	-	-	-	-	-	N	
50	6	qz vein	126	73	216	-	-	-	-	-	-	-	-	-	-	-	-	V6	-	700	-	-	-	N	**Fractured breccia quartz vein E block up offset**
50	10	qz vein	3	58	273	-	-	-	-	-	-	-	-	-	-	-	-	V6	-	50	-	-	-	N	Vein on thin fault plane
50	14	qz vein	149	57	239	-	-	qT	-	-	-	-	-	-	-	-	-	V2	-	100	-	-	-	N	FeO coatings
50	15	qz vein	20	45	290	-	-	qT	-	-	-	-	-	-	-	-	-	V2	-	100	-	-	-	N	Gently foliated vein
50	17	fault plane	175	53	265	-	-	-	-	-	-	-	-	-	-	-	-	SH7	-	-	-	-	-	N	Thin fault plane with irregular quartz infill
50	21	qz vein	12	78	102	-	-	-	-	-	-	-	-	-	-	-	-	V6	-	50	-	-	-	N	Quartz vein traverses entire face
50	22	qz vein	88	42	178	-	-	-	-	-	-	-	-	-	-	-	-	V6	-	-	-	-	-	N	Foliated quartz veins dipping out of face
50	22	e-limb	158	38	248	-	-	-	-	-	-	-	-	-	-	-	-	VL	-	-	-	-	-	N	Short limb of kink
50	24	fold axis	-	-	-	35	221	-	-	-	-	-	-	-	-	-	-	F1	-	-	-	-	-	N	Fold axis in quartz vein
50	24	w-limb	93	41	183	-	-	-	-	-	-	-	-	-	-	-	-	VL	-	-	-	-	-	N	Long limb of kink fold
50	25	foliation	27	85	117	-	-	-	-	-	-	-	-	-	-	-	-	CC	-	-	-	-	-	N	Intense wallrock foliation
50	25	faultbx zone	34	54	304	-	-	-	-	-	-	-	-	-	-	-	-	SH4	xprv	-	-	-	-	N	Intense breccia zone with shear alteration mafic and foliated quartz
50	25	faultbx zone	49	72	319	-	-	-	-	-	-	-	-	-	-	-	-	SH4	-	-	-	-	-	N	Shp upper bdy of previous breccia zone
50	27	foliation	165	49	255	-	-	-	-	-	-	-	-	-	-	-	-	CC	-	-	-	-	-	N	Intensely foliated pink weathered mafic
50	27	foliation	171	50	261	-	-	-	-	-	-	-	-	-	-	-	-	CC	-	-	-	-	-	N	Intensely foliated pink weathered mafic
50	29	cleavage	161	56	251	-	-	-	-	-	-	-	-	-	-	-	-	CS2	-	-	-	-	-	N	Pervasive cleavage
50	29	qz vein	167	50	257	-	-	qT	-	-	-	-	-	-	-	-	-	V2	-	-	-	-	-	N	Thin ferruginous vein
50	29	qz vein	60	43	150	-	-	-	-	-	-	-	-	-	-	-	-	V6	-	-	-	-	-	N	Foliated vein dipping out of face
51	3	qz vein	171	77	81	-	-	-	-	-	-	-	-	-	-	-	-	V6	-	-	-	-	-	N	Thin ferruginous vein
51	4	qz vein	126	73	216	-	-	qT	-	-	-	-	-	-	-	-	-	V2	-	140	-	-	-	N	Foliated vein with strongly sheared margin
51	6	foliation	150	46	240	-	-	-	-	-	-	-	-	-	-	-	-	CC	-	-	-	-	-	N	Strong foliation in wallrock
51	6	qz vein	124	60	214	-	-	qM	-	-	-	-	py	mu	-	-	-	V3	-	1000	-	WR	-	N	X-cut by EW trending fault
51	9	qz vein	165	53	255	-	-	qT	-	-	-	-	-	-	-	-	-	V2	-	-	-	-	-	N	Thin grey quartz vein
51	11	foliation	179	42	269	-	-	-	-	-	-	-	-	-	-	-	-	CC	-	-	-	-	-	N	Dominant foliation in wallrock
51	12	qz vein	34	48	124	-	-	qT	-	-	-	-	-	-	-	-	-	V2	-	-	-	vu	-	N	
51	15	foliation	140	41	230	-	-	-	-	-	-	-	-	-	-	-	-	CC	-	-	-	-	-	N	
51	16	qz vein	158	57	248	-	-	-	-	-	-	-	-	-	-	-	-	V6	-	30	-	-	-	N	Thin ferruginous vein
51	18	fault plane	44	68	314	-	-	-	-	-	-	-	-	-	-	-	-	SH7	-	-	-	-	-	N	Quartz vein at boundary of fault plane
51	18	foliation	163	60	253	-	-	-	-	-	-	-	-	-	-	-	-	SH7	-	-	-	-	-	N	Internal foliation in fault plane
51	20	foliation	16	45	286	-	-	-	-	-	-	-	-	-	-	-	-	CC	-	-	-	-	-	N	
51	22	foliation	23	73	293	-	-	-	-	-	-	-	-	-	-	-	-	CC	-	-	-	-	-	N	
51	25	qz vein	175	38	265	-	-	-	-	-	-	-	-	-	-	-	-	V6	-	30	-	-	-	N	Thin quartz vein subparallel to fault zone

LOCATION		Structural	Orientation					Defining Mineralogy					Alteration					Group	X-cut	Vein	Vein	Vein	Halo	Pos	DESCRIPTION
WALL	Metres	Element	Strike	Dip	Dip/Dir	Plunge	Dir	1	2	3	4	5	1	2	3	4	5		Rel.	Width	Style	Inc	Width		
51	29	qz vein	6	56	96	-	-	-	-	-	-	-	-	-	-	-	-	V6	-	30	-	-	-	N	
52	0	tension vein	47	42	317	-	-	ka	qz	cb	-	-	-	-	-	-	-	V8	-	3	-	-	-	N	Tension fractures sigmoidal
52	3	qz vein	16	40	106	-	-	-	-	-	-	-	-	-	-	-	-	V6	xprv	-	-	-	-	N	Thin veins
52	5	fault plane	110	65	200	-	-	-	-	-	-	-	-	-	-	-	-	SH7	-	-	-	-	-	N	Thin fault plane with 3cm intr vein
52	5	qz vein	5	26	275	-	-	qT	-	-	-	-	-	-	-	-	-	V2	-	30	-	-	-	N	Vein traverses face
52	7	qz vein	166	72	256	-	-	qT	-	-	-	-	-	-	-	-	-	V2	-	150	-	-	-	N	
52	11	qz vein	163	65	73	-	-	qT	-	-	-	-	-	-	-	-	-	V2	-	250	-	-	-	N	Vein in weakly foliated dolerite
52	19	qz vein	145	49	235	-	-	-	-	-	-	-	-	-	-	-	-	V6	-	-	-	-	-	N	
52	22	foliation	10	64	280	-	-	-	-	-	-	-	-	-	-	-	-	CC	-	-	-	-	-	N	Foliation parallel with quartz veins
52	22	qz vein	175	81	85	-	-	-	-	-	-	-	-	-	-	-	-	V6	-	30	mcs	-	-	N	Vein x-cuts foliation
52	27	qz vein	20	78	290	-	-	-	-	-	-	-	-	-	-	-	-	V6	-	-	-	-	-	N	
52	27	qz vein	169	49	259	-	-	-	-	-	-	-	-	-	-	-	-	V6	-	-	-	-	-	N	
53	3	foliation	164	84	254	-	-	-	-	-	-	-	-	-	-	-	-	CC	-	-	-	-	-	N	Intense foliation in strongly weathered maf
53	9	qz vein	127	52	217	-	-	qT	-	-	-	-	-	-	-	-	-	V2	-	150	-	-	-	N	
53	12	fault plane	26	73	296	-	-	-	-	-	-	-	-	-	-	-	-	SH7	-	-	-	-	-	N	**Nblock east**
53	12	qz vein	21	53	291	-	-	qT	-	-	-	-	-	-	-	-	-	V2	-	500	-	-	-	N	
53	12	qz vein	104	65	194	-	-	-	-	-	-	-	-	-	-	-	-	V6	-	100	-	-	-	N	
53	15	foliation	127	72	217	-	-	-	-	-	-	-	-	-	-	-	-	CC	-	-	-	-	-	N	
53	15	foliation	178	80	268	-	-	-	-	-	-	-	-	-	-	-	-	CC	-	-	-	-	-	N	
53	16	fault plane	8	73	278	-	-	-	-	-	-	-	-	-	-	-	-	SH7	-	-	-	-	-	N	
53	17	foliation	136	56	226	-	-	-	-	-	-	-	-	-	-	-	-	CC	-	-	-	-	-	N	
53	18	qz vein	11	62	281	-	-	qT	-	-	-	-	-	-	-	-	-	V2	-	50	-	-	-	N	Vein intrudes foliation defining lozenges
53	18	qz vein	118	62	208	-	-	qT	-	-	-	-	-	-	-	-	-	V2	-	50	-	-	-	N	Vein intrudes foliation defining lozenges
53	20	fault plane	24	34	294	-	-	-	-	-	-	-	-	-	-	-	-	SH7	-	-	-	-	-	N	
53	23	qz vein	142	28	52	-	-	-	-	-	-	-	-	-	-	-	-	V6	-	-	-	-	-	N	X cut veins with Wblock up
53	23	qz vein	116	51	206	-	-	-	-	-	-	-	-	-	-	-	-	V6	-	-	-	-	-	N	
53	26	fault plane	25	61	115	-	-	-	-	-	-	-	-	-	-	-	-	SH7	-	-	-	-	-	N	
53	27	stock vein	29	61	299	-	-	-	-	-	-	-	-	-	-	-	-	V6	-	-	-	-	-	N	Fine mm scale veins define stockwork fract
53	27	stock vein	148	83	58	-	-	-	-	-	-	-	-	-	-	-	-	V6	-	-	-	-	-	N	Fine mm scale veins define stockwork fract
53	27	stock vein	6	83	96	-	-	-	-	-	-	-	-	-	-	-	-	V6	-	-	-	-	-	N	Fine mm scale veins define stockwork fract
53	27	stock vein	15	50	105	-	-	-	-	-	-	-	-	-	-	-	-	V6	-	-	-	-	-	N	Fine mm scale veins define stockwork fract
54	0	fractures	23	25	293	-	-	-	-	-	-	-	-	-	-	-	-	CS1	-	-	-	-	-	N	Pervasive fracture stockwork
54	0	fractures	105	77	195	-	-	-	-	-	-	-	-	-	-	-	-	CS1	-	-	-	-	-	N	Pervasive fracture stockwork
54	0	fractures	132	63	222	-	-	-	-	-	-	-	-	-	-	-	-	CS1	-	-	-	-	-	N	Pervasive fracture stockwork
54	3	qz vein	135	74	225	-	-	qT	-	-	-	-	-	-	-	-	-	V2	-	30	-	vu	-	N	
54	6	shear zone	136	80	46	-	-	-	-	-	-	-	-	-	-	-	-	SH7	-	-	-	-	-	N	
54	9	foliation	150	70	240	-	-	-	-	-	-	-	-	-	-	-	-	CC	-	-	-	-	-	N	

LOCATION		Structural	Orientation					Defining Mineralogy					Alteration					Group	X-cut	Vein	Vein	Vein	Halo	Pos	DESCRIPTION
WALL	Metres	Element	Strike	Dip	Dip/Dir	Plunge	Dir	1	2	3	4	5	1	2	3	4	5		Rel.	Width	Style	Inc	Width		
54	16	sed	50	65	140	-	-	-	-	-	-	-	-	-	-	-	-	BED6	-	-	-	-	-	N	Block of sediment sheared out
54	16	foliation	131	57	221	-	-	-	-	-	-	-	-	-	-	-	-	CC	-	-	-	-	-	N	Foliation in wallrock at contact with GP
54	21	s-plane	114	80	204	-	-	-	-	-	-	-	-	-	-	-	-	SH1	-	-	-	-	-	N	
54	21	bx zone	74	75	344	-	-	-	-	-	-	-	-	-	-	-	-	SH4	-	-	-	-	-	N	Clasts of quartz and GP
54	24	qz vein	140	58	230	-	-	-	-	-	-	-	-	-	-	-	-	V6	-	100	-	-	-	N	
54	27	qz vein	130	88	40	-	-	-	-	-	-	-	-	-	-	-	-	V6	-	-	-	-	-	N	Quartz vein with sheared margins
55	0	foliation	130	87	220	-	-	-	-	-	-	-	-	-	-	-	-	CC	-	-	-	-	-	S	Intensely foliated talcose purple UM
55	5	foliation	134	86	224	-	-	-	-	-	-	-	-	-	-	-	-	CC	-	-	-	-	-	S	
55	10	foliation	146	67	236	-	-	-	-	-	-	-	-	-	-	-	-	CC	-	-	-	-	-	S	
55	10	sr-vein	8	54	278	-	-	-	-	-	-	-	-	-	-	-	-	SRPY	-	-	-	-	-	S	Very fine grained pyritic stringer veins
55	10	sr-vein	43	83	133	-	-	-	-	-	-	-	-	-	-	-	-	SRPY	-	-	-	-	-	S	
55	15	foliation	143	83	233	-	-	-	-	-	-	-	-	-	-	-	-	CC	-	-	-	-	-	S	Prominent foliation plane
56	0	sed/um	121	48	211	-	-	-	-	-	-	-	-	-	-	-	-	BED2	-	-	-	-	-	S	
56	0	foliation	136	80	226	-	-	-	-	-	-	-	-	-	-	-	-	CC	-	-	-	-	-	S	
56	11	foliation	142	70	232	-	-	-	-	-	-	-	-	-	-	-	-	CC	-	-	-	-	-	S	Foliation in crumbly talc schist
56	12	chillzone ct	141	66	231	-	-	-	-	-	-	-	-	-	-	-	-	BED1	-	-	-	-	-	S	
56	16	qz vein	36	84	306	-	-	-	-	-	-	-	-	-	-	-	-	V6	-	-	-	-	-	S	Thin ferruginous vein with fe banding
56	17	qz vein	112	55	202	-	-	qz	-	-	-	-	-	-	-	-	-	V6	-	50	-	-	-	S	Traverses face
56	24	foliation	169	78	259	-	-	-	-	-	-	-	-	-	-	-	-	CC	-	-	-	-	-	S	
56	28	foliation	154	60	244	-	-	-	-	-	-	-	-	-	-	-	-	CC	-	-	-	-	-	S	
57	0	foliation	8	61	278	-	-	-	-	-	-	-	-	-	-	-	-	CC	-	-	-	-	-	S	
57	1	foliation	154	66	244	-	-	-	-	-	-	-	-	-	-	-	-	CC	-	-	-	-	-	S	
57	5	foliation	158	60	248	-	-	-	-	-	-	-	-	-	-	-	-	CC	-	-	-	-	-	S	
57	11	c-plane	140	51	230	-	-	-	-	-	-	-	-	-	-	-	-	SH1	-	-	-	-	-	S	**Intense shear ta schist SS strike slip py tails**
57	11	s-plane	163	60	253	-	-	-	-	-	-	-	-	-	-	-	-	SH2	-	-	-	-	-	S	**Intense shear ta schist SS strike slip py tails**
57	15	foliation	146	63	236	-	-	-	-	-	-	-	-	-	-	-	-	CC	-	-	-	-	-	S	
57	21	foliation	151	59	241	-	-	-	-	-	-	-	-	-	-	-	-	CC	-	-	-	-	-	S	
57	26	fault plane	98	83	8	-	-	-	-	-	-	-	-	-	-	-	-	SH7	-	-	-	-	-	S	
58	0	foliation	33	59	303	-	-	-	-	-	-	-	-	-	-	-	-	CC	-	-	-	-	-	S	
58	7	foliation	178	60	268	-	-	-	-	-	-	-	-	-	-	-	-	CC	-	-	-	-	-	S	
58	13	foliation	28	59	298	-	-	-	-	-	-	-	-	-	-	-	-	CC	-	-	-	-	-	S	
58	13	foliation	48	51	318	-	-	-	-	-	-	-	-	-	-	-	-	CC	-	-	-	-	-	S	
58	14	foliation	34	60	304	-	-	-	-	-	-	-	-	-	-	-	-	CC	-	-	-	-	-	S	
58	14	foliation	161	82	71	-	-	-	-	-	-	-	-	-	-	-	-	CC	-	-	-	-	-	S	
58	14	foliation	177	75	267	-	-	-	-	-	-	-	-	-	-	-	-	CC	-	-	-	-	-	S	
58	19	foliation	30	44	300	-	-	-	-	-	-	-	-	-	-	-	-	CC	-	-	-	-	-	S	
59	12	foliation	115	80	205	-	-	-	-	-	-	-	-	-	-	-	-	CC	-	-	-	-	-	N	Foliation in Cashmans porphyry

LOCATION		Structural	Orientation					Defining Mineralogy					Alteration					Group	X-cut	Vein	Vein	Vein	Halo	Pos	DESCRIPTION
WALL	Metres	Element	Strike	Dip	Dip/Dir	Plunge	Dir	1	2	3	4	5	1	2	3	4	5		Rel.	Width	Style	Inc	Width		
59	23	sed	109	51	199	-	-	-	-	-	-	-	-	-	-	-	-	BED2	-	-	-	-	-	N	Quartz vein at lower CSH contact
60	1	tacb vein	102	47	192	-	-	-	-	-	-	-	-	-	-	-	-	V5	-	-	-	-	-	N	
60	3	fault plane	80	70	350	-	-	-	-	-	-	-	-	-	-	-	-	SH7	-	-	-	-	-	S	
60	3	fault plane	104	52	194	-	-	-	-	-	-	-	-	-	-	-	-	SH7	-	-	-	-	-	S	
60	9	fault plane	71	61	341	-	-	-	-	-	-	-	-	-	-	-	-	SH7	-	-	-	-	-	S	
60	23	fault plane	81	73	351	-	-	-	-	-	-	-	-	-	-	-	-	SH7	-	-	-	-	-	S	
61	15	qz vein	135	55	225	-	-	-	-	-	-	-	-	-	-	-	-	V6	-	-	-	-	-	S	Thin vein with ferruginous alteration selvedges
62	3	fault plane	96	83	6	-	-	-	-	-	-	-	-	-	-	-	-	SH7	-	-	-	-	-	S	Thin ferruginous fault plane
62	7	joint	157	50	67	-	-	-	-	-	-	-	-	-	-	-	-	J2	-	-	-	-	-	S	
62	7	joint	71	73	161	-	-	-	-	-	-	-	-	-	-	-	-	J2	-	-	-	-	-	S	
62	19	fault plane	114	89	24	-	-	-	-	-	-	-	-	-	-	-	-	SH7	-	-	-	-	-	S	**W Block up fault plane**
63	2	shear zone	37	76	127	-	-	-	-	-	-	-	-	-	-	-	-	SH1	-	-	-	-	-	S	10cm wide shear zone with intense mylonite
63	4	joint	66	80	336	-	-	-	-	-	-	-	-	-	-	-	-	J1	-	-	-	-	-	S	Prominent joint plane
63	4	joint	35	83	305	-	-	-	-	-	-	-	-	-	-	-	-	J2	-	-	-	-	-	S	Conjugate joint set?
63	4	joint	44	79	134	-	-	-	-	-	-	-	-	-	-	-	-	J2	-	-	-	-	-	S	Conjugate joint set?
63	4	joint	127	81	217	-	-	-	-	-	-	-	-	-	-	-	-	J2	-	-	-	-	-	S	Prominent joint plane
63	9	joint	40	86	130	-	-	-	-	-	-	-	-	-	-	-	-	J2	-	-	-	-	-	S	
63	9	joint	157	47	247	-	-	-	-	-	-	-	-	-	-	-	-	J2	-	-	-	-	-	S	
63	11	joint	59	81	329	-	-	-	-	-	-	-	-	-	-	-	-	J1	-	-	-	-	-	S	
63	11	joint	66	57	336	-	-	-	-	-	-	-	-	-	-	-	-	J1	-	-	-	-	-	S	
63	14	c-plane	136	49	226	-	-	-	-	-	-	-	-	-	-	-	-	SH1	-	-	-	-	-	S	**S-C myl Nblock west SS movement 1.5m zone**
63	14	s-plane	153	69	243	-	-	-	-	-	-	-	-	-	-	-	-	SH1	-	-	-	-	-	S	**S-C myl Nblock west SS movement 1.5m zone**
63	19	shear zone	9	81	279	-	-	-	-	-	-	-	-	-	-	-	-	SH6	-	-	-	-	-	S	
63	19	fault plane	113	47	23	-	-	-	-	-	-	-	-	-	-	-	-	SH7	xnxt	-	-	-	-	S	
64	0	joint	143	46	233	-	-	-	-	-	-	-	-	-	-	-	-	J2	-	-	-	-	-	S	
64	4	myl zone	42	52	312	-	-	-	-	-	-	-	-	-	-	-	-	SH1	-	-	-	-	-	S	Intense ductile deformation
64	6	joint	127	48	217	-	-	-	-	-	-	-	-	-	-	-	-	J2	-	-	-	-	-	S	
64	8	shear zone	32	88	122	-	-	-	-	-	-	-	-	-	-	-	-	SH1	-	-	-	-	-	S	**Nblock down ductile shear zone**
64	11	joint	33	63	123	-	-	-	-	-	-	-	-	-	-	-	-	J2	-	-	-	-	-	S	
64	11	joint	155	50	245	-	-	-	-	-	-	-	-	-	-	-	-	J2	-	-	-	-	-	S	
64	12	joint	76	63	346	-	-	-	-	-	-	-	-	-	-	-	-	J1	-	-	-	-	-	S	
64	13	s-plane	11	77	281	-	-	-	-	-	-	-	-	-	-	-	-	SH1	xnxt	-	-	-	-	S	
64	13	myl zone	50	82	320	-	-	-	-	-	-	-	-	-	-	-	-	SH1	-	-	-	-	-	S	Ductile shear zone cut by previous
64	13	c-plane	152	62	242	-	-	-	-	-	-	-	-	-	-	-	-	SH1	xnxt	-	-	-	-	S	Intense anastomosing ductile shear zone domainal
64	16	s-plane	31	58	301	-	-	-	-	-	-	-	-	-	-	-	-	SH1	-	-	-	-	-	S	Shear bands
64	16	c-plane	38	79	308	-	-	-	-	-	-	-	-	-	-	-	-	SH1	-	-	-	-	-	S	**Shear bands Nblock down**
64	16	shear zone	142	49	232	-	-	-	-	-	-	-	-	-	-	-	-	SH1	-	-	-	-	-	S	**Shear band Sinistral E Block north**

LOCATION		Structural	Orientation					Defining Mineralogy					Alteration					Group	X-cut	Vein	Vein	Vein	Halo	Pos	DESCRIPTION
WALL	Metres	Element	Strike	Dip	Dip/Dir	Plunge	Dir	1	2	3	4	5	1	2	3	4	5		Rel.	Width	Style	Inc	Width		
64	18	fault plane	170	42	80	-	-	-	-	-	-	-	-	-	-	-	-	SH7	-	-	-	-	-	S	**Undulating fault plane**
64	22	joint	151	61	241	-	-	-	-	-	-	-	-	-	-	-	-	J2	-	-	-	-	-	S	
64	25	fault plane	38	85	128	-	-	-	-	-	-	-	-	-	-	-	-	SH7	-	-	-	-	-	S	
64	27	fault plane	178	55	88	-	-	-	-	-	-	-	-	-	-	-	-	SH2	-	-	-	-	-	S	Talc schist fault plane
64	30	joint	3	42	273	-	-	-	-	-	-	-	-	-	-	-	-	J2	-	-	-	-	-	S	
65	0	foliation	178	72	268	-	-	-	-	-	-	-	-	-	-	-	-	CC	-	-	-	-	-	S	
65	1	qz vein	20	65	290	-	-	-	-	-	-	-	-	-	-	-	-	V6	-	-	-	-	-	S	Ferruginous quartz vein
65	6	shear zone	134	51	224	-	-	ta	ch	-	-	-	-	-	-	-	-	SH1	-	-	-	-	-	S	Intense shear zone euhedral py + asymmetric pressure shadows
65	6	qz vein	33	77	303	-	-	-	-	-	-	-	-	-	-	-	-	V6	-	-	-	-	-	S	Quartz vein in fault plane cut by ta schist shear zone
65	15	fault plane	33	64	303	-	-	-	-	-	-	-	-	-	-	-	-	SH7	-	-	-	-	-	S	Poorly developed discontinous cross faults
65	17	foliation	25	59	295	-	-	-	-	-	-	-	-	-	-	-	-	CC	-	-	-	-	-	S	
65	17	fault plane	21	83	111	-	-	-	-	-	-	-	-	-	-	-	-	SH7	xnxt	-	-	-	-	S	Cross fault
65	18	foliation	61	48	331	-	-	-	-	-	-	-	-	-	-	-	-	CC	-	-	-	-	-	S	
65	20	foliation	170	76	260	-	-	-	-	-	-	-	-	-	-	-	-	CC	-	-	-	-	-	S	Intense pervasive foliation in talc schist
65	21	foliation	27	86	297	-	-	-	-	-	-	-	-	-	-	-	-	CC	-	-	-	-	-	S	Internal foliation, vein boudins
65	21	fault plane	32	69	302	-	-	-	-	-	-	-	-	-	-	-	-	SH7	-	30	mcs	-	-	S	Vein on margin of fault 2.5m wide 030 structure
65	21	fault contact	47	86	317	-	-	-	-	-	-	-	-	-	-	-	-	SH7	-	-	-	-	-	S	West contact with major fault plane
65	26	joint	59	9	149	-	-	-	-	-	-	-	-	-	-	-	-	J2	-	-	-	-	-	S	
65	28	fault plane	143	78	53	-	-	-	-	-	-	-	-	-	-	-	-	SH7	-	-	-	-	-	S	
65	29	fault plane	28	83	298	-	-	-	-	-	-	-	-	-	-	-	-	SH7	-	-	-	-	-	S	**N Block down offset**
65	30	joint	25	66	115	-	-	-	-	-	-	-	-	-	-	-	-	J2	-	-	-	-	-	S	
66	3	foliation	42	52	312	-	-	-	-	-	-	-	-	-	-	-	-	CC	-	-	-	-	-	S	
66	7	sed lam	120	44	210	-	-	-	-	-	-	-	-	-	-	-	-	BED2	-	-	-	-	-	S	Pyritic lam on E side of SEF
66	7	sed lam	176	54	266	-	-	-	-	-	-	-	-	-	-	-	-	BED2	-	-	-	-	-	S	Pyritic lam on W side of SEF
66	7	fault plane	60	76	330	-	-	-	-	-	-	-	-	-	-	-	-	SEF	xprv	-	-	-	-	S	**SEF 2-3m app disp N Block E and down**
66	7	qz vein	119	38	209	-	-	qT	qM	-	-	-	-	-	-	-	-	V2	-	300	-	-	-	S	
66	12	qz vein	35	53	305	-	-	-	-	-	-	-	-	-	-	-	-	V10	-	150	-	-	-	S	Quartz vein in felsic porphyry
66	16	GP/sed ct	172	44	262	-	-	-	-	-	-	-	-	-	-	-	-	BED2	-	-	-	-	-	S	
66	17	shear fol	33	63	303	-	-	-	-	-	-	-	-	-	-	-	-	SH6	-	-	-	-	-	S	
66	17	qz vein	25	66	295	-	-	-	-	-	-	-	-	-	-	-	-	V6	-	-	-	-	-	S	Large quartz vein on fault plane
66	22	shear fol	50	53	320	-	-	-	-	-	-	-	-	-	-	-	-	SH6	-	-	-	-	-	S	
66	23	fault plane	179	83	89	-	-	-	-	-	-	-	-	-	-	-	-	SH7	-	-	-	-	-	S	
66	28	foliation	36	82	306	-	-	-	-	-	-	-	-	-	-	-	-	SH1	-	-	-	-	-	S	**N Block E movement**
67	0	qz vein	101	62	191	-	-	qT	-	-	-	-	-	-	-	-	-	V2	-	-	-	-	-	S	
67	3	foliation	28	49	298	-	-	-	-	-	-	-	-	-	-	-	-	CC	-	-	-	-	-	S	
67	3	qz vein	98	50	188	-	-	-	-	-	-	-	-	-	-	-	-	V6	-	-	-	-	-	S	
67	6	qz vein	99	48	189	-	-	qM	-	-	-	-	-	-	-	-	-	V3	-	300	-	-	-	S	Finely foliated margin

LOCATION		Structural	Orientation					Defining Mineralogy					Alteration					Group	X-cut	Vein	Vein	Vein	Halo	Pos	DESCRIPTION
WALL	Metres	Element	Strike	Dip	Dip/Dir	Plunge	Dir	1	2	3	4	5	1	2	3	4	5		Rel.	Width	Style	Inc	Width		
67	9	foliation	41	48	311	-	-	-	-	-	-	-	-	-	-	-	-	CC	-	-	-	-	-	S	Fg foliated basalt
67	11	fault plane	29	43	299	-	-	-	-	-	-	-	-	-	-	-	-	SH7	-	-	-	-	-	S	Fault plane with quartz vein intruding
67	17	foliation	37	37	307	-	-	-	-	-	-	-	-	-	-	-	-	CC	-	-	-	-	-	S	Foliated pillow basalt
68	0	qz vein	91	56	181	-	-	-	-	-	-	-	-	-	-	-	-	V6	-	20	mcs	-	-	S	Thin veins in m-cg dolerite
68	4	qz vein	112	48	202	-	-	-	-	-	-	-	-	-	-	-	-	V6	-	50	-	-	-	S	Limonitic quartz vein in cg ophitic dol/gabbro
68	7	joint	38	56	308	-	-	-	-	-	-	-	-	-	-	-	-	J2	-	-	-	-	-	S	
68	11	qz vein	112	55	202	-	-	qT	-	-	-	-	lm	-	-	-	-	V2	-	30	-	-	40	S	Pych alteration dol
68	13	qz vein	116	56	206	-	-	qM	-	-	-	-	lm	-	-	-	-	V3	-	50	-	-	40	S	Intense foliation wallrock
68	16	qz vein	119	49	209	-	-	qT	-	-	-	-	-	-	-	-	-	V2	-	150	-	-	-	S	
68	19	qz vein	93	49	183	-	-	qT	-	-	-	-	-	-	-	-	-	V2	-		-	-	-	S	Alt + foliated basalt
68	24	qz vein	97	63	187	-	-	qM	-	-	-	-	-	-	-	-	-	V3	-	-	-	-	-	S	Fg pillow? Basalt
68	28	foliation	39	39	309	-	-	-	-	-	-	-	-	-	-	-	-	CC	-	-	-	-	-	S	foliation in fg basalt
69	0	qz vein	103	29	193	-	-	qT	-	-	-	-	-	-	-	-	-	V2	-	80	-	-	-	S	Ferruginous vein
69	3	qz vein	116	45	206	-	-	qM	-	-	-	-	-	-	-	-	-	V3	-	-	-	-	-	S	Spotty porphyritic gabbro
69	14	qz vein	108	43	198	-	-	qz	-	-	-	-	-	-	-	-	-	V6	-	50	-	WR	-	S	
69	19	fault plane	6	38	276	-	-	-	-	-	-	-	-	-	-	-	-	SH7	-	-	-	-	-	S	Extensive fault plane intruded by quartz veins
69	26	qz vein	117	50	207	-	-	qM	-	-	-	-	lm	-	-	-	-	V3	-	100	-	-	-	S	
70	2	qz vein	109	38	199	-	-	qM	qT	-	-	-	-	-	-	-	-	V3	-	100	mcs	-	-	S	Foliated margins of vein
70	4	qz vein	18	39	288	-	-	-	-	-	-	-	-	-	-	-	-	V6	-	100	-	-	-	S	Ferruginous vein
70	7	foliation	13	52	283	-	-	-	-	-	-	-	-	-	-	-	-	CC	-	-	-	-	-	S	Foliation in gabbro
70	7	qz vein	106	44	196	-	-	-	-	-	-	-	-	-	-	-	-	V6	-	100	-	-	-	S	Ferruginous vein
70	9	qz vein	115	53	205	-	-	-	-	-	-	-	-	-	-	-	-	V6	-	100	-	-	-	S	
70	12	qz vein	117	50	207	-	-	-	-	-	-	-	-	-	-	-	-	V6	-	30	-	-	-	S	Thin vein with ferruginous margins
70	15	qz vein	87	62	177	-	-	-	-	-	-	-	-	-	-	-	-	V6	-	250	mcs	-	-	S	Vein intruding intensely foliated wallrock
70	18	qz vein	124	22	214	-	-	qM	-	-	-	-	-	-	-	-	-	V3	-	1500	-	-	-	S	
70	24	qz vein	84	51	174	-	-	qT	-	-	-	-	-	-	-	-	-	V2	-	180	-	-	-	S	
70	24	qz vein	89	44	179	-	-	-	-	-	-	-	-	-	-	-	-	V6	-	-	-	-	-	S	
70	28	qz vein	26	62	296	-	-	qM	-	-	-	-	-	-	-	-	-	V3	-	140	-	-	-	S	**Vein intrudes fault plane Wblock down**
71	2	qz vein	104	44	194	-	-	qT	-	-	-	-	-	-	-	-	-	V2	-	-	-	-	-	S	Intensely fractured foliation in wallrock
71	5	qz vein	89	48	179	-	-	qM	-	-	-	-	-	-	-	-	-	V3	-	30	-	-	-	S	
71	12	qz vein	101	53	191	-	-	-	-	-	-	-	-	-	-	-	-	V6	-	-	-	-	-	S	Ferruginous quartz vein
71	13	qz vein	90	58	180	-	-	-	-	-	-	-	-	-	-	-	-	V6	-	-	-	-	-	S	
71	15	qab vein	48	46	138	-	-	qz	ab	-	-	-	-	-	-	-	-	V6	-	-	-	-	-	S	Fibrous cockade texture
71	17	qz vein	18	43	288	-	-	-	-	-	-	-	-	-	-	-	-	V6	-	-	-	-	-	S	Ferruginous indurated zone
71	27	qz vein	98	52	188	-	-	-	-	-	-	-	-	-	-	-	-	V6	-	300	-	-	-	S	
71	29	foliation	5	42	275	-	-	-	-	-	-	-	-	-	-	-	-	CC	-	-	-	-	-	S	
72	2	qz vein	164	42	254	-	-	qT	-	-	-	-	-	-	-	-	-	V2	-	200	-	-	-	S	

LOCATION		Structural	Orientation					Defining Mineralogy					Alteration					Group	X-cut	Vein	Vein	Vein	Halo	Pos	DESCRIPTION
WALL	Metres	Element	Strike	Dip	Dip/Dir	Plunge	Dir	1	2	3	4	5	1	2	3	4	5		Rel.	Width	Style	Inc	Width		
72	5	foliation	140	35	230	-	-	-	-	-	-	-	-	-	-	-	-	CC	-	-	-	-	-	S	
72	6	qz vein	133	26	223	-	-	-	-	-	-	-	-	-	-	-	-	V6	-	-	-	-	-	S	
72	7	qz vein	59	48	149	-	-	-	-	-	-	-	-	-	-	-	-	V6	-	-	-	-	-	S	QZ vein with GP irregular contact
72	8	foliation	78	30	168	-	-	-	-	-	-	-	-	-	-	-	-	CC	-	-	-	-	-	S	
72	8	foliation	110	73	200	-	-	-	-	-	-	-	-	-	-	-	-	CC	-	-	-	-	-	S	
72	8	qz vein	164	73	74	-	-	qM	-	-	-	-	-	-	-	-	-	V3	-	-	-	-	-	S	
72	10	qz vein	111	43	201	-	-	qM	-	-	-	-	-	-	-	-	-	V3	-	-	-	-	-	S	Gently foliated quartz vein in int ka'd mafic
72	12	qz vein	96	51	186	-	-	qM	-	-	-	-	-	-	-	-	-	V3	-	-	-	-	-	S	Quartz vein no alteration halo
72	13	qz vein	179	30	269	-	-	-	-	-	-	-	-	-	-	-	-	V6	-	-	-	-	-	S	Ferruginous quartz vein
72	15	foliation	5	51	275	-	-	-	-	-	-	-	-	-	-	-	-	CC	-	-	-	-	-	S	Intensely foliated purple dolerite
72	19	qz vein	109	40	199	-	-	qM	-	-	-	-	-	-	-	-	-	V3	-	-	-	-	-	S	Thin vein no alteration halo
72	25	qz vein	109	56	199	-	-	-	-	-	-	-	-	-	-	-	-	V6	-	50	-	-	-	S	Ferrginous alteration margin
73	0	qz vein	88	60	178	-	-	-	-	-	-	-	-	-	-	-	-	V6	-	-	-	-	-	S	
73	5	foliation	161	37	251	-	-	-	-	-	-	-	-	-	-	-	-	CC	-	-	-	-	-	S	
73	8	qz vein	119	36	209	-	-	-	-	-	-	-	-	-	-	-	-	V6	-	-	-	-	-	S	
73	12	GP vein	110	45	200	-	-	-	-	-	-	-	-	-	-	-	-	V9	-	300	-	-	-	S	Fine grained porphyry veins
73	18	qz vein	106	41	196	-	-	qM	-	-	-	-	-	-	-	-	-	V3	-	100	-	-	-	S	
73	22	qz vein	91	51	181	-	-	qM	-	-	-	-	-	-	-	-	-	V3	-	100	-	-	-	S	
73	26	foliation	6	40	276	-	-	-	-	-	-	-	-	-	-	-	-	CC	-	-	-	-	-	S	
73	28	qz vein	102	46	192	-	-	qT	qM	-	-	-	-	-	-	-	-	V2	-	200	-	-	-	S	
74	0	qz vein	51	71	141	-	-	qT	-	-	-	-	-	-	-	-	-	V2	-	80	-	-	-	S	Quartz vein intruding fault plane
74	0	qz vein	165	66	75	-	-	-	-	-	-	-	-	-	-	-	-	V6	-	-	-	-	-	S	
74	6	qz vein	164	50	254	-	-	-	-	-	-	-	-	-	-	-	-	V6	-	-	-	-	-	S	Foliated quartz veins bending into fault plane
74	12	fault zone	74	69	344	-	-	-	-	-	-	-	-	-	-	-	-	SEF	-	-	-	-	-	S	0.5m fault zone SEF?
74	13	fault plane	69	42	339	-	-	-	-	-	-	-	-	-	-	-	-	SH7	-	-	-	-	-	S	Veins and foliation terminate against fault
74	15	foliation	122	56	212	-	-	-	-	-	-	-	-	-	-	-	-	CS1	-	-	-	-	-	S	Foliation in quartz feldspar porphyry
74	15	GP vein	99	74	189	-	-	-	-	-	-	-	-	-	-	-	-	V9	-	800	-	-	-	S	
75	2	qz vein	162	60	72	-	-	-	-	-	-	-	-	-	-	-	-	V6	-	50	-	-	-	N	**Small offsets on thin quartz veins NBlockE**
75	2	qz vein	166	17	76	-	-	-	-	-	-	-	-	-	-	-	-	V6	xnxt	300	-	-	-	N	Foliated quartz vein
75	4	fold limb	161	21	251	-	-	-	-	-	-	-	-	-	-	-	-	VL	-	-	-	-	-	N	E limb of s plunging fold in quartz vein
75	5	qz vein	20	39	290	-	-	qT	-	-	-	-	-	-	-	-	-	V2	-	50	-	-	-	N	Foliated quartz vein
75	8	qz vein	2	49	272	-	-	qM	-	-	-	-	-	-	-	-	-	V3	-	120	-	-	-	N	Western limb of kink in vein
75	8	qz vein	36	55	126	-	-	-	-	-	-	-	-	-	-	-	-	V6	-	-	-	-	-	N	Eastern limb of kink in vein
75	11	qz vein	155	41	245	-	-	-	-	-	-	-	-	-	-	-	-	V6	-	200	-	-	-	N	
75	16	foliation	151	23	241	-	-	-	-	-	-	-	-	-	-	-	-	CC	-	-	-	-	-	N	
75	16	qz vein	104	53	194	-	-	qM	-	-	-	-	-	-	-	-	-	V3	-	-	-	-	-	N	
75	16	qz vein	24	65	114	-	-	-	-	-	-	-	-	-	-	-	-	V6	-	-	-	-	-	N	

LOCATION		Structural	Orientation					Defining Mineralogy					Alteration					Group	X-cut	Vein	Vein	Vein	Halo	Pos	DESCRIPTION
WALL	Metres	Element	Strike	Dip	Dip/Dir	Plunge	Dir	1	2	3	4	5	1	2	3	4	5		Rel.	Width	Style	Inc	Width		
75	18	qz vein	150	15	60	-	-	-	-	-	-	-	-	-	-	-	-	V6	-	-	-	-	-	N	
75	20	foliation	155	41	245	-	-	-	-	-	-	-	-	-	-	-	-	CC	-	-	-	-	-	N	
75	22	qz vein	168	84	258	-	-	qM	-	-	-	-	-	-	-	-	-	V3	-	250	-	-	-	N	Foliated white quartz vein
75	23	qz vein	56	45	146	-	-	-	-	-	-	-	-	-	-	-	-	V6	-	50	-	-	-	N	Eastern limb of kink fold in vein
75	28	qz vein	81	41	171	-	-	qM	-	-	-	-	-	-	-	-	-	V3	-	200	-	-	-	N	Southern limb of gentle open fold in quartz
75	30	qz vein	56	58	146	-	-	qM	-	-	-	-	-	-	-	-	-	V3	-	200	-	-	-	N	Southern limb of gentle open fold in quartz
76	1	qz vein	35	34	125	-	-	qM	-	-	-	-	-	-	-	-	-	V3	-	100	mcs	-	-	N	3cm felsic porph vein intrudes centre of vein
76	2	GP vein	154	43	244	-	-	-	-	-	-	-	-	-	-	-	-	V9	-	1000	-	-	-	N	GP vein
76	5	qz vein	146	45	236	-	-	-	-	-	-	-	-	-	-	-	-	V6	-	50	-	-	-	N	Foliated quartz vein
76	8	foliation	4	40	274	-	-	-	-	-	-	-	-	-	-	-	-	CC	-	-	-	-	-	N	
76	10	fault plane	145	46	235	-	-	-	-	-	-	-	-	-	-	-	-	SH7	-	-	-	-	-	N	
76	10	qz vein	164	26	254	-	-	-	-	-	-	-	-	-	-	-	-	V6	-	-	-	-	-	N	
76	12	qz vein	35	43	125	-	-	qM	-	-	-	-	-	-	-	-	-	V3	-	60	-	-	-	N	
76	12	qz vein	160	39	250	-	-	-	-	-	-	-	-	-	-	-	-	V6	xprv	-	-	-	-	N	**W Block N offset of previous vein**
76	15	foliation	143	29	233	-	-	-	-	-	-	-	-	-	-	-	-	CC	-	-	-	-	-	N	
76	18	qz vein	154	44	244	-	-	-	-	-	-	-	-	-	-	-	-	V6	xprv	-	-	-	-	N	
76	18	qz vein	166	70	256	-	-	-	-	-	-	-	-	-	-	-	-	V6	-	-	-	-	-	N	
76	22	qz vein	174	74	84	-	-	qM	-	-	-	-	-	-	-	-	-	V3	-	200	-	-	-	N	
76	23	qz vein	174	54	84	-	-	qT	-	-	-	-	-	-	-	-	-	V2	-	-	-	-	-	N	
76	28	qz vein	130	18	220	-	-	-	-	-	-	-	-	-	-	-	-	V6	-	-	-	-	-	N	
77	4	qz vein	142	67	232	-	-	qM	-	-	-	-	-	-	-	-	-	V3	-	-	-	-	-	N	
77	8	qz vein	154	79	64	-	-	-	-	-	-	-	-	-	-	-	-	V6	-	50	-	-	-	N	
77	11	foliation	67	85	337	-	-	-	-	-	-	-	-	-	-	-	-	CC	xnxt	-	-	-	-	N	
77	11	foliation	98	45	188	-	-	-	-	-	-	-	-	-	-	-	-	CC	-	-	-	-	-	N	
77	12	qz vein	155	70	65	-	-	-	-	-	-	-	-	-	-	-	-	V6	-	50	-	-	-	N	
77	20	qz vein	18	86	108	-	-	qM	-	-	-	-	-	-	-	-	-	V3	-	-	-	-	-	N	Highly altered and foliated mafic
77	22	fault plane	176	79	86	-	-	-	-	-	-	-	-	-	-	-	-	SH7	-	-	-	-	-	N	**E Block down fault**
77	25	qz vein	10	81	100	-	-	qM	-	-	-	-	-	-	-	-	-	V3	-	1000	-	-	-	N	Foliation parallel vein
77	28	qz vein	35	32	125	-	-	-	-	-	-	-	-	-	-	-	-	V6	-	-	-	-	-	N	Eastern contact of previous vein
78	2	qz vein	5	56	95	-	-	qT	qM	-	-	-	-	-	-	-	-	V2	-	100	-	-	-	N	Intensely sheared mafic
78	6	fault plane	45	80	315	-	-	-	-	-	-	-	-	-	-	-	-	SH7	-	-	-	-	-	N	
78	6	qz vein	140	64	230	-	-	qT	-	-	-	-	-	-	-	-	-	V2	-	50	-	-	-	N	
78	10	qz vein	172	72	82	-	-	-	-	-	-	-	-	-	-	-	-	V6	-	-	-	-	-	N	Boudinaged quartz vein shear parallel
79	1	qz vein	2	50	272	-	-	-	-	-	-	-	-	-	-	-	-	V6	-	-	-	-	-	N	Vein intruding fault plane
79	2	qz vein	39	45	309	-	-	qT	-	-	-	-	-	-	-	-	-	V2	-	50	-	-	-	N	
79	5	shear fol	176	81	86	-	-	-	-	-	-	-	-	-	-	-	-	SH6	-	-	-	-	-	N	
79	8	qz vein	16	73	286	-	-	qM	-	-	-	-	-	-	-	-	-	V3	-	-	-	-	-	N	

LOCATION		Structural	Orientation					Defining Mineralogy					Alteration					Group	X-cut	Vein	Vein	Vein	Halo	Pos	DESCRIPTION
WALL	Metres	Element	Strike	Dip	Dip/Dir	Plunge	Dir	1	2	3	4	5	1	2	3	4	5		Rel.	Width	Style	Inc	Width		
79	10	qz vein	57	79	147	-	-	-	-	-	-	-	-	-	-	-	-	V6	-	500	-	-	-	N	
79	11	qz vein	145	30	55	-	-	-	-	-	-	-	-	-	-	-	-	V6	-	50	-	-	-	N	
79	19	qz vein	161	63	251	-	-	qT	-	-	-	-	-	-	-	-	-	V2	-	100	-	-	-	N	
79	21	foliation	37	73	307	-	-	-	-	-	-	-	-	-	-	-	-	CC	-	-	-	-	-	N	
79	21	qz vein	173	71	83	-	-	qT	-	-	-	-	-	-	-	-	-	V2	xnxt	200	-	-	-	N	**Offsets next vein with W Block up**
79	21	qz vein	164	60	74	-	-	-	-	-	-	-	-	-	-	-	-	V6	-	200	-	-	-	N	
79	24	foliation	134	40	224	-	-	-	-	-	-	-	-	-	-	-	-	CC	-	-	-	-	-	N	
79	26	qz vein	130	65	220	-	-	-	-	-	-	-	-	-	-	-	-	V6	-	-	-	-	-	N	Thin ferruginous quartz vein
79	28	qz vein	151	45	241	-	-	qM	-	-	-	-	-	-	-	-	-	V3	-	-	-	-	-	N	
80	1	fault plane	31	39	301	-	-	-	-	-	-	-	-	-	-	-	-	SH7	-	-	-	-	-	N	**W Block S disp**
80	1	qz vein	160	59	70	-	-	-	-	-	-	-	-	-	-	-	-	V6	-	-	-	-	-	N	
80	2	fault plane	34	76	304	-	-	-	-	-	-	-	-	-	-	-	-	SH7	-	-	-	-	-	N	
80	5	qz vein	19	46	289	-	-	-	-	-	-	-	-	-	-	-	-	V6	-	100	-	-	-	N	Ferruginous vein
80	8	fault plane	17	84	287	-	-	-	-	-	-	-	-	-	-	-	-	SH7	-	-	-	-	-	N	
80	8	foliation	163	60	253	-	-	-	-	-	-	-	-	-	-	-	-	SH7	-	-	-	-	-	N	Foliation in wallrock of fault
80	13	qz vein	48	64	318	-	-	-	-	-	-	-	-	-	-	-	-	V6	-	-	-	-	-	N	
80	16	qz vein	12	69	282	-	-	qT	-	-	-	-	-	-	-	-	-	V2	-	-	-	-	-	N	Quartz vein in fault plane
80	17	foliation	159	32	249	-	-	-	-	-	-	-	-	-	-	-	-	CC	-	-	-	-	-	N	
80	17	cleavage	39	89	129	-	-	-	-	-	-	-	-	-	-	-	-	CS2	-	-	-	-	-	N	Wide spaced cleavage
80	19	qz vein	19	43	109	-	-	qM	-	-	-	-	-	-	-	-	-	V3	-	200	-	-	-	N	
80	21	fault zone	80	71	350	-	-	-	-	-	-	-	-	-	-	-	-	NEF	-	-	-	-	-	N	NEF intense fault zone tension fractures
81	5	fault plane	147	48	237	-	-	-	-	-	-	-	-	-	-	-	-	SH7	-	-	-	-	-	N	
81	10	qz vein	162	53	252	-	-	-	-	-	-	-	fe	-	-	-	-	V6	-	150	-	-	20	N	
81	13	qz vein	133	54	223	-	-	-	-	-	-	-	-	-	-	-	-	V6	-	-	-	-	-	N	
81	16	fault plane	132	51	222	-	-	-	-	-	-	-	-	-	-	-	-	SH7	-	-	-	-	-	N	
81	20	qz vein	174	64	264	-	-	-	-	-	-	-	-	-	-	-	-	V6	-	-	-	-	-	N	
81	26	fault plane	157	65	247	-	-	-	-	-	-	-	-	-	-	-	-	SH7	-	-	-	-	-	N	Silicified ferruginous fault plane
81	28	qz vein	129	40	219	-	-	-	-	-	-	-	-	-	-	-	-	V6	-	-	-	-	-	N	Sugary quartz vein in thin fault plane
82	0	qz vein	169	49	259	-	-	-	-	-	-	-	-	-	-	-	-	V6	-	60	-	-	-	N	
82	4	qz vein	30	66	300	-	-	-	-	-	-	-	-	-	-	-	-	V6	-	-	-	-	-	N	Stretched boudinaged quartz vein
82	11	shear zone	24	38	294	-	-	-	-	-	-	-	-	-	-	-	-	SH6	-	-	-	-	-	N	
82	12	qz vein	131	56	221	-	-	-	-	-	-	-	-	-	-	-	-	V6	-	-	-	-	-	N	Sugary quartz vein
82	16	fault plane	155	45	245	-	-	-	-	-	-	-	-	-	-	-	-	SH7	-	-	-	-	-	N	
82	21	bx zone	133	53	223	-	-	-	-	-	-	-	-	-	-	-	-	SH4	-	-	-	-	-	N	
82	23	qz vein	146	45	236	-	-	qS	-	-	-	-	bi	ch	-	-	-	V6	-	-	-	-	-	N	Vfg sugar quartz vein
82	26	qz vein	80	53	170	-	-	-	-	-	-	-	-	-	-	-	-	V6	-	-	-	-	-	N	
82	29	qz vein	137	43	227	-	-	-	-	-	-	-	-	-	-	-	-	V6	-	-	-	-	-	N	

LOCATION		Structural	Orientation					Defining Mineralogy					Alteration					Group	X-cut	Vein	Vein	Vein	Halo	Pos	DESCRIPTION
WALL	Metres	Element	Strike	Dip	Dip/Dir	Plunge	Dir	1	2	3	4	5	1	2	3	4	5		Rel.	Width	Style	Inc	Width		
83	0	qz vein	166	70	76	-	-	-	-	-	-	-	-	-	-	-	-	V6	-	-	-	-	-	N	
83	0	qz vein	0	41	90	-	-	-	-	-	-	-	-	-	-	-	-	V6	xnxt2	50	-	-	-	N	**Vein x-cuts next 2 with NBLk E offset**
83	0	qz vein	82	49	172	-	-	-	-	-	-	-	-	-	-	-	-	V6	-	-	-	-	-	N	
83	6	qz vein	164	38	254	-	-	qM	-	-	-	-	-	-	-	-	-	V3	-	-	-	-	-	N	
83	17	qz vein	52	64	322	-	-	-	-	-	-	-	-	-	-	-	-	V6	-	-	-	-	-	N	
83	17	qz vein	150	39	240	-	-	-	-	-	-	-	-	-	-	-	-	V6	-	-	-	-	-	N	
83	29	shear zone	177	36	267	-	-	-	-	-	-	-	-	-	-	-	-	SH6	-	-	-	-	-	N	
84	2	qz vein	160	24	250	-	-	-	-	-	-	-	-	-	-	-	-	V6	-	-	-	-	-	N	
84	6	foliation	150	39	240	-	-	-	-	-	-	-	-	-	-	-	-	CC	-	-	-	-	-	N	
84	6	qz vein	89	51	179	-	-	qT	-	-	-	-	-	-	-	-	-	V2	-	30	-	-	-	N	
84	8	qz vein	151	56	241	-	-	-	-	-	-	-	-	-	-	-	-	V6	-	100	-	-	-	N	
84	11	GP vein	44	78	134	-	-	qz	fd	-	-	-	-	-	-	-	-	V9	-	600	-	-	-	N	Intrusive porphyry bar
84	21	qz vein	110	51	200	-	-	-	-	-	-	-	-	-	-	-	-	V6	-	50	-	-	-	N	
84	25	bx zone	89	45	179	-	-	-	-	-	-	-	-	-	-	-	-	SH4	-	-	-	-	-	N	Ferruginous quartz breccia
85	0	qz vein	63	56	153	-	-	qT	-	-	-	-	-	-	-	-	-	V2	-	30	-	-	-	N	
85	1	foliation	157	45	247	-	-	-	-	-	-	-	-	-	-	-	-	CC	-	-	-	-	-	N	
85	4	qz vein	31	38	121	-	-	qT	-	-	-	-	-	-	-	-	-	V2	-	-	-	-	-	N	
85	5	qz vein	169	55	259	-	-	qT	-	-	-	-	-	-	-	-	-	V2	-	-	-	-	-	N	**Vein intruding shear zone W Over E**
85	7	qz vein	25	55	115	-	-	qT	-	-	-	-	-	-	-	-	-	V2	-	-	-	-	-	N	
85	9	qz vein	159	55	249	-	-	qM	-	-	-	-	-	-	-	-	-	V3	-	-	-	-	-	N	
85	14	qz vein	75	49	165	-	-	-	-	-	-	-	-	-	-	-	-	V6	-	30	-	-	-	N	Quartz vein in limonitic mafic
85	15	foliation	13	68	103	-	-	-	-	-	-	-	-	-	-	-	-	CC	-	-	-	-	-	N	
85	22	aplite vein	140	45	230	-	-	-	-	-	-	-	-	-	-	-	-	V9	-	-	-	-	-	N	vfg saccaroidal txt like late facies of LHM
85	25	fault plane	153	69	243	-	-	-	-	-	-	-	-	-	-	-	-	SH7	-	-	-	-	-	N	
85	30	qz vein	100	57	190	-	-	qM	-	-	-	-	-	-	-	-	-	V3	-	-	-	-	-	N	
86	0	qz vein	158	67	248	-	-	qT	-	-	-	-	-	-	-	-	-	V2	-	-	-	-	-	N	
86	5	foliation	142	75	232	-	-	-	-	-	-	-	-	-	-	-	-	CC	-	-	-	-	-	N	
86	9	qz vein	89	47	179	-	-	-	-	-	-	-	-	-	-	-	-	V6	-	-	-	-	-	N	
86	11	qz vein	105	45	195	-	-	-	-	-	-	-	-	-	-	-	-	V6	-	-	-	-	-	N	
86	14	foliation	168	58	258	-	-	-	-	-	-	-	-	-	-	-	-	CC	-	-	-	-	-	N	
87	0	foliation	135	83	45	-	-	-	-	-	-	-	si	mu	ka	fu	-	CC	-	-	-	-	-	N	
87	1	fault plane	94	76	4	-	-	-	-	-	-	-	-	-	-	-	-	SH7	-	-	-	-	-	N	
87	9	qz vein	50	14	320	-	-	-	-	-	-	-	-	-	-	-	-	V6	-	-	-	-	-	N	
87	14	qz vein	43	26	313	-	-	qT	-	-	-	-	-	-	-	-	-	V2	-	400	-	-	-	N	
87	22	qz vein	168	40	258	-	-	-	-	-	-	-	-	-	-	-	-	V6	-	100	-	-	-	N	
87	23	qz vein	129	56	219	-	-	-	-	-	-	-	-	-	-	-	-	V6	-	-	-	-	-	N	
87	25	foliation	131	79	41	-	-	-	-	-	-	-	-	-	-	-	-	CC	-	-	-	-	-	N	

LOCATION		Structural	Orientation					Defining Mineralogy					Alteration					Group	X-cut	Vein	Vein	Vein	Halo	Pos	DESCRIPTION
WALL	Metres	Element	Strike	Dip	Dip/Dir	Plunge	Dir	1	2	3	4	5	1	2	3	4	5		Rel.	Width	Style	Inc	Width		
88	0	foliation	132	79	222	-	-	-	-	-	-	-	-	-	-	-	-	CC	-	-	-	-	-	N	Intense foliation in weathered UM
88	5	foliation	143	78	233	-	-	-	-	-	-	-	-	-	-	-	-	CC	-	-	-	-	-	N	
88	10	foliation	142	83	232	-	-	-	-	-	-	-	-	-	-	-	-	CC	-	-	-	-	-	N	
88	15	stock vein	97	76	187	-	-	-	-	-	-	-	-	-	-	-	-	V6	-	-	-	-	-	N	Ferruginous stockwork veining infill txt
88	15	stock vein	150	76	240	-	-	-	-	-	-	-	-	-	-	-	-	V6	-	-	-	-	-	N	Ferruginous stockwork veining infill txt

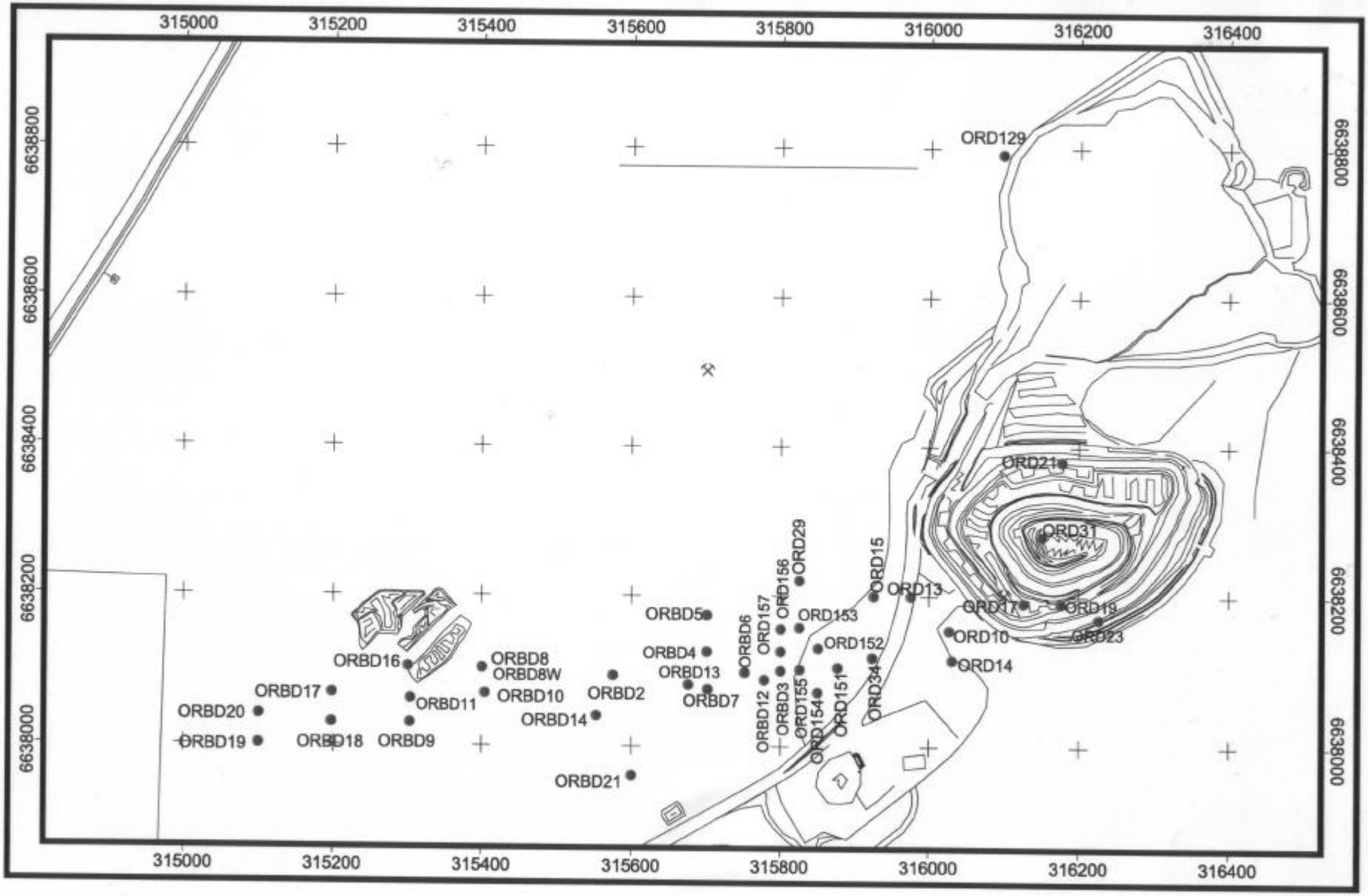

Figure A1.3 - Location plan of diamond drillholes sampled from the Enterprise mine.

Table A1.10 - Enterprise deposit, structural data from diamond drill core

HOLE NO	DEPTH	STRUCTURE	ALPHA	BETA	STRIKE	DIP	DIP DIRECTION	MINERALOGY	ALTERATION	GROUP	OVERPRINTING	HOLE DIP	HOLE AZIM	Au VALUE	COMMENTS
ORBD4	190.60	shear zone	15	70	173	67	83	ch, bi	-	SH6	-	58	2	-	Shear veins
ORBD4	203.50	shear zone	22	290	9	62	279	-	-	SH6	-	59	4	-	200mm wide shear zone
ORBD11	504.30	shear zone	30	240	161	71	251	si, hm	py,mu	SH6	-	72	19	0.59	Intense shear zone
ORBD11	522.60	shear zone	30	240	161	71	251	ch,bi	-	SH6	-	72	19	0.03	Sheared dolerite
ORBD11	564.75	shear/bx zone	38	220	138	66	228	ch, mu	-	CEF	-	73	15	0.46	Intense shear / breccia zone localised on main chloritic shear zone
ORBD11	592.00	shear zone	50	280	4	41	274	ch,bi	-	SH6	-	72	16	0.03	Intense shear zone
ORBD11	602.50	shear zone	50	220	136	55	226	ch,bi	-	SH6	-	72	16	0.03	Intense shear zone
ORBD12	258.09	quartz vein	20	130	48	89	318	qz	none	V2	-	58	5	5.70	Translucent quartz vein
ORBD12	264.64	qcb vein	25	170	85	84	355	qz,cb	-	V1	-	58	5	8.90	-
ORBD12	269.90	quartz vein	75	260	119	38	209	qz	bi,si	V2	-	58	5	2.00	30mm wide translucent quartz vein, 20mm wide selvedge
ORBD12	270.75	quartz vein	50	200	108	71	198	-	-	V1	-	58	5	4.46	Thin vein
ORBD12	271.20	qcb vein	13	90	11	80	101	-	-	V2	-	58	5	3.76	Low angle quartz-carbonate vein crosscut by comb textured quartz vein
ORBD12	273.57	quartz vein	70	360	94	12	184	-	cb,hm	V1	-	58	5	0.33	50mm quartz vein
ORBD12	274.19	quartz vein	85	180	95	37	185	-	-	V2	-	58	5	0.88	Translucent buck quartz vein with wallrock slivers and Mo sutures
ORBD12	291.53	quartz vein	60	150	75	60	165	-	hm	V2	-	58	2	2.13	Hematite alteration zone
ORBD12	293.58	quartz vein	55	120	55	58	145	-	cb,bi,hm	V2	-	58	2	0.19	-
ORBD12	360.65	shear zone	21	70	175	62	85	-	-	SH1	-	59	1	0.16	Mylonitic shear zone
ORBD14	166.50	qcb vein	10	50	145	63	55	-	-	V1	-	61	357	0.02	-
ORBD14	337.20	shear zone	50	240	130	59	220	-	-	SH6	-	62	360	0.03	-
ORBD14	393.80	shear zone	50	90	54	48	144	-	-	SH6	-	62	25	5.04	-
ORBD14	408.30	quartz vein	90	180	113	29	203	-	-	V3	-	62	23	0.55	Milky quartz vein
ORBD14	465.00	quartz vein	90	200	108	29	198	-	-	V3	-	61	18	0.03	Milky quartz vein
ORBD16	163.50	calcite vein	33	354	82	37	352	ca,ac	-	V4	-	69	1	0.10	Carbonate growth fibres sinistral NblockW movement sense
ORBD16	263.50	shear vein	26	264	167	68	257	ch,ac	-	SH6	-	69	3	0.14	Intense shear zone
ORBD16	289.30	fracture fol	18	310	32	60	302	-	-	CS1	-	69	360	0.01	Fracture foliation
ORBD16	430.00	calcite vein	68	144	71	41	161	ac,cb	-	SH6	-	70	1	0.02	Carbonate growth fibres sinistral NblockW movement sense
ORBD16	438.70	quartz vein	45	180	94	66	184	qz,cb	ch,po	V1	-	70	4	0.10	10mm thick recrystallised vein
ORBD16	438.90	quartz vein	5	280	11	82	281	qz	ch,bi,py	V3	-	70	4	0.10	20mm milky quartz vein
ORBD16	439.35	qcb shear vein	31	96	20	64	110	qM	py	V1	-	70	4	0.02	2mm quartz carbonate shear vein

HOLE NO	DEPTH	STRUCTURE	ALPHA	BETA	STRIKE	DIP	DIP DIRECTION	MINERALOGY	ALTERATION	GROUP	OVERPRINTING	HOLE DIP	HOLE AZIM	Au VALUE	COMMENTS
ORBD16	439.70	quartz vein	18	184	97	89	7	qM,cb	-	V3	-	70	4	0.02	30mm milky quartz vein
ORBD16	440.75	quartz vein	29	214	123	79	213	qz,cb,ac,ch	py,bi,ch	V3	-	70	4	0.05	3mm milky quartz vein with 5cm intense alteration halo
ORBD16	442.35	qcb vein	18	102	21	78	111	ac,cb,ch	py,ch	V1	-	70	4	0.07	5mm quartz carbonate vein
ORBD16	443.72	fracture fol	61	166	85	49	175	qz,cb	-	V1	-	70	4	0.05	5mm quartz carbonate vein with slickenfibres showing sinistral NblockW
ORBD16	448.46	qcb vein	42	330	49	32	319	qM	-	V1	-	70	4	0.10	Minor fracture veins
ORBD16	445.90	quartz vein	65	220	117	43	207	qz,cb	bi,py,hm	V3	-	70	4	0.21	0.2m milky quartz vein
ORBD16	451.28	qcb slicks	60	136	65	47	155	qz	-	V1	-	70	4	0.01	Slickenfibres step up to the west
ORBD16	453.77	quartz vein	47	276	168	45	258	qz,ab,cb	-	V3	-	70	4	0.95	0.5m milky quartz vein
ORBD16	457.70	qz ab vein	23	278	3	66	273	ch,bi,mu	-	V1	-	70	4	0.42	Slickenfibres step up to the south
ORBD16	462.20	shear zone	63	254	140	38	230	qz,cb,ch	-	SH6	-	70	5	0.27	Intense shear zone
ORBD16	475.50	shear contact	47	294	5	39	275	qz,cb,ab,mu,si	-	SH6	-	70	5	0.02	Contact shear zone between dolerite and porphyritic dolerite
ORBD16	492.65	shear zone	55	295	0	32	270	qz,ch,cb	mu,si,py	SH6	-	70	6	0.65	Intense shear zone with quartz carbonate veins
ORBD16	506.30	shear zone	40	277	176	51	266	qz,cb	bi,si,py	SH6	-	70	6	0.07	Intense shear zone
ORBD16	546.80	qcb vein	23	120	40	78	130	qz,cb,ch	-	V1	-	70	5	0.17	3mm quartz carbonate breccia fill vein
ORBD16	547.55	quartz vein	46	329	46	29	316	cb,ab,ch	-	V2	-	70	5	0.31	8mm translucent recrystallised quartz vein
ORBD16	548.43	shear fracture	70	330	170	11	260	qz,cb	-	CS1	-	70	5	0.08	1mm carbonate filled shear fracture
ORBD16	557.25	quartz vein	12	95	16	81	106	qz,cb	-	V3	-	70	8	0.01	5mm milky fracture fill vein
ORBD16	557.65	qcb vein	20	142	62	87	152	qz,cb	-	V1	-	70	8	0.01	3mm quartz carbonate vein
ORBD16	558.30	qcb vein	56	192	106	54	196	qz,cb	cb,ep,py	V1	-	70	8	0.05	3mm quartz carbonate vein
ORBD16	558.50	qcb vein	8	144	61	82	331	qz,cb	-	V1	xprev	70	8	0.05	3mm quartz carbonate vein
ORBD16	559.45	qcb vein	58	305	7	26	277	qz,cb	-	V1		70	8	0.02	10mm quartz carbonate vein
ORBD16	561.10	quartz vein	54	151	77	55	167	qT	ch,ep	V2	xnxt	70	8	0.02	10mm translucent quartz vein
ORBD16	561.40	qcb vein	17	279	10	71	280	qz,cb	-	V1	-	70	8	0.02	3mm quartz carbonate vein
ORBD16	563.15	qcb vein	39	327	51	36	321	qz,cb,hm	ch,hm	V1	-	70	8	0.04	10mm quartz carbonate vein
ORBD16	563.45	qcb vein	34	322	47	42	317	qz,cb,hm	hm	V1	-	70	8	0.04	10mm quartz carbonate vein
ORBD16	566.35	shear zone	18	97	20	76	110	qz,cb,ch	-	SH6	-	70	8	0.02	4cm shear zone, east dipping dextral
ORBD16	582.25	bedding	51	283	170	39	260	si,ep	-	BED3	-	70	3	-	Cherty sedimentary layering
ORBD16	586.90	bedding	48	299	7	36	277	si,hm,mu,py	-	BED6	-	70	3	-	Cherty sedimentary layering with carbonate-fluorite quartz breccia veins
ORBD16	598.00	bedding	54	274	160	40	250	si,hm,mu,qz,cb	-	BED6	-	70	3	-	Cherty sedimentary layering
ORBD16	600.50	bedding	51	277	165	41	255	-	-	BED6	-	70	3	-	-
ORBD16	602.90	shear zone	25	281	4	63	274	ch,bi,mu	-	SH6	-	70	3	-	Intense shear zone
ORBD16	604.80	quartz vein	16	89	7	75	97	qz	hm,si,se,mu	V2	-	70	3	-	-
ORBD17	322.95	mylonite	66	185	94	45	184	ch,ac,bi	-	SH1	-	69	2	0.01	Intense mylonite shear zone
ORBD17	329.50	breccia vein	10	124	35	88	305	ch,qz,cb	-	V1	-	69	360	0.01	Brecciated wallrock fragments in quartz vein

HOLE NO	DEPTH	STRUCTURE	ALPHA	BETA	STRIKE	DIP	DIP DIRECTION	MINERALOGY	ALTERATION	GROUP	OVERPRINTING	HOLE DIP	HOLE AZIM	Au VALUE	COMMENTS
ORBD17	344.75	foliation	65	226	116	43	206	fd,	-	BED1	-	69	360	0.03	Compositional layering
ORBD17	347.00	shear zone	40	16	114	31	24	ch,ac	-	SH1	-	69	360	0.04	Intense shear zone
ORBD17	494.80	shear zone	40	212	116	70	206	ch,cb,ac	-	SH2	-	68	1	0.01	Shear in talc ultramafic rocks
ORBD17	520.50	qcb vein	54	301	177	31	267	qz,cb	-	V1	xnxt	68	360	0.21	3mm quartz carbonate vein
ORBD17	520.60	qcb vein	27	70	172	58	82	qz,cb	-	V1	-	68	360	0.21	1mm quartz carbonate vein cross-cut by previous with E Block down movement
ORBD17	522.02	quartz vein	54	156	73	57	163	qz,	none	V3	-	68	360	0.07	20mm milky quartz vein
ORBD17	524.90	qcb vein	51	288	169	38	259	qz,cb,ch	si,ch,bi	V2	-	68	360	0.35	50mm translucent recrystallised quartz vein
ORBD17	525.60	qcb vein	58	334	28	16	298	qz,cb	-	V1	-	68	360	0.42	Fracture fill quartz carbonate vein
ORBD17	525.60	po stringer	20	185	94	89	4	po	-	Srpo	xprev	68	360	0.42	Fracture fill pyrrhotite stringer
ORBD17	529.85	quartz vein	16	280	3	72	273	ch,qz	-	V3	-	68	360	1.73	Contact of brecciated vein slickenfibres show Dextral E block down movement
ORBD17	534.00	qcb vein	36	279	172	54	262	qz,cb	-	V1	-	68	360	0.70	Quartz carbonate vein
ORBD17	543.00	shear zone	12	175	87	81	357	ch,ac	-	SH6	-	68	2	0.24	Intense shear zone slickenfibres show sinistral N block west movement
ORBD17	552.65	quartz vein	24	54	156	55	66	qz	-	V2	-	68	2	0.11	0.5m recrystallised quartz vein
ORBD17	561.10	quartz vein	39	193	102	73	192	qz,cb	bi,py,cb	V2	-	68	2	0.33	10mm translucent quartz vein
ORBD17	573.70	shear zone	23	137	53	83	143	mu,cb,ab,fl,py	-	SH4	-	69	3	0.69	Intense shear zone carbonate slickenfibres show dextral N block up movement
ORBD17	587.38	quartz vein	50	333	44	24	314	qM,cb	bi,py	V3	-	69	3	0.20	3mm milky quartz vein with carbonate
ORBD17	592.22	qcb vein	28	281	2	61	272	qz,cb	-	V1	-	69	3	0.03	5mm quartz carbonate vein
ORBD17	599.65	qcb vein	29	102	24	68	114	qz,cb,ch	bi,si	V1	xnxt	69	3	0.06	10mm quartz carbonate vein
ORBD17	599.90	qcb vein	30	232	138	74	228	qz,cb	-	V1	-	69	3	0.06	1mm quartz carbonate vein 3 per cm
ORBD17	602.45	qcb vein	28	109	30	71	120	qz,cb	-	V1	-	69	3	0.09	Abundant 1mm fracture fill quartz carbonate veins
ORBD17	606.60	quartz vein	66	53	20	20	110	qM	-	V3	-	69	4	0.04	20mm milky quartz vein with wallrock slivers
ORBD17	609.10	quartz vein	27	330	55	46	325	qM	-	V3	-	69	4	0.13	7mm milky quartz vein with pyrrhotite infill
ORBD17	629.25	cb vein	42	191	102	69	192	cb	-	V4	-	69	4	0.01	0.5m carbonate veins with brecciated wallrock fragments
ORBD17	631.15	foliation	36	204	114	74	204	cb,ch,bi	-	CC	-	69	4	0.02	Penetrative foliation with carbonate fill veins and ch,bi spots
ORBD17	630.90	qcb vein	22	165	80	89	170	qz,cb	-	V1	-	69	4	0.01	5mm quartz carbonate vein parallel to foliation
ORBD17	636.15	qcb vein	50	117	47	53	137	qz,cb	-	V1	xprev	69	4	0.04	3mm quartz carbonate vein cuts previous foliation
ORBD17	641.00	shear zone	23	180	94	89	184	qz,cb,ch,bi	-	SH6	-	69	4	0.05	Shear zone
ORBD17	651.50	foliation	39	208	119	71	209	ch,bi,cb	-	CC	-	69	7	0.05	Intensely foliated spotted Aod
ORBD17	655.50	qcb vein	21	257	167	75	257	ch,cb,fu,bi	-	V5	-	69	7	0.08	80mm quartz carbonate vein with wallrock slivers
ORBD17	655.60	ch vein	45	216	124	63	214	ch,cb,fu,bi	-	V5	-	69	7	0.08	Chlorite overprinting biotite spots in quartz carbonate vein
ORBD17	668.00	bedding	34	220	130	73	220	py,ch,bi	-	BED3	-	69	7	0.08	Contact sedimentary rocks on Enterprise dolerite Big Dick Basalt contact
ORBD17	669.70	bedding	36	277	178	55	268	py,ch	-	BED3	-	69	7	0.04	Contact sedimentary rocks on Enterprise dolerite Big Dick Basalt contact
ORBD17	691.00	bedding	35	249	154	65	244	bi,ch,qz,cb	-	SH6	-	69	7	0.05	Sheared interflow sedimentary rocks
ORBD18	498.85	qcb vein	43	15	113	29	23	qz,cb	-	V1	-	70	360	0.01	3mm quartz carbonate vein

HOLE NO	DEPTH	STRUCTURE	ALPHA	BETA	STRIKE	DIP	DIP DIRECTION	MINERALOGY	ALTERATION	GROUP	OVERPRINTING	HOLE DIP	HOLE AZIM	Au VALUE	COMMENTS
ORBD18	501.50	qcb,ta vein	49	158	73	60	163	qz,cb,ta	-	V1	-	70	360	0.02	10mm quartz carbonate vein
ORBD18	501.90	qcb shear vein	69	240	122	36	212	qz,cb,ta	-	V1	xnxt	70	360	0.02	3mm quartz carbonate vein
ORBD18	502.00	qcb shear vein	18	330	54	56	324	qz,cb,bi,ch	-	V1	-	70	360	0.01	5mm quartz carbonate vein
ORBD18	505.35	qcb vein	40	311	23	40	293	qz,cb	-	V1	-	70	360	0.01	2mm quartz carbonate vein
ORBD18	506.20	qcb,ta vein	42	65	174	43	84	qz,cb,ta	-	V1	-	70	360	0.01	20mm quartz carbonate vein
ORBD18	513.30	qcb,ta vein	5	123	32	85	302	qz,cb,ta	-	V1	-	70	360	0.01	20mm quartz carbonate vein
ORBD18	514.30	qcb,ta vein	19	147	58	89	148	qz,cb,ta	-	V1	-	70	360	0.01	3mm quartz carbonate vein
ORBD18	520.70	qcb,ta vein	9	59	153	72	63	qz,cb,ta	-	V1	-	70	360	0.01	5mm quartz carbonate vein
ORBD18	524.00	shear zone	43	223	124	63	214	qz,cb,ch,ta	bi,ch,ta,py	SH6	-	70	360	0.02	Shear zone
ORBD18	535.67	quartz vein	40	286	0	48	270	qM	bi,ch,ta	V3	-	70	2	0.33	0.7m milky quartz vein
ORBD18	536.90	shear zone	24	275	177	66	267	ch,bi	-	CC	-	70	2	0.16	Pervasive foliation parallel to shear zone
ORBD18	538.25	qcb vein	37	323	41	39	311	qz,cb	-	V1	-	70	2	0.03	2mm quartz carbonate vein
ORBD18	538.25	frac foliation	25	271	173	67	263	ch	-	CS1	xprev,xnxt	70	2	0.03	Fault plane E block down
ORBD18	538.25	py stringer	49	270	160	45	250	py,ch	-	SRPY	-	70	2	0.03	0.5mm pyrite stringer vein
ORBD18	539.75	qcb vein	24	281	3	64	273	qz,cb	-	V1	xnxt2	70	2	0.70	2mm quartz carbonate vein
ORBD18	539.75	qcb vein	54	275	160	39	250	qz,cb	-	V1	xprev	70	2	0.07	2mm quartz carbonate vein
ORBD18	539.85	qcb vein	70	144	72	38	162	qz,cb,ch	-	V1	-	70	2	0.07	Quartz carbonate vein
ORBD18	552.65	Sed laminae	63	233	124	42	214	po,py,si	-	BED2	-	70	2	0.02	Cashmans Sedimentary Horizon laminations
ORBD18	555.80	quartz vein	43	305	17	39	287	qM	-	V3	-	70	2	28.80	0.3m milky quartz vein
ORBD18	558.50	quartz vein	31	288	7	55	277	qM	bi,py	V3	-	70	2	10.20	10mm milky quartz vein 0.2m wide alteration halo
ORBD18	563.00	qcb vein	23	360	92	47	2	qz,cb,ch	ch	V1	-	70	2	0.01	1mm quartz carbonate vein
ORBD18	563.00	qcb vein	45	189	99	65	189	qz,cb,ch	-	V1	xprev	70	2	0.01	3mm quartz carbonate vein
ORBD18	563.40	qcb vein	13	201	112	85	22	qz,cb	ch	V1	-	70	2	0.01	5mm quartz carbonate vein
ORBD18	563.40	qcb vein	68	169	85	42	175	qz,cb	ch	V1	xnxt	70	2	0.01	5mm quartz carbonate vein
ORBD18	570.85	shear zone	21	48	148	57	58	bi,ch,qz,cb	-	SH6	-	70	2	0.60	Shear zone
ORBD18	585.30	qcb vein	12	304	30	68	300	qz,cb	ac	V1	-	70	2	0.04	Quartz carbonate vein with carbonate actinolite growth fibres
ORBD18	585.30	quartz vein	78	129	72	30	162	qm	bi,ch,py	V3	-	70	2	0.04	Sheared bi,py altered contact with 2cm vein
ORBD18	595.60	shear zone	47	285	174	42	264	qz	-	SH6	-	70	3	0.12	Shear zone
ORBD18	609.80	cb vein	21	278	1	68	271	cb,qz	-	V4	-	70	3	0.01	10mm recrystallised carbonate vein
ORBD18	611.00	qcb vein	23	240	146	78	236	qz,cb	-	V1	xnxt	70	3	0.01	2mm quartz carbonate shear vein
ORBD18	611.00	qcb vein	8	89	3	83	93	qz,cbq	-	V1	-	70	3	0.01	10mm quartz carbonate vein
ORBD18	617.60	shear zone	33	267	168	61	258	cb	bi,py	SH6	-	70	4	0.06	15mm vuggy quartz carbonate vein intensely altered shear zone
ORBD19	352.40	qcb vein	53	206	114	54	204	qz,cb	-	V1	-	72	5	-	10mm recrystallised quartz carbonate vein
ORBD19	359.00	shear zone	67	167	89	41	179	bi,qz	-	SH1	-	72	7	-	Mylonite zone

HOLE NO	DEPTH	STRUCTURE	ALPHA	BETA	STRIKE	DIP	DIP DIRECTION	MINERALOGY	ALTERATION	GROUP	OVERPRINTING	HOLE DIP	HOLE AZIM	Au VALUE	COMMENTS
ORBD19	542.70	shear zone	66	267	153	30	243	qz,cb,ch	-	SH6	-	73	9	-	0.3m shear zone
ORBD19	556.36	CSZ	58	205	116	48	206	ch,cb,ac	-	CSZ	-	73	9	0.01	Cashmans Shear Zone, intense talc schist
ORBD19	572.30	qcb vein	21	13	115	53	25	qz,cb	-	V1	-	73	10	0.01	-
ORBD19	572.20	qcb vein	15	72	177	71	87	qz,ta,ch	-	V1	-	73	10	0.01	Recrystallised vein
ORBD19	575.60	shear zone	65	197	110	42	200	ch,qz,cb	-	SH6	-	73	10	0.01	0.2m shear vein
ORBD19	583.95	qcb vein	26	55	163	56	73	qz,cb	-	V1	xnxt	73	10	0.01	2mm comb textured quartz carbonate vein
ORBD19	583.95	qcb vein	58	273	167	36	257	qz,cb	-	V1	-	73	10	0.01	1mm quartz carbonate vein stringer
ORBD19	584.05	shear zone	14	22	124	61	34	ch,cb	-	SH6	xprev	73	10	0.01	4mm shear zone apparent N block down movement
ORBD19	584.35	cb vein	22	129	52	80	142	cb,ta,ch,ac	-	V1	-	73	10	0.01	Ladder vein set with truncating set
ORBD19	584.45	qcb vein	23	323	56	54	326	qz,cb	-	V1	xprev	73	10	0.01	1mm quartz carbonate vein truncates previous
ORBD19	584.70	qcb vein	15	327	63	62	333	qz,cb	-	V1	xprev2	73	10	0.01	Offsets truncated vein in ladder array
ORBD19	585.00	shear zone	62	230	133	41	223	ch,py	-	SRPY	-	73	10	0.02	5mm pyrite stringer offsets core-axis-parallel recrystallised carbonate vein
ORBD19	585.10	qcb vein	57	117	54	44	144	qz,cb,py	-	V1	-	73	10	0.02	2mm quartz carbonate vein conjugate with next
ORBD19	585.45	qcb vein	16	343	80	58	350	-	-	V1	xprev	73	10	0.02	2mm quartz carbonate vein conjugate with previous
ORBD19	586.00	shear zone	9	165	85	83	355	qz,cb,ch	-	SH6	-	73	10	0.01	3mm shear zone
ORBD19	587.25	bedding	59	175	96	48	186	qz,cb,py	-	BED6	-	73	10	0.01	Interflow sedimentary unit, pyrite carbonate
ORBD19	589.00	qcb vein	22	321	54	56	324	qz,cb	-	V1	-	73	10	0.01	10mm laminated quartz carbonate vein, (WR/cb/qz/cb/WR)
ORBD19	590.20	quartz vein	56	149	77	50	167	qT	-	V2	-	73	10	0.01	20mm laminated translucent quartz vein
ORBD19	591.00	qcb vein	7	93	14	85	104	py,qz,ch,cb	-	V1	-	73	10	0.01	10mm recrystallised carbonate pyrite vein with brecciated wallrock fragments
ORBD19	594.35	bedding	64	195	110	44	200	si,qz,cb,py	-	BED2	-	72	11	0.02	Finely laminated Cahsmans Sedimentary Horizon sharp upper contact
ORBD19	604.55	qcb vein	48	142	71	58	161	qz,cb	-	V1	-	72	11	0.01	1mm quartz carbonate vein in dominant fracture orientation E-W slickenfibres
ORBD19	607.00	qcb vein	13	227	146	90	236	qz,cb	ch,ac	V1	-	72	11	0.01	10mm shear vein
ORBD19	611.10	quartz vein	54	46	172	27	82	qT,qM	-	V2	-	72	11	0.03	50mm milky quartz vein brecciated by clear quartz
ORBD19	618.00	bedding	61	135	71	44	161	qT,qM	cb,py,bi,mu	BED6	-	72	11	0.01	Sedimentary unit? parallel quartz vein
ORBD19	619.50	shear zone	51	166	90	57	180	ch,bi,cb	py,bi,ch,mu	SH6	-	72	11	0.01	Fine-grained foliation
ORBD19	619.50	quartz vein	47	114	49	53	139	qT	-	V2	xprev	72	11	0.01	Translucent quartz vein with brecciated milky quartz, intense shear zone at angle to vein
ORBD19	661.00	shear zone	39	109	44	59	134	mu,si,py	-	SH7	-	73	14	0.16	Intense fault zone bleached brittle-ductile fault
ORBD19	677.00	quartz vein	42	255	165	55	255	bi,ch,mu,py	-	V3	-	73	13	1.25	Intense shear zone with white recrystallised quartz vein
ORBD20	327.00	fault	17	256	173	79	263	qz,cb,ch,bi	-	SH7	-	70	12	0.02	Intense northwest fault zone, strike-slip
ORBD20	538.90	qcb vein	24	273	9	67	279	qz,cb	-	V1	-	71	15	0.01	3mm shear vein
ORBD20	539.90	qcb vein	40	304	32	42	302	qz,cb	-	V1	-	71	15	0.01	5mm quartz carbonate vein
ORBD20	540.20	qcb vein	28	341	80	45	350	qz,cb	-	V1	-	71	15	0.01	5mm quartz carbonate vein
ORBD20	541.25	qcb vein	25	265	1	69	271	qz,cb	-	V1	-	71	15	0.01	3mm comb textured quartz carbonate vein
ORBD20	541.90	py stringer	56	132	71	49	161	py	-	SRpy	-	71	15	0.01	Fine-grained pyrite stringer vein

HOLE NO	DEPTH	STRUCTURE	ALPHA	BETA	STRIKE	DIP	DIP DIRECTION	MINERALOGY	ALTERATION	GROUP	OVERPRINTING	HOLE DIP	HOLE AZIM	Au VALUE	COMMENTS
ORBD20	541.95	qcb vein	62	257	154	37	244	qz,cb	-	V1	-	71	15	0.01	Very fine crackle-breccia veins
ORBD20	542.10	shear zone	62	143	81	45	171	qz,cb,ch,bi	-	SH6	-	71	15	0.02	0.2m wide intense brittle-ductile fault
ORBD20	547.50	shear zone	22	329	67	53	337	qz,cb	-	SH6	-	71	15	0.01	Intense fault with wallrock fragments
ORBD20	548.35	qcb vein	39	296	24	46	294	qz,cb	-	V1	-	71	15	0.01	5mm quartz carbonate vein
ORBD20	552.60	qcb vein	33	270	3	60	273	qz,cb	-	V1	-	71	15	0.01	10mm recrystallised quartz carbonate vein
ORBD20	554.30	shear zone	8	41	149	68	59	ch,qz,cb	-	SH7	-	71	15	0.01	Intense shear/breccia zone
ORBD20	554.30	shear zone	34	201	123	74	213	ch,qz,cb	-	SH7	-	71	15	0.01	Splay off previous shear zone
ORBD20	554.30	shear zone	14	191	115	86	25	ch,qz,cb	-	SH7	-	71	15	0.01	Splay off previous shear zone
ORBD20	555.30	shear zone	30	218	138	76	228	qz,cb	-	SH6	-	71	15	0.01	Sigmoidal quartz vein show N block east movement
ORBD20	557.30	bedding	41	225	141	64	231	si,py	-	BED2	-	71	15	0.01	Cherty laminations
ORBD20	563.70	qcb vein	18	21	129	55	39	qz,cb	-	V1	-	71	15	0.02	5mm quartz carbonate vein
ORBD20	569.40	quartz vein	23	256	172	74	262	qz	-	V2	-	70	14	0.02	0.2m quartz vein with po,py,cp sutures
ORBD20	570.85	qcb vein	23	237	155	79	245	qz,cb	-	V1	-	70	14	0.01	5mm quartz carbonate vein fault related
ORBD20	570.85	qcb vein	27	57	172	54	82	qz,cb	-	V1	xprev	70	14	0.01	N block down 2mm quartz carbonate shear vein
ORBD20	570.85	qcb vein	20	199	121	89	211	qz,cb	-	V1	xprev2	70	14	0.01	5mm crackle breccia shear vein
ORBD20	571.20	qcb vein	27	180	103	84	193	qz,cb	-	V1	-	70	14	0.01	10mm quartz carbonate vein with wallrock brecciation
ORBD20	571.20	qcb vein	36	28	142	38	52	qz,cb	-	V1	xprev	70	14	0.01	5mm quartz carbonate vein
ORBD20	571.40	qcb vein	31	208	128	77	218	qz,cb	-	V1	-	70	14	0.01	5mm quartz carbonate vein
ORBD20	572.20	qcb vein	13	131	56	90	326	qz,cb	-	V1	-	70	14	0.14	Quartz carbonate vein
ORBD20	575.90	shear vein	7	239	162	87	72	qz,cb	-	V1	-	70	14	0.04	10mm quartz carbonate filled shear vein
ORBD20	577.20	shear zone	26	196	118	84	208	qz,cb,mu	-	SH6	-	70	14	0.40	Shear zone
ORBD20	577.60	shear zone	42	199	119	68	209	py,po	-	SH7	-	70	14	0.40	Intense shear zone
ORBD20	577.90	qcb vein	21	214	135	86	225	qz,cb,ch,ab	-	V1	-	70	14	0.42	Quartz carbonate vein on shear zone contact
ORBD20	578.30	quartz vein	51	10	123	20	33	qz	-	V2	-	70	14	0.42	0.3m translucent quartz vein
ORBD20	588.15	foliation	35	44	161	43	71	po,py,cb	-	CC	-	70	14	0.57	Pervasive foliation
ORBD20	590.30	foliation	32	41	156	45	66	po,py,cb	-	CC	-	70	14	0.86	Pervasive foliation
ORBD20	592.10	foliation	11	44	152	66	62	py,po	-	CC	-	70	14	1.16	Intense shear foliation and mill breccia
ORBD20	609.20	shear zone	10	180	104	81	14	qz,cb	ch	SH7	-	70	16	0.05	2mm shear fracture
ORBD20	612.45	cb vein	27	123	53	75	143	cb	-	V4	-	70	16	0.10	0.3m recrystallised carbonate vein
ORBD20	617.20	quartz vein	31	167	92	79	182	qT	-	V2	-	70	16	0.02	5mm translucent quartz vein with carbonate
ORBD20	621.45	qcb vein	19	220	141	87	231	qz,cb,ch	po	V1	-	70	16	0.03	20mm quartz carbonate shear vein
ORBD20	624.20	quartz vein	53	295	10	34	280	qz,py,po,si	-	V2	-	70	16	0.02	1mm clear quartz vein with breccia
ORBD20	625.20	qcb vein	21	282	17	67	287	qT	-	V1	-	70	16	0.02	10mm crack-seal quartz vein
ORBD20	626.10	quartz vein	36	284	12	52	282	qT	-	V2	-	70	16	0.01	20mm translucent quartz vein
ORBD20	629.70	qcb vein	12	272	11	79	281	qz,cb	-	V1	-	70	16	0.01	Quartz carbonate extensional vein

HOLE NO	DEPTH	STRUCTURE	ALPHA	BETA	STRIKE	DIP	DIP DIRECTION	MINERALOGY	ALTERATION	GROUP	OVERPRINTING	HOLE DIP	HOLE AZIM	Au VALUE	COMMENTS
ORBD20	640.15	qcb vein	50	178	102	60	192	qz,cb,ch	-	V1	-	70	16	0.12	1mm quartz carbonate vein parallel to pervasive foliation
ORBD20	645.20	foliation	41	220	136	66	226	cb,mu,si,py	-	CC	-	70	16	0.32	Foliated main contact of breccia zone
ORBD20	645.25	breccia zone	52	236	144	52	234	cb,mu,si,py,cb	-	SH4	-	70	16	0.32	Intense hydraulic breccia
ORBD20	653.80	foliation	42	195	116	68	206	bi,si,ch	-	CC	-	70	16	0.08	Intense shear foliation slickenfibres show sinistral N block up movement
ORBD20	659.60	cb vein	50	248	154	51	244	cb,qz	-	V4	-	70	16	3.54	Coarse-grained recrystallised carbonate vein with some crack-seal quartz bands
ORBD20	667.90	quartz vein	44	293	16	42	286	qM	-	V3	-	70	16	-	50mm milky quartz vein parallel to shear zone
ORBD21	309.00	fault zone	4	87	9	86	99	qz,cb,ch	-	SH7	-	71	11	0.01	Intense shear zone
ORBD21	317.20	shear vein	17	195	115	89	25	qz,cb,ch	-	SH6	-	71	11	0.03	50mm shear/breccia vein with wallrock fragments
ORBD21	319.10	fault plane	10	269	6	81	276	qz,cb,ch	-	SH7	-	71	11	0.01	10mm shear/fault plane with quartz carbonate infill
ORBD21	354.00	qcb vein	42	159	83	66	173	qz,cb	py,ep	V1	-	72	11	0.01	10mm vuggy quartz carbonate vein
ORBD21	366.20	qcb vein	51	259	161	46	251	qz,cb	py,ep	V1	-	72	11	0.01	2mm quartz carbonate vein on boundary of Cashmans Shear Zone
ORBD21	366.20	qcb vein	35	259	168	61	258	qz,cb	py,ep	V1	-	72	11	0.01	2mm quartz carbonate vein on boundary of Cashmans Shear Zone
ORBD21	381.50	chlorite vein	32	279	8	57	278	ch,bi	cb,py	V5	-	72	11	0.01	10mm vuggy quartz vein
ORBD21	414.50	bedding	70	275	154	26	244	py,po	-	BED2	-	72	12	0.09	Pyrite laminae in Cashmans Sedimentary Horizon
ORBD21	416.00	quartz vein	39	323	52	38	322	qT	cb	BED2	-	72	12	0.08	30mm translucent quartz vein on basal contact of CSH
ORBD21	417.00	qcb vein	25	333	69	50	339	qz,cb	-	V1	-	72	12	0.03	1mm quartz carbonate veins breccia fill with striped rock texture
ORBD21	418.00	qcb vein	24	338	75	50	345	qz,cb	-	V1	-	72	12	0.03	3mm quartz carbonate vein breccia fill
ORBD21	437.60	qcb vein	59	135	71	46	161	qz,cb	ch,bi,py	V1	-	72	12	0.02	1mm quartz carbonate vein with 10mm alteration halo
ORBD21	437.95	qcb vein	34	303	32	48	302	qz,cb	-	V1	-	72	12	0.02	1mm quartz carbonate vein
ORBD21	437.95	qcb vein	33	286	15	54	285	qz cb	ch	V1	-	72	12	0.02	2mm quartz carbonate vein
ORBD21	440.25	shear contact	40	302	28	43	298	qz,cb	bi,cb,py	BED3	-	72	12	0.05	Intensely sheared upper contact of Enterprise dolerite?
ORBD21	468.80	quartz vein	62	110	54	38	144	qT,cb	ch,bi	V2	-	72	11	-	10mm translucent quartz vein with carbonate
ORBD21	474.38	quartz vein	51	271	170	43	260	qz,cb,ch,bi,lx	-	BED3	-	72	11	-	Upper contact of porphyritic dolerite, quartz carbonate vein
ORBD21	476.26	quartz vein	28	6	108	45	18	qz,cb	ch,po,ep	V2	-	72	11	-	20mm translucent comb textured quartz vein
ORBD21	479.00	shear zone	61	134	70	44	160	qz,cb,ch,bi	bi,ep,py	V6	-	72	11	-	Intense shear zone with chlorite slivers 60mm thick
ORBD21	479.00	qcb vein	38	301	27	45	297	qz,cb	ch,bi	V1	-	72	11	-	2mm quartz carbonate vein with sharp bi ch defined contact
ORBD21	480.15	qcb vein	34	350	87	39	357	qz,cb	ch	V1	-	72	11	-	-
ORBD21	481.00	qcb vein	15	302	37	67	307	qz,cb	-	V1	-	72	11	-	2mm recrystallised quartz carbonate vein
ORBD21	483.05	quartz vein	56	198	113	52	203	qT	py,ep	V2	-	72	11	-	3mm translucent quartz vein with 3mm pyrite selvedge
ORBD21	483.05	shear fracture	37	319	47	41	317	ch,bi	ch	SH7	xprev	72	11	-	<1mm chlorite filled fracture showing dextral W block down movement
ORBD21	488.80	quartz vein	30	102	32	66	122	qz,cb	ch	V2	-	72	11	0.02	20mm translucent recrystallised quartz vein
ORBD21	490.10	shear zone	38	390	141	38	51	bi,ch	qz,cb	V6	-	72	11	0.03	60mm shear zone with quartz carbonate veins
ORBD21	491.50	quartz vein	53	236	142	50	232	qT,qM	bi,ch,po	V2	-	72	11	0.03	0.18m translucent quartz vein with milky quartz breccia
ORBD21	493.65	quartz vein	46	318	41	33	311	qT	ch,bi,py	V2	-	72	11	0.19	20mm translucent quartz vein with 20mm py halo

HOLE NO	DEPTH	STRUCTURE	ALPHA	BETA	STRIKE	DIP	DIP DIRECTION	MINERALOGY	ALTERATION	GROUP	OVERPRINTING	HOLE DIP	HOLE AZIM	Au VALUE	COMMENTS
ORBD21	494.45	quartz vein	53	180	101	56	191	qM	si,bi,lx	V3	-	72	11	0.02	0.3m milky quartz vein with wallrock fragments
ORBD21	495.90	quartz vein	60	232	136	44	226	qT	bi,si,ch	V2	-	72	11	0.01	Translucent quartz vein with brecciated milky quartz and wallrock fragments
ORBD21	503.20	qcb vein	26	267	179	67	269	qz,cb	ch,py	V1	-	72	11	0.01	1mm quartz carbonate vein slickenfibres show dextral W block down movement
ORBD21	506.20	quartz vein	32	30	139	44	49	qT	ch,lx	V2	-	72	11	0.05	0.1m quartz vein
ORBD21	506.60	GP contact	59	341	60	16	330	ep	si,ep,qz	BED4	-	72	11	0.05	0.3m porphyry bar
ORBD21	525.60	shear zone	40	111	46	59	136	bi,ch,qz	-	SH6	-	72	14	0.35	Intense shear zone (mod ESE dip)
ORBD21	527.40	quartz vein	47	118	55	54	145	qz,cb,ch,bi	bi,ch,po	V1	-	72	14	0.02	50mm quartz vein
ORBD21	528.83	quartz vein	49	249	157	50	247	qT	cb,ch	V2	-	72	14	0.01	10mm translucent recrystallised quartz vein
ORBD21	530.30	cb vein	29	263	177	65	267	qz,cb	-	V4	-	72	14	0.02	20mm recrystallised carbonate vein
ORBD21	532.70	qcb vein	38	153	81	69	171	qz,cb	ch	V1	-	72	14	0.02	2mm quartz carbonate vein
ORBD21	532.75	qcb vein	32	284	16	56	286	qz,cb	ch	V1	-	72	14	0.02	2mm quartz carbonate vein
ORBD21	534.60	qcb vein	42	182	105	66	195	qz,cb	-	V1	-	72	14	0.01	10mm recrystallised quartz carbonate vein
ORBD21	539.50	quartz vein	62	286	175	29	265	qT	cb	V2	-	72	14	0.04	3mm translucent quartz vein E-W slickenfibres
ORBD21	539.60	quartz vein	38	330	63	38	333	qT	bi,py	V1	-	72	14	0.04	20mm quartz carbonate vein 30% py selvedge
ORD10	127.93	quartz vein	50	180	97	71	187	-	-	V6	-	59	7	0.32	White buck quartz vein
ORD10	167.09	quartz vein	70	200	108	51	198	-	-	V6	-	59	10	2.68	-
ORD10	167.09	quartz vein	72	190	104	49	194	-	-	V6	-	59	10	2.68	-
ORD10	167.09	quartz vein	60	100	56	46	146	-	-	V6	-	59	10	2.68	-
ORD10	182.36	shear zone	65	290	149	32	239	-	-	SH6	-	59	10	-	Brecciated quartz vein with fragments of biotite altered Aod
ORD10	182.36	shear zone	60	280	152	39	242	-	-	V6	-	59	10	-	Brecciated quartz vein with fragments of biotite altered Aod
ORD10	191.83	quartz vein	45	310	10	33	280	-	-	V6	-	59	8	1.29	-
ORD10	192.60	quartz vein	55	90	44	46	134	-	-	V6	-	59	8	-	-
ORD10	198.89	shear zone	8	240	157	83	67	-	-	SH6	-	59	8	-	-
ORD10	215.09	shear zone	36	305	16	43	286	-	-	C1	-	59	8	6.03	-
ORD10	215.09	shear zone	64	295	150	31	240	-	-	S1	-	59	8	6.03	-
ORD10	224.58	quartz vein	43	290	177	45	267	-	-	V6	-	59	9	0.12	-
ORD10	239.80	shear zone	55	270	152	46	242	-	-	SH6	-	59	9	0.94	-
ORD10	249.90	quartz vein	90	210	101	30	191	-	-	V6	-	60	12	0.08	-
ORD10	249.90	quartz vein	85	180	102	35	192	-	-	V6	-	60	12	0.08	-
ORD10	249.90	quartz vein	65	270	145	39	235	-	-	V6	-	60	12	0.08	-
ORD10	252.36	quartz vein	65	290	152	32	242	-	-	V6	-	60	12	-	-
ORD10	255.60	quartz vein	90	30	101	30	191	-	-	V6	-	60	12	-	-
ORD10	265.40	shear zone	20	200	120	82	30	-	-	SH6	-	60	12	-	-
ORD10	265.40	quartz vein	60	240	135	52	225	-	-	V6	-	60	12	-	-

HOLE NO	DEPTH	STRUCTURE	ALPHA	BETA	STRIKE	DIP	DIP DIRECTION	MINERALOGY	ALTERATION	GROUP	OVERPRINTING	HOLE DIP	HOLE AZIM	Au VALUE	COMMENTS
ORD10	265.40	shear zone	30	160	84	89	174	-	-	SH6	-	60	12	-	-
ORD10	265.40	quartz vein	90	180	101	30	191	-	-	V6	-	60	12	-	-
ORD10	274.35	shear zone	34	180	102	86	192	-	-	C2	-	60	12	-	-
ORD10	274.35	shear zone	90	180	101	30	191	-	-	S2	-	60	12	-	-
ORD13	110.33	quartz vein	35	270	164	61	254	-	-	V6	-	59	4	2.80	-
ORD13	121.60	quartz vein	54	180	94	67	184	-	-	SH1	-	59	4	1.80	-
ORD13	123.33	quartz vein	40	160	78	80	168	-	-	V6	-	59	4	1.03	-
ORD13	123.33	shear zone	34	240	142	75	232	-	-	V6	-	59	4	1.03	-
ORD13	123.33	qcb vein	60	100	50	46	140	-	-	SH6	-	59	4	1.03	-
ORD13	124.50	quartz vein	54	233	127	60	217	-	-	SH1	-	59	4	1.22	-
ORD13	127.47	quartz vein	40	280	167	52	257	-	-	V6	-	59	4	0.37	-
ORD13	133.33	quartz vein	45	290	170	44	260	-	-	V6	-	59	4	0.55	-
ORD13	133.33	quartz vein	20	220	131	86	41	-	-	V6	xnxt	59	4	0.55	-
ORD13	134.87	quartz vein	30	300	12	50	282	-	-	V6	-	59	4	1.27	-
ORD13	136.56	quartz vein	40	300	3	42	273	-	-	V6	xall veins	59	4	-	-
ORD13	136.56	quartz vein	50	100	41	54	131	-	-	V6	-	59	4	-	-
ORD13	140.55	GP dyke	90	180	94	31	184	-	-	V9	xprev	59	4	0.88	50cm wide quartz porphyry dyke
ORD13	170.20	shear zone	16	243	153	90	243	-	-	SH6	-	59	4	6.31	-
ORD13	170.20	shear zone	50	223	123	66	213	-	-	SH6	-	59	4	6.31	-
ORD14	224.20	shear zone	30	210	119	88	209	-	-	SH6	-	61	12	0.13	Shear zone defined by bi,ch slives, vein emplaced parallel to shear zone
ORD17	119.50	quartz vein	90	180	101	32	191	-	-	V1	-	58	11	0.16	Translucent quartz vein offsets milky quartz vein with fluorite
ORD17	120.70	quartz vein	90	180	101	32	191	-	-	V1	-	58	11	0.50	0.25m quartz vein with molybdenite sutures
ORD17	146.86	shear zone	40	210	123	79	213	-	-	SH6	-	58	11	0.06	Thin shear bands
ORD19	121.77	quartz vein	35	30	156	30	66	qz	cb,si,mu	V6	-	56	10	2.20	Quartz vein with molybdenite, chalcopyrite and biotite stringers, 20% pyrite
ORD19	134.30	shear zone	30	290	7	55	277	-	-	SH6	-	56	10	1.57	Dextral shear sense
ORD19	134.30	quartz vein	35	240	147	76	237	mo,cp,py	-	V6	-	56	10	1.57	-
ORD19	147.40	shear zone	35	210	124	86	214	-	-	SH6	-	56	10	0.60	-
ORD19	176.50	shear zone	40	260	159	63	249	mu	-	SH6	-	56	11	1.54	-
ORD19	185.80	shear zone	35	220	133	83	223	si,mu,ch	-	SH6	-	56	11	3.29	Intensely silicified shear foliation
ORD19	196.60	shear zone	40	240	145	72	235	mu,ch	-	SH6	-	56	11	6.00	Intense shear foliation

HOLE NO	DEPTH	STRUCTURE	ALPHA	BETA	STRIKE	DIP	DIP DIRECTION	MINERALOGY	ALTERATION	GROUP	OVERPRINTING	HOLE DIP	HOLE AZIM	Au VALUE	COMMENTS
ORD21	139.00	qcb vein	35	70	178	51	268	-	-	V1	-	60	175	0.91	Minor quartz carbonate veining
ORD21	139.00	qcb vein	30	260	150	70	60	-	-	V1	-	60	175	0.91	-
ORD21	139.00	quartz vein	35	350	65	26	155	-	-	V2	-	60	175	0.91	40mm vein with mo, py,cp
ORD21	151.36	GP contact	35	270	155	61	65	-	-	BED2	-	60	175	0.04	Aod clasts in quartz porphyry
ORD21	164.70	quartz vein	35	80	6	56	276	qz,cb	bi,ch	V6	-	60	175	0.66	150mm quartz carbonate vein
ORD21	168.69	qcb vein	20	350	69	42	159	cb,mo,py	cb,mu	V1	-	61	174	1.33	-
ORD21	168.69	foliation	25	70	169	59	259	mu	cb	CC	-	61	174	1.33	Intense carbonation
ORD27	100.90	qcb vein	10	10	116	52	26	-	ta,zb,ch	V1	-	61	14	0.01	Minor quartz carbonate veining
ORD27	100.90	qcb vein	45	120	60	64	150	-	ta,zb,ch	V1	-	61	14	0.01	-
ORD27	107.43	qcb vein	55	340	34	13	304	-	ta,ch,cb,bi	V1	-	61	14	0.01	-
ORD27	107.43	qcb vein	30	80	21	60	111	-	ta,ch,cb,bi	V1	-	61	14	0.01	Euhedral pyrite to 5mm
ORD27	107.43	shear zone	55	340	34	13	304	-	ta,ch,cb,bi	SH6	-	61	14	0.01	-
ORD27	107.80	shear zone	60	110	64	48	154	-	-	SH6	-	61	14	0.01	-
ORD27	107.80	qcb vein	30	330	57	37	327	-	-	V1	-	61	14	0.01	-
ORD27	110.73	shear zone	20	60	177	59	87	ch,ta,cb	-	SH4	-	61	14	0.01	Chaotic shear zone with breccia
ORD27	111.12	shear zone	65	230	129	49	219	ch,ta,cb	-	SH6	-	61	14	0.01	Contact with massive rock
ORD27	117.81	shear zone	87	220	107	32	197	ch,ta,cb	-	SH2	-	61	14	0.01	Cashmans Shear Zone, sharp contact
ORD27	122.05	talc,cb vein	60	70	43	33	133	ta,cb	-	V5	-	61	14	0.01	Minor veins
ORD27	122.05	talc,cb vein	45	110	53	60	143	ta,cb	-	V5	-	61	14	0.01	Minor veins
ORD27	129.00	talc,cb vein	20	110	39	82	129	ta,cb	-	V5	-	61	13	0.18	-
ORD27	141.00	talc,cb vein	45	90	38	52	128	ta,cb	-	V5	-	61	13	0.01	Fine-grained mafic rocks
ORD27	142.05	talc,cb vein	35	240	151	73	241	ta,cb	-	V5	-	61	13	0.01	Abundant pyrite
ORD27	143.00	talc,cb vein	30	320	44	41	314	ta,cb	-	V5	-	61	13	0.01	Abundant pyrite
ORD27	147.50	talc,cb vein	35	320	40	37	310	ta,cb	-	V5	-	61	13	0.01	Abundant pyrite
ORD27	153.00	quartz vein	60	240	137	51	227	-	-	V2	-	61	13	0.01	Large vuggy vein with sheared contact
ORD27	153.30	quartz vein	80	180	102	40	192	qz	-	V2	-	61	13	0.01	Buck vein
ORD27	153.30	qcb vein	50	220	130	65	220	ta,cb	-	V1	-	61	13	0.02	Minor veins
ORD27	173.42	quartz vein	40	250	161	65	251	qz,po,mp,cp	-	V1	-	61	18	2.92	-
ORD27	170.40	foliation	50	220	135	65	225	-	-	CC	-	61	18	3.00	-
ORD27	177.40	quartz vein	89	170	107	30	197	qz	-	V2	-	61	18	0.46	1m biotite alteration halo
ORD27	180.30	foliation	30	230	150	81	240	bi,ta,ch	-	CC	-	61	18	0.14	Stretched wallrock slivers
ORD27	187.54	foliation	30	230	150	81	240	-	-	CC	-	61	18	0.21	Approximately vertical foliation
ORD29	100.00	qcb vein	38	120	45	72	135	qz,cb	-	V1	-	59	2	-	Veins in foliation

HOLE NO	DEPTH	STRUCTURE	ALPHA	BETA	STRIKE	DIP	DIP DIRECTION	MINERALOGY	ALTERATION	GROUP	OVERPRINTING	HOLE DIP	HOLE AZIM	Au VALUE	COMMENTS
ORD29	106.83	shear zone	70	180	92	51	182	bi,ta	-	SH6	-	59	2	-	En echelon vein array at 90 to shear plane
ORD29	108.40	talc,cb vein	90	180	92	31	182		-	V5	-	59	2	-	-
ORD29	122.30	foliation	40	70	10	47	100	ch,ta	-	CC	-	59	2	-	Intense foliation
ORD29	122.30	qcb vein	35	70	6	51	96	qz,cb	-	V1	-	59	2	-	Minor quartz carbonate veining
ORD29	124.43	quartz vein	50	80	27	45	117		-	V2	-	59	2	-	0.5m buck vein at centre of foliation
ORD29	124.43	foliation	40	80	18	52	108	bi,ch	-	CC	-	59	2	-	-
ORD29	124.43	quartz vein	60	80	39	39	129	qz	-	V6	-	59	2	-	Large vein
ORD29	124.43	foliation	30	320	31	40	301	qz	-	CC	-	59	2	-	Contact with massive Aod
ORD29	147.25	shear zone	40	290	173	47	263	qz,ch,cb	ch,bi	SH6	-	59	2	0.13	Quartz carbonate veins parallel to shear foliation
ORD29	150.25	quartz vein	40	290	173	47	263	qz,cb,fl	si,py,hm	V6	-	59	2	1.80	Vein in biotite altered brecciated Aod
ORD29	151.30	qcb vein	40	310	10	37	280	qz,cb	py,bi,ch	V6	-	59	2	0.33	Brecciation and tension gash infill
ORD29	152.50	quartz vein	70	220	109	48	199	qz,ch,mo	ch,bi,py	V6	-	59	2	0.16	20cm alteration halo
ORD29	153.05	quartz vein	60	100	48	46	138	qz,fl,mo	si,bi,ch	V6	-	59	2	0.25	Wallrock brecciation
ORD29	154.25	quartz vein	80	160	86	41	176	qz,cb	py	V6	-	59	2	0.04	Quartz vein
ORD29	154.25	qcb vein	30	290	1	55	271	qz,cb	py	V1	-	59	2	0.04	Minor veining
ORD29	160.80	quartz vein	5	270	179	86	269	qz,cb	hm	V1	-	59	2	0.21	Thin vein
ORD29	164.13	quartz vein	35	340	54	28	324	qz	hm,py,bi,si	V1	-	59	2	0.42	-
ORD29	171.40	shear zone	40	220	122	76	212	ch,bi	py,qz,bi	CC	-	59	2	0.11	Large buck quartz veins
ORD29	178.10	shear zone	30	220	125	86	215	ch,bi	py,lx,bi,ch	SH6	-	59	2	3.36	Intense alteration near shear zone
ORD29	180.46	foliation	40	310	10	37	280	ch,bi	bi,si,qz	CC	-	59	2	2.86	Intense alteration
ORD29	194.36	quartz vein	55	350	34	7	304	qz	si,bi	V6	-	59	2	0.85	Large buck quartz vein
ORD29	196.65	quartz vein	50	270	150	49	240	qz	mo,si,py	V6	-	59	2	0.11	Large buck vein with wallrock brecciation and Mo sutures
ORD29	199.35	quartz vein	30	330	43	36	313	qz		V6	-	59	2	0.05	Large buck veins
ORD29	224.38	quartz vein	45	310	5	33	275	qz	ch,bi,si	V6	-	59	3	0.36	0.2m alteration selvedge with 20% pyrite
ORD151	246.50	quartz vein	70	250	124	38	214	qz	bi,ch,cb,si	V2	-	64	3	2.35	Large buck quartz vein with intense alteration halo
ORD155	219.90	shear zone	40	220	122	74	212	bi,ta,ch	-	SH6	-	62	2	-	Intense shear zone
ORD155	222.80	shear zone	28	230	135	82	225	-	-	SH6	xall	62	2	-	Shear zone
ORD155	223.90	quartz vein	27	235	139	81	229	qz,cb	-	V1	-	62	2	-	2mm vein, 2 veins/cm
ORD155	228.60	shear zone	25	260	163	73	253	py,ch	-	SH6	-	62	4	3.90	Intense shear zone
ORD155	229.56	qcb vein	60	30	9	15	99	qz,cb	-	V1	xnxt	62	4	1.66	-
ORD155	229.56	shear zone	26	270	171	68	261	ch,bi,py	-	SH6	-	62	4	1.66	Intense shear zone
ORD155	229.87	quartz vein	75	190	97	43	187	qz,cb	-	V2	-	62	4	1.66	Buck quartz vein
ORD155	235.65	quartz vein	53	320	8	23	278	qz,mo	-	V2	xall	62	4	1.17	Buck quartz vein with fracturerd milky quartz fragments

HOLE NO	DEPTH	STRUCTURE	ALPHA	BETA	STRIKE	DIP	DIP DIRECTION	MINERALOGY	ALTERATION	GROUP	OVERPRINTING	HOLE DIP	HOLE AZIM	Au VALUE	COMMENTS
ORD157	207.85	py stringer	40	210	113	71	203	py,ch	-	SRPY	-	67	360	0.01	3mm pyritic veinlet
ORD157	208.30	qcb vein	40	180	90	73	180	qz,cb	-	V1	-	67	360	0.03	2mm quartz carbonate vein
ORD157	208.40	shear vein	35	170	81	78	171	ch,cb,ta,bi	-	V1	-	67	360	0.03	0.1m comb textured vein
ORD157	209.13	talc,cb vein	15	248	154	85	244	ch,cb,ta,bi	-	V1	xnxt	67	360	0.01	5mm shear vein
ORD157	209.43	talc,cb vein	35	230	131	72	221	ta,cb	-	V1	-	67	360	0.01	-
ORD157	211.10	talc,cb vein	55	60	6	30	96	ta,cb	-	V1	-	67	360	0.01	2mm shear vein
ORD157	214.00	shear zone	45	190	97	68	187	qz,ta,bi	-	SH6	-	67	360	2.68	Shear foliation
ORD157	214.65	qcb vein	25	330	50	46	320	qz,cb,ch	-	V1	-	67	360	2.68	Comb textured vein
ORD157	216.10	qcb vein	10	330	55	61	325	qz,cb,ta	-	V1	-	67	360	0.37	3mm vein
ORD157	216.20	qcb vein	30	160	72	82	162	qz,cb,ch	-	V1	xprev	67	360	0.37	50mm shear vein
ORD157	219.10	fracturing	32	185	94	81	184	qz,ch,py	-	CS1	-	67	360	0.62	Spaced hydrofracturing, 3/cm
ORD157	220.00	qcb vein	20	180	360	88	360	qz,bi,cb	-	CS1	xnxt	67	360	2.67	5mm shear vein with parallel foliation
ORD157	220.00	qcb vein	65	60	23	24	113	qz,cb	-	V1	-	67	360	2.67	10mm vein
ORD157	220.44	qcb vein	45	320	26	31	296	qz,cb	-	V1	-	67	360	2.67	2mm vein with wallrock fragments
ORD157	220.70	qcb vein	40	30	136	32	46	qz,cb	-	V1	-	67	360	2.67	6mm vein
ORD157	220.70	qcb vein	25	145	58	85	148	qz,cb	-	SH6	xnxt/xprev	67	360	2.67	10mm shear/breccia vein
ORD157	220.70	qcb vein	40	260	153	58	243	qz,cb	-	V1	-	67	360	2.67	10mm quartz vein cut by previous with sinistral offset
ORD157	224.00	qcb vein	30	190	98	83	188	qz,cb	-	V1	-	67	360	1.85	3mm quartz carbonate vein cross-cut by core axis parallel shear vein
ORD157	224.25	qcb vein	45	75	8	44	98	qz,cb	-	V1	xnxt	67	360	2.08	3mm vein
ORD157	224.25	shear zone	5	270	178	86	268	qz,cb	-	SH6	xnxt	67	360	2.08	15mm shear/breccia vein
ORD157	224.25	shear zone	25	185	94	88	184	qz,cb	-	SH6	-	67	360	2.08	15mm shear/breccia vein
ORD157	225.60	qcb vein	25	15	110	44	20	qz,cb,bi,fd	-	CC	-	67	360	1.88	Fine pervasive foliation with parallel veins
ORD157	225.60	qcb vein	60	180	90	54	180	qz,cb	-	V1	xall	67	360	1.88	Crack-seal vein cross-cuts all structures
ORD157	225.60	qcb vein	60	185	93	53	183	qz,cb	-	V1	xnxt	67	360	1.88	1mm cbx fill vein
ORD157	225.60	qcb vein	50	35	153	25	63	qz,cb	-	V1	xnxt	67	360	1.88	1mm cbx fill vein
ORD157	225.60	qcb vein	2	30	122	69	32	qz,cb	-	V1	-	67	360	1.88	1mm cbx fill vein
ORD157	226.60	quartz vein	30	160	72	82	162	qz,ch	-	V2	-	67	360	0.21	0.75m quartz vein
ORD157	227.10	foliation	30	160	72	82	162	ch,bi,py	-	CC	-	67	360	0.19	Foliation on lower vein contact
ORD157	227.30	quartz vein	35	240	139	69	229	qz,cb,ch	-	V1	-	67	360	0.19	6cm laminated edges with slivers of wallrocks + py,po
ORD157	227.30	qcb vein	70	250	124	35	214	qz,cb	-	V1	xprev	67	360	0.19	1mm quartz carbonate vein
ORD157	227.75	quartz vein	58	245	131	47	221	qz	-	V2	-	67	360	0.19	15cm translucent quartz vein with milky vein fragments and bi altered WR fragments
ORD157	228.25	quartz vein	68	30	21	12	111	qz	-	V2	-	67	3	0.21	0.2m translucent quartz vein
ORD157	228.80	quartz vein	56	295	171	32	261	qz,ch	-	V2	-	67	3	0.21	Translucent quartz vein with milky vein fragments and parallel quartz carbonate veins
ORD157	229.50	qcb vein	50	80	20	42	110	qz,cb	-	SH4	xnxt	67	3	5.82	2mm cbx fill vein

HOLE NO	DEPTH	STRUCTURE	ALPHA	BETA	STRIKE	DIP	DIP DIRECTION	MINERALOGY	ALTERATION	GROUP	OVERPRINTING	HOLE DIP	HOLE AZIM	Au VALUE	COMMENTS
ORD157	229.50	qcb vein	60	210	111	52	201	qz,cb	-	SH4	-	67	3	5.82	1mm cbx vein
ORD157	229.50	qcb vein	80	90	68	25	158	qz,cb	-	SH4	xprev2	67	3	5.82	1mm cbx vein
ORD157	233.40	foliation	30	210	119	81	209	ch,bi,cb	-	CC	-	67	3	9.36	Foliation
ORD157	240.00	shear zone	40	250	148	61	238	ch,bi,mu	-	CEF	-	67	3	1.04	Close spaced foliation and shearing
ORD157	240.75	quartz vein	85	90	80	24	170	ch,qz	-	V2	-	67	3	1.04	3cm quartz vein with milky quartz fragments
ORD157	241.90	shear zone	20	260	165	76	255	qz,mu,cb	-	SH5	-	67	3	12.10	Shear/breccia zone with streaming textures
ORD157	244.00	shear zone	12	20	116	57	26	qz,cb,fu	-	CEF	-	67	3	1.38	Lower contact of south Enterprise fault
ORD157	248.25	qcb vein	12	70	169	72	79	qz,cb	-	V1	-	67	3	0.23	1mm quartz carbonate vein
ORD157	248.25	qcb vein	35	265	163	60	253	qz,cb	-	V1	xprev	67	3	0.23	1mm quartz carbonate vein
ORD157	248.25	qcb vein	20	55	157	59	67	qz,cb	-	V1	-	67	3	0.23	1mm quartz carbonate vein
ORD157	254.40	quartz vein	5	140	51	78	321	qz,ch	-	V2	-	67	3	0.49	1.5m translucent quartz vein
ORD157	257.40	shear zone	40	140	61	69	151	ch,bi	-	CC	-	67	3	0.15	Close spaced foliation and shearing
ORD157	259.10	quartz vein	50	150	74	61	164	qz	-	V2	-	67	6	2.59	Translucent quartz vein with brecciated milky vein fragments +WR slivers
ORD157	276.55	shear zone	2	260	176	88	86	qz,cb,fl,ch,hm	-	SH6	-	67	6	10.70	Zone of core axis parallel veins and shear zones
ORD157	283.80	qcb vein	30	320	42	44	312	qz,cb	-	CC	-	67	6	0.04	End of zone marked by foliation
ORD157	285.50	qcb vein	20	310	36	57	306	qz,cb	-	V1	-	67	6	0.04	10mm quartz carbonate vein
ORD157	286.45	qcb vein	70	220	115	41	205	qz,cb	-	V1	-	67	6	0.59	20mm quartz vein with coarse-grained fragments of laminated wallrock
ORD157	288.60	qcb vein	25	90	16	68	106	qz,cb	-	V1	-	67	6	0.07	5mm vein slivers of chlorite
ORD157	291.33	qcb vein	20	360	96	47	6	qz,cb,fl,hm	fl,hm	V1	-	67	6	0.03	10mm quartz vein with intese alteration halo
ORD157	294.45	qcb vein	25	355	89	43	359	qz,cb,ch	hm	V1	-	67	6	0.04	20mm vein with hematite alteration
ORD157	308.87	shear zone	10	90	9	81	99	qz,cb,ch	-	SH6	-	67	6	0.79	Shear zone at boundary of fault
ORD157	313.70	shear zone	30	220	130	79	220	qz,ch,py	-	SH6	-	67	6	0.79	Shear zone and vein at boundary of fault
ORD157	314.40	shear zone	15	310	38	62	308	qz,cb,py,bi,mu	-	SH5	-	67	6	0.33	Intense mill breccia in fault
ORD157	314.70	shear zone	20	300	26	61	296	py,qz,cb,si	-	SH5	-	67	6	0.33	Intense mill breccia in fault
ORD157	322.54	quartz vein	85	180	95	28	185	qz	-	V2	-	67	5	0.04	Quartz vein in fault lithon
ORD157	339.20	qcb vein	88	190	95	25	185	qz,cb	-	V1	-	67	5	-	3mm quartz carbonate vein
ORD157	339.20	qcb vein	28	220	130	81	220	qz,cb	-	V1	xprev	67	5	-	3mm quartz carbonate vein
ORD157	340.30	shear zone	20	85	8	70	98	ch,bi	-	SH6	-	67	5	-	Shear zone

Table A1.11 - Gimlet South Deposit, structural data from undergound face mapping

Drive	Structure	Orientation					Offset	Fault Width	Northing	Easting	RL
		Strike	Dip	Dip direction	Plunge	Plunge dir					
1130e	fault	87	70	357	-		-	500	6637026.282	313933.479	1130
1130e	fault	17	85	107	-		-	-	6637027.156	313932.994	1130
1130e	fault	67	80	337	-		-	-	6637030.654	313931.055	1130
1130e	shear zone	71	85	341	10	257	-	-	6637031.519	313940.864	1130
1130e	joint	45	75	135	-		-	-	6637032.394	313940.379	1130
1130e	vein	103	60	13	-		-	-	6637033.268	313939.895	1130
1130e	shear zone	43	90	313	-		-	-	6637035.891	313938.440	1130
1130e	shear zone	42	85	312	-		-	-	6637033.458	313944.362	1130
1130e	shear zone	62	80	332	-		-	-	6637035.207	313943.392	1130
1130e	fault	77	80	347	-		-	-	6637036.956	313942.423	1130
1130e	fault	64	88	334	-		-	-	6637034.913	313946.985	1130
1130e	fault	73	64	343	-		-	-	6637035.787	313946.501	1130
1130e	fault	70	90	340	-		-	-	6637038.410	313945.046	1130
1130e	fault	62	70	332	-		-	-	6637035.493	313950.093	1130
1130e	vein	117	65	27	-		-	-	6637038.990	313948.154	1130
1130e	shear zone	67	80	157	-		-	500	6637039.865	313947.670	1130
1130e	shear zone	121	86	31	-		-	-	6637036.557	313954.076	1130
1130e	shear zone	68	86	158	-		-	-	6637037.432	313953.591	1130
1130e	shear zone	73	45	343	-		-	-	6637038.306	313953.106	1130
1130e	fault	60	75	150	-		-	-	6637039.181	313952.622	1130
1130e	fault	48	81	318	-		-	-	6637040.055	313952.137	1130
1130e	shear zone	65	88	335	-		-	-	6637040.055	313952.137	1130
1130e	shear zone	72	80	342	-		-	50	6637037.622	313958.059	1130
1130e	fault	50	87	140	-		-	40	6637038.496	313957.574	1130
1130e	fault	125	59	35	-		-	50	6637039.371	313957.089	1130
1130e	fault	51	87	321	-		-	30	6637041.120	313956.119	1130
1130e	fault	116	54	26	-		-	150	6637041.120	313956.119	1130
1130e	shear zone	89	84	359	-		-	-	6637041.994	313955.635	1130
1130e	fault	62	80	332	-		-	-	6637039.951	313960.197	1129
1130e	shear zone	42	90	312	-		-	-	6637041.700	313959.228	1129
1130e	fault	67	90	337	-		-	-	6637044.323	313957.773	1129
1130e	fault	67	90	337	-		-	-	6637039.656	313963.790	1130
1130e	fault	67	90	337	-		-	-	6637043.344	313966.318	1130

Drive	Structure	Orientation					Offset	Fault Width	Northing	Easting	RL
		Strike	Dip	Dip direction	Plunge	Plunge dir					
1130e	fault	44	84	314	7	130	-	-	6637045.968	313964.864	1130
1130e	fault	67	85	337	-		-	-	6637043.924	313969.426	1130
1130e	fault	69	87	159	90	150	-	50	6637044.799	313968.941	1130
1130e	fault	130	55	40	-		-	50	6637044.799	313968.941	1130
1130e	fault	63	70	153	-		-	-	6637045.673	313968.457	1130
1130e	fault	162	45	72	-		-	30	6637045.673	313968.457	1130
1130e	fault	99	82	9	-		-	50	6637046.547	313967.972	1130
1130e	shear zone	60	80	330	-		-	50	6637046.253	313971.565	1130
1130e	fault	125	42	35	-		-	-	6637047.127	313971.080	1130
1130e	joint	70	78	160	-		-	-	6637048.002	313970.595	1130
1130e	shear zone	39	90	309	-		-	-	6637048.002	313970.595	1130
1130e	fault	82	85	352	-		-	50	6637048.876	313970.110	1130
1130e	shear zone	79	80	349	-		-	-	6637047.223	313973.314	1130
1130e	fault	70	86	340	-		-	-	6637050.720	313971.375	1130
1130e	shear zone	97	90	187	-		-	500	6637051.300	313974.483	1130
1130e	shear zone	37	90	307	-		-	200	6637053.049	313973.513	1130
1130e	shear zone	72	90	162	-		-	400	6637052.365	313978.465	1130
1130e	shear zone	57	90	147	-		-	600	6637054.988	313977.011	1130
1130e	fault	62	73	332	-		-	50	6637055.083	313979.245	1130
1130e	fault	72	77	342	-		-	50	6637055.958	313978.760	1130
1130e	fault	77	72	347	-		-	100	6637055.274	313983.712	1130
1130e	fault	30	65	300	-		-	-	6637055.274	313983.712	1130
1130e	fault	84	72	354	-		-	100	6637057.022	313982.742	1130
1130e	fault	64	48	334	-		-	50	6637055.369	313985.946	1130
1130e	shear zone	74	40	164	-		-	-	6637055.369	313985.946	1130
1130e	fault	78	82	168	-		-	100	6637056.243	313985.461	1130
1130e	fault	20	85	110	-		-	10	6637057.992	313984.491	1130
1130e	fault	54	78	324	-		r	100	6637058.866	313984.006	1130
1130e	fault	80	75	350	-		-	50	6637056.823	313988.569	1130
1130e	fault	50	87	320	-		r	100	6637057.697	313988.084	1130
1130e	fault	37	76	127	-		-	-	6637058.572	313987.599	1130
1130e	fault	84	77	354	-		-	-	6637059.446	313987.114	1130
1130e	fault	80	80	350	-		-	50	6637058.762	313992.067	1130
1130e	fault	74	85	164	-		-	150	6637059.637	313991.582	1130
1130e	fault	69	85	339	90	324	-	50	6637062.260	313990.127	1130

Drive	Structure	Orientation					Offset	Fault Width	Northing	Easting	RL
		Strike	Dip	Dip direction	Plunge	Plunge dir					
1130e	fault	117	58	27	-		-	20	6637059.342	313995.175	1130
1130e	fault	27	85	117	-		-	50	6637060.217	313994.690	1130
1130e	shear zone	32	74	122	-		-	-	6637061.965	313993.720	1130
1130e	fault	71	87	341	-		-	50	6637062.840	313993.236	1130
1130e	shear zone	52	70	322	-		-	200	6637060.312	313996.924	1130
1130e	shear zone	68	76	338	-		-	50	6637061.186	313996.439	1130
1130e	shear zone	67	79	157	-		-	-	6637062.061	313995.954	1130
1130e	shear zone	72	88	162	-		-	200	6637063.809	313994.984	1130
1130e	shear zone	62	75	152	-		-	500	6637020.759	313919.393	1130
1130e	shear zone	57	90	327	-		-	500	6637026.005	313916.484	1130
1130e	fault	87	78	177	-		-	-	6637020.378	313910.458	1130
1130e	shear zone	91	70	1	-		-	-	6637021.253	313909.973	1130
1130e	vein	91	50	1	-		-	-	6637022.127	313909.489	1130
1130e	shear zone	69	89	339	-		-	500	6637023.002	313909.004	1130
1130e	shear zone	49	87	319	-		-	-	6637021.642	313908.614	1130
1130e	shear zone	60	73	150	-		-	500	6637022.517	313908.129	1130
1130e	fault	62	80	152	-		-	100	6637017.470	313905.212	1130
1130e	fault	32	80	122	-		-	-	6637019.218	313904.242	1130
1130e	shear zone	77	75	347	-		-	-	6637020.093	313903.757	1130
1130w	fault	47	75	137	-		-	-	6637013.877	313904.917	1130
1130w	shear zone	67	80	337	-		-	200	6637014.751	313904.432	1130
1130w	shear zone	52	85	142	-		-	-	6637017.374	313902.978	1130
1130w	fault	67	88	337	-		-	-	6637015.236	313905.307	1130
1130w	fault	57	82	147	-		-	-	6637016.110	313904.822	1130
1130w	fault	56	81	326	18	54	-	-	6637017.859	313903.852	1130
1130w	shear zone	82	82	172	-	-	-	200	6637008.839	313891.705	1130
1130w	fault	62	82	332	-		-	-	6637009.713	313891.221	1130
1130w	joint	53	68	143	-		-	-	6637004.181	313887.428	1130
1130w	joint	68	68	158	-		-	-	6637005.055	313886.943	1130
1130w	joint	95	30	5	-		-	-	6637005.930	313886.459	1130
1130w	joint	82	69	172	-		-	-	6637005.930	313886.459	1130
1130w	fault	56	88	146	-		-	-	6637006.804	313885.974	1130
1130w	fault	62	85	332	-		-	-	6637007.679	313885.489	1130
1130w	shear zone	62	80	152	-		-	150	6637005.350	313883.351	1130
1130w	vein	32	90	122	-		-	-	6637006.224	313882.866	1130

Drive	Structure	Orientation					Offset	Fault Width	Northing	Easting	RL
		Strike	Dip	Dip direction	Plunge	Plunge dir					
1130w	fault	62	80	332	-		-	1000	6637003.506	313882.087	1130
1130w	vein	102	60	12	-		-	50	6637006.129	313880.632	1130
1130w	fault	62	85	152	-		d	-	6637002.052	313879.463	1130
1130w	shear zone	72	80	342	-		-	200	6637002.926	313878.978	1130
1135e	shear zone	62	68	332	-		-	-	6637098.315	314069.597	1135
1135e	fault	92	61	182	-		-	-	6637099.190	314069.112	1135
1135e	shear zone	102	55	192	-		-	-	6637100.064	314068.628	1135
1135e	shear zone	118	67	208	-		-	-	6637100.064	314068.628	1135
1135e	shear zone	79	81	349	-		-	-	6637101.813	314067.658	1135
1135e	shear zone	65	76	335	-		-	-	6637102.687	314067.173	1135
1135e	shear zone	84	74	354	-		-	-	6637098.505	314074.065	1135
1135e	vein	110	61	200	-		-	-	6637099.380	314073.580	1135
1135e	joint	80	81	170	-		-	-	6637100.254	314073.095	1135
1135e	joint	77	80	167	-		-	-	6637101.129	314072.610	1135
1135e	joint	70	84	160	-		-	-	6637101.129	314072.610	1135
1135e	shear zone	86	64	176	-		-	-	6637102.003	314072.125	1135
1135e	shear zone	76	83	166	-		-	-	6637102.878	314071.641	1135
1135e	shear zone	72	70	162	-		-	-	6637102.878	314071.641	1135
1135e	shear zone	84	78	354	-		-	150	6637097.726	314076.783	1135
1135e	shear zone	82	73	172	-		-	-	6637098.600	314076.298	1135
1135e	shear zone	71	88	161	-		-	-	6637099.475	314075.813	1135
1135e	shear zone	82	80	172	-		-	-	6637099.475	314075.813	1135
1135e	shear zone	81	75	351	-		-	-	6637102.098	314074.359	1135
1135e	shear zone	57	70	327	-		-	200	6637098.401	314082.125	1135
1135e	shear zone	80	81	170	-		-	-	6637099.276	314081.640	1135
1135e	fault	77	81	167	-		-	-	6637100.150	314081.155	1135
1135e	vein	102	57	12	-		-	-	6637101.024	314080.670	1135
1135e	shear zone	64	87	154	-		-	-	6637101.899	314080.186	1135
1135e	shear zone	82	80	172	-		-	-	6637100.920	314088.731	1135
1135e	shear zone	87	60	357	-		-	-	6637102.669	314087.761	1135
1135e	shear zone	69	25	159	-		-	-	6637103.543	314087.276	1135
1135e	shear zone	67	85	157	-		-	500	6637104.418	314086.792	1135
1260e	fault	138	84	228	-		-	-	6636829.840	313587.391	1260
1260e	fault	66	60	336	-		-	-	6636832.853	313584.577	1260
1260w	shear zone	153	87	63	-		-	-	6636737.998	313448.536	1260

Drive	Structure	Orientation					Offset	Fault Width	Northing	Easting	RL
		Strike	Dip	Dip direction	Plunge	Plunge dir					
1260w	shear zone	41	80	311	-		-	-	6636739.747	313447.567	1260
1260w	shear zone	39	70	129	-		-	-	6636740.621	313447.082	1260
1260w	shear zone	145	78	55	-		-	-	6636738.578	313451.644	1260
1260w	shear zone	83	71	353	-		-	-	6636739.452	313451.159	1260
1260w	shear zone	51	65	321	-		-	-	6636742.075	313449.705	1260
1260w	shear zone	143	60	233	-		-	-	6636742.950	313449.220	1260
1260w	fault	177	88	267	-		-	-	6636741.002	313456.016	1260
1260w	fault	128	64	38	-		-	-	6636741.876	313455.532	1260
1260w	fault	162	78	72	-		-	-	6636742.751	313455.047	1260
1260w	fault	45	64	315	-		-	-	6636743.625	313454.562	1260
1260w	fault	64	90	334	-		-	-	6636744.499	313454.077	1260
1260w	fault	32	75	302	-		-	-	6636745.374	313453.593	1260
1260w	fault	17	75	287	-		-	-	6636746.248	313453.108	1260
1260w	shear zone	66	25	156	-		-	-	6636743.625	313454.562	1260
1260w	shear zone	52	70	322	-		-	-	6636741.971	313457.765	1260
1260w	shear zone	33	68	303	-		-	-	6636741.971	313457.765	1260
1260w	shear zone	22	70	292	-		-	-	6636742.846	313457.281	1260
1260w	shear zone	107	72	17	70	43	-	-	6636744.595	313456.311	1260
1260w	shear zone	17	75	287	70	43	-	-	6636745.469	313455.826	1260
1260w	shear zone	40	66	310	-		-	-	6636743.521	313462.622	1260
1260w	shear zone	6	83	276	-		-	-	6636744.395	313462.138	1260
1260w	shear zone	171	80	81	77	16	-	-	6636745.270	313461.653	1260
1260w	shear zone	103	75	193	-		-	-	6636747.018	313460.683	1260
1260w	shear zone	29	66	299	-		-	-	6636747.893	313460.198	1260
1260w	shear zone	2	65	92	-		-	1000	6636749.728	313471.756	1260
1260w	fault	42	88	312	-		-	-	6636751.667	313475.254	1260
1260w	fault	0	80	90	-		-	-	6636753.416	313474.285	1260
1260w	fault	166	85	256	-		d	-	6636755.165	313473.315	1260
1260w	fault	70	65	340	-		d	200	6636759.822	313477.592	1260
1260w	shear zone	62	80	332	-		-	500	6636756.515	313483.999	1260
1270e	shear zone	90	80	0	25	269	-	200	6636799.565	313559.590	1266
1270e	fault	76	78	346	-		-	-	6636799.470	313557.356	1266
1270e	vein	72	85	342	-		-	-	6636799.765	313553.763	1267
1270e	fault	82	85	352	-		-	-	6636796.951	313550.751	1268
1270w	fault	13	85	103	-		-	-	6636775.145	313501.107	1272

Drive	Structure	Orientation					Offset	Fault Width	Northing	Easting	RL
		Strike	Dip	Dip direction	Plunge	Plunge dir					
1270w	fault	7	80	97	36	181	-	-	6636774.565	313497.999	1272
1270w	fault	158	85	68	41	161	-	-	6636775.440	313497.514	1272
1270w	fault	163	85	73	17	163	-	-	6636749.252	313460.588	1273
1270w	fault	170	78	80	-		-	10	6636751.001	313459.618	1273
1270w	fault	160	75	70	25	157	-	-	6636747.408	313459.324	1273
1270w	fault	105	62	195	-		-	10	6636748.283	313458.839	1273
1270w	fault	79	50	349	-		-	50	6636749.157	313458.354	1273
1270w	fault	170	62	80	-		-	10	6636750.031	313457.870	1273
1270w	fault	82	82	352	-		-	10	6636746.828	313456.216	1273
1270w	fault	144	72	54	-		-	10	6636750.326	313454.277	1273
1270w	fault	65	60	335	-		-	50	6636751.200	313453.792	1273
1270w	fault	95	89	185	-		-	-	6636746.248	313453.108	1273
1270w	vein	150	70	60	-		-	-	6636747.997	313452.138	1273
1270w	fault	76	40	346	-		-	100	6636748.872	313451.653	1273
1270w	vein	62	50	332	-		-	150	6636747.807	313447.671	1273
1270w	shear zone	54	78	144	-		-	-	6636743.244	313445.627	1273
1270w	shear zone	54	78	324	-		-	-	6636744.119	313445.143	1273
1270w	shear zone	160	84	70	-		-	-	6636741.790	313443.004	1273
1270w	shear zone	27	68	297	-		-	-	6636742.665	313442.519	1273
1270w	joint	60	79	150	-		-	-	6636745.288	313441.065	1273
1270w	shear zone	40	79	130	-		-	-	6636739.461	313440.866	1273
1270w	fault	27	77	117	-		-	-	6636741.210	313439.896	1273
1270w	shear zone	65	85	335	-		-	100	6636738.007	313438.242	1272
1270w	shear zone	78	79	168	-		-	100	6636738.881	313437.757	1272
1270w	shear zone	74	90	344	-		-	100	6636736.553	313435.619	1274
1270w	shear zone	73	85	163	-		-	-	6636737.427	313435.134	1274
1270w	joint	5	76	95	-		-	-	6636740.925	313433.195	1274
1270w	shear zone	60	86	150	-		-	-	6636734.613	313432.121	1274
1270w	shear zone	83	85	353	-		-	-	6636735.488	313431.636	1274
1270w	vein	70	20	340	-		-	100	6636735.488	313431.636	1274
1270w	shear zone	61	86	331	-		-		6636736.362	313431.152	1274
1270w	shear zone	173	74	83	-		-	-	6636738.111	313430.182	1274
1270w	shear zone	170	76	80	-		-	-	6636738.986	313429.697	1274
1270w	vein	61	32	331	-		-	200	6636732.190	313427.749	1274
1270w	shear zone	16	75	286	-		-	150	6636733.064	313427.264	1274

Drive	Structure	Orientation					Offset	Fault Width	Northing	Easting	RL
		Strike	Dip	Dip direction	Plunge	Plunge dir					
1130e	fault	44	84	314	7	130	-	-	6637045.968	313964.864	1130
1130e	fault	67	85	337	-		-	-	6637043.924	313969.426	1130
1130e	fault	69	87	159	90	150	-	50	6637044.799	313968.941	1130
1130e	fault	130	55	40	-		-	50	6637044.799	313968.941	1130
1130e	fault	63	70	153	-		-	-	6637045.673	313968.457	1130
1130e	fault	162	45	72	-		-	30	6637045.673	313968.457	1130
1130e	fault	99	82	9	-		-	50	6637046.547	313967.972	1130
1130e	shear zone	60	80	330	-		-	50	6637046.253	313971.565	1130
1130e	fault	125	42	35	-		-	-	6637047.127	313971.080	1130
1130e	joint	70	78	160	-		-	-	6637048.002	313970.595	1130
1130e	shear zone	39	90	309	-		-	-	6637048.002	313970.595	1130
1130e	fault	82	85	352	-		-	50	6637048.876	313970.110	1130
1130e	shear zone	79	80	349	-		-	-	6637047.223	313973.314	1130
1130e	fault	70	86	340	-		-	-	6637050.720	313971.375	1130
1130e	shear zone	97	90	187	-		-	500	6637051.300	313974.483	1130
1130e	shear zone	37	90	307	-		-	200	6637053.049	313973.513	1130
1130e	shear zone	72	90	162	-		-	400	6637052.365	313978.465	1130
1130e	shear zone	57	90	147	-		-	600	6637054.988	313977.011	1130
1130e	fault	62	73	332	-		-	50	6637055.083	313979.245	1130
1130e	fault	72	77	342	-		-	50	6637055.958	313978.760	1130
1130e	fault	77	72	347	-		-	100	6637055.274	313983.712	1130
1130e	fault	30	65	300	-		-	-	6637055.274	313983.712	1130
1130e	fault	84	72	354	-		-	100	6637057.022	313982.742	1130
1130e	fault	64	48	334	-		-	50	6637055.369	313985.946	1130
1130e	shear zone	74	40	164	-		-	-	6637055.369	313985.946	1130
1130e	fault	78	82	168	-		-	100	6637056.243	313985.461	1130
1130e	fault	20	85	110	-		-	10	6637057.992	313984.491	1130
1130e	fault	54	78	324	-		r	100	6637058.866	313984.006	1130
1130e	fault	80	75	350	-		-	50	6637056.823	313988.569	1130
1130e	fault	50	87	320	-		r	100	6637057.697	313988.084	1130
1130e	fault	37	76	127	-		-	-	6637058.572	313987.599	1130
1130e	fault	84	77	354	-		-	-	6637059.446	313987.114	1130
1130e	fault	80	80	350	-		-	50	6637058.762	313992.067	1130
1130e	fault	74	85	164	-		-	150	6637059.637	313991.582	1130
1130e	fault	69	85	339	90	324	-	50	6637062.260	313990.127	1130

Drive	Structure	Orientation					Offset	Fault Width	Northing	Easting	RL
		Strike	Dip	Dip direction	Plunge	Plunge dir					
1130e	fault	117	58	27	-		-	20	6637059.342	313995.175	1130
1130e	fault	27	85	117	-		-	50	6637060.217	313994.690	1130
1130e	shear zone	32	74	122	-		-	-	6637061.965	313993.720	1130
1130e	fault	71	87	341	-		-	50	6637062.840	313993.236	1130
1130e	shear zone	52	70	322	-		-	200	6637060.312	313996.924	1130
1130e	shear zone	68	76	338	-		-	50	6637061.186	313996.439	1130
1130e	shear zone	67	79	157	-		-	-	6637062.061	313995.954	1130
1130e	shear zone	72	88	162	-		-	200	6637063.809	313994.984	1130
1130e	shear zone	62	75	152	-		-	500	6637020.759	313919.393	1130
1130e	shear zone	57	90	327	-		-	500	6637026.005	313916.484	1130
1130e	fault	87	78	177	-		-	-	6637020.378	313910.458	1130
1130e	shear zone	91	70	1	-		-	-	6637021.253	313909.973	1130
1130e	vein	91	50	1	-		-	-	6637022.127	313909.489	1130
1130e	shear zone	69	89	339	-		-	500	6637023.002	313909.004	1130
1130e	shear zone	49	87	319	-		-	-	6637021.642	313908.614	1130
1130e	shear zone	60	73	150	-		-	500	6637022.517	313908.129	1130
1130e	fault	62	80	152	-		-	100	6637017.470	313905.212	1130
1130e	fault	32	80	122	-		-	-	6637019.218	313904.242	1130
1130e	shear zone	77	75	347	-		-	-	6637020.093	313903.757	1130
1130w	fault	47	75	137	-		-	-	6637013.877	313904.917	1130
1130w	shear zone	67	80	337	-		-	200	6637014.751	313904.432	1130
1130w	shear zone	52	85	142	-		-	-	6637017.374	313902.978	1130
1130w	fault	67	88	337	-		-	-	6637015.236	313905.307	1130
1130w	fault	57	82	147	-		-	-	6637016.110	313904.822	1130
1130w	fault	56	81	326	18	54	-	-	6637017.859	313903.852	1130
1130w	shear zone	82	82	172	-	-	-	200	6637008.839	313891.705	1130
1130w	fault	62	82	332	-		-	-	6637009.713	313891.221	1130
1130w	joint	53	68	143	-		-	-	6637004.181	313887.428	1130
1130w	joint	68	68	158	-		-	-	6637005.055	313886.943	1130
1130w	joint	95	30	5	-		-	-	6637005.930	313886.459	1130
1130w	joint	82	69	172	-		-	-	6637005.930	313886.459	1130
1130w	fault	56	88	146	-		-	-	6637006.804	313885.974	1130
1130w	fault	62	85	332	-		-	-	6637007.679	313885.489	1130
1130w	shear zone	62	80	152	-		-	150	6637005.350	313883.351	1130
1130w	vein	32	90	122	-		-	-	6637006.224	313882.866	1130

Drive	Structure	Orientation					Offset	Fault Width	Northing	Easting	RL
		Strike	Dip	Dip direction	Plunge	Plunge dir					
1130w	fault	62	80	332	-		-	1000	6637003.506	313882.087	1130
1130w	vein	102	60	12	-		-	50	6637006.129	313880.632	1130
1130w	fault	62	85	152	-		d	-	6637002.052	313879.463	1130
1130w	shear zone	72	80	342	-		-	200	6637002.926	313878.978	1130
1135e	shear zone	62	68	332	-		-	-	6637098.315	314069.597	1135
1135e	fault	92	61	182	-		-	-	6637099.190	314069.112	1135
1135e	shear zone	102	55	192	-		-	-	6637100.064	314068.628	1135
1135e	shear zone	118	67	208	-		-	-	6637100.064	314068.628	1135
1135e	shear zone	79	81	349	-		-	-	6637101.813	314067.658	1135
1135e	shear zone	65	76	335	-		-	-	6637102.687	314067.173	1135
1135e	shear zone	84	74	354	-		-	-	6637098.505	314074.065	1135
1135e	vein	110	61	200	-		-	-	6637099.380	314073.580	1135
1135e	joint	80	81	170	-		-	-	6637100.254	314073.095	1135
1135e	joint	77	80	167	-		-	-	6637101.129	314072.610	1135
1135e	joint	70	84	160	-		-	-	6637101.129	314072.610	1135
1135e	shear zone	86	64	176	-		-	-	6637102.003	314072.125	1135
1135e	shear zone	76	83	166	-		-	-	6637102.878	314071.641	1135
1135e	shear zone	72	70	162	-		-	-	6637102.878	314071.641	1135
1135e	shear zone	84	78	354	-		-	150	6637097.726	314076.783	1135
1135e	shear zone	82	73	172	-		-	-	6637098.600	314076.298	1135
1135e	shear zone	71	88	161	-		-	-	6637099.475	314075.813	1135
1135e	shear zone	82	80	172	-		-	-	6637099.475	314075.813	1135
1135e	shear zone	81	75	351	-		-	-	6637102.098	314074.359	1135
1135e	shear zone	57	70	327	-		-	200	6637098.401	314082.125	1135
1135e	shear zone	80	81	170	-		-	-	6637099.276	314081.640	1135
1135e	fault	77	81	167	-		-	-	6637100.150	314081.155	1135
1135e	vein	102	57	12	-		-	-	6637101.024	314080.670	1135
1135e	shear zone	64	87	154	-		-	-	6637101.899	314080.186	1135
1135e	shear zone	82	80	172	-		-	-	6637100.920	314088.731	1135
1135e	shear zone	87	60	357	-		-	-	6637102.669	314087.761	1135
1135e	shear zone	69	25	159	-		-	-	6637103.543	314087.276	1135
1135e	shear zone	67	85	157	-		-	500	6637104.418	314086.792	1135
1260e	fault	138	84	228	-		-	-	6636829.840	313587.391	1260
1260e	fault	66	60	336	-		-	-	6636832.853	313584.577	1260
1260w	shear zone	153	87	63	-		-	-	6636737.998	313448.536	1260

Drive	Structure	Orientation					Offset	Fault Width	Northing	Easting	RL
		Strike	Dip	Dip direction	Plunge	Plunge dir					
1260w	shear zone	41	80	311	-		-	-	6636739.747	313447.567	1260
1260w	shear zone	39	70	129	-		-	-	6636740.621	313447.082	1260
1260w	shear zone	145	78	55	-		-	-	6636738.578	313451.644	1260
1260w	shear zone	83	71	353	-		-	-	6636739.452	313451.159	1260
1260w	shear zone	51	65	321	-		-	-	6636742.075	313449.705	1260
1260w	shear zone	143	60	233	-		-	-	6636742.950	313449.220	1260
1260w	fault	177	88	267	-		-	-	6636741.002	313456.016	1260
1260w	fault	128	64	38	-		-	-	6636741.876	313455.532	1260
1260w	fault	162	78	72	-		-	-	6636742.751	313455.047	1260
1260w	fault	45	64	315	-		-	-	6636743.625	313454.562	1260
1260w	fault	64	90	334	-		-	-	6636744.499	313454.077	1260
1260w	fault	32	75	302	-		-	-	6636745.374	313453.593	1260
1260w	fault	17	75	287	-		-	-	6636746.248	313453.108	1260
1260w	shear zone	66	25	156	-		-	-	6636743.625	313454.562	1260
1260w	shear zone	52	70	322	-		-	-	6636741.971	313457.765	1260
1260w	shear zone	33	68	303	-		-	-	6636741.971	313457.765	1260
1260w	shear zone	22	70	292	-		-	-	6636742.846	313457.281	1260
1260w	shear zone	107	72	17	70	43	-	-	6636744.595	313456.311	1260
1260w	shear zone	17	75	287	70	43	-	-	6636745.469	313455.826	1260
1260w	shear zone	40	66	310	-		-	-	6636743.521	313462.622	1260
1260w	shear zone	6	83	276	-		-	-	6636744.395	313462.138	1260
1260w	shear zone	171	80	81	77	16	-	-	6636745.270	313461.653	1260
1260w	shear zone	103	75	193	-		-	-	6636747.018	313460.683	1260
1260w	shear zone	29	66	299	-		-	-	6636747.893	313460.198	1260
1260w	shear zone	2	65	92	-		-	1000	6636749.728	313471.756	1260
1260w	fault	42	88	312	-		-	-	6636751.667	313475.254	1260
1260w	fault	0	80	90	-		-	-	6636753.416	313474.285	1260
1260w	fault	166	85	256	-		d	-	6636755.165	313473.315	1260
1260w	fault	70	65	340	-		d	200	6636759.822	313477.592	1260
1260w	shear zone	62	80	332	-		-	500	6636756.515	313483.999	1260
1270e	shear zone	90	80	0	25	269	-	200	6636799.565	313559.590	1266
1270e	fault	76	78	346	-		-	-	6636799.470	313557.356	1266
1270e	vein	72	85	342	-		-	-	6636799.765	313553.763	1267
1270e	fault	82	85	352	-		-	-	6636796.951	313550.751	1268
1270w	fault	13	85	103	-		-	-	6636775.145	313501.107	1272

Drive	Structure	Orientation					Offset	Fault Width	Northing	Easting	RL
		Strike	Dip	Dip direction	Plunge	Plunge dir					
1270w	fault	7	80	97	36	181	-	-	6636774.565	313497.999	1272
1270w	fault	158	85	68	41	161	-	-	6636775.440	313497.514	1272
1270w	fault	163	85	73	17	163	-	-	6636749.252	313460.588	1273
1270w	fault	170	78	80	-		-	10	6636751.001	313459.618	1273
1270w	fault	160	75	70	25	157	-	-	6636747.408	313459.324	1273
1270w	fault	105	62	195	-		-	10	6636748.283	313458.839	1273
1270w	fault	79	50	349	-		-	50	6636749.157	313458.354	1273
1270w	fault	170	62	80	-		-	10	6636750.031	313457.870	1273
1270w	fault	82	82	352	-		-	10	6636746.828	313456.216	1273
1270w	fault	144	72	54	-		-	10	6636750.326	313454.277	1273
1270w	fault	65	60	335	-		-	50	6636751.200	313453.792	1273
1270w	fault	95	89	185	-		-	-	6636746.248	313453.108	1273
1270w	vein	150	70	60	-		-	-	6636747.997	313452.138	1273
1270w	fault	76	40	346	-		-	100	6636748.872	313451.653	1273
1270w	vein	62	50	332	-		-	150	6636747.807	313447.671	1273
1270w	shear zone	54	78	144	-		-	-	6636743.244	313445.627	1273
1270w	shear zone	54	78	324	-		-	-	6636744.119	313445.143	1273
1270w	shear zone	160	84	70	-		-	-	6636741.790	313443.004	1273
1270w	shear zone	27	68	297	-		-	-	6636742.665	313442.519	1273
1270w	joint	60	79	150	-		-	-	6636745.288	313441.065	1273
1270w	shear zone	40	79	130	-		-	-	6636739.461	313440.866	1273
1270w	fault	27	77	117	-		-	-	6636741.210	313439.896	1273
1270w	shear zone	65	85	335	-		-	100	6636738.007	313438.242	1272
1270w	shear zone	78	79	168	-		-	100	6636738.881	313437.757	1272
1270w	shear zone	74	90	344	-		-	100	6636736.553	313435.619	1274
1270w	shear zone	73	85	163	-		-	-	6636737.427	313435.134	1274
1270w	joint	5	76	95	-		-	-	6636740.925	313433.195	1274
1270w	shear zone	60	86	150	-		-	-	6636734.613	313432.121	1274
1270w	shear zone	83	85	353	-		-	-	6636735.488	313431.636	1274
1270w	vein	70	20	340	-		-	100	6636735.488	313431.636	1274
1270w	shear zone	61	86	331	-		-		6636736.362	313431.152	1274
1270w	shear zone	173	74	83	-		-	-	6636738.111	313430.182	1274
1270w	shear zone	170	76	80	-		-	-	6636738.986	313429.697	1274
1270w	vein	61	32	331	-		-	200	6636732.190	313427.749	1274
1270w	shear zone	16	75	286	-		-	150	6636733.064	313427.264	1274

Drive	Structure	Orientation					Offset	Fault Width	Northing	Easting	RL
		Strike	Dip	Dip direction	Plunge	Plunge dir					
1270w	fault	58	84	328	-		d	-	6636734.813	313426.295	1274
1270w	shear zone	52	81	322	-		-	-	6636734.813	313426.295	1274
1270w	shear zone	59	75	329	-		-	-	6636735.687	313425.810	1274
1270w	vein	70	22	340	-		-	200	6636730.640	313422.892	1274
1270w	shear zone	59	80	329	-		-	200	6636731.515	313422.407	1274
1270w	fault	97	52	187	-		-	20	6636732.389	313421.922	1274
1270w	shear zone	57	78	147	-		-	200	6636732.389	313421.922	1274
1270w	vein	63	32	333	-		-	150	6636729.575	313418.909	1274
1270w	shear zone	64	52	334	-		-	200	6636730.450	313418.425	1274
1270w	shear zone	73	75	343	-		-	200	6636731.324	313417.940	1274
1270w	fault	70	76	160	-		-	-	6636785.810	313520.344	1272
1270w	fault	12	84	102	27	180	-	-	6636789.308	313518.405	1272
1270w	fault	23	86	293	19	193	-	-	6636791.057	313517.436	1272
1270w	fault	177	90	267	20	179	-	-	6636792.806	313516.466	1272
1300w	fault	26	80	116	-		-	-	6636718.312	313417.151	1300
1300w	fault	162	55	72	-		-	-	6636720.061	313416.182	1300
1300w	fault	48	62	138	-		-	-	6636720.935	313415.697	1300
1300w	fault	65	40	335	-		-	-	6636721.810	313415.212	1300
1300w	shear zone	47	84	317	-		-	-	6636722.485	313420.554	1300
1300w	vein	33	38	303	-		-	100	6636725.108	313419.100	1300
1300w	shear zone	67	77	337	-		-	-	6636725.982	313418.615	1300
1300w	shear zone	64	89	334	-		-	-	6636723.065	313423.662	1300
1300w	shear zone	42	90	312	-		-	-	6636723.939	313423.177	1300
1300w	vein	70	85	340	-		-	-	6636725.688	313422.208	1300
1300w	shear zone	96	84	186	-		-	-	6636726.562	313421.723	1300
1300w	shear zone	62	70	332	-		-	500	6636728.207	313428.814	1300
1300w	fault	177	60	267	-		-	-	6636729.081	313428.329	1300
1300w	fault	57	70	327	-		-	-	6636729.272	313432.796	1300
1300w	shear zone	54	78	324	-		-	-	6636730.241	313434.545	1300
1300w	shear zone	43	78	133	-		-	-	6636731.990	313433.576	1300
1300w	fault	67	80	337	-		-	-	6636731.696	313437.168	1300
1300w	shear zone	32	90	302	-		-	-	6636732.371	313442.510	1298
1300w	fault	62	80	332	-		-	-	6636733.245	313442.025	1298
1300w	fault	127	60	37	-		-	-	6636734.994	313441.056	1298
1300w	shear zone	61	74	331	-		-	-	6636734.699	313444.649	1298

Drive	Structure	Orientation					Offset	Fault Width	Northing	Easting	RL
		Strike	Dip	Dip direction	Plunge	Plunge dir					
1300w	shear zone	39	87	129	-		-	-	6636736.448	313443.679	1298
1300w	fault	2	85	92	30	72	s	-	6636758.264	313483.029	1298
1300w	fault	48	76	318	-		-	-	6636757.969	313486.622	1298
1300w	fault	80	25	350	-		s	-	6636801.645	313513.852	1298
1300w	fault	65	74	335	-		-	-	6636759.423	313489.245	1298
1300w	fault	116	79	206	-		-	-	6636762.047	313487.791	1298
1300w	fault	42	80	312	-		-	-	6636761.363	313492.743	1298
1300w	fault	56	75	326	-		-	-	6636762.237	313492.258	1298
1300w	fault	60	76	330	-		-	-	6636765.051	313495.271	1298
1300w	fault	47	75	317	-		-	-	6636766.115	313499.254	1298
1300w	fault	56	80	326	-		-	-	6636769.414	313503.141	1298
1300w	fault	177	86	267	45	197	d	-	6636771.163	313502.172	1298
1300w	fault	37	88	307	-		-	-	6636769.994	313506.249	1298
1300w	fault	58	79	328	-		-	-	6636770.868	313505.764	1298
1300w	fault	58	74	328	-		-	-	6636771.933	313509.747	1298
1300w	fault	63	75	333	-		-	-	6636772.807	313509.262	1298
1300w	fault	87	85	357	-		-	-	6636773.682	313508.777	1298
1300w	fault	60	75	330	-		-	-	6636773.387	313512.370	1298
1300w	fault	64	85	334	-		-	-	6636775.136	313511.401	1298
1300w	fault	62	75	332	-		-	-	6636775.906	313518.976	1298
1300w	fault	60	84	330	-		-	-	6636777.655	313518.007	1298
1300w	fault	32	70	302	-		-	-	6636779.300	313525.097	1297
1300w	fault	39	85	309	-		-	-	6636780.174	313524.612	1297
1300w	fault	70	65	340	-		-	-	6636781.048	313524.128	1297
1300w	fault	4	82	274	30	197	s	-	6636781.048	313524.128	1297
1300w	fault	70	90	340	-		-	-	6636781.923	313523.643	1297
1300w	shear zone	172	70	82	-		-	500	6636766.990	313498.769	1298
1300w	fault	172	80	82	-		-	500	6636767.864	313498.284	1298
1300w	fault	162	70	252	-		-	-	6636769.613	313497.315	1298
1300w	fault	39	80	129	-		-	50	6636765.830	313492.553	1298
1300w	fault	64	87	154	-		-	-	6636767.579	313491.583	1298
1300w	fault	52	85	142	-		-	-	6636768.453	313491.098	1298
1300w	joint	49	89	139	-		-	-	6636762.627	313490.899	1298
1300w	shear zone	52	78	322	-		-	200	6636763.501	313490.414	1298
1300w	fault	67	83	337	-		-	-	6636763.501	313490.414	1298

Drive	Structure	Orientation					Offset	Fault Width	Northing	Easting	RL
		Strike	Dip	Dip direction	Plunge	Plunge dir					
1300w	fault	84	83	354	-		-	-	6636763.501	313490.414	1298
1300w	shear zone	52	86	322	-		-	200	6636759.328	313487.011	1298
1300w	shear zone	59	76	329	-		-	100	6636760.203	313486.527	1298
1300w	shear zone	49	83	319	-		-	250	6636761.077	313486.042	1298
1300w	shear zone	80	88	350	-		-	100	6636761.952	313485.557	1298
1300w	fault	137	80	47	-		-	-	6636757.874	313484.388	1298
1300w	fault	92	80	2	-		-	-	6636759.623	313483.419	1298
1300w	slickensides	-	-	-	60	52	-	-	6636761.372	313482.449	1298
1300w	fault	32	90	302	-		-	-	6636751.372	313478.847	1298
1300w	fault	71	90	341	-		-	-	6636752.247	313478.362	1298
1300w	fault	97	45	7	-		-	-	6636753.121	313477.877	1298
1300w	fault	37	80	307	-		-	-	6636753.996	313477.393	1298
1300w	fault	165	88	75	-		-	-	6636746.620	313472.336	1298
1300w	fault	160	69	70	-		-	-	6636746.620	313472.336	1298
1300w	shear zone	149	78	59	-		-	-	6636747.494	313471.851	1298
1300w	vein	80	37	350	-		-	-	6636748.369	313471.367	1298
1300w	shear zone	162	77	72	-		-	100	6636744.291	313470.198	1298
1300w	shear zone	147	76	57	-		-	100	6636746.040	313469.228	1298
1300w	shear zone	172	67	82	-		-	100	6636746.914	313468.743	1298
1300w	vein	52	50	322	-		-	100	6636748.663	313467.774	1298
1300w	shear zone	138	78	48	-		-	-	6636742.352	313466.700	1298
1300w	fault	144	67	54	-		-	-	6636743.226	313466.215	1298
1300w	fault	153	74	63	-		-	-	6636744.101	313465.730	1298
1300w	fault	73	37	343	-		-	100	6636745.849	313464.761	1298
1300w	fault	140	88	50	-		-	-	6636746.724	313464.276	1298
1320w	vein	82	50	352	-		-	-	6636729.281	313422.502	1319
1320w	fault	26	58	296	-		-	-	6636737.133	313438.727	1319
1320w	fault	77	35	347	-		-	-	6636738.007	313438.242	1319
1320w	fault	61	51	331	-		-	-	6636739.072	313442.225	1319
1320w	fault	111	78	21	-		-	-	6636739.946	313441.740	1319
1320w	fault	144	70	54	30	138	s	-	6636741.106	313447.956	1319
1320w	fault	60	86	150	28	233	d	-	6636743.920	313450.969	1319
1320w	fault	59	59	329	-		-	-	6636699.102	313396.935	1319
1320w	fault	8	60	98	-		-	-	6636700.851	313395.965	1319
1320w	fault	42	85	312	-		-	-	6636735.175	313455.817	1320

Drive	Structure	Orientation					Offset	Fault Width	Northing	Easting	RL
		Strike	Dip	Dip direction	Plunge	Plunge dir					
1320w	fault	107	75	197	-		-	100	6636736.050	313455.332	1320
1320w	fault	82	70	352	-		-	100	6636733.825	313445.133	1320
1320w	vein	32	37	302	-		-	-	6636733.825	313445.133	1320
1320w	vein	97	78	7	-		-	300	6636734.699	313444.649	1320
1320w	fault	87	28	357	-		-	-	6636736.448	313443.679	1320
1320w	shear zone	62	75	152	-		-	-	6636731.886	313441.636	1320
1320w	fault	72	85	342	-		-	-	6636730.432	313439.012	1320
1320w	shear zone	72	80	162	-		-	-	6636731.306	313438.528	1320
1320w	fault	70	83	340	-		-	-	6636730.726	313435.420	1320
1320w	fault	62	89	332	-		d	150	6636729.272	313432.796	1320
1320w	fault	56	46	326	-		-	-	6636726.848	313428.424	1320
1320w	fault	58	90	328	-		-	200	6636727.722	313427.939	1320
1320w	vein	97	45	7	35	-	-	-	6636723.939	313423.177	1320
1320w	shear zone	77	85	347	165	-	-	250	6636726.562	313421.723	1320
1320xc	shear zone	177	70	87	-		-	100	6636755.468	313459.428	1318
1320xc	fault	62	85	332	-		-	-	6636749.053	313466.415	1320
v1270e	fault	147	90	237	-		-	-	6636823.234	313589.910	1262
v1270e	fault	177	85	87	-		-	-	6636824.108	313589.425	1262
v1270e	fault	27	80	297	-		-	-	6636825.857	313588.456	1262
v1270e	fault	56	90	326	30	240	-	-	6636819.061	313586.507	1262
v1270e	fault	17	87	107	-		-	-	6636815.858	313584.854	1262
v1270e	vein	17	85	107	-		-	-	6636815.858	313584.854	1262
v1270e	shear zone	56	90	326	30	240	-	150	6636814.204	313588.057	1262
v1270e	shear zone	50	78	320	-		-	-	6636809.546	313583.780	1262
v1270e	fault	171	88	81	-		-	-	6636811.295	313582.810	1262
v1270e	vein	48	85	318	-		-	-	6636811.970	313588.152	1262
v1270e	fault	17	87	107	-		-	-	6636812.845	313587.667	1262
v1270e	vein	45	85	315	-		-	-	6636808.577	313582.031	1263
v1270e	shear zone	69	71	339	-		-	-	6636803.824	313575.520	1265
v1270e	vein	69	80	339	-		-	-	6636801.885	313572.022	1265
v1270e	shear zone	82	80	352	29	263	-	-	6636800.431	313569.399	1264
v1270e	shear zone	79	90	349	-		-	-	6636798.025	313544.439	1270
v1270e	fault	177	75	267	84	1	-	-	6636798.900	313543.954	1270
v1270e	vein	72	75	342	-		d	50	6636796.086	313540.941	1270
v1270e	vein	82	50	352	-		-	150	6636799.584	313539.002	1270

Drive	Structure	Orientation					Offset	Fault Width	Northing	Easting	RL
		Strike	Dip	Dip direction	Plunge	Plunge dir					
v1270e	vein	105	39	15	-		-	150	6636799.004	313535.894	1272
v1270e	fault	69	80	339	-		-	-	6636794.536	313536.084	1272
v1270e	fault	87	85	357	-		-	-	6636795.411	313535.600	1272
v1270e	vein	92	35	2	-		-	-	6636798.909	313533.660	1272
v1270e	shear zone	66	80	336	-		-	150	6636793.567	313534.336	1272
v1270e	fault	71	44	341	-		-	-	6636794.441	313533.851	1272
v1270e	fault	62	73	152	-		-	-	6636795.316	313533.366	1272
v1270e	fault	64	70	334	24	254	-	-	6636792.987	313531.227	1271
v1270e	fault	96	68	186	-		-	-	6636795.610	313529.773	1271
v1270e	fault	67	79	337	-		-	-	6636790.173	313528.214	1271
v1270e	fault	100	70	190	22	272	d	-	6636793.671	313526.275	1271
v1270e	fault	67	70	337	-		d	-	6636789.204	313526.466	1272
v1270e	vein	92	80	182	-		-	-	6636792.702	313524.526	1272
v1270e	shear zone	63	89	333	13	238	-	-	6636787.265	313522.968	1272
v1270e	fault	70	76	160	-		-	-	6636785.810	313520.344	1272
v1270e	fault	12	84	102	27	180	-	-	6636789.308	313518.405	1272
v1270e	fault	23	86	293	19	193	-	-	6636790.183	313517.921	1272
v1270e	fault	177	90	267	20	179	-	-	6636791.931	313516.951	1272
v1270e	fault	82	54	352	-		-	-	6636793.680	313515.981	1272
v1270e	fault	71	82	161	32	250	-	-	6636790.772	313510.735	1272
v1270e	fault	102	44	12	-		-	-	6636792.520	313509.765	1272
v1270e	fault	16	7	106	80	10	-	-	6636796.893	313507.341	1272
v1270e	shear zone	67	40	337	6	257	-	-	6637586.512	313069.581	1272
v1270e	shear zone	32	60	302	36	232	-	-	6636779.508	313508.977	1271

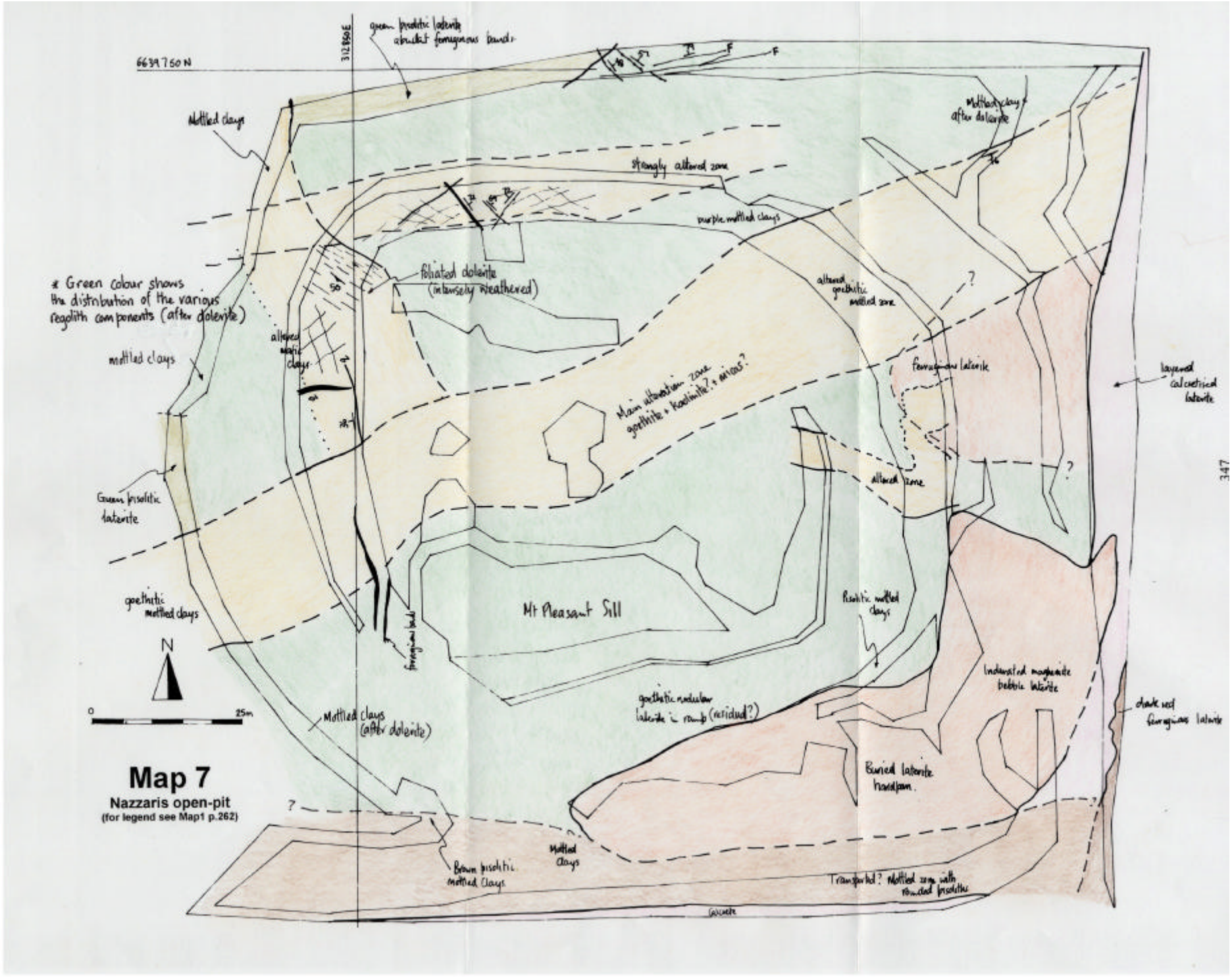
6639750 N
312850E
green fisolitic laterite
abundant ferruginous bauxite
Mottled clays
Mottled clay after dolerite
strongly altered zone
purple mottled clays
foliated dolerite
(intensely weathered)
altered goethitic mottled zone
* Green colour shows the distribution of the various regolith components (after dolerite)
altered mafic clays
mottled clays
Main alteration zone goethite + kaolinite? + gibbsite?
ferruginous laterite
layered calcretised laterite
altered zone
Green fisolitic laterite
Mt Pleasant Sill
goethitic mottled clays
fisolitic mottled clays
ferruginous bauxite
N
0
25m
Mottled clays (after dolerite)
goethitic nodular laterite in rumpy (residual?)
Indurated magnetite pebble laterite
dark red ferruginous laterite
Buried laterite hardpan.
Brown fisolitic mottled clays
Mottled clays
Transported? Mottled zone with rounded fisolithes
Map 7
Nazzaris open-pit
(for legend see Map1 p.262)

Table A1.12 - Nazzaris Deposit, structural data from diamond drill core (from G. Adams)

HOLE NO	DEPTH	STRUCTURE	ALPHA	BETA	STRIKE	DIP	DIP DIRECTION	MINERALOGY	ALTERATION	GROUP	OVERPRINTING	HOLE DIP	HOLE AZIM	Au VALUE	COMMENTS
NOBD4	120.20	quartz vein	-	-	20	69	290	-	-	V6	-	62	180	0.04	1cm quartz vein with parallel pyrite and fracturing
NOBD4	120.24	shear zone	-	-	30	70	300	-	-	SH6	-	62	180	0.04	Shear zone with slip lineation and 1mm quartz infill
NOBD4	120.24	slip lineation	-	-	-	66	328	-	-	Lslk	-	62	180	0.04	Slip lineations
NOBD4	120.48	joint	-	-	15	88	105	-	-	J2	-	62	180	0.04	Fracture parallel to core with quartz biotite pyrite infill
NOBD4	122.22	shear zone	-	-	146	48	236	-	-	SH6	-	62	180	0.03	Shear zone with slip lineation
NOBD4	122.22	slip lineation	-	-	-	2	148	-	-	Lslk	-	62	180	0.03	Slip lineations
NOBD4	122.77	shear zone	-	-	47	33	317	-	-	SH6	-	62	180	0.03	Shear zone with slip lineation and 1mm quartz infill
NOBD4	122.77	slip lineation	-	-	-	27	335	-	-	Lslk	-	62	180	0.03	Slip lineations
NOBD4	122.80	quartz vein	-	-	360	90	360	-	-	V6	-	62	180	0.03	6mm quartz vein with biotite
NOBD4	123.58	quartz vein	-	-	61	66	331	-	-	V6	-	62	180	0.03	1cm quartz vein
NOBD4	125.26	joint	-	-	92	59	182	-	-	J2	-	62	186	0.02	Pyrite filled fracture
NOBD4	125.45	joint	-	-	37	43	307	-	-	J1	xprev	62	186	0.02	Fracture with quartz carbonate pyrite infill
NOBD4	126.63	quartz vein	-	-	42	46	312	-	-	V6	xnxt	62	186	0.01	3mm quartz carbonate vein
NOBD4	126.70	quartz vein	-	-	66	71	156	-	-	V6	-	62	186	0.01	5mm quartz carbonate vein with pyrite + chlorite
NOBD4	127.81	quartz vein	-	-	86	75	356	-	-	V6	-	62	186	0.06	4mm quartz carbonate vein with chlorite and biotite
NOBD4	128.00	quartz vein	-	-	76	85	166	-	-	V6	-	62	186	0.04	2mm quartz vein
NOBD4	128.65	quartz vein	-	-	134	31	224	-	-	V6	-	62	186	0.04	1cm quartz vein with biotite pyrite
NOBD4	129.73	quartz vein	-	-	84	79	354	-	-	V6	-	62	186	0.01	2mm quartz carbonate vein
NOBD4	131.58	layering	-	-	-	27	335	-	-	Lslk	-	62	186	0.07	Layering
NOBD4	131.76	joint	-	-	65	86	335	-	-	J1	-	62	186	0.07	Fracture filled with quartz, feldspar, chlorite
NOBD4	131.83	quartz vein	-	-	360	90	360	-	-	V6	-	62	186	0.07	Quartz carbonate vein
NOBD4	131.85	joint	-	-	7	47	277	-	-	FR	-	62	186	0.07	Fracture filled with calcite pyrite
NOBD4	133.27	calcite vein	-	-	45	46	315	-	-	V6	-	62	186	0.02	4mm fibrous calcite vein
NOBD4	134.80	schistosity	-	-	126	44	216	-	-	CC	-	62	186	0.03	Weak schistosity
NOBD4	135.69	quartz vein	-	-	29	56	299	-	-	V6	-	63	177	0.02	6mm quartz carbonate vein
NOBD4	136.00	schistosity	-	-	135	38	225	-	-	CC	-	63	177	0.02	Weak schistosity
NOBD4	137.51	quartz vein	-	-	103	16	193	-	-	V6	-	63	177	0.02	35mm quartz carbonate vein with pyrite chlorite
NOBD4	139.24	quartz vein	-	-	23	17	293	-	-	V6	-	63	177	0.02	2mm quartz carbonate vein
NOBD4	146.06	quartz vein	-	-	65	88	155	-	-	V6	-	63	180	0.07	10mm quartz vein
NOBD4	148.05	quartz vein	-	-	86	88	356	-	-	V6	-	63	180	0.02	5mm quartz vein with chlorite
NOBD4	150.69	joint	-	-	67	67	337	-	-	J1	-	63	180	0.02	Fracture
NOBD4	150.70	quartz vein	-	-	67	67	337	-	-	V6	-	63	180	0.02	10mm quartz carbonate vein
NOBD4	150.86	quartz vein	-	-	28	77	298	-	-	V6	-	63	180	0.02	20mm quartz carbonate vein

HOLE NO	DEPTH	STRUCTURE	ALPHA	BETA	STRIKE	DIP	DIP DIRECTION	MINERALOGY	ALTERATION	GROUP	OVERPRINTING	HOLE DIP	HOLE AZIM	Au VALUE	COMMENTS
NOBD4	152.59	quartz vein	-	-	17	24	287	-	-	V6	-	63	180	0.02	5mm quartz carbonate vein with chlorite
NOBD4	152.64	quartz vein	-	-	27	88	117	-	-	V6	-	63	180	0.02	2mm quartz carbonate vein
NOBD4	154.06	quartz vein	-	-	172	26	82	-	-	V6	-	63	180	0.02	1mm quartz carbonate vein
NOBD4	154.10	quartz vein	-	-	20	61	290	-	-	V6	-	63	180	0.02	1mm quartz carbonate vein
NOBD4	154.12	schistosity	-	-	15	45	105	-	-	CC	-	63	180	0.02	Moderate schistosity defined by biotite
NOBD4	154.64	quartz vein	-	-	146	50	236	-	-	V6	-	63	180	0.02	Quartz carbonate vein with biotite and chlorite
NOBD4	154.64	schistosity	-	-	146	50	236	-	-	CC	-	63	180	0.02	Strong schistosity defined by biotite and chlorite around vein
NOBD4	157.05	joint	-	-	2	40	272	-	-	J2	-	63	180	0.02	Fracture plane with biotite
NOBD4	157.22	quartz vein	-	-	22	67	292	-	-	V6	-	63	180	0.02	Quartz carbonate vein with biotite
NOBD4	157.30	schistosity	-	-	152	40	242	-	-	CC	-	63	180	0.02	Moderate schistosity
NOBD4	158.00	calcite vein	-	-	30	87	300	-	-	V6	-	63	180	0.02	Calcite vein
NOBD4	159.04	quartz vein	-	-	21	47	291	-	-	V6	-	63	180	0.02	Quartz carbonate vein with biotite and chlorite
NOBD4	159.05	shear zone	-	-	21	47	291	-	-	SH6	-	63	180	0.02	Shear vein
NOBD5	120.72	joint	-	-	80	44	170	-	-	J1	-	63	175	2.35	2mm fracture with calcite and pyrite
NOBD5	121.00	quartz vein	-	-	42	79	312	-	-	V6	-	63	175	1.12	0.3m quartz vein with pyrite and minor calcite-biotite
NOBD5	121.45	quartz vein	-	-	61	60	331	-	-	V6	-	63	175	1.12	20mm quartz carbonate vein rimmed by pyrite
NOBD5	121.76	quartz vein	-	-	103	80	193	-	-	V6	-	63	175	1.12	3mm fractured quartz carbonate vein
NOBD5	121.88	quartz vein	-	-	49	63	319	-	-	V6	xprev	63	175	1.12	6mm quartz vein cross-cuts bedding and schistosity
NOBD5	121.95	layering	-	-	323	42	233	-	-	BED6	-	63	175	1.12	Layering with a faint parallel schistosity
NOBD5	122.22	quartz vein	-	-	99	79	189	-	-	V6	-	63	175	0.08	4mm quartz carbonate vein
NOBD5	122.30	quartz vein	-	-	68	57	338	-	bi	V6	-	63	175	0.08	10mm quartz carbonate vein
NOBD5	124.68	quartz vein	-	-	75	62	345	-	-	V6	-	63	175	0.04	5mm quartz carbonate vein
NOBD5	124.80	shear zone	-	-	16	10	286	-	-	SH6	-	63	175	0.04	Small shear zone with calcite cross-cuts schistosity
NOBD5	124.92	quartz vein	-	-	73	56	343	-	-	V6	-	63	175	0.04	5mm quartz carbonate vein
NOBD5	125.18	shear zone	-	-	167	35	257	-	-	SH6	-	63	175	0.03	Small shear zone with calcite cross-cuts schistosity
NOBD5	125.30	schistosity	-	-	137	53	227	-	-	CC	-	63	175	0.02	Schistosity defined by biotite and chlorite
NOBD5	125.38	shear zone	-	-	163	37	253	-	-	SH6	-	63	175	0.03	Shear zone with biotite
NOBD5	125.48	quartz vein	-	-	76	83	346	-	-	V6	-	63	175	0.03	4mm quartz carbonate vein
NOBD5	125.61	shear zone	-	-	58	18	148	-	-	SH6	-	63	175	0.03	10mm shear zone with calcite infill and biotite
NOBD5	132.14	quartz vein	-	-	18	45	288	-	-	V6	xnxt2	64	174	0.01	3mm quartz carbonate vein
NOBD5	132.18	quartz vein	-	-	6	58	96	-	-	V6	-	64	174	0.01	2mm quartz carbonate vein
NOBD5	132.50	calcite vein	-	-	36	85	126	-	-	V6	-	64	174	0.01	3mm calcite vein
NOBD5	132.60	calcite vein	-	-	71	55	161	-	-	V6	-	64	174	0.01	2mm calcite vein
NOBD5	132.73	schistosity	-	-	123	44	213	-	-	CC	-	64	174	0.01	Weak schistosity

HOLE NO	DEPTH	STRUCTURE	ALPHA	BETA	STRIKE	DIP	DIP DIRECTION	MINERALOGY	ALTERATION	GROUP	OVERPRINTING	HOLE DIP	HOLE AZIM	Au VALUE	COMMENTS
NOBD5	133.47	calcite vein	-	-	64	60	334	-	-	V6	xnxt	64	174	0.02	4mm calcite vein
NOBD5	133.60	calcite vein	-	-	52	68	142	-	-	V6	-	64	174	0.02	2mm calcite vein
NOBD5	133.68	schistosity	-	-	118	47	208	-	-	CC	-	64	174	0.02	Weak schistosity
NOBD5	135.23	schistosity	-	-	122	44	212	-	-	CC	-	64	174	0.01	Strong schistosity around sheared quartz carbonate vein
NOBD5	135.27	shear zone	-	-	122	44	212	-	bi	V6	-	64	174	0.01	12mm quartz carbonate vein with biotite alteration
NOBD5	135.34	calcite vein	-	-	103	36	193	-	-	V6	-	64	174	0.01	1mm calcite vein
NOBD5	136.52	calcite vein	-	-	110	55	200	-	-	V6	-	64	174	0.01	1mm calcite vein
NOBD5	136.56	schistosity	-	-	125	50	215	-	-	CC	-	64	174	0.01	Weak schistosity defined by biotite
NOBD5	136.70	shear zone	-	-	1	44	271	-	-	SH6	-	64	174	0.01	Shear zone with biotite
NOBD5	137.00	quartz vein	-	-	125	60	215	-	-	V6	-	64	174	0.62	3mm calcite vein parallel to schistosity
NOBD5	137.80	calcite vein	-	-	129	31	219	-	-	V6	-	64	174	0.62	1mm calcite vein
NOBD5	137.84	schistosity	-	-	129	45	219	-	-	CC	-	64	174	0.62	Weak schistosity
NOBD5	137.89	quartz vein	-	-	62	67	152	-	-	V6	-	64	174	0.62	3mm calcite vein
NOBD5	137.93	quartz vein	-	-	109	28	19	-	-	V6	xprev	64	174	0.62	50mm quartz vein
NOBD5	138.13	quartz vein	-	-	75	52	165	-	ch	V6	-	64	174	0.16	5mm quartz carbonate vein
NOBD5	138.43	quartz vein	-	-	154	32	64	-	-	V6	-	64	174	0.16	3mm quartz vein
NOBD5	138.57	shear zone	-	-	34	71	304	-	-	V6	-	64	174	0.16	10mm quartz vein
NOBD5	138.69	quartz vein	-	-	101	45	11	-	-	V6	-	64	174	0.16	50mm quartz vein
NOBD5	138.69	shear zone	-	-	101	45	11	-	-	SH6	-	64	174	0.16	Shear zone on top of quartz vein with slip lineations
NOBD5	138.69	slip lineation	-	-	-	30	350	-	-	Lslk	-	64	174	0.16	Slip lineation in the shear plane
NOBD5	138.79	quartz vein	-	-	125	32	215	-	ch,bi	V6	-	64	174	0.16	15mm quartz carbonate vein
NOBD5	138.84	quartz vein	-	-	127	43	217	-	bi,ch	V6	-	64	174	0.16	2mm Quartz carbonate vein with biotite chlorite alteration
NOBD5	138.86	quartz vein	-	-	58	57	328	-	bi	V6	-	64	174	0.16	3mm quartz carbonate vein with biotite alteration
NOBD5	140.57	quartz vein	-	-	41	70	311	-	-	V6	-	64	174	1.15	7mm quartz vein with calcite-pyrite
NOBD5	140.68	quartz vein	-	-	92	35	182	-	-	V6	-	64	174	1.15	4mm quartz carbonate vein with pyrite
NOBD5	140.75	schistosity	-	-	120	44	210	-	-	CC	-	64	174	1.15	Moderate schistosity defined by biotite
NOBD5	162.74	calcite vein	-	-	78	57	348	-	-	V6	-	64	175	0.01	2mm calcite vein in brecciated rock
NOBD5	163.19	calcite vein	-	-	72	80	342	-	-	V6	xnxt	64	175	0.00	1mm calcite vein
NOBD5	163.24	calcite vein	-	-	39	55	129	-	-	V6	-	64	175	0.01	1mm calcite vein
NOBD5	163.87	calcite vein	-	-	46	80	316	-	-	V6	-	64	175	0.01	10mm boudinaged calcite vein
NOBD5	165.49	calcite vein	-	-	360	60	360	-	-	V6	-	64	175	0.01	4mm calcite vein on fracture
NOBD5	165.54	calcite vein	-	-	44	68	314	-	-	V6	-	64	175	0.01	10mm stretched calcite vein
NOBD5	166.04	quartz vein	-	-	70	90	-	-	bi,ch	V6	-	64	175	0.01	4mm calcite vein on fracture
NOBD5	166.17	calcite vein	-	-	67	60	337	-	ch	V6	-	64	175	0.01	20mm calcite vein with chlorite alteration
NOBD5	166.25	calcite vein	-	-	360	90	-	-	ch	V6	-	64	175	0.01	6mm calcite vein with chlorite alteration

HOLE NO	DEPTH	STRUCTURE	ALPHA	BETA	STRIKE	DIP	DIP DIRECTION	MINERALOGY	ALTERATION	GROUP	OVERPRINTING	HOLE DIP	HOLE AZIM	Au VALUE	COMMENTS
NOBD5	166.62	calcite vein	-	-	71	56	341	-	ch,py	V6	-	64	175	0.01	10mm calcite vein with chlorite pyrite alteration
NOBD5	167.55	calcite vein	-	-	81	57	351	-	-	V6	-	64	175	0.29	1mm calcite vein
NOBD5	168.05	shear zone	-	-	156	67	66	-	-	SH6	-	64	175	0.01	Shear zone with slip lineations
NOBD5	168.05	slip lineation	-	-	-	30	121	-	-	Lslk	-	64	175	0.01	Slip lineation in the shear plane
NOBD5	168.08	quartz vein	-	-	38	83	308	-	bi,ch	V6	-	64	175	0.01	10mm quartz carbonate vein with biotite chlorite alteration
NOBD5	168.12	quartz vein	-	-	87	59	357	-	-	V6	-	64	175	0.01	5mm quartz vein
NOBD5	169.37	shear zone	-	-	1	64	271	-	-	SH6	-	64	175	0.02	Shear zone
NOBD5	169.37	calcite vein	-	-	1	64	271	-	-	V6	-	64	175	0.02	10mm calcite vein with chlorite pyrite alteration
NOBD5	169.51	calcite vein	-	-	80	82	350	-	-	V6	-	64	175	0.02	10mm calcite vein partly boudinaged
NOBD5	173.00	calcite vein	-	-	57	73	327	-	-	V6	-	64	175	0.01	35mm calcite vein with minor biotite and chorite
NOBD5	174.55	schistosity	-	-	26	85	296	-	-	CC	-	64	175	0.04	Strong schistosity defined by biotite chlorite and pyrite
NOBD5	175.82	calcite vein	-	-	20	67	290	-	ch	V6	-	64	175	0.01	10mm calcite vein with chlorite alteration
NOBD5	176.20	shear zone	-	-	31	77	121	-	-	SH6	-	64	175	0.01	Shear zone defined by biotite chlorite
NOBD5	176.65	calcite vein	-	-	42	86	312	-	-	V6	-	64	175	0.01	8mm quartz carbonate vein
NOBD5	178.59	quartz vein	-	-	36	86	306	-	-	V6	-	64	175	0.06	50mm quartz carbonate vein with biotite chlorite alteration
NOBD5	180.30	calcite vein	-	-	22	88	292	-	-	V6	-	64	175	0.01	2mm calcite veins spaced at 50mm
NOBD5	181.35	quartz vein	-	-	42	75	312	-	-	V6	-	64	175	0.01	5mm quartz carbonate vein
NOBD5	182.08	quartz vein	-	-	74	67	344	-	-	V6	-	64	175	0.01	30mm foliated quartz carbonate vein
NOBD5	184.00	calcite vein	-	-	171	74	261	-	-	V6	-	64	175	0.04	10mm calcite vein with biotite
NOBD5	184.52	shear zone	-	-	360	90	360	-	-	SH6	-	64	175	0.04	20mm shear zone with calcite veins
NOBD5	186.16	calcite vein	-	-	63	86	153	-	-	V6	-	64	175	0.01	150mm calcite vein with biotite chlorite alteration
NOBD5	186.60	quartz vein	-	-	118	55	28	-	-	V6	-	64	175	0.01	10mm quartz carbonate vein with pyrite chlorite alteration
NOBD5	188.05	calcite vein	-	-	93	80	3	-	-	V6	-	64	175	0.10	5mm calcite vein
NOBD5	188.60	quartz vein	-	-	76	77	166	-	-	V6	-	64	175	0.10	8cm zone of calcite veins
NOBD5	189.28	quartz vein	-	-	86	66	356	-	-	V6	-	64	175	0.01	15mm quartz carbonate vein
NOBD5	189.56	quartz vein	-	-	360	90	360	-	-	V6	-	64	175	0.01	10mm stretched quartz carbonate vein
NOBD5	195.07	quartz vein	-	-	38	51	308	-	-	V6	-	64	175	0.01	7mm fibrous quartz carbonate vein with pyrite
NOBD5	195.56	calcite vein	-	-	45	70	315	-	-	V6	-	64	175	0.01	5mm calcite vein with rare quartz and pyrite
NOBD5	195.78	quartz vein	-	-	109	28	199	-	bi,ch	V6	-	64	175	0.01	120mm quartz carbonate vein with pyrite biotite alteration
NOBD5	195.90	shear zone	-	-	45	33	315	-	-	SH6	-	64	175	0.01	Shear zone with slip lineations
NOBD5	195.90	slip lineation	-	-	-	28	336	-	-	Lslk	-	64	175	0.01	Slip lineation in the shear plane
NOBD5	196.00	quartz vein	-	-	59	78	329	-	-	V6	-	64	175	0.01	2mm quartz carbonate vein
NOBD5	196.73	quartz vein	-	-	68	80	338	-	-	V6	-	64	175	0.01	20mm quartz carbonate vein
NOBD5	197.05	quartz vein	-	-	83	73	353	-	-	V6	-	64	175	0.01	50mm quartz carbonate vein
NOBD5	198.37	quartz vein	-	-	62	79	332	-	-	V6	-	64	175	0.01	10mm quartz carbonate vein

HOLE NO	DEPTH	STRUCTURE	ALPHA	BETA	STRIKE	DIP	DIP DIRECTION	MINERALOGY	ALTERATION	GROUP	OVERPRINTING	HOLE DIP	HOLE AZIM	Au VALUE	COMMENTS
NOBD5	198.54	quartz vein	-	-	360	90	360	-	-	V6	-	64	175	0.01	2mm quartz carbonate vein
NOBD5	200.09	quartz vein	-	-	38	63	308	-	-	V6	-	65	175	0.01	4mm quartz carbonate vein with chlorite
NOBD5	200.15	schistosity	-	-	104	45	194	-	-	CC	-	65	175	0.01	Schistosity
NOBD5	200.83	shear zone	-	-	74	53	344	-	-	SH6	-	65	175	0.01	Shear zone with slip lineations
NOBD5	200.83	slip lineation	-	-	-	25	41	-	-	Lslk	-	65	175	0.01	Slip lineation in the shear plane
NOBD5	200.95	layering	-	-	311	51	221	-	-	BED6	-	65	175	0.01	Layering
NOBD5	201.85	quartz vein	-	-	360	90	360	-	-	V6	-	65	175	0.01	5mm quartz vein
NOBD5	202.00	quartz vein	-	-	114	68	24	-	-	V6	-	65	175	0.01	2mm quartz carbonate vein
NOBD5	202.91	quartz vein	-	-	57	63	327	-	bi,ch	V6	-	65	175	0.01	5mm quartz carbonate vein with biotite chlorite alteration
NOBD5	205.84	quartz vein	-	-	88	64	358	-	bi	V6	-	65	175	0.01	5mm quartz-pyrite-chlorite vein
NOBD5	205.85	joint	-	-	61	60	151	-	-	J1	-	65	175	0.01	Fracture
NOBD5	208.25	schistosity	-	-	124	38	214	-	-	SH6	-	65	175	0.02	Schistosity
NOBD5	208.95	quartz vein	-	-	42	76	312	-	-	V6	-	65	175	0.02	5mm quartz vein
NOBD5	209.10	quartz vein	-	-	48	89	318	-	-	V6	-	65	175	0.02	2mm quartz vein
NOBD5	211.50	quartz vein	-	-	360	90	360	-	-	V6	-	65	175	0.02	10mm quartz vein
NOBD5	213.70	shear zone	-	-	21	46	291	-	-	SH6	-	65	175	0.01	Shear zone with slip lineations
NOBD5	213.70	slip lineation	-	-	-	29	350	-	-	Lslk	-	65	175	0.01	Slip lineation in the shear plane
NOBD5	213.78	quartz vein	-	-	42	86	312	-	-	V6	-	65	175	0.01	2mm quartz vein
NOBD5	213.88	quartz vein	-	-	32	54	302	-	bi,ch	V6	-	65	175	0.01	2mm quartz carbonate vein with biotite
NOBD5	215.14	quartz vein	-	-	21	53	291	-	-	V6	-	65	175	0.02	30mm quartz vein with biotite
NOBD5	215.17	shear zone	-	-	21	53	291	-	-	SH6	-	65	175	0.02	Shear zone on base of quartz vein
NOBD5	219.32	quartz vein	-	-	75	74	345	-	-	V6	-	65	175	0.02	2mm quartz carbonate vein
NOBD5	219.40	quartz vein	-	-	14	62	284	-	-	V6	-	65	175	0.02	3mm quartz carbonate chlorite vein

Map 8

Sleeping Beauty open-pit

(for legend see Map1 p.262)

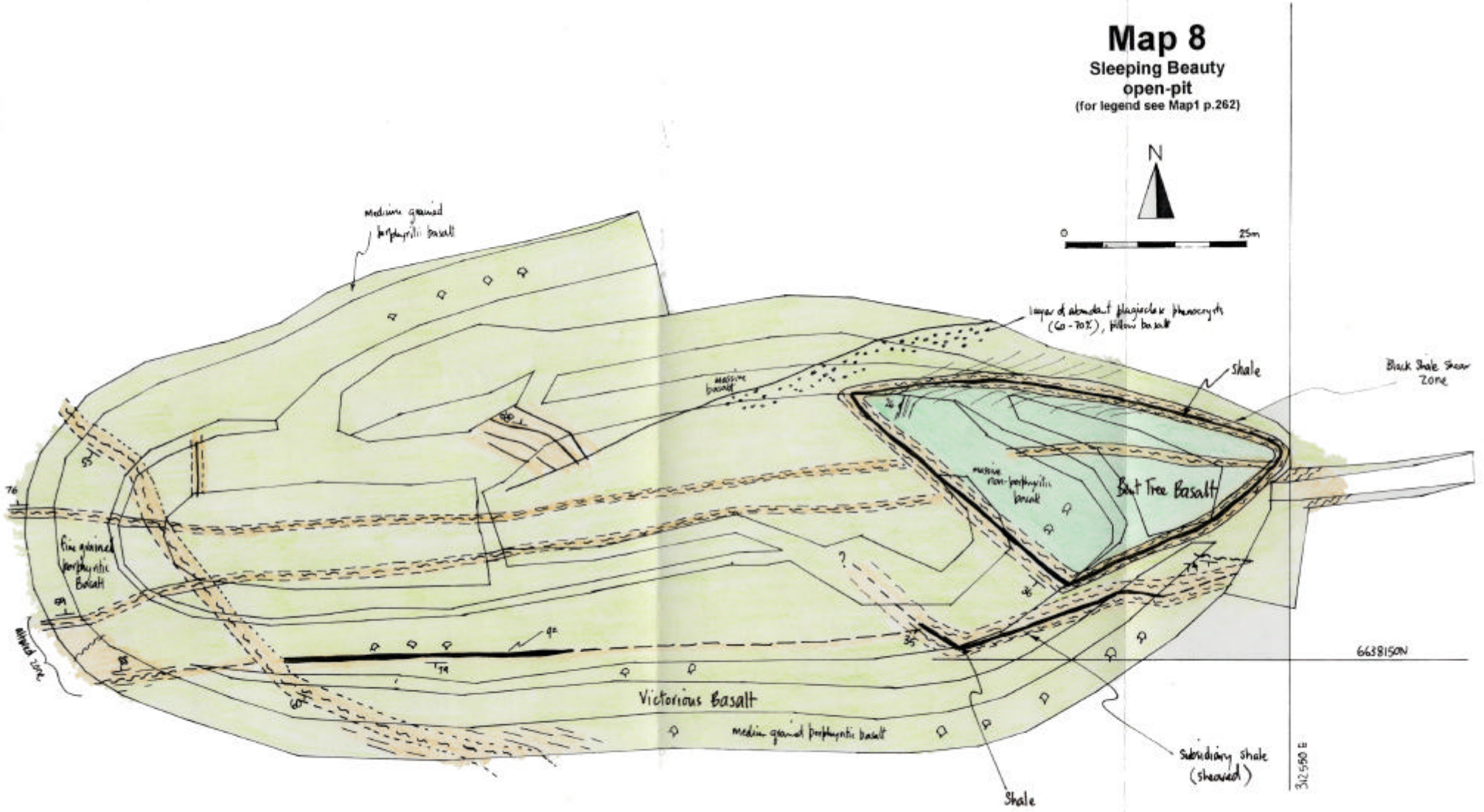

Table A1.13 - Sleeping Beauty Deposit, structural data from diamond drill core and open pit mapping

HOLE NO	DEPTH	STRUCTURE	ALPHA	BETA	STRIKE	DIP	DIP DIRECTION	MINERALOGY	ALTERATION	GROUP	OVERPRINTING	HOLE DIP	HOLE AZIM	Au VALUE	COMMENTS
GIMCD4	128.50	foliation	48	96	35	55	305	qz,cb	ch,py	CS1	-	57	181	-	Spaced fracture foliation
GIMCD4	128.80	breccia zone	45	97	34	57	304	qz,cb	py,bi,ch	SH5	-	57	181	-	Bounding breccia contact slickenfibres show S Blk W and down
GIMCD4	129.70	shear zone	45	70	16	44	286	py,po,mu	-	SH6	-	57	181	-	5mm bounding shear zone
GIMCD4	130.80	qcb vein	50	269	147	51	57	qz,cb	py,po	V1	-	57	181	-	3mm quartz carbonate vein
GIMCD4	130.80	py,po stringer	28	90	17	67	287	py,po,qz,cb	-	SRPO	xprev	57	181	-	4mm quartz carbonate pyrrhotite stringer vein
GIMCD4	132.00	qcb vein	72	195	96	51	6	qz,cb	-	V1	-	57	181	-	2mm quartz carbonate breccia infill vein
GIMCD4	141.00	bx contact	41	173	85	82	355	qz,cb,po,ep	ch,ab	SH4	-	57	181	-	Sharp contact with 0.1m breccia zone
GIMCD4	146.10	qcb vein	47	289	162	43	72	qz,cb	-	V1	-	57	181	-	2mm quartz carbonate vein
GIMCD4	151.65	qcb vein	23	210	118	84	208	qz,cb,bi	ch	V1	-	57	181	-	3mm quartz carbonate vein
GIMCD4	153.30	qcb vein	64	139	70	55	340	qz,cb	-	V1	-	57	181	-	5mm quartz carbonate vein
GIMCD4	159.45	qcb ab vein	52	166	81	71	351	qz,cb,ab	po	V1	-	57	181	-	15mm quartz carbonate vein at an angle to a shear foliation
GIMCD4	159.45	shear zone	27	155	68	87	158	qz,cb	-	SH6	-	57	181	-	Intense shear zone with stretched phenocrysts
GIMCD4	159.80	bx contact	39	165	79	84	349	qz,cb	po,py	SH4	-	57	181	-	Sharp contact of breccia zone with chlorite muscovite alteration
GIMCD4	160.65	quartz vein	49	90	33	51	303	qz,cb,py,po,asp	-	V1	-	57	181	-	Vuggy 5mm quartz carbonate vein with abundant sulphides
GIMCD4	161.15	qcb vein	53	94	39	50	309	qz,cb	po,py	V1	-	57	181	-	3mm comb textured quartz vein
GIMCD4	167.35	qcb vein	44	181	91	79	1	qz,cb	-	V1	-	57	181	-	10mm quartz carbonate vein
GIMCD4	170.15	qcb vein	34	129	50	80	320	qz,cb,bi,ch	-	V1	-	57	181	-	Shear zone parallel quartz carbonate vein
GIMCD4	183.05	qcb shear vein	48	61	12	37	282	qz,cb	-	V1	-	57	180	-	Quartz carbonate shear vein slickenfibres show S Blk W and down
GIMCD4	200.30	po,py stringer	68	202	99	54	9	po,py	-	SRPO	-	57	180	0.03	Pyrrhotite-pyrite stringer vein qith quartz carbonate
GIMCD4	200.35	quartz vein	42	185	93	81	3	qz,cb,mu	-	V3	-	57	180	0.03	Quartz vein in intense breccia zone
GIMCD4	200.55	po stringer	43	177	87	80	357	po,py	-	SRPO	-	57	180	0.03	1mm pyrrhotite stringer vein
GIMCD4	200.60	quartz vein	66	41	41	22	311	qT	po,py	V2	-	57	180	0.03	3mm tranlucent quartz vein with sulphides
GIMCD4	202.40	qcb vein	29	259	154	72	64	qz,cb,ch	-	V1	-	57	180	0.01	5mm quartz carbonate vein
GIMCD4	204.80	qcb vein	21	332	48	42	138	qz,cb	-	V1	-	57	180	-	1mm quartz carbonate vein
GIMCD4	204.80	qcb vein	30	192	100	88	190	qz,cb	-	V1	xprev	57	180	-	2mm quartz carbonate vein N Blk down movement sense
GIMCD4	207.15	qcb vein	61	193	97	62	7	qz,cb,	-	V1	-	57	180	-	2mm recrystallised quartz carbonate vein
GIMCD4	215.60	qcb shear vein	35	135	54	81	324	qz,cb,ch,bi	-	V1	-	57	180	-	15mm shear vein
GIMCD4	220.40	qcb vein	31	27	137	33	227	qz,cb	mu,cb,si	V1	-	57	180	-	1mm quartz carbonate vein
GIMCD4	233.80	qcb shear vein	32	30	142	33	232	qz,cb,mu,ch	-	SH6	-	57	180	0.02	Black Shale shear zone with stretched sedimentary rock fragments
GIMCD4	263.00	shear zone	10	348	74	49	164	qz,mu	-	SH6	-	58	180	0.02	Intense shear zone at upper contact of Bent Tree Basalt
GIMCD4	268.60	shear zone	12	190	100	71	190	qz,cb,mu,po	-	SH6	-	58	180	0.01	10mm wide intense shear zone
GIMCD4	275.20	shear vein	40	282	164	51	74	qz,cb,po	-	SH6	-	58	180	0.01	Shear vein
GIMCD4	276.33	qcb vein	65	33	37	17	307	qz,cb	-	V1	-	58	180	0.54	2mm quartz carbonate vein

HOLE NO	DEPTH	STRUCTURE	ALPHA	BETA	STRIKE	DIP	DIP DIRECTION	MINERALOGY	ALTERATION	GROUP	OVERPRINTING	HOLE DIP	HOLE AZIM	Au VALUE	COMMENTS
GIMCD4	279.00	qcb vein	90	180	360	32	360	qz,cb,ch,py	-	V1	-	58	180	0.01	Recrystallised 10mm quartz carbonate chlorite pyrite vein
GIMCD4	282.00	qcb vein	36	129	49	77	319	qz,cb,ch	-	V1	-	58	180	0.02	6mm quartz carbonate vein
GIMCD4	282.00	qcb vein	51	273	148	48	58	qz,cb	-	V1	-	58	180	0.02	3mm quartz carbonate vein
GIMCD4	282.70	breccia zone	44	251	140	63	50	qz,ch,si,hm,mu	py,po,ep,sph	SH4	-	58	180	0.02	70mm breccia zone veins
GIMCD4	283.70	shear zone	42	249	140	65	50	qM,cb,mu	py,po,cp,asp,Au	SH6	-	58	180	20.30	60mm shear zone with Au specks
Pit	-	shear zone	-	-	60	84	330	-	-	SH6	-	-	-	-	Southern lode in base of pit
Pit	-	shear zone	-	-	74	69	344	-	-	SH6	-	-	-	-	North lode
Pit	-	fracturing	-	-	115	83	205	-	-	J2	-	-	-	-	Cross fracturing

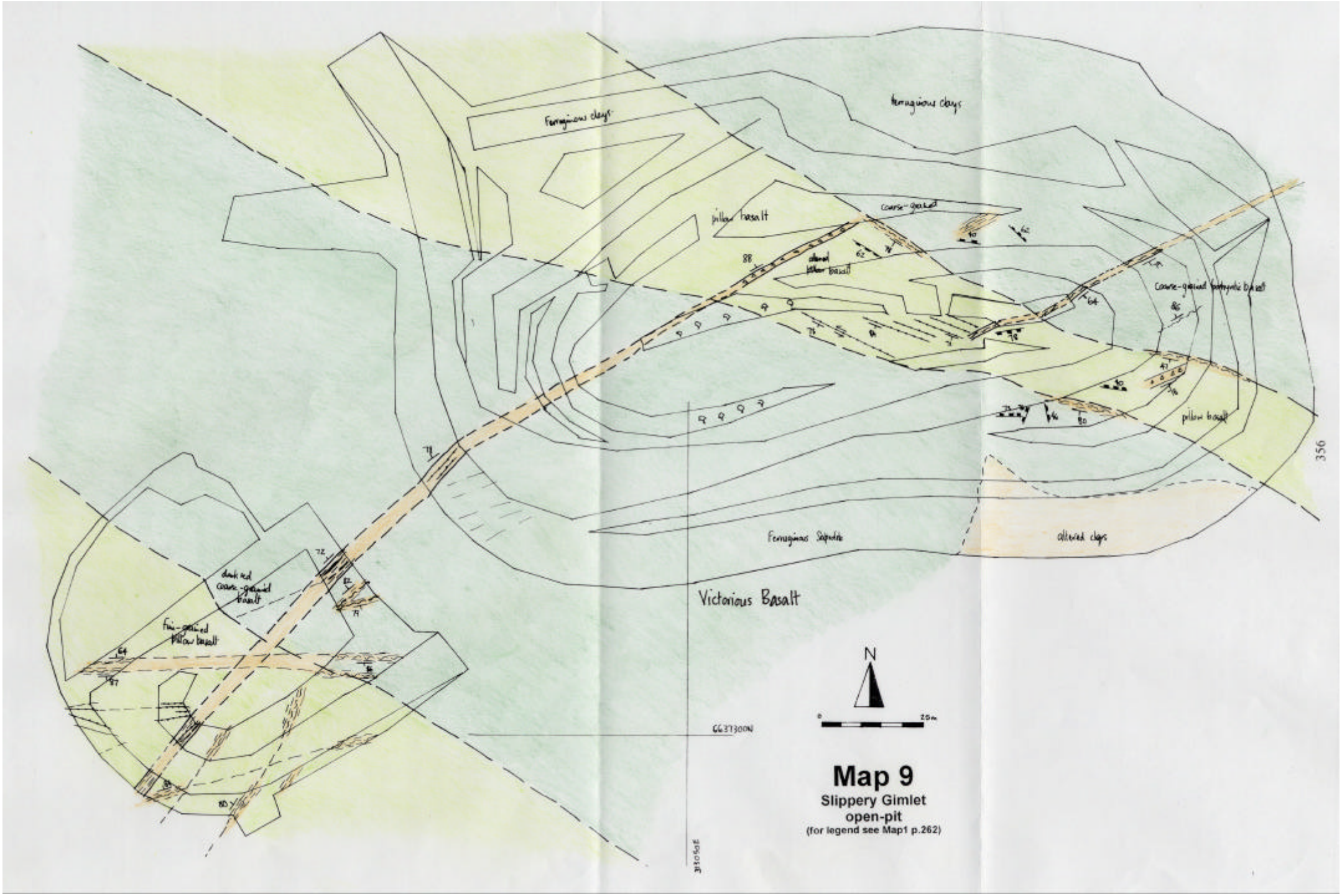

Map 9

Slippery Gimlet open-pit

(for legend see Map1 p.262)

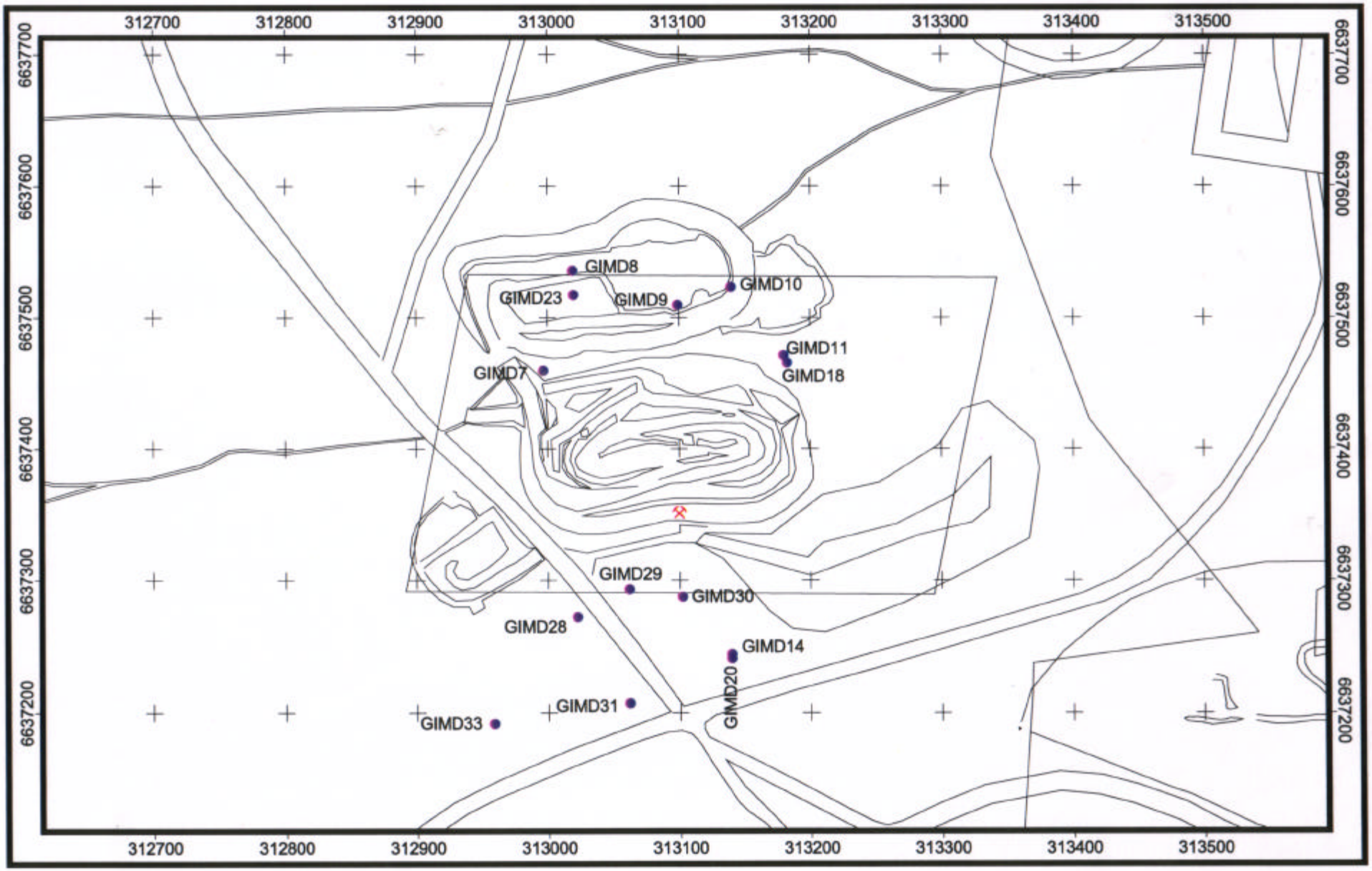

Figure A1.4 - Location plan of drillholes sampled from the Slippery Gimlet mine

Table A1.14 - Slippery Gimlet Deposit, structural data from pit mapping and diamond drill core

HOLE NO	DEPTH	STRUCTURE	ALPHA	BETA	STRIKE	DIP	DIP DIRECTION	MINERALOGY	ALT/SELVEDGE	GROUP	OVERPRINTING	HOLE DIP	HOLE AZIM	Au VALUE	COMMENTS
East Pit	wall 1	joint	-	-	91	42	1	-	-	J2	-	-	-	-	
East Pit	wall 1	joint	-	-	23	76	293	-	-	J2	-	-	-	-	
East Pit	wall 1	joint	-	-	167	46	77	-	-	J2	-	-	-	-	
East Pit	wall 1	joint	-	-	288	40	198	-	-	J2	-	-	-	-	
East Pit	wall 1	joint	-	-	100	40	10	-	-	J2	-	-	-	-	
East Pit	wall 1	joint	-	-	45	88	315	-	-	J1	-	-	-	-	Intensely altered porphyritic pillowed basalt
East Pit	wall 1	joint	-	-	154	36	64	-	-	J2	-	-	-	-	Fracture zone on pillow margin
East Pit	wall 1	joint	-	-	283	37	193	-	-	J2	-	-	-	-	Fracture zone on pillow margin
East Pit	wall 1	fracture zone	-	-	245	78	155	-	-	J2	-	-	-	-	5m fracture zone
East Pit	wall 1	C-plane sh zn	-	-	279	47	189	-	-	SH6	-	-	-	-	C-plane of shear zone left-lateral strike slip, south block east and up
East Pit	wall 1	S-plane sh zn	-	-	326	67	236	-	-	SH6	-	-	-	-	
East Pit	wall 1	shear zone	-	-	229	75	139	-	-	SH6	x-cuts prev	-	-	-	Moderately sheared zone with undeformed lithons
East Pit	wall 1	sh bx zone	-	-	56	86	326	-	-	SH4	-	-	-	-	0.5m wide breccia zone, some shearing
East Pit	wall 1	joint	-	-	75	64	345	-	-	J1	-	-	-	-	
East Pit	wall 2	joint	-	-	78	70	348	-	-	J1	-	-	-	-	
East Pit	wall 2	joint	-	-	88	34	358	-	-	J2	-	-	-	-	
East Pit	wall 2	joint	-	-	81	68	351	-	-	J2	-	-	-	-	
East Pit	wall 2	joint	-	-	47	48	317	-	-	J1	-	-	-	-	
East Pit	wall 2	shear zone	-	-	245	79	155	-	-	SH4	-	-	-	-	Hanging wall contact of main lode
East Pit	wall 2	shear zone	-	-	248	75	158	-	-	SH4	-	-	-	-	Footwall contact of main lode
East Pit	wall 2	shear zone	-	-	252	66	162	qz,hm	-	SH4	-	-	-	-	C-Plane of main lode ferruginous vein in centre of main lode
East Pit	wall 2	shear zone	-	-	244	54	154	qz,hm	-	SH4	-	-	-	-	S-Plane of main lode ferruginous vein at angle to previous
East Pit	wall 2	quartz vein	-	-	256	64	166	-	-	V3	-	-	-	-	Cross-cutting quartz vein
East Pit	wall 3	lineation	-	-	-	22	245	-	-	lslk	-	-	-	-	
East Pit	wall 3	joint	-	-	284	80	194	-	-	J2	-	-	-	-	Pervasive joint set
East Pit	wall 3	joint	-	-	137	62	47	-	-	J2	-	-	-	-	
East Pit	wall 3	joint	-	-	86	46	356	-	-	J1	-	-	-	-	
East Pit	wall 3	joint	-	-	100	40	10	-	-	J2	-	-	-	-	Jointing in very coarse grained gabbro
East Pit	wall 3	joint	-	-	63	39	333	-	-	J1	-	-	-	-	Pervasive jointing with comb textured quartz veins
East Pit	wall 3	joint	-	-	294	72	204	qz,cb	-	J2	-	-	-	-	
East Pit	wall 3	joint	-	-	155	38	65	-	-	J2	-	-	-	-	
East Pit	wall 3	shear zone	-	-	302	78	212	-	-	SH4	-	-	-	-	East bounding shear of central lode system
East Pit	wall 3	joint	-	-	302	62	212	-	-	J2	-	-	-	-	

HOLE NO	DEPTH	STRUCTURE	ALPHA	BETA	STRIKE	DIP	DIP DIRECTION	MINERALOGY	ALT/SELVEDGE	GROUP	OVERPRINTING	HOLE DIP	HOLE AZIM	Au VALUE	COMMENTS
East Pit	wall 3	joint	-	-	34	15	304	-	-	J1	-	-	-	-	
East Pit	wall 3	joint	-	-	29	58	299	-	-	J1	-	-	-	-	
East Pit	wall 3	breccia zone	-	-	56	88	326	py,po,qz	-	SH4	-	-	-	-	Western main lode 1.1m shear / crackle breccia zone
East Pit	wall 3	qzpo stringer	-	-	99	46	9	-	-	SRPO	-	-	-	-	
East Pit	wall 3	quartz vein	-	-	94	83	4	-	-	V2	-	-	-	-	
East Pit	wall 4	qzpo stringer	-	-	242	61	152	-	-	SRPO	-	-	-	-	
East Pit	wall 4	joint	-	-	226	46	136	-	-	J2	-	-	-	-	
East Pit	wall 4	joint	-	-	299	60	209	-	-	J2	-	-	-	-	
East Pit	wall 5	shear zone	-	-	227	64	137	-	-	SH4	-	-	-	-	Intense shear breccia zone, main lode
East Pit	wall 5	joint	-	-	88	43	358	-	-	J1	-	-	-	-	
East Pit	wall 5	joint	-	-	89	53	359	cb,py,po	-	J1	-	-	-	-	
East Pit	wall 5	joint	-	-	92	41	2	-	-	J1	-	-	-	-	
East Pit	wall 5	joint	-	-	261	82	171	-	-	J2	-	-	-	-	
East Pit	wall 5	quartz vein	-	-	297	71	207	qz,hm,py	mu,si,hm	SH4	-	-	-	-	Central lode system, dilational quartz vein with alteration halo
East Pit	wall 5	quartz vein	-	-	291	84	201	-	-	SH4	-	-	-	-	
East Pit	wall 5	joint	-	-	82	61	352	-	-	J1	-	-	-	-	
East Pit	wall 5	shear zone	-	-	295	73	205	-	-	SH4	-	-	-	-	West bounding shear of central lode system C-plane
East Pit	wall 5	shear zone	-	-	335	70	245	-	-	SH4	-	-	-	-	West bounding shear of central lode system S-plane
East pit	W wall	shear zone	-	-	60	78	330	-	-	SH6	-	-	-	-	2.5m wide main shear zone, boudinaged quartz veins in sheared basalt
West Pit	-	shear zone	-	-	38	80	308	-	-	SH6	-	-	-	-	0.5m wide altered schistose zone
West Pit	-	quartz vein	-	-	74	84	344	-	-	V6	-	-	-	-	Ferruginous veins in thin shear zone 1m wide within fg pillowed basalt
West Pit	-	shear zone	-	-	40	80	310	-	-	SH6	-	-	-	-	1.1m wide shear zone, shallow to horizontal slip lineation
West Pit	-	quartz vein	-	-	87	87	177	-	-	V6	-	-	-	-	Quartz veins in alteration zone in corner of western wall
West Pit	-	shear zone	-	-	82	64	352	-	-	SH6	-	-	-	-	0.3m wide shear/breccia zone
West Pit	-	shear zone	-	-	70	72	340	-	-	SH6	-	-	-	-	Main shear in eastern wall, 3.7m wide with pinch and swell qz veins
West Pit	-	shear zone	-	-	54	82	324	-	-	SH6	-	-	-	-	Shear zone
West Pit	-	shear zone	-	-	79	79	169	-	-	SH6	-	-	-	-	Shear zone
West Pit	-	shear zone	-	-	90	86	180	-	-	SH6	-	-	-	-	Shear zone
GIMD7	131.58	shear zone	50	65	173	37	263	po	-	SH6	-	60	159	10.4	Intensely altered basalt with pyrrhotite stringer veins
GIMD7	132.80	qcb vein	40	130	30	72	300	qz,cb	-	V1	-	60	159	0.01	Quartz carbonate veins
GIMD7	134.70	epidote vein	10	100	172	82	262	ep,mu	-	V6	-	60	159	0.01	Epidote alteration selvedge around vein with comb texture
GIMD7	185.40	breccia zone	50	150	50	66	320	cb,ep,se	-	SH4	-	60	161	0.03	Intensely altered and bleached breccia zone
GIMD8	182.55	breccia zone	45	140	61	71	331	-	cb,hm,si	SH4	-	59	180	0.4	Breccia zone with sharp boundaries
GIMD8	272.26	stringer vein	45	210	109	74	19	po	-	SRPO	-	59	178	2.31	Pyrrhotite stringer veins in jigsaw breccia fractures

HOLE NO	DEPTH	STRUCTURE	ALPHA	BETA	STRIKE	DIP	DIP DIRECTION	MINERALOGY	ALT/SELVEDGE	GROUP	OVERPRINTING	HOLE DIP	HOLE AZIM	Au VALUE	COMMENTS
GIMD8	273.66	stringer vein	50	210	108	69	18	po	-	SRPO	-	59	178	1.22	Pyrrhotite stringer veins in jigsaw breccia fractures
GIMD8	303.65	qcb vein	55	220	112	62	22	po	-	V1	-	59	178	0.17	Pyrrhotite stringer veins in jigsaw breccia fractures
GIMD8	373.68	qcb vein	45	130	55	69	325	-	-	V1	-	59	181	5.32	Quartz carbonate vein
GIMD8	402.00	shear zone	10	210	117	74	207	-	-	SH1	-	59	177	0.12	Intensely sheared Black Shale/Bent Tree Basalt contact
GIMD9	184.45	fracture vein	38	215	115	85	25	qcb	-	V1	-	53	178	-	1mm quartz-carbonate fracture fill vein
GIMD9	186.40	carbonate vein	62	186	91	65	1	cb,bi,py	-	V4	-	53	178	-	Comb textured carbonate vein growth fibres at 90 to vein wall
GIMD9	189.40	qcb fract vein	69	196	102	58	12	qz,cb,ch	-	V1	-	53	186	-	Comb textured fracture fill vein
GIMD9	193.80	qcb vein	43	163	83	83	353	qcb,po,cp,am	-	V1	-	53	186	-	1mm quartz-carbonate vein
GIMD9	201.10	qcb vein	13	301	23	62	113	acb,py,cp	-	V1	-	53	186	0.01	5mm quartz-carbonate vein
GIMD9	204.25	qz breccia vein	59	190	101	68	11	qcb	po,mu,hm	V3	-	53	186	6.64	5cm milky quartz vein, stretched phenocrysts, south block down offset
GIMD9	204.35	stringer vein	71	192	100	56	10	po,cp,as	-	SRPO	po x-cuts bi	53	186	6.64	1mm pyrrhotite stringer vein, pyrrhotite mimics bi plates in zone
GIMD9	204.40	stringer vein	54	205	111	72	21	po,cp,as	-	SRPO		53	186	6.64	2mm pyrrhotite stringer with fracture fill texture
GIMD9	204.75	stringer vein	37	197	109	89	19	po,cp	-	SRPO		53	186	6.64	1mm pyrrhotite stringer
GIMD9	204.75	stringer vein	71	229	114	52	24	po,cp	-	SRPO	x-cuts prev	53	186	6.64	1mm pyrrhotite stringer
GIMD9	204.80	quartz vein	32	185	100	86	190	qz	po	V3	-	53	186	6.64	3cm milky quartz vein
GIMD9	205.20	fracture vein	21	197	112	76	202	bi,qcb	-	V1	-	53	186	0.21	5mm bi filled fracture with quartz carbonate
GIMD9	205.20	qcb vein	63	213	112	62	22	qcb	-	V1	-	53	186	0.21	1mm quartz carbonate vein
GIMD9	228.30	carbonate vein	58	172	84	69	354	qcb,bi,mu,po	po,cp,as	V1	-	53	179	0.48	5mm fracture vein with sulphide stringers
GIMD9	242.50	qcb vein	44	344	33	14	123	qcb	po,cp,py,as	V1	-	53	179	5.44	5mm fracture vein with sulphide stringers
GIMD9	242.60	stringer vein	51	176	86	76	356	po,py	bi,lx,si	SRPO	-	53	179	5.44	0.5mm pyrrhotite stringer
GIMD9	243.30	quartz vein	67	169	84	60	354	qcb	bi	V1	x-cuts next	53	179	0.02	3mm quartz carbonate vein with south block down offset
GIMD9	243.40	qcb vein	19	335	49	40	139	qzM	po	V3	-	53	179	0.02	3mm fracture fill vein
GIMD9	244.65	shear zone	69	189	92	58	2	qcb,po,cp,am	ch,po,Au	SH4	-	53	179	98.1	Breccia zone with open space growth fibres, south block down offset
GIMD9	245.30	qcb vein	62	94	48	47	318	qcb	ch,bi	V1	x-cuts next	53	179	0.16	6mm fine grained recrystallised quartz carbonate vein
GIMD9	245.50	quartz vein	29	313	15	42	105	qzT	po	V2	-	53	179	0.16	5mm translucent quartz vein
GIMD9	247.50	quartz vein	63	160	78	63	348	qzM	mu,po,as	V3	-	53	179	2.16	2cm milky quartz vein
GIMD9	259.00	quartz vein	56	195	95	71	5	qz,cb,ch,ac	mu,hm,po	V1	-	53	184	0.36	5cm quartz carb vein with crack-seal texture and pyrrhotite stringers
GIMD9	282.05	qcb vein	56	178	92	71	2	qcb	mu,si,py,po,as	V1	-	53	184	0.39	Quartz carbonate fracture fill vein with pyrrhotite stringers
GIMD9	284.10	stringer vein	57	195	102	70	12	po,qz	mu,cb,po,bi	V1	-	53	184	27.2	Quartz carbonate vein with parallel pyrrhotite stringers
GIMD9	284.20	stringer vein	78	175	92	49	2	po	-	SRPO	x-cuts next	53	184	27.2	3mm pyrrhotite stringers
GIMD9	284.25	stringer vein	22	201	113	78	203	po	-	SRPO	-	53	184	27.2	1mm pyrrhotite stringer
GIMD9	284.85	breccia zone	56	217	115	67	25		qcb,mu,po	SH4	-	53	184	27.2	Contact of breccia zone with crackle brecciated basalt
GIMD9	285.00	stringer vein	72	143	80	53	350	py,bi,qcb	bi	SRPY	-	53	184	78.5	2mm pyrite stringer vein with biotite selvedge
GIMD9	285.00	stringer vein	18	45	156	50	246	py,bi,qcb	bi	SRPY	x-cuts prev	53	184	78.5	2mm pyrite stringer vein
GIMD9	285.60	stringer vein	25	237	143	88	53	po	-	SRPO	-	53	184	78.5	Pyrrhotite strringer vein parallel to gold bearing quartz veins

HOLE NO	DEPTH	STRUCTURE	ALPHA	BETA	STRIKE	DIP	DIP DIRECTION	MINERALOGY	ALT/SELVEDGE	GROUP	OVERPRINTING	HOLE DIP	HOLE AZIM	Au VALUE	COMMENTS
GIMD9	295.40	quartz vein	58	149	76	67	346	qzT	cb,mu,po	V2	-	53	184	5.46	1cm quartz vein
GIMD9	310.50	quartz vein	36	201	110	90	20	qzM	mu,po,bi	V3	-	53	184	1.91	Quartz vein with wide intense alteration selvedge
											-				
GIMD10	153.18	qcb vein	52	180	360	67	360	qz,cb	-	V1	-	61	180	-	3mm recrystallised quartz carbonate vein
GIMD10	155.60	qcb vein	58	136	63	57	333	qz,cb	-	V1	-	61	180	-	3mm recrystallised quartz carbonate vein
GIMD10	159.70	qcb vein	45	205	108	73	18	qz,cb	-	V1	x-cuts next	61	180	-	3mm recrystallised quartz carbonate vein
GIMD10	159.70	qcb vein	9	351	78	53	168	qz,cb	-	V1	-	61	180	-	3mm recrystallised quartz carb vein slickensides show south block up
GIMD10	172.90	shear zone	54	101	38	50	308	ch,se,bi,cb	-	SH6	-	61	178	-	4cm shear zone
GIMD10	175.90	qcb vein	58	100	41	46	311	qz,cb	-	V1	-	61	178	-	3cm quartz carbonate vein
GIMD10	184.00	cb breccia vein	54	187	92	65	2	ch,cb	-	V4	-	61	178	-	0.3m recrystallised carbonate vein with wallrock breccia fragments
GIMD10	184.35	qcb vein	9	125	33	83	123	cb,qz,ep	-	V1	-	61	178	-	5mm quartz carbonate vein
GIMD10	186.85	qcb shear vein	51	206	105	67	15	qz,cb	-	V1	-	61	178	-	10mm quartz carbonate vein
GIMD10	196.65	sediment	32	49	158	43	248	gp	-	BED5	-	61	178	0.01	Thin interflow black shale contact
GIMD10	199.45	qcb vein	13	345	68	50	158	qz,cb,py	-	V1	-	61	178	0.01	2mm quartz vein
GIMD10	222.00	qcb vein	58	272	143	41	53	qz,cb	-	V1	-	62	179	0.01	20mm recrystallised comb textured quartz carbonate vein
GIMD10	236.80	shear zone	18	38	137	52	227	po,py,mu	-	SH6	-	62	179	0.01	Intense shear zone
GIMD10	238.26	breccia zone ct	39	121	43	69	313	po,mu	-	SH4	-	62	179	3.15	Sharp contact of breccia zone
GIMD10	238.30	breccia zone ct	38	185	93	80	3	po	-	SH4	-	62	179	3.15	Main shear direction, pyrrhotite stringer
GIMD10	279.85	shear zone	23	53	153	53	243	ch,po,cb	-	SH6	-	62	176	0.01	Intense shear zone
GIMD10	306.10	breccia zone ct	47	196	97	71	7	qz,cb,mu,po	-	SH4	-	62	176	2.75	Moderately sharp contact of breccia zone
GIMD10	309.15	po stringer	39	174	81	79	351	-	-	SR60	-	62	176	0.44	Pyrrhotite stringer in breccia zone
GIMD11	131.10	qcb vein	44	151	70	72	340	qz,cb	-	V1	-	62	182	0.01	3mm quartz carbonate vein
GIMD11	132.70	qcb vein	24	190	101	87	191	qz,cb	-	V1	-	62	182	0.01	2mm quartz carbonate vein
GIMD11	134.15	qcb vein	12	270	176	80	86	qz,cb	-	V1	-	62	182	0.01	1mm crack-seal quartz carbonate vein
GIMD11	148.80	quartz vein	25	4	99	38	189	qz,cb	-	V1	-	62	183	0.01	Vein filled dilation fracture
GIMD11	158.00	qcb vein	51	139	65	636	335	qz,cb	-	V1	-	62	183	0.01	1mm quartz carbonate vein
GIMD11	158.45	qcb vein	52	182	94	66	4	qz,cb	ch	V1	-	62	183	0.01	2mm quartz carbonate vein
GIMD11	158.45	qcb vein	26	7	103	37	193	qz,cb,po	ch	V1	-	62	183	0.01	Sigmoidal fractures with pyrrhotite infill
GIMD11	159.00	qcb shear vein	40	117	44	67	314	qz,cb,ch	-	V1	-	62	183	0.01	2mm shear vein
GIMD11	161.60	breccia zone	63	160	81	55	351	qz,cb,matrix	-	SH4	-	62	183	0.09	Muscovite carbonate altered basalt, angular fragments
GIMD11	162.00	shear zone	43	5	104	0	194	cb	-	SH7	-	62	183	0.09	1mm chlorite filled shear fracture
GIMD11	162.15	breccia zone	57	172	88	61	358	cb,py,po	cb,mu	SH4	-	62	183	4.02	Upper contact of intensely altered breccia zone
GIMD11	162.20	po stringer	54	184	95	64	5	po,py	-	SRPO	-	62	183	4.02	1mm pyrrhotite stringer
GIMD11	162.30	qcb vein	18	59	163	60	253	qz,cb	cb,mu	V1	x-cuts prev	62	183	4.02	2mm quartz carbonate vein
GIMD11	162.35	breccia zone	45	140	63	69	333	po,py	-	SH4	-	62	183	4.02	Contact of intense crackle breccia zone

HOLE NO	DEPTH	STRUCTURE	ALPHA	BETA	STRIKE	DIP	DIP DIRECTION	MINERALOGY	ALT/SELVEDGE	GROUP	OVERPRINTING	HOLE DIP	HOLE AZIM	Au VALUE	COMMENTS
GIMD11	168.35	qcb vein	44	172	88	74	358	qz,cb	ch	V1	-	62	184	0.01	5mm recrystallised quartz carbonate vein
GIMD11	191.00	qcb vein	37	193	104	81	14	qz,cb,ch,po	-	V1	-	62	184	0.09	2cm crack-seal pyrrhotite carbonate vein
GIMD11	191.73	qcb vein	12	175	88	75	178	qz,cb	-	V1	-	62	184	0.09	1mm recrystallised quartz carbonate vein
GIMD11	194.00	po stringer	13	179	92	76	182	po	-	SRPO	-	62	184	2.65	1mm pyrrhotite stringer
GIMD11	194.38	po stringer	34	238	141	74	51	po	-	SRPO	-	62	184	2.65	3mm pyrrhotite stringer vein
GIMD11	231.40	qcb vein	26	104	26	74	296	qz,cb	ch,ep	V1	-	63	182	0.04	4mm quartz carbonate vein
GIMD11	233.40	breccia zone	31	147	63	83	333	qz,cb,po	cb,mu	SH4	-	63	182	0.56	10cm pyrrhotite, chalcopyrite breccia zone
GIMD11	234.40	qcb vein	30	134	52	81	322	qz,cb	-	V1	-	63	182	0.08	Shear parallel quartz carbonate vein
GIMD11	244.10	qcb vein	57	143	68	57	338	qz,cb	-	V1	-	63	182	0.01	2mm quartz carbonate vein
GIMD11	244.10	qcb vein	24	113	32	79	302	qz,cb	-	V1	x-cuts prev	63	182	0.01	5mm quartz carbonate vein, right-lateral south block down offset
GIMD11	246.50	qcb vein	9	145	56	77	146	qz,cb	-	V1	-	63	182	0.01	5mm quartz carbonate vein
GIMD11	256.55	qcb vein	57	10	136	8	226	qz,cb,bi,ch	-	V1	-	63	182	0.48	10mm vuggy quartz carbonate vein in shear zone
GIMD11	256.80	py stringer	25	22	123	41	213	py	-	SRPY	-	63	182	1.29	<1mm pyrite filled fracture
GIMD11	256.85	po stringer	24	162	75	89	165	po,cb,py	-	SRPO	-	63	182	1.29	5mm pyrrhotite stringer vein
GIMD11	256.90	qcb vein	43	193	101	74	11	qz,cb	po,py	V1	-	63	182	1.29	6mm quartz carbonate vein with pyrrhotite stringers
GIMD11	257.50	shear zone	21	167	77	85	167	qz,cb,ch,py	po,cb	SH6	-	63	180	1.11	Intense shear zone, right-lateral south block down offset
GIMD11	260.00	qcb vein	22	164	75	86	165	qz,cb	ch,bi	V1	-	63	180	0.01	Recrystallised quartz carbonate vein
GIMD11	260.00	qcb vein	54	152	71	61	341	qz,cb	-	V1	-	63	180	0.01	5mm quartz carbonate vein
GIMD14	125.40	qcb vein	16	300	20	61	290	qz,cb,ch	-	V1	x-cuts all	58	3	-	2mm quartz carbonate vein
GIMD14	126.50	qcb vein	28	95	22	70	112	qz,cb	-	V1	-	58	3	-	1mm quartz carbonate vein joint fill?
GIMD14	126.55	qcb vein	53	129	60	62	150	qz,cb	-	V1	-	58	3	-	1mm quartz carbonate vein joint fill?
GIMD14	127.25	qcb vein	43	157	75	78	165	qz,cb	mu,cb	V1	-	58	3	-	3mm quartz carbonate vein
GIMD14	127.50	qcb vein	52	241	131	60	221	qz,cb	-	V1	-	58	3	-	3mm quartz carbonate vein
GIMD14	129.10	qcb vein	55	283	152	41	242	qz,cb	-	V1	-	58	3	-	5mm quartz carbonate vein
GIMD14	130.10	qcb vein	9	343	71	51	341	qz,cb	-	V1	-	58	3	-	1mm quartz carbonate vein
GIMD14	131.80	qcb vein	5	347	76	54	346	qz,cb	ch?	V1	-	58	3	-	5mm quartz carbonate vein
GIMD14	132.00	qcb vein	30	1	94	29	4	qz,cb	-	V1	-	58	3	-	3mm quartz carbonate vein
GIMD14	138.00	qcb vein	9	163	74	69	344	qz,cb	-	V1	-	58	3	-	5mm quartz carbonate vein
GIMD14	141.70	shear zone	49	259	144	55	234	ch,bi	bi	SH1	-	58	3	-	1mm shear zone
GIMD14	147.60	qcb vein	6	339	67	55	337	qz,cb,ch	ch	V2	-	58	3	-	5mm translucent quartz vein
GIMD14	159.90	quartz vein	34	18	129	28	39	qzT	-	V2	-	59	6	0.01	15mm translucent quartz vein
GIMD14	171.00	qcb vein	17	127	46	88	316	qz,cb	ch,ep	V1	-	59	6	0.01	1mm comb textured quartz carbonate vein
GIMD14	171.10	qcb vein	1	19	118	60	28	qz,cb	ch	V1	-	59	6	0.01	3mm quartz carbonate vein
GIMD14	174.70	shear zone	18	179	95	78	5	mu,cb,bi,po	-	SH1	-	59	6	0.01	Intense shear zone on edge of mineralised breccia
GIMD14	175.30	breccia zone	31	208	119	88	209	po	-	SR60	-	59	6	0.8	Pyrrhotite stringer on edge of silicified breccia zone

HOLE NO	DEPTH	STRUCTURE	ALPHA	BETA	STRIKE	DIP	DIP DIRECTION	MINERALOGY	ALT/SELVEDGE	GROUP	OVERPRINTING	HOLE DIP	HOLE AZIM	Au VALUE	COMMENTS
GIMD14	206.00	qcb vein	20	0	94	39	4	qz,cb	si	V1	-	59	4	0.17	1mm quartz carbonate vein
GIMD14	222.30	po stringer	27	227	134	86	224	qz,cb,po	si,po	SR60	-	59	4	2.37	Pyrrhotite stringer near quartz carbonate breccia vein
GIMD14	224.70	qcb vein	8	96	13	87	103	qz,cb	-	V1	-	59	4	0.01	1mm quartz carbonate vein
GIMD14	224.90	qcb vein	29	3	99	31	9	qz,cb	-	V1	-	59	4	0.01	2mm quartz carbonate vein
GIMD14	233.50	quartz vein	47	285	165	45	255	qzM	si,mu,po,py,as	V3	-	59	4	2.67	4cm milky white quartz vein
GIMD14	262.70	bedding	47	283	164	46	254	qz,si	si	BED6	-	59	5	0.01	Bedded cherty sediment
GIMD18	137.00	breccia zone	25	145	59	87	149	ch,po	-	SH4	-	56	181	3.19	Sharp contact of breccia zone, some shearing
GIMD18	137.70	ep/mu vein	23	131	46	90	136	qz,ep,mu	po	V1	-	56	181	3.19	20mm vein with muscovite, epidote infill
GIMD18	150.60	po vein	43	135	58	74	328	po,cb	-	V5	-	56	181	3.69	30mm massive pyrrhotite vein
GIMD18	156.70	po stringer	71	262	122	40	32	po,ch	-	SRPO	-	57	182	0.46	1mm pyrrhotite stringer vein
GIMD18	184.20	shear foliation	18	114	31	88	301	po,ch	-	SH6	-	57	182	3.81	Fine grained pervasive shear foliation
GIMD18	184.50	breccia zone	19	168	80	77	170	po,mu,cb	-	SH4	-	57	182	29.2	Sharp contact of main breccia zone
GIMD18	196.75	po/cb vein	18	139	51	83	141	po,qz,cb	-	V5	-	57	181	0.62	5mm quartz carbonate vein with pyrrhotite
GIMD20	289.20	bedding	60	269	147	39	237	po	-	BED5	-	66	3	0.09	Interflow sediment contact black shale
GIMD20	290.20	bedding	79	191	96	35	186	pyrite	-	BED5	-	66	3	0.07	Sheared interflow sediment contact, black shale
GIMD23	340.00	rxt cb vein	45	185	91	76	1	ca,qz	mu,bi,po	V4	-	59	178	0.31	7cm recrystallised carbonate vein with 6cm selvedge
GIMD23	340.30	qcb vein	37	93	21	61	291	qz,cb	po	V1	-	59	178	0.41	5mm quartz carbonate vein with irregeular margins
GIMD23	341.10	qcb vein	24	319	30	46	120	qz,cb	-	V1	x-cuts all	59	178	0.41	5mm crack-seal quartz carbonate vein with carbonate infill
GIMD23	341.10	qcb vein	43	160	73	77	343	qz,cb	-	V1	-	59	178	0.41	1mm quartz carbonate vein
GIMD23	341.35	qcb vein	48	199	101	72	11	qz,cb	bi,po	V1	-	59	178	5.32	5mm quartz carbonate vein at margin of alteration zone
GIMD23	341.65	po,bi stringer	47	191	95	74	5	po,bi	-	SRPO	-	59	178	5.32	<1mm pyrrhotite stringer
GIMD23	341.85	qcb vein	54	225	116	62	26	qz,cb	po,py,to	V1	-	59	178	5.32	20mm crack-seal quartz carbonate vein
GIMD23	342.30	po stringer	39	195	99	82	9	po	-	SRPY	-	59	178	5.32	<1mm pyrrhotite stringer
GIMD23	366.00	qz,to vein	70	339	119	15	29	qz,to,po	si	V2	-	59	179	0.02	8cm grey quartz vein euhedral tourmaline crystals and pyrrhotite spots
GIMD23	366.25	qz,to vein	43	357	81	17	171	qz,to,po,cb	-	V1	-	59	179	0.45	3mm quartz tourmaline vein
GIMD23	366.85	rxt qcb vein	57	205	104	63	14	qz,cb,ch,po,to	ch,po	V2	x-cuts next	59	179	0.45	3cm recrystallised quartz carbonate chlorite vein
GIMD23	367.00	qcb,to vein	23	7	99	37	189	qz,cb,to	ch,cb	V1	-	59	179	0.45	5mm quartz carbonate tourmaline vein
GIMD23	447.60	bedding	28	349	70	33	160	-	-	BED4	-	60	179	0.09	Sharp conatact of unaltered and altered porphyritic basalt
GIMD23	447.65	bedding	50	53	152	38	242	-	-	BED5	-	60	179	0.09	Thin graphitic shale horizon
GIMD23	448.05	bedding	33	41	4	32	274	-	-	BED5	-	60	179	0.09	20mm sheared pyritic graphitic shale with quartz carbonate veining
GIMD28	191.00	Au qz vein	16	91	12	77	102	-	-	V2	-	60	3	-	Grey quartz vein with visible gold and minor pyrite

HOLE NO	DEPTH	STRUCTURE	ALPHA	BETA	STRIKE	DIP	DIP DIRECTION	MINERALOGY	ALT/SELVEDGE	GROUP	OVERPRINTING	HOLE DIP	HOLE AZIM	Au VALUE	COMMENTS
GIMD29	139.50	sh bx zone	26	195	102	86	12	qz,cb,ch	-	SH3	-	59	359	-	Intense shear/breccia zone
GIMD29	153.00	shear zone	24	209	115	87	25	po,qz,cb	-	SH1	-	59	359	-	Pyrrhotite stringer at the edge of shear zone, contains wallrock slivers
GIMD29	159.30	shear zone	36	169	80	85	170	-	-	SH1	-	59	359	-	Intense ductile shear zone at edge of breccia zone
GIMD29	160.60	shear zone	18	177	86	78	356	-	-	SH1	-	59	359	-	Intense shear zone at edge of orebody
GIMD30	148.75	quartz vein	31	94	20	66	110	qzM	-	V3	-	59	360	-	10cm milky quartz crack-seal vein
GIMD30	149.05	breccia zone	51	123	52	61	142	qz,py	-	SH3	-	59	360	-	Contact of breccia zone, thin shear zone at contact
GIMD30	149.70	breccia zone	51	229	122	64	212	-	-	SH3	-	59	360	-	Lower contact of breccia zone, shearing with very fine grained pyrite
GIMD31	266.80	cb vein	33	207	122	69	32	ca	-	SH1	-	61	8	-	Large euhedral calcite vein sub-parallel to core axis
GIMD31	269.10	shear zone	5	203	120	84	210	-	-	V4	-	61	8	-	Intense ductile shear zone at edge of orebody
GIMD31	282.20	shear zone	23	151	71	88	341	-	-	SH1	-	61	8	-	Intense brittle-ductile shear zone
GIMD33	253.60	breccia zone	34	145	60	82	150	-	-	SH3	-	60	359	-	

A2 SAMPLE LISTS

The following lists tabulate the diamond drill holes logged from each of the study areas and the specific samples collected for thin sectioning and microscopic analysis.

A2.1 Drill hole lists

Table A2.1 - Diamond drill holes logged in this study

Zuleika district

Porphyry mine					
ZULD10	-60	49	252.00	6624729.443	310130.063
ZULD14	-60	229	162.00	6624757.114	310194.220
ZULD15	-60	229	120.00	6624743.059	310179.229
Bowerbird mine					
ZULD8	-60	229	354.40	6622589.426	312265.262
Wattlebird mine					
ZULD7	-60	49	426.40	6621666.279	312785.710
ZULD17	-60	49	328.80	6621747.448	312730.378
Bullant mine					
ZULD9	-60	229	291.60	6621118.428	313637.969
ZULD2	-60	229	466.00	6621041.712	313668.548
ZULD18	-60	229	277.00	6620919.295	313657.761

Ora Banda district

Hole no.	Dip	Azimuth	Depth	AMG-North	AMG-East
Sleeping Beauty mine					
GIMCD4	-60	180	285.40	6638214.670	312210.540
Slippery Gimlet mine					
GIMD7	-60	160	240.50	6637459.398	312996.584
GIMD8	-60	180	459.50	6637535.441	313019.189
GIMD9	-60	180	331.50	6637509.538	313098.907
GIMD10	-60	180	324.40	6637522.974	313139.832
GIMD11	-60	180	273.40	6637470.989	313179.814
GIMD14	-60	360	273.20	6637244.264	313139.763
GIMD18	-55	180	304.20	6637465.155	313182.621
GIMD20	-65	360	343.60	6637240.904	313139.921
GIMD23	-55	180	474.60	6637516.969	313019.663
GIMD28	-60	360	192.60	6637271.940	313022.132
GIMD29	-60	360	259.24	6637292.780	313061.834
GIMD30	-60	360	195.00	6637287.300	313102.194
GIMD31	-60	360	305.80	6637206.857	313061.691
GIMD33	-60	360	341.90	6637191.557	312958.642
Boundary mine					
NOBD1	-60	180	315.40	6638816.980	312738.359
NOBD2	-60	180	297.40	6638900.864	312859.760
Nazzaris mine					
NOBD4	-60	180	162.00	6639767.120	312758.810
NOBD5	-60	180	220.00	6639769.850	312598.548
Enterprise mine					
ORBD2	-65	360	429.00	6638093.096	315575.194
ORBD3	-60	355	350.50	6638099.862	315800.198
ORBD4	-65	355	453.00	6638124.621	315700.294
ORBD5	-65	355	150.00	6638173.814	315700.129
ORBD6	-65	355	402.50	6638097.142	315751.782
ORBD7	-65	355	452.00	6638075.206	315701.507
ORBD8	-72	355	402.50	6638102.229	315400.134
ORBD8W	-72	355	567.00	6638102.229	315400.134

Hole no.	Dip	Azimuth	Depth	AMG-North	AMG-East
ORBD9	-72	355	554.00	6638029.394	315303.049
ORBD10	-72	355	462.30	6638068.828	315403.742
ORBD11	-72	355	617.20	6638060.898	315303.403
ORBD12	-60	355	390.50	6638087.903	315777.617
ORBD13	-60	355	200.00	6638080.854	315675.773
ORBD14	-60	355	483.50	6638039.700	315552.676
ORBD16	-70	355	606.50	6638103.617	315300.219
ORBD17	-70	355	699.70	6638068.883	315198.919
ORBD18	-70	355	651.60	6638029.521	315198.309
ORBD19	-70	355	742.60	6638000.402	315099.687
ORBD20	-70	355	693.70	6638040.000	315100.000
ORBD21	-70	355	541.40	6637960.000	315600.000
ORD10	-60	360	329.90	6638153.860	316025.590
ORD13	-60	360	229.20	6638199.351	315975.213
ORD14	-60	360	303.00	6638114.419	316029.780
ORD15	-60	360	498.00	6638199.511	315925.038
ORD17	-60	360	262.00	6638190.734	316124.780
ORD19	-60	360	240.00	6638190.042	316175.189
ORD21	-60	180	210.10	6638379.935	316176.450
ORD23	-60	360	156.10	6638169.683	316225.476
ORD29	-60	360	231.00	6638220.038	315824.751
ORD31	-60	360	95.60	6638279.524	316149.498
ORD34	-60	360	300.70	6638117.365	315923.000
ORD129	-60	360	289.00	6638791.841	316095.454
ORD151	-60	355	342.70	6638104.545	315876.701
ORD152	-60	355	354.40	6638130.004	315850.048
ORD153	-60	355	312.00	6638157.154	315825.099
ORD154	-60	355	357.00	6638071.559	315849.900
ORD155	-60	355	359.00	6638101.851	315825.689
ORD156	-60	355	327.00	6638154.952	315800.430
ORD157	-60	355	348.00	6638125.520	315800.357

A2.2 Petrographic samples

Table A2.2 –Thin section samples

Zuleika samples

HoleID	Depth	Strike	Dip	DipDir	Au	Group	Description	Distance from shear zone (m)
Faults								
ZULD18	252.30	28	70	118	0.21	EW	cataclasite	1m W
Shear zones								
ZULD9	208.14	0	76	90	**4.12**	NS	mylonite	Main shear
ZULD9	209.30	8	68	98	0.05	NS	mylonite	Main shear
ZULPIT1	pit					NW	mylonite	Main shear
ZSZ-1	pit	146	84	56	-	NW	ductile shear zone	UM/MB contact
Schistosity and Cleavage								
ZULD9	202.40	138	72	48	**2.51**	NW	shear foliation	Main shear

Enterprise samples

Hole No.	Depth	Strike	Dip	DipDir	Au	Group	Description	Depth(m) below CSH*	Enterprise dolerite unit
Faults									
ORD13	110.33	164	61	254	**2.80**	NW	brittle fault	4	8
ORD157	282.25	47	61	317	**1.78**	NE	cataclasite	62	4
ORBD12	264.50	85	84	355	**8.90**	EW	foliated cataclasite	8.5	7
ORDB17	573.70	53	83	143	0.69	NE	foliated cataclasite	55	5
ORD13	170.20	153	90	-	**6.31**	NW	foliated cataclasite	63	4
ORD27	174.00	-	-	-	**3.87**	-	mesofracture array	14.5	7
ORBD18	570.85	30	68	300	0.60	NE	mesofracture array	36	6
ORD157	283.30	7	42	277	0.15	NE	mesofracture array	63	4
ORD29	150.50	173	47	263	**1.80**	NS	mesofracture array	12	7
ORBD18	617.60	168	61	258	0.06	NW	mesofracture array	83	4
ORD10	239.80	152	46	242	0.94	NW	mesofracture array	117.5	2
Shear zones									
ORD14	224.20	99	88	9	0.13	EW	banded mylonite	77	4
ORBD12	360.65	175	62	85	0.16	NS	banded mylonite	104	3
ORD10	274.35	102	86	192	**4.95**	EW	S-C mylonite	163.5	2
ORBD16	506.00	176	51	266	0.07	NS	S-C mylonite	69	4
ORD10	215.09	7	42	277	0.05	NS	S-C mylonite	91	3
ORBD16	602.90	4	63	274	-	NS	S-C mylonite	34m below ED	Big Dick Basalt
ORD13	124.50	127	60	217	**1.22**	NW	S-C mylonite	12.5	7
ORBD21	525.60	46	59	136	0.35	NE	S-C-C' mylonite	105	3
ORDB17	543.00	87	81	357	0.24	EW	shear zone	24	6
ORD10	265.40	120	82	30	0.18	EW	shear zone	150.5	2
ORBD19	661.00	44	59	134	0.16	NE	shear zone	56	5
ORD29	180.40	10	37	280	**2.86**	NS	shear zone	42	5
ORD157	340.30	8	70	98	0.26	NS	shear zone	121	2

ORD19	176.50	159	63	249	**1.54**	NW	shear zone	147	2
ORBD16	492.65	0	32	270	0.65	NS	ultramylonite	55	5
Quartz veins									
ORBD12	273.57	94	12	184	0.33	EW	quartz vein	13	7
ORBD12	291.53	75	60	165	**2.13**	EW	vein parallel foliation	35	6
ORBD12	270.75	108	71	198	**4.46**	EW	vein parallel to shear	14.5	7
ORD29	194.36	34	7	304	0.85	NE	vein parallel to shear	56	5
ORBD12	269.90	119	38	209	**2.00**	EW	vein x-cuts foliation	8.5	7
ORD10	249.90	101	30	191	0.09	EW	vein x-cuts foliation	118.5	2
ORBD12	258.09	48	89	318	**5.70**	NE	vein x-cuts shear	2	8
Schistosity and Cleavage									
ORD157	225.60	110	44	20	**1.88**	EW	continuous cleavage	5.5	8
ORDB17	631.15	114	74	204	0.02	EW	continuous cleavage	112	3
ORBD20	547.50	67	53	337	0.01	NE	continuous cleavage	11m above CSH	Mt Pleasant Sill
ORD21	168.69A	69	42	159	**1.33**	NE	continuous cleavage	146	2
ORD157	244.00	148	61	238	**1.04**	NW	continuous cleavage	24	6
ORD157	257.40	61	69	151	0.15	NE	spaced cleavage	37	6
ORD157	240.00	148	61	238	**1.04**	NW	spaced cleavage	20	7
ORD27	180.30	150	81	240	0.14	NW	spaced cleavage	21	7

*** Cashmans Sedimentary Horizon**

A3 GOLD PRODUCTION DATA SHEETS

A large component of the data in the following tables is compiled from Witt (1993b) and combined with structural and resource/reserve data from Centaur Mining and Exploration records.

Table A3.1 - Mines of the Siberia - Mt Pleasant district - Tonnes,grade and contained Au metal vs orientation

MINE	TONNES	KG	GRADE	STR	Gp	STRK	DIP	DIR	O/S	HOST	Tonne code	Kg code	Grade code	North	East
BELLEVUE	10189	214	21.0	SH	2	360	30	270		ED	10000-55000t	150-220kg	15-90g/T	6627000	325500
BENT TREE	249000	779	7.1	SH	1	330	55	240	S	BTB	55000-1.1Mt	220-900kg	5-10g/T	6631650	320350
BLACK FLAG	46500	521	11.2	SH	2	10	65	280	D	BTB	10000-55000t	220-900kg	10-15g/T	6619650	330250
BLACK RABBIT		30		SH	1	115	45	25		SK	35-150t	<60kg	15-90g/T	6641200	296200
BONNIDOON	2938	88	29.9	SH	2	10	65	100		MB	150-3500t	80-150kg	15-90g/T	6653350	302550
BOUNDARY	1150000	2301	2.0	SH	3	45	65	315		BTB	1.1M-5.5Mt	1800-6000kg	<5g/T	6638781	312697
CAMPERDOWN	165000	792	4.8	SH	2	20	75	110	D	MB	55000-1.1Mt	220-900kg	<5g/T	6657000	304000
CAVE HILL	802	65	81.5	SH	3	250	80	160		SK	150-3500t	60-80kg	15-90g/T	6648250	299900
CAWSE	177000	591	3.3	BX	3	250	55	340	D	G	55000-1.1Mt	220-900kg	<5g/T	6636750	322950
DARK HORSE	147	40	273.8	SH	2	360	40	270		BTB	35-150t	<60kg	>250g/T	6629900	322250
DENVER CITY	659	18	26.9	SH	2	190	60	280		MPS	150-3500t	<60kg	15-90g/T	6637100	317700
DEVON CONSOLS GM	1	15	14969.4	VN	1	115	75	25		VB	<35t	<60kg	>250g/T	6616200	334400
DIXIE	4118	204	49.5	SH	1	295	75	205	S	SK	3500-8000t	150-220kg	15-90g/T	6629650	328450
ENTERPRISE	18000000	39600	2.2	SH	4	80	80	350		ED	>5.5Mt	>8000kg	<5g/T	6638300	316300
EXPECTATION	362	12	31.8	SH	3	240	85	330		BDB	150-3500t	<60kg	15-90g/T	6641000	298650
FAIR ADELAIDE	3856	17	4.5	VN	4	270	60	180		G	3500-8000t	<60kg	<5g/T	6646950	306300
GIMLET DUKE	1221	19	15.5	SH	4	270	75	180		ED	150-3500t	<60kg	15-90g/T	6639270	314829
GIMLET SOUTH	6200000	31135	5.0	BX	3	60	75	330		VB	>5.5Mt	>8000kg	5-10g/T	6636800	313000
GK SHOOT	1700000	7558	4.4	VN	4	270	70	360	S	MPS	1.1M-5.5Mt	>8000kg	<5g/T	6622250	330250
GLENROCK	2364	70	29.5	SH	2	165	80	255		OBS	150-3500t	60-80kg	15-90g/T	6637250	301550
GOLDEN	340	29	85.6	SH	1	340	40	70		WB	150-3500t	<60kg	15-90g/T	6652150	299900
GOLDEN BUCKLE	79	7	85.4	SH	2	10	70	100	D	MPS	35-150t	<60kg	15-90g/T	6624500	334000
GOLDEN MOUNT	2215	39	17.5	SH	4	290	35	200		ED	150-3500t	<60kg	15-90g/T	6637250	317100
GRANTS PATCH	180421	2446	13.6	BX	4	290	70	20	D	VB	55000-1.1Mt	1800-6000kg	10-15g/T	6629500	320300
GREAT ORA BANDA	1720	27	15.6	VN	4	278	60	188		MPS	150-3500t	<60kg	15-90g/T	6640793	311781
HENNING	1800000	9540	5.3	SH	3	60	85	330		VB	1.1M-5.5Mt	>8000kg	5-10g/T	6619400	330200
JACK HUGH	173	21	121.2	SH	4	260	45	170		MPS	150-3500t	<60kg	90-250g/T	6644900	304650
KING EDWARD	1489	86	57.6	SH	1	330	30	240		MPS	150-3500t	80-150kg	15-90g/T	6623600	327700
LADY B	8017	371	46.3	SH	4	270	75	360		MPS	8000-10000t	220-900kg	15-90g/T	6624300	327900
LADY EVELYN	9658	321	33.3	SH	1	330	45	240		MPS	8000-10000t	220-900kg	15-90g/T	6635800	318000
LAST HOPE	794	11	14.0	SH	2	190	75	280		MPS	150-3500t	<60kg	10-15g/T	6640150	313750
LBE	1000000	4000	4.0	SH	4	270	75	360		G	55000-1.1Mt	1800-6000kg	<5g/T	6623800	328250
LIBERTY	10353	188	18.1	VN	1	308	50	218		G	10000-55000t	150-220kg	15-90g/T	6625850	331550
LIGHT OF THE SWAN	483	10	20.6	VN	3	215	90	0		G	150-3500t	<60kg	15-90g/T	6627000	331400
MAGPIE	1719	34	19.5	SH	1	135	60	225		BTB	150-3500t	<60kg	15-90g/T	6632200	319650

Table A3.1 - Mines of the Siberia - Mt Pleasant district - Tonnes,grade and contained Au metal vs orientation

MINE	TONNES	KG	GRADE	STR	Gp	STRK	DIP	DIR	O/S	HOST	Tonne code	Kg code	Grade code	North	East
MAJESTIC	105	5	47.0	VN	2	15	70	285		MB	35-150t	<60kg	15-90g/T	6655900	305150
MASCOTTE	983	2	1.6	SH	1	300	55	210		OS	150-3500t	<60kg	<5g/T	6632150	313800
MERRY DANCE		5		SH	2	7	40	97		SK	35-150t	<60kg	15-90g/T	6646900	298350
MISSED CHANCE	721	14	20.0	SH	1	330	60	240	D	MPS	150-3500t	<60kg	15-90g/T	6636600	317600
MISSOURI	300000	900	3.0	VN	1	315	70	45	D	MB	55000-1.1Mt	900-1800kg	<5g/T	6655000	302900
MONTE CARLO	809	13	16.6	SH	4	290	70	20		ED	150-3500t	<60kg	15-90g/T	6641410	312666
MT PLEASANT	1411	10	7.1	SH	3	35	80	305		MPS	150-3500t	<60kg	5-10g/T	6622800	331800
NEW MEXICO	8979	430	47.9	SH	4	270	55	180		ED	8000-10000t	220-900kg	15-90g/T	6645250	303600
ORINDA	3083	69	22.3	SH	1	300	55	210		OS	150-3500t	60-80kg	15-90g/T	6631500	314850
POLE	1407	70	50.0	SH	4	75	85	345		MB	150-3500t	60-80kg	15-90g/T	6647800	296900
PRIDE OF ERIN	548	27	49.5	SH	3	70	70	160		SK	150-3500t	<60kg	15-90g/T	6650800	301450
QUARTERS CENTRAL	11900000	35700	3.0	SH	3	60	80	330		BTB	>5.5Mt	>8000kg	<5g/T	6621200	330300
QUEENSLANDER	545	6	10.1	SH	3	245	70	335	S	MPS	150-3500t	<60kg	10-15g/T	6622300	331150
RACETRACK	1800000	5782	4.9	BX	3	240	70	330		VB	1.1M-5.5Mt	1800-6000kg	<5g/T	6618000	330800
RENOWN	269	22	83.5	SH	3	230	80	320		MES	150-3500t	<60kg	15-90g/T	6630200	322150
ROYAL STD	866	14	15.9	VN	2	10	80	280	D	VB	150-3500t	<60kg	15-90g/T	6618300	332050
SANDKING	2240000	6794	3.1	SH	3	50	75	320		MB	1.1M-5.5Mt	6000-8000kg	<5g/T	6655450	303350
SIBERIA CONSOLS	2320	173	74.4	SH	3	65	70	155		SK	150-3500t	150-220kg	15-90g/T	6650000	300900
SLEEPING BEAUTY	546000	1856	3.4	BX	4	90	70	360		VB	55000-1.1Mt	1800-6000kg	<5g/T	6638192	312535
SLIPPERY GIMLET	1300000	9331	7.0	BX	3	57	87	327		VB	1.1M-5.5Mt	>8000kg	5-10g/T	6637290	313013
SOUTHERN SHOOT	1700000	7558	4.4	VN	3	240	70	330		MPS	1.1M-5.5Mt	>8000kg	<5g/T	6622700	330250
TAIPO	39	7	174.6	VN	2	350	47	80		BTB	35-150t	<60kg	90-250g/T	6619150	334100
THIEL WELL	600000	3000	5.0	SH	2	195	30	105		BDB	55000-1.1Mt	1800-6000kg	5-10g/T	6641000	298700
THREE EIGHTS	2087	158	22.3	SH	1	130	45	40		SK	150-3500t	150-220kg	15-90g/T	6646000	297500
TUART	9100000	25480	2.8	SH	3	60	45	330		BTB	>5.5Mt	>8000kg	<5g/T	6621250	329700
WELLINGTON		25		SH	2	170	70	260	S	SK	35-150t	<60kg	15-90g/T	6631700	327050
WENTWORTH	83000	201	2.5	SH	2	360	70	270	D	VB	55000-1.1Mt	150-220kg	<5g/T	6630850	320250
WHITEHAVEN	642	10	15.5	SH	1	320	60	230		MPS	150-3500t	<60kg	15-90g/T	6640280	313446
WOTAN	139	7	50.7	SH	3	220	80	310		MPS	35-150t	<60kg	15-90g/T	6640080	313297
XMAS LONE HAND	38	6	155.1	SH	4	110	80	20		MPS	35-150t	<60kg	90-250g/T	6644850	306250
YELLOW BELLE	122	14	139.2	SH	2	170	85	80		SK	35-150t	<60kg	90-250g/T	6645100	296900

Table A3.2 - Mines of the Siberia - Mt Pleasant district - Tonnes,grade and contained Au metal versus orientation of subsidiary structures

MINE	TONNES	KG	GRADE	STR	Gp	STRK	DIP	DIR	O/S	HOST	Tonne code	Kg code	Grade code	North	East
BENT TREE	249000	779	7.1	SH	1	320	55	230	S	BTB	55000-1.1Mt	220-900kg	5-10g/T	6631650	320350
BLACK RABBIT		30		SH	1	155	50	65		SK	35-150t	<60kg	15-90g/T	6641200	296200
BONNIDOON	2938	88	29.9	SH	2	60	70	330		MB	150-3500t	80-150kg	15-90g/T	6653350	302550
CAMPERDOWN	165000	792	4.8	SH	2	350	75	80	D	MB	55000-1.1Mt	220-900kg	<5g/T	6657000	304000
CAWSE	177000	591	3.3	BX	3	275	55	5	D	G	55000-1.1Mt	220-900kg	<5g/T	6636750	322950
DARK HORSE	147	40	273.8	SH	2	15	90	105		BTB	35-150t	<60kg	>250g/T	6629900	322250
DIXIE	4118	204	49.5	SH	1	2	85	272	S	SK	3500-8000t	150-220kg	15-90g/T	6629650	328450
ENTERPRISE	18000000	39600	2.2	SH	4	35	77	305		ED	>5.5Mt	>8000kg	<5g/T	6638300	316300
GIMLET DUKE	1221	19	15.5	SH	4	360	70	270		ED	150-3500t	<60kg	15-90g/T	6639270	314829
GK SHOOT	3400000	15116	4.4	VN	4	245	90	335	S	MPS	1.1M-5.5Mt	>8000kg	<5g/T	6622250	330250
GOLDEN	340	29	85.6	SH	1	180	50	90		WB	150-3500t	<60kg	15-90g/T	6652150	299900
GOLDEN BUCKLE	79	7	85.4	SH	2	330	70	60	D	MPS	35-150t	<60kg	15-90g/T	6624500	334000
GRANTS PATCH	180421	2446	13.6	BX	4	340	50	250	D	VB	55000-1.1Mt	1800-6000kg	10-15g/T	6629500	320300
LADY B	8017	371	46.3	SH	4	45	70	315		MPS	8000-10000t	220-900kg	15-90g/T	6624300	327900
LIBERTY	10353	188	18.1	VN	1	250	70	160		G	10000-55000t	150-220kg	15-90g/T	6625850	331550
LIGHT OF THE SWAN	483	10	20.6	VN	3	145	70	235		G	150-3500t	<60kg	15-90g/T	6627000	331400
MAGPIE	1719	34	19.5	SH	1	35	90	305		BTB	150-3500t	<60kg	15-90g/T	6632200	319650
MAJESTIC	105	5	47.0	VN	2	250	80	160		MB	35-150t	<60kg	15-90g/T	6655900	305150
MISSED CHANCE	721	14	20.0	SH	1	290	70	200	D	MPS	150-3500t	<60kg	15-90g/T	6636600	317600
MISSOURI	300000	900	3.0	VN	1	350	60	260	D	MB	55000-1.1Mt	900-1800kg	<5g/T	6655000	302900
MONTE CARLO	809	13	16.6	SH	4	242	65	332		ED	150-3500t	<60kg	15-90g/T	6641410	312666
QUARTERS CENTRAL	11900000	35700	3.0	SH	3	20	90	290		BTB	>5.5Mt	>8000kg	<5g/T	6621200	330300
QUEENSLANDER	545	6	10.1	SH	3	100	70	10	S	MPS	150-3500t	<60kg	10-15g/T	6622300	331150
ROYAL STD	866	14	15.9	VN	2	235	65	325	D	VB	150-3500t	<60kg	15-90g/T	6618300	332050
SANDKING	2240000	6794	3.1	SH	3	35	55	125		MB	1.1M-5.5Mt	6000-8000kg	<5g/T	6655450	303350
SIBERIA CONSOLS	2320	173	74.4	SH	3	50	45	140		SK	150-3500t	150-220kg	15-90g/T	6650000	300900
TAIPO	39	7	174.6	VN	2	360	60	270		BTB	35-150t	<60kg	90-250g/T	6619150	334100
THIEL WELL	600000	3000	5.0	SH	2	90	80	360		BDB	55000-1.1Mt	1800-6000kg	5-10g/T	6641000	298700
WELLINGTON		25		SH	2	245	70	335	S	SK	35-150t	<60kg	15-90g/T	6631700	327050
WENTWORTH	83000	201	2.5	SH	2	320	70	230	D	VB	55000-1.1Mt	150-220kg	<5g/T	6630850	320250
WHITEHAVEN	642	10	15.5	SH	1	300	90	210		MPS	150-3500t	<60kg	15-90g/T	6640280	313446
XMAS LONE HAND	38	6	155.1	SH	4	335	40	245		MPS	35-150t	<60kg	90-250g/T	6644850	306250
YELLOW BELLE	122	14	139.2	SH	2	287	90	197		SK	35-150t	<60kg	90-250g/T	6645100	296900

Table A3.3 - Host rock groups for the main orientations and number of structures in each

NW-SE	%	N-S	%	ENE-WSW	%	E-W	%	ALL
		MPS	**17.6**					
MPS	26.7	ED	5.9	MPS	21.1	ED	33.3	
OS	13.3	OBS	5.9	MES	5.3	MPS	33.3	
Sills	**40**	**Sills**	**29.4**	**Sills**	**26.4**	**Sills**	**66.6**	**39.3**
VB	6.7	BTB	17.6	BTB	15.7			
BTB	13.3	MB	17.6	VB	21.1	VB	13.3	
MB	6.7	VB	11.8	MB	5.2	MB	6.7	
Tholeiites	**26.7**	**Tholeiites**	**47**	**Tholeiites**	**42**	**Tholeiites**	**20**	**34.8**
SK	20	SK	17.6	SK	15.8	SK	0	
Ultramafics	**20**	**Ultramafics**	**17.6**	**Ultramafics**	**15.8**	**Ultramafics**	**0**	**13.6**
G	6.7	G	0	G	10.5	Granites	13.3	
Granites	**6.7**	**Granites**	**0**	**Granites**	**10.5**	**Granites**	**13.3**	**7.6**
WB	6.6	BDB	5.9	BDB	5.3			
High Mg Basalts	**6.6**	**High Mg Basalts**	**5.9**	**High Mg Basalts**	**5.3**	**High Mg Basalts**	**0**	**4.5**
TOTAL MINES	**22.7**		**25.8**		**28.8**		**22.7**	

Table A3.4 - Ranges for tonnage, grade and kg Au, and mines in the various categories for each host rock

HOSTROCK	TONNES	%	>55000t	GRADE	%	<10g/T	KG	%	>900kg
Enterprise dolerite 9.10%	**150-3500**	**50.0**	**16.6**	**<5**	**16.7**	**16.7**	**<60**	**50.0**	**16.7**
	8000-10000	16.7		15-90	83.3		150-220	16.7	
	10000-55000	16.7					220-900	16.7	
	>5.5M	16.6					>8000	16.7	
Mount Ellis Sill 1.50%	**150-3500**	**100.0**	**0**	**15-90**	**100.0**	**0**	**<60**	**100.0**	**0**
Mount Pleasant Sill 24.20%	**35-150**	**18.8**	**12.5**	**<5**	**12.5**	**18.8**	**<60**	**68.8**	**12.5**
	150-3500	56.3		5-10	6.3		80-150	6.3	
	8000-10000	12.5		10-15	12.5		200-900	12.5	
	1.1M-5.5M	12.5		15-90	56.3		>8000	12.5	
				90-250	12.5				
Ora Banda Sill 1.50%	**150-3500**	**100.0**	**0**	**15-90**	**100.0**	**0**	**60-80**	**100.0**	**0**
Orinda Sill 3.00%	**150-3500**	**100.0**	**0**	**<5**	**50.0**	**50**	**<60**	**50.0**	**0**
				15-90	50.0		60-80	50.0	
Bent Tree Basalt 12.10%	**35-150**	**25.0**	**25**	**<5**	**37.5**	**50**	**<60**	**37.5**	**37.5**
	150-3500	12.5		5-10	12.5		220-900	25.0	
	10000-55000	12.5		10-15	12.5		1800-6000	12.5	
	55000-1.1M	12.5		15-90	12.5		>8000	25.0	
	1.1M-5.5M	12.5		90-250	12.5				
				>250	12.5				
Missouri Basalt 9.10%	**35-150**	**16.7**	**50**	**<5**	**50.0**	**50**	**<60**	**16.6**	**33.2**
	150-3500	33.3		15-90	50.0		60-80	16.6	
	55000-1.1M	33.3					80-150	16.6	
	1.1M-5.5M	16.7					220-900	16.6	
							900-1800	16.6	
							6000-8000	16.6	
Victorious Basalt 13.60%	**<35**	**11.1**	**77.7**	**<5**	**33.3**	**66.6**	**<60**	**22.2**	**66.6**
	15-350	11.1		5-10	33.3		>8000	33.3	
	55000-1.1M	33.3		10-15	11.1		150-220	11.1	
	1.1M-5.5M	33.3		15-90	11.1		1800-6000	33.3	
	>5.5M	11.1		>250	11.1				
Siberia Komatiite 13.60%	**35-150**	**44.4**	**0**	**15-90**	**88.9**	**0**	**<60**	**55.6**	**0**
	150-3500	44.4		90-250	11.1		150-220	33.3	
	3500-8000	11.2					60-80	11.1	
Granites 7.60%	**150-3500**	**20.0**	**40**	**<5**	**60.0**	**60**	**<60**	**40.0**	**20**
	3500-8000	20.0		15-90	40.0		150-220	20.0	
	10000-55000	20.0					220-900	20.0	
	55000-1.1M	40.0					1800-6000	20.0	
Big Dick Basalt 3.00%	**150-3500**	**50.0**	**50**	**5-10**	**50.0**	**50**	<60	**50.0**	**50**
	55000-1.1M	50.0		15-90	50.0		1800-6000	50.0	
Wongi Basalt 1.50%	**150-3500**	**100.0**	**0**	**15-90**	**100.0**	**0**	**<60**	**100.0**	**0**

Table A3.5 - Tonnage,grade and kg Au, and mines in various categories for each structural direction

ORIENTATION	TONNES	%	>55000t	GRADE	%	<10g/T	KG	%	>900kg
NW-SE	**150-3500**	**53.3**	**13.3**	**15-90**	**73.3**	**20**	**<60**	**46.7**	**6.7**
	55000-1.1M	13.3		<5	13.3		150-220	20.0	
	<35	6.7		5-10	6.7		220-900	13.3	
	35-150	6.7		>250	6.7		60-80	6.7	
	3500-8000	6.7					80-150	6.7	
	8000-10000	6.7					900-1800	6.7	
	10000-55000	6.6							
N-S	**35-150**	**41.2**	**17.7**	**15-90**	**52.9**	**17.7**	**<60**	**58.8**	**5.9**
	150-3500	29.4		<5	11.8		150-220	11.8	
	55000-1.1M	17.7		10-15	11.8		220-900	11.7	
	10000-55000	11.7		90-250	11.7		60-80	5.9	
				5-10	5.9		80-150	5.9	
				>250	5.9		1800-6000	5.9	
ENE-WSW	**150-3500**	**42.1**	**52.6**	**15-90**	**36.8**	**57.8**	**<60**	**36.8**	**47.3**
	1.1M-5.5M	31.6		<5	36.8		1800-6000	10.5	
	35-150	5.3		5-10	21.0		>8000	31.5	
	55000-1.1M	5.3		10-15	5.3		60-80	5.3	
	>5.5M	15.7					150-220	5.3	
							220-900	5.3	
							6000-8000	5.3	
E-W	**150-3500**	**40.0**	**33.3**	**15-90**	**46.7**	**33.3**	**<60**	**46.7**	**33.3**
	55000-1.1M	20.0		<5	33.3		1800-6000	20.0	
	8000-10000	13.3		90-250	13.3		220-900	13.3	
	35-150	6.7		10-15	6.7		>8000	13.3	
	3500-8000	6.7					60-80	6.7	
	1.1M-5.5M	6.7							
	>5.5M	6.6							

A4 SEISMIC SURVEY SPECIFICATIONS

The following information is transcribed from Goleby *et al.* (1993)

The subset of seismic data used in this study comes from a 213km long, deep seismic reflection profile oriented about E-W, 30km north of Kalgoorlie. The data were acquired by the Australian Geological Survey Organisation using an SN368 seismic telemetry acquisition system. Seismic source was 8kg explosive charges buried at a maximum depth of 36m. Seismic signals were acquired using 96 active data channels (geophones) spaced at 40m along the traverse. Shots were recorded for 20 seconds at a 2sec sampling rate.

A5 AEROMAGNETIC SURVEY SPECIFICATIONS

Several aeromagnetic data sets are used for this study compiled from existing multi-client aeromagnetic surveys as well as recent high-resolution aeromagnetic surveys flown over the Ora Banda / Mount Pleasant areas. Surveys at 50m line-spacing, 40m sensor height and 6m nominal sampling interval were flown in the late 1990's over Ora Banda and Mt Pleasant by Aerodata. Lines were oriented at 045°, approximately orthogonal to stratigraphy.

A single aeromagnetic data set compiled from these sources was used by Vearncombe (1998b) for an interpretation at 1:100,000 scale. This data set was processed to produce a series of up to 70 images including total magnetic intensity, first and second vertical derivatives, auto gain control filtering and reduction to the pole, in a range of sun angles to highlight strike variations in linear features.